Christian Schorn

NMR Spectroscopy: Data Acquisition

WILEY-VCH

Weinheim · New York · Chichester · Brisbane · Singapore · Toronto

Dr. Christian Schorn
Institute for Molecular Biology
ETH Zürich
Hoenggerberg
CH-8093 Zürich
Switzerland

A CD-ROM containing a teaching version of the program NMR-SIM (© Bruker Analytik GmbH) is included with this book. Readers can obtain further information on this software by contacting: Dr. Pavel Kessler, Bruker Analytik GmbH, Silberstreifen, D-76287 Rheinstetten, Germany; Pavel.Kessler@bruker.de

Preface

The application of NMR spectroscopy into new fields of research continues on an almost daily basis. High-resolution NMR experiments on compounds of low molecular mass in the liquid phase are now routine and modern NMR spectroscopy is aimed at overcoming some of the inherent problems associated with the technique. Thus higher magnetic field strengths can be used to help overcome the problems associated with low sample concentration enabling the analysis of complex spectra of large macromolecules such as proteins whilst also helping to advance the study of non liquid samples by MAS and solid state NMR spectroscopy. Apart from the chemical and physical research fields NMR spectroscopy has become an integral part of industrial production and medicine, e.g. by MRI (magnetic resonance imaging) and MRS (magnetic resonance spectroscopy). The basic principles of acquiring the raw time domain data, processing this data and then analysing the spectra is similar irrespective of the particular technique used. The diversity of NMR is such that a newcomer to NMR spectroscopy might train in the field of high resolution NMR and establish his career in solid state NMR. A distinct advantage of NMR spectroscopy is that the basic knowledge of acquisition, processing and analysis may be transferred from one field of endeavour to another. These ideas and perspectives were the origin for the series entitled ***Spectroscopic Techniques: An Interactive Course***. The section relating to ***NMR Spectroscopy***, consists of four volumes

- Volume 1 – *Processing Strategies*
- Volume 2 – *Data Acquisition*
- Volume 3 – *Modern Spectral Analysis*
- Volume 4 – *Intelligent Data Management*

and deals with all the aspects of a standard NMR investigation, starting with the definition of the structural problem and ending – hopefully – with the unravelled structure. This sequence of events is depicted on the next page. The central step is the transformation of the acquired raw data into a NMR spectrum, which may then be used in two different ways. The NMR spectrum can be analysed and the NMR parameters such as chemical shifts, coupling constants, peak areas (for proton spectra) and relaxation times can be extracted. Using NMR parameter databases and dedicated software tools these parameters may then be translated into structural information. The second way follows the strategy of building up and making use of NMR databases. NMR spectra serve as the input for such data bases, which are used to directly compare the measured spectrum of an unknown compound either with the spectra of known compounds or with the spectra predicted for the expected chemical structure. Which of
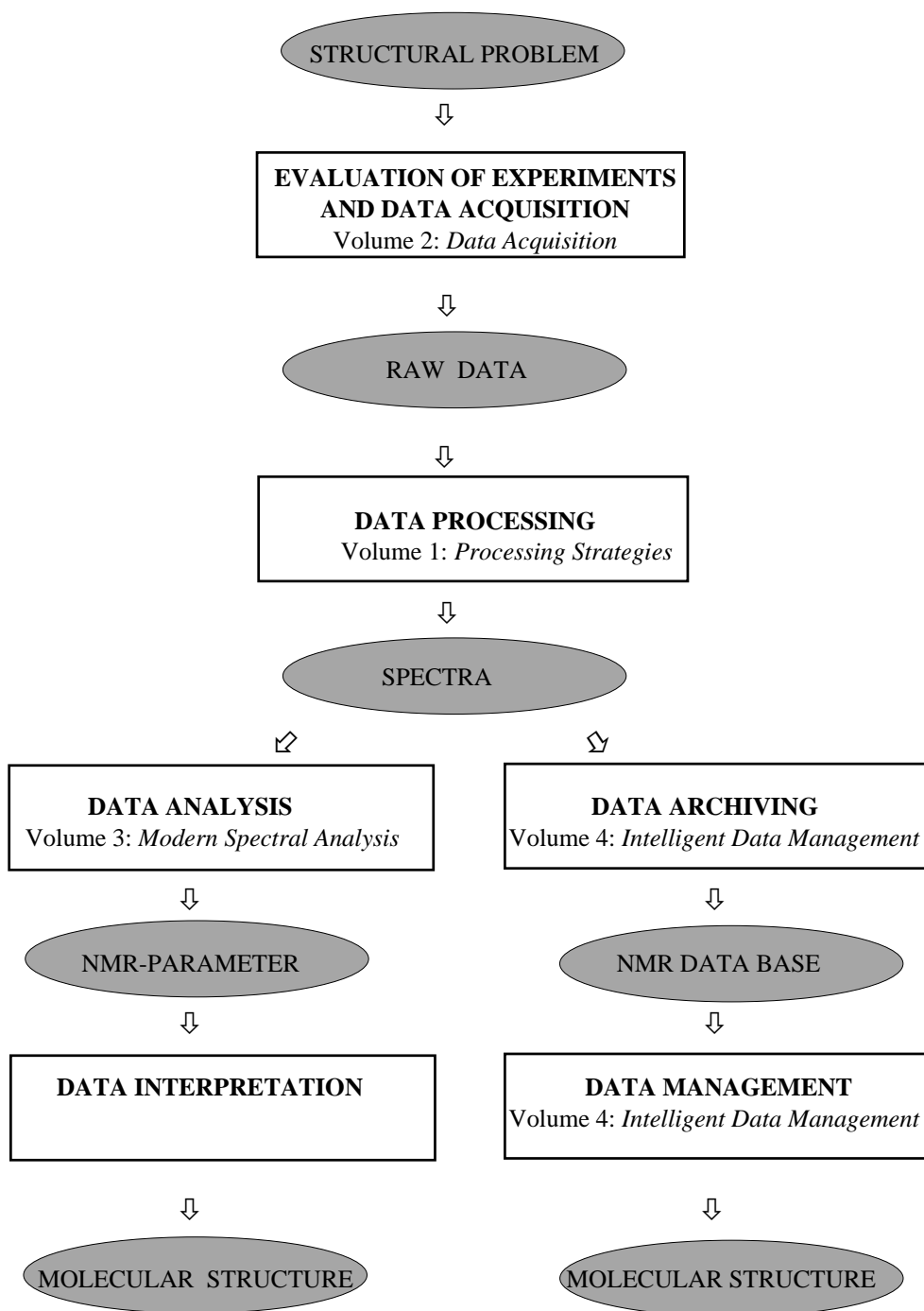
the two approaches is followed depends on the actual structural problem. Each of them has its own advantages, limitations and field of application. However, it is the combined application of both techniques that makes them such a powerful tool for structure elucidation.

The contents of volumes 1 – 4 may be summarized as follows:

Volume 1: ***Processing Strategies***

Processing NMR data transforms the acquired time domain signal(s) – depending on the experiment – into 1D or 2D spectra. This is certainly the most central and important step in the whole NMR analysis and is probably the part, which is of interest to the vast majority of NMR users. Not everyone has direct access to an NMR spectrometer, but most have access to some remote computer and would prefer to process their own data according to their special needs with respect to their spectroscopic or structural problem. This also includes the graphical layout for the presentation of reports, papers or thesis. It is essential for the reliability of the extracted information and subsequent conclusions with respect to molecular structure, that a few general rules are followed when processing NMR data. It is of great advantage that the user is informed about the many possibilities for data manipulation so they can make the best use of their NMR data. This is especially true in more demanding situations when dealing with subtle, but nevertheless important spectral effects. Modern NMR data processing is not simply a Fourier transformation in one or two dimensions, it consists of a series of additional steps in both the time and the frequency domain designed to improve and enhance the quality of the spectra.

Processing Strategies gives the theoretical background for all these individual processing steps and demonstrates the effects of the various manipulations on suitable examples. The powerful Bruker 1D WIN-NMR, 2D WIN-NMR and GETFILE software tools, together with a set of experimental data for two carbohydrate compounds allow you to carry out the processing steps on your own remote computer, which behaves in some sense as a personal "NMR processing station". You will learn how the quality of NMR spectra may be improved, experience the advantages and limitations of the various processing possibilities and most important, as you work through the text, become an expert in this field. The unknown structure of one of the carbohydrate compounds should stimulate you to exercise and apply what you have learnt. The elucidation of this unknown structure should demonstrate, how powerful the combined application of several modern NMR experiments can be and what an enormous and unexpected amount of structural information can thereby be obtained and extracted by appropriate data processing. It is this unknown structure which should remind you throughout this whole educational series that NMR data processing is neither just "playing around" on a computer nor some kind of scientific "l'art pour l' art". The main goal for measuring and processing NMR data and for extracting the structural information contained in it is to get an insight into how molecules behave. Furthermore, working through ***Processing***

STRUCTURAL PROBLEM

⇩

**EVALUATION OF EXPERIMENTS
AND DATA ACQUISITION**
Volume 2: *Data Acquisition*

⇩

RAW DATA

⇩

DATA PROCESSING
Volume 1: *Processing Strategies*

⇩

SPECTRA

⇗   ⇖

DATA ANALYSIS
Volume 3: *Modern Spectral Analysis*

DATA ARCHIVING
Volume 4: *Intelligent Data Management*

⇩   ⇩

NMR-PARAMETER

NMR DATA BASE

⇩   ⇩

DATA INTERPRETATION

DATA MANAGEMENT
Volume 4: *Intelligent Data Management*

⇩   ⇩

MOLECULAR STRUCTURE

MOLECULAR STRUCTURE

Strategies should encourage you to study other topics covered by related volumes in this series. This is particularly important if you intend to operate a NMR spectrometer yourself, or want to become familiar with additional powerful software tools to make the best of your NMR data.

Volume 2: ***Data Acquisition***

Any NMR analysis of a structural problem usually starts with the selection of the most appropriate pulse experiment(s). Understanding the basic principles of the most common experiments and being aware of the dependence of spectral quality on the various experimental parameters are the main prerequisites for the successful application of any NMR experiment. Spectral quality on the other hand strongly determines the reliability of the structural information extracted in subsequent steps of the NMR analysis. Even if you do not intend to operate a spectrometer yourself it would be beneficial to acquire some familiarity with the interdependence of various experimental parameters e.g. acquisition time and resolution, repetition rate, relaxation times and signal intensities. Many mistakes made with the application of modern NMR spectroscopy arise because of a lack of understanding of these basic principles.

Data Acquisition covers these various aspects and exploits them in an interactive way using the Bruker software package NMR-SIM. Together with 1D WIN-NMR and 2D WIN-NMR, NMR-SIM allows you to simulate routine NMR experiments and to study the interdependence of a number of NMR parameters and to get an insight into how modern multiple pulse NMR experiments work.

Volume 3: ***Modern Spectral Analysis***

Following the strategy of spectral analysis, the evaluation of a whole unknown structure, of the local stereochemistry in a molecular fragment or of molecular dynamic properties, depends on NMR parameters. Structural information can be obtained from chemical shifts, homonuclear and heteronuclear spin-spin connectivities and corresponding coupling constants and from relaxation data such as NOEs, ROEs, T_1s or T_2s. It is assumed that the user is aware of the typical ranges of these NMR parameters and of the numerous correlation's between the NMR and structural parameters, i.e. between coupling constants, NOE enhancements or linewidths and dihedral angles, internuclear distances and exchange rates. However, the extraction of these NMR parameters from the corresponding spectra is not always straightforward,

- The spectrum may exhibit extensive signal overlap, a problem common with biomolecules.
- The spectrum may contain strongly coupled spin systems.
- The molecule under investigation may be undergoing dynamic or chemical exchange.

Modern Spectral Analysis discusses the strategies needed to efficiently and competently extract the NMR parameters from the corresponding spectra. You will be shown how to use the spectrum simulation package WIN-DAISY to extract chemical shifts, coupling constants and individual linewidths from even highly complex NMR spectra. In addition, the determination of T_1s, T_2s or NOEs using the special analysis tools of 1D WIN-NMR will be explained. Sets of spectral data for a series of

representative compounds, including the two carbohydrates mentioned in volume 1 are used as instructive examples and for problem solving. NMR analysis often stops with the plotting of the spectrum thereby renouncing a wealth of structural data. This part of the series should encourage you to go further and fully exploit the valuable information "hidden" in the carefully determined NMR parameters of your molecule.

Volume 4: ***Intelligent Data Management***

The evaluation and interpretation of NMR parameters to establish molecular structures is usually a tedious task. An alternative way to elucidate a molecular structure is to directly compare its measured NMR spectrum – serving here as a fingerprint of the investigated molecule – with the corresponding spectra of known compounds. An expert system combining a comprehensive data base of NMR spectra with associated structures, NMR spectra prediction and structure generators not only facilitates this part of the NMR analysis but makes structure elucidation more reliable and efficient.

In ***Intelligent Data Management***, an introduction to the computer-assisted interpretation of molecular spectra of organic compounds using the Bruker WIN-SPECEDIT software package is given. This expert system together with the Bruker STRUKED software tool is designed to follow up the traditional processing of NMR spectra using 1D WIN-NMR and 2D WIN-NMR in terms of structure-oriented spectral interpretation and signal assignments. WIN-SPECEDIT offers not only various tools for automatic interpretation of spectra and for structure elucidation, including the prediction of spectra, but also a number of functions for so-called "authentic" archiving of spectra in a database, which links molecular structures, shift information and assignments with original spectroscopic data. You will learn to exploit several interactive functions such as the simple assignment of individual resonances to specific atoms in a structure and about a number of automated functions such as the recognition of signal groups (multiplets) in ^{1}H NMR spectra. In addition, you will also learn how to calculate and predict chemical shifts and how to generate a local database dedicated to your own purposes. Several examples and exercises, including the two carbohydrate compounds from volume 1, serve to apply all these tools and to give you the necessary practice for your daily spectroscopic work.
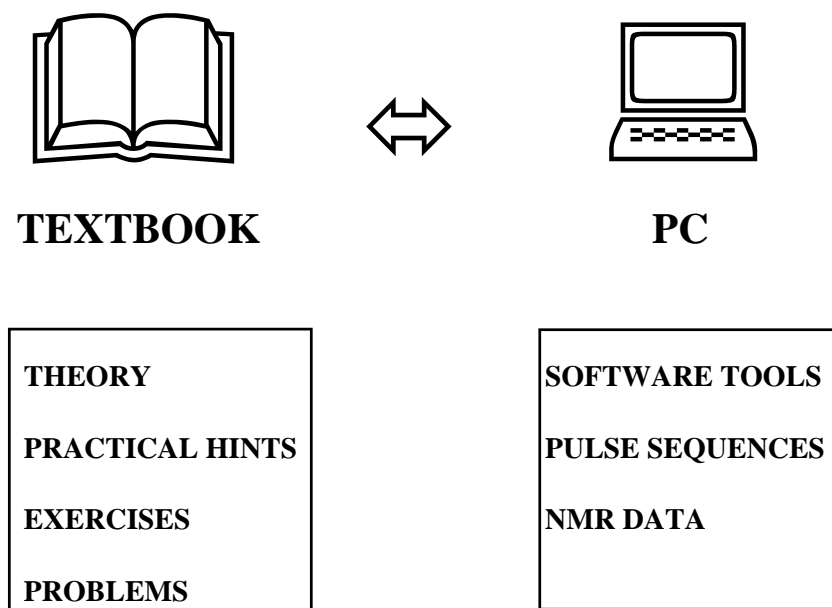
It is the primary aim of the series ***Spectroscopic Techniques: An Interactive Course*** to teach the user how NMR spectra may be obtained from the data acquired on a spectrometer and how these spectra may be used to establish molecular structure following one of the two strategies outlined before. The series of volumes therefore emphasises the methodical aspect of NMR spectroscopy, rather than the more usual analytical aspects *i.e.* the description of the various NMR parameters and of how they depend on structural features, presented in numerous textbooks.

This series of books is to give the newcomer to physical NMR spectroscopy the necessary information, the theoretical background and the practice to acquire NMR spectra and to process the measured raw data from modern routine homonuclear and heteronuclear 1D and 2D NMR experiments. They will also enable the user to evaluate NMR parameters, to generate and exploit dedicated databases and finally to establish the molecular structure.

Each of the four volumes consists of three parts:

- A written part covers the theoretical background and explains why things are done in particular manner. Practical hints, examples, exercises and problems are also included.
- Software tools dedicated to the items discussed in the corresponding volume are supplied on CD-ROM.
- The most popular 1D and 2D pulse sequences together with the corresponding NMR raw data and spectra are supplied on CD-ROM. They are used to simulate NMR experiments, to exercise data processing and spectral analysis and serve as a database for spectral interpretation.

It is this combination of written text, the software tools and supplied data, that make it different from other books on NMR spectroscopy and which should draw your attention to the many possibilities and the enormous potential of modern NMR. Sitting in front of your PC , which becomes your personal "PC-NMR spectrometer", you experience in a very direct and practical way, how modern NMR works. According to the approved rule "Learning by Doing" you perform NMR experiments without wasting valuable spectrometer time, handle experimental data in different ways, plot 1D and 2D spectra, analyse spectra and extract NMR parameters and learn to build up and use NMR data bases.

TEXTBOOK   **PC**

THEORY **PRACTICAL HINTS** **EXERCISES** **PROBLEMS**	**SOFTWARE TOOLS** **PULSE SEQUENCES** **NMR DATA**

It is recommended that you use all these educational tools in a complementary and interactive way switching from textbook to the software tools and the sets of data stored on the PC and back again and that you proceed at your own rate. It is assumed that you verify the numerous examples and solve the exercises in order to improve your skill in

using the various software tools and to consolidate the theoretical background. In this way, the strongly interconnected components of this series of books are best utilised and will guarantee the most efficient means to become an expert in this field.

Furthermore it is recommended that NMR newcomers start with the central volume ***Processing Strategies*** and complete their education in modern NMR spectroscopy according to their special needs by working through the appropriate volumes, ***Data Acquisition***, ***Modern Data Analysis*** and ***Intelligent Data Management***.

This interactive course in practical NMR spectroscopy may be used in dedicated courses in modern NMR spectroscopy at universities, technical schools or in industry, or may be used in an autodidactic way for those interested in this field.

Acknowledgement

Table of Contents

1 Introduction

1.1 Scope and Audience

The aim of this book is to illustrate the use of the NMR-SIM simulation program; in common with the other volumes in the series *Spectroscopic Techniques: An Interactive Course* a teaching version of NMR-SIM is included with this book. Thus the basics of NMR as described in manifold monographs [1.1 – 1.14] can be visualized. It is necessary to draw a distinction between the program WIN-DAISY covered in *NMR Spectroscopy: Modern Spectral Analysis* [1.11] and NMR-SIM, both are simulation programs but both have very different uses in NMR spectroscopy. Essentially WIN-DAISY uses chemical shifts and coupling constants to simulate a NMR spectrum using standard quantum mechanical calculations whilst NMR-SIM uses experimental parameters in conjunction with pulse sequences to simulate the experimental 1D and 2D NMR data which may then be processed to produce the appropriate NMR spectrum. NMR-SIM assumes a perfect spectrometer and certain sample specific variables such as probe matching, probe tuning, shimming and temperature control cannot be incorporated into the simulation. However other experimental variables such as the effect of non-optimized pulse angles, delays and a non-uniform excitation range due to limited transmitter power (off-resonance effects) may be simulated. In these cases the effect of the experiment parameters in a specific pulse sequence can be studied and their influence on the overall result evaluated. NMR-SIM may also be used to study and optimize pulse sequences published in the literature; in this way new pulse sequences may be completely debugged before implementing the new pulse sequence on an NMR spectrometer saving a considerable amount of spectrometer time. The applications of NMR-SIM can be summarized as follows:

- To demonstrate and understand the basic principles of pulse sequences by means of the resulting NMR spectra.
- To analyze the dependence of particular parameters, such as spin systems variables, on the experiment result
- To visualize the effect of new pulse sequences on complex spin systems
- To check the performance of a real spectrometer and to assist in evaluating experimental errors

The focus of this book is data acquisition using NMR-SIM to simulate the raw experimental data. In common with the other volumes in this series the emphasis is on "learning by doing" and there are many simulations to help the reader become familiar with the simulation program. This book will be of use to all NMR spectroscopist ranging from the newcomer to the more experienced user. The newcomer can use this book and

software to understand how pulse sequences work and to check and evaluate the flood of new pulse sequences appearing in the literature prior to testing a proposed pulse sequence on a spectrometer. This approach is a much more efficient use of spectrometer time because the pulse sequences used in NMR-SIM can be used directly on a BRUKER DRX spectrometer with only minor modifications.

The advanced NMR spectroscopist may use this book in a different manner using NMR-SIM for teaching and demonstration purposes. They may also use it in the evaluation or the design of new pulse sequence particularly when applied to a complex spin system where analysis using mathematical methods is cumbersome, less obvious and time-consuming compared to the visual results of NMR-SIM.

1.1.1   Simulation environment

The NMR-SIM program*:* NMR-SIM is based on a density matrix approach to generate data that is as comparable to real experimental data as possible. Although the calculation is based on an ideal spectrometer and ignores effects such as magnet field inhomogenity, several parameters can be set to study the impact of non-optimum conditions in a spectrum. There are also a number of other constraints in the current version of NMR-SIM aimed at reducing computer resources. Relaxation effects are implemented using the Bloch equations and can be "switched off" or restricted to only the acquisition period instead of the whole experiment. Transverse relaxation is defined for the linewidth calculation. Furthermore transverse and longitudinal relaxation can be taken into account in the simulation to reproduce relaxation artefacts. Due to this simple approach relaxation related processes and phenomena such as cross-relaxation and NOE effects which are used experimentally to detect and measure spatial proximity among nuclear spins, are neglected.

NMR-SIM — Generation of raw data for 1D and 2D NMR experiments

1D WIN-NMR | 2D WIN-NMR — Transformation of 1D and 2D raw data into corresponding spectra to analyse and understand experiments and to study influences of experimental or spin system parameters
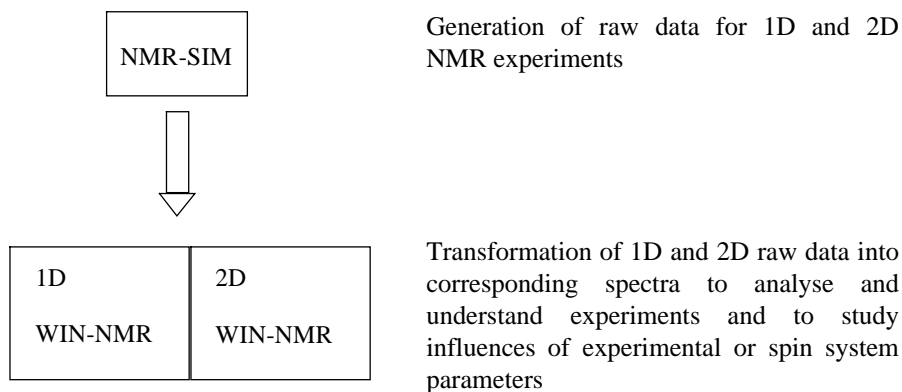
Fig. 1.1:   Flow of raw data simulation and data processing.

Similarly incoherent magnetisation transfer due to chemical exchange is also not part of the current version of NMR-SIM. Only chemical shift and coupling evolution that

occur during the execution of a pulse sequence are considered whilst relaxation processes are simplified. Finally in this teaching version of NMR-SIM the simultaneous execution of a selective pulse and a hard or selective pulse on a second rf channel is not enabled.

The Reader: It is assumed that the reader understands the fundamental principles of pulse Fourier transform spectroscopy (PFT) and is proficient in using the MS-Windows operating system and Windows based programs. The references at the end of section 1.4 list both introductory and comprehensive texts on the main principles of NMR spectroscopy. Furthermore the reader should be familiar with computer environments, as working on a spectrometer inevitable requires computer management skills.

The Personal PC: The NMR-SIM program can be run on any IBM-compatible PC with an 80486 or higher processor. The operating system has to be MS-Windows NT 4.0 or MS-Windows 2000, NMR-SIM will not install on a PC running MS-Windows 9x. For the correct operation of the teaching version of both NMR-SIM and the WIN-NMR the operating system must be installed properly. The basic hardware configuration is set by the requirements of the operating system but the program requires a minimum of 32 MB RAM memory and a free hard disk partition of approximately 300 MB for temporary files and stored data. To ensure that the calculation times are no longer than two minutes all the C*heck its* have been optimized and the simulations tested on a PC equipped with a 300 MHz Intel Celeron processor and 128 MB RAM memory.

The full version of the NMR-SIM program can be purchased either as the Windows NT/Windows 2000 version or the UNIX version from BRUKER. These versions use the same program set-up and commands as the Teaching version or though by necessity the directory structure of the UNIX version is different. For further details the reader is invited to contact BRUKER or their local representative directly, the contact addresses are listed on BRUKER's worldwide web homepage [1.13, 1.14].

1.1.2   Book content

The book is separated into five main chapters with the overall layout designed to cater for both the new and the experienced NMR spectroscopist. Chapter 1 describes the installation of NMR-SIM and the processing software packages 1D WIN-NMR and 2D WIN-NMR, it also contains a brief description of NMR-SIM. Chapter 2 uses NMR-SIM to illustrate the theoretical background of the NMR experiment instead of the normal mathematical approach and shows that even when using complex pulse sequences NMR-SIM can be used to simulate realistic experimental data. The concepts introduced in this chapter form the basis for understanding the pulse sequences discussed in chapter 5 as well as the pulse sequences that appear in the literature. Chapter 3 briefly discusses data processing using 1D WIN-NMR and 2D WIN-NMR. Chapter 4 is essentially a reference chapter and using *Check its* extensively looks in detail at various aspects of using NMR-SIM such as editing spin systems, the pulse programming language and using the Bloch simulator. Chapter 5 is the main part of the volume and examines the pulse sequences routinely used for studying non-biopolymer molecules in a modern NMR laboratory. In

many cases the differences between the standard sequence and its variants are demonstrated. This chapter also looks in detail at the building blocks that often occur in pulse sequences such as hard and shaped pulses and filter elements.

1.2   Software

The CD-ROM enclosed with this book contains the special teaching version of the commercially available simulation program NMR-SIM and the NMR data processing programs 1D WIN-NMR and 2D WIN-NMR. The versions of the WIN-NMR programs are the same as included with the books in this series *Processing Strategies* and *Modern Spectral Analysis* [1.10, 1.11].

The NMR-SIM program is based on the full commercial version of NMR-SIM 2.8.5. Both versions will only run under MS Windows NT 4.0 or Windows 2000 operating system. There are some minor differences between the teaching and full program version:

- the type of experiment that can be studied is restricted to two rf channels
- the number of pre-defined nuclei is reduced to a minimum and the examples used in this volume have taken this into account
- the number of magnetically non-equivalent spins which form a coupling system is reduced to 9 spins
- all data which is generated by the NMR-SIM teaching version can only be processed by the teaching versions of WIN-NMR.

If the teaching versions of 1D WIN-NMR and 2D WIN-NMR have not been installed already as part of *Spectroscopic Techniques: An interactive Course* they must be installed as outlined below. The CD-ROM also contains the NMR-SIM, 1D WIN-NMR and 2D WIN-NMR manuals as pdf files plus a copy of Adobe Acrobat Reader required to read pdf files. Finally the CD-ROM contains a file ***result.pdf*** containing additional information and results appertaining to the various *Check its* in this book.

1.2.1   Installation

All the programs and files required to perform the *Check its* in this book are contained on the CD-ROM which is enclosed in this book. The CD-ROM is configured with an autorun function such that program installation starts automatically after the CD-ROM has been inserted in the CD-ROM drive. A self-instructing menu guides the reader through the whole installation procedure. If the autorun facility has been disabled or is not available the programs must be installed using the Run command and Windows Explorer as shown in *Check its 1.2.1.1* and *1.2.1.2*. The default pathnames used by the installation procedure are also used by the *Check its* in this book, if the default pathways are altered in any way the files used in the *Check its* must be modified accordingly. Users who already have the full version of NMR-SIM installed should take care during the installation procedure not to overwrite the existing executable program and related files.

It must be emphasized that the simulation results calculated with the teaching version of NMR-SIM can only be processed with the teaching version of 1D WIN-NMR and 2D WIN-NMR.

1.2.1.1 Check it in WINDOWS

Insert the software CD-ROM in the CD-ROM drive. If the autorun facility is available the introductory window will appear and it is only necessary to follow the dialogue. If the autorun facility is not available use the **Run** option of the **Start** pop-up menu in the bottom menu bar. In the pop-up window select *[CD-ROM drive letter]:SETUP.EXE*. Confirm the introductory window with the **Next** button. In the Product Selection window select the programs WINNMR, NMRSIM and AcroRead 4.0. Click the **Next** button to start the installation. During the installation procedure a number of different windows appears as shown in the flow diagram below. Most of these windows can be passed unchanged by clicking the **Next** button. During the installation of the Adobe Acrobat Reader several user-friendly and self-explanatory windows will appear.

Windows ⇒ User interaction

"Welcome" ⇒ **Next**

"Custom Options Sections" ⇒ **Next**

"Choose Destination Location": 1D C:\TEACH\WIN1D etc. ⇒ **Next**

"Choose Destination Location": Spectra C:\TEACH\NMRData etc. ⇒ **Next**

"Choose Destination Location": Other Files C:\TEACH\ etc. ⇒ **Next**

"Select Components": make no selection ⇒ **Next**

"WIN-NMR Teaching Version Folder": *BRUKERTeach* ⇒ **Next** or enter the *new name*

"Information": "Setup Complete" ⇒ **Finish**

1D / 2D WIN-NMR installation.

Windows ⇒ User interaction

"Welcome" ⇒ **Next**

"Select the installation type" ⇒ choose *User installation*, **Next**

"Choose Destination Location": C:\Teach\NMR-SIM ⇒ **Next** or **Browse** (to select a new path)

"Choose Program Folder": *BRUKERTeach* ⇒ **Next** or enter the *new name*

"Information": "NMR-SIM setup is complete" ⇒ **Ok**

NMR-SIM installation

The configuration files used in the *Check its* can be used with the full version of NMR-SIM but the experimental data can only be processed using the full version of 1D

WIN-NMR and 2D WIN-NMR or by another processing software package after file conversion from the BRUKER format. It is convenience to have the icons for each program of the teaching software displayed on the main Windows desktop for fast access. *Check it 1.2.1.2* describes the procedure for setting up these shortcuts and gives the recommended icon names which will also be used in the later *Check its*.

Windows desktop

1.2.1.2 Check it in WINDOWS

Open NT-Explorer and if necessary resize the window so that part of the Desktop is also visible. Locate the file *C:\Teach\NMR-SIM\nmrsim_w.exe*. Select the file by holding down the right-hand mouse button and then drag the file onto the Desktop. Release the right-hand mouse button and in the on-the-fly-pop-up menu choose the **Create Shortcut(s) Here** option. To rename the icon click on the icon using the right-hand mouse button and select the **Rename** command from the on-the-fly pop-up menu. Using the keyboard enter the new name NMRSIMTeach followed by **RETURN**. Repeat the procedure for the 1D and 2D WIN-NMR programs using the file and path names *C:\Teach\Win1d\Demo1D.exe* and. *C:\Teach\Win2D\Demo2D.exe* respectively to create the icons named 1DWINTeach and 2DWINTeach.

In *Check it 1.2.1.3* the program manual files and the *result.pdf* file are installed.

1.2.1.3 Check it in MS-Windows

Using Windows NT Explorer create in the directory *C:\Teach* the subdirectories *Manuals* and *Results*. Copy the corresponding pdf-files from the CD-ROM to the newly created directories. On the CD-ROM the manuals and the result file are stored in the directories *\NMR-Sim\Manuals* and *\NMR-Sim\Results* respectively. To open the pdf-files move the cursor onto the filename in the Explorer directory tree and double click with the left-hand mouse button.

Nmrsim.pdf manual of NMR-SIM (Version 2.8)

Winnmr1d.pdf manual of 1D WIN-NMR

Winnmr2d.pdf manual of 2D WIN-NMR (16bit)

result.pdf documented simulation results of the *Check its*

Fig. 1.2 shows the directory structure generated by the software installation using the recommended directory. The main TEACH directory contains the program subdirectories Getfile, NMR-Sim, Win1D and Win2D plus the data subdirectory Nmrdata. The subdirectories Manuals and Results contain the software documentation for the programs and the additional information and results for most of the *Check its*.
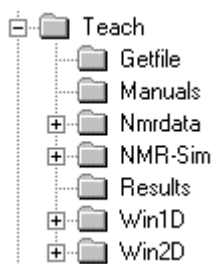
Fig. 1.2:   Directory structure - Software, data and documentation subdirectories installed according *Check its 1.2.11* and *1.2.1.3*.

1.2.2   The User Interfaces of NMR-SIM, 1D WIN-NMR and 2D WIN-NMR

The programs NMR-SIM, 1D WIN-NMR and 2D WIN-NMR are started using a double left-hand mouse button click on the appropriate icons on the Windows desktop.

The main window of NMR-SIM is subdivided in the **title bar** with the program name, the **menu bar** with the pull-down menu commands **File**, **NMR-Wizard**, **Edit** etc., the **rf channel option bar** with two accessible rf channel combo boxes and the **main status** window, see Fig. 1.3. Each command in the menu bar opens a pull-down menu that may contain sub-menus or commands that can be selected and opened/executed. The rf channel option bar uses isotope identifier to assign a specific nucleus and hence NMR frequency to the F1 or F2 channel. The main status window is built up in line order and shows the pulse program name, spin system name and other optional files associated with the current simulation.
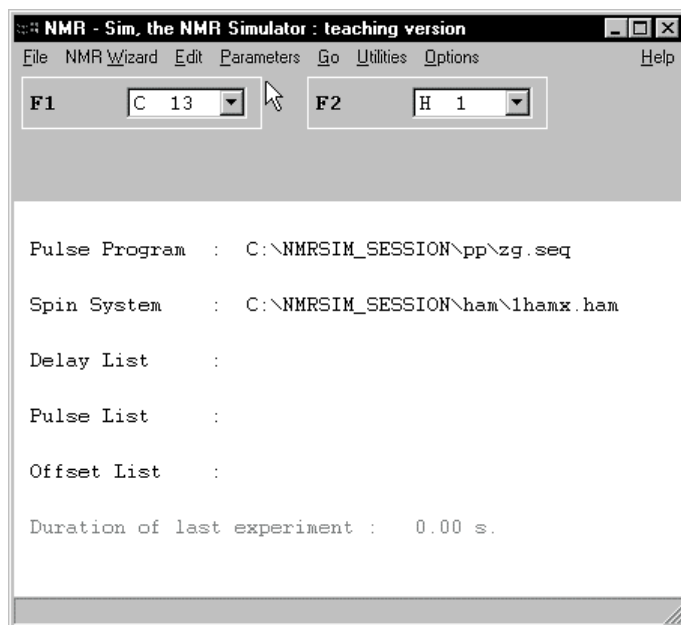
Fig. 1.3:   NMR-SIM - main window.

By default the calculated data is transferred automatically to the appropriate WIN-NMR processing software; 1D data is transferred to 1D WIN-NMR and 2D data to 2D WIN-NMR. When the simulation of a 1D NMR data set in NMR-SIM is completed 1D WIN-NMR is loaded into the foreground as the active program and the resulting FID displayed in the spectrum window as shown in Fig. 1.4. On the left-hand side of the 1D WIN-NMR window is a button panel containing a number of buttons that can be used to change the contents of the spectrum window in addition to performing a variety of processing commands such as **Window!** and **Zero Filling!** The commands in the menu bar open pull-down menus containing both sub-menus and processing commands. Section 3.2.3 and 3.3.2 give a brief description of the different processing steps and functions of 1D WIN-NMR and 2D WIN-NMR. For a full description the reader is referred to the WIN-NMR manuals on the CD or to the BRUKER WWW homepage [1.13] and [1.14].
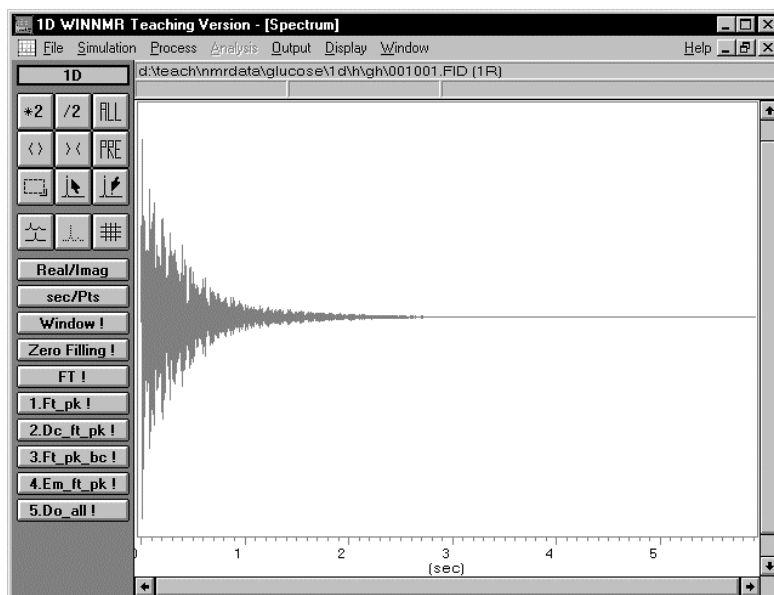
Fig. 1.4:   1D WIN-NMR - spectrum window.

After the simulation of a 2D NMR data set the 2D WIN-NMR main window, Fig. 1.5, opens for data processing. In a similar manner to 1D WIN-NMR the main window is subdivided into a menu bar, a spectrum window and a special 2D button panel. In contrast to 1D WIN-NMR 2D time domain data is not displayed in the spectrum window and a blank display is shown instead.

1.2.3   Data Organization

After the software installation two new directories will have been created in the root directory of the local PC. Assuming that the default pathway was used in the installation the program directory **C:\Teach\…** has the directory structure shown in Fig. 1.2. The second directory **C:\NMRSIM_SESSION** created contains all the pulse programs, spin systems and experimental set-ups files in the subdirectories **C:\...\CONFIG** configuration files, **C:\...\HAM** spin system files, **C:\...\PP** pulse program files, **C:\...\WAVE** pulse shape files, **C:\...\LIST** lists files and **C:\...\JOB** job files. Table 1.1 lists the different file extensions that might be helpful for identification and working with external text editors. The full version of NMR-SIM also creates two additional subdirectories **C:\...\PP.AMX** and **C:\...\PP.DMX** containing the different pulse programming language versions of the pulse programs for BRUKER AM/AMX and DMX/DRX spectrometers.

Table 1.1:   File extensions of NMR-SIM files.

*.cfg	configuration files
*.ham	spin system files
*.job	job files
*.ld	delay list
*.lo	offset list
*.lp	pulse list
*.pr	job protocol file
*.seq	pulse sequence file
*.sp	saved excitation profile file

In the following discussion it is assumed that the default pathways have been used during the installation process. If different pathways have been selected during the installation this must be taken into account when using the *Check its* and other references in this book.
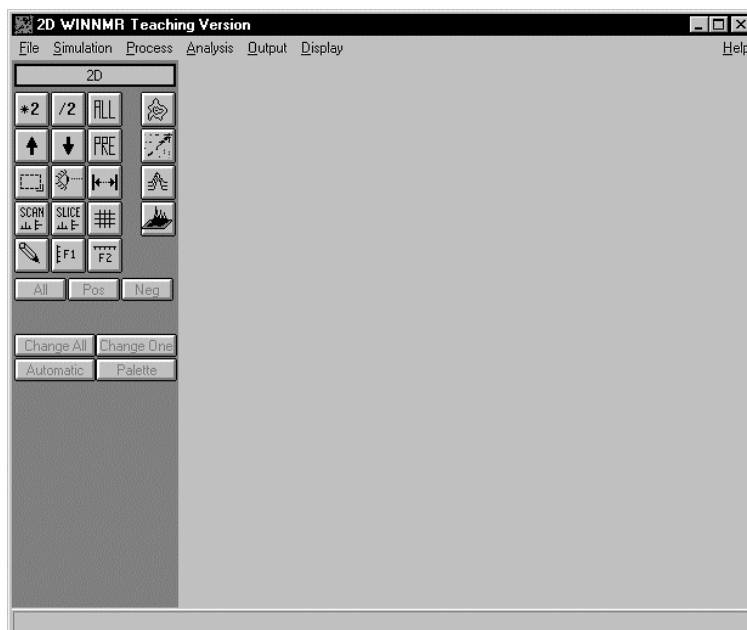
Fig. 1.5:   2D WIN-NMR - spectrum window.

1D WIN-NMR and 2D WIN-NMR Data Sets

Each NMR-SIM simulation creates a number of different files in a single subdirectory. The number and format of these files are similar to those obtained when converting experimental data from a BRUKER spectrometer into WIN-NMR format. Table 1.2 lists some of the file extensions used by WIN-NMR. For copyright protection the data sets created by NMR-SIM are encoded and can only be processed by the teaching version of the 1D WIN-NMR or 2D WIN-NMR processing software.

Table 1.2:   File extensions of WIN-NMR files.

	1D Data Set	2D Data Set
Acquisition Parameters	*.AQS	*.FA1 and *.FA2
Processing Parameters	*.FQS	*.FP1 and *.FP2
Raw Data	*.FID	*.SER
Processed Data - Real	*.1R	*.RR
Processed Data - Imaginary	*.1I	*.II, *.IR and *.RI

1.3   The Check its

In all the books in the series *Spectroscopic Techniques: An Interactive Course* the emphasis is on the interactive method of learning and this volume follows the same approach. The remaining chapters in this book all have a similar format, a short written introduction and number of *Check its* for the reader to complete. Before each *Check it* is a short introduction which may include the discussion of new concepts or the advantage or disadvantage of a particular pulse sequence etc. The *Check its* are then used to illustrate the points being discussed either by displaying the processed data in 1D WIN-NMR or 2D WIN-NMR or in the case of the Bloch simulator in a spherical or other display modes.

Each *Check it* is usually based on a configuration file which contains the complete experimental set-up (Fig. 1.6). After starting the simulation the reader will be prompted to define the output file to which the calculated data is stored. If no configuration file exists the pulse program, rf channels, spin system, acquisition and processing parameters have to be chosen by the reader before the simulation is run (Fig. 1.6 left hand side).

```
┌─────────────────────────────┐          ┌─────────────────────────────┐
│  selection of pulse program │          │                             │
│  spin system                │          │  loading a configuration file│
│                             │          │                             │
│  rf channel(s):             │          │  and check of experiment    │
│  assignment of radiofrequency│          │                             │
│                             │          │  parameters                 │
│  experiment parameters      │          │                             │
│                             │          │                             │
│    NMR-SIM settings         │          │                             │
│    processing parameters    │          │                             │
└─────────────────────────────┘          └─────────────────────────────┘
              │   "Run Experiment"                    │   "Run Experiment"
              ▼                                       ▼
┌─────────────────────────────┐          ┌─────────────────────────────┐
│  definition of output file  │          │  definition of output file  │
└─────────────────────────────┘          └─────────────────────────────┘
              │   transfer to                         │   transfer to
              ▼   1D or 2D WIN-NMR                     ▼   1D or 2D WIN-NMR
┌─────────────────────────────┐          ┌─────────────────────────────┐
│  processing, analysis and   │          │  processing, analysis and   │
│  optional plot              │          │  optional plot              │
└─────────────────────────────┘          └─────────────────────────────┘

         a new simulation                          a Check it
```

Fig. 1.6:   Flow chart of simulations based on a new experiment setup (left) and on a configuration file (right).

In each *Check it* the reader has to perform a series of tasks in the correct order. To reduce the text part of each *Check it* to the minimum and to stop being repetitive these operations and commands will be described in more detail here. The three main tasks are:

- loading a configuration file, replacing a pulse program or a spin system
- modification (editing) of the spin system file or the pulse program files and
- checking and eventual adjustment of experiment parameters or NMR-SIM options

The loading of a configuration file (cfg files) is done using the **Load from file...** command in the **File** pull-down menu. In the *Check its* this operation is described by the short hand notation **File│Experiment setup│Load from file...**. A left-hand mouse button click on the command field opens a standard Windows file list box. In this file list box it is possible to select a specific cfg file either directly from the keyboard or by using the mouse; it is also possible to change the directory and/or disk drive if necessary.
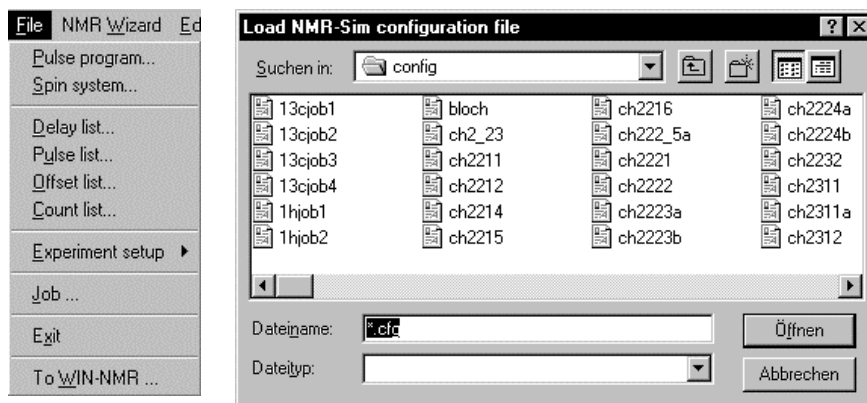
Fig. 1.7: Loading a configuration file - the **File** pull-down menu and **Experiment setup Load from file…** dialog box.

A different pulse sequence or spin system can be selected using the **Pulse program...** or **Spin system...** command of the **File** pull-down menu respectively. Again a standard Windows file list box appears displaying the existing pulse programs (*.seq) or spin system files (*.ham). In some *Check its* the same experiment is simulated using different NMR-SIM options or experiment parameters and the results compared. The NMR-Sim settings dialog box is opened by selecting the **NMR-Sim settings** command in the **Options** pull-down menu (**Options|NMR-SIM settings**) while the experimental parameters dialog box is opened using the **Check Experiment parameters** command of the **Go** pull-down menu (**Go|Check Experiment parameters**).

After loading a configuration file pulse programs or spin systems can be modified using the internal NMR-SIM text editor. Selecting either the **Pulse program** or **Spin system** command from the **Edit** pull-down menu activates the appropriate editor. The short hand annotations are **Edit|Pulse program** and **Edit|Spin system**. New pulse sequences or spin system files may be created using the **Create new|Pulse program** or **Create new |Spin system** sub menus of the **Edit** pull-down menu. In either case the editor has the standard Windows functionality, see the **File** pull-down menu in Fig. 1.8. Alternatively any text editor may be used provided that the correct filename extensions is appended.
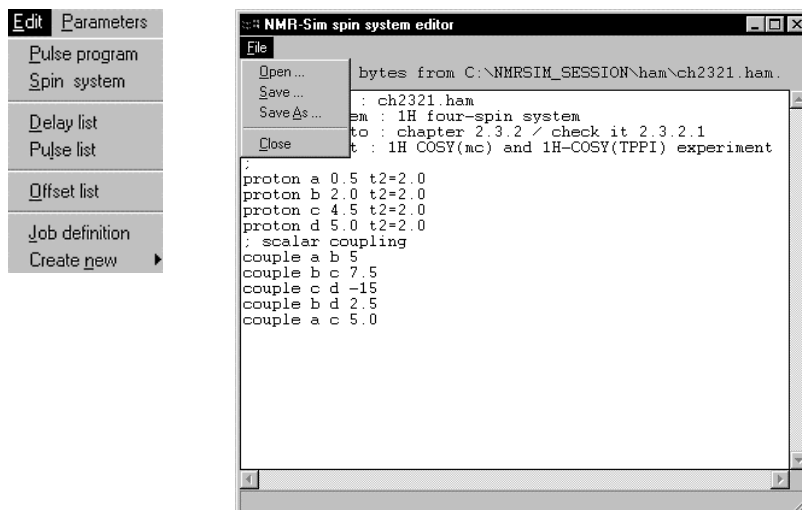
Fig. 1.8:   Editing a spin system file - **Edit** pull-down menu and NMR-SIM editor window.

Simulations are started using either the **Run Experiment** or **Check Parameters & Go** commands in the **Go** pull-down menu. The **Check Parameters & Go** command opens the Experiment parameter dialog box to enable the parameters to be checked before the simulation is started. By default the configuration file used in the *Check its* require the output filename must to be entered prior to the calculation starting (Fig. 1.9).
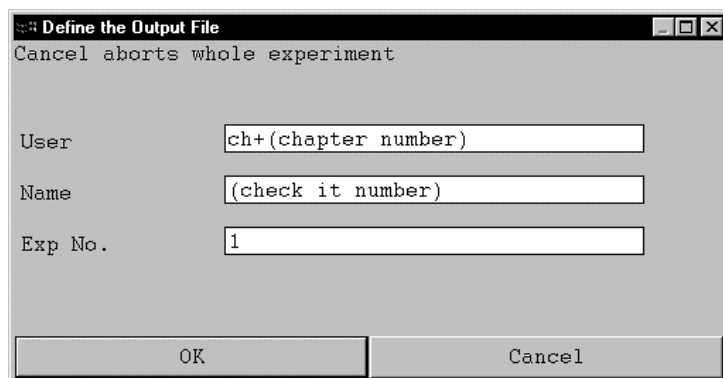
Fig. 1.9:   The Define the Output File dialog box.

It is recommended that the output files are named systematically with the entry fields **User**, **Name** and **Exp No.** derived from the *Check it* number. Thus the **User** field consists of the letters "ch" combined with the number of the *Check it* excluding the last

number; the **Name** field is the last *Check it* number and the **Exp No.** is the simulation number. As an example the output file of the second simulation of *Check it 5.2.6.11* would be named: **User**: *ch526*; **Name**: *11*; **Exp No.**: *2* with the simulated raw data stored in the new subdirectory *C:\Teach\Spectra\ch526\11*. The type of data created depends upon the type of experiment; a 1D experiment generates a FID (*002001.fid*) and a 2D experiment a 2D matrix (*002001.ser*) together with the appropriate experiment parameters files. When the simulation is completed either 1D WIN-NMR or 2D WIN-NMR is started depending on the type of experiment. Both the output filename and the automatic program start options can be changed by selecting the **NMR-Sim settings** in the **Options** pull-down menu (Fig. 1.10).
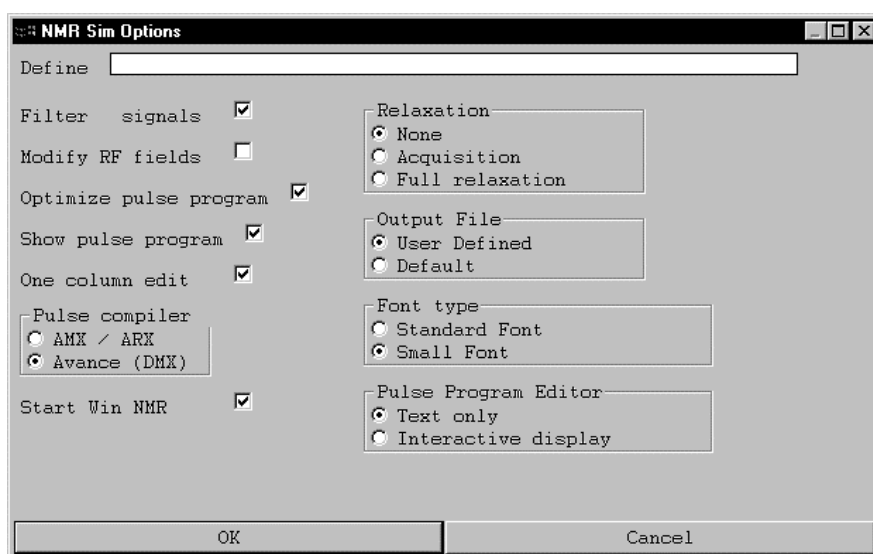
Fig. 1.10:   Dialog box - **NMR-SIM options**.

There are many *Check its* in this volume where the reader is instructed to edit a pulse program and to help with this task a diagram of the pulse sequence is often shown. The reader is strongly advised when editing a pulse program to number the pulses and delays using an ordinal scheme based upon the order of execution. This approach allows the pulse program to be exported to any type of NMR spectrometer as well as allowing the discussion of a pulse program to be based on the individual pulses and delays. However the configuration files used in the *Check its* are based on the standard BRUKER pulse program nomenclature, syntax and definitions as described in chapter 4.2.1.4, Table 4.6. Using this approach if two 90° pulses with the same power level are executed on the same rf channel they will have the same name irrespective of where the pulses appear in the pulse sequence. In Fig 1.11 the conversion from an ordinal naming scheme to the standard Bruker scheme is illustrated. The pulse names in brackets correspond to the execution order in the pulse sequence scheme while the preceding names are the one

which appears in the final pulse program and which correlate with the configuration file parameters.

p1 (p1, p4): 90° pulse (f1)
p2(p2): 180° pulse (f1)
p4(p3): 180° pulse (f2)
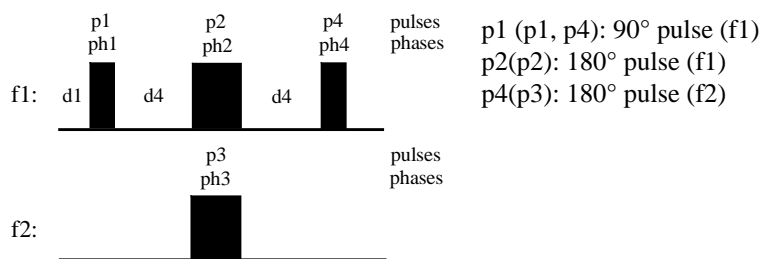
pulse sequence scheme

first step to edit the pulse sequence	final pulse sequence
d1	d1
(**p1** ph1):f1	(**p1** ph1):f1
d4	d4
(**p2** ph2):f1 (**p3** ph3):f2	(**p2** ph2):f1 (**p4** ph3):f2
d4	d4
(**p4** ph4):f1	(**p1** ph4):f1

Fig. 1.11:   Conversions of pulse names to fit with configuration files.

1.4   Book Layout

In keeping with the overall philosophy of *Spectroscopic Techniques: An Interactive Course* the reader is encouraged by a series of *Check its* to become familiar with the software tools NMR-SIM, 1D WIN-NMR and 2D WIN-NMR and to try their own simulations. To assist the reader the character format used is the same as used in the other books in this series:

Italic letters designate filenames and pathnames used for storing data on the local hard disk drive of the PC. Likewise *Italic* text is used for entries in edit fields or for selecting the options in list or combo boxes.

Bold letters, words and expressions refer to commands and controls, particularly in the *Check its* and simulation examples.

Small capitals identify people's names.

1.5   References

[1.1] Duddeck, H., Dietrich, W., *Structure Elucidation by Modern NMR*, Darmstadt, 2. Aufl., Steinkopff, 1992.

[1.2] Friebolin, H. P., *Basic One- and Two-Dimenisional NMR Spectroscopy*, 3. Aufl., Weinheim, WILEY-VCH, 1998.

[1.3] Harris, R. K., *Nuclear Magnetic Resonance Spectroscopy*, New York, Wiley & Sons Inc. 1989.

[1.4] Günther, H., *NMR Spectroscopy - Basic Principles, Concepts and Applications in Chemistry*, 2nd Ed., Chichester, WILEY-VCH, 1995.

[1.5] Kleinpeter, E., *NMR Spektroskopie, Struktur, Dynamik und Chemie des Moleküls*, Leipzig, J. Barth-Verlag, 1992.

[1.6] Martin, G. E., Zektzer, A. S., *Two-Dimensional NMR Methods for Establishing Molecular Connectivity*, Weinheim, WILEY-VCH, 1988.

[1.7] Derome, A. E., *Modern NMR Techniques for Chemistry Research*, Oxford, Pergamon Press, 1987.

[1.8] Brevard, C., Granger, P., *Handbook of High Resolution Multinuclear NMR*, New York, John Wiley & Sons, 1981.

[1.9] Sanders, J. K. M., Hunter, B. K., *Modern NMR Spectroscopy - A guide for chemists*, Oxford, Oxford University Press, 2nd Ed., 1994.

[1.10] King, R. W., Kathryn, R., J. Chem. Educ. 1989, 66, A213.
The Fourier transform in chemistry. Part I. Nuclear magnetic resonance - introduction

[1.11] Kessler, H., Gehrke, M., Griesinger, C., Angew. Chem. Int. Ed. Engl. 1988, *27*, 490.
Two-Dimensional NMR Spectroscopy: Background and Overview of the Experiments

[1.12] Kessler, H., Mronga, S., Gemmecker, G., Magn. Reson. Chem. 1991, 29, 527.
Multi-Dimensional NMR Experiments Using Selective Pulses

[1.13] NMR-SIM program, Rheinstetten, Germany, Bruker Analytik GmbH.
(internet homepage: http://www.bruker.com)

[1.14] 1D and 2D WIN-NMR program, Rheinstetten, Germany, Bruker Analytik, GmbH.
(internet homepage: http://www.bruker.com)

2 Background on Simulation

In this chapter NMR-SIM is used to illustrate the theoretical principles of NMR spectroscopy instead of the more usual pure mathematical description. There are many textbooks, reviews and original papers in the literature dealing with the fundamentals of NMR spectroscopy and the reader is referred to them [2.1 – 2.7]. Alternatively the reader can use the list of references at the end of chapter 5 but these relate primarily to the pulse sequences discussed in that chapter. The design of any new experiment always starts with a formal analysis of the problem and an examination of the coherence transfer processes necessary to obtained the required information. The present chapter focuses on three items:

- **2.1 Description of real samples**
  A multitude of spin system parameters exist and all of them influence the response of a molecule to a particular experiment to a lesser or greater extent. Conversely the pulse sequence can induce processes on the spin system such that a response can be obtained which can be attributed to a spin system parameter that is not directly available. In this section a short overview of spin system parameters is given including the parameters available for use with NMR-SIM and the spin system processes which can currently be simulated using NMR-SIM.

- **2.2 Description of pulse sequences**
  This section examines the theoretical approach to pulse sequences using the density matrix method and product operator formalism. It also looks at the pictorial representations of coherence levels and energy level schemes. This section summarizes the terms and methods that provide the arguments for a particular pulse sequence layout. The concepts introduced in this section are used in chapter 5 when discussing possible improvements to a specific pulse sequence.

- **2.3 Signal detection**
  This final section examines the methods of signal detection and signal selection and covers:
  - quadrature detection in one and two dimensions
  - decoupling
  - coherence selection by phase cycling and gradients

In section 2.2 and 2.3 *Check its* are used extensively and indirectly these *Check its* demonstrate the power of NMR-SIM and its ability to simulate complex experiments. The interactive nature of these *Check its* prompts the reader to create and modify various pulse sequences and to examine the results, consequently the reader new to NMR-SIM may prefer to read chapter 4 first before studying these sections. As an additional aid, the

file *result.pdf* on the enclosed CD-ROM contains both the pulse sequence listing and the results for all the *Check its* in this compendium.

2.1 Description of real samples - spin systems and processes on spin systems

NMR-SIM is very powerful simulation tool based on a density matrix approach and is designed to make low demands on computer resources. The spin system parameters consist of a small basic set of spin parameters: chemical shift, weak/strong scalar J coupling, dipolar coupling, quadrupolar coupling, longitudinal and transverse relaxation time. Currently the calculated coherence transfer processes are limited to polarization transfer and cross polarization.

2.1.1 Spin system parameters

The most important spin system parameters can often be obtained directly from a NMR spectrum by simply measuring the signal positions, the line separation in multiplets and the linewidths. It must be stressed that a molecular parameter measured directly from a NMR spectrum, particularly in second order spectra, is not necessarily the same as the spin system parameter.

Table 2.1:　　Molecular Parameters and Spectrum Parameters.

Molecular Parameter	Spectrum Parameter
shielding constant	position relative to a reference substance: chemical shift δ or ν[Hz]
scalar J coupling constant [Hz]	multiplet splitting, line separation
dipolar coupling constant [Hz]	multiplet splitting, line separation
quadrupolar coupling constant [Hz]	multiplet splitting, linewidth
relaxation time 　　- longitudinal (T_1)	
- transverse (T_2)	linewidth
exchange rate	linewidth, separate spectra of the individual exchanging conformers

The chemical shift can be traced back to the shielding which a nucleus experiences due to its neighbours in the same molecule or from the surrounding solvent. Scalar J coupling arises from the possible spin states of the neighbouring NMR active nuclei. In a homonuclear AX spin system with $s(A) = s(X) = 1/2$, there are two possible states for the nuclei A and X, $\alpha = +1/2$ and $\beta = -1/2$, and a doublet is observed for both A and X in the NMR spectrum. In contrast dipolar coupling can occur between nuclei that are not directly bound and through space dipole-dipole relaxation is the basis of the well-known homonuclear and heteronuclear NOE and ROE experiments used for molecular distance measurements. Quadrupolar coupling must be considered for nuclei with spin $s > 1/2$.

These nuclei possesses a nuclear quadrupole moment that can interact with the electric fields present in all molecules to produce a very efficient relaxation mechanism. In the B_0 field the nuclear energy levels are split asymmetrically by the ZEEMAN and quadrupolar interaction; in solution rapid tumbling averages the quadrupolar contribution to the nuclear energy level splitting. Because the quadrupolar moment provides a very efficient relaxation mechanism for non-spin 1/2 nuclei the linewidth of such nuclei are generally significantly greater than for spin s = 1/2 nuclei. The relaxation processes are described by two time constants: the transverse relaxation time T_2 and the longitudinal relaxation time T_1. In the case of pulsed NMR the term relaxation means the return of the coherence generated by the pulse sequence back to the thermal equilibrium state. Dynamic processes such as tautomerism or rotational conformation which occur on the NMR time scale give rise to spectra which can display either separate signals for the individual conformers or simply line broadening depending on the rate of exchange.

2.1.2   Coherence transfer processes

Any pulse sequence that uses more than one excitation pulse make use of coherence evolution and coherence transfer. The coherence evolves due to chemical shift or scalar coupling while at the same time or in a different time period coherence transfer processes are generated or occur. The four normal coherence transfer processes are given in Table 2.2 and according to [2.8 – 2.10] they must be categorized as either *coherent* and *incoherent* transfer processes. Coherent transfer processes rely on scalar (indirect) coupling interaction whereas incoherent processes are based on dipolar (indirect) coupling interaction or exchange among spins. The current version of NMR-SIM only permits calculations of coherent transfer processes.

Table 2.2:   Coherence evolution and transfer processes.

coherence evolution	coherence evolution due to chemical shift or scalar coupling
coherence transfer processes	*coherent transfer processes* polarization transfer cross polarization *incoherent transfer processes* cross relaxation chemical exchange

Coherent transfer processes induced by polarization transfer or cross polarization differ by the preparation pulse sequence as shown in Fig. 2.1 for a heteronuclear IS spin system. Using polarization transfer two RF pulses create antiphase coherence with the S spin retaining the antiphase coherence state whereas for cross polarization using two spinlock pulses, which obey the HARTMANN-HAHN condition, in-phase coherence is generated for both the I and the S spins.
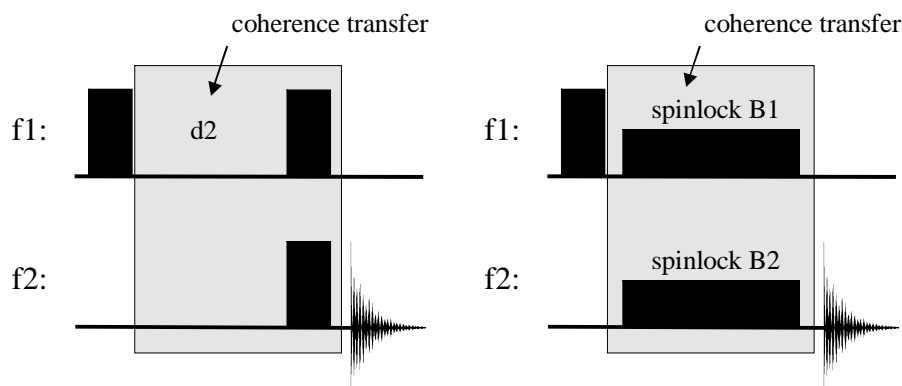
Fig. 2.1:   Basic coherence transfer preparation sequence on a heteronuclear IS spin system (I = sensitive nucleus *e.g.* ^{1}H, S = insensitive nucleus *e.g.* ^{13}C): (a) by polarization transfer or (b) by cross polarization.

The effect of the coherence transfer for an IS spin system can be summarized as follows:

- Coherence transfer by polarization transfer results in a population exchange for one of the I transitions, *e.g.* the transition between the $\alpha_I\beta_S$ and $\beta_I\beta_S$ states, with a signal enhancement for spin S of $|\gamma_I/\gamma_S|$.
- Coherence transfer by cross polarization step generates the same maximum signal enhancement as coherence transfer using rf pulses.

2.2   Description of Pulse Sequences

The detection of NMR signals is based on the perturbation of spin systems that obey the laws of quantum mechanics. The effect of a single hard pulse or a selective pulse on an individual spin or the basic understanding of relaxation can be illustrated using a classical approach based on the BLOCH equations. However as soon as scalar coupling and coherence transfer processes become part of the pulse sequence this simple approach is invalid and fails. Consequently most pulse experiments and techniques cannot be described satisfactorily using a classical or even semi-classical description and it is necessary to use the density matrix approach to describe the quantum physics of nuclear spins. The density matrix is the basis of the more practicable product operator formalism.

2.2.1   Density Matrix Formalism

NMR signals are the response of a quantum mechanic system, the spin systems, to a sequence of rf pulses. Since the recorded signal is only the macroscopic expectation value of an observable quantity, knowledge of the quantum mechanical background is necessary for a complete understanding of NMR. To study the overall effect of a pulse sequences it is necessary to understand how the spin systems behave under the influence

of rf pulses or free precession evolution, which are the fundamental units of any pulse sequences. For this purpose the conversion from the spin wave functions to the density matrix approach will be outlined. The step from the density matrix approach [2.11 – 2.14] to the more popular product formalism is then a minor one.

The spin system, the source of the NMR signal, consists of a multitude of spins and in a pure state each spin state can be described as the superposition of n wave functions whose contributions are scaled by the coefficient c_n:

$$|\varphi> = \sum_{n=1}^{N} c_n |n>$$ [2-1].

Thus the expectation value <A> of a macroscopic observable quantity A, such as the transverse coherence, is given by:

$$< A > = \sum c_m^* c_n A_{mn}$$ [2-2].

For a given basis set, *i.e.* a set of defined wavefunctions, A_{mn} are constants and the product $c_m^* c_n$ determines the observable quantity A for a particular state. Both A_{mn} and $c_m^* c_n$ represent a NxN matrix. The product of the coefficients $c_m^* c_n$ can be represented by an operator P and <A> by:

$$< A > = \sum_{nm} P_{nm} A_{nm} = Tr\{PA\}$$ [2-3]

where Tr{} is the trace or sum of the diagonal elements of the matrix.

For a macroscopic sample it is necessary to define a different set of wave functions because the spins are in a mixed state. The mixed state indicates that the wave functions of a particular nuclear spin are subject to additional molecular contributions that might differ over the whole sample. The expectation value of a mixed state now uses the averaged coefficients and is defined as the trace of the density matrix σ where $\overline{c_n c_m} = \sigma_{nm}$:

$$\overline{<A>} = Tr\{\sigma A\}$$ [2-4]

For the description of a pulse sequence as a time-related series of processes the density matrix must be described in time-evolution terms. Starting from the time-dependent SCHRÖDINGER equation the LIOUVILLE-VON NEUMANN equation is obtained in density matrix formalism as:

$$\frac{d\,\sigma(t)}{dt} = -i[\sigma(t), H]$$ [2-5]

Thus if the effect of a rf pulse or a free precession period on a spin system with the initial density matrix $\sigma_{initial}$ can be described by the time-independent Hamiltonian H_i then because:

$$\sigma(t) = \exp(-i \cdot H \cdot t)\sigma(t=0)\exp(i \cdot H \cdot t)$$ [2-6]

the evolution of a spin system in the course of a pulse sequence starting from thermal equilibrium can be written as illustrated in Fig. 2.2.
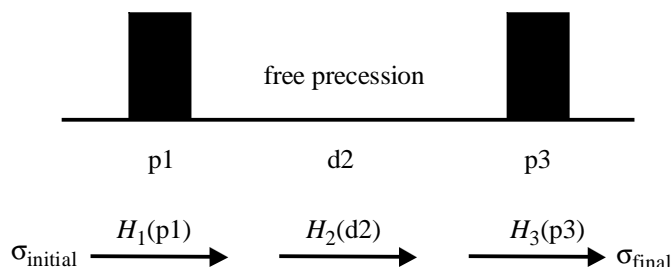
$$\sigma_{final} = \exp(-i \cdot H_1 \cdot t) \exp(-i \cdot H_2 \cdot t) \exp(-i \cdot H_3 \cdot t) \; \sigma_{initial} \; \exp(i \cdot H_1 \cdot t) \exp(i \cdot H_2 \cdot t) \exp(i \cdot H_3 \cdot t)$$

Fig. 2.2:   A pulse sequence in density matrix nomenclature.

The explicit density matrix calculation is accomplished by the definition of a density matrix for a particular spin system and by the operation of the Hamiltonian's on the density matrix. In the resulting density matrix σ_{final} the diagonal elements provide the population of the corresponding spin states whilst the off-diagonal elements represent the transitions.

2.2.2   Product Operator Formalism

As shown for the simple example in Fig. 2.2 explicit density matrix calculation can be cumbersome and this approach is often not recommended for complex pulse sequences, particularly if large data matrices of multi-spin systems or multi-pulse sequences must be evaluated. Consequently different operator formalisms [2.15 - 2.19] using CARTESIAN, spherical, shift, polarization and tensor operators, based on different coordinate systems or basic functions, have been developed where each formalism is suitable for a particular type of problem. The criteria used to select the appropriate formalism depend on the spin system being described:

- individual components of a multiplet
- multi-exponential relaxation
- magnetically non-equivalent and non spin-1/2 nuclei

With respect to the pulse sequences the suitable formalism must derive:

- the effect of common 90° and 180° pulses
- arbitrary pulses
- phase cycles and/or composite rotations

Taking into account all the relevant criteria spin-1/2 nuclei in the liquid phase can generally be described using CARTESIAN, spherical and shift product operators as shown in Table 2.3. The spherical operators are not shown because they can be easily derived from the shift operators, see Table 2.5.

Table 2.3: Suitable product operators for spin-1/2 nuclei in liquids [2.17].

spin systems attributes	multiplet components	multi-exponential relaxation	magnetically equivalent and spin S > 1/2 nuclei	
Cartesian	✗	✓	✗	
Shift	✓	✓	✗	

pulse sequences attribute	90° and 180° pulses	arbitrary pulses	phase cycles	composite rotations
Cartesian	✓	✗	✗	✓
Shift	✗	✓	✓	✗

In Table 2.3 the ✓ denotes the preferred formalism to analyse the particular spin system attribute. Irrespective of the chosen formalism, any formalism can be modified to describe any attribute of spin system or pulse sequence.

The derivation of the product operator formalism from the density matrix is relatively straightforward. Starting with the density matrix of an arbitrary defined spin system, the density matrix is expanded into a linear combination of orthogonal matrices, the so-called product operators O_k which specify an orthogonal coherence component

e.g. I_x or I_xS_y in terms of CARTESIAN product operators:

$$O_k = \sum_k b_k O_k \qquad\qquad [2\text{-}7]$$

where O_k is the orthogonal matrices describing a particular coherence and b_k the coefficients. For a coupled two spin system IS with $s_I = s_S = 1/2$ as outlined in references [2.18, 2.19], there are $2^{2n} = 16$ possible CARTESIAN product operators:

E (indentity operator)	I_x S_x I_xS_x	I_z I_y S_y I_yS_y	S_z I_xS_z I_zS_x I_xS_y	I_zS_z I_yS_z I_zI_y I_yS_x

The application of this expansion to the product operator formalism is then based on the following principles [2.20]:

- The execution of a rf pulse or the evolution of chemical shift or J-scalar coupling is described by an operator. The operation of this operator on the expanded density matrix is exclusively related to the coefficients of the corresponding operator matrix $\sigma_{expanded}$.
- Application of pulses, precession and J-coupling modifies the product operators, annihilates some and creates new operators in the expansion according to a defined set of rules.

The Cartesian Product Operator

The CARTESIAN product operators are the most common operator basis used to understand pulse sequences reduced to one or two phase combinations. This operator formalism is the preferred scheme to describe the effects of hard pulses, the evolution of chemical shift and scalar coupling as well as signal enhancement by polarization transfer. The basic operations can be derived from the expressions in Table 2.4. The evolution due to a rf pulse, chemical shift or scalar coupling can be expressed by equation [2-8].

$$I_{initial} \xrightarrow{\quad A \cdot t \cdot I_{evolution} \quad} \cos(A \cdot t)I_{initial} + \sin(A \cdot t)I_{new} \qquad [2\text{-}8]$$

Table 2.4:   Shorthand notation and conversion schemes for CARTESIAN product operators.

rotation under a rf pulse

$$I_{1z} \xrightarrow{\quad \omega_1 \cdot I_x \cdot t \quad} \cos(\omega_1 \cdot t)I_{1z} + \sin(\omega_1 \cdot t)(-I_{1y})$$

$$I_{1x} \xrightarrow{\quad \omega_1 \cdot I_y \cdot t \quad} \cos(\omega_1 \cdot t)I_{1x} + \sin(\omega_1 \cdot t)(-I_{1z})$$

chemical shift evolution

$$I_{1x} \xrightarrow{\quad \Omega_1 \cdot I_z \cdot t \quad} \cos(\Omega_1 \cdot t)I_{1x} + \sin(\Omega_1 \cdot t)I_{1y}$$

evolution under scalar coupling

$$I_x \xrightarrow{\quad 2\pi \cdot J_{IS}I_zS_z \cdot t \quad} \cos(\pi \cdot J_{IS} \cdot t)I_x + \sin(\pi \cdot J_{IS} \cdot t)(2I_yS_z)$$

$$-2I_yS_z \xrightarrow{\quad 2\pi \cdot J_{IS}I_zS_z \cdot t \quad} \cos(\pi \cdot J_{IS} \cdot t)(-2I_yS_z) + \sin(\pi \cdot J_{IS} \cdot t)(I_x)$$

x-pulse

$$I_z \longrightarrow -I_y$$
$$\uparrow \qquad \downarrow$$
$$I_y \longleftarrow -I_z$$

y-pulse

$$I_z \longrightarrow I_x$$
$$\uparrow \qquad \downarrow$$
$$-I_x \longleftarrow -I_z$$

$$I_x \longrightarrow I_y$$
$$\uparrow \qquad \downarrow$$
$$-I_x \longleftarrow -I_y$$

$$I_y \longrightarrow -2I_xS_z$$
$$\uparrow \qquad \downarrow$$
$$2I_xS_z \longleftarrow -I_y$$

$$I_x \longrightarrow 2I_yS_z$$
$$\uparrow \qquad \downarrow$$
$$-2I_yS_z \longleftarrow -I_x$$

$I_{initial}$ corresponds therefore to the operator before a pulse or a free precession delay *e.g.* I_z for the thermal equilibrium state. The $I_{evolution}$ operator denotes the effective operator during the shift or coupling evolution or the rotation due to a rf pulse. From the schematic circles which are subdivided according to the current evolution the I_{new} operator can be found. For instance, if a x-pulse with a tilt angle $\varphi \neq n \cdot \pi/2$ is executed the $I_{initial}$ operator I_z is transferred to the operator $-I_y$ and a residual I_z. Because the operators are commutable the evolution of chemical shift and scalar coupling can be calculated in any order. So the operations $\xrightarrow{\Omega \cdot t \cdot I_z} \xrightarrow{2\pi \cdot t \cdot J_{IS} I_z S_z}$ and $\xrightarrow{2\pi \cdot t \cdot J_{IS} I_z S_z} \xrightarrow{\Omega \cdot t \cdot I_z}$ have the same effect on the spin systems IS. In their current form the CARTESIAN product operators cannot be used to understand phase cycling or gradients because the operators do not have any information about either the coherence level or the phase shift a particular coherence has experienced during the previous pulse sequence.

The Product Operators in Spherical Coordinates

For the description of coherence transfer pathways, the basis for understanding phase cycling or gradients, spherical coordinate product operators should be used. The spherical coordinate product operators can be derived from the CARTESIAN operators using the simple transformation operations in Table 2.5. The advantage of spherical operators is that they indicate the coherence order instead of the simple CARTESIAN coordinates. It is the coherence order or more precisely the steps in the coherence pathway of the generated coherence and the discrimination of a particular coherence using phase cycling or gradients that is of particular relevance. As shown in section 2.3.3 the spherical tensor operators can be helpful because they describe both the introduced overall phase shift on a particular coherence and the coherence order steps.

Table 2.5: Conversion of spherical product operators, spherical coordinate product operators and the basic operations of these operators [2.31].

product operators in spherical coordinates	product operators in Cartesian coordinates	shift operators
$I_+ = (I_x + i \bullet I_y)/\sqrt{2}$	$I_x = 1/\sqrt{2} \, (I_+ - I_-)$	$I^+ = -\sqrt{2} \bullet I_{+1} = I_x + i \cdot I_y$
$I_- = (I_x - i \bullet I_y)/\sqrt{2}$	$I_y = 1/(i \bullet \sqrt{2}) \, (I_+ - I_-)$	$I^- = \sqrt{2} \bullet I_{-1} = I_x - i \cdot I_y$
$I_0 = I_z$	$I_0 = I_z$	

chemical shift evolution during the period t

$$I_{k, p} \xrightarrow{\Omega_k \cdot I_{kz} \cdot t} I_{k, p} \exp(-i \cdot p \cdot \Omega_k \cdot t)$$

$p = 0, \pm 1$ (coherence order), Ω_k = chemical shift frequency

scalar coupling of the nuclei k and l

$$I_{k,\pm1} \xrightarrow{\quad 2\pi\cdot J_{kl}\cdot t\cdot I_{kz}I_{lz} \quad} I_{k,\pm1}\cdot\cos(\pi J_{kl}\cdot t) \mp 2iI_{k,\pm1}I_{l,0}\cdot\sin(\pi\cdot J_{kl}\cdot t)$$

$$2I_{k,\pm1}I_{l,0} \xrightarrow{\quad 2\pi\cdot J_{kl}\cdot t\cdot I_{kz}I_{lz} \quad} 2I_{k,\pm1}I_{l,0}\cdot\cos(\pi J_{kl}\cdot t) \mp I_{k,\pm1}\cdot\sin(\pi\cdot J_{kl}\cdot t)$$

$$2I_{k,\pm1}I_{l,\pm1} \xrightarrow{\quad 2\pi\cdot J_{kl}\cdot t\cdot I_{kz}I_{lz} \quad} 2I_{k,\pm1}I_{l,\pm1}$$

rotation using arbitrary pulses aligned to the axis of the rotational coordinate system

$$I_{k,0} \xrightarrow{-\varphi I_{kz}} \xrightarrow{\beta I_{kz}} \xrightarrow{\varphi I_{kz}}$$

$$\frac{-i}{\sqrt{2}}I_{k,+1}\cdot\sin\beta\cdot\exp(-i\varphi) + I_{k,0}\cdot\cos\beta + \frac{-i}{\sqrt{2}}I_{k,-1}\cdot\sin\beta\cdot\exp(+i\varphi)$$

$$I_{k,\pm1} \xrightarrow{-\varphi I_{kz}} \xrightarrow{\beta I_{kz}} \xrightarrow{\varphi I_{kz}}$$

$$I_{k,\pm1}\cdot(\cos\beta+1)/2 + \frac{-i}{\sqrt{2}}I_{k,0}\cdot\sin\beta\cdot\exp(\pm i\varphi) + I_{k,\mp1}[(\cos\beta-1)/2]\cdot\exp(\pm2i\varphi)$$

- a 90° x-pulse on $I_{z,0}$ has the notation:

$$I_{z,0} \xrightarrow[\varphi=0]{-\varphi\cdot I_z} \xrightarrow{\pi/2 I_z} \xrightarrow[\varphi=0]{\varphi\cdot I_z} \quad \frac{-1}{\sqrt{2}}(I_{k,+1}+I_{k,-1})$$

- a 90° y-pulse on $I_{z,0}$:

$$I_{z,0} \xrightarrow[\varphi=\pi/2]{-\varphi\cdot I_z} \xrightarrow{\pi/2 I_z} \xrightarrow[\varphi=\pi/2]{\varphi\cdot I_z} \quad \frac{-i}{\sqrt{2}}(I_{k,+1}+I_{k,-1})$$

Some elementary rules on the meaning of the operator formalism can be summarized as follows [2.22]:

(1)　By convention a pure absorption signal using the quadrature detection procedure is composed of a real part $I_{k,y}$ and a imaginary part $I_{k,x}$. Conversion to spherical operators means that $i\cdot I_{k,-1} = (I_{k,y} + i \bullet I_{k,x})/\sqrt{2}$ represents a pure absorption signal, while $I_{k,+1}$ represents a pure dispersion signal. The operator $I_{k,+1}$ corresponds to the "quad image".

(2)　The coherence level associated with a particular product operator is just the sum of the indices of the nuclear spin operators in the product operator, for example $I_{k,-1}I_{l,-1}$ has a coherence level $p = -2$.

2.2.3　Coherence Level Scheme

The concept of longitudinal and transverse magnetization must be extended if the discussion of multi-pulse experiments is to include multiple quantum states and coherence transfer. The concept of *coherence*, the transition between two eigenstates, is preferable to using the expression transverse magnetization. Each transition may involve

a nuclear magnetic quantum number change and the term *coherence order* describes the quantum number difference between the spin states involved in the transition. In Table 2.6 the coherence order of different spin system states are listed for a two-spin system.

Table 2.6: Possible coherence order for two scalar coupled spins I_1 and I_2 [2.19].

coherence order	coherence state	CARTESIAN product operator
	longitudinal magnetization,	I_{1z}, I_{2z} and $I_{1z}I_{2z}$
p = 0	zero-quantum coherence	$2I_{1x}I_{2x} + 2 I_{1y}I_{2y}$, $2 I_{1y}I_{2x} - 2 I_{1x}I_{2y}$
p = 1	single-quantum coherence	I_{1x}, I_{1y}, I_{2x}, I_{2y}, $I_{1x}I_{2z}$, $I_{1y}I_{2z}$, $I_{1z}I_{2x}$, $I_{1z}I_{2y}$
p = 2	double-quantum coherence	$2I_{1x}I_{2x} - 2 I_{1y}I_{2y}$, $2 I_{1y}I_{2x} + 2 I_{1x}I_{2y}$

For completeness the transverse (I_{1x}, I_{1y}, I_{2x}, I_{2y}) and longitudinal magnetization are explicitly listed in Table 2.6 although the later discussion of coherences does not differentiate between these states or any other coherence state of the same order. Coherence order or more precisely the coherence pathway is an important concept in the design of a phase program or gradient selection used in pulse sequences. In addition to simple coherence suppression in 1D sequences, these procedures are also used for frequency discrimination and for the measurement of pure absorption spectra in 2D experiments.

Phase cycling and gradient selection procedures are based on the *coherence transfer pathway* of the complete pulse sequence. The corresponding *coherence level scheme* depicts the coherence evolution starting with the longitudinal magnetization at the beginning of the pulse sequence and finishing just before signal detection. The conventions regarding the general attributes of each coherence level scheme can be summarised as follows:

- For any pulse sequence which starts with the spin system in thermal equilibrium the initial coherence level must be denoted by p = 0.
- Using quadrature detection in the acquisition period only coherences of order p = -1 prior to detection are observed. (Some publications define the level p = +1 for quadrature detected coherences.)
- The first pulse can only create single quantum coherence.

Coherence transfer pathways (CT pathway) fall in the domain of spherical product operators instead of CARTESIAN operators. Before proceeding any further it is recommended to a necomer to read section 2.2.2 and for addition information references [2.20 – 2.31]. To illustrate the use of coherence transfer pathways in coherence selection, three pulse sequences will be examined.

The one-pulse experiment: A one-pulse experiment consists of an excitation pulse, often with a 90° tilt angle and phase 0 or 2 for the first two scans. According to the conventions in section 2.2 the phase values corresponds to the x-axis (phase value: 0, phase shift: $\varphi = \pi/2$) and the y-axis (phase value: 1, phase shift: $\varphi = 0$). The coherence

transfer pathway for the x- and y-pulse can then be easily derived from the expressions given in Table 2.5.
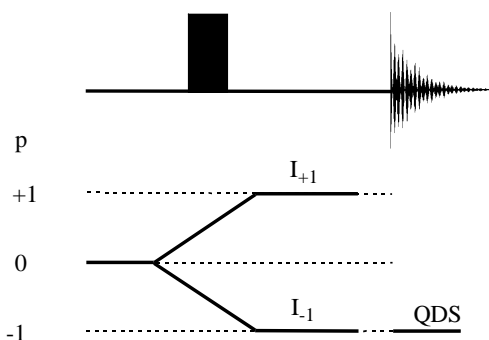
Fig. 2.3: Coherence transfer pathway for a one-pulse experiment.

The heteronuclear polarization transfer step: The simplest sequence unit to create coherence transfer from a sensitive nucleus I to a insensitive nucleus S is a 90°(I) pulse and a 90°(S) pulse enclosing a scalar coupling evolution delay. This unit forms part of many pulse sequences including the HMQC and the HMBC experiment.
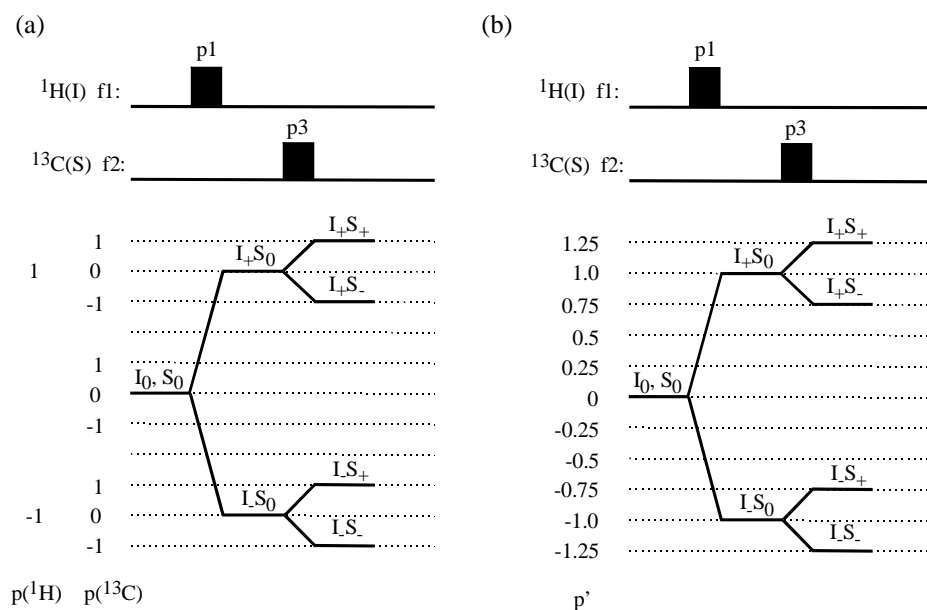
Fig. 2.4: Alternative coherence level schemes for the heteronuclear polarization transfer step of a ^{13}C, ^{1}H spin system.

The coherence transfer pathway can be represented in two ways. The first way, shown on the left of Fig. 2.4, is based on the straightforward use of coherence order

schemes to separate single and double quantum coherences. The second way, shown on the right of Fig. 2.4, uses a weighted factor p' based on the gyromagnetic ratio of the nuclei involved to scale the individual coherence order [2.29]. The weighted scheme is recommended for the determination of gradient strengths for CT pathway selection and is illustrated in *Check it 2.3.3.12*, section 2.3.3. The coherence order p' of a two spin system ^1H, ^nX is calculated according to equation [2.9]:

$$p' = p(^1H) + p(^nX) \cdot \frac{\gamma(^nX)}{\gamma(^1H)}$$

[2-9]

The disadvantages of this representation is that the coherence scheme is specific for a particular spin combination as in Fig. 2.4 which is for a ^1H, ^{13}C spin system and that the individual coherence order of I or S cannot be read directly from the scale.

2.2.4 Energy Level Scheme

Energy level schemes are very instructive representations for describing the line splitting of simple spin systems such as AX or AMX spin systems and for visualizing the quantum mechanical allowed and forbidden transitions. The relative population of each state can be calculated and the signal enhancement by polarization transfer using a double-quantum, forbidden transition calculated.
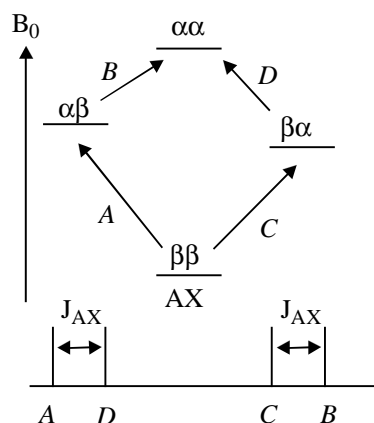
AX spin system with $J_{AX} > 0$: energy level scheme and spectrum, α and β denotes the spin state (α = antiparallel to B_0).
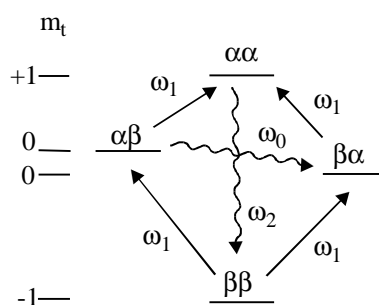
Transitions in a AX spin system: ω_1 = allowed transitions with $m_t = \pm 1$ (total magnetic spin quantum number), ω_0, ω_2 = forbidden transitions with a total magnetic quantum change of 0 and 2 respectively.

Fig. 2.5: Energy level scheme to describe a spin system and the transitions.

However the description of complex pulse sequences soon becomes cumbersome and less instructive and consequently the main application of the energy level scheme is for describing processes such as the population changes associated with a transition in a SPI experiment. NMR-SIM can be used to construct energy level schemes for a spin system in the state of thermal equilibrium.

2.2.4.1 Check it in NMR-SIM

Open NMR-SIM and use the **Edit⎮Create new⎮Spin system** command to create a new file called *myax.ham*. Enter the parameters for an ^{1}H AX spin system by defining two proton spins a and b with an arbitrary chemical shift and a strong scalar coupling of 10 Hz as shown below. Save the new spin system (**File⎮Save…**). Inspect the energy level scheme (**Utilities⎮Show energy levels**) and then the energy level list (**Utilities⎮List energy levels**). The Energy Levels can be used to draw the energy level scheme in Hz while the Lines information enables the allowed transitions between energy levels to be assigned to the appropriate lines in the one-pulse spectrum.

Spin system file	Energy Levels [Hz][1]		Lines		
	1 : | >	452.5	transitions	Frequency	Intensity
;filename : myax.ham	2 : | >	147.583	2 -> 1 :	304.92	25.84
proton a 1.0	3 : | >	-152.583	3 -> 1 :	605.08	24.17
proton b 2.0	4 : | >	-447.5	4 -> 2 :	595.08	25.84
couple a b 10			4 -> 3 :	-294.92	24.17

[1]Energy levels and transition frequencies for SF = 300 MHz.

2.3   Signal Detection

2.3.1   Quadrature Detection

Quadrature Detection in one dimension

After a single excitation pulse or a series of pulses the signal detection period begins where the response of the spin system to the pulse sequence is recorded. The basic configuration for quadrature detection [2.32, 2.33] is two detectors in the x,y-plane with a 90° phase difference where each detector may be assigned to the x- or y-axis. As illustrated in Fig. 2.6 there are two detection methods, in simultaneous detection both detectors are sampled at the same time whilst in sequential detection the detectors are sampled alternatively.
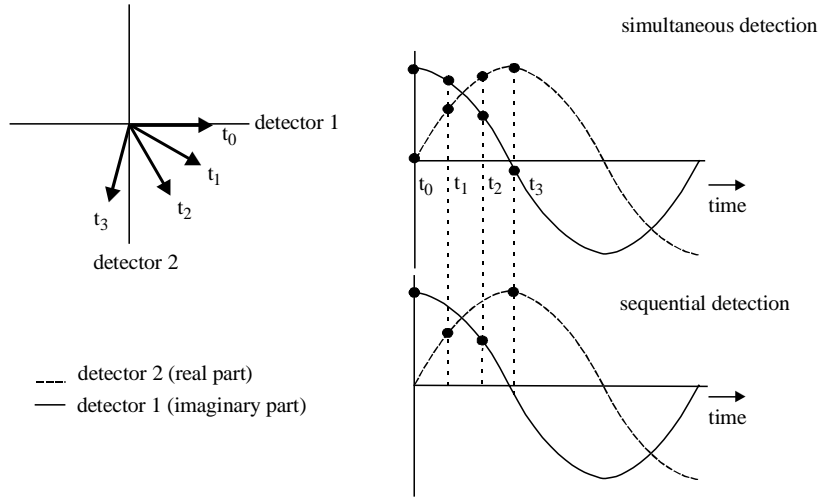
Fig. 2.6: Quadrature detection modes: QSIM and QSEQ.

In the single detection method the transmitter frequency must be positioned outside of the expected chemical shift range because it cannot discriminate between frequencies that are higher or lower than the transmitter frequency. In quadrature detection the transmitter frequency is in the centre of the observed frequency range halving the bandwidth of the observed frequency range compared to the single detection method. The detected signal is mixed with the transmitter frequency and by using two detectors it is possible to discriminate whether the frequencies are lower or higher than the transmitter frequency. Quadrature detection has two advantages compared with a single component detection method. The narrower frequency range reduces the pulse power requirements necessary to generate a 90° over the complete spectral width and there is a signal-to-noise advantage of $\sqrt{2}$ due to the smaller bandwidth which the analogue filter has to control.

If a 90° pulse with phase y is applied to the equilibrium magnetization the signal recorded by the detectors aligned along the x- and y-axis, see Fig. 2.6 is given by:

Detector 1 $\qquad S_x(t) = \lambda \cos(\varpi \cdot t) \exp(-t / T_2)$ $\qquad$ [2-10]

Detector 2 $\qquad S_y(t) = \lambda \sin(\varpi \cdot t) \exp(-t / T_2)$ $\qquad$ [2-11]

$\qquad \lambda =$ intensity scaling factor which is a function of experimental parameters

The components S_x and S_y can be combined into a single complex function:

$$S(t) = S_x(t) + i \cdot S_y(t)$$
$$= \lambda(\cos(\varpi \cdot t) + i \sin(\varpi \cdot t)) \exp(-t / T_2)$$
$$= \lambda \exp(i \cdot \varpi \cdot t) \exp(-t / T_2) \qquad [2\text{-}12]$$

The Fourier transformation of the complex time domain signal in equation [2-12] yields:

$$S(\Delta\omega) = \lambda \, (A(\Delta\omega) + i \bullet D(\Delta\omega))$$

$\Delta\omega$ = difference between the resonance frequency and transmitter frequency

The real part of the complex frequency domain signal, $A(\Delta\omega)$, represents the absorption lineshape of the detected signal and includes the frequency information required to determine whether the detected signal is at a lower or a higher frequency with respect to the transmitter frequency. The corresponding imaginary part $D(\Delta\omega)$ represents the dispersive lineshape and also includes the frequency information.

Quadrature Detection in two dimensions

Quadrature detection in the second f1 dimension in a 2D experiment [2.34 – 2.45] is not a simple proposition because the second dimension is not directly detected, but generated by the modulation of the signal response as a function of the incremented evolution period t1. However quadrature detection in the second dimension is required to discriminate frequencies to prevent the folding of signals and to obtain pure phase spectra. Lineshapes in pure phase spectra are superior to the signals in magnitude spectra being shaper without the wide dispersive base. As shown in Table 2.7 there are several methods for recording two-dimensional experiment and achieving quadrature detection in f1. All two dimension experiments, even magnitude mode 2D spectra, must be acquired using either phase cycling or field gradients for frequency discrimination in f1. The method for obtaining pure phase 2D spectra is usually based on a combination of the acquisition procedure and the processing of the time domain 2D data matrix.

Table 2.7:   Quadrature detection modes for two-dimensional experiments.

Co-Addition (magnitude processing)	not phase sensitive	[2.39, 2.36]
Ruben-States-Haberkorn (RSH)	phase sensitive	[2.40]
TPPI	phase sensitive	[2.41]
States-TPPI	phase sensitive	[2.44]
Echo/Antiecho (E/A)	phase sensitive, requires gradients	[2.45]

To understand the role of phase cycling or field gradients in frequency discrimination in the f1 dimension it is necessary to examine in more detail the theoretical background of 2D experiments. The extension of a 1D pulse sequence to a 2D experiment is achieved by adding a evolution delay t1 which is then incremented in succeeding experiments resulting in signal modulation in the f1 dimension. Depending on the type of experiment the recorded signal in the t1 dimension can be either phase or amplitude modulated and both types of modulation must be considered for the quadrature detection in the second dimension. In Table 2.8 the results of Fourier transforming data based on phase and amplitude modulated signals are compared: amplitude modulation is shown as a sine and cosine modulation as detected by the x- and y-detector. For simplicity only frequency and time-related terms are included, all relaxation terms have been ignored. By analogy with the corresponding terms used for quadrature detection in one dimension, the final

results of the data processing are given in terms of A and D where A denotes an absorptive lineshape and D a dispersive lineshape. The subscripts "+" and "-" signify if the frequency of a line is of lower or higher frequency relative to centre of the spectrum and the superscripts denotes the f1 or f2 dimension. In addition for amplitude modulated data the transformation with respect to t1 after discarding the imaginary part of the data arising from the transformation with respect to t2 is also shown.

Table 2.8:   Processing of phase and amplitude modulated 2D data [2.38].

phase modulated data

$$s(t_1, t_2) = \gamma \cdot \exp(i \cdot \Omega_1 \cdot t_1) \cdot \exp(i \cdot \Omega_2 \cdot t_2)$$

$\xrightarrow{\text{FT(t2)}} \xrightarrow{\text{FT(t1)}}$ $s(\omega_1, \omega_2) = \gamma \cdot [A_+^1 + i \cdot D_+^1] \cdot [A_+^2 + i \cdot D_+^2]$

real part $\mathbf{Re}[s(\omega_1, \omega_2)] = \gamma \cdot \{[A_+^1 \cdot A_+^2] - [D_+^1 \cdot D_+^2]\}$

amplitude modulated data

cosine modulation $s(t_1, t_2) = \gamma \cdot \cos(\Omega_1 \cdot t_1) \cdot \exp(i \cdot \Omega_2 \cdot t_2)$

$\xrightarrow{\text{FT(t2)}} \xrightarrow{\text{FT(t1)}}$ $s(\omega_1, \omega_2) = 1/2\, \gamma \cdot \{[A_+^1 + i \cdot D_+^1] + [A_-^1 + i \cdot D_-^1]\} \cdot [A_+^2 + i \cdot D_+^2]$

FT in t1 of only the real part of $s(t_1, \omega_2)$ $\mathbf{Re}[s(\omega_1, \omega_2)]^{\mathbf{Re}\omega_2} = 1/2\, \gamma \cdot A_+^1 A_+^2 + 1/2\, \gamma \cdot A_-^1 A_+^2$

sine modulation $s(t_1, t_2) = \gamma \cdot \sin(\Omega_1 \cdot t_1) \cdot \exp(i \cdot \Omega_2 \cdot t_2)$

$\xrightarrow{\text{FT(t2)}} \xrightarrow{\text{FT(t1)}}$ $s(\omega_1, \omega_2) = 1/2i\, \gamma \cdot \{[A_+^1 + i \cdot D_+^1] + [A_-^1 + i \cdot D_-^1]\} \cdot [A_+^2 + i \cdot D_+^2]$

FT in t1 of only the real part of $s(t_1, \omega_2)$ $\mathbf{Im}[s(\omega_1, \omega_2)]^{\mathbf{Re}\omega_2} = -1/2\, \gamma \cdot A_+^1 A_+^2 + 1/2\, \gamma \cdot A_-^1 A_+^2$

The phase modulated data shows a real part $Re[s(\omega_1, \omega_2)]$ which includes frequency discrimination corresponding to a single peak at $(\omega_1, \omega_2) = (\Omega_1, \Omega_2)$ but with a phase twisted lineshape $(D_+^1 D_+^2)$. The amplitude modulated data does not allow frequency discrimination ($A_+^1 A_+^2$ and $A_+^1 A_-^2$ terms) and corresponds to two peaks at (Ω_1, Ω_2) and $(-\Omega_1, \Omega_2)$ again with a phase twisted lineshape ($D_+^1 D_+^2$ and $D_+^1 D_-^2$). The clue to obtaining pure phase and frequency discriminated data sets from amplitude modulated data as outlined in Table 2.8 is the summation of the real part $Re(\omega_1, \omega_2)^{Re(\omega_2)}$ and the imaginary part $Im(\omega_1, \omega_2)^{Re(\omega_2)}$ of the data as shown in equation [2-13] and [2-14].

In the following discussion the experimental procedures to extract frequency discriminated spectra with pure absorptive lines from amplitude modulated data is outlined. The analogous procedure for phase modulated data is discussed in the paragraph on the Echo/Antiecho detection mode. As shown in equation [2-15] taking the

difference between the real and the imaginary part enables the representation of pure absorption lineshape with frequency discrimination in f1:

cosine modulated data

$s(t_1, t_2) \quad \longrightarrow \quad \longrightarrow \quad \longrightarrow \quad \longrightarrow \quad \mathbf{Re}[s(\omega_1, \omega_2)]^{\mathbf{Re}\omega_2}$ 　　　[2-13]

　　　　　　 FT(t_2)　real part　FT(t_1)　real part
　　　　　　　　　　　selection　　　　　selection

sine modulated data

$s(t_1, t_2) \quad \longrightarrow \quad \longrightarrow \quad \longrightarrow \quad \longrightarrow \quad \mathbf{Im}[s(\omega_1, \omega_2)]^{\mathbf{Re}\omega_2}$ 　　　[2-14]

　　　　　　 FT(t_2)　real part　FT(t_1)　imaginary
　　　　　　　　　　　selection　　　　　part selection

$\mathrm{Re}[s(\omega_1, \omega_2)]^{\mathbf{Re}\omega_2} - \mathrm{Im}[s(\omega_1, \omega_2)]^{\mathbf{Re}\omega_2} =$ 　　　[2-15]

$$= 1/2\, \gamma \cdot (A_+^1 A_+^2 + A_-^1 A_+^2) - 1/2\, \gamma \cdot (-A_+^1 A_+^2 + A_-^1 A_+^2)$$

$$= \gamma \cdot A_+^1 A_+^2$$

　　 With amplitude modulation the cosine and sine components may be handled in two ways to achieve quadrature detection in f1. They may be acquired in subsequent scans by either incrementing the pulse or receiver phase and the data co-added in the computer memory or they may be acquired sequentially and stored separately. With the first approach direct Fourier transformation yields frequency discrimination in f1 but no absorptive lineshapes whilst with the second approach additional processing steps are necessary to achieve both, frequency discrimination and absorptive lineshapes.

The Co-Addition (magnitude mode) [2.39]: This quadrature detection mode, often synonymously called magnitude mode due to the later processing, is probably the most commonly applied detection mode. Although the signals all have positive intensities they do not have pure phase and are very broad at the base being composed of both absorption and dispersive lineshape. This method is also called Co-Addition because the time domain data set for each experiment is based on the combination of multiples of two scans. Each scan uses the appropriate phase cycling to create either sine or cosine amplitude modulation data that is then combined allowing frequency discrimination. The underlying acquisition and processing procedure is illustrated in the scheme below.

$s(t_1, t_2)_{cos} \searrow$ 　　Co-Addition　　　　　FT(t_2), FT(t_1)　　　magnitude
　　　　　　　　　　　　　　　　　　　　　　　　　　　calculation

　　　　　　$s(t_1, t_2) = \quad s(t_1, t_2)_{cos} \longrightarrow \quad [A_1 - i \cdot D_1] \longrightarrow [A_1^2 + D_1^2]^{1/2}$
　　　　　　　　　　　　　 $+\, i \cdot s(t_1, t_2)_{sin} \quad\quad \cdot [A_2 - i \cdot D_2] \quad\quad\quad \cdot [A_2^2 + D_2^2]^{1/2}$

$s(t_1, t_2)_{sin} \nearrow$
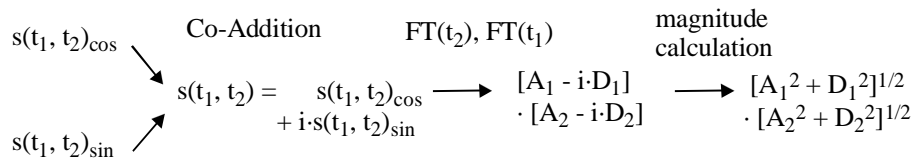
　　 Processing procedure for "magnitude" 2D spectra.

　　 For the same time increment, there is no phase difference between the pulses and receiver for the sine modulated data but for the cosine modulated data there is a 90° phase shift between the first pulse and second pulse and the second pulse and the receiver. In *Check it 2.3.1.1* this phase relationship is examined.

2.3.1.1 Check it in NMR-SIM

Load the configuration file *ch2311.cfg* and simulate the ^{1}H COSY spectrum of a four spin system (**Go⎮Run Experiment**). Save the spectrum as **Exp. No.**: *1*. In 2D WIN-NMR Fourier transform the 2D data set (**Process⎮2D transform [xfb]**). Note that the spectrum has no frequency discrimination in f1 and the spectrum is symmetrical about the centre of the f1 dimension. Using the **Edit|Pulse program** command modify the phase cycling as shown below and save the pulse program (**File⎮Save...**). Repeat the simulation saving the data as **Exp No.**: *2*. In the transformed spectrum there is now frequency discrimination in f1 but the frequencies have been inverted. Modify the pulse program again to include the correct phase cycling for the magnitude spectrum. Save the data as **Exp No.**: *3*. The spectrum has frequency discrimination in f1 with no inverted frequencies.

simulation 1	simulation 2	simulation 3
ph1=0	ph1=0 0	ph1=0 0
ph2=0	ph2=0 1	ph2=0 1
ph31=0	ph31=0 0	ph31=0 2

In this magnitude COSY experiment it is possible to obtain sine and cosine modulated data with co-addition using a simple two step phase cycle and consequently the minimum number of scans per increment is 2 or for long acquisitions a multiple of 2. The simplicity of this pulse program is in contrast to the phase sensitive COSY experiment and other Bruker two dimension pulse programs which utilize phase increment commands such as ip1 to achieve frequency discrimination in f1.

The Ruben/State/Haberkorn mode [2.40]: This quadrature detection mode leads to phase sensitive 2D spectra and is based on the different symmetry properties of the sine and cosine functions after Fourier transformation. As shown in equation [2-15] the first term of imaginary part of the sine data set $Im[s(\omega_1, \omega_2)]$ has a negative sign in contrast to the real part of the cosine data set. Simple mathematical addition of the real part and the imaginary part of the sine and cosine modulated data sets after Fourier transformation and selection of the real or imaginary part leads to the term $A_+^1 A_+^2$ which describes a pure absorptive line at $(\omega_1, \omega_2) = (\Omega_1, \Omega_2)$.

This algorithm is the basic of the States et al. quadrature detection mode. In practice the following equivalent data combination and processing steps are used:

new data set

$$s(t_1, t_2)_{cos} \xrightarrow{FT(t_2)} s(t_1, \omega_2)_{cos} \longrightarrow s(t_1, \omega_2)_{cos}^{real} \searrow$$

$$s(t_1, \omega_2)_{cos}^{real} + i \cdot s(t_1, \omega_2)_{sin}^{real}$$

$$s(t_1, t_2)_{sin} \longrightarrow s(t_1, \omega_2)_{sin} \longrightarrow s(t_1, \omega_2)_{sin}^{real} \nearrow$$

$$\xrightarrow{FT(t_1)} s(\omega_1, \omega_2) \xrightarrow{\text{real part selection}} Re[s(\omega_1, \omega_2)] = A_+^1 A_+^1$$
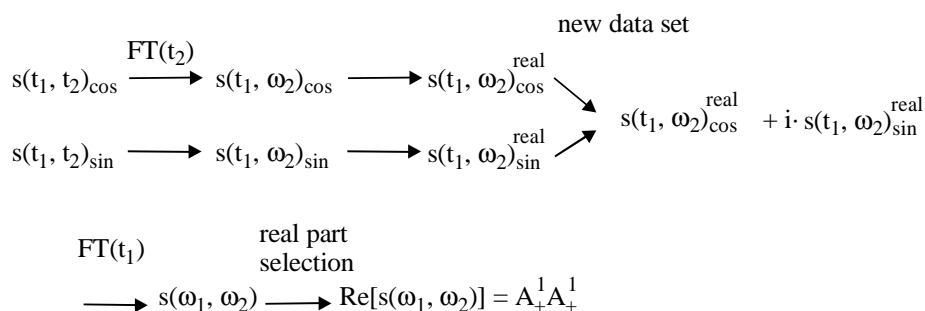
Ruben-States-Haberkorn quadrature detection procedure.

The TPPI-method or Marion/Wüthrich-method [2.41]: In the TPPI method the transmitter frequency ω_{trans} is positioned at the centre of the detected frequency range SW. Frequency discrimination is achieved by shifting the apparent sweepwidth from $\pm 1/2SW$ to 0 to SW. This apparent frequency shift is obtained by incrementing the phase of the selection pulse by 90° for each successive t1 increments and sampling the data faster than normal by modifying the value of t1 by the phc-factor (see section 3.3.1). The TPPI method guaranties both frequency discrimination and pure absorption lineshapes.

The States-TPPI method [2.44]: This method combines elements from both the States et al. and TPPI method to obtain phase sensitive spectra.

The Echo/Antiecho method [2.45]: In the introduction to the discussion of phase and amplitude modulated 2D data sets, see Table 2.8, it was emphasized that frequency discrimination in the f1 dimension was inherent in phase modulated data sets. However the lineshapes was phase twisted because of the absorptive and dispersive contributions to the real part of $s(\omega_1, \omega_2)$ which describes the lineshapes in the final spectrum.

The Echo/Antiecho procedure relies on the possibility of generating two experiments simply by changing the sign of a gradient pulse. Thus the applied gradients select in two scans different coherence transfer pathways which contribute to the detected signal. In both cases the coherence order is -1 but the signal functions obtained differ by the sign of the frequency term $\exp(i\Omega t_1)$. In Fig. 2.7 the pulse sequence and applied gradients, the coherence transfer pathways and the resulting signal functions are shown for a gradient selected homonuclear ^{1}H COSY experiment using the Echo/Antiecho (abbreviated to E/A) detection mode.

$$s(t_1, t_2)_{N\text{-type}} = \exp(-i\Omega t_1) \cdot \exp(i\Omega t_2)$$

$$s(t_1, t_2)_{P\text{-type}} = \exp(i\Omega t_1) \cdot \exp(i\Omega t_2)$$
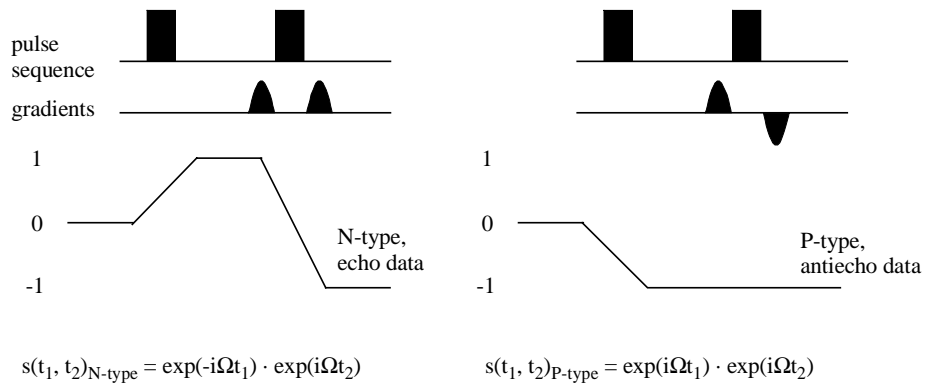
Fig. 2.7:   Combination of gradients amplitudes and stored signal functions in the Echo/Antiecho detection mode.

The p- and n-type data sets are stored separately and by taking the sum and difference it is possible to obtain the standard sine and cosine modulated functions. These functions can then be processed in a similar manner to the States et al data.

$$1/2 \cdot [s(t_1, t_2)_{P-type} + s(t_1, t_2)_{N-type} = \cos(\Omega \cdot t_1) \cdot \exp(i \cdot \Omega \cdot t_2)$$

$$1/2i \cdot [s(t_1, t_2)_{P-type} - s(t_1, t_2)_{N-type} = \sin(i \cdot \Omega \cdot t_1) \cdot \exp(i \cdot \Omega \cdot t_2)$$

Definition of new data sets obtained from the Echo/Antiecho signals.

In *Check it 2.3.12* a homonuclear COSY magnitude calculation spectrum [2.34] is converted into its various phase sensitive analogues. Fig. 2.8 shows the phase incrementation and loop commands necessary for this conversion. Table 3.5 in chapter 3 lists the recommended processing parameters to use for the different types of experiment. The gradient based Echo/Antiecho COSY experiment is discussed further in section 2.3.3, which considers gradient application in more detail.
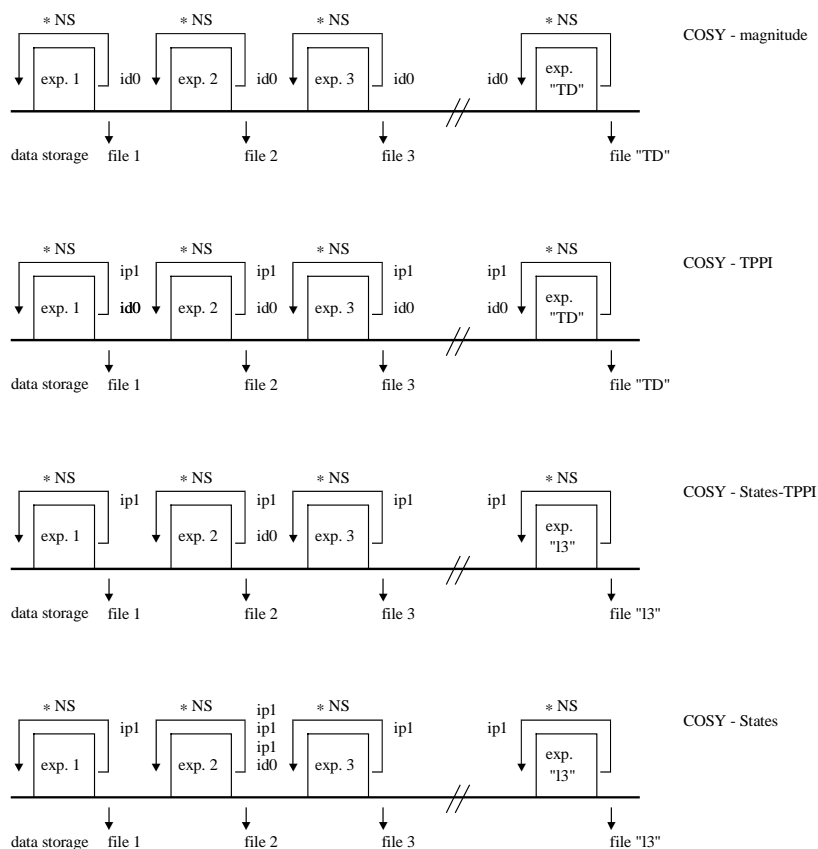
Fig. 2.8: Sequence procedures to obtain magnitude and phase sensitive homonuclear COSY spectra.

COSY (magnitude)

ph1 = 0 0 0 0 1 1 1 1...
ph2 = 0 1 2 3
ph31 = 0 2 0 2 3 1 3 1...

phase sensitive COSY

ph1 = 0 2 2 0 1 3 3 1
ph2 = 0 2 0 2 1 3 1 3
ph31 = 0 2 2 0 1 3 3 1

2.3.1.2 Check it in NMR-SIM

Load the configuration file *ch2312.cfg* to set the basic experiment parameters for the ^{1}H COSY magnitude spectrum of the four spin system. Check the pulse program (**Edit|Pulse program**). Simulate the spectrum saving the data as **Exp:** *1*. Transform the data using the **Process|2D transform [xfb]** command and scale the levels of the spectrum using the **∗2** or **/2** button in the button panel. Return to NMR-SIM and using Fig. 2.8 as a guide convert the COSY(mc) pulse sequence to the COSY(TPPI) sequence by inclusion of the ip1 command. Change the pulse program to the values shown above for the phase

sensitive COSY experiments. Save the modified file as *mycosytp.seq* (**File|Save As…**). Simulate the COSY(TPPI) spectrum (**Exp:** *2*) and process the data in 2D WIN-NMR ensuring that **MC2** parameter is set accordingly. Continue to convert the pulse sequence for the COSY(States), *mycosysh.seq,* and COSY(States-TPPI), *mycosyst.seq,* experiments. In both these experiments replace td1 by the loop counter l3 and ensure that there is always a delay preceding the incrementation commands id0 and ip1. In all cases take care to apply the correct processing parameters for window-function and related parameter SSB (see Table 3.5) and ensure that the **MC2** parameter is set correctly. If necessary the *result.pdf* file lists the correct pulse sequences.

2.3.2 Decoupling Methods

Decoupling is an important operation in data acquisition. Indeed it is standard practise when recording the NMR spectra of X nuclei such as ^{13}C, ^{29}Si or ^{31}P to use proton decoupling. The effect of either a continuous rf field or rf pulse sequence applied to the proton channel of an NMR spectrometer is to set all the proton nuclei in the same "decoupled" spin state suppressing the multiplet splitting which arises from the heteronucleus coupling to the protons. Proton decoupled spectra show only single lines for every magnetically non-equivalent X nucleus and compared to a proton coupled spectrum the signal-to-noise increases significantly due to the collapse of the $^{n}J(X, {}^{1}H)$ multiplets. Although coupling information relating to the number of neighbouring protons is lost, coupling to other X nuclei i.e. $^{n}J(^{19}F, {}^{13}C)$ is still visible.

Fig. 2.9: Typical decoupling periods in a pulse sequence. Period 2 might also be executed as pulses instead of decoupling.

Different decoupling techniques and methods have been developed as shown in Fig. 2.9. The decoupling sequence can be applied prior to any excitation pulse (period 1), as part of the pulse sequence (period 2), d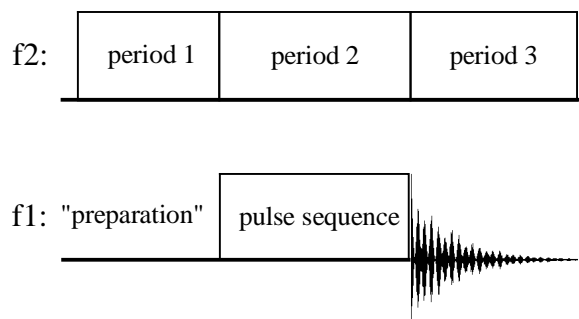uring the acquisition period (period 3) or as a combination of the three different periods. A similar decoupling regime can be applied to homonuclear spin systems. Technical methods for decoupling vary from the older noise decoupling through to the modern composite and adiabatic pulse decoupling. In addition the bandwidth of the decoupling can differ from a narrow to a very wide frequency range.

In NMR-SIM broadband heteronuclear decoupling can be "switched on" by assigning a rf channel to the decoupled nucleus. As shown in Fig. 2.9 decoupling can be switched on during acquisition and/or prior to the detection pulse. In the following section the most common decoupling methods will be briefly discussed.

^{1}H off-resonance decoupling technique

In this method the proton decoupler frequency is set at approximately -5 ppm and the protons irradiated using low power continuous wave irradiation. The effect is to remove all the small long-range $^nJ(X, {}^1H)$ coupling constants and reduce the splitting caused by the large $^1J(X, {}^1H)$ coupling constants. The exact reduction depends on the frequency difference and decoupler power. For ^{13}C the ^1H off-resonance decoupled spectra allows the multiplicity of the CH_n groups to be determined, CH groups appearing as a doublet, CH_2 groups as a triplet and CH_3 groups as a quartet. Unfortunately compared to the basic broadband ^1H decoupled spectrum there is a considerable reduction in the signal-to-noise. It is also necessary to measure the spectrum twice. Also multiplicity information may be obtained using techniques such as APT (JMODulation), DEPT or INEPT.

Homonuclear decoupling technique

In a homonuclear decoupling experiment a particular multiplet is irradiated suppressing the coupling interaction between the irradiated nucleus and its coupling partners. A comparison of the standard coupled 1D spectrum and the selectively homonuclear decoupled spectrum reveals which nuclei are coupled. Whether a homonuclear decoupling experiment or a 2D homonuclear COSY experiment would be the best solution for multiplet analysis in a one-dimensional spectrum depends very much on the nature of the problem under investigation. If a large number of multiplets need to be irradiated then a two-dimension approach may be preferable.

Homonuclear selective decoupling is the preferred experiment if a multiplet structure is to be simplified for use in spectral analysis. However the homonuclear decoupling affects chemical shifts and coupling constants in a non-uniform manner (BLOCH-SIEGERT shift). These changes in chemical shift and reduction in the coupling splitting depend on the difference between the irradiated frequency and the resonance frequency of the affected nucleus. In heteronuclear selective decoupling experiments the BLOCH-SIEGERT shift affects only the magnitude of the heteronuclear coupling constants.

Technically homonuclear decoupling has to be implemented in a special way. In order to be selective the irradiation power (in Hz) is comparable to the sweepwidth so to prevent the detected signals being masked by the decoupler output the decoupler and the receiver are alternatively gated-on and off during the detection period.

Gated ^{1}H and inverse gated ^{1}H decoupling technique

Although both experiments have a similar name the gated decoupling experiment results in a proton coupled heteronuclear spectrum (normally *with* nuclear Overhauser enhancement) while a inverse gated experiment results in a proton decoupled spectrum (normally *without* nuclear Overhauser enhancement). In the gated ^{1}H decoupling technique the ^{1}H decoupling sequence is gated on prior to the detection pulse (period 1 in Fig. 2.9). This allows a magnetization transfer by cross relaxation from protons to the X nuclei to build up and the X signal intensities are enhanced by the heteronuclear Overhauser effect. Since the decoupler is gated-off during the acquisition time the heteronuclear coupling can evolve. If the observed nucleus has a negative gyromagnetic ratio the nuclear Overhauser enhancement can cause complete suppression of signal intensity when using normal broadband proton decoupling, *i.e.* ^{29}Si. In the inverse gated ^{1}H decoupling experiment the decoupling is switched on only during the acquisition time (period 3 in Fig. 2.9) giving a proton decoupled heteronuclear spectrum without any nuclear Overhauser enhancement. This technique is used for the quantitative evaluation of ^{13}C spectra.

2.3.3   Coherence Selection - Phase Cycling and Gradients

Coherence selection or more correctly the selection of coherence transfer pathways (CT pathways) which contribute to the acquired data is an important part of any pulse sequence. The coherence selection is relevant for

- suppression of quadrature detection artefacts ("quad image")
- suppression of undesired signals
  - suppression of solvent signal(s)
  - suppression of signals which rely on multiquantum states during the t1 period of a 2D experiment
  - suppression of ^{1}H signals which belong to ^{12}C isotopomers
- suppression of coherences due to relaxation during the pulse sequence
- frequency discrimination in 2D data

The methods available for selecting a particular pathway are phase cycling and pulsed field gradients.

Phase Cycling for Coherence Selection

CT pathway selection using phase cycling procedures depends on the signal accumulation of repeated scans. In each scan the same pulse sequence is executed but the phase of the excitation pulses and the receiver is shifted. The coherence selection is based on a difference method such that the unwanted coherences are cancelled because the effect of the phase shift is different for the coherence and the receiver phase. The wanted coherences are constructively added to the detected signal because the coherence and receiver have the same behaviour with respect to the phase shift. The best way to

trace the overall phase shift of a selected CT pathway is by using a CT pathway scheme. The rules for these schemes are [2.20, 2.25, 2.27]:

(1)   If the phase of a pulse is changed by Ω, then a coherence undergoing a change in coherence level Δp experiences a phase shift of $\Delta p \bullet \Omega$.

(2)   In N experiments the desired pathway is obtained by setting the receiver in phase with the pathway. Unwanted pathways add to zero after N experiments. The overall change in the receiver phase Ω_{rec}, can be expressed using the applied phase shifts and coherence levels by equation [2-16].

$$\Omega_{rec} = - (p_1 \cdot \Omega_1 + p_2 \cdot \Omega_2 + p_3 \cdot \Omega_3 + ...)$$ [2-16]

(3)   If a phase cycle uses N steps of 360/N degrees, pathways $\Delta p \pm n \cdot N$ with n = 1, 2, 3... will be allowed to contribute to the detected signal.

(4)   If a particular value of Δp is to be chosen from r consecutive values, N must be at least the same or geater than r.

The following *Check its* demonstrates rules (1) and (2) while the phase cycling in rules (3) and (4) can be checked in references [2.20, 2.25, 2.27]. The easiest way to show the basic condition for addition is to simulate a series of one-pulse experiments keeping the pulse phase constant and incrementing the receiver phase from 0° to 270° in 90° steps. As an additional exercise the reader might wish to confirm that the signal cancels after two scans by adding an additional step to the receiver phase program, the second step being shifted 180° in phase with respect to the first step.

2.3.3.1 Check it in NMR-SIM

Load the configuration file *ch2331.cfg*. Open the current pulse program *zg.seq* (**Edit│Pulse program**) and change the phase program as shown below. Save the pulse program with a new filename *myzg1ph.seq*: (**File│Save as…**). Replace the current pulse program with the newly created pulse program (**File│Pulse program**). Run the simulation saving the data as **Exp No:** *1*. In 1D WIN-NMR apply a window function and transform the data. Save the spectrum (**File|Save as…**). Repeat the simulation for the three remaining receiver phase programs, saving each simulation using a different **Exp No:**. Finally modify the phase program for **Exp No:** *5* and confirm that no signal is obtained.

	Exp No.: 1	Exp No.: 2	Exp No.: 3	Exp No.: 4	Exp No.: 5
ph1=	0	0	0	0	0
ph31=	0	1	2	3	0 2

It is obvious from *Check it 2.3.3.1* that the accumulation of all four scans where the receiver phase is incremented whilst the excitation pulse phase remains constant results in an observed signal with zero intensity. (This may also be confirmed manually in 1D WIN-NMR by using the **Process|File Algebra** command and clicking on the **Add./Sub.** button in the button panel to add all four FID or spectra together.) However if the phase

of the excitation pulse and receiver are shifted in parallel the accumulation of four scans results in a signal with four times the intensity when compared to a one scan spectrum. Both these results are in accordance with statement (1) and (2) above.

A second example of coherence selection using phase cycling is the suppression of the quaternary carbon signals in a polarization transfer ^{13}C spectrum. DEPT and INEPT type pulse sequences use a polarization transfer step to enhance the signal of an NMR insensitive nucleus such as ^{13}C which exhibits scalar coupling to a NMR sensitive nucleus such as ^{1}H.

2.3.3.2 Check it in NMR-SIM

(a) Load the configuration file *ch2332.cfg*. Create a pulse program that corresponds to the pulse sequence scheme and first phase program below. Open the editor (**Edit⎪Create new⎪Pulse program**) and enter the filename *myinept.seq* for the new pulse program. In the edit window enter the necessary commands for pulses and delays and then save the pulse program (**File⎪Save…**). Using the **Utilities|Show pulse program…** check that the pulse program corresponds to the pulse sequence below. If necessary compare the new pulse program with the INEPT sequence *ineptnd.seq*. Run four simulations corresponding to the phase programs shown below saving each data set using a different value of **Exp No:**. In 1D WIN-NMR apply a window function and transform the data. The loaded spin system file contains a quaternary carbon atom at 15 ppm and a ^{13}C^{1}H group at 10 ppm with a scalar coupling of 125 Hz. In the polarization transfer spectra the CH group appears as an antiphase doublet. A comparison of Exp. No. 1 and 2 shows that changing the phase values of ph4 and ph5 produces a 180° phase shift for the quaternary carbon. The combination of phase program 1 and 2 in Exp. No. 3 then leads to the complete suppression of the quaternary carbon signal. The final phase cycle, Exp. No. 4, cancels the enhancement due to the polarization transfer and the CH signals have the same intensity as a simple ^{13}C experiment.
(b) Using the pulse sequence as part (a) find an alternative phase program based on a constant receiver phase for suppressing the quaternary carbon signal whilst enabling polarization transfer enhancement for the CH signal (as a hint consider changing only ph4 and ph5).
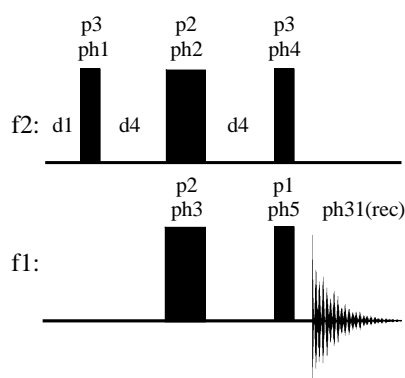
Exp. No.1:
ph1=0, ph2=0, ph3=0, ph4=1,
ph5=1, ph31=3

Exp. No.2:
ph1=0, ph2=0, ph3=0, ph4=3,
ph5=1, ph31=1

Exp. No.3:
ph1=0, ph2=0, ph3=0, ph4=1 3,
ph5=1, ph31=3 1

Exp. No.4:
ph1=0 2, ph2=0, ph3=0, ph4=3,
ph5=1, ph31=3

Another example of CT pathway selection using phase cycling is the EXORCYCLE phase cycle which is used to suppress artefacts due to imperfect refocusing in a spin echo. *Check it 2.3.3.3* shows how it is possible to compensate for an incorrect pulse length, 140° instead of a 180° pulse, using a four step phase cycle.

2.3.3.3 Check it in NMR-SIM

Load the configuration file *ch2333.cfg*. Using the pulse program scheme below create a pulse program saving the new pulse program with the name *myhospec.seq*. Perform four simulations using different phase cycles and pulse p2 pulse angle combinations saving the data as **Exp No.**: *1* to *4*. Simulation 1: one phase pulse program with **p2**: *180d*. Simulation 2: EXORCYCLE phase program with **p2**: *180d*. Simulation 3: one phase pulse program with **p2**: *140d*. Simulation 4: EXORCYCLE phase program with **p2**: *140d*. In 1D WIN-NMR use the **Display|Dual Display** mode to compare the signal intensities. Use the **Move Trace** button to move the second trace horizontally for a better comparison.
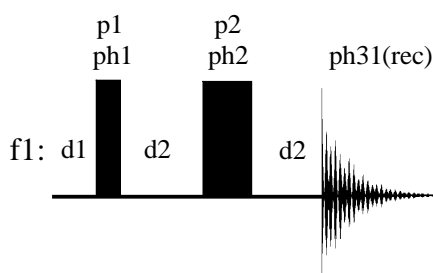
one phase program
ph1 = 2
ph2 = 0
ph31= 0
EXORCYCLE phase
program
ph1= 2
ph2= 0 1 2 3
ph31= 0 2 0 2

Gradients for Coherence Selection [2.46 – 2.51]

The effect of a z-gradient on transverse magnetization is often depicted using a "disk" representation that is sometimes called a "salami-slice". Fig. 2.10 illustrates how the on-resonance transverse magnetization in the rotating coordinate system evolves spatially

under the influence of an applied z-gradient. To simplify the following discussion only on-resonance magnetization will be considered because off-resonance transverse magnetization evolves simultaneously under the influence of both the chemical shift and the applied gradient. If the individual magnetization component of each spatial compartment is symbolised by a vector M(r), the influence of the gradient can be expressed as a phase evolution due to a dephasing motion of the M(r) vector with respect to each other (Fig. 2.10c). Starting with the magnetization aligned along the y-axis, the dotted arrows in Fig. 2.10 indicate the evolution due to the gradient field. Inverting the gradient field reverses the phase evolution refocusing the magnetization along the y-axis (Fig. 2.10c to d).
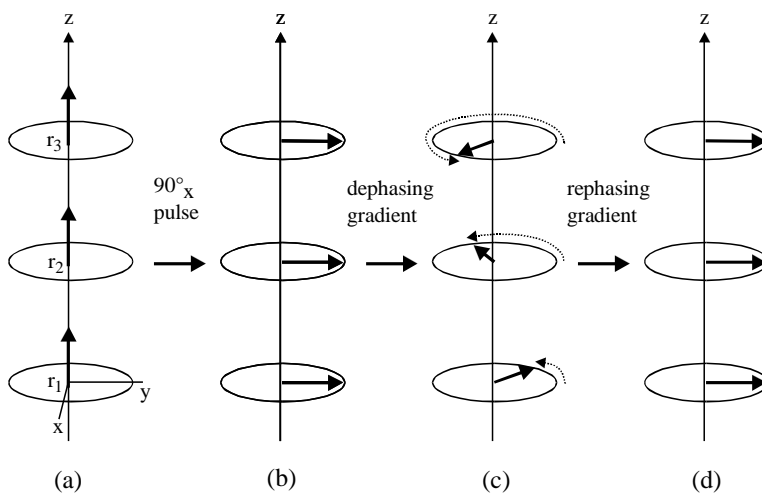
Fig. 2.10: Transverse magnetization in gradient fields.

The effect of the gradient is that the dephased magnetization components combine destructively to give a signal of zero intensity (Fig. 2.10c) whereas the rephased magnetization components can be detected in a similar manner to the signal directly observed after the initial $90°_x$ pulse (Fig. 2.10d). The use of gradients for coherence selection is very popular but what is often forgotten is that the spatial evolution depends upon the following properties of the spin system:

(1)　the gyromagnetic ratio γ of the nuclei whose transverse or multi-quantum coherence evolves under the gradient

(2)　the coherence order **p** of the dephased or rephased magnetization coherence.

The spatially dependent phase evolution $\varphi(r, \tau)$ of the transverse magnetization or coherence in a gradient field is given by equation [2-17]:

$$\varphi(r, \tau) = s \cdot p \cdot \gamma \cdot B_g(r) \cdot \tau \qquad\qquad [2\text{-}17]$$

where　s = form factor of the gradient; B_g = gradient field strength;

　　　　r = field coordinate; τ = gradient pulse length

Pictorially the relation for two spins 1 and 2 can be interpreted as a double-quantum coherence, $I_{1y}I_{2y}$, that evolves twice as fast as the single-quantum coherence, $I_{1y}I_{2z}$.

2.3.3.4 Check it in NMR-SIM

Load the configuration file *ch2334.cfg* and modify the basic one pulse experiment to include a gradient pulse prior to the data acquisition. Open the current pulse program *zg.seq* (**Edit│Pulse program**), add the gradient pulse line **p16: gp1** before the go-command and save the pulse sequence as *myzggrad.seq*. (**File│Save as…**). Replace the current pulse program by the newly created *myzggrad.seq* (**File│Pulse program**). Run five simulations using different values of the pulse **p16**: *1u*, *10*, *20*, *50* and *100u*. Transform the data and compare the non-linear signal intensity lost as a function of the dephasing pulse gradient field strength using the **Stack plot** option of the **Display|Multiple Display** mode. If necessary use the **Mouse Grid** option to shift the spectra for a clearer display.
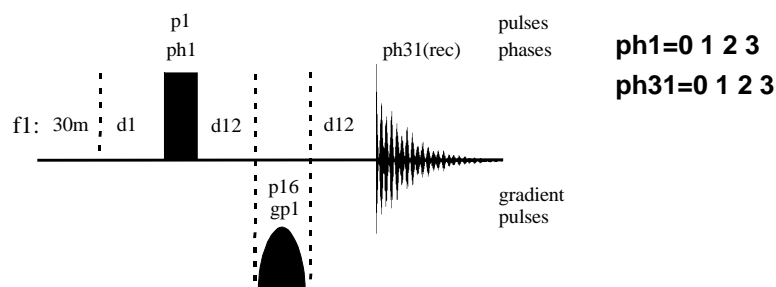
The application of one gradient, two gradients or several gradients as part of a pulse program has to be considered separately. The following discussion is restricted to z-gradients only and makes the assumption that the spatial shape of the gradient remains constant during the course of the experiment. In addition the explicit differentiation between transverse magnetization and coherence is neglected because it is not relevant.

The combination of two or more gradients has a similar effect as phase cycling and in a similar way to phase cycling coherence transfer pathways can be selected to contribute to the final quadrature detection signal (QDS) with a coherence level $p_{final} = -1$. By analogy with equation [2-16] for phase cycling, a similar equation can be derived for selection by gradients assuming that the gradients have the same shape and length:

$$\sum_i (\sum_n p_{i,n}) \cdot B_{g,\,i} = 0 \qquad\qquad [2\text{-}18]$$

$\sum p_{i,n}$: coherence order of the selected coherence pathway during the gradient field;
$p_{i,n}$: coherence level of spin n; $B_{g,i}$: gradient field amplitude of gradient i.

In practical terms equation [2-18] means that the refocusing of the selected coherences requires that the net phase of the selected pathways returns to zero prior to

detection. For heteronuclear gradient experiments each term in equation [2-18] must be modified to include the magnetogyric ratio of the coherence components:

$$\sum_i \left(\sum_n \gamma_n \cdot p_{i,n}\right) \cdot B_{g,i} = 0 \qquad\qquad [2-19]$$

γ_n: magnetogyric ratio of the spin n.

Although both phase cycling and gradient selection can be used for coherence selection there are differences between the two methods [2.46]:

- Phase cycling is a difference method and therefore is very susceptible to changes in the experiment conditions such as magnetic field changes or probehead temperature variations which leads to the incomplete subtraction (suppression) of undesirable signals.

- Combination of gradient pulses selects coherence transfer pathways of a particular ratio of coherence orders.

- Phase cycling selects coherence transfer pathways which are characterized by a particular change of coherence orders and further pathways with $\Delta p_{total} = \sum \Delta p_i \pm N \cdot r$ and $N = 0, 1, 2, 3...$ (N, r see equation [2-16]).

- Due to the application of several gradients a lost of signal intensity must be accepted because of the suppression of coherence transfer pathways which otherwise would contribute to the detected signal and which are not suppressed by phase cycling.

The order of the following three subsections reflect the number of gradients applied prior to data acquisition and use examples to illustrate gradient selection.

Application of one gradient

The effect of a gradient depends upon the coherence order (equation [2-17]) so that unlike single and multiquantum coherences, zero-quantum coherence and longitudinal magnetization are not dephased by a z-gradient. Consequently a single gradient can be used to dephase single and multiquantum coherences and separate these coherences from zero-quantum coherence. The required coherences are stored as zero-quantum coherence or longitudinal magnetization during the gradient pulse then brought back to detectable transverse coherence using a 90° pulse. In Fig. 2.11 there are two examples of zero-quantum coherence selection with the corresponding pulse sequences. The first example, *Check it 2.3.3.5*, is the suppression of a solvent signal and the second example, *Check it 2.3.3.6*, is the separation of a ^{13}C, ^{1}H spin system from its ^{12}C, ^{1}H isotopomers.

(a)

(b)
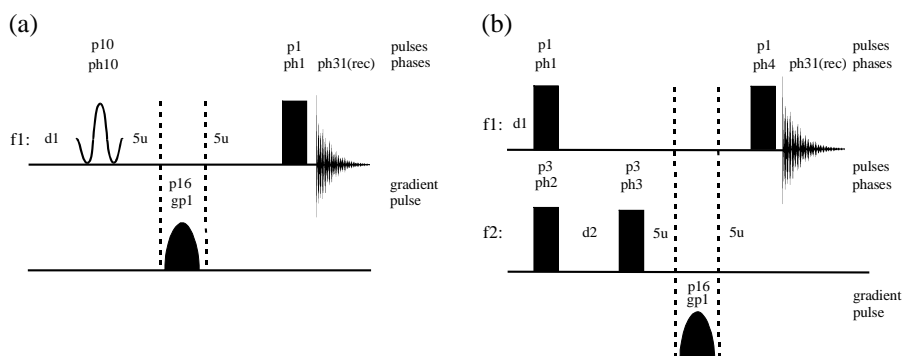
Fig. 2.11: (a) Solvent signal suppression, (b) ^{12}C coherence suppression (^{1}H signals of ^{12}C isotopomers).

2.3.3.5 Check it in NMR-SIM

Load the configuration file *ch2335.cfg*. Create a new pulse sequence as depicted in Fig. 2.11(a) implementing the shaped pulse and phase program shown below. Save the new sequence as *myzgshpg.seq* (**File⎮Save as…**). Run two simulations using the new pulse program : **Exp No.**: *1* with **gp1**: *0* % and **Exp No.**: *2* with **gp1**: *50* % (**Go⎮Check Parameters & Go**). Process the data in 1D WIN-NMR and compare the spectra using the **Dual Display** mode. The shaped pulse transfers the solvent signal into transverse magnetization, which is then dephased by the gradient pulse.

Shaped pulse implementation: **Phase program:**
p10:sp0 ph10   ph10=0, ph1=0, ph31=0

2.3.3.6 Check it in NMR- SIM

Load the configuration file *ch2336.cfg*. Create a new pulse program, called *myzgnxse.seq*, using the sequence scheme in Fig. 2.11(b) and the phase program listed below. Use the **Utilities|Show pulse program…** to check the pulse sequence. Run two simulations, **Exp No.**: *1* with **gp1**: *0* % and **Exp No.:** *2* with **gp2**: *10* %. Use the **Dual Display** mode to compare the processed spectra. Only the ^{1}H signal from the ^{12}C isotopomer is suppressed because the ^{13}C isotopomer coherence is converted to zero-quantum coherence by the second p3 pulse prior to the gradient pulse.

phase program	**ph3=1**
ph1=0	**ph4=1**
ph2=0	**ph31=1**

Application of two gradients

Two gradient pulses can be combined in three basic ways:

g1 : g2 with   **(I)**   **g2 = - g1**

                          (II)   **g2 = g1**

                          (III)   **g2 = A • g1**

Two gradients can only be used for coherence selection if the coherence order changes between the gradient pulses because the application of a gradient of inverse sign after the dephasing gradient would simply refocus the original magnetization. Consequently if two gradient pulses are to be used for coherence selection the coherence order of both the wanted and unwanted coherences must be changed differently by the rf pulses applied in the period between the gradient pulses. Three popular applications using two gradients of the same intensity, both with and without sign inversion are:

- The application of two gradients in homonuclear 2D COSY experiments
- The WATERGATE sequence
- The excitation sculpting procedure

The application of two gradients in homonuclear 2D COSY experiments: The use of gradients in 2D experiments enables frequency discrimination in the indirectly detected f1 dimension using only one scan per increment. In Fig. 2.12 the Echo/Antiecho method for generating phase sensitive spectra is illustrated using coherence transfer pathways, the mathematical principles have already been discussed in section 2.3.1. Depending on

g1 = g2: n-type (echo) COSY spectrum   g1 = -g2: p-type (antiecho) COSY spectrum
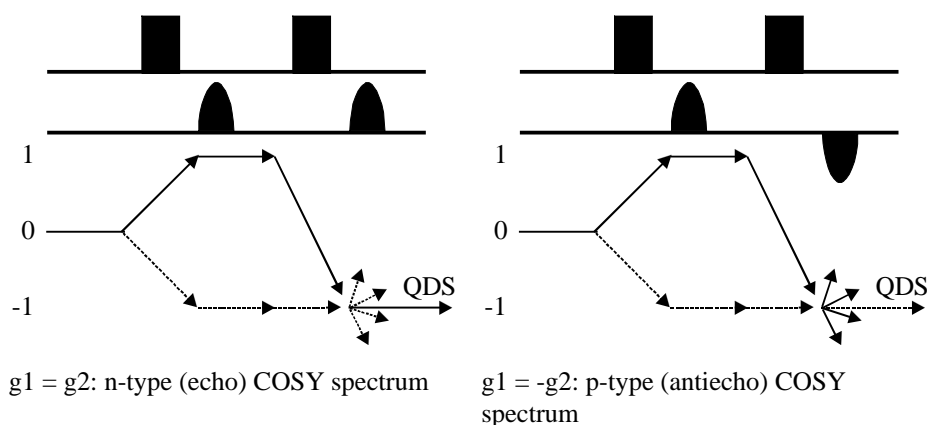
Fig 2.12:   Coherence transfer pathways that contribute to the p- and n-type COSY spectrum.

the gradient sign two different CT pathways can contribute to the final detected signal. If both gradients have the same sign the CT pathway with coherence order +1 (n-type, bold arrows) in the period between the two rf pulses is transferred to the detector. In contrast the CT pathway with coherence order -1 (p-type, dotted arrows) is fanned out by the second gradient during the evolution period and does not reach the detector. The

selection of the p-type coherence pathway can be achieved if the second gradient has negative amplitude. In this situation it is the coherence order +1 (n-type, bold arrows) that is fanned out by the second gradient and does not reach the detector. Using only one of both types results in a 2D experiment with frequency discrimination in f1. If the data is collected in the co-addition mode it can only be processed in the magnitude mode. However using appropriate gradients and the separate storage of the detected signals from the p- and n-type coherence pathways, the data can be processing according to the States et al. method, for instance, to provides the both frequency discriminated and phase sensitive spectra.

In *Check its 2.3.3.7* and *2.3.3.8* a phase-cycled COSY magnitude spectrum is converted into a gradient selected COSY spectrum. The *Check its* also show how the choice of either the n- or p-type CT pathways influences the frequency display in the f1 dimension.

2.3.3.7 Check it in NMR-SIM

Load the configuration file *ch2337.cfg*. Open the current pulse program *cosy.seq* in the NMR-SIM editor (**Edit**⎮**Pulse program**). Add the gradient command lines listed below and replace the phase program by the phase program also listed below. Save the pulse sequence with the new name *mycosygp.seq* (**File**⎮**Save as…**). Replace the current pulse program with the new pulse program that will be used in the simulation (**File**⎮**Pulse program…**). Check the pulse sequence for correct syntax using the pulse program viewer (**Utilities**⎮**Show pulse program...**).

50u ; first gradient g1	**ph1=0 2**
p16:gp1	**ph2=0 0 2 2**
d16	**ph31=0 2**
50u ; second gradient g2	
p16:gp2	
d16	

The homonuclear 2D gradient selected COSY(mc) experiment.   Gradient commands

2.3.3.8 Check it in NMR-SIM

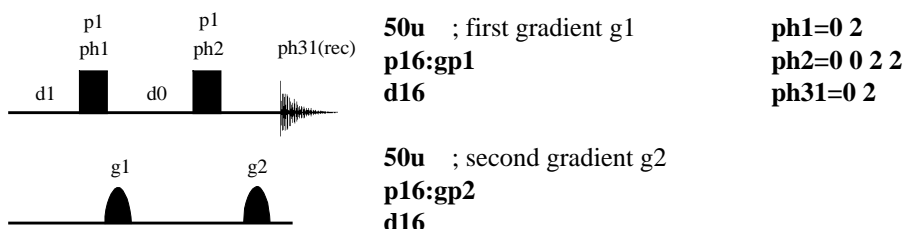Load the configuration file *ch2338.cfg*. To simulate the n- and p-type gradient-selected COSY magnitude mode spectra of the ^{1}H-AMX spin system load the pulse sequence *mycosygp.seq* written in *Check it 2.3.3.7* (**File**⎮**Pulse program…**). Simulate the spectra **Exp No.**: *1* **g1**:**g2** *10:10* for the n-type and **Exp No.**: **g1**:**g2** *10:-10* for the p-type COSY spectrum. Transform the data using the **Process|2D transform [xfb]** command. A

comparison of the spectra shows the spectrum is inverted about the centre of the f1 dimension.

In gradient selected 2D experiments the data is phase modulated and frequency discrimination in the f1 dimension is inherent in the method. As shown in *Check it 2.3.3.9* the combination of n- and p-type data leads to a phase sensitive spectrum.

;filename: mycosyea.seq

define list<gradient> EA=<EA>

```
1 ze
2 30m
3 30m
4 d1
...
p16:gp2*EA
...
30m wr #0 if #0 zd
3m igrad EA
lo to 3 times 2
30m id0
lo to 4 times l3
exit

ph1=0 2 2 0
ph2=0 2 0 2
ph31=0 2 2 0
```

Modifications for the pulse sequence *mycosyea.seq*.

2.3.3.9 Check it in NMR-SIM

(a) Load the configuration file *ch2339.cfg* and replace the current pulse program with *mycosygp.seq* from *Check it 2.3.3.7*. Use the NMR-SIM Editor to convert the program to a phase sensitive experiment replacing or adding the commands listed in bold on the left side of this *Check it*. Note that in the define list there is a space between <gradient> and EA. Save the sequence with the name *mycosyea.seq* (**File│Save as…**). Note that for each d0 value there are two data sets stored separately corresponding to the different gradient settings. Simulate the spectrum but prior to the 2D Fourier transformation check in the Parameters dialog box box (**Process│General parameter setup**) that **MC2** is set to *echo-antiecho*.
(b) Compare your pulse sequence with the phase sensitive echo/antiecho COSY sequence *cosyetgp.seq* in the standard BRUKER pulse program library.

The pulse sequence created in the *Check it 2.3.3.9* produces a echo/antiecho COSY spectrum that may be phased is slightly different from the commonly used pulse sequence *cosyetgp.seq* included in the standard BRUKER pulse program library. The first difference is the introduction of two 180° pulses which refocus any coherence evolution during the long gradient pulses. The second difference is alternation in the sign of the amplitude of the first gradient pulse; this is based on experimental observations which have shown that alternating the last gradient can rephased and reintroduce unwanted coherences [2.52].

The WATERGATE sequence: In its simplest form the WATERGATE sequence for solvent suppression consists of two gradients with inverted amplitudes and a selective pulse which inverts the solvent coherence. The effect of this gradient selective pulse combination is to refocus the coherences of the wanted resonance signals that can then

be detected while the solvent coherence is dephased by each gradient. Fig. 2.13 shows the CT pathway for this simple WATERGATE experiment illustrated in *Check it 2.3.3.10*.

wanted coherences   suppressed solvent coherence
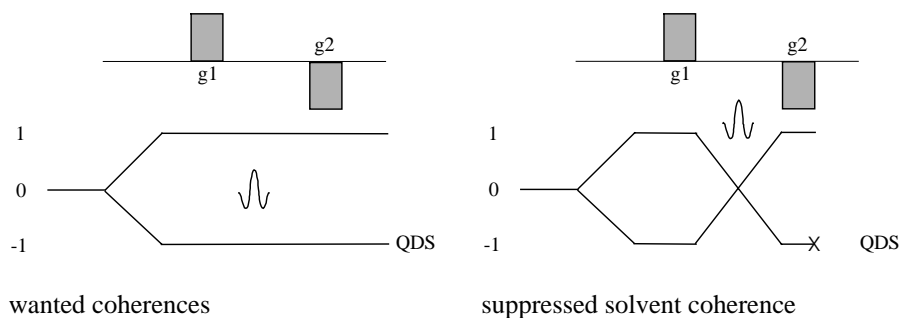
Fig. 2.13:   Coherence transfer pathways for simple WATERGATE experiment.

2.3.3.10 Check it in NMR-SIM

Load the configuration file *ch23310.cfg* with all the necessary experiment parameters and a suitable test spin system - the reduced spin system of cis-3-amino-DL-proline (2%) in water (98%). Create a new pulse program corresponding to the pulse sequence shown below (**Edit│Create new│Pulse program**) saving the sequence as *mywaterg.seq*. Run the simulation using the current experimental parameters and a 100ms REBURP pulse. Transform the data in 1D WIN-NMR. Note the phase distortion across the whole spectrum due to the overall phase shift introduced by the selective pulse. To confirm this phase shift, open the Bloch module (**Utilities│Bloch module…**) and calculate the excitation profile.
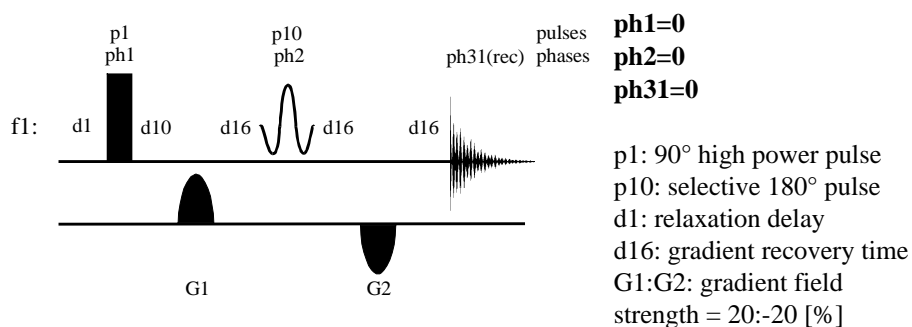
Simple WATERGATE sequence.

Unfortunately this simple sequence produces a phase distorted spectrum due to the selective 180° pulse inverting the on-resonance coherences and at the same time

introducing a phase shift for the neighbouring frequency range. Thus, the commonly used WATERGATE sequence differs from the sequence in *Check it 2.3.3.10* by using two gradients with the same sign and a selective 180° spin echo pulse that refocuses the whole detected frequency range except for the solvent frequency. Thus, the wanted coherences are exchanged between coherence orders ± 1 prior to the second gradient pulse while the solvent coherence is kept constant suppressing the transfer of the solvent signal to the detector. This sequence is easily implemented using a binomial pulse or a composite of two 90° selective pulses and a hard 180° pulse between the two gradients. For further details on the WATERGATE sequence the reader is referred to section 5.2.3.

The Excitation Sculpting procedure: Excitation sculpting essentially consists of two pulsed field gradient spin echo units which may be represented as ***...G_1 - S - G_1 - G_2 - S - G_2....*** To prevent the refocusing of dephased coherence by the second spin echo, the first pair and second pair of gradients differ in strength as indicated by the terms ***G_1*** and ***G_2***. The effect of the combined spin echoes can be mathematically derived in density matrix terms [2.53, 2.54] and involves solving the basic equation: $\mathbf{M}$ (M_x, M_y, M_z) = T $\cdot\mathbf{m}$ (m_x, m_y, m_z). The most import term is the matrix T, a 3x3 matrix corresponding to the three orthogonal axes. The dominant parameters for each matrix element are the probability P that the 180° refocusing sequence S flip a spin and the phase shift β of the transverse magnetization arising from the sequence. A comparison of the single pulsed field gradient spin echo (SPFGE) represented by ***...G_1 - S - G_1...*** and the double pulsed field gradient spin echo (DPFGSE) is shown below. It is obviously that for the single pulsed field gradient spin echo the matrix T incorporates both diagonal elements for M_x, M_y and M_z as well as non-diagonal elements which are attributed to transitions to phase shifted transverse components. In contrast for the double pulsed field gradient spin echo, represented by the product T^2 of the matrix T, the matrix only contains diagonal elements which can be interpreted as the scaling of the transverse components M_x and M_y and the longitudinal component M_z by the probability P.

$$G - S - G \qquad\qquad G_1 - S - G_1 - G_2 - S - G_2$$

$$T = \begin{bmatrix} P \cdot \cos\beta & P \cdot \sin2\beta & 0 \\ P \cdot \sin\beta & -P \cdot \cos2\beta & 0 \\ 0 & 0 & (1\text{-}2) \cdot P \end{bmatrix} \qquad T^2 = \begin{bmatrix} P \cdot \cos\beta & 0 & 0 \\ 0 & -P \cdot \cos2\beta & 0 \\ 0 & 0 & (1\text{-}2) \cdot P \end{bmatrix}$$

Matrix representation of the effect of a single (SPFGE) and double pulsed field gradient spin echo (DPFGSE).

The mathematical results of the double pulsed field gradient spin echoes can also be formulated as a set of rules [2.54]:

- Independent of the initial magnetization and the particular refocusing sequence S, the transverse magnetization is brought back to its initial position in three-

  dimensional space with its magnitude attenuated by a factor P.
- Different magnetization components are not mixed.
- The excitation profile depends only on the inversion profile of S, not its phase properties.
- The sequence S must be anti-symmetric in time or have a net rotation axis that is stable as a function of the offset. This implies that sequence S separates the wanted and unwanted coherences using a selective coherence level change for one of both types of coherence. However S must also refocus any chemical shift evolution (which is anti-symmetric in time) as well as any offset dependent phase and tilt modulation (the net rotation axis that is stable as a function of the offset).
- The role of the gradients is to dephase all magnetization components that do not experience a perfect 180° pulse.

It can be concluded [2.53]: *A double pulsed field gradient spin echo of any pulse sequence S returns any transverse magnetization to its original position, attenuated by the square of the probability that a spin is flipped by the sequence S.*

The excitation sculpting procedure is usually implemented in 1D and 2D pulse sequences using a selective 180° refocusing element. However as shown in Table 2.9 there are also a number of applications where non-selective pulses are used. In all cases the choice of a particular pulse sequences depends upon the phase distortions the refocusing units introduce into the spectrum.

Table 2.9:   Examples of pulse sequence using Excitation sculpting.

1D improved WATERGATE experiment	[2.53]
1D selective COSY and TOCSY experiment	[2.55, 2.56]
1D single and double selective ROESY experiments	[2.57]
2D selective J-HSQC experiment (EXSIDE)	[2.58]
Band-selective 2D ^{1}H-TOCSY experiment	[2.59]
2D HSQC experiment	[2.60]
GBIRD pulse sequence element	[2.61]

In *Check it 2.3.3.11* the excitation sculpting procedure is demonstrated using the GBIRD sequence, an interesting alternative for suppressing the ^{1}H signals of ^{12}C isotopomers. Finally the performance of the ^{1}H-GBIRD pulse sequence is compared to the alternative BIRD-t_{null} sequence.

2.3.3.11 Check it in NMR-SIM

(a) Create a pulse program *mygbird.seq* based upon the pulse sequence scheme below (**Edit│Create new│Pulse program**). Load the configuration file *ch23311a.cfg* containing the experimental and processing parameters and the spin system *13c12c.ham*. Simulate a standard ^{1}H spectrum (**File|Pulse program…**) using the *zg.seq* pulse sequence and the ^{1}H

GBIRD spectrum using the newly created *mygbird.seq*. Store the data using different **Exp. No:**'s and process the data in 1D WIN-NMR by clicking the **Zero Filling!**, **Window!** and **FT!** buttons. Compare the results using the **Dual Display** mode and note that for the ^{1}H GBIRD spectrum the ^{1}H signals of the ^{13}C isotopomer have nearly the same intensity as the corresponding ^{13}C satellites in the standard ^{1}H spectrum.

(b) To compare the performance of the BIRD-t_{null} sequence (*birdd7.seq*) and the GBIRD sequence (*mygbird.seq*) load the configuration file *ch23311b.cfg*. The spin system *13C1hrng.ham* contains five CH fragments with a range of $^1J(^{13}C, ^1H)$ values from 100 Hz to 180 Hz while the experimental parameter d2 = 1/(2 • J(C, H)) has been optimized for a value of 140 Hz. Perform three simulations: the first using the *zg.seq* pulse sequence, the second with the BIRD-d7 pulse sequence (t_{null} = d7) available from the pulse sequence library and the third with the GBIRD pulse sequence. Process the data in 1D WIN-NMR. Compare the signal intensities of the ^{13}C satellites in all three ^{1}H spectra. There is some loss of signal intensity and phase distortion in the ^{1}H GBIRD spectrum for unmatched d2 values compared to the BIRD-t_{null} sequence but it is only a minor aberration. In turn the suppression of the ^{1}H signals of the ^{12}C isotopomer in the BIRD-t_{null} sequence requires all the protons to have the same relaxation time. Consequently on a practical basis the GBIRD sequence might be the preferred option.
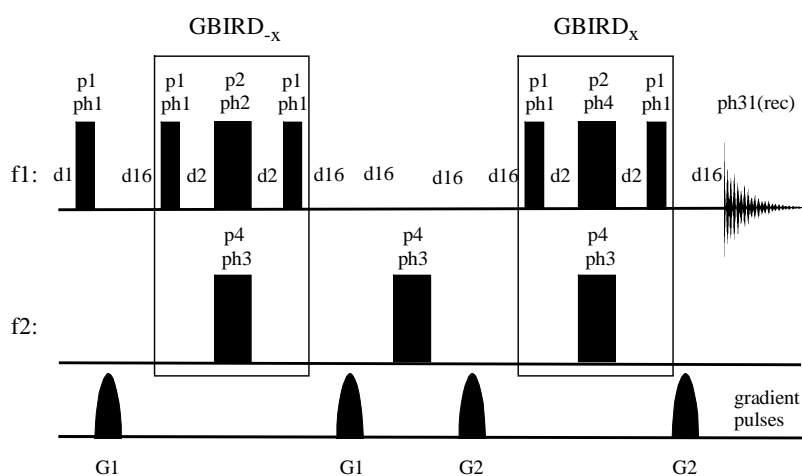
p1: 90° pulse (f1), p21: 180° pulse (f1); p4: 180° pulse (f2), p16: gradient pulse = 1.0 ms, d16: gradient recovery time = 100u, d1: relaxation delay (1 - 2 s); d2: = 1/(2 • $^1J(C, H)$), phase program: ph1, ph3, ph4, ph31=0, ph2=2.

[1]H-GBIRD pulse sequence.

Further examples of the use of excitation sculpting to minimize the phase distortions introduced by a spin echo unit are discussed in section 5.2.3 on the WATERGATE sequence and in section 5.4.1.1 for a 1D selective COSY experiment.

Application of three and more gradients

The application of three and more gradients is necessary if multiquantum states are to be suppressed as in the double-quantum filtered COSY experiment or if CT pathways in heteronuclear spin systems should be selected in sequences which include magnetization transfer steps.

2.3.3.12 Check it in NMR-SIM

Load the configuration file *ch23312.cfg* and create a new pulse sequence (**Edit│Create new│Pulse program**) that corresponds to the sequence scheme and phase program in Fig 2.14. Ignore the numbered arrows as they refer to *Check it 2.3.3.13*. Save the new pulse sequence file with the name *my1Dhmqc.seq* (**File│Save as…**). Check the pulse sequence for correct syntax using the pulse program viewer (**Utilities│Show pulse program...**). Run two simulations using the new pulse sequence and the standard one-pulse sequence *zg.seq*. Transform the data and use the **Dual Display** mode in 1D WIN-NMR to compare the spectra, note that the ^{1}H signal intensities for both the ^{12}C and ^{13}C isotopomers is the same.
(b) To suppress the ^{1}H signal of the ^{12}C isotopomer phase cycling is necessary. Modify the phase program in *my1Dhmqc.seq* changing ph2 and ph31 to: *ph2=1 3* and *ph31=2 0*. Transform the data and compare the spectra with and without phase cycling and note the suppression of the ^{1}H signal of the ^{12}C isotopomer.

This second case is illustrated in *Check its 2.3.3.12* and *2.3.3.13* for the one-dimensional version of the gradient selected ^{n}X, ^{1}H HMQC experiment. In this particular sequence three gradients are used to suppress the ^{1}H signals of the ^{12}C isotopomers which in the 2D experiment would cause a t1 noise ridge parallel to the f1 dimension. As shown in the previous *Check it*, the BIRD-t_{null} unit (see section 5.8.1) or similar type of unit can cause incomplete suppression of the ^{12}C isotopomers ^{1}H signals. To implement gradient selection to suppress the ^{12}C isotopomers ^{1}H signals in a single scan, it is necessary to analyze the CT pathways shown in Fig. 2.14. According to the CT diagram, pathway A and B contribute to the detected signal in the absence of any applied gradient. In the gradient selected HMQC sequence one pathway must be suppressed and this is normally achieved by using three gradients with the strengths G1:G2:G3 = 5:3:4. Using the coherence level diagram in Fig 2.14 the solution of equation [2-19] for CT pathway A and B results in only pathway A contributing to the recorded signal ($\sum_i p_i \bullet G_i = 0$)

because the signals of pathway B are dephased for the same ratio ($\sum_i p_i \bullet G_i \neq 0$).

CT pathway A: $1.25 \bullet G1 + (-0.75 \bullet G2) + (-1 \bullet G3) = 6.25 \ - 2.25 - 4 = 0$

CT pathway B: $0.75 \bullet G1 + (-1.25 \bullet G2) + (-1 \bullet G3) = 3.75 \ - 3.75 - 4 = -4$

ph1 = 0
ph2 = 1
ph3 = 0
ph4 = 3
ph31 = 2

Pulse program scheme of a 1D HMQC experiment.

Coherence level scheme of a 1D ^{13}C, ^{1}H HMQC pulse sequence using the p' scale.
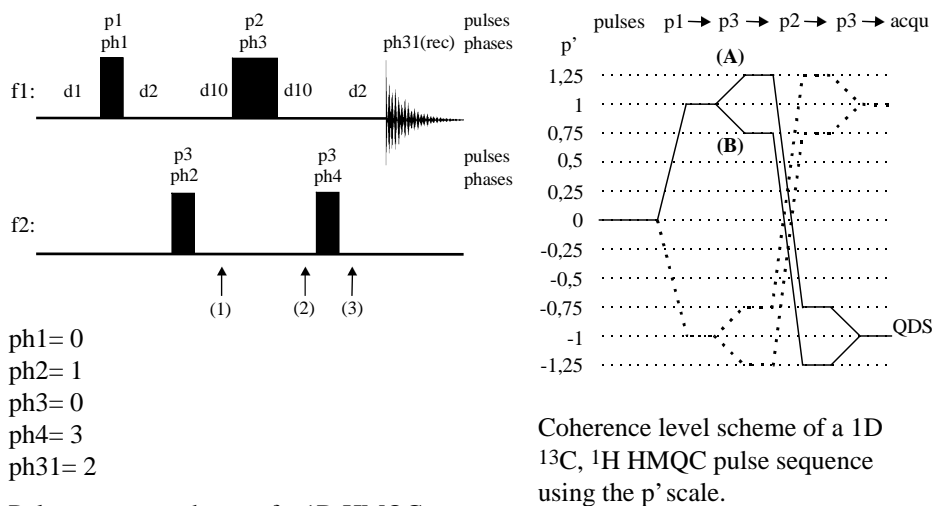
Fig. 2.14:   1D HMQC experiment - Pulse sequence scheme and CT diagram.

position (1)
p16:gp1
d16

position (2)
p16:gp2
d16

position (3)
p16:gp3
d16

Implementation of gradients G1, G2 and G3 in the 1D HMQC experiment.

2.3.3.13 Check it in NMR-SIM

Edit (**Edit│Pulse progam**) the 1D HMQC pulse program from *Check it* 2.3.3.12 and using the gradient commands shown on the left, add the gradient pulses to the sequence at the positions denoted by arrows in Fig. 2.14. Save the new sequence with the name *my1ghmqc.seq*. Run the simulation using the new sequence and notice that even only using one scan, the ^{1}H signal from the ^{12}C isotopomer is suppressed. Using the **Dual Display** mode compare the spectra without and with gradient selection and note that a reduction in signal intensity of a factor of 2 can be observed. As shown in Fig. 2.14, this signal lost is due to the suppression of CT pathway B which would otherwise contribute to the observed signal.

As shown by *Check it 2.3.3.12* and *2.3.3.13* the ^{1}H signals from the ^{12}C isotopomers can be successfully suppressed using either phase cycling or gradient selected experiment. However using gradient selection this suppression is possible in a single

scan saving a considerable amount of time in 2D experiments. In addition phase cycling is more susceptible to fluctuations in the experiment conditions between succeeding scans i.e. sample temperature variations, and to relaxation artefacts.

2.4   References

[2.1] Ernst R. R., Bodenhausen, G., Wokaun, A., *Principles of Nuclear Magnetic Resonance in One and Two Dimensions*, Oxford, Clarendon Press, 1994.

[2.2] Cavanagh, J., Fairbrother, W. J., Palmer, A. G. III, Skelton, N. J*., Protein NMR Spectroscopy - Principles and Practice*, San Diego, Academic Press, 1995.

[2.3] Harris, R. K., *Nuclear Magnetic Resonance Spectroscopy*, Harlow, Longman Scientific & Technical, 1986.

[2.4] Freeman, R., *Spin Choreography*, Oxford, Oxford University Press, 1998.

[2.5] Slichter, C. P., *Principles of Magnetic Resonance*, 3rd Ed., Berlin, Springer-Verlag, 1989.

[2.6] Neuhaus, D., Williamson, M., *The Nuclear Overhauser Effect in Structural and Conformational Analysis*, New York, WILEY-VCH, 1989.

[2.7] Hoch, J. C., Stern, A. S., *NMR Data Processing*, New York, WILEY-Lyss, 1996.

[2.8] Eberstadt, M., Gemmecker, G., Mierke, D. F., Kessler, H., Angew. Chem. 1995, *107*, 1813 - 1838.

[2.9] Hwang, T.-L., Kadkhodaei, M., Mohebbi, A., Shaka, A. J., Magn. Reson, Chem. 1992, *30*, S24 - S34.

[2.10] Macura, S., Westler, W. M., Markley, J. L., Methods Enzymol. 1994, *239*, 106 - 144.

[2.11] Bain, A. D., Martin, J. S., J. Magn. Reson. 1978, *29*, 125 - 135.

[2.12] Farrar, T. C., Concepts Magn. Reson., 1990, *2*, 1 - 12.

[2.13] Mulkern, R. Bowers, J., Concepts Magn. Reson. 1994, *6*, 1 - 23.

[2.14] Johnston, E. R., Concepts Magn. Reson. 1995, *7*, 219 – 242.

[2.15] Vega, S., J. Chem. Phys. 1978, *68*, 5518 - 5527.

[2.16] Packer, K. J., Wright, K. M., Mol. Phys. 1983, *50*, 797 - 813.

[2.17] Bodenhausen, G., NATO ASI Ser. C, 1990, *322*, 51 - 61.

[2.18] Van de Ven, F. J. M., Hilbers, C. W., J. Magn. Reson. 1983, *54*, 512 - 520.

[2.19] Sørensen, O. W., Eich, G. W., Levitt, M. H., Bodenhausen, G., Ernst, R. R., Prog. NMR Spectrosc. 1983, *16*, 163 - 192.

[2.20] Shriver, J., Concepts Magn. Reson. 1992, *4*, 1 - 33.

[2.21] Kingsley, P. B., Concepts Magn. Reson. 1995, *7*, 29 - 47.

[2.22] Nakashima, T. T., McClung, R. E. D., J. Magn. Reson. 1986, *70*, 187 - 203.

[2.23] Brown, L. R., Bremer, J., J. Magn. Reson. 1986, *68*, 217 - 231.

[2.24] Bain, A. D., J. Magn. Reson. 1984, *56*, 418 - 427.

[2.25] Bodenhausen, G., Kogler, H., Ernst, R. R., J. Magn. Reson. 1984, *58*, 370 - 388.

[2.26] Counsell, C. J. R., Levitt, M. H., Ernst, R. R., J. Magn. Reson. 1985, *64*, 470 - 478.

[2.27] Keeler, J., NATO ASI Ser. C, 1990, *322*, 103 - 129.

[2.28] McClung, R. E. D., Concepts Magn. Reson. 1999, *11*, 1 - 28.

[2.29] Zhu, J.-M., Smith, I. C. P., Concepts Magn. Reson. 1995, *7*, 281 - 291.

[2.30] Kingsley, P. B., J. Magn. Reson. Ser. A, 1994, *107*, 14 - 23.

[2.31] Kingsley, P. B., Concepts Magn. Reson. 1995, *7*, 29 - 47.

[2.32] Stejskal, E. O., Schäfer, J., J. Magn. Reson. 1974, *14*, 160 - 169.

[2.33] Stejskal, E. O., Schäfer, J., J. Magn. Reson. 1974, *13*, 249 - 251.

[2.34] Aue, W. P., Bartholdi, E., Ernst, R. R., J. Chem. Phys. 1976, *64*, 2229 - 2250.

[2.35] Bodenhausen, G., Freeman, G., Niedermeyer, R., Turner, D. L., J. Magn. Reson. 1977, *26*, 133 - 164.

[2.36] Nagayama, K., Kumar, A., Wüthrich, K., Ernst, R. R., J. Magn. Reson. 1980, *40*, 321 - 334.

[2.37] Bain, A. D., Burton, I. W., Concepts Magn. Reson. 1996, *8*, 191 - 204.

[2.38] Keeler, J., "Lectures on NMR-Spectroscopy 1998 (1.-4.)", University of Cambridge, U. K., (contact James.Keeler@ch.cam.ac.uk)

[2.39] NM Group, Analytical Instrument Technical and Engineering Division, JEOL News, 1986, *22A*, 14 - 19.

[2.40] States, D. J., Haberkorn, R. A., Ruben, D. J., J. Magn. Reson. 1982, *48*, 286 - 292.

[2.41] Marion, D., Wüthrich, K., Biochem. Biophys. Res. Commun. 1983, *113*, 967 - 974.

[2.42] Keeler, J., Neuhaus, D., J. Magn. Reson. 1985, *63*, 454 - 472.

[2.43] Nagayama, K., J. Magn. Reson. 1986, *66*, 240 - 249.

[2.44] Marion, D., Ikura, M., Tschudin, R., Bax, A., J. Magn. Reson. 1989, *85*, 393 - 399.

[2.45] Kay, L. E., Keifer, P., Saarinen, T., J. Am. Chem. Soc. 1992, *114*, 10663 -10665.

[2.46] Keeler, J., Crowes, R. T., Davis, A. L., Laue E. D., Methods Enzymol. 1994, *239*, 145 - 207.

[2.47] Davis, A. J., Keeler, J., Laue, E. D., Moskau, D., J. Magn. Reson. 1992, *98*, 207 - 216.

[2.48] Ruiz-Cabello, J., Vuister, G. W., Moonen, C. T. W., v. Gelderen, P., Cohen, J. S., v. Zijl, P. C. M., J. Magn. Reson. 1992, *100*, 282 - 302.

[2.49] Bax, A., Pochapsky, S. S., J. Magn. Reson. 1992, *99*, 638 - 643.

[2.50] Willker, W., Leibfritz, D., Kerssebaum, R. Bermel, W., Magn. Reson. Chem. 1993, *31*, 287 - 292.

[2.51] Parella, T., Magn. Reson. Chem. 1996, *34*, 329 - 347.

[2.52] Moskau, D., private communication, BRUKER application laboratory, Fällanden, CH.

[2.53] Hwang, T.-L., Shaka, A. J., J. Magn. Reson. Ser. A, 1995, *112*, 275 - 279.

[2.54] Stott, K., Stonehouse, J., Keeler, J., Hwang, T.-L., Shaka, A. J., J. Am. Chem. Soc. 1995, *117*, 4199 - 4200.

[2.55] Xu, G., Evans, J. S., J. Magn. Reson. Ser. B, 1996, *111*, 183 - 185.

[2.56] Xu, G., Evans, J. S., J. Magn. Reson. Ser. A, 1996, *123*, 105 - 110.

[2.57] Gradwell, M. J., Kogelberg, H., Frenkiel, T. A., J. Magn. Reson. 1997, *124*, 267 - 270.

[2.58] Krishnamurthy, V. V., J. Magn. Reson. Ser. A, 1996, *121*, 33 - 41.

[2.59] Krishnamurthy, V. V., Magn. Reson. Chem. 1997, *35*, 9 - 12.

[2.60] Heikkinen, S., Rahkamaa, E., Kilpeläinen, I., J. Magn. Reson. 1997, *127*, 80 - 86.

[2.61] Emetarom, Ch., Hwang, T.-L., Mackin, G., Shaka, A. J., J. Magn. Reson. Ser. A, 1995, *115*, 137 - 140.

3   Acquisition and Processing

The results of the analysis of the coherence evolution at each stage of a pulse sequence using density matrix representation or product operator (PO) formalism is usually a series of mathematical expressions which are often difficult for the experimental NMR spectroscopist to visualize and interpret. In contrast the result of a NMR-SIM simulation is either a FID (1D experiment) or a series of FIDs (2D experiment) very similar to the raw data acquired from a real NMR experiment. Consequently, with the exception of Bloch simulator operations, the processing of NMR data is an integral part of evaluating the results of a NMR-SIM simulation. The purpose of this chapter is to introduce the reader to the basics of NMR data processing using 1D WIN-NMR and 2D WIN-NMR prior to using NMR-SIM to examine and evaluate pulse sequences. It also examines how the appearance of both 1D and 2D spectra depend upon the choice of the experimental parameters.

The present introduction is a brief overview of the steps necessary to process the simulated NMR data to obtain the appropriate spectra. The chapter also contains short paragraphs entitled **How to...** which describe in slightly greater detail the various processing functions of 1D WIN-NMR. The manipulation of 2D data sets using 2D WIN-NMR is a little more complicated and is illustrated using a number of *Check its*. For a comprehensive introduction to 1D WIN-NMR and 2D WIN-NMR the reader is referred to the companion volume of this series *NMR Spectroscopy: Processing Strategies* [3.1] and the BRUKER manuals [3.2, 3.3] contained in pdf format on the enclosed CD-ROM.

3.1 Excitation of nuclear spins and their response detection

A free induction decay or FID is obtained by applying a rf pulse to a sample placed in a magnetic field via the transmitter/receiver coil of a probehead. Only the NMR-active nuclei whose resonance frequencies are close to the frequency of the rf pulse are excited and their nuclear magnetic moments induces a voltage inside the coil. For uncoupled nuclei the resonance experiment can be described by a simple vector representation based on the concept of macroscopic magnetization. For a spin-1/2 nucleus the ensemble of nuclei can be aligned either with the external magnetic B_0 field of the spectrometer magnet along the +z axis (lower energy state) or against the magnetic field along the –z

axis (higher energy state). Due to the BOLTZMANN distribution, at equilibrium there are slightly more nuclei in the lower energy state and although there is no phase coherence, the population excess aligned along the +z-axis may be represented by a single vector M_z. Introducing the concept of the rotating frame, where the CARTESIAN axis rotate at the frequency of the rf field, it is possible to simplify the spatial description of the magnetization components. A rf pulse with a 90° tilt angle and a phase x tips the M_z vector from the +z-axis to the +y-axis of the rotating frame. If there is a difference between the resonance frequency of the nuclei and the frequency of the rotating frame, the chemical shift, the magnetization M_y evolves in the x,y-plane during the data acquisition period. After the pulse longitudinal relaxation returns the magnetization vector to its equilibrium state along the +z-axis. For simplicity transverse relaxation is ignored.
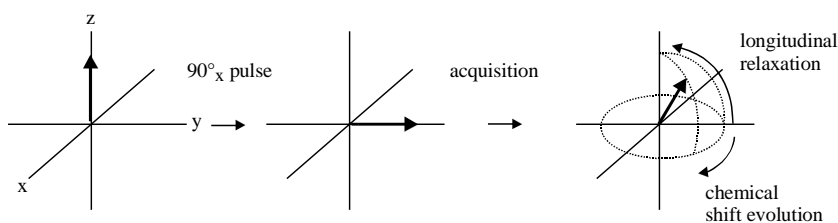
Fig. 3.1:   Vector picture of a one-pulse excitation experiment.

Starting with the initial value of the M_y component, the detection process measures the evolution of the magnetization in the x,y-plane during the acquisition period and the return of magnetization to its equilibrium state. When a non-frequency selective excitation pulse excites nuclear spins with different resonance frequencies the individual responses of the different nuclear spins are superimposed upon each other to form the overall free induction decay. The recording of n-dimensional spectra is also based on this general scheme. A series of FIDs are acquired but between each FID there is an increment in an evolution period based on a spin system parameter such as the chemical shift or coupling evolution or incoherent molecular effects such as chemical exchange. The number of these evolution periods determining the number of processed dimensions.

3.2   One dimensional Experiments

In its simplest form the recording of a one dimensional experiment consists of the excitation of the spins by a rf pulse and acquisition of their response. The response of the excited nuclear spins generates a rf signal which, after pre-amplification, is combined with the initial excitation frequency and converted into a low frequency signal in the kHz range. This signal is then digitized in an analog-to-digital converter (ADC) and stored in the computer memory. On modern spectrometers the x- and y-component of the rf signal are detected and stored separately, see section 2.3.1 on quadrature detection. This time

domain signal is referred to as the raw data or free induction decay. Often the appearance of the FID is quite complicated and before it can be used the time domain signal must be converted to a frequency domain signal using Fourier transformation (FT).

Fig. 3.2: Flow chart - acquisition and processing.

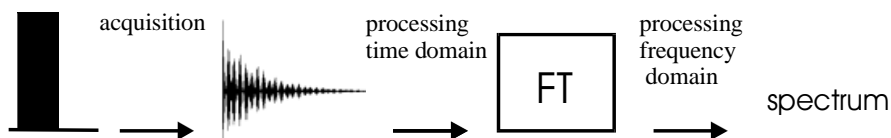In the context of the NMR-SIM simulation, the recording of a one-dimensional experiment consists of the definition of the spin system, the pulse sequence and the experiment parameters. The result of the simulation is a FID that is loaded into the 1D WIN-NMR processing program. Both the time domain and the frequency domain data may be processed using a variety of domain specific mathematical functions.

3.2.1 Recording a Free Induction Decay

Prior to the data acquisition (simulation) a number of experimental parameters have to be set. Because these parameters can effect the appearance of the final spectrum and are common to all pulse sequences they will be discussed in more detail under the following headings:

- Spectral width, acquisition time and time domain data points
- the accumulation of repeated experiments
- the effect of the magnetic field strength

Spectral width, acquisition time and time domain data points

Normally a FID is acquired using simultaneous quadrature detection, sequential quadrature detection is explained in section 2.3.1. The FID consists of the values of the x- and y-components of the magnetization measured at discrete intervals during the acquisition period T_{aq}. The time interval between two successive pairs of data points is called the dwell time τ_d. For a given (chosen) spectral width SW [Hz], a total number of data points TD and acquisition time T_{aq}, the following relation is valid (NYQUIST theorem):

$$SW = \frac{TD}{2} \bullet \frac{1}{T_{aq}} = \frac{1}{\tau_d} \text{ , with } \nu_{transmitter} \text{ at the spectrum centre.} \qquad [3\text{-}1].$$

Two consequences of this relation must be stressed:
- The highest frequency that can be correctly detected is the NYQUIST frequency:
  $\nu_{NYQUIST} = SW / 2$.
- The digital spectral resolution is defined by the number of time domain data points for a given spectral width and is directly proportional to the length of the acquisition

time: TD/SW $\propto$ T$_{aq}$. A lineshape can be correctly reproduced provided that the reciprocal of the acquisition time is less than the linewidth of a resonance signal at half-height: $1/T_{aq} < \delta\nu_{1/2}$.

In *Check it 3.2.1.1* the correct measurement of two sets of signals is demonstrated. In addition the effect of the number of time domain data points TD on the digital resolution using the same spectral width recorded at higher magnetic field strengths is illustrated.

3.2.1.1 Check it in NMR-SIM

(a) Load the configuration file *ch3211.cfg* (**File│Experiment setup│Load from file...**). Simulate the ^{1}H spectrum of the AX spin system (**Go│Check Parameters & Go**). In 1D WIN-NMR click on the **FT!** button in the button panel to Fourier transform the calculated FID. Expand the signal at 0.5 ppm to observe the poorly resolved doublet. In NMR-SIM open the *Check the experiment parameters* dialog box (**Go│Check Parameters & Go**) and either decrease the spectral width **SW**: *5* ppm or increase the number of time domain data points TD: *64*k and repeat the simulation. Decreasing SW or increasing **TD** increases the digital resolution and improves the doublet splitting.

(b) Load the *ch3211.cfg* file again to reset the experiment parameters. Set the spectrometer ^{1}H reference frequency to **SF**: *600* MHz. Simulate two experiments: one with the original **TD**: *32*k and a second experiment with **TD**: *64*k. Fourier transform the FIDs and examine the signal at 0.5 ppm. The lineshape for the second experiment with **SF**: *600 MHz* and **TD**: *64*k corresponds to the digital resolution of the first simulation of session (a).

The accumulation of repeated experiments

Because NMR is a relatively insensitive technique, a NMR experiment is usually repeated several times (multi-scan accumulation) with the data from successive experiments accumulated in the computer memory in order to improve the signal-to-noise ratio in the final spectrum. It is a common misconception that the statistical noise is destructively superimposed to a constant level; the signal intensity of the real resonance signals is directly proportional to the number of scans n while the random noise is directly proportional to the square root number of scans.

$$\text{noise} \quad \propto \sqrt{n}$$
$$\text{signal intensity} \quad \propto n \quad \Rightarrow \quad \text{Signal-to-noise ratio} \quad \propto \sqrt{n} \quad [3\text{-}2]$$

From equation [3-2] the expected intensity gain in a multi-scan accumulation can be easily deduced. As shown in the table the signal-to-noise ratio of a single scan experiment can be increased by a factor of two by acquiring four scans and taking four times the experimental time. On the other hand the same signal-to-noise ratio may be obtained in one fourth of the time by doubling the sample amount.

Number of scans, NS	relative Intensity, $I_{rel.}$	experiment time, t_{exp}
1	100	t_{exp}
4	200	$\times 4$
16	400	$\times 16$

In simulations NMR-SIM does not employ a statistical noise generator and consequently the relationship between signal intensity and multi-scan experiment can not be simulated. Nevertheless the reader should keep this relationship in mind since this is one reason for the tendency to reduce the number of scans and to increase the signal intensity by particular methods like magnetization transfer from resp. to sensitive nuclei rather than by using repetitive accumulations.

The effect of the magnet field strength

The application of higher and higher magnetic field strengths for NMR spectrometer magnets is driven by the desire for a wider chemical shift dispersion which is particularly valuable for the study of biomolecules where the signals are normally crowded into a narrow frequency range. The signal-to-noise ratio is field dependent and for the same sample better signal-to-noise ratios can be achieved at higher magnetic fields: $S/N \propto B_0^{3/2}$. A further effect of higher magnetic field strength is the transition of complex higher order spectra to first-order spectra although even complex higher order spectra may be analysed and chemical shifts, coupling constants and linewidths be extracted using specialist software tools such as WIN-DAISY [3.4]. The effect of different magnetic field strengths on the appearance of a spectrum may be demonstrated using NMR-SIM where the scalar coupling interaction can be defined using the options **weak** and **couple** for weakly or strongly coupled spins.

Check it 3.2.1.2 illustrates magnetic field effects on a weakly and strongly coupled nuclear spins using a AX and AB spin system.

3.2.1.2 Check it in NMR-SIM

To simulate the 400MHz ^{1}H spectrum containing the individual AX and AB spin systems, load the configuration file *ch3212.cfg*. The spin system is defined in the file *abax.ham*. Run the simulation and save the FID as **Exp No.**: *1*. Process the FID using zero filling **SI(r+i)**: *64k* and an exponential window (wdw function: **EM**, **LB**: *0.2* Hz), see section 3.2.3. Repeat the simulation replacing the spectrometer reference frequency **SF**: *100* MHz (**Run│Check Parameters & Go**) and **Exp No.**: *2*. Process and Fourier transform the FID as before. Change the spectrometer reference frequency **SF**: *400* MHz and replace the spin system by the file *axax.ham* (**File│Spin system...**). Simulate and process the spectrum saving the data as **Exp No.**: *3*. Using the **Multiple Display** command (**Display│Multiple Display**), see section 3.2.3, compare the three spectra. Note that the root effect is less pronounced with increasing field strength. To enhance the appearance of

the multiple display, click the **File Param.** button and for the first and third spectrum set **Y-Scaling**: *0.250.*

AB spin system

AX spin system

$\delta(^1H)$ 2   1   0
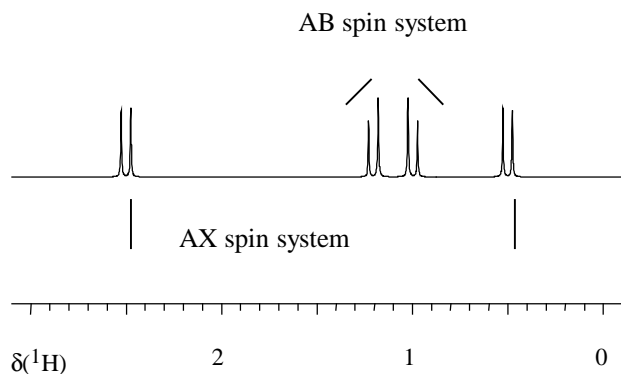
Fig. 3.3: ^1H spectrum of an AX and AB spin system
(second simulation of *Check it 3.2.1.2*).

In Fig. 3.3 the roof effect, a typical indication of strongly coupled spins, can be observed for the AB spin system, whereas the line intensities of the AX spin system indicate that it may be analysed on a simple first order basis. Normally a first order spin system can be assumed if the chemical shift difference in Hz for the coupled spins i and k is a lot greater than the scalar coupling constant J_{ik}.

$$\left| \nu_i - \nu_k \right| >> \left| J_{ik} \right| \qquad\qquad [3\text{-}3]$$

3.2.2   Simulation of a Free Induction Decay

In NMR-SIM the simulation of an NMR experiment is based on the density matrix approach with relaxation phenomena implemented using a simple model based on the BLOCH equations. Spectrometer related difficulties such as magnetic field inhomogeneity, acoustic ringing, radiation damping or statistical noise cannot be calculated using the present approach. Similarly neither can some spin system effects such as cross-relaxation and spin diffusion can be simulated.

The FID is calculated from the solution of the LIOUVILLE-VON NEUMANN equation, which is often called the density operator equation, and which describes the dynamics of quantum mechanical systems.

density operator equation [3-4]   matrix   response equation [3-5]
                                   multiplication

$$\frac{d}{dt} \rho(t) = -i[H(t), \rho(t)] \qquad \Rightarrow \qquad FID(n) = f(H(0), H_{rf}(t), U_g, \rho(0))$$

The hamiltonian H(t) can be subdivided in a time-dependent part H(t) and a time-independent part H(0). The time-dependent part H(t) contributes the interaction between nuclei and the applied radio frequency fields of the pulse sequence while the time-invariant part H(0) defines the nuclear spin system, the so-called sample. The coherence evolution during the pulses and delays of a pulse sequence are described by the individual propagators U_i and are combined by matrix multiplication to give the complete propagator U_g. If the ***Full relaxation*** option has been selected in the NMR-Sim settings dialog box the density matrix is modified throughout the pulse sequence whilst the ***Acquisition*** option restricts relaxation phenomena to the acquisition time only. The possibility to be able to switch relaxation on and off and to modify the rf pulse lengths as a function of the rf frequency are two important options of the NMR-SIM simulation environment and will be described in detail. In *Check it 3.2.2.1* effect of transverse relaxation on the linewidth is demonstrated by simulating two spectra using the same spin system with the ***Acquisition*** relaxation option enabled and disabled. Longitudinal relaxation effects are discussed in more detail in chapter 5.

3.2.2.1 Check it in NMR-SIM

Load the configuration file *ch3221.cfg* (**File│Experiment Setup│Load from file...**). Open the NMR-Sim settings dialog box (**Options│NMR-Sim settings...**) and select the option **Relaxation**: *Acquisition.* Run the simulation (**Go│Run experiment**). Apply an exponential window function (**Window!** button) but no DC correction. Fourier transform the FID (**FT!** button). (The effects of window functions are explained in section 3.2.3). Save the spectrum (**File|Save**) for comparison with the second calculation. For the second simulation select the option **Relaxation**: *None* and run the simulation saving the file with a new name. Process the data in exactly the same way as for the first simulation (**Window!** and then the **FT!** button) and compare the two spectra using the dual display mode of 1D WIN-NMR (**Display|Dual Display**) (see section 3.2.3.4).

The gyromagnetic ratio of a nucleus influences both the resonance frequency and, more importantly for NMR-SIM simulations, the rf pulse lengths. The resonance frequency of a nucleus is a function of its gyromagnetic ratio and is related to the basic ^{1}H frequency of the spectrometer as shown in equation [3-6]. The gyromagnetic ratio of the excited nucleus effects both the rf power and the pulse length, equations [3-7] and [3-8]. Consequently NMR-SIM has the option to modify the rf pulse behaviour according nucleus being excited and to generate spectra that are close to real experiments.

$$\frac{SF_1}{SF_{ref}} = \frac{\gamma_1}{\gamma_{ref}} \quad [3\text{-}6] \qquad \frac{pl_1}{pl_2} = \frac{\gamma_1}{\gamma_2} \quad [3\text{-}7] \qquad p_1 = \frac{(\alpha/360)}{(100000 \bullet \gamma)} \quad [3\text{-}8]$$

SF_1 = radio frequency of a nucleus 1
SF_{ref} = basic ^{1}H reference frequency
pl_l = pulse power level of pulse p_1

γ_I = gyromagnetic ratio of nucleus i
p_1 = pulse length in units of time
α = the normalized pulse angle [degrees]

In NMR-SIM a 90° excitation pulse can be described in two possible ways:

- A normalized pulse can be defined by its rotation angle, e.g. 90d. If the **Modify RF fields** option is off the pulse is calculated according to equation [3-8] with $\alpha = 90$ and $\gamma = 1$ and is independent of the rf channel assignment. So a 90° ^{1}H pulse and a 90° ^{13}C pulse would have the same length. If the **Modify RF fields** option is enabled the pulse is corrected with respect to the nucleus that is assigned to the rf channel on which the pulse is transmitted. So if a rf channel is set for a 90° ^{1}H pulse and then the channel assigned to ^{13}C, the 90° ^{13}C pulse would be γ^1H/γ^{13}C times longer than the 90° ^{1}H pulse.
- A pulse can be defined in the time units: us, ms or s. The corresponding tilt angle is calculated with or without γ correction depending on the **Modify RF fields** option.

Check it 3.2.2.2 illustrates the correct pulse definition using the ^{13}C spectra of a single carbon atom.

3.2.2.2 Check it in NMR-SIM

Load the configuration file *ch3222.cfg*. Open the NMR-Sim settings dialog box (**Options⏐NMR-Sim settings...**) and disable the **Modify RF fields** option. Set the p1 pulse length to **p1**: *90d* (**Check Parameters & Go**) and run the simulation (**Go⏐Run experiment**) and save the data as **Exp No.**: *1*. Fourier transform the FID (**FT!** button) and save the spectrum (**File|Save**). Repeat the simulation for **p1**: 2.5*u* saving the data as **Exp No.**: *2*. Enable the **Modify RF fields** option and simulate two FIDs with p1: *2.5u* (**Exp No.: 3**) and *10u* (**Exp No.: 4**). Process and save the spectra and then compare all four spectra using the **Display|Multiple Display** option of 1D WIN-NMR (see section 3.2.3.4).

The carbon signal intensity is the same in simulations 1 and 2 because a 90° excitation pulse is applied in both cases. In the third simulation the rf pulse tilt angle has been modified by the internal NMR-SIM algorithm using equation [3-8] and the signal intensity is reduced. In the fourth simulation the signal intensity again corresponds to a 90° excitation pulse because the appropriate pulse length of 10us has been entered manually. The dependence of pulse power and pulse length on the γ-correction is an important aspect in making simulated data mimic experimental data as close as possible.

3.2.3   Processing and Analysis of 1D NMR data

All the processing methods of 1D NMR data [3.1, 3.5] can be categorized on the basis of whether the processing is applied to the time domain or frequency domain data. The time domain data can be the output of an NMR experiment performed on a spectrometer or of an NMR-SIM calculation. In either case the Fourier Transformation (FT) is always the central step and is handled as a "black box" tool. Because the NMR-SIM simulation environment corresponds to the "ideal spectrometer" several processing steps designed to overcome spectrometer imperfections are irrelevant. Consequently the

time domain processing step of linear prediction and the frequency domain processing steps of baseline correction, smoothing or magnitude/power calculation are omitted from the following discussion. The one exception to this approach is the DC correction function; although redundant for the processing of NMR-SIM data its inadvertent application can cause misleading results as explained below. Fig. 3.4 shows the processing steps performed to transform the data from the original FID to the final spectrum.
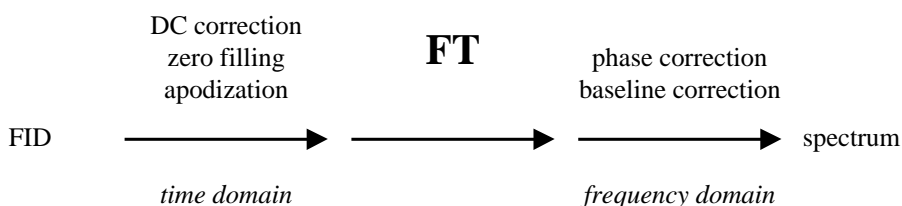
Fig. 3.4:   One dimensional NMR Data processing - flow of processing.

Simulated data generally requires fewer 1D WIN-NMR data analysis steps than experimental data. The most usual operations performed are listed below:

- chemical shift calibration
- peak picking
- linewidth measurement
- integration
- multiplet analysis

In 1D WIN-NMR the processing and analysis tools are available from the **Process** or **Analysi**s pull-down menus in the menu bar. The **Process** pull-down menu is context sensitive such that before the Fourier transformation only time domain processing functions are available whilst after Fourier transformation the **Process** pull-down menu is updated to include frequency domain related processing functions. The 1D WIN-NMR **Process** and **Analysi**s pull-down menus are shown in Fig. 3.5.

Process menu **before**   **Process** menu **after**   **Analysis** pull-down menu
Fourier Transformation   Fourier Transformation

Fig. 3.5:   1D WIN-NMR - **Process** and **Analysis** pull-down menus.

After the command selection the window mode will change and the functionality of the button panel will be modified to incorporate any command specific buttons. It is also possible that some of the standard buttons will be deactivated.
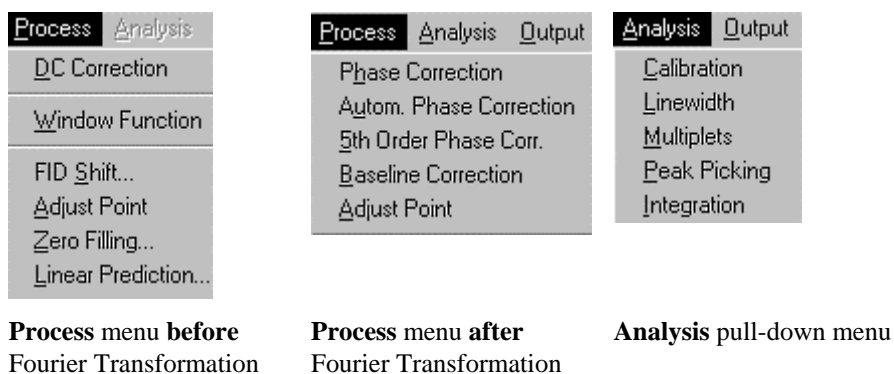
3.2.3.1 Time Domain Processing of raw NMR data

All the processing steps in this section are intended to enhance the time domain data leading to the suppression of distortions or artefacts and an improvement in the overall spectral quality. The suitability of the methods can be estimated from the appearance of the FID in the main spectrum window of 1D WIN-NMR as illustrated in the schematic FID shown in Fig. 3.6. The envelope of the exponentially decaying FID has a dc offset as it is not symmetrical about the zero line whilst the spectrum lineshape may be improved by either zero filling or apodization or possibly both.
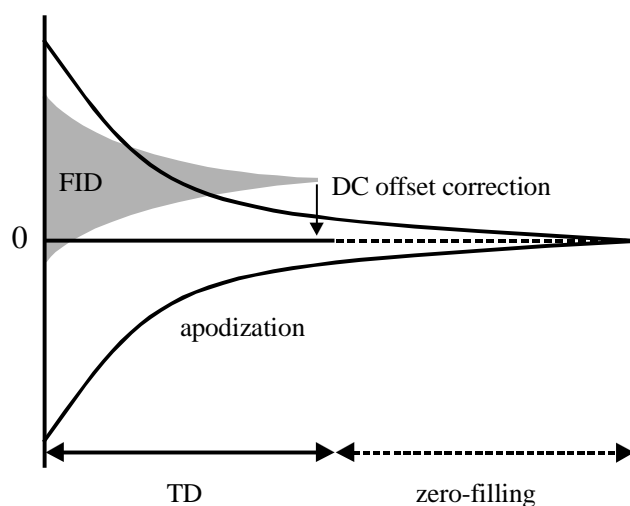
Fig. 3.6:   Time domain processing steps - dc offset correction, zero filling and apodization.

How to use the button panel of 1D WIN-NMR...

The primary function of the buttons in the top part of the button panel is to change the appearance of the data displayed in the spectrum window irrespective of whether the data is a FID or spectrum. The functionality of these buttons is independent of the current processing command whilst the lower part of this panel may contain addition buttons specific to the current task. The special buttons for allowing the comparison of two or more spectra discussed in section 3.2.3.4 in combination with the output options.

Upper Part of the Button panel

(a)   (b)   (c)

(d)   (e)   (f)

Particular buttons
(a) Zoom button
(b) Maximum Cursor button
(c) Perpendicular Cursor button
(d) Split-Screen button
(e) Point button
(f) Grid button

The upper part of the 1D WIN-NMR button panel, in conjunction with the scroll bars along the edge of the window, contains all the functions necessary for expanding and panning through the data displayed in the main spectrum window. This panel also contains the buttons for changing the cursor mode. With the exception of the **Zoom** button all the buttons are activated by a single click of the left mouse button.

The functions of most of the button are obvious from the pictogram; thus the ***2** and **/2** buttons increase and decrease the y-scale of the displayed data respectively whilst the **<>** and **><** buttons expand and contract the x-scale. The **ALL** button resets the display. The **PRE** button toggles the view between the current display and the previous expansion. Using the **Zoom** button (a) a specific region can be expanded in both the x- and y-direction. The mouse cursor is positioned at the appropriate place in the display window, holding down the left mouse button down to position the cursor the expanding box is dragged to encompass the region of interest. Releasing the left mouse button and clicking with the right mouse button the content of the frame is zoomed to occupy the main window. The **Maximum Cursor** button (b) positions the cursor at the top of the highest peak immediately to the left of its current position. The **Perpendicular Cursor** (c) button can be used to position the cursor anywhere in the spectrum. In either mode the cursor may be dragged to any position by holding down the left mouse button. The different cursor modes are particularly useful with the analysis functions such as peak picking or integration. The **Split-Screen** (d) button splits the spectrum window into two sections; the upper section displays the complete spectrum and the lower section the expanded region. The **Point** button (e) toggles between the individual data point display and the vector line display.

The **Grid** button (f) superimposes a regular grid on the display. The **Real/Imag** buttons toggles the FID or spectrum between the real and the imaginary data. The **ppm/Hz/Pts** button toggles the x-axis units between ppm, Hz or points. The δ scale would generally be used for simple chemical shift assignment while the Hz scale would be helpful for the determination of line distances, e.g. for the estimation of coupling constants. After this brief description of the button panel functions the 1D WIN-NMR

processing commands applicable to the NMR-SIM simulations will be illustrated in the following *Check its*.

How to execute a DC correction...

The DC offset is a spectrometer based effect which is related to an unwanted DC voltage added to one or both of the two detection channels used with quadrature detection. The response of the nuclear spin system is imposed upon the resonance frequency, which serves as a carrier, and any DC offset is added to this response prior to the signal being digitized. An uncorrected DC offset gives rise to a spike at the middle of the spectrum. An imbalance between quad detectors gives rise to quad images, small signals that are a reflection of real signals about the centre of the spectrum.

NMR-SIM does not permit such spectrometer imperfections to be simulated so that the DC offset correction is redundant. Indeed this correction must never be applied if a resonance signal is placed directly on-resonance, i.e. a nuclear spin is defined with $\delta =$ O1 ppm (the transmitter frequency). In 1D WIN-NMR the DC Correction dialog box opens automatically before processing of the current FID data but for the processing of NMR data generated by NMR-SIM the **No** option should always be selected. The effect of the DC offset correction is shown in *Check it 3.2.3.1* using a data set containing a pseudo DC offset.

3.2.3.1 Check it in NMR-SIM

Load the configuration file *ch3231.cfg* to simulate the ^{1}H spectrum of 1-chloropropane. The pseudo DC offset is defined as an intense on-resonance signal (δ = O1 = 3.75 ppm). Run the simulation (**Go**⏐**Run Experiment**) saving the FID as **Exp No.**: *1*. Inspect the DC offset of the FID in the main spectrum window of 1D WIN-NMR. Using the **FT!** button, Fourier transform the data. Do not apply a DC correction, zero filling or apodization. Observe the very intense signal, the O1 spike, at the centre frequency (δ = 3.75 ppm). Using the **File**⏐**Recall last** command reload the FID and reprocess the data using a DC correction. Note that the intensity of the O1 spike has been reduced by several orders of magnitude.

How to apply a zero filling to a FID...

Another important processing procedure is zero filling which improves the signal lineshape by appending data points to the end of the FID. The increase in the digital resolution permits the lineshape of individual signals to be defined more precisely although the improvement possible using this procedure should not be overestimated. Experimentally zero filling will not overcome the problems associated with poor sample preparation and sample shimming.

1D WIN-NMR

Zero Filling dialog box

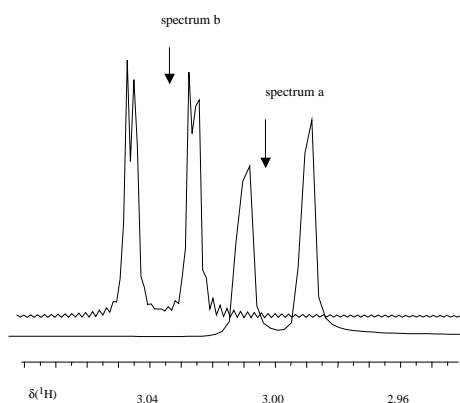Clicking the **Zero Filling !** button in the button panel of 1D WIN-NMR applies zero filling to the current FID using the default parameters of SI = 2 • TD. If the **Process│Zero Filling** command is used the Zero Filling dialog box opens showing the acquired and used TD values plus the current spectrum size **SI(r+i)**. For spectral improvement zero filling of SI = 2 • TD is normally recommended; 16k (TD = 8k = 8192 words), 32k (TD = 16k = 16384 words), 64k (TD = 32k = 32768 words) or 128k (TD = 64k = 65536 words) for instance. A disadvantage of zero filling is the discontinuity that occurs if the FID has not decayed away to zero before the additional data points with zero amplitude are appended, which after Fourier transformation, causes wiggles at the base of each signal. This effect can be minimized by using a suitable apodization function.

For further details on zero filling, apodization and the NZP command the reader is referred to the corresponding companion volume in this series [3.1].

Effect of zero filling
(a) without zero filling,
(b) with single zero filling (SI = 2 • TD).

3.2.3.2 Check it in NMR-SIM

To simulate the ^{1}H spectrum of the AMX spin system, load the configuration file *ch3232.cfg*. Run the calculation (**Go│Run Experiment**), Fourier transform the FID (**FT!** button) and save the spectrum using the **File│Save** command. Reload the FID (**File│Recall last**) using the **Process│Zero filling...** command open the Zero Filling dialog box and set **SI:** *16k*. Note the discontinuity in the FID. Fourier transform the data. Using the **File|Save as** command save the spectrum using a different processing number e.g. *001002.1r*. Compare the two spectra using the dual display mode (**Display|Dual Display**) (see section 3.2.3.4).

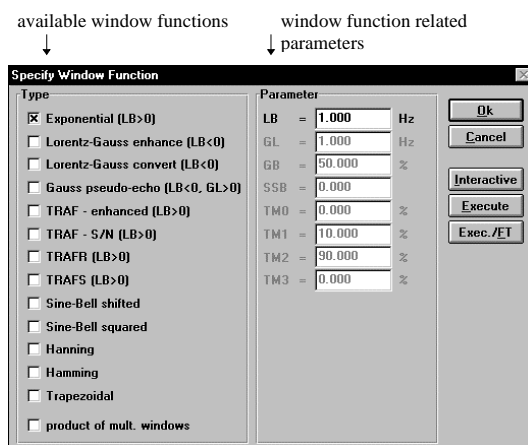A comparison of *Check it 3.2.3.2* of the FID processed with and without zero filling illustrates clearly the advantage of the technique in improving the lineshape and the ability to resolve small couplings. The "wiggles" at the base of the signals are also apparent but these may be minimized by using a suitable apodization function. In practise zero filling is used in conjunction with apodization, the overall result being a

compromise because whilst reducing the line distortions, apodization decreases the resolution by increasing the overall linewidth.

How to apodize a spectrum...

Apodization is the process of multiplying the FID prior to Fourier transformation by a mathematical function. The type of mathematical or window function applied depends upon the enhancement required: the signal-to-noise ratio in a spectrum can be improved by applying an exponential window function to a noisy FID whilst the resolution can be improved by reducing the signal linewidth using a LORENTZ-GAUSS function. 1D WIN-NMR has a variety of window functions, abbreviated to wdw function, such as exponential (EM), shifted sine-bell (SINE) and sine-bell squared (QSINE). Each window function has its own particular parameters associated with it; LB for EM function, SSB for sine functions etc.

1D WIN-NMR

available window functions   window function related
↓   ↓ parameters

Window function dialog box

The command **Process│Window Function** opens the Specify Window Function dialog box where a window function can be selected and the associated parameters selected. Clicking the **Interactive** button the parameters may be optimized interactively; both the FID and the window function are loaded into the main spectrum window and the parameters adjusted using the slider box in a special button panel. Clicking the **Window!** button using the right mouse button opens the Window Function dialog box where both the function and parameters may be selected.

Clicking the **Execute** button the window function is applied to the FID whilst clicking the **Exec./FT** button performs both apodization and Fourier transformation. Clicking the **Window!** button using the left mouse button applies the window function currently defined in the Window Function dialog box to the FID. *Check it 3.2.3.3* demonstrates how the lineshape of the zero filled FIDs in *Check it 3.2.3.2* can be improved using apodization.

Effect of apodization on a zero filled FID
(a) without any apodization
(b) with an exponential apodization
(LB = 0.3)

3.2.3.3 Check it in NMR-SIM

Repeat the simulation of *Check it 3.2.3.2* or load the calculated FID into 1D WIN-NMR (**File|Open…**). Process the FID with zero filling of **SI**: *16k.* Fourier transform the data (**FT! button**) and using the zoom facility inspect the small splitting of the intense signals. Reload the calculated FID (**File|Recall last**) and using the same zero filling parameters apply an **Exponential** window function with a **LB**: *0.3* Hz (**Process⎪Window Function**). The transformed spectrum displays less distortion at the base of the multiplet lines but the line broadening applied by the apodization makes the splitting of the small coupling constants less apparent.

The FIDs simulated using NMR-SIM should always be processed using the zero filling and apodization parameters shown in Table 3.1. This table also lists the abbreviations used for these parameters in the *Check its.* Occasionally parameters different from the recommended values may be used in a *Check it*; this is particularly true in simulations where the relaxation option is disabled, the values of the parameters are chosen to improve the spectrum appearance by minimizing line distortions. The *Check it* may contain the phrase "use zero filling and an apodization (EM, LB: 2.0 Hz)" implying zero filling of **SI**(r+i): 2 • TD and an exponential apodization with a **LB** factor of *2.0.*

Table 3.1: Recommended processing parameters for one dimensional NMR data.

| processing step	function	abbreviation	parameter
zero filling	SI(r+i) = 2 • TD	SI:	SI = 16k (TD = 8192 or 8k), 32k (TD = 16384 or 16k) or 64k (TD = 32768 or 32k)
apodization	exponential window function	EM	LB = 2.0

3.2.3.2 FOURIER Transformation

A free induction decay is a display of observed signal intensity as a function of time. To be able to interpret the response of the spins this time domain data has to be transformed into frequency domain data, the spectrum.

The FID s(t) and spectrum S(ν) form a Fourier pair which can be transferred into one another by (forward) Fourier and inverse Fourier transformation.

$$s(t) \xrightleftharpoons[\text{inverse FT}]{\text{FT}} S(\nu)$$
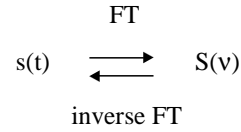
A time domain function can be expressed as a FOURIER series, an infinite series of sines and cosines. However in practise integrals related to the FOURIER series, rather than the series themselves are used to perform the FOURIER transformation. Linear response theory shows that in addition to NMR time domain data and frequency domain data, pulse shape and its associated excitation profile are also a FOURIER pair. Although a more detailed study [3.5] has indicated that this is only a first order approximation, this approach can form the basis of an introductory discussion.

Two further aspects of Fourier transformation with respect to NMR data must be mentioned. With quadrature detection a complex FOURIER transformation must be performed, there is a 90° phase shift between the two detectors and the sine and cosine dependence of the sequential or simultaneous detected data points are different. In addition because the FID is a finite number of data points, the integral of the continuous Fourier transform pair must be replaced by a summation.

As an introduction to the concept of the Fourier transform consider the macroscopic magnetization vector M_0, which represents the nuclear spins in an uncoupled spin system, shown in Fig. 3.7. To simplify the mathematics the coordinate system rotates at the resonance frequency, the on-resonance magnetization vectors remaining static in the rotating frame. At thermal equilibrium the magnetization lies along the z-axis but the application of a rf pulse with a tilt angle β and phase y rotates M_0 into the x,z-plane where the magnetization evolves and in quadrature mode the sine and cosine dependence of the magnetization recorded:

$$M_x(t) = M_0 \sin\beta \bullet \cos(\Omega \bullet t) \exp(-t/T_2)$$

and

$$M_y(t) = M_0 \sin\beta \bullet \sin(\Omega \bullet t) \exp(-t/T_2).$$

In a complex notation the signal is described as:

$$M^+(t) = M_x(t) + i \bullet M_y(t)$$
$$= M_0 \sin\beta \exp(i\,\Omega\,t - t/T_2).$$

Since the complex signal s+(t) is proportional to $M^+(t)$ the complex Fourier transform pair s+(t), S(w) is given by: $S(\omega) = \int_0^\infty s^+(t) \exp(-i\omega t)\, dt$.
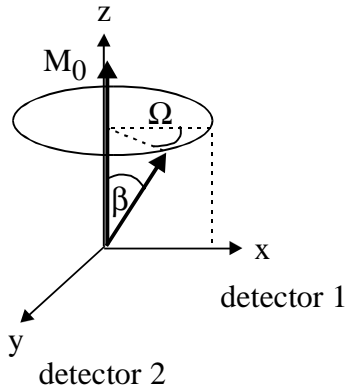
Fig. 3.7: Signal response.

After complex Fourier transformation the spectrum signal $S(\omega)$ is described by:

$S(\omega) = R(\omega) + i \cdot I(\omega)$ with $\qquad$ $R(\omega) = M_0 \sin\beta \; A(\Delta\omega)$

$$I(\omega) = -M_0 \sin\beta \; D(\Delta\omega)$$

$\Delta\omega = \omega - \Omega$; $\Delta\omega$ = frequency offset,
ω = resonance frequency,
Ω = transmitter frequency

absorptive signal part: $\qquad\qquad$ **dispersive signal part:**

$$A(\Delta\omega) = \frac{1/T_2}{(1/T_2)^2 + (\Delta\omega)^2} \qquad\qquad D(\Delta\omega) = \frac{\Delta\omega}{(1/T_2)^2 + (\Delta\omega)^2}$$

The function $S(\omega)$ can be subdivided into a real and imaginary part. The real part $R(\Delta\omega)$ corresponds to a signal with a absorptive LORENTZIAN lineshape which is normally displayed while the imaginary part $I(\Delta\omega)$ corresponds to a dispersive LORENTZIAN lineshape. To phase a spectrum both real and imaginary parts are required.

3.2.3.3 Frequency Domain processing of NMR data

There are two basic processing steps in the frequency domain, phase correction followed by baseline correction. These steps are necessary because in a real NMR experiment the spectrometer, the sample and the experimental parameters are not perfect in contrast to NMR-SIM which represents the ideal experiment. These imperfections can lead to distortions in the lineshape and a non-linear baseline that must be corrected to enable reliable spectral analysis and interpretation using integration and multiplet analysis. Although not a typical application for NMR-SIM these distortions can be simulated as illustrated in *Check its 3.2.3.4* to *3.2.3.6*.
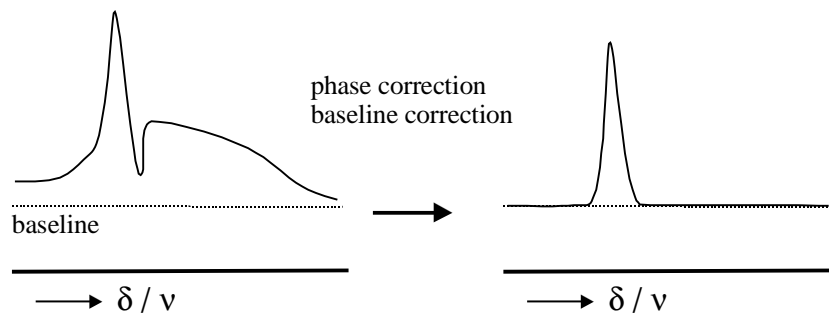

Fig. 3.8: Frequency related processing steps - phase and baseline correction.

How to execute a phase correction...

A property of excitation pulses and the receiver channel is their phases and as outlined in section 2.3.3 appropriate phase cycling is necessary for both coherence selection and also to compensate for the phase differences between the detected

transverse magnetization (coherence) and the detector phase. In NMR-SIM, because of the ideal spectrometer approach these phases will always be orthogonal and phase correction is unnecessary. However for compatibility with experimental data, it is often necessary for simulated spectra to have a zero-order phase correction of n • π /2 (for phc0) because the pulse programs taken from literature or from the BRUKER pulse program library usually have a phase difference of n • π /2 between the detected coherence in the x,y-plane and the receiver phase. Shaped pulses and if selected the ***Full relaxation*** option in the NMR-Sim settings dialog box are another source of phase distortion which must be corrected using the phase routine.

1D WIN-NMR
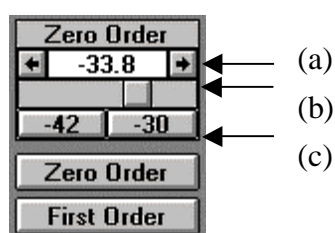
Phase Correction mode

part of the button panel: (a) the slider arrow buttons and current phase correction value, (b) the slider scroll bar and (c) the limit buttons

In 1D WIN-NMR the phase correction routine is chosen from the menubar using the **Process⏐Phase Correction** command. Automatically the mouse cursor is set at the top of the largest signal in the display as reference peak. The reference peak can also be selected manually. Simultaneously the **Zero Order** phase correction is activated (button highlighted) in the button panel. The zero-order phase correction is performed by either dragging the slider button in the scroll bar (see figure on the left) or by clicking on the slider arrows. The phase value range and the step size can be modified by clicking the right and left arrow respectively. Clicking the **First Order** button with the left mouse button switches to the first-order phase correction mode that is performed in a similar manner to the zero-order phase correction. The phase constant parameters are called phc0 (zero-order phase correction constant) and phc1 (first-order phase correction constant). If the numerical values for the phase correction are known clicking the **Numerical** button opens a dialog box where the values of **phc0** and **phc1** can be entered directly. Clicking the **Undo** button cancels the current phase correction and clicking the **Return** button exits from the phase routine.

In real experiments after Fourier transformed the lineshapes are mixtures of absorptive and dispersive signals and are related to the delayed FID acquisition (first-order phase error). The delayed acquisition is a consequence of the minimum time required to change the spectrometer from transmit to receive mode, during this delay the magnetization vectors precess according to their chemical shift frequencies. The zero-order phase error arises because of the phase difference between the magnetization vectors and the receiver. In NMR-SIM the delayed acquisition is not necessary because the ideal spectrometer approach does not require any switching time and the first order phase correction is normally zero if no other sources of phase deviations are present.

In *Check it 3.2.3.4* the reader is introduced to the phase correction procedure in 1D WIN-NMR whilst examining zero- and first-order phase distortions. An advantage of the

NMR-SIM simulation is that the zero- and first-order phase distortions can be investigated separately in contrast to experimental spectra where both errors occur simultaneously. In the first part of *Check it 3.2.3.4* the zero-order phase distortion is simulated using a 40° phase shift difference between the excitation pulse and the receiver phase, in the second part the first-order phase distortion is simulated using a delay d10 before the data acquisition. The spin system used in the *Check it* consists of a number of singlets evenly spaced over a frequency range of 3200 Hz.

3.2.3.4 Check it in NMR-SIM

(a) simulation of zero-order phase distortion

Load the configuration file *ch3234a.cfg* (**File│Experiment Setup│Load from File...**). Use the pulse program editor (**Edit│Pulse program**) to inspect the pulse program paying particular attention to the phase program. Close the pulse program editor without any modification (**File│Close**). Run the simulation (**Go│Run Experiment**) and process the FID (zero filling **SI(r+i)**: *64k*, wdw function **EM**, **LB**: *1.0* Hz, **FT!** button). Note that all the signals have the same zero-order phase error clearly illustrating that this type of distortion is frequency independent. Using the **Process│Phase Correction** command click on the **Numerical** button in the button panel and enter the values **phc0**: *-40* and **phc1**: *0*. Click the **Ok** button to perform the phase correction - all the peaks should now be correctly phased.

δ(¹H)   7   6   5   4   3   2   1   0
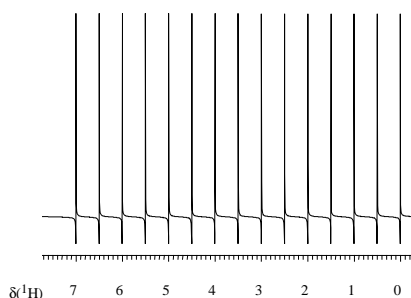
Fig. 3.9 (a): The zero-order phase error is independent on the rf offset.

There are two forms for the ideal phase program depending on the type of NMR hardware

ph1=0 2 2 0 1 3 3 1
ph31=0 2 2 0 1 3 3 1

or

ph1=(360) 0 180 180 0 90 270 270 90
ph31=0 2 2 0 1 3 3 1

Phase program with a phase difference of 40° between the pulse and receiver phase

ph1=(360) 40 220 220 40 130 310 310 130
ph31=0 2 2 0 1 3 3 1

(b) simulation of a first-order phase distortion

Load the configuration file *ch3234b.cfg*. Check the pulse program for the delay **d10** between last pulse and start the acquisition process. Exit from the pulse program and run the simulation processing the data in exactly the same manner as part a. Note the symmetrical phase error of all the signals about the centre of the spectrum at 3.75 ppm illustrating the frequency dependence of the first order phase distortion.
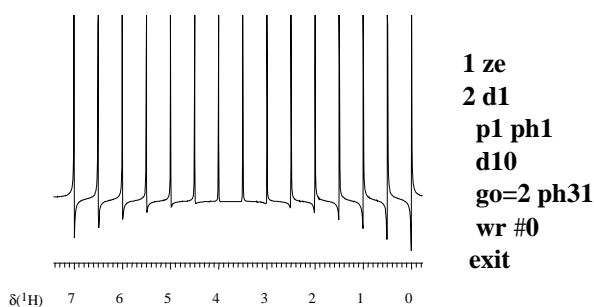


```
1 ze
2 d1
  p1 ph1
  d10
  go=2 ph31
  wr #0
exit
```

δ(¹H)   7   6   5   4   3   2   1   0

Fig. 3.9 (b): Effect of first-order phase distortion as a function of different rf offsets.

(c) simulation of zero- and first order phase distortion

Load the configuration file *ch3234c.cfg*. Run the simulation and process the data as in part a. Using the **Numerical** option correct the zero-order phase (**Process│Phase Correction**, **phc0**: *-40* and **phc1**: *0*). Ensure that the cursor is set on top of the peak at 3.75 ppm click the **First Order** button and adjust the phase of the off-resonance signals for the correct absorptive lineshape.

The second processing step for experimental data is baseline correction, a flat baseline is essential for the correct integration of signals and for spin system analysis using an iterative approach for comparing theoretical and experimental results. As such baseline correction is not necessary for simulated data but nevertheless NMR-SIM can be used to simulate and study non-linear baseline effects. There are main two reasons of non-linear baselines, the background signal arising from the materials used to make the probehead or sample tube and pulse breakthrough. In *Check it 3.2.3.5* the appearance of Teflon, a probehead material, in a ¹⁹F spectrum is simulated, the baseline roll in the spectrum is typical for ¹¹B, ¹⁹F and ²⁹Si NMR spectra obtained using a standard probehead and sample tube. Pulse breakthrough can generate a rapidly decaying signal, which is superimposed on the first few data points of the FID distorting the signal. In these cases the FID can be "repaired" by cutting the first data points (see the function **FID shift** in reference [3.1]) before transforming the data. *Check it 3.2.3.6* simulates pulse breakthrough distortion by the manual manipulation of the first data points in the FID.

3.2.3.5 Check it in NMR-SIM

Load the configuration file *ch3235.cfg*. Select the **Go⎮Run Experiment** command from the pull-down menubar to start the simulation. Process the FID prior to Fourier transformation using zero filling (**SI(r+i)**: *64k*) and apodization (wdw function: **EM**, **LB**: *2.0* Hz). The Fourier transformed FID should resemble the spectrum in Fig. 3.10a.

3.2.3.6 Check it in NMR-SIM

Load the configuration file *ch3236.cfg*. Execute the simulation (**Go⎮Run Experiment command**). In 1D WIN-NMR use the **sec/Pts button** of the button panel to toggle the x-axis scale from seconds to points. Using the **<>** button, the **zoom cursor mode** and the slider bar along the bottom of the window, expand the first few data points of the FID. Select the fourth data point of the FID and then change to the **Adjust Point** mode (**Process⎮Adjust Point**). Click on the point **Shift** button and move the new mouse cursor to a position that has the same x-coordinate as the fourth data point but a lower y-value. Click the right mouse button to set the fourth data point to this new position. Save the changed FID as *001002.fid*. After processing of the FID (zero filling: **Si(r+i)**: *32k*, wdw-function: **EM**, **LB**: *0.5* Hz) Fourier transform the FID which should resemble the spectrum in Fig. 3.10b.
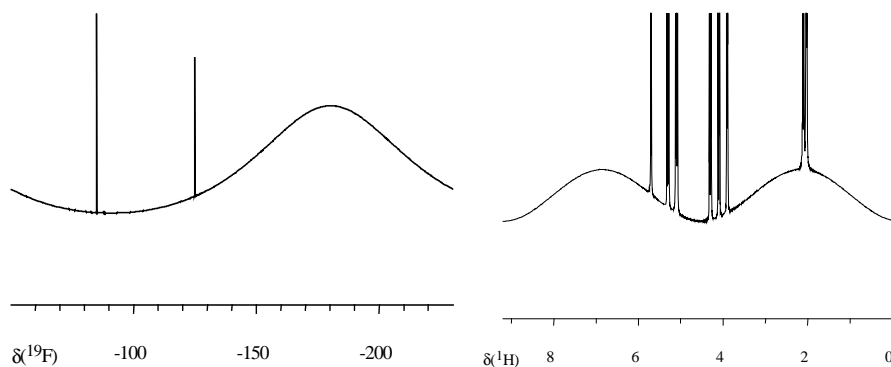

Fig. 3.10: Non-linear baselines effect (a) absorption of broad background signals (left side, *Check it 3.2.3.5*), (b) pulse breakthrough (right side, *Check it 3.2.3.6*).

For further details on the baseline correction function of 1D WIN-NMR the reader is referred to the relevant pages of the 1D WIN-NMR manual which is part of the teaching software.

3.2.3.4 Analysis, Display and Output Tools in 1D WIN-NMR

Several analysis and output tools are available in 1D and 2D WIN-NMR [3.1]. A number of these tools are used in the *Check its* in this book and it is relevant at this stage to look at a few of the most important analysis feature such as calibration, linewidth measurement, multiplet analysis using the AX approximation, peak picking and integration. In 1D WIN-NMR these functions are accessible as shown in Fig. 3.5 from the **Analysis** pull-down menu. The order of the commands in the pull-down menu is a guideline to the order of processing steps required for the correct analysis. Thus peak picking is only relevant after the spectrum has been calibrated. Each analysis tool has its own window mode and additions to the standard button panel. In all cases clicking the **Return** button in the button panel exits from the analysis routine.

How to calibrate a spectrum...

The calibration of a NMR spectrum is based on the assignment of a reference signal to a known chemical shift. For heteronuclear spectra the ^nX standard frequency is based on the ^1H standard frequency SF and calculated according to equation [3-6]. The teaching version of NMR-SIM only support two rf channels and it is only necessary to set the parameters SF and O1 and O2. The radio frequency applied during the experiment is called SFOi where i refers to either the rf channel 1 or 2 and is defined in equation [3-9]. The parameter **SR** is used for the manual calibration according to equation [3-10]. All the parameters are defined in Hz.

$$SFOi = SF \bullet \frac{\gamma_{channel\ i}}{\gamma_{proton}} + Oi \qquad\qquad [3\text{-}9]$$

$$SFOi_{calibrated} = SF \bullet \frac{\gamma_{channel\ i}}{\gamma_{proton}} + Oi + SR \qquad [3\text{-}10]$$

In NMR-SIM spectrum calibration is not normally necessary, since the chemical shifts in the spin system file are already defined on the ppm scale. However occasionally it might be necessary to calibrate a spectrum, particularly if comparing a simulated spectrum with an experimentally measured spectrum. In 1D WIN-NMR the calibration mode is selected by choosing the **Calibrate** command in the **Analysis** pull-down menu. The calibration can be performed in two ways:

1. A signal can be set to a known chemical shift value. The mouse cursor is placed at the top of the reference signal by selecting the maximum cursor mode and with the cursor close to the reference peak clicking with the left mouse button. Clicking the **Calibrate** button in the button panel opens the Calibration dialog box where the chemical shift of the selected line can be entered in the **X:** entry field. Closing the dialog box by clicking the **Ok** button calibrates the spectrum to the entered chemical shift value.

2. The second method is to click the **Num. Comp.** button in the button panel and in the Numerical Component dialog box enter the **X-Scaling (SR):** value directly. The **SR** value depends upon the solvent and detected nucleus but once the SR value has been determined experimentally the

value may be used for spectrum calibration. This is particularly important for ⁿX nuclei where the samples do not generally contain the reference compound.
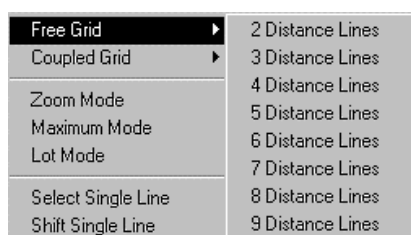
How to measure the linewidth ...

1D WIN-NMR offers a simple routine to measure the linewidth at half-height of each signal. After Fourier transformation the **Linewidth** command can be chosen from the **Analysis** pull-down menu. To measure the linewidth select the maximum cursor mode, place the mouse cursor slightly to the right of the appropriate signal and click the left mouse button. Click the right mouse button to start the linewidth calculation, the result is shown in the information bar at the top of the spectrum window and a black bar appears on the signal at half-height.

How to perform a multiplet analysis...

Multiplet analysis is one of the most useful analytical tools in 1D WIN-NMR; it simplifies the measurement of coupling constants, it is the first step in disentangling overlapping multiplets of complex multi-spin systems and it provides the input parameters for the WIN-DAISY computer analysis program. It is based on the AX approximation and uses distance measurement to build up coupling patterns by recognizing lines split by a common coupling constant.

1D WIN-NMR

Free Grid ▶	2 Distance Lines
Coupled Grid ▶	3 Distance Lines
	4 Distance Lines
Zoom Mode	5 Distance Lines
Maximum Mode	6 Distance Lines
Lot Mode	7 Distance Lines
Select Single Line	8 Distance Lines
Shift Single Line	9 Distance Lines

*on-the-fly menu and sub-menu of the **Free Grid** command*

To start the analysis the **Multiplets** command is selected from the **Analysis** pull-down menu. With the mouse cursor in maximum cursor mode the cursor is positioned on top of one of the signals making up the multiplet. The mouse cursor is fixed in position by clicking the left mouse button. Clicking the right mouse button in the main window opens a pop-up menu where it is possible to chose the number of equidistant lines which should be assigned (**Free grid| 2 Distances**, for instance).

Holding down the left mouse button grid lines can be dragged over the multiplet until the grid lines and lines of the multiplet coincide defining the line splits by a common coupling constant. The grid is fixed by releasing the left mouse button and clicking on the **Define Mult.** button in the button panel. To build up the complete coupling pattern the **Coupled Grid** command is used to generate a grid of grids (the multiplicity is selected from the on-the-fly pull-down menu) which is dragged over the multiplet until there is a match. Once all the lines in a multiplet have been assigned click the **Define Mult.** button. Other multiplets can be assigned in the same way using the **Free Grid/Coupled Grid** command. Most of the buttons in the button panel are self-explanatory but for further details the reader is referred to the on-line manual and the first volume of this series [3.1].

How to use the peak picking...

The Peaking Picking mode measures and displays the chemical shifts of the individual signals in a calibrated spectrum. Selecting **Peak Picking** from the **Analysis** pull-down menu opens the Peak Picking Options dialog box where a number of options are available. Normally this box is closed by clicking the **OK** button, depending on the options clicking the **Execute** button can generate a large pick listing. Clicking on the **Option…** button in the button panel in the peak picking routine also opens this box.

1D WIN-NMR
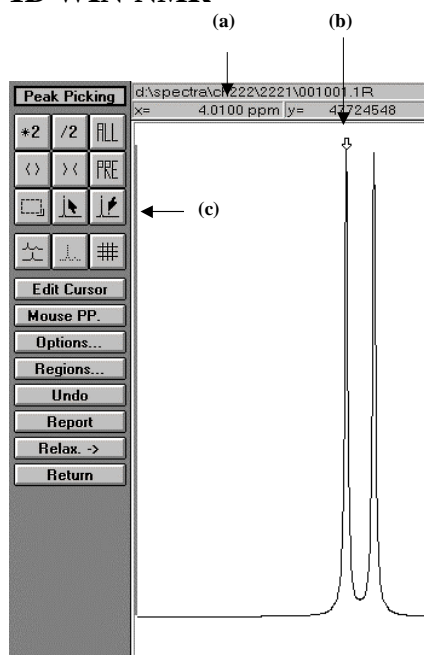
Peak picking mode

(a) actual chemical shift of the arrow indicator, (b) the arrow indicator, (c) Minimum/ Maximum Cursor mode buttons

Automatically the **Mouse PP.** mode is activated which can be used to define the region where the signals are to be labelled with their chemical shift. The mouse cursor is positioned to the left and above the region of the spectrum where the peak picking is required. Holding down the left mouse button and dragging the mouse a rectangle can be drawn above the relevant region. The rectangle is fixed by clicking the left mouse button again. Clicking the right mouse button performs the peak picking. Chemical shifts can be assigned manually by changing the cursor to **Maximum Cursor** mode, placing the cursor at the top of a peak and clicking the right mouse button. Assigned chemical shifts can be deleted using the **Edit Cursor** button. Position the cursor close to the peak, click the left mouse and an arrow indicator is set on the peak. Click the right mouse button to delete the chemical shift label. Clicking the **Report** button generates a list of chemical shifts that may be printed.

How to integrate signals...

The integration of the signals in an NMR spectrum can be used to determine the relative ratio of nuclei in a pure sample or the ratio of two or more components in a mixture. Signal integration can be performed in a number of different ways in 1D WIN-NMR; clicking the **Integration!** button in the button panel or by selecting from the **Analysis** pull-down menu the commands **Integration**, **Special integration**,

Deconvolution 1 and **Deconvolution 2**. In this book integration is performed using the **Analysis|Integration** command.

1D WIN-NMR

Integration mode

integral bar

After selecting this command the spectrum window changes to the Integration mode and the perpendicular mouse cursor mode is activated. Positioning the cursor on the left side of a signal and clicking the left mouse button, the integral limit can be selected. The position is fixed using a right mouse button click. The right integral limit is defined in the same manner. After the selection an integral bar appears below the integration range. It is possible to integrate all the signals in the spectrum using the slider at the bottom of the spectrum window. By default the last defined integral is set as the active integral as indicated by the colour change of the integral bar. To change the active integral, position the cursor on the appropriate signal and click the left mouse button. Clicking the **Options…** button in the button panel opens the Integral Options dialog box where it is possible to calibrate the selected integral by entering a value in the option **Selected Integral** field of the **Manual Calibration** option. Clicking the **Delete** button in the button panel deletes the active integral.

How to use the dual and multiple display modes…

In many of the *Check its* in this book different spectra are compared using the **Dual** and **Multiple Display** modes which are selected from the **Display** pull-down menu. This pull-down menu contains a number of different options for changing colours, fonts and miscellaneous display parameters, most are mostly self explanatory [3.2]. Although in the dialog boxes associated with both display modes it is possible to toggle the selection between **FID** and **Spectrum**, in the following discussion it is assumed that only spectra are to be displayed.

When the **Dual Display** mode is started the Select the Second File dialog box opens where the filename for the second spectrum is entered in the **Filename:** field or else selected from the standard Windows search pathway. The spectrum originally in the display window when the Dual Display mode is started is labelled the first trace. Once the second trace has been selected there are two possible display modes. The default

setting is the **Overlay mode** where both spectra are superimposed. The spectra can be disentangled by clicking the **Move Trace** button and dragging the second spectrum horizontally whilst holding down the left mouse button. Clicking the **Separate** button activates the second display mode which subdivides the spectrum window into an upper section (first trace) and a lower section (second trace) each with its own x- and y-scale.
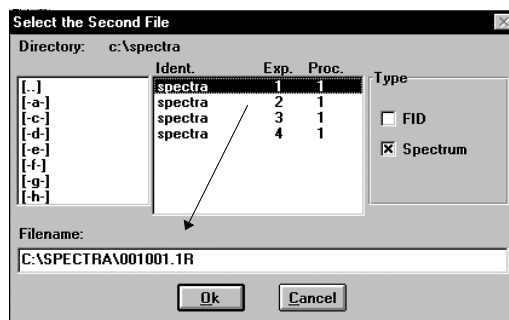
Fig. 3.10:   Dialog box of the Dual Display mode. The arrow denotes the selection of the second trace by clicking the left mouse button on the filename in the upper selection field.

The **Multiple Display** mode can be used to compare two or more spectra. Files for display are selected in the Select Multi Display **Files** dialog box. Clicking a filename in the upper part of the dialog box with the left mouse button transfers the filename into the
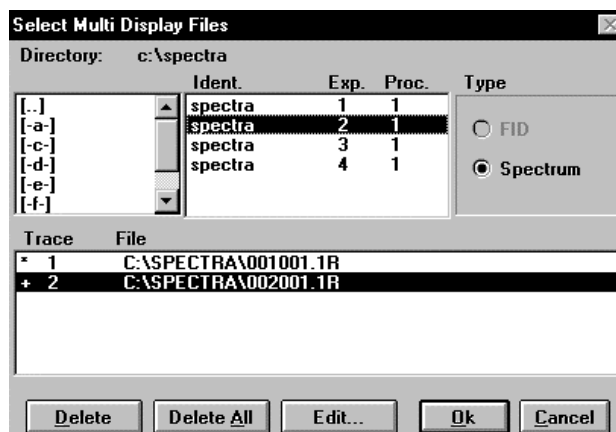
Fig. 3.11:   Dialog box of the **Multiple Display mode**. Upper part is used for the path search of a spectrum by its filename. The lower part lists the selected files.

lower part of the dialog box. Files are displayed in 1D WIN-NMR in the order they have been selected. Once selected one or all of the files may be deleted using the **Delete** or **Delete All** button respectively. Search pathways may be altered using the directories

listed in the top part of the dialog box. Closing the dialog box all files are displayed as an overlaid 3D spectrum. It is possible to toggle the appearance of the display by clicking the **Overlay**, **Stack Plot**, **3D** or **Separate** button in the button panel. The display modes and the **Options** button are used extensively in chapter 4 and 5.

How to plot a spectrum...

If available clicking the **Print!** button in the button panel will print the current contents of the spectrum window irrespective of whether it is a spectrum, a FID or a series of spectra in the Dual or Multiple Display mode that is displayed. The appearance of the output depends upon the page layout and options such as axis, integral values and peak picking should always be checked first. Selecting the **Page Layout…** command from the **Output** pull-down menu opens the Page Layout dialog box that contains many printing options. In a similar way clicking the **Print** button in the appropriate Report: dialog box, opened by clicking the **Report** button, will print reports such as peak picking or multiplet lists.

Although spectra and reports can be rapidly produced using the **Print** button an alternative approach is to use the **Preview** command selected either from the **Output** pull-down menu or by using the **Preview** button in the button panel or Report: dialog boxes. Using this approach the contents of the spectrum window or report dialog box is transferred to the Preview window which is loaded into the foreground. The Preview window, which can also be selected from the **Window** pull-down menu, is essentially a virtual piece of paper with the same dimensions as the paper in the currently selected printer. In the Preview window individual elements can be sized, moved and deleted allowing complex figures to be built up. Positioning the mouse cursor on an element and double clicking the left mouse button opens a dialog box where a number of parameters associated with the object can be modified. Fig. 3.12 shows the NMR Options dialog box associated with the spectrum. After the final adjustment of the layout the final figure can be plotted in three different ways:

(a)   The preview can be printed on the connected printer using the **Print!** button.

(b)   The preview can be transferred to the Windows clipboard using the **Output| Copy** command.

(c)   The preview can be saved as Windows metafile using the **File|Save File** command.
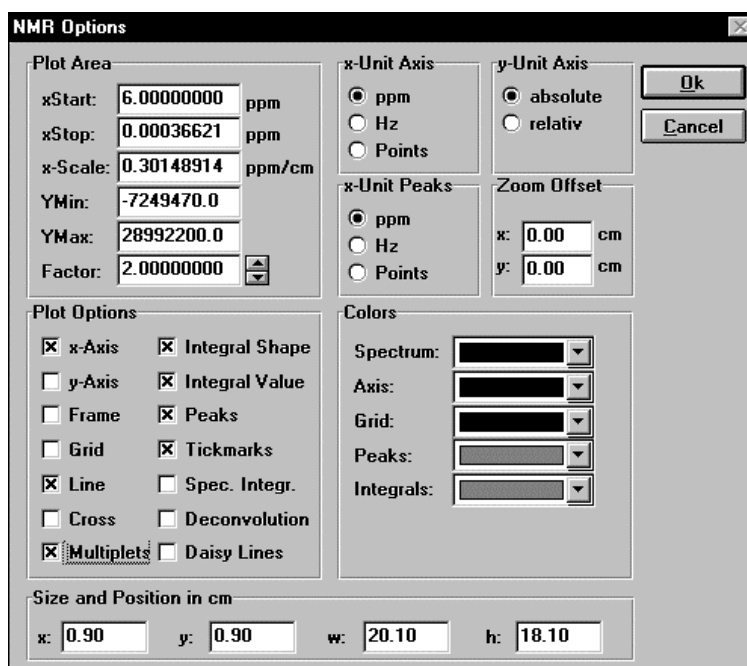
Fig. 3.12:   Preview window - spectrum pop up dialog box.

This short introduction to 1D WIN-NMR is by necessity restricted to those functions required for processing the simulated spectra in this book. Further information on 1D WIN-NMR can be obtained from the online-CD manual and the companion volume of this series [3.1].

3.3   Two dimensional Experiments

In a 2D experiment one or more scans are acquired with a delay t1 that is incremented in subsequent acquisitions to generate a time domain t1. The time domain t1 in conjunction with the acquisition time domain t2 generates a 2D data set that upon double Fourier transform gives a 2D spectrum. In a very simplified view all 2D experiments can be described as series of 1D experiments but in practise the situation is rather more complicated because to achieve quadrature detection in both dimensions phase cycling or pulse field gradients must be used. Consequently the processing of 2D data sets depends upon the detection mode and the experimental setup.

For the successful simulation and processing of 2D experiments knowledge of some of the more fundamental 2D parameters is essential and the first part of this section will briefly examine these parameters. For a comprehensive review of 2D parameters the reader is referred to sections 2.3.1 and 2.3.2.
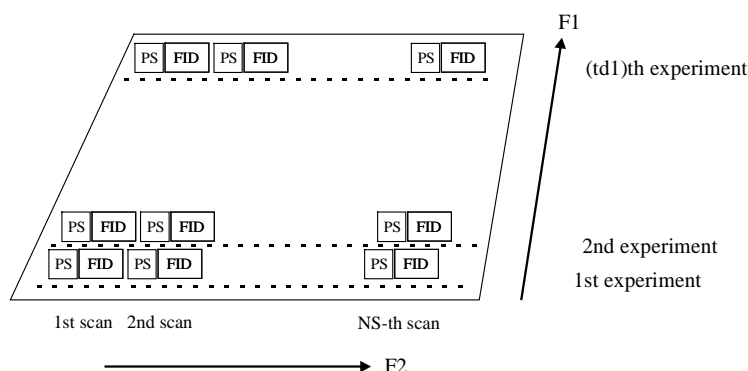
Fig. 3.13: The 2D matrix as combination of "scans" and "experiments". The acronym PS replaces the term pulse sequence. The phase cycling procedure for 2D quadrature detection is not implemented in the scheme.

The second part of this section examines the processing of 2D NMR data using 2D WIN-NMR. By necessity the description of 2D data processing is very brief and the raw 2D data is processed in a single step rather than the stepwise approach used for 1D data. Table 3.5 at the end of this section summarizes the recommended processing parameters for a number of the more common 2D experiments.

3.3.1   Recording and Simulation of 2D Experiments

This section examines some of the general experiment parameters required to create a 2D data matrix and the special experiment setup in NMR-SIM. The most important experimental parameters are in0, NS, delays di and the type of quadrature detection in f1. The user-related entries for the experiment setup are:
- The calculation of the correct increment in0 for the second dimension
- The minimum number of scans per experiment
- The calculation of the coherence evolution delays di
- The definition of gradient amplitudes where applicable

Calculation of the increment in0

In a 2D experiments a series of FIDs are acquired using an incremented delay t1 to build up a 2D data matrix, each row of the matrix corresponding to a specific value of t1. The effect of the incremented delay is to modulate the FIDs from the experiments, which can be interpreted and analysed as a pseudo FID with respect to the time delay t1. By convention the incremented delay is called d0 and the increment in0. The detected frequency range in the f1 dimension is given by ΔSW [Hz] = 1/(in0 • nd0*). Normally there is only one time increment variable but in special pulse sequences based upon for instance the ACCORDION-principle, see section 5.9.3, additional increment variable in1, in2… can be defined. Usually for the first experiment d0 = 3 us and for the second and subsequent experiments d0 = 3u + in0 • (n -1). In a number of 2D experiments the

incremented delay d0 is applied twice, centred about for instance a 180° pulse designed to refocus the unwanted coherence evolution in t1. This is taken into account in the in0 calculation by the factor nd0* - equation [3-13] which also depends on the detection mode. In Table 3.2 the relevant equations used to calculate in0 are shown based on the SW in ppm, the scale most commonly used experimentally.

Table 3.2:   Calculation of the Increment in0 in NMR-SIM.

f1 = f2:   **in0 = 1/ (nd0* • SW[ppm] • SF)**   [3-11]

f1 ≠ f2:   **in0 = 1/ (nd0* • SW[ppm] • SF • γ(^{n}X)/γ(^{1}H))**   [3-12]

nd0* = nd0 • phc-factor   [3-13]

nd0 = number of repeated delays d0 in a experiment, SF = spectrometer reference frequency [MHz], γ(^{1}H) = gyromagnetic ratio of ^{1}H, γ(^{n}X) = gyromagnetic ratio of the ^{n}X nucleus, phc-factor is related to the detection mode

Use in NMR-SIM:
homonuclear experiments: in0 = SW or = 1 / SW, except for TPPI: in0 = 1 / 2 • SW
                            and always nd0* = 1
heteronuclear experiments: Co-Addition (magnitude): in0 = 1 / 2 • SW and nd0 = 2
                            TPPI: in0 = 1/ 4 • SW and nd0 = 2

NMR-SIM does not differentiate Co-Addition, TPPI and States-TPPI concerning nd0, but the sweep width has to be calculated correspondingly to Table 3.2. In NMR-SIM for homonuclear 2D experiments with SW(f1) = SW(f2) the calculation of in0 is extremely simple, the sweep width SW is entered in the in0 field and the value calculated by an internal algorithm based on equation [3-11]. This procedure is illustrated in *Check it 3.3.1.1*.

3.3.1.1 Check it in NMR-SIM

Load the configuration file *ch3311.cfg* to simulate the ^{1}H COSY magnitude spectrum of an AMX spin system. In the NMR-SIM main window check the name of the pulse program: *cosy.seq* and spin system: *h3_amx.ham*. Check that in the rf channel bar the correct nuclei have been selected for F1 and F2. Using the **Go│Check Parameters & Go** command open the Check the experiment parameters dialog box and examine the parameters **nd0**: *1* and **in0**: *sw*. Click on the **Ok** button to start the simulation. After the calculation is completed the data is automatically loaded into 2D WIN-NMR. Fourier transformation using the **Process|2D transform [xfb]** command. To scale the levels of the spectrum use the *∗2 or /2* button in the button panel or the **Change All** button (for further details see section 3.3.2). The result should be similar to the spectrum below.
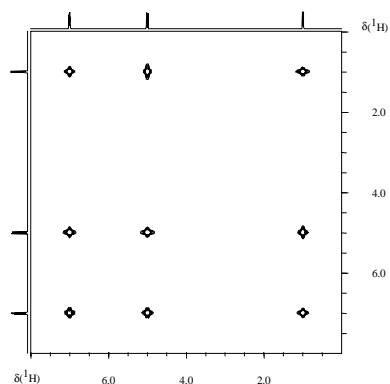
rf channel bar:

f1: H 1   f2: H 1

Check the experiment parameters
dialog box

...

nd0 = 1

...

in0 = *sw*

One further difference between the two frequency dimensions of a 2D spectrum should be mentioned. In contrast to direct acquisition in t2 no filters (analogue or digital) can be applied in the t1 dimension. As a consequence signals outside of the f1 spectral limits are folded back and give rise to "ghost" peaks in the 2D spectrum. To prevent this occurring in either the f1 spectral width and observation frequency have to be adjusted or a more sophisticated pulse sequence with region selective pulses in f1 has to be used. NMR-SIM can also produce folded peaks in the f1 dimension as demonstrated in *Check it 3.3.1.2.*

3.3.1.2 Check it in NMR-SIM

Load the configuration file *ch3312.cfg* to simulate the "narrow frequency range" ^{1}H COSY spectrum using the *h3_amx.ham* file. Run the simulation storing the 2D data as **Exp No.**: *1* (**User**: *ch331*, **Name**: *2*). Process and Fourier transform the 2D data matrix using the **Process│2D transform [xfb]** command. Observe the folded peaks at 0.0 ppm which can be identified as ghost peaks of the resonance signal at 7.0 ppm.

In *Check it 3.3.1.3* the explicit calculation of the in0 increment is demonstrated using equation [3-11] for two different quadrature detection modes.

3.3.1.3 Check it in NMR-SIM

Load the *ch3313b.cfg* file to simulate the ^{1}H COSY magnitude spectrum of an ABMX spin system. Using the **Go│Check Parameters & Go** command open the Check the experiment parameters dialog box and set the following parameters: **nd0**: 1, **in0**: 1 / (1 • 8 • 400) = *3.125e-04s* and run the simulation storing the 2D data as **Exp No.**: *1*. Transform the 2D data in 2D WIN-NMR (**Process│2D transform [xfb]**). For comparison the simulation can be repeated setting **in0**: *sw* and storing the data as **Exp No.**: *2*. Finally the ^{1}H COSY (TPPI) spectrum can be simulated using the file *ch3313c.cfg*. In the Check the experiment parameters dialog box note that **nd0**: *1* and **in0**: 1 / (2(!) • 8 • 400) = *1.563e-04s*. The Fourier transformed 2D data

matrix gives the same frequency range as for the previous simulations. Compared to the magnitude spectrum the cross peaks are resolved better while the diagonal peaks are less well defined. These differences are explained in section 5.4.1.1. If required the ^{1}H spectrum to use for the projections can be calculated using the *ch3313a.cfg* file.

The spectrometer reference frequency is defined for the ^{1}H nucleus and the frequency for all ^nX nuclei are calculated with respect to this frequency. Consequently if a heteronuclear frequency is assigned to the f1 dimension the value of in0 must be modified by the factor $\gamma(^nX)/\gamma(^1H)$ as shown in equation [3-12].

3.3.1.4 Check it in NMR-SIM

(a) To simulate the ^{1}H spectrum of the $^1H^{13}C^{31}P$ spin system (*1h13c31p.ham*), load the file *ch3314a.cfg*. Run the simulation saving the file as **Exp. No.**: *1*. Process the FID (no zero filling; apodization: wdw function **EM**, **LB**: *1.0* Hz) and save the Fourier transformed spectrum (**File│Save**). Simulate the ^{13}C spectrum by changing the **F1** nucleus in the rf channel bar to *C 13* and in the Check the experiment parameters dialog box setting **O1**: *35* ppm and **SW**: *70* ppm. Store the file as **Exp. No.**: *2*. Process the data (**EM**, **LB**: *2.0* Hz) and store the spectrum. Finally simulate the ^{31}P spectrum: **F1** *P 31*, **O1**: *60* ppm, **SW**: *200* ppm, **EM**, **LB** = *4.0* Hz. Saving the Fourier transformed spectra for use as the projection in the HMQC experiments.

(b) To simulate the ^{13}C, ^{1}H HMQC spectrum, load the file *ch3314b.cfg*. In the rf channel bar set **F1**: *H 1* and **F2**: *C 13*. In the Check the experiment parameters dialog box ensure that **O1**: *4* ppm, **O2**: *35* ppm, **SW**: *8* ppm, **nd0**: *2*, **in0**: *7.1e-05s*, **d2**: *0.042s*. Run the simulation storing the 2D data as **Exp. No.**: 4. Process the 2D data (**Process│2D transform xfb**) and add the projections to the f1 and f2 dimension. To obtain the ^{31}P, ^{1}H correlation spectrum repeat the simulation changing the **F2** nucleus: *P 31* and **O1**: *4* ppm, **O2**: *60* ppm, **SW**: *8* ppm, **nd0**: *2*, **in0**: *1.54e-05s*, **d2**: *0.01s*. Process the data in 2D WIN-NMR and add the appropriate f1 and f2 projections.

in0 values for the ^nX, ^{1}H magnitude HMQC experiments

	SW / O2	in0 (approx.)
$\gamma(^{13}C) = 6.73$	**70 / 35**	**7.10 • 10^{-5}sec**
$\gamma(^{31}P) = 10.84$	**200 / 60**	**1.54 • 10^{-5}sec**

Minimum number of scans

Phase cycling is an important part of any pulse program enabling signal selection and the suppression of artefacts. To help in setting up an experiment, particularly a 2D experiment, the minimum number of scans required for the correct phase cycling is usually listed in the commentary section of the pulse program. *Check it 3.3.1.5* briefly

examines the effect of phase cycling on the suppression of unwanted signals in a homonuclear COSY experiment by using a pulse program with two different phase program arguments. Further signal suppression is discussed in detail in chapter 5. This example introduces the way in which NMR-SIM can be used to manipulate pulse programs to understand the effects that individual elements such as phase cycling have on the experimental results.
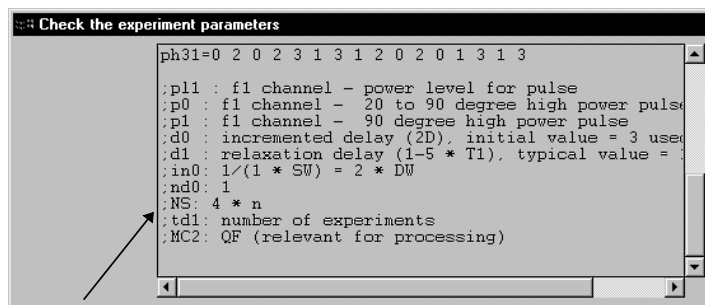
phase program of
cosyp1.seq

ph1=0
ph2=1
ph31=0

phase program of
cosyp12.seq

ph1=0
ph2=1 2
ph31=0 2

3.3.1.5 Check it in NMR-SIM

Load the configuration file *ch3315.cfg* and simulate the ^{1}H COSY spectrum using the pulse program *cosyp1.seq* with the simple phase program based on one scan per increment (**Go│Run Experiment**). Save the spectrum as **Exp. No.**: *1*. In 2D WIN-NMR Fourier transform the 2D data set (**Process│2D transform [xfb]**). Inspect the spectrum for the apparent signals at 3.0 ppm in the f1 dimension. For a second simulation replace the pulse program with the sequence *cosyp12.seq* (**File│Pulse program...**) which is based on two scans per increment. Save the data as **Exp No.**: *2*. In the transformed spectrum the ghost signals at 3.0 ppm have disappeared. The standard four step phase program for each pulse phase and the receiver phase was imposed by the EXORCYCLE phase cycle which was originally used to compensate for imperfections in the 180° pulse. If required the ^{1}H spectrum calculated in *Check it 3.3.1.1* may be used as the projection files.

```
Check the experiment parameters

ph31=0 2 0 2 3 1 3 1 2 0 2 0 1 3 1 3

;pl1 : f1 channel — power level for pulse
;p0  : f1 channel —  20 to 90 degree high power pulse
;p1  : f1 channel —  90 degree high power pulse
;d0  : incremented delay (2D), initial value = 3 use
;d1  : relaxation delay (1-5 * T1), typical value =
;in0 : 1/(1 * SW) = 2 * DW
;nd0 : 1
;NS  : 4 * n
;td1 : number of experiments
;MC2 : QF (relevant for processing)
```

minimum number of scans of each experiment

Fig. 3.14:   Scroll window of the Check the experiment parameters dialog box.

Calculation of coherence evolution delays

The step from 2D homonuclear correlation spectroscopy to 2D heteronuclear correlation spectroscopy is relatively straight forward but there is one important point to consider relating to the evolution of the antiphase coherence for magnetization transfer. Irrespective of whether direct or indirect detection is used, the delay times for optimum

antiphase coherence is a function of the coupling constants involved. By convention these delays are called d2, d4, d6 and d8 and are defined in Table 3.3. In *Check it 3.3.1.6* the ^{13}C, ^{1}H HMQC spectrum is simulated using different values of d2 based on the one-bond and long-range ^{13}C-^{1}H scalar couplings.

3.3.1.6 Check it in NMR-SIM

To simulate the one-bond ^{13}C, ^{1}H HMQC (mc) spectrum of the spin system file *c4h6.ham*, load the configuration file *ch3316.cfg*. In the Check the experiment parameters dialog box ensure that **d2**: 1/ (2 • $^{1}J(^{13}C, ^{1}H)$) = *0.0357m* before running the simulation and saving the data as **Exp. No.**: *1*. Repeat the simulation using **d2**: 1/ (2 • $^{n}J(^{13}C, ^{1}H)$) = *0.05s* and an **Exp. No.**: *2*. In 2D WIN-NMR Fourier transform both data sets (**Process│2D transform [xfb]**). To scale both spectra use the ∗**2** or **/2** button in the button panel or alternatively use the **Change All** button (section 3.3.2). Inspect the first spectrum for $^{1}J(^{13}C, ^{1}H)$ correlation peaks and the second spectrum for long-range $^{n}J(^{13}C, ^{1}H)$ correlation peaks. The ^{1}H spectrum can be calculated using the file *ch3316a.cfg*.

Definition of gradient amplitudes

An important development in modern 2D experiments is the use of gradients for coherence selection, which minimizes phase cycling and effectively suppresses unwanted coherences, see section 2.3.3. The relevant parameters to use for NMR-SIM simulations are the gradient pulse length and the gradient field strength. Usually two or more gradients are applied as part of a pulse sequence with the gradient amplitude depending, not only on the selected coherence pathways, but also on the gyromagnetic ratio of the nuclei involved. The pulse programs contained in this book all contain a short description in the comment section on the correct gradient field strengths to use for several isotope combinations. The guidelines to calculate gradient field strengths for other isotope combinations are given in section 2.3.3.

3.3.1.7 Check it in NMR-SIM

Load the configuration file *ch3317a.cfg* to simulate the gradient-selected ^{13}C, ^{1}H HMQC (mc) spectrum of uracil. Using the values shown below enter the gradient field strengths **GPZ1**... **GPZ3** in the Check the experiment parameters dialog box. Run the simulation and process the 2D data in 2D WIN-NMR. Using the *ch3317b.cfg* file calculate the gradient-selected ^{15}N, ^{1}H HMQC (mc) spectrum. Enter the gradient field strengths **GPZ1** ... **GPZ3** for the ^{15}N, ^{1}H correlation as shown in the table. Load the file *ch3317c.cfg* file to calculate the ^{1}H spectrum of uracil to use for the f2 projection (no zero filling, exponential apodization **EM**, **LB**: *1.0* [Hz]).
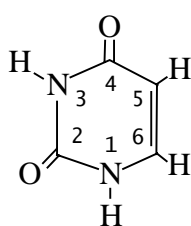
gradient ratio	**GPZ1**	**GPZ2**	**GPZ3**
$^{13}C/^{1}H$	*50*	*30*	*40*
$^{15}N/^{1}H$	70	30	60

structure of uracil.

Table 3.3 is a checklist of the parameters required specifically for either the simulation or experimental measurement of 2D data. Usually the default starting value of d0 is 3usec. To prevent misleading results, the value of nd0 should always be checked prior to starting any type of 2D simulation or experiment.

Table 3.3: Checklist of 2D specific experimental parameters.

data matrix related parameter

Parmode: 2D

f1 dimension related parameters

O2:	spectrum centre of the f1 dimension	**nd0**:	1, 2, 4 = scaling factor taking into account the type of 2D transform and the number of incremented d0 delay
TD1:	number of experiments		
in0:	increment of the d0 delay for successive experiments	**d0**:	initial value of the incremented d0 delay(s)

gradient related parameters[1)]

p16:	gradient pulse length	**gpz**:	gradient field strength

coherence evolution delay related parameters[1)]

d2:	$1/(2 \bullet {}^{1}J(^{n}X, {}^{1}H))$	**d6**:	$1/(2 \bullet {}^{1}J(^{n}X, {}^{1}H))$
d4:	$1/(4 \bullet {}^{n}J(^{n}X, {}^{1}H))$	**d8**:	$1/(4 \bullet {}^{n}J(^{n}X, {}^{1}H))$

[1)]Gradients and coherence evolution delays are not specific to 2D experiments but the correct setup of these parameters is particularly important for 2D experiment.

3.3.2   Processing of 2D NMR data

The basic processing steps for 1D NMR data can also be applied to the processing of 2D NMR data with similar effects. Of particular importance for the processing of 2D data matrices are zero filling and apodization. Usually 2D experiments are recorded with a relatively small number of time domain data points TD2, compared with a 1D experiment, and small number of increments TD1 in order to minimize data acquisition times. Typical time domain values are 512, 1k or 2k words. Small values of TD2 and TD1 and the correspondingly short acquisition times cause poor spectral resolution and

because the recorded FID has not decayed completely to zero before the end of the acquisition period inadequate data processing causes line distortion. Table 3.4 lists the general flow of 2D NMR data processing that will be briefly discussed in this section. At the end of this section there is a brief description on the analysis and output functions of 2D WIN-NMR.

Table 3.4:　　General Flow of 2D data processing for NMR-SIM 2D data.

• check and modification of the processing parameters	• calibration
• Fourier transformation in both dimensions	• choice of representation, intensity scale, projections, printer output
• phase correction	• (decomposition of a 2D matrix)

Data decomposition is not a common part of 2D data processing, but in the course of evaluating a pulse sequence the comparison of the same row or column which belong to different data sets can be very helpful. Similarly if a kinetic experiment has been performed as a pseudo 2D experiment it is easy to process the data to determine the rate constants if the data is treated as a set of 1D spectra.

Checking and modifying processing parameters

The time domain processing parameters for 2D experiments can be defined in NMR-SIM and be transferred automatically with the simulated 2D data matrix to 2D WIN-NMR for use in processing. These parameters can be checked in NMR-SIM using the **Options|Processing parameters…** command. The configuration files used in the *Check its* in this book already have the processing parameters defined such that the simulated 2D data matrix can be Fourier transformed immediately in 2D WIN-NMR. To allow the possibility of user-defined configuration files this introduction will examine the effect these processing parameters have on the 2D spectrum.

After the 2D data matrix is loaded into 2D WIN-NMR the filename and path on the local PC is shown in a separate bar below the menubar. The **Process|General parameter setup [edp]** command opens the Parameters dialog box and using the **Set** and **Data** check boxes the *Acquisition* or *Processing* parameters for the *f1* or *f2* dimensions can be selected and modified. The most important parameters are **SI**, **WDW** the type of window function plus its related parameters **LB**, **SSB** and **GB**, **MC2** (for f1), **Ph_mod** and **BC_mod**. Many of these parameters are analogous to the 1D processing parameters and their values may be set by following the guideline outlined for processing 1D data. The parameter **MC2** relates to the quadrature detection mode used in the f1 dimension and the value of MC2 is normally listed in the comment section of the pulse sequence file. MC2 can have the value magnitude, States or TPPI. After the Fourier transformation **PH_mod** determines the phase correction applied to the 2D spectrum. Normally PH_mod should be set to *no* except for magnitude spectra where it should be set to *mc*. PH_mod can also have the values *pk*, meaning use the current values of PHC0 and PHC1, and *ps*, calculate the power spectrum. The **BC_mod** parameter refers to the

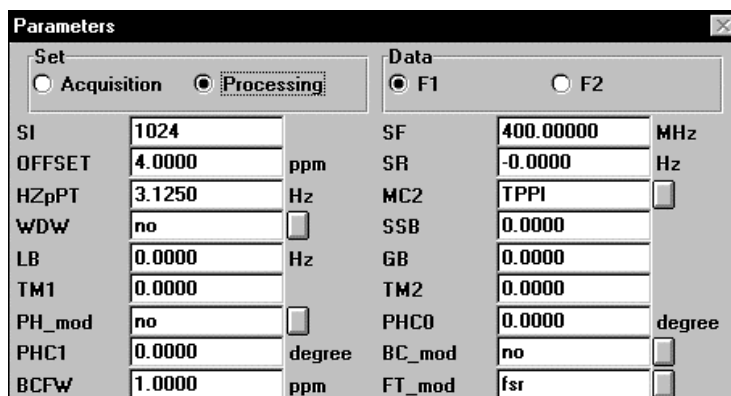baseline correction that should be applied and for simulated data BC_mod should always be set to *no*.

Set			Data		
○ Acquisition	⦿ Processing		⦿ F1	○ F2	
SI	1024		SF	400.00000	MHz
OFFSET	4.0000	ppm	SR	-0.0000	Hz
HZpPT	3.1250	Hz	MC2	TPPI	
WDW	no		SSB	0.0000	
LB	0.0000	Hz	GB	0.0000	
TM1	0.0000		TM2	0.0000	
PH_mod	no		PHC0	0.0000	degree
PHC1	0.0000	degree	BC_mod	no	
BCFW	1.0000	ppm	FT_mod	fsr	

Fig. 3.15: 2D WIN-NMR - partial view of the Processing parameter dialog box.

3.3.2.1 Check it in NMR-SIM

Load the configuration file *ch3321.cfg* (**File|Experiment setup|Load from file...**). To demonstrate the effect of different processing parameters start the calculation with the **Go|Run Experiment** command and in 2D WIN-NMR use the **Process|2D transform [xfb]** command to transform the data. Adjust the intensity levels of the contour plot using the ∗**2** and **/2** buttons of the button panel. Reload the 2D raw data matrix with the **File|Recall last** command. In the Parameters dialog box box (**Process|General parameter setup**) alter the processing parameter **SSB** from *0* to *2.0* for both the f1 and f2 dimension. Exit from the dialog box by clicking the **Save** button. Fourier transform the data and scale the spectrum until its looks similar to the right hand side of Fig. 3.16.
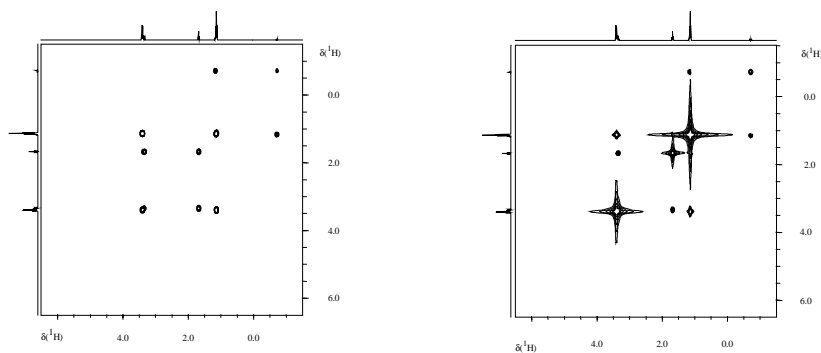

Fig. 3.16: 2D ¹H magnitude COSY spectra of *Check it 3.3.2.1*, both processed with WDW: QSINE. SSB: 0 (left hand side); SSB: 2.0 (right hand side).

In *Check it 3.3.2.1* the ^{1}H magnitude COSY spectrum of a ternary mixture of diethylether (1.0 (molar ratio)), ethyl bromide (0.2) and ethylmagnesium bromide (0.15) is simulated to demonstrate the importance of choosing the correct apodization parameters, particularly in a sample with a wide range of signal intensities.

Check it 3.3.2.1 clearly illustrates that the appearance of the spectrum depends upon the weighting function and its associated parameters which have to be adjusted to both the experiment and the detection mode employed e.g. magnitude or phase sensitive. With the magnitude mode of detection the best results are achieved using a SINE or QSINE weighting function with SSB = 0 in both dimensions whilst for the phase sensitive detection mode e.g. TPPI the best results are obtained with SSB = 2. At the end of this section Table 3.5 lists the recommended zero filling and apodization values to use for processing the data from a variety of 2D experiments. The 2D processing parameters used in the *Check its* in this book follow these guidelines.

FOURIER transformation of 2D data

In a similar manner to 1D data, the Fourier transformation used for 2D data can be treated as a blackbox function but with the additional consideration of the quadrature detection mode used in the second dimension. This aspect has already been discussed in section 2.3.1 and the reader is referred to this chapter for further details on the data processing and selection.

In 2D WIN-NMR the Fourier transformation of 2D raw data is accomplished in one step using the **xfb** command or stepwise using the **xf2** and then the **xf1** command. In either case the processing parameters including the selection of the appropriate FT mode must be set in the General parameter setup dialog box prior to the Fourier transformation.

Phase correction in both dimensions in 2D WIN-NMR

The phase correction of a 2D spectrum follows essentially the same procedure as a 1D spectrum except that the phase correction for the rows, the f2 dimension, and columns, the f1 dimension, must be executed separately. The following discussion describes the phase correction in the f2 dimension; the phase correction of the f1 dimension is achieved in a similar way. After Fourier transformation the **Manual phase correction** command is selected from the **Process** pull-down menu. The phasing procedure is divided into three steps.

Step 1: selection of rows or columns

Step 1: Select three representative rows containing both cross and diagonal peaks. The first row is selected by clicking the **Rows** and then the **Ch1** button. Move the mouse cursor in the spectrum window until the horizontal cross hair is positioned on a suitable row. As the horizontal cross hair is moved through the spectrum the row appear in a separate display window on top of the spectrum. Fix the position by clicking the left mouse button. Use a similar procedure to select two more rows for use with the phase correction by clicking the **Ch2** and then the **Ch3** button.

Big.Point	Cursor
Display	
Correct the Phase	
Back	Return

Step 2: choosing the data point of zero phase correction

Zero Order	First Order
Range+	Range-
Add 180°	Sub 180°
◄	►
P0: 0.00	P1: 0.00
Accept	Back
Return	

Step 3: slider panel for interactive phase correction

Step 2: With the cursor in the spectrum window click the right mouse button. The button panel changes to the layout shown on the left and at the same time a cursor appears at the top of the spectrum window designating the reference peak to be used for the zero-order phase adjustment. By default the cursor is set on the maximum signal (**Big Point**), clicking the **Cursor** button allows the reference peak to be set manually. Click on the **Correct the Phase** button to continue with the zero-order phase correction.

Step 3: The **Zero Order** correction is automatically selected, the phase of the reference signal is adjusted using the horizontal slider button in a similar manner to phasing a 1D spectrum. Clicking on the **First Order** button switches to the first-order phase correction which is performed in an analogous way. When the spectrum is correctly phased the phase correction is started using the **Accept** button.
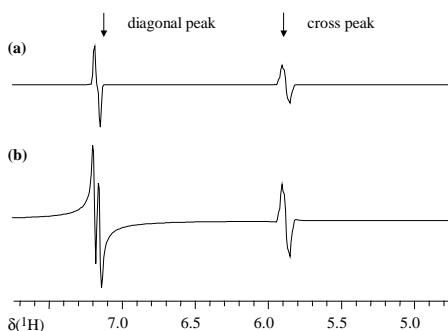
Once the rows have been correctly phased the columns are phased in a similar way except that in step 1 the **Columns** button is used instead of the **Rows** button.

Check it 3.3.2.2 illustrates the phase correction of a phase sensitive ^{1}H COSY TPPI spectrum whilst in *Check it 3.3.2.3* a phase sensitive COSY spectrum with double quantum filter is simulated. The double quantum filter effects the lineshape in the spectrum such that the diagonal and cross peaks have a narrower absorptive lineshape.

3.3.2.2 Check it in NMR-SIM

Load the file *ch3322.cfg*. Run the simulation and in the **Go|Check Parameters & Go** dialog box check the value of **nd0** and **in0**. Process the 2D data matrix in 2D WIN-NMR (**Process|2D transform [xfb]**). Scale the spectrum using the ∗**2** or **/2** button in the button panel or alternatively use the **Change All** button (section 3.3.2). Entering the phase routine by selecting the **Manual phase correction** command in the **Process** pull-down menu automatically activates the **Ch1** button in the button panel. Move the mouse cursor onto row 71 and assign this row to Ch1 by clicking the left mouse button. Toggle to the Ch2 selection by clicking on the **Ch2** button and assign row 235 to Ch2. Finally select and assign row 753 to **Ch3**. With the mouse cursor anywhere in the spectrum window click the right mouse button to start the second step of the phase correction. Click the **Correct the Phase** button with the left mouse button and start the **Zero Order** phase correction by using the slider panel to set the **phc0** value to

40 (the predefined difference between the transmitter and receiver phase). Click the **First Order** button and execute the first-order phase correction observing the tails of the signal at 1.8 ppm in the first channel. Click the **Accept** button to return to the phase corrected 2D contour plot. To phase the f1 dimension repeat the procedure using rows instead of columns.

Row 80 of ^{1}H DQF COSY(TPPI) spectrum **(a)** and ^{1}H COSY(TPPI) spectrum **(b)** of *Check it 3.3.2.3.*

3.3.2.3 Check it in NMR-SIM

Using the file *ch3323a.cfg* simulate the 2D phase sensitive ^{1}H DQF COSY (TPPI) spectrum of crotonic acid (**File│Experiment Setup│Load from File**). Prior to the calculation check that the value of **nd0** in the **Go|Check Parameters & Go** dialog box. Transform the data in 2D WIN-NMR (**Process│2D transform [xfb]**). Use the **∗2** or **/2** buttons to scale the contour plot intensity to an optimum level. Click the **Scan** button and in conjunction with the bottom information bar, move the cross hairs to a position near row 80 and inspect the diagonal peak at 7.2 ppm for an absorptive lineshape as shown in spectrum (a). For comparison simulate the ^{1}H COSY (TPPI) spectrum of the same spin system replacing the pulse program by the file *cosytp.seq* (**File│Pulse program…**). Prior to running the simulation check the value of **nd0** and **in0** in the Check experiment parameters dialog box. Process the spectrum in a similar manner to the previous data set and then select the same row as in the previous spectrum. The selected row should be similar to spectrum (b) above. Note the dispersive signal contribution in spectrum (b) (see section 5.4.1). If required the ^{1}H spectrum to use for the projections can be simulated using the file *ch3323b.cfg*.

Manual calibration of the frequency dimensions

Even though the NMR-SIM spin system files are defined using chemical shift values instead of frequency values, occasionally it is necessary to calibrate the second dimension (f1). In 2D WIN-NMR the calibration is enabled using the **Manual calibration** command of the **Analysis** pull-down menu. In the calibration mode the standard mouse cursor is replaced by a crosshair which is positioned on a signal of known chemical shift. Clicking the left mouse button fixes the cursor position and opens a dialog box where the appropriate chemical shift values can be entered in both dimensions. The **Ok** button closes the dialog box and starts the calibration.

Choice of representation, intensity scale, projections, output

The final processing steps before plotting or the export to the clipboard are the definition of the 1D spectra to be used as projections, the choice of the number and relative intensity of the contour levels and the selection of the plot parameters. The main functions of the spectrum window are combined in the upper part of the button panel as shown in Fig. 3.17 and are executed or enabled by a click of the left mouse button. Some functions have their own special cursor mode and it is only possible to leave these functions by clicking the function button again.

Most functions such as *2 and /2 have the same functionality as in 1D WIN-NMR and have been explained already whilst some are specifically for the manipulation of 2D data. The utmost right column of four buttons can be used to toggle between the different 2D representation modes: contour plot, density mode, stacked mode and 3D mode (from top to bottom). The |↔| button measures distances in the spectrum window; the first point is fixed using a left mouse button click and as the crosshair is moved the distance is displayed in the information bar at the bottom of the window. A right mouse button click releases the fixed point for a new distance measurement. The buttons marked with a frequency scale and f1 or f2 can be used to toggle the chemical shift scales between ppm, Hz or data points.

The **Change all** button is used to change the intensity of the contours in the 2D spectrum. Clicking the **Options** button opens a dialog box shown on the right hand side of Fig. 3.17. The **First level**: entry field is the most important parameter and sets the lowest level of the displayed contour. If the **Multiply** option is selected the **Factor** value determines the intensity difference between two adjacent contour levels: intensity (level (n+1)) = factor • intensity (level n). Finally for the correct representation of phasesensitive detected spectra containing signals with positive and negative intensity the [**+/-**] option must be selected.
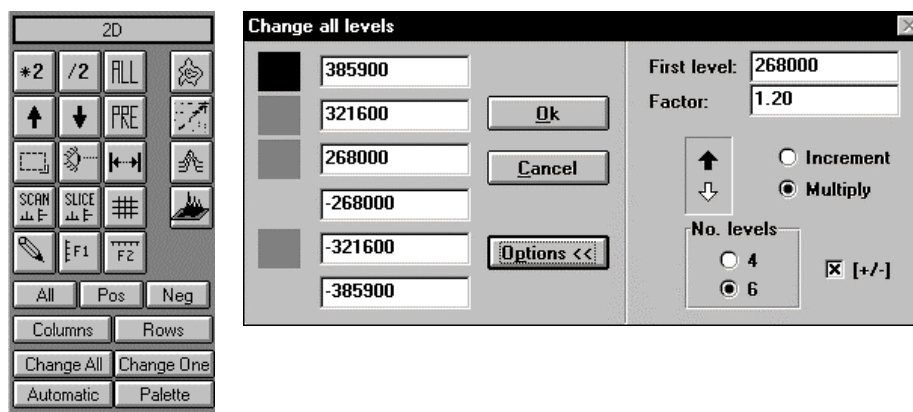

Fig. 3.17: 2D WIN-NMR - upper part of the button panel and the Change All dialog box (right).

A 2D spectrum is usually plotted together with its projections along f1 and f2 to simplify the signal assignment. It is recommended to use separately simulated 1D spectra instead of the internal projections of the 2D spectrum, which often have a low digital resolution, and for this purpose most *Check its* have a .cfg file to simulate the corresponding 1D spectrum. After processing and storing the 1D spectra in 1D WIN-NMR the spectra must be linked to the appropriate axis in 2D WIN-NMR. Select the **Layout** command from the **Display** pull-down menu and in the submenu select **Spectrum…**. A dialog box appears as shown in Fig. 3.18 containing a standard Windows file browser. First select **Type F1** and then the file for the f1 projection by double clicking on the appropriate filename. For the f2 projection select **Type F2** and then choose the file in the same manner.
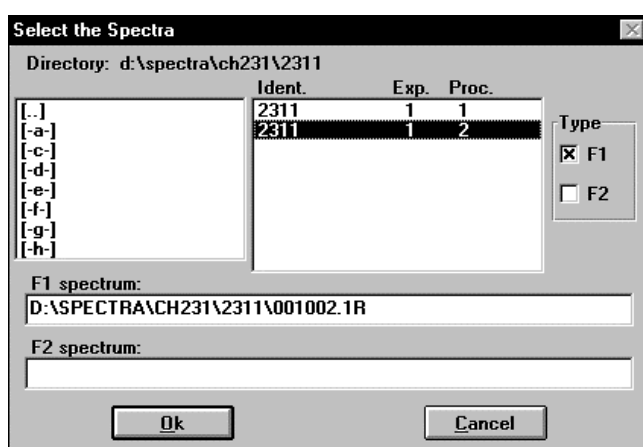

Fig. 3.18:   Projections - the **Display|Spectrum** dialog box.

The output to a printer or to the Windows Clipboard is accessible from the **Output** pull-down menu. The **Copy** command allows a direct transfer of the spectrum window contents to the clipboard which can then be loaded in to a text or graphic processing program such as Word by using the **Paste** function. The spectrum can be printed directly using the **Print** command selected from the **Output** pull-down menu or indirectly via the Page Setup dialog box. The Page Setup dialog box, shown in Fig. 3.19, enables a number of plot options to be modified as well as enabling the spectrum window contents to be displayed in the **Preview** window where the plot elements can be modified interactively in a similar manner to 1D WIN-NMR.
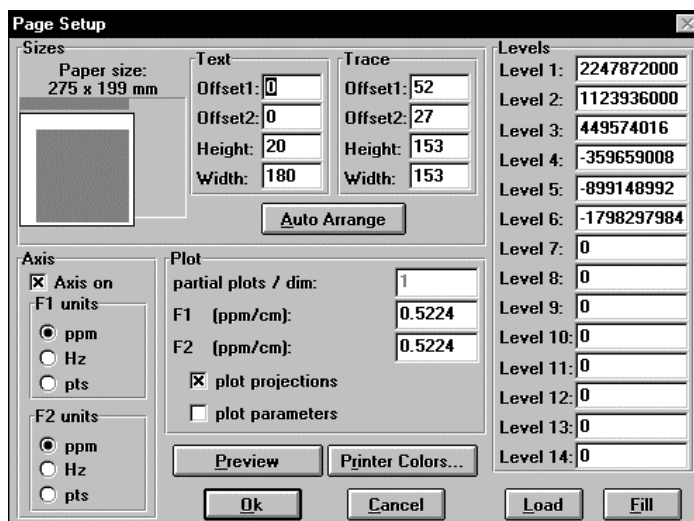
**Fig. 3.19:**   Page Setup dialog box.

Decomposition of a 2D matrix

The comparison of 2D spectra is often simplified by the decomposition or splitting of a 2D data matrix into a series of 1D spectra. Time domain data can be used to optimize weighting functions prior to processing the 2D data matrix whilst frequency domain data can be used in the evaluation and development of modified pulse sequence. 1D spectra can also be used to optimize the phase correction in a phase sensitive experiment.

In 2D WIN-NMR the 2D time domain data matrix can only be split into rows corresponding to the acquired FID as shown in Fig. 3.13. In a 2D frequency domain data matrix both rows (f2) and columns (f1) can be extracted with the proviso that the column data is only available after the 2D Fourier transformation. Zero filling may cause the results obtained from the extraction of rows in the frequency domain to be different from the results obtained from the time domain. This is particular true for the f1 dimension where the zero filling will effect the modulation in f1 as well as altering the overall row numbering.

(a) Decomposition of a 2 D data matrix in the time domain

A row of the data matrix prior to Fourier transformation can be extracted using the **FID-Transmission** command in the **File** pull-down menu.

A dialog box, see Fig. 3.20, is opened where the required row number **FID-number** must be entered as well as the **Filename** of the extracted FID. By clicking the **Transfer** button the FID is saved under the new file name, 1D WIN-NMR is started and the FID is loaded for further processing.
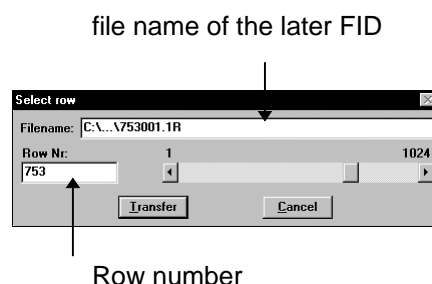
file name of the later FID

Row number

Fig. 3.20: FID-Transmission dialog box.

(b) Decomposition of a 2D data matrix in the frequency domain.

After Fourier transformation of the time domain data the 2D frequency data, the spectrum, can be described in terms of horizontal rows and vertical columns. To extract an individual row or column the **Slice** command of the button panel is used. The next step is to choose between the extraction of **Rows** or **Columns** by clicking the corresponding button in the button panel. A dialog box similar to Fig. 3.20 appears on the screen and the currently selected row or column is shown in the spectrum window with the associated number appearing in the **Row Nr:** or

Columns / Rows option

Slice button

Fig. 3.21: Button panel - Slice, Column and Row buttons.
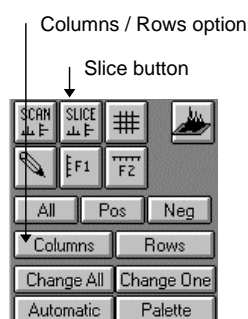
Column Nr: field. A different number can be entered from the keyboard or selected interactively using the slider button in the dialog box panel. Clicking the **Transfer** button extracts and saves the selected row or column and the data is automatically transferred and loaded in 1D WIN-NMR.

In *Check it 3.3.3.4* the decomposition technique is illustrated by extracting three rows from a 2D data matrix and using this raw data to optimize the apodization function and related parameters prior to transforming the data set.

3.3.2.4 Check it in NMR-SIM

Load the configuration file *ch2334.cfg* and run the simulation checking the value of **nd0** in the Check the experiment parameters dialog box. Transform the data and click the **Slice** button. Using the **Rows** option select rows *71*, *235* and *753* and transfer the data to 1D WIN-NMR using a suitable filename, *e.g. \071001.1r*, *\235001.1r* and *\753001.1r*. In 1D WIN-NMR open each 1r file in turn and use the **Process|Inverse FT** command to recreate the corresponding FID. Process each FID using a Sine-Bell squared wdw function with **SSB**: *0* and *2* saving each spectrum with a

different processing number, *e.g. \071002.1r, \071003.1r.* Alternatively

select the **Window Function** from the **Process** pull-down menu, click the **Interactive** button and use the slider bar to adjust the value of **SSB** interactively. Once all the FIDs have been processed use the **Multiple Display** mode to compare the spectra. Note how the unshifted Sine-Bell squared window-function (SSB = 0) suppresses the wiggles at the base of the peaks compared with the original spectra that have been processed without a window function. The shifted Sine-Bell squared function also reduces the distortions of the inner multiplet structure.

FIDs of the decomposed ^{1}H DQ COSY spectrum of *Check it 3.3.2.4*, corresponding to rows 71, 235 and 753. Note the applied zero filling.
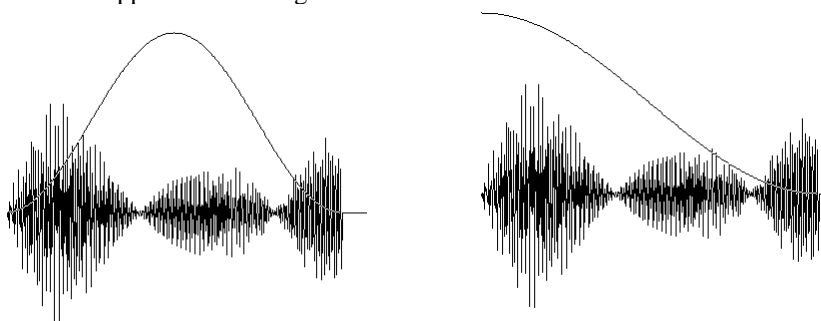
FID of row 71 and unshifted, Sine-Bell squared window function

FID of row 71 and π/2-shifted, Sine-Bell squared window function

Fig. 3.22:   t2 FID of a decomposed 2D spectrum and apodization functions to eliminate line distortion, see *Check it 3.3.2.4.*

It is apparent from *Check it 3.3.2.1* that the π/2-shifted Sine-Bell squared window function is the most appropriate apodization procedure for the 2D ^{1}H phase sensitive COSY spectrum, see Fig. 3.16. The reason that the Sine-Bell squared function is the best choice is because the last data points are zero and this type of window function ensures that there is no discontinuity in the FID. However the position of the function also has an important effect on the intensity of the data points in the first third of FID and this is why several values of SSB should be tried prior to making a final selection.

Table 3.5: Recommend Processing Parameters for homonuclear 2D $^1H/^1H$ Experiments.

Experiment	*Dim.*	*SI*	*WDW*	*SSB*	*PH_mod*	*BC_mod*	*MC2*
COSY	f2	512, 1K	SINE, QSINE	0	no	no, quad	
(magnitude)	f1	512, 1K	SINE, QSINE	0	mc	no	Qf
COSY	f2	512, 1K	SINE, QSINE	2	pk	no, quad	
(phased)	f1	512, 1K	SINE, QSINE	2	pk	no	TPPI
TOCSY	f2	512, 1K	SINE, QSINE	2	pk	no, quad	
(phased)	f1	512, 1K	SINE, QSINE	2	pk	no	TPPI
JRES	f2	512, 1K	SINE, QSINE	0	no	no, quad	
(magnitude)	f1	512, 1K	SINE, QSINE	0	mc	no	Qf

Recommended Processing Parameters for heteronuclear 2D $^{13}C/^1H$ Experiments.

Experiment	*Dim.*	*SI*	*WDW*	*SSB*	*PH_mod*	*BC_mod*	*MC2*
C/H COSY	f2	512, 1K	QSINE, SINE	0	no	no, quad	
(magnitude)	f1	512, 1K	QSINE, SINE	0	mc	no	QF
comment : ^{13}C detected							
C/H COSY	f2	512, 1K	QSINE, SINE	2	pk	no, quad	
(phased)	f1	512, 1K	QSINE, SINE	2	pk	no	TPPI, E/A
comment : ^1H detected HMQC, HSQC(TPPI), HSQC (E/A)							
C/H COSY H/H TOCSY	f2	512, 1K	QSINE, SINE	2	pk	no, quad	
(phased)	f1	512, 1K	QSINE, SINE	2	pk	no	TPPI, E/A
comment : ^1H detected HMQC, HSQC(TPPI), HSQC (E/A)							
C/H COSY	f2	512, 1K	QSINE, SINE	0	no	no, quad	
(magnitude)	f1	512, 1K	QSINE, SINE	2	mc	no	QF
comment : ^1H-detected HMBC							

3.4   NMR-SIM options

Irrespective of the dimension of the experiment the NMR-SIM option dialog box offers the possibility to alter the simulation environment to be as realistic as possible. In addition some options can be toggled on and off depending upon the simulation routine.
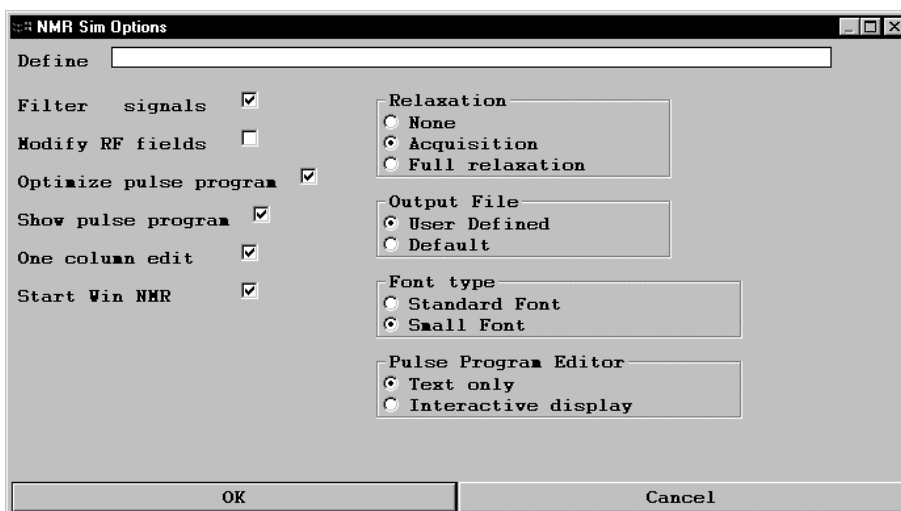

Fig. 2.23:   NMR-SIM options dialog box.

Options **for the simulation routine**

Normally the experiment parameter dialog box displays the pulse program and a list of parameters with a brief comment beside each parameter. This scroll window can be changed into a more compact form by disabling the options **Show pulse program** and **One column edit**. The option **Start Win NMR** allows either 1D WIN-NMR or 2D WIN-NMR to be started automatically as soon as the calculation is completed with the current simulated data loaded into the main display window.

The option **Output File** enables the user to choose whether the simulation result is stored in the default NMR-SIM directory structure or with a user defined pathname. The *Font type* enables the fonts used in the selection boxes to be altered to the user's preference. Finally the **Pulse Program Editor** option enables the pulse program editor to be started in either *Text* mode or *Interactive display* mode. In the interactive display mode a window displaying a graphical representation of the pulse program opens automatically enabling modifications to the pulse sequence to be visualized. Depending upon the speed of the computer this option seriously may degrade computer performance.

Options for the considered calculation parameters

Digital filtering is now a common spectrometer option and is used to suppress folded signals. Folded signals arise if a resonance is excited but is not part of the acquired frequency range. NMR-SIM can also suppress such folded peaks by selecting the **Filter signals** option. If the option **Optimize pulse program** is enabled NMR-SIM detects which sequence units might be combined to speed up the calculation time. For instance in an INEPT unit it is assumed that the refocusing units will refocus the chemical shift evolution and it is necessary to only calculate the coupling evolution explicitly. The **Modify RF fields** option is an important function because the pulse length can be adjusted for the resonance frequency of the nucleus (see section 3.2.2). Thus a ^{13}C pulse is calculated to be approximately four times longer than the corresponding ^{1}H pulse because the ratio of the gyromagnetic ratios is approximately four.

The **Relaxation** option becomes important if relaxation effects should be considered either during the pulse program execution or just during the data acquisition period. Set to *Acquisition* the simulated FID can be processed in a similar manner to experimental data. Although relaxation cannot be excluded in real experiments, NMR-SIM has the option to turn off relaxation effects when analysing a pulse sequence by selecting the *None* option and so reduce the simulation time.

3.5   References

[3.1] Bigler, P., *NMR Spectroscopy: Processing Strategies*, Weinheim, VCH Wiley, 2nd Ed. 2001.

[3.2] BRUKER, *1D WIN-NMR Software Manual, Release 6.0*, Bremen, Bruker-Franzen Analytik 1997.

[3.3] BRUKER, *2D WIN-NMR Software Manual, Release 6.01*, Bremen, Bruker-Franzen Analytik 1997.

[3.4] Weber, U., Thiele, H., *NMR Spectroscopy: Modern Spectral Analysis*, Weinheim, VCH Wiley, 1998.

[3.5] Ernst R. R., Bodenhausen, G., Wokaun, A., *Principles of Nuclear Magnetic Resonance in One and Two Dimensions*, Oxford, Clarendon Press, 1994.

4   Experiment Setup in NMR-SIM

The information that may be obtained from an NMR spectrum depends to some extent on the experimental parameters used to record the spectrum. Before recording an NMR spectrum a number of acquisition parameters have to be defined which depend on both the type of sample and the pulse sequence being used. Often the various parameters interact with each other making the optimization of the acquisition parameters difficult. Once the data has been acquired it may be processed and analysed in a number of different ways to extract the required information.

NMR-SIM can be seen as a software tool to analyse separately the effects on a NMR spectrum of different experimental variables such as spin system, pulse sequence and experimental parameters. The simulation program reduces the number of experimental parameters to a minimum to resemble as closely as possible a real experiment. This reduction in the number of variable parameters is a basic principle of scientific research because often the relationship between only a limited number of parameters can be interpreted unambiguously. The parameter reduction also speeds up calculation time. As illustrated in Fig. 4.1 the NMR spectrometer, represented by the magnet and computer, can be replaced by a computer plus software and the NMR sample by a defined theoretical spin system. Such an "ideal spectrometer" is the basis of the NMR-SIM or NMR experiment simulator software tool.
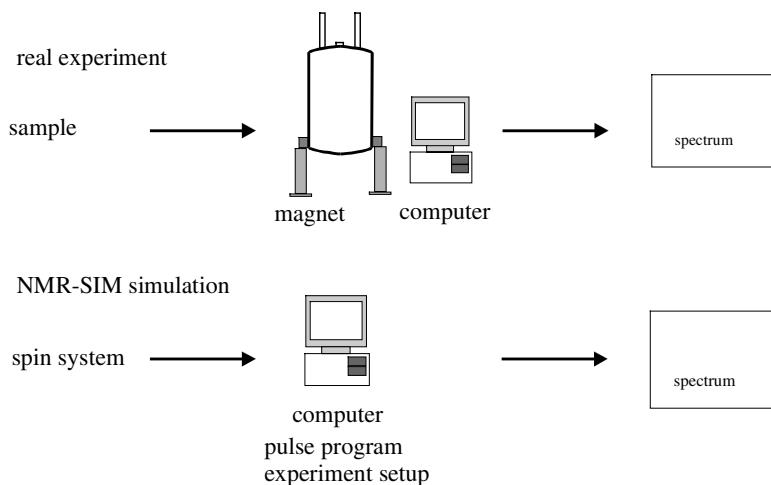

Fig. 4.1:   Comparison of a real experiment and a simulation environment.

Magnetic field inhomogenity, field drift or temperature fluctuation effects cannot be calculated but other experimental effects such as incorrectly set pulse lengths or phases that the NMR spectroscopist may come across can be easily simulated.

In the first section of this chapter spin systems and pulse sequences are discussed. Starting with the definition of a spin system and a description of the various spin parameters used by NMR-SIM. Using suitable examples the correct definition of spin system parameters, how to reduce the number of spin system parameters and the application of variable spin system parameters is illustrated. Following on, pulse sequences are discussed in some detail and the difference between a pulse sequence and a pulse program is emphasized. The pulse program language of NMR-SIM should be familiar to users of Bruker NMR spectrometers as it uses the same syntax. However, because this is not covered in the NMR-SIM manual, pulse sequence elements such as pulses, phases and delays are explained in detail and illustrated using a variety of examples.

The second section examines setting up experimental and processing parameters both manually and using the automatic NMR Wizard. The concept of configuration and job files is introduced and examples used to show how using this approach simulation experiments may be quickly set up and modified. Finally the use of NMR-SIM to optimize experimental parameters is discussed and different ways of displaying the results examined.

The final section looks at the Bloch module simulator. This remarkable software tool is virtually a stand alone package and enables the effects of shaped pulses and pulse sequence fragments to be examined and the results displayed in a number of different ways including an animated macroscopic magnetization vector diagram.

This chapter can be used either as an introduction to spin system definition and pulse programming or as a reference section. In either case the emphasis is on "learning by doing" and to this end there are numerous examples and *Check its* to follow. It is recommended that readers unfamiliar with simulation experiments refer to sections 2.2.2 and 2.3.2 before starting this chapter. This teaching version of NMR-SIM does not have all the features of the full version, consequently some topics that appear in the full version may not appear in this text and in these cases the NMR-SIM manual should be consulted for further information.

4.1 Spin Systems and Pulse Programs

A simulation using NMR-SIM is arranged into four different steps: spin system definition, pulse program selection, experimental and processing parameter selection and the output of the NMR data. For all these different steps NMR-SIM has an appropriate input device. Spin systems and pulse programs are simple text files which may be edited using either an external editor e.g. Notepad or by the internal editor of NMR-SIM whilst experimental and processing parameters are modified using pop-up dialog boxes.
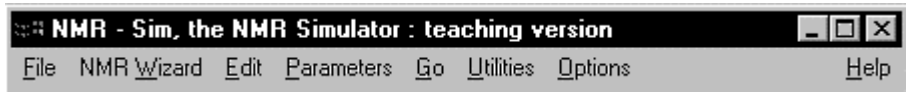
editing of pulse
programs, spin
systems, delay and
pulse lists
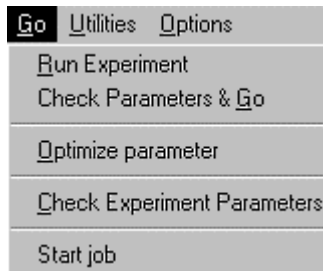
editing of experiment
parameters
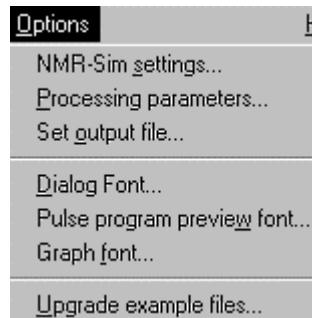
editing of simulation
conditions and processing
parameters

Fig. 4.2: The pull-down menus to edit spin systems, pulse programs and
related parameters, and the experiment and processing parameters.

4.1.1 Editing a Spin System

In NMR-SIM spin systems are defined as a plain ASCII text file and are denoted by
the file extension .ham. After the correct installation the spin system files supplied with
the program are saved in the sub-directory *...\Ham*. Spin systems can be modified like
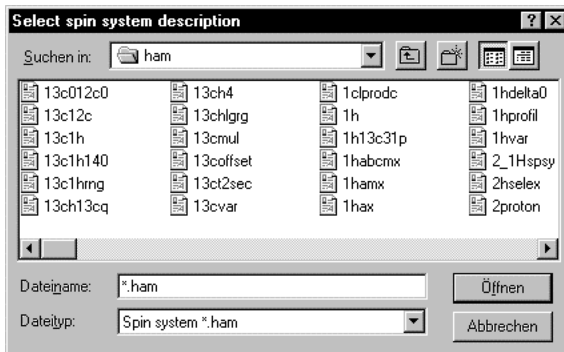
4.1.1.1 Check it in NMR-SIM

Start NMR-SIM, in the
main display window the
name of the currently
selected spin system, if
any, is shown. Using the
Edit│Spin   system
command start the internal
text editor. The text editor
window will open in the
foreground showing the

current spin system file. Close the text editor using the **File│Close** command in the menu bar. Now select the **Edit│Create new│Spin system** option. In the pop-up dialog box enter a new filename in the **Dateiname** (brit.: filename) input field e.g. *test.ham*. Take care not to leave **Dateiname** empty otherwise the current spin system will be replaced by a blank file. Close the window using the **Close** button and the text editor window will open in the foreground with a blank screen ready for input.

any conventional text file using either a standard Windows text editor or the integrated text editor of NMR-SIM. The integrated text editor of NMR-SIM is started using the **Edit│Spin system** pull-down menu and it is advisable to use this default editor because some other text editors may append a .txt to the **.ham** extension. New spin systems can be created using the **Edit│Create new│Spin system** pull-down menu, the name of a new spin system is entered and an empty edit window opens ready for input.

The labels used in the definition of the NMR-SIM spin system parameters depend to some extent upon personal preference. As with any programming language it is important to include comments; comments not only makes the spin system file more readable, they also make it easier to keep track of any modifications to the file and help other users to understand the spin system definitions. Comment lines start with a semicolon (**;**) and both the semicolon and the following text are ignored by the NMR-SIM processor.

The full version of NMR-SIM allows the use of externally defined pulse sequence units e.g. composite pulse decoupling sequences and arrays of constants e.g. delay lists, using pre-processor commands. These pre-processor commands correspond to the standard C pre-processor commands #ifdef, #if, #else, #endif and #include. Pre-processor commands are not supported by this teaching version and consequently the description of these commands is excluded. For further information on pre-processor commands consult the NMR-SIM manual.

4.1.1.1 Defining a Spin System

The drawing of a molecular structure will show all the bond connectivities between neighbouring atoms and, if a stereochemistry representation is used, the configuration and the conformation of the molecule. The NMR experiment is based on the detection of spin systems and consequently the molecular structure can be defined in terms of spin systems using chemical shifts, coupling networks and, for stereochemical information, the relaxation times of the NMR active nuclei.

In NMR-SIM, simulations are based on the definition of either a single spin system or two or more spin systems. The simultaneous simulation of several independent spin systems becomes relevant if molecules with two or more mutually isolated spin systems are investigated or if the spectrum of two or more compounds have to be described. In the latter case it is also necessary to include the concentration ratio for the correct correlation of intensities and integrals. Even for a chemically pure compound the definition of several spin systems is necessary to completely define the molecule if the structure contains NMR active isotope of low natural abundance e.g. ^{13}C. NMR-SIM

treats molecules with different labelling sites or containing different NMR active isotopes as different compounds and this is reflected in the syntax used. If a molecule contains nuclei of two different isotopes, it must be defined as two separate spin systems taking into consideration the natural abundance of each isotope and the effect of each isotope upon the scalar couplings and chemical shifts. However if the NMR spectrum of only the most sensitive nucleus is to be calculated, the number of spin systems can be reduced to only the main isotopomer or isotopomers.

NMR-SIM uses the predefined command **molecule** and **endmol** to set up the individual spin systems or molecules within the spin system definition file. All statements relating to nuclei, interactions and initial spin states are defined in a block that begins with the command **molecule** and ends with the command **endmol**. All the statements that occur in this block only relate to that particular spin system. Each spin system defined in this way has to be named, the name appearing on the same line as the **molecule** command separated by a space. Finally the relative concentration of the individual spin systems is added, separated from the name by a space.


```
molecule name weight
    nucleus statement
    ...                        first
    interaction
    statement
    ...                        spin
    initial spin state
    statement                  system
    ...
endmol
;
molecule name weight
    nucleus statement
    ...                        second
    interaction
    statement                  spin
    ...
    initial spin state         system
    statement
    ...
endmol
```

NMR-Sim spin syste...

File

574 bytes saved to

```
molecule alpha 0.98
proton 3*a 1.19
proton 2*b 3.56
proton c 5.27
;
couple a b 9
couple b c 4.76
endmol
;
molecule beta 0.01
proton 3*a 1.19
proton 2*b 3.56
proton c 5.27
carbon d 16
;
couple a b 9
couple b c 4.76
weak a d 125
endmol
```

Fig. 4.3:   Layout of the spin system definition; on the left hand side is shown the general scheme and on the right hand side a typical NMR-SIM text file for comparison.

The command **molecule** has the highest priority in the internal hierarchy of the spin system definition. Next comes the **nucleus** statement, each magnetically non-equivalent nucleus is defined, one nucleus per line followed by the coupling interaction between nuclei, one interaction per line. It is also possible to define a non-thermal equilibrium spin system state such as produced in multiple quantum coherence experiments. The required coherence may be selected using the spin state definition rather than by a pulse sequence, this not only simplifies the pulse sequence but also reduces calculation times. Fig. 4.3 illustrates the general layout of a spin system file. In the case of a single spin system, the **molecule** and **endmol** commands are redundant and may be omitted.

Defining the chemical shifts with the nucleus statement

This statement for each magnetic non-equivalent nucleus appears on one line and is grouped in three parts. First the *identifier* of the defined nucleus have to be given, all the possible identifiers are listed in Table 4.1. For the definition of nuclei not listed in Table 4.1 the wildcard identifier **nucleus** can be used. If the new nucleus does not have the default spin quantum number of 1/2, the correct spin quantum number must be appended in the form j3/2 or j2 separated from the **label** by a space. Separated by a space from the *identifier* the *multiplicity* and the nucleus *label* have to be denoted. The *multiplicity* has to be a number between 1 and 4 and is not allowed for nuclei with a spin quantum number greater than 1/2. The *label* has to be a character and can appear only once in any **molecule** definition. The expressions *multiplicity* and *label* are combined with a "*".

Table 4.1: Options for the command **nucleus**.

Isotope	Natural abundance [%]	Identifier	Spin (quantum number)	Relative gyromagnetic ratio ($\gamma(^nX)/\gamma(^1H)$)
^1H	99,985	proton	1/2	1
^2H (=D)	0,015	deuterium	1	0,15351
^{11}B	80.42	bor11	3/2	0.32809
^{13}C	1,108	carbon	1/2	0,25144
^{14}N	99,63	nitrogen14	1	0.07229
^{15}N	0,37	nitrogen	1/2	0,10133
^{19}F	100	fluorine	1/2	0.94077
^{29}Si	4,70	silicon	1/2	0,19867
^{31}P	100	phosphor	1/2	0,40481
^nX	[1]	nucleus	1/2 (default)	-

[1] For isotopes not defined in this table these values can be set by the user.

In the second part the chemical shift of the defined nucleus must be specified either in ppm units or Hz. If the chemical shifts are entered in Hz, then the units Hz must also be entered. The pre-processor uses the spectrometer frequency **SF** defined in the **Parameters|Frequencies…** dialog box, to convert the chemical shifts in ppm into Hz.

Finally the relaxation times T_1 and T_2 for each nucleus has to be given in units of seconds. In the **Options│NMR-SIM settings…** dialog box if the **Relaxation** option **Bloch model** is selected, both the T_1 and T_2 relaxation times are used in the simulation during the whole experiment whereas the option **Acquisition** allows relaxation only during the acquisition period. Selecting this option greatly increases the simulation time. Different permutations of the default values and individual set values are possible.

defined value:	automatically set value
t1 = value	t1 = t2
t2 = value	t1 = infinity
t1 = value, t2 = value	

Defining the couplings with the interaction statement

This statement of interactions appears on one line and consists of three arguments. First of all the type of interaction must be specified, the possible options are **couple**, **weak**, **dipolar** and **qpolar**. Using the previously defined *labels*, spaces are used to separate the nuclei whose interaction is defined by the current statement. The final argument is the estimated coupling constant in Hz units, again separated from the interaction labels by a space.

The options **couple** and **weak** denote a scalar coupling interaction. **Couple** is adequate for a strongly coupled second order spin system and **weak** for a coupling that can be described by an AX approximation. **Dipolar** describes a dipolar coupling, only the energy conserving part of the dipolar Hamiltonian are implemented. The **qpolar** option is reserved for the coupling interaction of a quadrupolar nucleus. Before a nucleus can appear in the interaction statement it must be defined in the nucleus statement.

Defining the initial spin system state statement

It is also possible to start a simulation with a spin system whose spin state is different from the thermal equilibrium state using the **add** command. **Add** modifies the density matrix that is the basis of the simulation and allows spin states that correspond to multiple quantum transitions to be defined. Each spin of a coherence state is specified on a separate line using product operator formalism as for example A_x or A_zX_y (pure single quantum state). Each line consists of the command **add** and three arguments. The first and second argument **ro0** and **1** allow the matrix element that represents the initial spin system state to be selected and the third argument consists of the spin label plus CARTESIAN coordinate, as usual the arguments are separated for each other by a space. Thus a single quantum state of an AM spin system A_zM_y is defined by the two lines: **add ro0 1 az** and **add ro0 1 my**.

4.1.1.2 Spin Systems with variable Arguments

It is also possible to study the effect of pulse sequences using the variable definition feature. Using variable definitions it is possible to increment the chemical shift to

generate the excitation profile of a pulse or to compare the chemical shift evolution of several spins during a definite delay.

A chemical shift may be defined as a variable by replacing the constant value in the nucleus or interaction statement by the argument **var***identifier* where the variable *identifier* is a number between 1 and 32. An operator **ihv** included in the pulse program, outside of the acquisition loop used for multiple scan operation, changes the value of the variable parameter. The modifications required in a pulse program to implement the use of variable parameters are shown in Fig. 4.4.
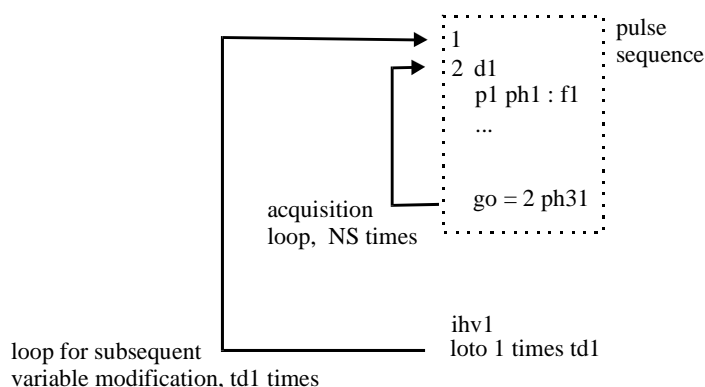

Fig. 4.4: The implementation of spin system variables in a pulse program.

Table 4.2: Variable Parameter Definitions, Initialization and Operators.

var1...32	A variable parameter is defined using the string var and the number 1 to 32. A maximum of 32 variables can be used in one simulation.

The initial value and increment parameters are set in the **Go│Check Experiment Parameters** dialog box.

HV1...32	The initial values, in Hz, of the variable var1...32.
HS1...32	The increment or decrement value, in Hz, of the variable var1...32.

Variable operators: These operators have to be placed in the pulse sequence outside of the acquisition loop.

dhc, ihc and **rhc**	Decrement, increment or reset **all** variables.
dhv*identifier* **ihv***identifier* **rhv***identifier*	Perform a selective decrement, increment, or a reset to the initial value of the spin system variable *identifier*.

The operators and arguments **loto** and **td1 times** corresponds to the expressions used in the pulse sequence language described in section 4.1.2.3. Table 4.2 summarizes the parameter definition, initialisation and variable parameter operators.

4.1.1.3 Editing a partial Spin System – The Molecule Bromomethylcrotonate

To simulate a NMR spectrum that is as close as possible to the experimental data, the spin system of a compound would have to be defined containing all the NMR parameters of all possible isotopomers. However if a pulse sequence is being used to study specific effects such as what effect do the multiplicity and homonuclear and heteronuclear scalar coupling constants have on an NMR spectrum, it is unnecessary to define all the possible spin system parameters. Often a spin system composed of fragments such as CH, CH_2 and CH_3 is a better choice for use in a simulation rather than a complex spin system that represents all the NMR parameters of a particular compound. A further advantage in reducing the number of spin system parameters is that the calculation time is dramatically reduced. For the comparison of simulated and experimental spectra it is often advantageous to use small molecules such as the hypothetical compound bromomethylcrotonate. In the following *Check its* bromomethylcrotonate is used to illustrate the use of NMR-SIM and to show how the molecule can be split into different partial spin systems depending upon the sequence being studied.

The NMR parameters and the structure of bromomethylcrotonate are shown in Fig. 4.5. The NMR parameters are based upon values given in literature for similar types of compounds. To simplify the analysis the scalar coupling along the ester bond and isotope shifts have been ignored.
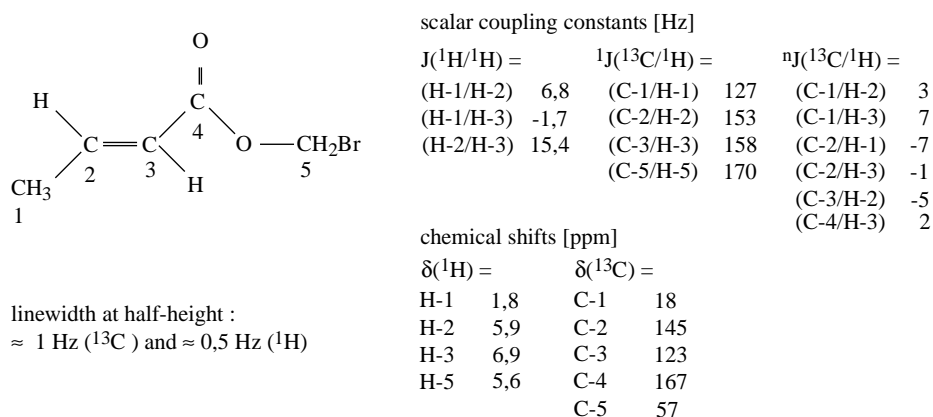
scalar coupling constants [Hz]

$J(^1H/^1H) =$		$^1J(^{13}C/^1H) =$		$^nJ(^{13}C/^1H) =$	
(H-1/H-2)	6,8	(C-1/H-1)	127	(C-1/H-2)	3
(H-1/H-3)	-1,7	(C-2/H-2)	153	(C-1/H-3)	7
(H-2/H-3)	15,4	(C-3/H-3)	158	(C-2/H-1)	-7
		(C-5/H-5)	170	(C-2/H-3)	-1
				(C-3/H-2)	-5
				(C-4/H-3)	2

chemical shifts [ppm]

$\delta(^1H) =$		$\delta(^{13}C) =$	
H-1	1,8	C-1	18
H-2	5,9	C-2	145
H-3	6,9	C-3	123
H-5	5,6	C-4	167
		C-5	57

linewidth at half-height :
≈ 1 Hz (^{13}C) and ≈ 0,5 Hz (^1H)

Fig. 4.5: Structure and NMR parameters of bromomethylcrotonate.

Example 1: Simulating a ^1H spectrum

Because of the low natural abundance of ^{13}C, in the simulation of the ^1H spectrum and the homonuclear ^1H COSY or TOCSY spectra of bromomethylcrotonate the effect of the ^{13}C can be safely ignored and the spin system reduced to a purely ^1H only spin system. In the figure below the reduced spin system is drawn and all nuclei which are not relevant are represented by a dot.
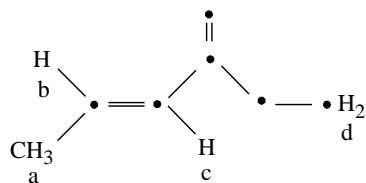
proton 3*a 1.8 t2=2
proton b 5.9 t2=2
proton c 6.9 t2=2
proton 2*d 5.6 t2=2
couple a b 6.8
couple a c -1.7
couple b c 15.4

4.1.1.2 Check it in NMR-SIM

Load the configuration file *stan1h.cfg* using the **File│Experiment Setup│Load from file…** command. Using the **File│Spin system…** command replace the spin system file *dummy.ham* with the file *exam1.ham*. Open the file (**Edit│Spin system**) and complete the spin system entries using the parameters shown on the left to create the reduced ^{1}H only spin system. Save the edited spin system (**File│Save…**) and then start a simulation using **Go│Run Experiment**. The FID will be transferred automatically to 1D WIN-NMR, use zero filling of **SI(r+i)**: *32k* and apply an exponential window function with a **LB** value of *1* Hz. After Fourier transformation of the data the simulated spectrum should resemble the one in the *result.pdf* file.

Example 2: Simulating a ^{13}C spectrum

The ^{13}C spectrum of a "pure" compound is actually the result of recording a mixture of different ^{13}C isotopomers. Although this fact is usually ignored, it must be taken in account for NMR-SIM simulations. For instance the ^{13}C spectrum of ethanol is measured for a mixture of the ^{12}C isotopomer and several ^{13}C isotopomers. Of course the ^{12}C isotopomer where all the carbon atoms of the molecular backbone are ^{12}C nuclei does not contribute to the ^{13}C spectrum. The ^{13}CH$_3$^{12}CH$_2$OH isotopomer contributes to the resonance signal of the CH$_3$ group and the ^{12}CH$_3$^{13}CH$_2$OH isotopomer contributes to resonance signal of the methylene group. Except for INADEQUATE experiments, the isotopomers of any compound where two carbon atoms are substituted by ^{13}C nuclei can normally be neglected. Generally homonuclear coupling involving NMR active nuclei with low natural abundance can also be ignored. It is important to be able to define spin systems for different isotopomers correctly as it would be completely wrong to define a virtual compound where all the carbon atoms were replaced by ^{13}C nuclei because such a spin system occurs nearly undetectable in an isotope non-enriched sample.

Fig. 4.6 shows as separate molecules the isotopomers used to define the various spin systems required to simulate correctly the ^{13}C spectrum of bromomethylcrotonate.
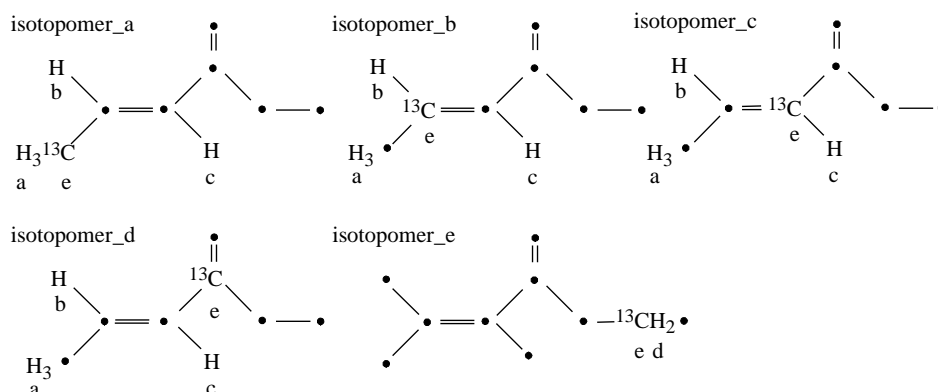
Fig. 4.6: ^{13}C isotopomers of bromomethylcrotonate.

4.1.1.3 Check it in NMR-SIM

Load the configuration file *stan13C.cfg* using the **File⎪Experiment Setup⎪Load from file…** command. Using the **File⎪Spin system…** command replace the spin system file *dummy.ham* with the file *exam2.ham*. Open the spin system file (**Edit⎪Spin system**). The spin system of the isotopomer A called *isotopomer_a* in the molecule command line has already been defined. Using this as a guide and the data given in Fig. 4.5 complete the spin systems parameters for isotopomers B to E. Add the T_2 values for both the proton (*t2=2*) and the carbon signals (*t2=1*). Save the edited spin system (**File⎪Save…**) with the new name *exam3.ham* and simulate the ^{13}C spectrum using **Go⎪Run Experiment**. The FID will be transferred automatically to 1D WIN-NMR. Process the spectrum with a zero filling of **SI(r+i)**: *32k* and a exponential window function with a **LB** value of *3* Hz. Inspect the spectrum for the multiplet splitting due to ^1H, ^{13}C coupling.

Example 3: Simulating a ^1H spectrum with ^{13}C satellites

In ^1H detected correlation type experiments such as HMQC, HMBC or HSQC the spectra obtained are the responses of the individual ^{13}C isotopomers to the excitation and coherence selection of the pulse sequence. The pulse sequence also has to suppress the unwanted ^1H signals of the ^{12}C isotopomer, how efficiently these signals are suppressed can be studied using NMR-SIM. In any simulation it is necessary to take into account the abundance of the ^{12}C isotopomer and the various ^{13}C isotopomers. This may be achieved by adding the appropriate weighting factors such as the natural abundance or relative concentrations to the molecule statement in the spin system file.

In *Check it 4.1.1.4* the ^{12}C isotopomer and ^{13}C isotopomers of bromomethylcrotonate are defined and weighting factors applied according to the natural abundance of a particular isotopomer. The appearance of the ^{13}C satellites in the simulated ^1H spectrum indicates that the spin systems have been correctly defined.

4.1.1.4 Check it in NMR-SIM

Load the configuration file *stan1h.cfg*. Using the **File│Spin system…** command replace the spin system file *dummy.ham* with the file *exam3.ham*. Open the file (**Edit│Spin system**) and extend the spin system file to include the spin system of the ^{12}C isotopomer using the values given in *Check it 4.1.1.2*. The spin system file should contain six molecule statements, each starting with the command *molecule* and concluding with the command *endmol* as shown in the result file. The approximate natural abundance of each isotopomer should be added to the same line as the molecule command. Start the simulation using the **Go│Run Experiment** command. In 1D WIN-NMR process the FID using zero filling of **SI(r+i)**: *32k* and an exponential window function with a **LB** value of *1.0* Hz.

Increase the signal intensity in the Fourier transformed spectrum to observe the so-called ^{13}C satellites of the ^{13}C isotopomers. In an experimental spectrum a small chemical shift difference can be detected between the centre of the ^{13}C satellite doublet and the main signal of the ^{12}C isotopomer. This primary isotope effect is related to the different chemical nature of the ^{13}C-^{1}H bond with respect to the ^{12}C-^{1}H bond and has been neglected in this example.

Example 4: Simulating the ^{1}H spectrum of a mixture

The original purpose of the molecule weight statement was to allow the simulation of mixtures containing compounds with very different concentrations. In this context it would be of interest to simulate the ^{1}H spectrum run using water suppression of a water-bromomethylcrotonate mixture in the ratio 100:1 which might be used experimentally.
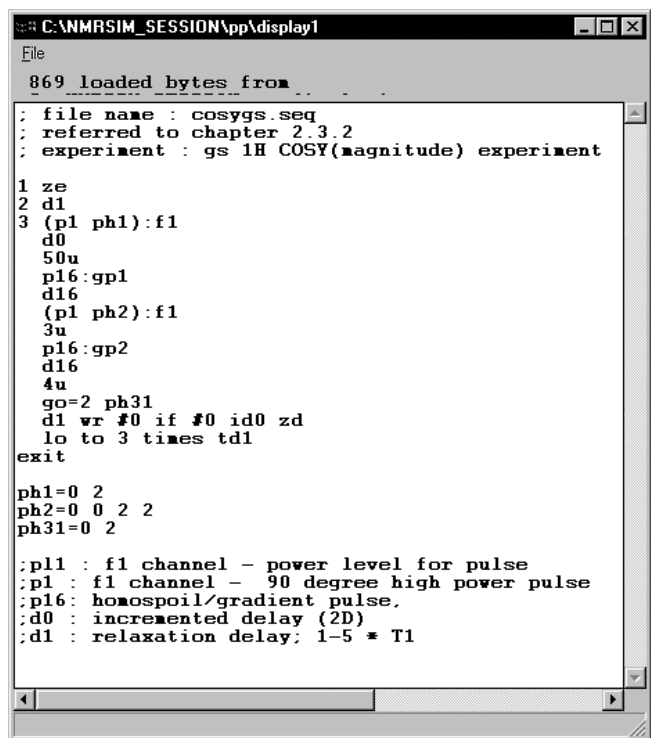
4.1.1.5 Check it in NMR-SIM

Load the configuration file *stan1h.cfg* and replace the spin system *dummy.ham* by the file *exam4.ham* using the **File│Spin system** command. Open the spin system file (**Edit│Spin system**) and compare the molecule definition and the weight factors with the molecular ratio of water and bromomethylcrotonate given in the spectrum. Run a simulation using the **Go│Run Experiment** command. In 1D WIN-NMR process the FID using zero filling of **SI(r+i)**: *32k* and a exponential window function with a **LB** value of *2.0* Hz.

In conclusion it should now be possible for the reader to define their own spin systems depending upon the types of problems they want to simulate by NMR-SIM. If required, the spin systems defined in this section may be used as a starting point and modified accordingly. It is very important, particularly when simulating 2D experiments, that the number of spin system parameters, where possible, be reduced to the minimum consistent with the type of analysis that is being performed.

4.1.2 Pulse Programming

It is often assumed that a pulse sequence is the same as a pulse program and that the two terms are interchangeable. A pulse sequence is a set of instructions relating to pulses, phases, delays and gradients whilst a pulse program, in addition to containing the pulse sequence instructions, also contains a list of executable commands that an NMR spectrometer computer requires to run a complete NMR experiment. A pulse program will include instructions relating to data acquisition, data storage, the accumulation of several free induction decays and possibly a number of different comments. Adding comments to a pulse program as with standard programming, is a thankless task but comments help improve the readability of the pulse program as well as helping other users understand what the pulse program is doing. Semicolons mark the start of a commentary text block and allow the NMR-SIM program interpreter to differentiate between commentary text and executable commands.

Fig. 4.7:   An example of a pulse program: a gradient selected magnitude COSY experiment.

Program documentation usually consists of a header block of text starting with a headline containing the program name and notes including literature citation marks and modification annotations made by the user. Secondary comments may be added at the end of the program summarizing experimental parameters such as pulse angles, pulse power, delays, acquisition mode and processing options.

The NMR Wizard function in NMR-SIM also makes use of comments. The NMR Wizard will analyze the spin system data, the pulse program and commentary text and automatically extract the appropriate experimental parameters required for a simulation based on the current pulse program.

As shown in Fig. 4.7, the main blocks of the pulse program are the pulse sequences and data acquisition commands. A pulse program may also contain gradient pulses, loops for time averaging experiments and 2D extensions. The final part of the pulse program contains the phase cycling instructions to be used by the pulse sequence.

4.1.2.1 Modifying an existing pulse program or creating a new one

There are two ways to create a new pulse program; modify an existing pulse program or start with a completely empty text file, of the two methods the former is probably the easiest. To modify an existing pulse program use the pull-down menu command **Edit|Pulse program**, the NMR-SIM integrated text editor starts and displays the current pulse program in a text editor window. The pulse program displayed may be selected either during the NMR-SIM program start up, by loading a configuration file (**File|Experiment setup|Load from file…**) or by using the **File|Pulse program** command. Before editing a pulse program it is recommended that in the **Options|NMR-SIM settings…** dialog box the **Pulse Program Editor** is set to the *Text only* option. With this option selected only the text editor is started, by selecting the alternative option *Interactive Display* both the text editor window and the pulse program viewer are started. Depending on the type of computer system, there can be a dramatic reduction in computer performance using the *Interactive Display* option. Using the **File|Open…** command in the menu bar of the integrated text editor other pulse programs can be loaded into the text window for editing. The text editor commands **Save…** and **Save as…** enable the modified pulse program to be written to the hard disk using either the same name or with a new name respectively. The command **Close** closes the text editor. Completely new pulse programs may be created using the **Edit|Create new|Pulse program** command. An interactive dialog box opens and the filename that will be used to save the new pulse program to disk must be entered. The integrated text editor then opens displaying an empty text window.

4.1.2.1 Check it in NMR-SIM

In the NMR-SIM options dialog box (**Options|NMR-SIM settings…**) set the **Pulse Program Editor** to the *Text only* option. The name of the currently selected pulse program is shown in the main display window next to the entry **Pulse Program**. Using the **Edit|Pulse program** command, start the integrated text editor to display the currently selected pulse program in the text editor window. Set the **Pulse**

Program Editor to the *Interactive Display* option and repeat the above procedure. The pulse sequence is displayed graphically in the pulse program viewer window and then the text editor window opens up in the foreground to display the pulse program text. To create a new pulse program use the **Edit⎮Create new⎮Pulse program** command. In the dialog box enter the filename *test.seq* in the **Filename** field and click on the **OK** button. The editor window now opens with a blank screen.

The **pulse program viewer** is a very important tool for comparing pulse programs or for analysing sequences because the graphical representation is often easier to understand than a text file. The program viewer can be opened using the **Utilities⎮Show Pulse program…** command and the current pulse program, whose name is given in the main window line **Pulse Program**, is displayed in the viewer window. Using the **File** pull-down menu, other pulse sequences may be selected using the **File|Select…** command while the currently displayed pulse sequence may either be printed using the **File|Print…** command or copied to the clipboard for use with other programs using the **File|Copy to clipboard…** command. The **Options** pull-down menu and the other viewer commands are of minor importance and are self-explanatory but if required, full details of these various commands are given in the NMR-SIM manual.

4.1.2.2 Check it in NMR-SIM

Select the file *cosygmfq.seq* (**File⎮Pulse Program…**). Open the pulse program viewer using the command **Utilities⎮Show Pulse program…**. The pulse program for the gradient selected double quantum filtered homonuclear COSY experiment is displayed in the main window.

4.1.2.2   The Syntax for using Pulses, Gradients, Delays and Decoupling

Pulses, delays and gradients are the basic elements of a pulse sequence. They are often used repeatedly and may be changed in a very versatile way. Their exact definition and time related execution follows a specific set of rules which the pulse program interpreter uses to translate the line ordered execution commands into a computer readable list of commands.

High power pulses, shaped pulses and gradients

Pulses are extremely versatile and can have a number of different properties:
- pulse length (duration)/pulse angle   • pulse phase
- frequency   • pulse shape
- rf power (amplitude).

With the design of a modern NMR spectrometer some of these properties, such as frequency and power, do not have to be explicitly defined for each pulse. Normally rf pulses with the same NMR frequency are transmitted from the spectrometer to the probehead using the same rf channel. In normal and reverse detection mode the rf

channel that is used for signal detection is always called F1. If available a second, third or fourth channel can be used to transmit pulses at different NMR frequencies and power levels to the probehead. This teaching version of NMR-SIM will only support two rf channels and consequently the simulation of only two types of experiments is possible. The first type of experiment is a homonuclear experiment that involves only one NMR frequency and where the pulses used in the experiment do not have to be assigned to a specific rf channel. The second type is a heteronuclear experiment where the pulses have different NMR frequencies and have to be assigned to the appropriate rf channel. Unless specified in the pulse sequence the same pulse level and frequency offset is applied to all the pulses on a specific channel and unless specified by an explicit command, all pulses will be generated as hard pulses.

High power pulses are defined by a variable p1....p31. The command line to specify a pulse **pi**, with phase **phj** applied to channel **F1**, has the form **pi :f1 phj**. It is also possible to do simple maths on the pulse length using the "*" operator. Any pulse p0...31 can be multiplied by a factor N, where N is a positive number, using the expression **pi*N**. Thus if **pi** represents a 90° pulse, the expression **pi*0.33** represents a 30° pulse and **pi*2** a 180° pulse. It is also possible to set the power level used during an experiment for all the pulses on the same rf channel using the parameter **pli**; the command **1u pl1** sets the default power level for channel F1 during a switch time of 1u and **1u pl2:f2** the default power level for F2. Power level commands without a rf channel specification use as default rf channel F1. To change the power level during the pulse program as for example in a spinlock or cp decoupling sequence the command line used for power switching must specify a delay time, a power level and the appropriate rf channel e.g. **d13 pl10:f2**. The delay period is necessary to mimic the power level switching time that occurs in a real spectrometer. To reset the pulse power back to its previous value a command line containing the appropriate settings has to be added after the pulse statement line. To specify the phase of a pulse each pulse execution command pi is combined with a phase argument phj in the form **(p1 ph3)**. Phj can have the values 0, 1, 2, 3 which corresponds to the CARTESIAN axis +x (= 0), +y (= 1), -x (= 2) and -y (= 3). The phase values of all the pulses and of the receiver used in a phase cycled time averaging experiment are combined into a set of phase cycling programs specified at the end of the pulse program. Each pulse has it's own phase cycling program. The reason for phase cycling is discussed in section 3.3.2. At the start of each pulse sequence the value for each phase phj is set to the first value in the appropriate phase cycling program. At the end of the pulse sequence the phase value is then incremented to the next value in the phase program. This continues until the last value in a phase program is reached, when the phase program "rolls-over" back to the first value. It is also possible to change the phase value in increments other than 90° using a phase program of the form **phj = (M) 0 1 5 6**, where M is an integer between 1 and 65536. In this example the phase phj on subsequent scans would be (0 • 360° / M), (1 • 360° / M), (5 • 360° / M) and (6 • 360° / M).

Shaped pulses use the command **spi**; the argument **spi** denotes the corresponding shape and power level together. Before they can be used in a pulse sequence the shaped pulse power level and shape have to be specified in the **Parameters│Shapes …** dialog

box. NMR-SIM can simulate pulse sequences containing up to a maximum of seven shaped pulses.

Gradient pulses are executed in similar way to rf pulses using commands such as **p16:gp1**. The argument **p16** describes the gradient duration and the **gpi** term the amplitude or strength of the gradient field. NMR-SIM only supports z-gradients. Following standard Bruker pulse program syntax it is recommended that the pulse p16 is used exclusively for gradient pulses.

Delays

Delays are an important part of pulse sequences and may be characterized by their duration and the effect they cause. Short delays in the micro-second region such as the pre-scan delay **de** or power switching delays, are not normally illustrated explicitly in pulse sequences and NMR-SIM simulations do not take these types of delay into consideration because an ideal spectrometer is assumed. Such delays may seem superfluous but they should nevertheless be considered and included sometimes in the interpretation of experimental artefacts or signal distortions. These effects are discussed in detail in sections 2.2.1 and 5.8.2.

For the NMR spectroscopist delays of between 20 microseconds and 1 second are of the most interest. During this type of delay the magnetization will evolve under the influence of coupling constants and chemical shift. Often in a pulse program delays are labelled according to what is happening to the magnetization during the delay period as for example "long-range coupling evolution delay".

All delays fall into one of three categories:

- fixed delays   30u, 30m, 1s
- constant delays   d1...d31   Note that d0 and d10 are recommended exclusively for use as the incremented delay in 2D and 3D experiments.
- variable delays   vd

A fixed delay is entered directly into a pulse program and is normally used for mundane tasks such as writing data to disk or turning the decoupler off before exiting a pulse program. In contrast, the values of constant and variable delays are entered independently of the pulse program; constant delays are entered during the experimental setup procedure whilst variable delays are stored in a variable delay or **vd** list, the name of which must be entered during the experimental setup procedure. How a delay is defined effects the way that a particular delay can be manipulated during the experiment execution, fixed delays cannot be manipulated.

The simplest operator is the multiplication "*****" operator which increases a delay by a fixed positive multiplier. The multiplier may be either an integer or a real number. The "*" operator must be placed after the delay not before it; a delay **d2*2** lasts twice as long as the original d2 delay but the delay **2*d2** would be illegal. The "*" operator can also be used for variable delays as in **vd*4**.

Constant and variable delays may also be incremented or decremented by a fixed argument and reset to their original value. To increment and decrement a delay the

commands **id0...id31** and **dd0...dd31** are available, the constants which are added or subtracted are defined by the parameters **in0...in31**. The command **rd0...rd31** resets the delay to the original value entered during the experiment setup procedure. If a delay **d1** has an initial value of **t**, the constant, which is added by the **id1** command or subtracted by the **dd1** command, is stored in the parameter **in1**. The command **rd1** resets **d1** back to its initial value **t**. For internal reasons the commands idi, ddi and rdi must be specified after a delay that is not related to the variable delay di such as **0.1m idi** or **d1 rdi**. In these cases the length of the delay is not important provided that the delay is correctly defined.

The **vd** command can be used for variable delays which cannot be expressed by simple arithmetic calculations as in a kinetic experiment or a T_1 inversion recovery sequence. The variable delay **vd** used in the pulse program is exchanged for the values defined in a delay list. In NMR-SIM a delay list is selected using the **File|Delay list...** command and edited using the **Edit│Delay list** command. The command **ivd** in the pulse program increments a pointer in the delay list to the next value. If the ivd command is included inside the loop for a time averaging multi-scan experiment the delay vd will be changed for each scan. If the command vd is part of the external loop of a multi-dimensional experiment, different vd delays will be used for each experiment as for example a 2D serial file. As with the increment/decrement commands ivd must be specified after a correctly defined delay.

Decoupling

In modern pulse sequences heteronuclear decoupling is performed using composite pulse decoupling using a command such as **cdpi:f2**. The rf channel used for decoupling is sometimes called the decoupler channel although with a modern spectrometer this definition is rather an anachronism. The instructions for the decoupling sequence are stored in an external file and consist of an endless loop of pulses with different duration and phase. The type of decoupling sequence is defined in the experiment setup parameters. The cpd command is really a macro-instruction that switches the decoupling sequence on. The decoupling sequence is switched off using the **do** command which is an acronym for **decoupler off**. The only other heteronuclear decoupling command used in a pulse program is the command to set the pulse power used for the composite decoupling.

The effect of the decoupling sequence is to permanently exchange the magnetization of the nuclei involved in the coupling between the various possible spin states. Since NMR-SIM represents an ideal spectrometer the decoupling procedure is not simulated explicitly, instead while the decoupler is switched on all the heteronuclear coupling constants involved are set to zero. For instance, if ^{1}H decoupling is applied during the acquisition of the ^{13}C spectrum of a ^{13}CF$_2$H-group the ^{13}C-^{1}H interaction is set to zero, but the ^{13}C-^{19}F coupling will still be observed in the spectrum. The decoupling sequence is started by the command **cpdi:fi**, where the index i in fi denotes the rf channel on which the decoupling sequence is executed. The **cpdi** command on the other hand is related to the applied cpd sequence which can be explicitly chosen on real spectrometer. In contrast to a real NMR spectrometer where the cw command involving the selective

irradiation at one radio frequency is very specific, the **cw** command is not available. The decoupler off command **do** would also switch off the cw irradiation.

Also the simulation of homodecoupling is not available in the current version of NMR-SIM.

Interaction of delays and pulses

The timing relationship involving sequential or simultaneous delays and pulses is governed by a set of pulse program compiler rules. The most important rule is that the pulse program compiler does not distinguish between a pulse and a delay. To control the start or beginning of these time periods, line feed, parentheses and round brackets, are used. Fig. 4.8 illustrates the different timing alternatives.
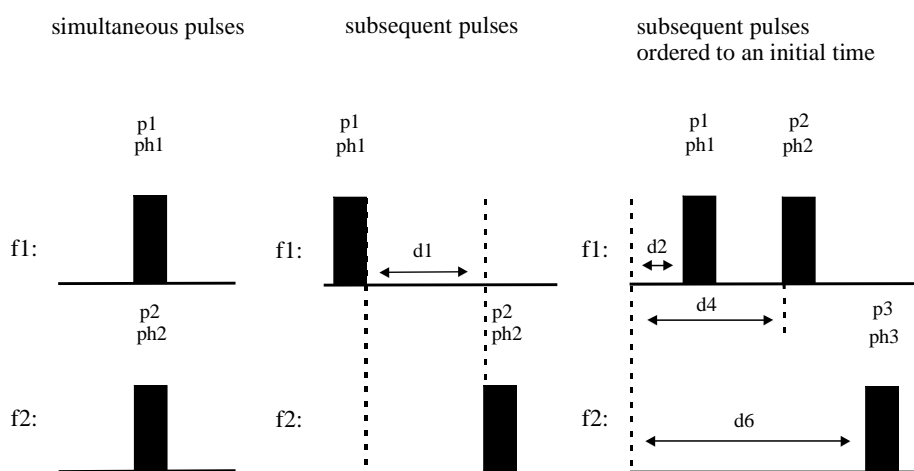

Fig. 4.8:   Combinations of delays and pulses.

The simplest form is the sequential execution of two elements such as two pulses or the combination of a pulse and a delay. In this case the commands have to be written on sequential lines or in one line enclosed by parenthesis. The sequence in the middle of Fig. 4.8 illustrates the sequential execution of a pulse p1 followed by a delay d1 and a pulse p2 which corresponds to the commands **(p1 ph1)/d1/(p2 ph2)**. The symbol "/" denotes a line feed. Alternatively, since commands on the same line inside the same parenthesis are executed sequentially, the three lines may be combined in a single statement **(p1 ph1 d1 p2 ph2)**. The simultaneous execution of two pulses as shown on the left hand side of Fig. 4.8 occurs if both pulses are placed on the same line in parenthesis **(p1 ph1) (p2 ph2)**, the first item in each set of parenthesis starting at the same time. A delay and a pulse or two delays can also be applied in the same way. The combination of parenthesis and the correct order of commands inside the same set of parenthesis are important when specifying the order of pulses and delays relative to a fixed starting point. Thus the sequence illustrated on the right side of Fig. 4.8 corresponds to the statement **(d2 p1) (d4 p2) (d6 p3)**.

In Table 4.3 the various ways of combining two pulses or a pulse and a delay are given.

Table 4.3:   The execution rules for pulses and delays.

Rule :	(1)	Commands on sequental lines are executed sequentially.
	(2)	Commands on the same line enclosed by the same parenthesis are executed sequentially.
	(3)	Commands on the same line, which are enclosed by different sets of parenthesis, are executed simultaneously.

	Examples:	Two pulses	A pulse and a delay
Simultaneous execution		(p1 ph1):f1 (p2 ph2):f2	(p1 ph1):f1 (d1)
Sequential execution		p1	p1
		p2	d2
		(p1 ph1 p2 ph2):f1	(p1 ph1 d2):f1

Because of the combination of line, parenthesis and the position in the parenthesis, there are often several alternative ways to write a particular pulse sequence. Consequently the program scheme viewer should always be used to ensure the correct sequence of pulses and delays.

4.1.2.3 Check it in NMR-SIM

Start NMR-SIM and load the pulse sequence *dummy.seq* using the **File⎪Pulse program…** command. In the NMR-SIM options dialog box (**Options⎪NMR-SIM settings…**) set the **Pulse Sequence editor** to *Text only*. Open the pulse program *dummy.seq* using the **Edit⎪Pulse program** command and enter the first example of Table 4.3 in the text editor window. Use the **Save as** command save the file under the new name *test.seq*. Open the pulse program viewer (**Utilities⎪Show Pulse program…**) and use the **File|Select** command in the menu bar of the viewer to load the file *test.seq*. Compare the display with the left-hand side of Fig. 4.8. Test out the other examples in Table 4.3 or alternatively write an original pulse sequence fragment and view the results.

4.1.2.3   Acquisition Loops and Data Storage

Loops and acquisition commands are often related. Two typical applications of loops are the execution of a time averaging experiment and the measurement of a series of spectra to generate a two dimensional matrix during a 2D experiment. Both examples implement data acquisition and data storage in a specific way. The acquisition commands used in NMR-SIM pulse programs have to be structured to be consistent with the pulse programs used on BRUKER NMR spectrometers.

The first data handling command is the **ze** command which is entered at the beginning of a pulse program and which deletes all the data currently stored in the temporary memory. The size of the temporary memory, also called the buffer, is specified by the value of **TD** and is reserved during the current experiment for the acquired data. At the beginning of an experiment this temporary memory consists only of "zero" values which are later replaced by the data from each scan during the accumulation. The command to write the digitized data points of a FID to the temporary memory is implemented by the **go=...** command. The transfer of data from temporary memory to persistent memory, such as the hard disk, is performed using the write command **wr #0**. The time averaging loop is constructed from the go command and a **loop label**; the loop label appears at the start of the first line of the pulse sequence to be repeated. The **loop counter,** given by the **NS** parameter, determines how many times the pulse sequence is executed.

In contrast to a 1D experiment, at the beginning of a 2D experiment a serial file containing a fixed number of blank FID data files is generated in persistent memory. The two dimensional matrix consists of **td1** files, with a size of **TD** with each file corresponding to one time increment in the 2D matrix. A pointer is used to instruct the computer to transfer the accumulated data for each time increment from temporary memory to the correct persistent file. The pointer is then incremented for the next element. This whole procedure is executed by the **pointer command if #0**. The **zd** command occurs after the if #0 command and deletes the buffer contents. The 2D loop is closed by the command **lo to label**. In this instance **label** is a number or a string that is entered in the first position of the line where the next time increment in the 2D matrix will be started.

4.1.2.4 Non-standard Bruker Pulse Program Commands

The use of variable spin system parameters and the visualization of magnetization vectors using the Bloch simulator module require additional commands to be implemented in the NMR-SIM pulse programs that do not appear in the standard BRUKER pulse programs. The increment or decrement of a spin system parameter is triggered by a command line in the pulse program. The Bloch simulator module uses the increment of the virtual chemical shift to generate the offset dependence of a pulse.

To generate a multi-scan 1D spectrum using an incremented spin system parameter for each scan or a pseudo 2D experiment where each experiment in the second dimension represents a changed spin system parameter, the appropriate spin system parameter in the *.ham file must be replaced by a variable definition. For instance a nucleus statement would have to be altered from **proton a 1.99 t=2** to **proton a var1 t=2** and a coupling interaction statement from **couple a b 9.2** to **couple a b var2**. The pulse program used to investigate the influence of chemical shift or coupling constant variation also has to be modified to include two additional command lines. The first line contains the command *ihvi* used to increment the variable **vari** and the second line the loop **lo to N times M** command which must be external to the acquisition **go=…** loop.

A typical application for these commands is to display the excitation profile of a pulse or shaped pulse as a spectrum. The frequency of the pulse is held constant and the chemical shift of a spin is incremented. The signal intensity is then measured as a function of the frequency difference or offset between the spin's chemical shift and the pulse frequency. This method essentially corresponds to a sweep over the excitation range of the pulse and offers an alternative representation to the Bloch simulator approach.

4.1.2.4 Check it in NMR-SIM

Load the configuration file *dsweep.cfg*. Open the spin system file (**Edit⎪Spin system…**) and note the spin system variable definition. Examine the pulse sequence (**Edit⎪Pulse program…**) and note the additional loop command to increment the chemical shift. Using the **Go|Run Experiment** command simulate the spectrum which corresponds to the excitation profile of a 90° TOPHAT pulse. In 1D WIN-NMR process the FID using zero filling of **SI(r+i)**: *32k* and an exponential window function with a **LB** value of *2* Hz.

The Bloch simulator module in NMR-SIM enables the offset dependence between the frequency of a pulse and the resonance frequency of an uncoupled single spin to be visualized graphically in a manner similar to the diagrams in the literature. Essentially the BLOCH equations describe two simultaneous processes; the effect of a radio frequency pulse on a macroscopic magnetization vector and the relaxation of the macroscopic magnetization back to its equilibrium value with the assumption that the T_1 and T_2 relaxation can be treated as a simple first order process. The NMR-SIM Bloch simulator only uses the equations for the first process and ignores any relaxation processes. It is not necessary to define a spin system because the BLOCH equations are based on an ensemble of identical spins that can be represented by a single macroscopic vector. To simulate the influence of the difference between the resonance frequency of the spin and the pulse frequency, the Bloch simulator calculates how the magnetization generated using a shaped pulse or a pulse sequence fragment, of a single macroscopic spin evolves, as the chemical shift is incremented. To enable the chemical shift to be incremented the pulse sequence or fragment must be modified:

1. After the ze command the command line "1 sample" is inserted.
2. The command line "go=..." is replaced by the command "sample".
3. After the command "sample" the lines "ihc" and "lo to 1 *loop_counter*" are inserted before the final command "exit". The term "*loop_counter*" can be a loop counter variable such as li, which must be set with the experiment parameters.

ze
1 sample
  p1 ph1
  p2 ph2
  p3 ph3
  sample
  ihc
  lo to 1 times l1
 exit
ph1=0
ph2=1
ph3=0

4.1.2.5 Check it in NMR-SIM

Using the **File│Pulse program…** command load the pulse program *cp121.seq* into NMR-SIM. Open the file (**Edit│Pulse program…**) from *c:\nmrsim_session\pp\ppfrag* and examine the text file for the execution commands **sample**, **ihc** and **lo to**. The pulse sequence is shown on the left-hand side of this *Check it*.

4.1.2.5   Editing Pulse Programs - from one pulse to the DEPT experiment

In this section a number of examples will be discussed illustrating the editing of pulse programs, starting with the simple one-pulse experiment for ^nX (X = ^1H, ^{13}C...) nuclei. This pulse program is then extended to a heteronuclear experiment with ^1H decoupling. The DEPT experiment is used as an example of experiments with pulses on different rf channels. The starting point is always the pulse sequence representation that appears in the literature so that this section and the following section, concerning gradients and 2D experiments, can serve as a guide on how to edit and simulate pulse sequences described in the literature. The spin systems used in these examples are those used in section 4.1.1.3 so that it is possible to compare the simulated spectra with those displayed in that section. Again the difference between a pulse program and a pulse sequence has to be emphasized; a pulse program contains computer related commands for data processing and spectrometer relevant execution tasks including the pulse sequence whilst a pulse sequence only contains commands relating to pulses, delays, gradients and phases.

For all the examples the development of the pulse sequence should be checked using the pulse sequence viewer utility (**Utilities│Show Pulse program…**).

Example 1: The ^nX experiment (= ^1H, ^{13}C, ^{19}F, ...)

p1
ph1   ph31 (rec)

ph1=0 2 2 0 1 3 3 1
ph31=0 2 2 0 1 3 3 1

p1(p1) : 90° pulse (f1)

f1:   d1
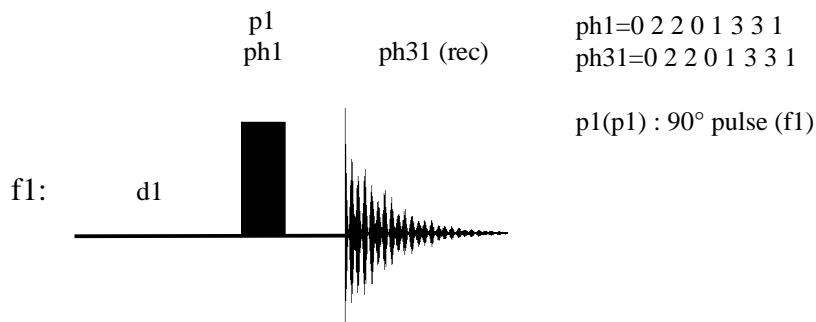
The common representation of a nX pulse sequence, including the phase cycling program, is shown above. The sequence can be used for any NMR active nucleus; the correct rf frequency is set by the experiment parameters. In *Check it 4.1.2.6(a)* the first elements of the pulse sequence are entered starting with the delay and pulse as line ordered commands.

4.1.2.6(a) Check it in NMR-SIM

To create a new pulse program select the pull-down menu command **Edit│Create new│Pulse program** and enter the name *ppexam1.seq* in the **Filename** field. In the text editor window enter the two lines as shown below and save the new pulse program using the **File│Save…** command. View the pulse sequence using the **Utilities│Show pulse program…** command and compare the diagram with the figure below.

d1
(p1 ph1):f1
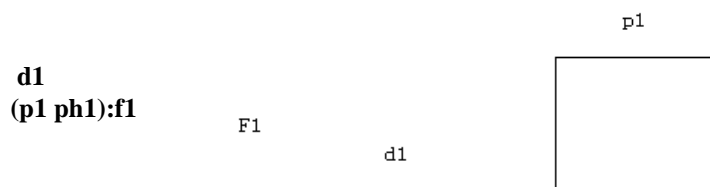
As explained in section 2.3.3 for time averaging experiments the pulse phase and the receiver phase are cycled. One major reason for phase cycling is that the performance of the electronic devices used to detect the x- and y-components of coherence for quadrature detection are not identical. In *Check it 4.1.2.6(b)* the most common phase cycling procedure is listed. In both NMR-SIM and the BRUKER pulse program language phase ph31 is recommended exclusively for the receiver phase.

4.1.2.6(b) Check it in NMR-SIM

...
ph1= 0 2 2 0 1 3 3 1
ph31= 0 2 2 0 1 3 3 1

Open the pulse program *ppexam1.seq* created in the *Check it 4.1.2.6(a)* using the **Edit│Pulse program** command. Add the two phase program lines after the lines for d1 and (p1 ph1):f1. Using the **File│Save As…** command save the file with the new name *ppexam2.seq*.

Because NMR spectroscopy is such an insensitive technique, spectra are recorded in a time averaging procedure with the FID of each scan being added to the FID from the previous scans stored in the computer memory. The time averaging procedure is initialized by the loop command go =... Because the same rf coil is used for the transmission of the rf pulse and for the acquisition of the induced voltage, the go command also performs various electronic switching tasks. Once the acquisition has started the accumulated data is saved in a temporary file and is saved at the end of the

experiment in a pre-defined output file by the wr #0 command. The exit command on the last line closes the pulse program.

4.1.2.6(c) Check it in NMR-SIM

Open the pulse program file *ppexam2.seq* using the **Edit⏐Pulse program** command. Before the accumulation can start the data currently stored in the computer memory must be deleted, enter *1 ze* as the first line in the text window. Amend the second line by placing the loop label *2*, separated by a space, in front of the delay *d1*. Add *go = 2 ph31*, *wr #0* and *exit* on three additional lines between the command *(p1 ph1):f1* and the phase program. Save the modified file as *ppexam3.seq* using the command **File|Save As…**. Check the pulse program by selecting the command **Utilities⏐Show Pulse program**.

1 ze
2 d1
  ...
  go=2 ph31
  wr #0
  exit

ph1 =...
ph31=...
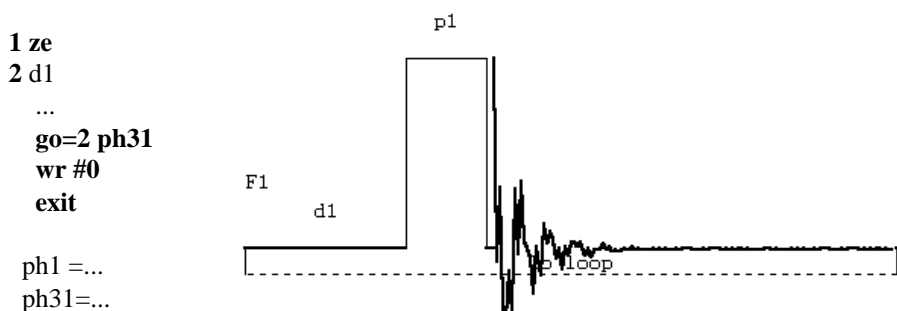
To check that the new pulse program works correctly complete *Check it 4.1.2.6 (d)*.

4.1.2.6(d) Check it in NMR-SIM

Load the configuration file *stan1h.cfg* using the **File⏐Experiment Setup⏐Load from file…** command and replace the spin system either by the file *exam1.ham* previously created in *Check it 4.1.1.2* or the file *exam1p.ham* delivered with the program. Load the pulse program *ppexam3.seq* and start the simulation by the command **Go⏐Run Experiment**. In 1D WIN-NMR process the FID using zero filling of **SI(r+i)** = *32k* and an exponential window function with a **LB** value of *1* Hz. The spectrum should be identical to the one displayed in *Check it 4.1.1.2*.

To test the pulse program for a ^{13}C spectrum repeat the process using the configuration file *stan13C.cfg* and using either the spin system file *exam3.ham* previously created in *Check it* 4.1.1.3 or the file *exam2p.ham* delivered with the program. Process the FID with zero filling (**SI(r+i)** = *32k*) and an exponential window function (**LB** value of *3* Hz). The spectrum should correspond to the plotted spectrum in *Check it 4.1.1.3*.

Example 2: The $^nX\{^1H\}$ experiment

Generally the NMR spectra of ^nX nuclei which have a low natural abundance are recorded with ^1H decoupling during acquisition because the multiplets caused by the ^1H-^nX scalar coupling considerably reduces signal intensity. Decoupling is achieved by applying a decoupling sequence during data acquisition. For simplification NMR-SIM does not calculate the decoupling explicitly, instead the ^nX-^1H scalar coupling constants are simply set to zero. Scalar coupling involving ^nX and another NMR active nuclei ^mY is not suppressed so that in the ^1H decoupled ^{13}C spectrum of a CF_2H- group the ^{19}F spin coupling would still be visible. The decoupling command **cpdi** is the same as used on BRUKER NMR spectrometers and may also have appended the rf channel on which the decoupling pulse sequence is executed e.g. **cpd2:f2**. In a ^1H decoupled ^nX detected experiment the second rf channel F2 used for ^1H decoupling must be assigned to the ^1H frequency during the experiment parameter setup procedure. Because of the way the effect of composite decoupling is simulated the commands used in the pulse sequence on a real spectrometer to switch between high pulse power levels and low composite pulse decoupling power levels are not necessary in NMR-SIM. This leads to a simplification of the pulse sequences used in NMR-SIM to study composite decoupling experiments.
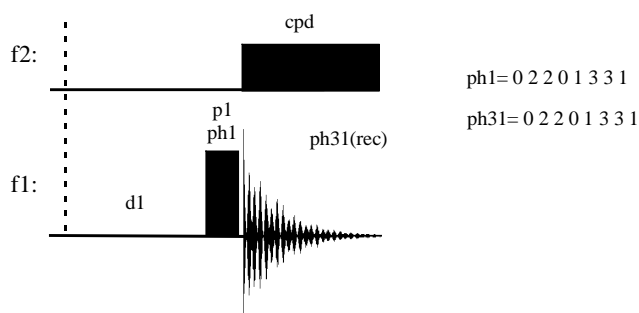

Fig. 4.9:   The $^nX\{^1H\}$ experiment. The curly brackets $\{^1H\}$ denote ^1H decoupling during data acquisition.

4.1.2.7(a) Check it in NMR-SIM

Open the pulse program *ppexam3.seq* (**Edit|Spin system**) and after the go=2 ph2 statement add the decoupling command *cpd2:f2*. Save the modified pulse program as *ppexam4.seq* (**File|Save as…**). Check the pulse program by selecting the command **Utilities|Show pulse program…**.

```
1 ze
2 d1 do:f2
...
go = 2 ph 31 cpd2:f2
wr #0
exit

ph1=...
ph2=...
```
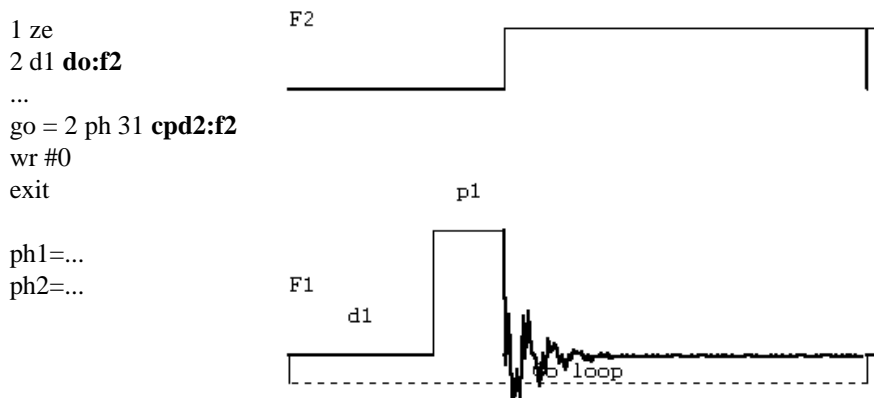

4.1.2.7(b) Check it in NMR-SIM

Load the configuration file *stan13c.cfg* and replace the pulse program by the file *ppexam4.seq* and the spin system by either the file *exam3.ham* previously created in *Check it 4.1.1.3* or the file *exam3p.ham* delivered with the program. Simulate the spectrum (**Go|Run Spectrum**) and process the FID using zero filling of **SI(r+i)** = *32k* and an exponential window function with a **LB** value of *3* Hz. The spectrum should correspond to the figure in the result file.

Example 3: The DEPT135-$^{13}C\{^{1}H\}$ experiment

The DEPT experiment is representative of pulse programs where pulses are executed on two different rf channels either simultaneously or sequentially. This example will illustrate how pulses and delays have to be defined to construct the correct pulse sequence. It will also introduce the use of the operator "*" as a way of reducing the number of fixed pulses.
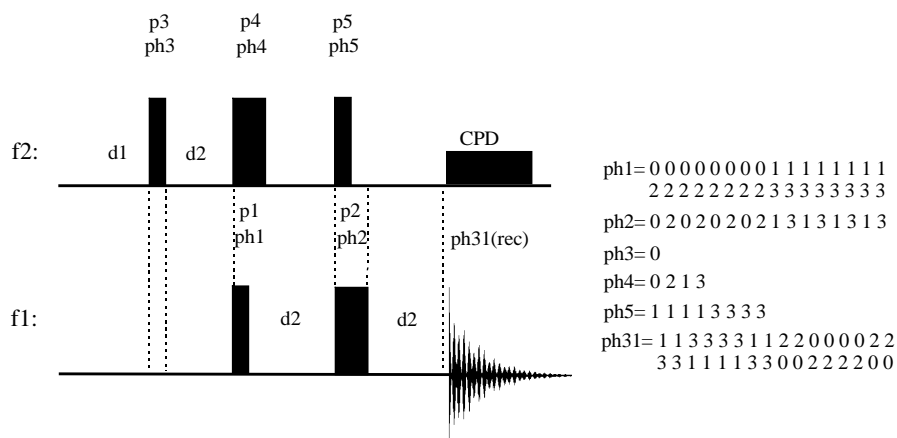

Fig. 4.10: The DEPT135 pulse sequence.

The first step is to construct a partial pulse program with pulses and delays in a simple sequence. As users of BRUKER spectrometers are already aware, the scheme of the DEPT experiment imposes a number of restrictions on the pulse sequence; the rf channel used for detection is designated F1 while the second rf channel is designated F2. For each pulse in the pulse sequence the pulse length, pulse phase and rf channel has to be specified as for example (p1 ph1):f1 or (p3 ph3):f1. As shown in the table below pulses p1 to p4 are generally used to describe 90° and 180° pulses, however it is strongly recommended that these pulse definitions are used in all pulse sequences. This approach not only helps other users understand the pulse program more easily and allows the experiment parameters to be set up faster, but more importantly it allows the use of the NMR-SIM's NMR Wizard.

rf channel	90° pulse	180° pulse	p5 - p31[1]
F1	p1	p2	any other pulse
F2	p3	p4	any other pulse

[1]The parameter p16 is recommended for the gradient pulse.

1 ze
2 d1 do:f2
  (p3 ph3):f2
  d2
  (p4 ph4):f2
  (p1 ph1):f1
  d2
  (p5 ph5):f2
  (p2 ph2):f1
  d2
go=2 ph31 cpd2:f2
exit

4.1.2.8(a) Check it in NMR-SIM

Create a new file named *ppexam5.seq* using the **Edit│Create new│Pulse program** command. Using a separate line for each pulse (including the simultaneous pulses p1, p4 and p2, p5) enter the pulses, phases, rf channels and delays. Add the data acquisition command *go =,* the memory deletion command *1 ze* and the loop label *2 d1*. Finally enter the terminating *exit* command and the phase cycling program shown in Fig. 4.10. Using the command **Utilities│Show pulse program…** compare the new pulse program with the scheme in the *result.pdf* file.

The second step is to derive all pulses from the 90° pulse using the "*" operator. If p1 is a 90° pulse, then a 180° pulse p2 on the same rf channel can be expressed as p1*2. A further advantage of this procedure is the fact that only the 90° pulse has to be entered during the experiment parameter setup. However it is not always practical to derive all pulses from the 90° pulse. For instance there are three DEPT experiments DEPT45, DEPT90 and DEPT135, each experiment differs from the other by the value of pulse p5 which corresponds to 45°, 90° or 135° respectively. Defining p5 in terms of the 90° pulse using a fixed multiplier e.g. p1*0.5, p1*1, p1*1.5 would require the pulse program to be corrected for each type of DEPT experiment. Consequently in this case it is advisable to define p5 explicitly.

As shown in the *Check it 4.1.2.8(a),* the execution of delays and pulses is not quite correct, the execution of p1, p4 and p2, p5 should be simultaneous. The next step is to place the pulses p1, p4 and p2, p5 on the same line.

```
1 ze
2 d1 do:f2
 (p3 ph3):f2
 d2
 (p4 ph4):f2 (p1 ph1):f1
 d2
 (p5 ph5):f2 (p2 ph2):f1
 d2
 go=2 ph31 cpd2:f2
 exit
```

4.1.2.8(b) Check it in NMR-SIM

Open the pulse program *ppexam5.seq* using the **Edit│Pulse program** command and replace p2 by *p1*2* and place the simultaneous pulses p1 / p4 and p2 / p5 on the same line as shown below. Save the file as *ppexam6.seq* using **File│Save as…**. Using the command **Utilities│Show pulse program…** compare the pulse program scheme with the scheme from *Check it 4.1.2.8(a).*

Comparing the "literature" sequence scheme with the scheme above there is a difference concerning the second delay d2 between the pulses p1 and (p1*2). This difference arises because the delay d2 cannot be executed until either p1 or p4 has finished depending on which pulse is the longest. To start the delay d2 directly after the execution of the pulse p1, it has to be enclosed in the expression for the p1 pulse (p1 ph1 d2):f1.

4.1.2.8(c) Check it in NMR-SIM

Edit the pulse program *ppexam6.seq* and change the expression (p1 ph1): f1 to include the delay d2 *(p1 ph1 d2):f1*. Delete d2 on the following line. Save the modified file as *ppexam7.seq* and using the command **Utilities│Show pulse program…** compare the new pulse sequence with the "literature" pulse sequence.

It is now possible to use the DEPT pulse program just created to simulate the DEPT135 $^{13}C\{^1H\}$ spectrum of bromomethylcrotonate using the ^{13}C spin system created in *Check it 4.1.1.3.*

4.1.2.8(d) Check it in NMR-SIM

Load the configuration file *st13cde.cfg* (**File│Experiment Setup│Load from file…**) and replace the spin system file either with the file *exam3.ham* previously created in *Check it 4.1.1.3* or the file *exam3p.ham* delivered with the program. Load the pulse program *ppexam7.seq* from the *Check it 4.1.2.8(c).* Run a simulation (**Go|Run Spectrum**) and process the FID with zero filling (**SI(r+i)** = *32k*) and an exponential window function (**LB** value of *2* Hz). Phase the spectrum as shown in the result file.

As the spectrum shows the signals of the methyl and methine carbons are in pure absorption whilst the methylene signal of the CH_2Br group shows a small distortion. This distortion arises because the value of d2 can only be optimized for one value of

$^1J_{CH}$. In *Check it 4.1.2.8(d)* the delay d2, 0.00357s, was optimized for a coupling constant of 140 Hz which is an adequate compromise for the coupling constants of the methyl and methine carbon. However for the CH_2Br group $^1J_{CH}$ is 170 Hz, d2 is not the optimum value and consequently there will be a phase distortion in the DEPT spectrum of the methylene signal. As an exercise *Check it 4.1.2.8(d)* can be repeated using a d2 value of 0.00294s ($= (2 \bullet 170)^{-1}$)) and the results of the two simulations compared.
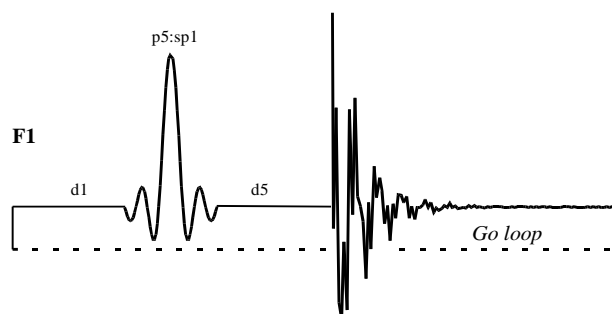
Example 4: Selective excitation

The final example demonstrates the use of selective pulses. As discussed in section 4.1.2.2 a selective pulse is defined using a combination of pulse label and shape label; the command to execute a shaped pulse with a pulse length p5 and a shape sp1 is p5:sp1. The pulse shape must be defined and stored in a file and the pathway to this file must be defined in the **Parameters│Shapes …** dialog box. In *Check it 4.1.2.9(a)* there is a delay d5 prior to acquisition, in the region of 10 µs, to simulate the ordinary pre-scan delay.

4.1.2.9(a) Check it in NMR-SIM

Create a new file named *ppexam8.seq* using the **Edit│Create new│Pulse program** command. In the window enter the pulse program shown in the listing below. Save the pulse program using **File|Save…**. Using the pulse program viewer of NMR-SIM (**Utilities│Show pulse program…**), compare this new pulse sequence with the sequence plotted below.


```
1 ze
2 d1
  (p5:sp1 ph1):f1
  d5
  go=2 ph31
  wr #0
  exit


ph1= 0 2 1 3
ph31= 0 2 1 3
```

To illustrate the new selective excitation pulse sequence the ^1H NMR spectrum of bromomethylcrotonate will be simulated for several frequency offsets.

4.1.2.9(b) Check it in NMR-SIM

Load the configuration file *sel1h.cfg* (**File│Experiment setup│Load from file**. Replace the pulse program by the file *ppexam8.seq* from *Check it 4.1.2.9(a)* and the spin system by either the file *exam1.ham* created in *Check it 4.1.1.2* or the file *exam1p.ham* delivered with the program. Using the pull-down menu **Parameters│Shapes …** open the ***Pulse Shapes Definition*** dialog box and check that **Waveform 1** contains the correct pathway for the shaped pulse e.g. *c:\...\wave\gauss.shp*. Set the value of **SP1** to *50* Hz and close the dialog

box with the command **OK**. Because there will be four simulations with different values of O1 and pulse length p5 it is more convenient to use the **Go|Check Parameters&Go** command to execute the simulation. In the ***Check the experimental parameters*** dialog box set **p5**: *100ms* and **O1** to the following values: *6.9* ppm (H-3), *5.9* ppm (H-2), *5.6* ppm (H-5) and *1.8* ppm (H-1). Process the FIDs using zero filling (**SI(r+i)**: *32k*) and an exponential window function (**LB**: *0.5* Hz).

4.1.2.6 Gradients and the second dimension - The gs-^{13}C, ^{1}H HMQC experiment

In this section the use of gradients and the generation of two dimensional spectra is illustrated using the gradient selected ^{13}C, ^{1}H HMQC experiment as an example. As in the previous section, the starting point is the pulse scheme represented in literature.
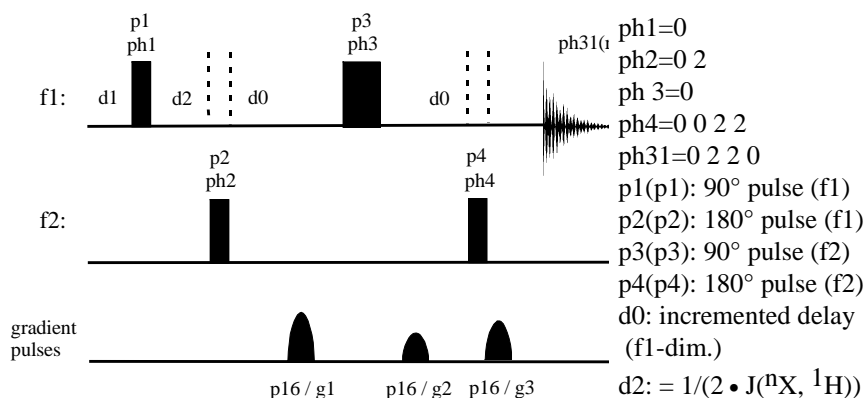

$ph1=0$
$ph2=0\ 2$
$ph\ 3=0$
$ph4=0\ 0\ 2\ 2$
$ph31=0\ 2\ 2\ 0$
$p1(p1)$: 90° pulse (f1)
$p2(p2)$: 180° pulse (f1)
$p3(p3)$: 90° pulse (f2)
$p4(p4)$: 180° pulse (f2)
$d0$: incremented delay (f1-dim.)
$d2$: = $1/(2 \bullet J(^nX, {}^1H))$

Fig. 4.11: The gradient selected ^{13}C, ^{1}H HMQC pulse sequence.

The first step is to define the pulses, phases, delays and the rudimentary acquisition commands according to the scheme shown above using the BRUKER convention for pulse names, see section 4.2.1.4.

4.1.2.10(a) Check it in NMR-SIM

Create a new pulse program file called *ppexam9.seq* using the **Edit|Create new|Pulse program** command. Enter the lines listed below in the blank text editor screen and then add the "literature scheme" phase program above except for the changed pulse names. Take care when entering the delay d0. Now save the file (**File|Save…)** and use the pulse sequence viewer of NMR-SIM (**Utilities|Show pulse program…**) to compare the pulse program with the scheme below.

1 ze
2 d1
  (p1 ph1):f1
  d2
  (p3 ph3):f2
  d0
  (p2 ph2):f1
  d0
  (p3 ph4):f2
 **go=2 ph 31**
  wr #0
  exit
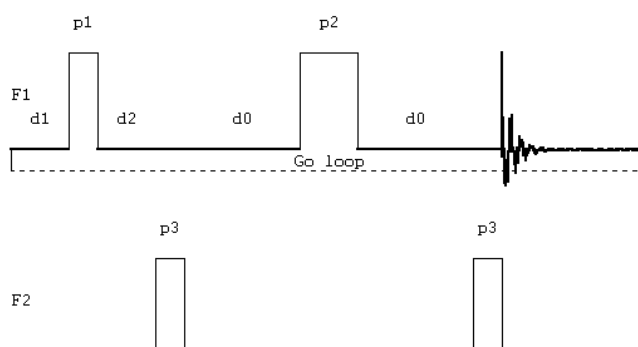
ph1=...

    The scheme corresponds to the standard HMQC experiment without gradient selection and as such does not indicate whether the experiment is either a 1D or 2D data acquisition. To generate a 2D spectrum, the pulse sequence will have to be extended to include commands to increment the delay d0. It is the incrementation of delay d0 that generates the second time domain which is Fourier transformed into the f1 dimension. To increment the delay d0, the command **id0** is appended to the wr #0 statement. The individual experiments that make up the 2D data set are generated using an external loop that saves the FID measured for each value of d0 in a separate data file. This is achieved using the statement **lo to 3 times td1**, the loop counter td1 corresponding to the number of experiments required to make up the f1 dimension.

1 ze
2 d1
3 (p1 ph1):f1
  ...
  go=2 ph 31
  d1 wr #0 **if #0 id0 zd**
  lo to 3 times td1
 exit
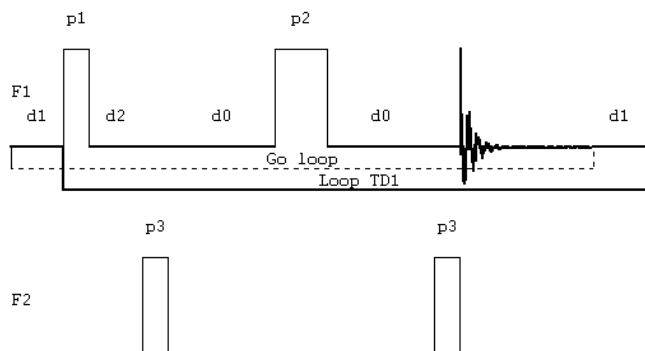
ph1=...

4.1.2.10(b) Check it in NMR-SIM

Open the pulse program file *ppexam9.seq* using the **Edit│Pulse program** command. Add to the pulse sequence the loop label *3* in front of the command *(p1 ph1):f1*, append to the line wr #0 the increment instructions and

> add the line for the external loop for the f1 dimension. Save the file (**File**│**Save)** and use the pulse sequence viewer of NMR-SIM (**Utilities**│**Show pulse program…**) to compare the pulse program with the plotted scheme above.

It should now be possible to recognize this sequence as a 2D experiment. Conversely it is also possible to convert a 2D experiment into a 1D sequence by removing the specific 2D commands and removing the d0 increment loop. The final step is to add the gradient commands. As explained in section 2.3.3 a gradient is always accompanied by a delay before and after its execution. In the "literature" scheme at the beginning of this section the first gradient is executed immediately after the d0 delay and the second gradient is applied before the second delay d0 so that in this case the extra delay before the first gradient and after the second gradient may be omitted. The gradient command consists of two arguments, the gradient length p16 and the gradient amplitude gpi.

4.1.2.10(c) Check it in NMR-SIM

> Open the pulse program file *ppexam9.seq* using the **Edit**│**Pulse program** command. Add the gradient instructions shown in bold below. Save the file (**File**│**Save…)** and use the pulse sequence viewer of NMR-SIM (**Utilities**│**Show pulse program…**) to compare the pulse program with the plotted scheme below.

```
...
(p3 ph3):f2
d0
p16:gp1
d16
(p2 ph2):f1
d13
p16:gp2
d16
d0
(p3 ph4):f2
d13
p16:gp3
d16
go=2...
```
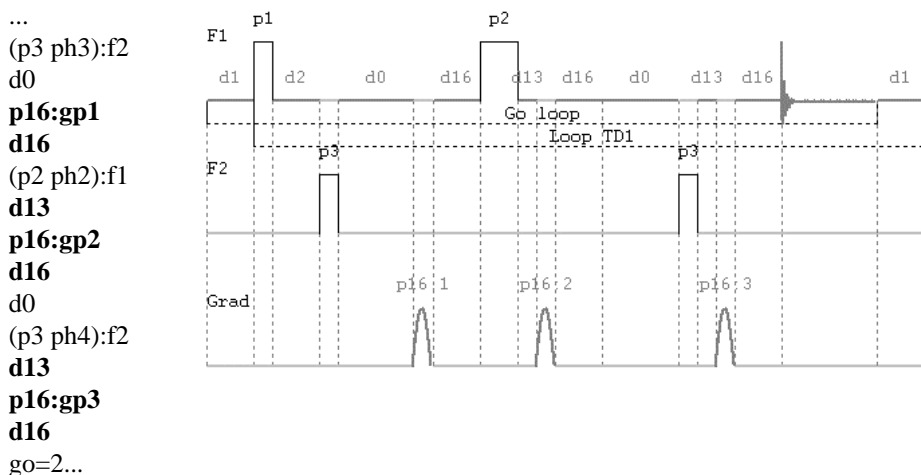

The final *Check it* in this section draws together a number of different threads using spin system definitions and pulse sequences from other *Check its* to simulate both the gradient selected ^{13}C, ^1H HMQC spectrum and the f1/f2 projections of bromomethylcrotonate. To speed up the 2D simulation the virtual spin system definition should only contain the ^1H and ^{13}C chemical shifts and the values of $^1J_{CH}$ shown in the Fig. 4.12.

4.1.2.10(d) Check it in NMR-SIM

The first step is to calculate the ^{1}H and ^{13}C spectra to be used for the 1D projections of the 2D spectrum. Load the file *stan1h.cfg* and replace the spin system by the file *exam1.ham*. Simulate the ^{1}H spectrum. It will be necessary to decrease the value of **SI** because 2D WIN-NMR cannot use large data sets for projections. Process the FID in 1D WIN-NMR using zero filling of **SI(r+i)**:*8k* and an exponential window function with **LB**: *2* Hz. Save the spectrum with a suitable filename e.g. c:\....*projf2*\. Simulate the ^{13}C{^{1}H} spectrum using the configuration file *stan13CH.cfg* and the spin system *exam3.ham*. Process the FID and in a similar way to the ^{1}H data and save the spectrum using a suitable filenamee.g. *c:\....\projf1*\.

To simulate the gs-^{13}C, ^{1}H spectrum, load the configuration file *stghmqc.cfg*. Replace the pulse program by your edited file *ppexam9.seq* from *Check it 4.1.2.10(c)*. Using the **Edit|Create new|Spin system** command create a new file *exam5.ham* and enter the spin system shown in Fig. 4.13. Save the edited spin system (**File⎸Save…**) and replace the spin system by the file. Start the simulation and process the data in 2D WIN-NMR using the **Process⎸xfb** pull-down command. Add the appropriate projections using the **Utilities** button and the **ext** command for each frequency domain.
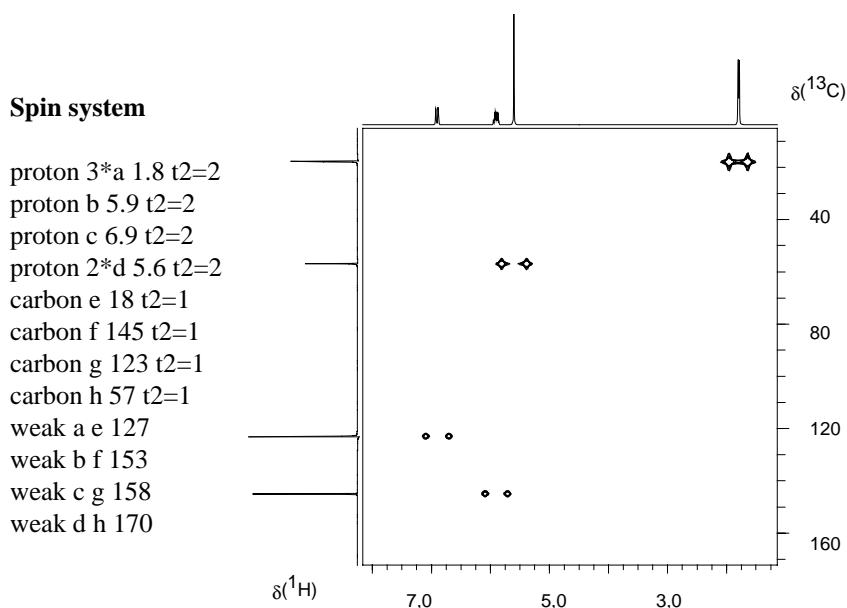
Spin system

proton 3*a 1.8 t2=2
proton b 5.9 t2=2
proton c 6.9 t2=2
proton 2*d 5.6 t2=2
carbon e 18 t2=1
carbon f 145 t2=1
carbon g 123 t2=1
carbon h 57 t2=1
weak a e 127
weak b f 153
weak c g 158
weak d h 170

Fig. 4.12:   The gradient selected ^{13}C, ^{1}H HMQC of bromomethylcrotonate.

At the start of this section it was stressed how important it was to add comments both to spin system definitions and pulse sequences. Comments not only improve the "readability" of pulse programs but also indicate what modifications have been made to standard sequences as illustrated by the examples in this section. In a complex pulse

program the modifications can often be very subtle and without comments it would be very time consuming to cross check several similar pulse programs.

4.2 Experiment and Processing Parameters

4.2.1 Editing the experiment parameters

Pulse programs are written independently of a particular spin system or spectrometer configuration such as magnetic field strength or transmitter pulse power so that, for instance, the same HMQC pulse sequence can be used for a $^{13}C/^1H$, $^{13}C/^{19}F$ or a $^{15}N/^1H$ HMQC experiment. To simulate an experiment it is necessary to select not only, the spin system and pulse sequence, but also the experimental parameter relating to the simulation. The configuration file and job file features in NMR-SIM enables tested simulation parameters to be edited and stored for use in later sessions. Configuration files have been used extensively in the previous sections in this chapter and are used extensively throughout this text. The NMR Wizard can also be used to set up the necessary simulation parameters; this is achieved by searching the spin system and the pulse sequence and, provided that the pulse sequence has been written following the rules in section 4.1.2, the parameters relevant to the simulation are extracted automatically. In the current version the NMR Wizard is restricted to homonuclear spin systems and to the following types of experiments:

1. Standard one-pulse experiment.
2. ^1H or ^{19}F COSY experiments.
3. J-resolved experiments.

The **Go|Optimize parameter** command can be used to determine the optimum parameters for use in a particular experiment. A typical example would be to determine the delay necessary to generate antiphase coherence for several coupled spins, which have very different coupling constant values.

4.2.1.1 Manual Parameter Selection

The setup of experiment parameters can be separated in different categories. The entry of experiment parameters is not just restricted to the dialog box of the **Go│Check Experiment Parameters** pull-down menu command. The **rf channel option bar** is an integral part of the NMR-SIM main window whilst the **Parameters│...** pull-down menu command opens several different dialog boxes. The various different categories of experiment parameters are listed in Table 4.4.

Table 4.4: Categories of Experiment Parameters in NMR-SIM.

Category	Experiment Parameters
Radio frequencies	Rf channel and frequency offsets (O1, O2, OFS)
Signal detection	Dimension of data acquisition (Parmode), detection mode (AQ_mod), spectrometer proton frequency (SF), time domain (TD, TD1), scans (NS), delay, sweep width (SW), incrementation for n dimensional acquisition (nd0 and in0)
Pulse program commands	Delays (d0...d31), pulses (0...p31), pulse power levels (pl1...pl31)
Gradient pulse commands	Gradient pulse duration (p16), gradient amplitude (GPZ0...31)
Selective pulse commands	Pulse duration/ angle (AW0...7) and pulse shape (SPNAM0...16)
Spin system variable start values and increments	Start value (HV1...32), increments (HS1...32)

The experiment parameters are usually defined in the **Go|Check Experiment Parameters** dialog box. As shown in Fig. 4.13 the dialog box is separated into an upper part and a lower part. In the upper part of the dialog box the current pulse program is opened in a text window, the pulse program may be scrolled to examine parameter definitions and comments but cannot be altered in anyway. In the bottom part of the dialog box the experimental parameters selected by the internal pulse program processor may be entered in the various data fields. As an alternative to the **Go|Check Experiment Parameters** command the **Go|Check Parameter & Go** command can be chosen. In this case the simulation process is started automatically after the **Check the experiment parameter** dialog box is closed.

Following the order shown in Table 4.4, the first step is to assign the rf channels to the correct nuclei. During the experiment, pulses on each rf channel are executed at the resonance frequency of the selected nucleus. Each rf channel is assigned to a specific nucleus using it's isotope label, selected from the rf channel option bar as shown below. As shown in Table 4.5 all resonance frequencies are calculated with respect to the ^{1}H resonance frequency. Once the correct NMR resonance frequency has been selected the **Go|Check Experiment Parameters** dialog box can be used to set additional frequency parameters for each rf channel.
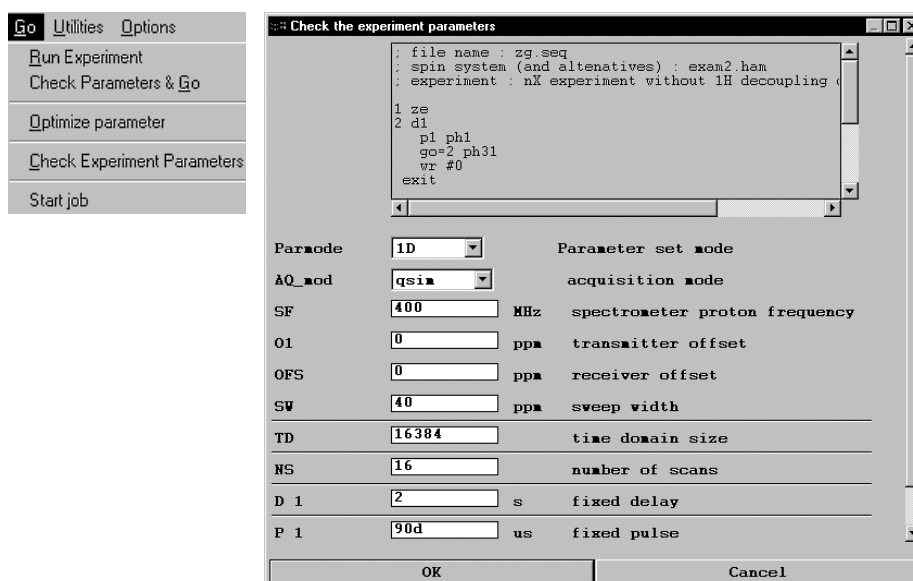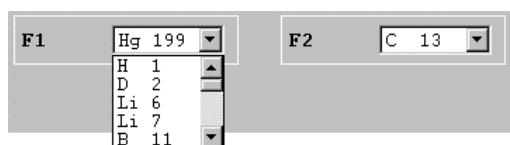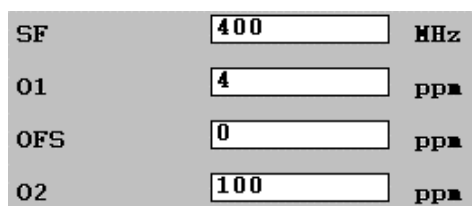
Fig. 4.13: Pull-down menu (left side) and dialog box (right side) of the **Go│Check Experiment Parameter** command.

Rf channel option bar

Check Experiment Parameter dialog box

For the F1 channel the nucleus specified in the **Obs** channel of the rf channel option bar denotes the transmitter frequency **SFO** used for the transmitted pulses and the reference frequency of the spectrum. The centre of the spectrum is **SFO1** (receiver frequency) and is the sum of **SFO** and the offset frequency **O1**. A second parameter **OFS** can be used if a particular pulse sequence requires an additional offset between the transmitter and receiver frequency. Both **O1** and **OFS** must be specified in ppm. The radio frequency of the optional second channel F2 used for decoupling or 2D experiments is specified in the **Dec** channel of the rf channel option bar. The parameter **O2** works in an analogous way to O1 and may be adjusted in the **Go│Check Experiment Parameters** dialog box. See section 2.2 for an introduction and comprehensive explanation of radio frequencies, sweep widths and offsets.

In 2D experiments the term's F1 and F2 channel must not be confused with the expressions for the f1 and f2 dimensions. The F1 channel, which on older spectrometers

is also called the observe channel (Obs), is the rf channel on which the acquired resonance signal is transmitted back from the probehead to the spectrometer to record a FID. The F2 channel or decoupler channel (Dec) is a second rf channel on which a decoupling sequence is executed during acquisition, as for example during a ^{1}H decoupled ^{13}C spectrum. Pulses can also be transmitted on the F2 channel; in an ^{1}H, ^{n}X heteronuclear correlation experiment there are both simultaneous and sequential pulses at the ^{1}H and ^{n}X resonance frequency. In a 2D experiment the f2 dimension corresponds to the normal acquisition domain of a 1D experiment, the signal being acquired on the F1 channel while the f1 dimension is the frequency domain generated by the increment in the delay d0.

The parameters that must be specified for correct data acquisition depends upon the pulse program being used but the most important parameters used in a simulation are shown below. The **Parmode** field is self-explanatory and sets the dimension of the experiment; the two options are *1D* and *2D*. The **AQ_mode** relates to the different acquisition modes that can be used to acquire the data and can be defined as *qf, qsim, qseq*. The **qf** option corresponds to signal detection by a single detector in the x,y-plane of the rotating frame (single phase detection) whilst the *qsim* and *qseq* options correspond to signal detection by two virtual detectors with a 90° phase difference (quadrature phase detection) which is common standard on modern spectrometers. In *qsim* mode both detectors detect the signal simultaneously while in *qseq* mode the signal is detected alternatively, one data point at a time, by each detector. The different acquisition modes are explained in detail in section 2.3.1.

Parmode	2D	
AQ_mod	qseq	
SF	400	MHz
SW	10	ppm
TD	512	
TD1	512	
ND0	2	
NS	2	
D 0	0.003	s
IN 0	0.025	s

The parameter **SF**, following common convention, describes the spectrometer magnetic field strength in terms of the ^{1}H proton resonance frequency in MHz. As shown in Table 4.5 all resonance frequencies are calculated with respect to the ^{1}H resonance frequency. The sweep width **SW** used for the acquisition has to be entered in ppm.

The parameters **TD** and **TD1** relate to the number of time domain data points in a data set. **TD** determines the number of data points used to acquire the data in a standard 1D experiment or in the f2 dimension of a 2D experiment. **TD1** determines the number of data points in the f1 dimension and describes the number of experiments and increments in d0 used to generate the f1 dimension of a 2D matrix. The total number of time domain data points has to be specified in multiples of 2 words. Alternatively k values can be used, where for example: 1k = 1024 words, 2k = 2048 words...There are three additional parameters for a 2D experiment **d0** (start value 3μs), **nd0** and **IN0** which are used to calculate the f1 sweep width. **nd0** is the number of times the delay d0 occurs in a pulse sequence, if the TPPI phase increments

option is selected nd0 must be multiplied by 2. **IN0** is calculated as shown in equation [4-4] in Table 4.5. For homonuclear experiments the sweep width may be entered directly for both frequency domains as **in0**: *SW*.

Table 4.5:   The relationship between radio frequency intensity, frequency, pulse duration and pulse power.

radio frequency field intensity (pulse power)

B_1(nucleus i) = B_1(proton) • (γ(nucleus i) / γ(proton))   [4-1]

reference radio frequency of nucleus i

SFO = SF • (γ(Obs) / γ(proton))   [4-2]

radio frequency of the spectrum centre (receiver frequency)

SFO1 = SFO + O1   [4-3]

spectral range of the f1 dimension

SW(f1) [ppm] = 1 / (nd0 • IN0 [1/Hz] • SFO [Hz])   [4-4]

pulse duration of a pulse assigned to the resonance frequency of a nucleus i

τ [μs] = normalized pulse angle [deg] / 360[deg] / (B_1[Hz] • (γ(nucleus i)))   [4-5]

The pulse program processor selects all the relevant pulse and delay variables and lists them in the **Go|Check Experiment Parameters** dialog box.

D16	0.02■	s
D20	0.00257	s
P 1	90d	us
P 2	180d	us
PL 1	1e+006	Hz
PL 2	1e+006	Hz

Delays **d0...d31** can be entered in units of seconds [s], milliseconds [ms] or microseconds [u] as shown on the left. Pulses **p0..p.31** can be specified as normalized pulses using the option *d* (=degree). So for instance the entry *180d* corresponds to a 180° pulse. In the **Options|NMR-SIM settings** dialog box, if the option *Modify rf fields* is checked, the NMR-SIM processor calculates the pulse duration taking into consideration the pulse power, the selected nucleus and the rf channel. If a pulse is entered as a time a pulse of that duration is executed virtually. The time unit options for pulse duration are exactly the same as for delays. The pulse power identifiers **pl0.. pl.31** sets the radio frequency strength in Hz units and have the value 0 to 1e007 [Hz].

For gradient pulses both amplitude and pulse duration must be specified.

P16	1000	us

The gradient field strength is multiplied by the gradient intensity modifier **GPZ0...31**. The

GPZ 1	50
GPZ 2	30
GPZ 3	40

possible value are from -100 to 100 [%]. The gradient pulse length **p16** follows the same rules as the high power pulses p0...31. Typical values of a gradient pulse are in the range of 1000 to 1500 μs. In this book the variable p16 is used exclusively for gradient pulses. This teaching version of NMR-SIM will only support z-gradients with a GAUSSIAN shape. For selective pulses the pulse shape and the pulse power must be defined. The filename of the shaped pulse are assigned to the NMR-SIM variable parameters **SPNAM0...16** and are defined in the **Parameters│Shapes** dialog box. The power levels are assigned to the variable parameters **SP0...7** and are defined in the **Go│Check Experiment Parameters** dialog box. With the exception of adiabatic pulses, all shaped pulses can be specified as normalized pulses.
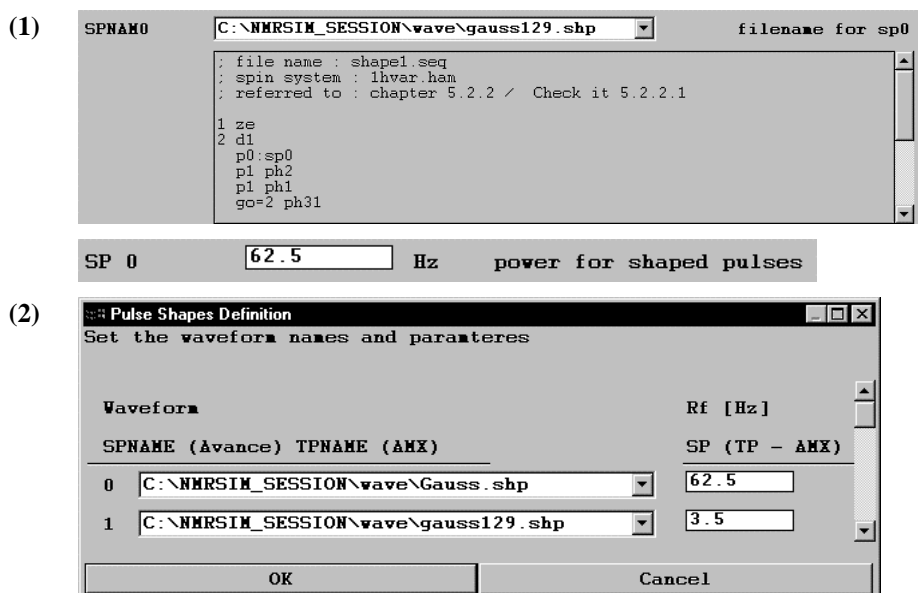
(1)

SPNAM0   `C:\NMRSIM_SESSION\wave\gauss129.shp`   filename for sp0

```
; file name : shape1.seq
; spin system : 1hvar.ham
; referred to : chapter 5.2.2 /  Check it 5.2.2.1

1 ze
2 d1
  p0:sp0
  p1 ph2
  p1 ph1
  go=2 ph31
```

SP 0   62.5   Hz   power for shaped pulses

(2)

Pulse Shapes Definition

Set the waveform names and parameteres

Waveform   Rf [Hz]

SPNAME (Avance) TPNAME (AMX)   SP (TP – AMX)

0 `C:\NMRSIM_SESSION\wave\Gauss.shp`   62.5

1 `C:\NMRSIM_SESSION\wave\gauss129.shp`   3.5

OK	Cancel

Fig. 4.14:   (1) Shaped pulses related parameter of the **Go|Check Experiment Parameters** dialog box; (2) **Parameters│Shapes** dialog box.

If variable spin system parameters are used the increment step **HS1...32**, the start value **HV1...32** and the loop limit **L0...L31** must be assigned. The range over which a variable parameter is varied depends upon the increment step size and the loop limit. If required by the pulse program these parameters will appear the **Go│Check Experiment Parameters** dialog box. As discussed in previous sections, loop definitions are not only restricted to spin system variable incrementation.

L0...L31 must be a positive integer. The start values **HV1...32** and the increment values **HS1...31** of the spin system variables must be defined in Hz.

Most experiment parameters can be modified independently of the **Go│Check Experiment Parameters** dialog box by using the pull-down menu command **Parameters│..**. This command opens a number of different dialog boxes relating to pulses, delays, increment steps or pulse shapes etc., where it possible to enter the appropriate parameters. Fig. 4.15 shows the **Parameters│Pulses…** dialog box for setting the high power pulses.
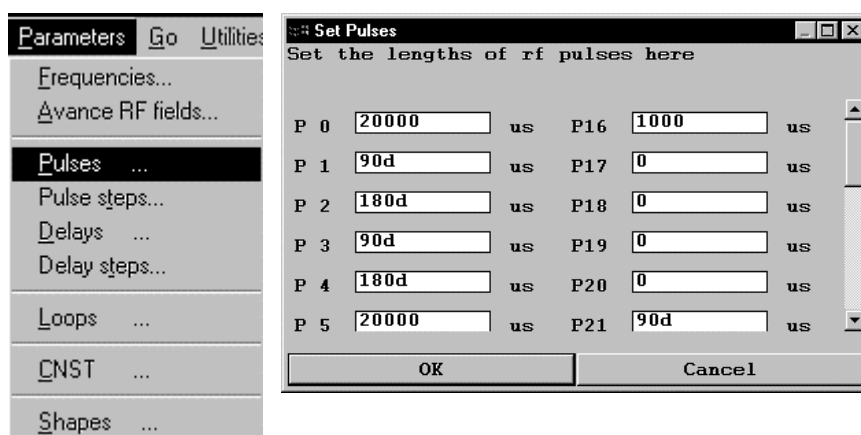

Fig. 4.15: Dialog box opened using the pull-down menu **Parameters|…** command for the sub-menu **Pulses**.

Only the most significant experimental parameters have been discussed in this section, the reader is referred to the NMR-SIM manual for a description of the remaining parameters. The simulations in this book only use the experimental parameters discussed in this chapter.

4.2.1.2 Using Configuration Files

If a simulation has been completed successfully it would be extremely useful to be able to save all the relevant parameters such as the spin system, pulse program, experimental and processing parameters in a file. In NMR-SIM this type of file is called a **configuration** file. Configuration files have been used extensively in this chapter allowing the same experiment parameters to be used in different NMR-SIM simulations. To perform a set of simulations on different spin systems using the same experimental setup, it is only necessary to load the appropriate configuration file and to replace the spin system accordingly.

The configuration file commands **Load from file…** and **Save to file…** are called from the **File│Experiment setup** pull-down menu. As shown on the right hand side of Fig. 4.16, configuration file are simple ASCII text file containing the file names of the spin system, pulse program and, if required, experiment parameter lists such as a delay list etc. Additional experiment and processing parameters are saved in the later sections of the configuration file.
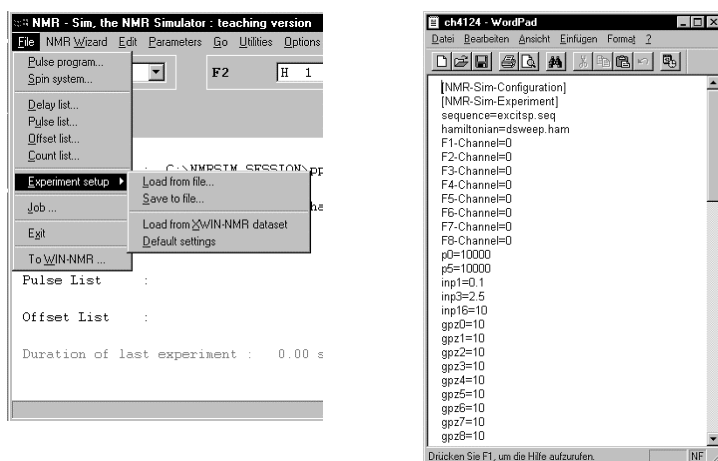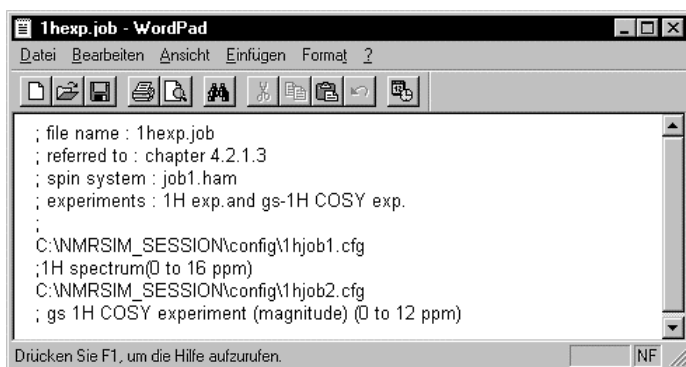

Fig. 4.16:   Pull-down menu **File│Experiment setup** to handle configuration files (left side) and view of a configuration file to calculate a ^{1}H spectrum.

To load an existing configuration file the **File|Experiment Setup|Load from file…** command is used to select the filename of the required configuration file from a standard windows file list box. There are a number of steps required to create a new configuration file, the first is to specify the spin system, pulse program and to assign the nuclei and frequencies for the Obs- and Dec-channel. In the next step all the experiment parameters must be entered in the **Go│Check Experiment Parameters** dialog box, if required optional delays, pulse or offset lists can be loaded and edited. Finally the processing parameters which are automatically transferred to 1D WIN-NMR or 2D WIN-NMR for data processing are entered in the **Options│Processing Parameters…** dialog box. Once all the parameters have been entered and a successful test simulation completed the configuration is saved using the **File│Experiment setup│Save to file…** command, the name for the new configuration file being entered in the dialog box. Configuration file have the extension **.cfg**.

Because configuration files are text files, existing configuration files can be easily amended using either NMR-SIM or a simple text editor and the modified file stored under the same or a new filename. If a text editor is used the file must be stored as a plain ASCII text file.

4.2.1.3 Using Job Files

A job file is a text file containing a number of different configuration files, which are loaded, sequentially into NMR-SIM and the corresponding experiment simulated. As shown in Fig. 4.17, the job file can also contain optional comments. Job files maybe modified by deleting or adding further parameters to the configuration files.
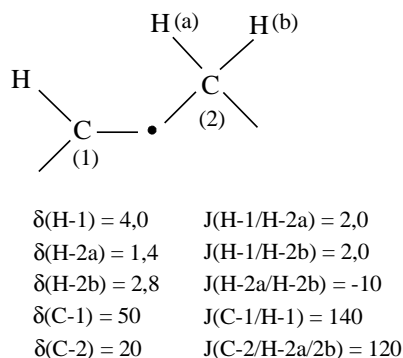

Fig. 4.17:   Listing of the *1hexp.job* file.

The definition and execution of "jobs" uses three pull-down menu commands. A job is selected using the **File⏐Job…** command. It is also possible to change an existing job or to create a new job based on an existing file using the **Edit⏐Job definition** command. To create a new job file an old job file has to be opened, the text modified to include the required configuration files and the file saved under a new name using the **File|Save as…** command. Finally the series of simulations is started by the **Go⏐Start job** command.

In *Check it 4.2.1.1* a job file is used to simulate a typical experimental combination used for routine structure analysis; a standard 1D ^{1}H spectrum and a 2D gradient selected ^{1}H COSY experiment.

δ(H-1) = 4,0   J(H-1/H-2a) = 2,0
δ(H-2a) = 1,4   J(H-1/H-2b) = 2,0
δ(H-2b) = 2,8   J(H-2a/H-2b) = -10
δ(C-1) = 50   J(C-1/H-1) = 140
δ(C-2) = 20   J(C-2/H-2a/2b) = 120

4.2.1.1 Check it in NMR-SIM

Using the **File⏐Job…** command select the job file *1hexp.job*. Modify the spin system (**Edit⏐Spin system)** by replacing the existing spin system parameters with those listed on the left-hand side of this *Check it*. In the **Options⏐NMR-SIM settings…** dialog box select the option *Output File* to *User defined*. Start the job using the **Go⏐Start Job** command. Enter appropriate output file names and process the spectra at the end of the job execution in 1D WIN-NMR and respectively 2D WIN-NMR.

In *Check it 4.2.1.2* a second job, listed in Fig. 4.18, is used to simulate a ^{13}C, a DEPT135-^{13}C{^{1}H} and a gradient selected ^{13}C, ^{1}H HMQC experiment which are typically used for the routine structure analysis of hydrocarbons.

```
; file name : 13cexp.job
; referred to : chapter 4.2.1.3
; spin system : job2.ham
; experiments :
; 13C{1H} spectrum (0 to 220 ppm)
; DEPT135-13C{1H} spectrum
; gs 13C, 1H HMQC spectrum
; [1H: 0 to 12 ppm; 13C: 0 to 220 ppm]
;
13cjob1.cfg
13cjob2.cfg
13cjob3.cfg
.
```

Fig. 4.18: Listing of the *13cexp.job* file.

4.2.1.2 Check it in NMR-SIM

Using the **File│Job…** command select the job file *13cexp.job*. If necessary modify the spin system (**Edit│Spin system)** by replacing the existing spin system parameters with those listed in *Check it 4.2.1.1*. In the **Options│NMR-SIM settings…** dialog box toggle the option *Output File* to *User defined*. Start the job using the **Go│Start Job** command. Enter appropriate output file names and process the spectra at the end of the job execution in 1D WIN-NMR or 2D WIN-NMR.

4.2.1.4 NMR Wizard for homonuclear experiments

In this teaching version of NMR-SIM the NMR Wizard may only be used for setting up homonuclear experiments, any attempt to set up a heteronuclear experiment will generate an error. Consequently this version of the NMR Wizard is only really suitable for nuclei with high receptivity to the NMR experiment such as ^{1}H, ^{19}F and possibly ^{31}P. Shaped pulses are not supported in any form. In addition to selecting the experimental parameters, the NMR-Wizard can also select the appropriate processing parameters but if necessary this function can be switched off and the parameters can be entered manually.

Before using the Wizard the correct nucleus must first be specified in the **Obs** channel of the rf channel option bar and the various options in the **Options|NMR-SIM settings** dialog box set. The NMR Wizard is started using the **Wizard** command which opens the dialog box shown in Fig. 4.19.
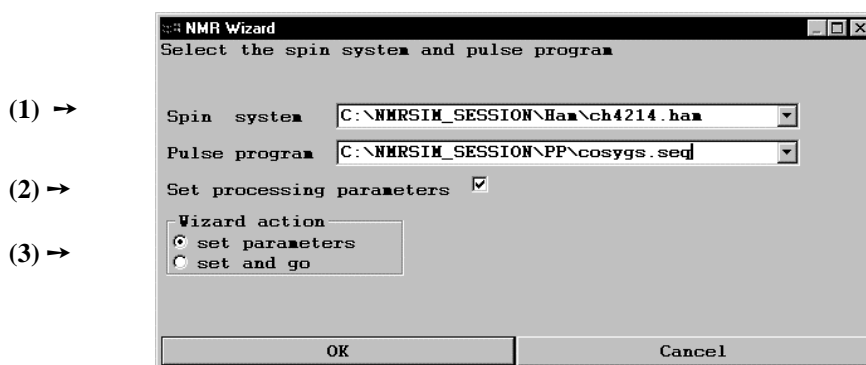
Fig. 4.19: NMR Wizard dialog box.

The dialog box of the wizard contains several different options that can be specified.

1. The current spin system and pulse program can be changed using the file selection box.
2. The wizard can set the processing parameters.
3. The wizard can either just set the appropriate parameters or set the appropriate parameters and simulate the experiment.

For the wizard to work correctly some rules have to be obeyed. The wizard's work is based on the information contained in the pulse program and assumes that the pulses and delays conform to the standard Bruker pulse programming language definitions. The most common of these definitions are listed in Table 4.6. For manual spectrometer operation any convention may be used, but if the NMR Wizard is to be used successfully the standard definition must be strictly adhered to.

Table 4.6: Standard BRUKER pulse programming language definitions.

Rf channels, pulse angles and power levels		Delay Times	
p0	no default value	d0	incremented delay (2D) [3 u]
p1	f1; 90 degree; high power pulse.	d1	relaxation delay; 1-5 • T_1
p2	f1; 180 degree; high power pulse.	d2	1/(2J)
p3	f2; 90 degree; high power pulse	d3	1/(3J)
p4	f2; 180 degree; high power pulse	d4	1/(4J)
p5	f1; 60 degree; low power pulse	d5	DE/2
p6	f1; 90 degree; low power pulse	d6	delay for evolution of long range couplings
p7	f1; 180 degree; low power pulse	d7	delay for inversion recovery
p8	f2; 60 degree; low power pulse	d8	mixing time
p9	f2; 90 degree; low power pulse	d9	random delay

p10	f2; 180 degree; low power pulse	d10	incremented delay (3D)
p11	f1; 90 degree; shaped pulse	d11	delay for disk I/O [30 m]
p12	f1; 180 degree; shaped pulse	d12	delay for power switching [20 u]
p13	f2; 90 degree; shaped pulse	d13	short delay (e.g. to compensate delay line) [4 u]
p14	f2; 180 degree; shaped pulse	d14	delay for evolution after shaped pulse
p17	f1; trim pulse [2.5 m]	d16	delay for homospoil/gradient recovery
p18	f1; shaped pulse for off-resonance presaturation	d17	delay for DANTE pulse train
p19	2nd homospoil / gradient pulse	d27	delay for shaped gradient
p20	f2; trim pulse [2.5 m]		

If a conflict occurs between the standard pulse program definitions and the current pulse program or spin system the wizard function displays an error warning and the value have to be entered manually.
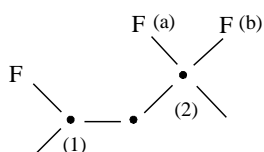
In *Check it 4.2.1.3* the NMR Wizard is used to automatically adapt experimental parameters from one nucleus to another. Starting with the ^{1}H spin system and the simulation of the ^{1}H COSY spectrum the spin system is changed to the analogous ^{19}F spin system and the wizard used to determine the correct parameters to simulate the ^{19}F COSY spectrum.
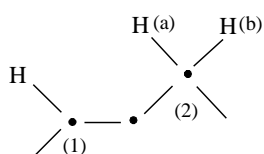
4.2.1.3 Check it in NMR-SIM

Load the configuration file *ch4213.cfg* using the **File│Experiment Setup│Load from file…** command. Start the NMR Wizard using the **NMR Wizard** command. Select the options *Set processing parameters* and *set and go*. Click on the **OK** button. Process the ^{1}H COSY spectrum in 2D WIN-NMR using the following parameters:

δ(H-1) = 4,0   J(H-1/H-2a) = 2,0
δ(H-2a) = 1,4   J(H-1/H-2b) = 2,0
δ(H-2b) = 2,8   J(H-2a/H-2b) = -10

	F2	F1
SI	512k	512k
WDW	QSINE	QSINE
SSB	0	0
PH-mod	no	mc

The SF frequency value should be the same for both dimensions. If required the spectrum can be calibrated. The calculated spectrum should be the same as in the result file.

δ(F-1) = -160   J(F-1/F-2a) = 10
δ(F-2a) = -110   J(F-1/F-2b) = 10
δ(F-2b) = -105   J(F-2a/F-2b) = 160

In NMR-SIM replace the spin system by the file *ch4213b.ham* (**File|Spin system…**). Select *F19* for the Obs channel and start the NMR wizard again. In 2D WIN-NMR select the same options as before and process the data. The simulated ¹⁹F COSY spectrum should be the same as the spectrum in the *result.pdf* file.

4.2.1.5   Parameter Optimization

The parameter optimizer routine can be used to find the optimum delay for a particular 1D sequence or to determine the pulse length for a specific power level and pulse angle combination. A series of spectra are calculated that differ by a constant increment in the parameter being optimized, the optimum delay or pulse length is then determined by examining the signal intensities in the simulated spectra.

The calculated spectra may be represented either as a 1D spectrum, a series of 1D spectra or as a pseudo 2D spectrum. As such the delay or pulse angle in any 1D pulse sequence can be optimized without the pulse sequence having to be modified in anyway. For 2D experiments the pulse program must be converted to its 1D analogue. The optimization process is started using the menu bar command **Go⎮Optimize parameter**. Fig. 4.19 shows the **Parameter optimizer** dialog box where a number of different options may be selected.
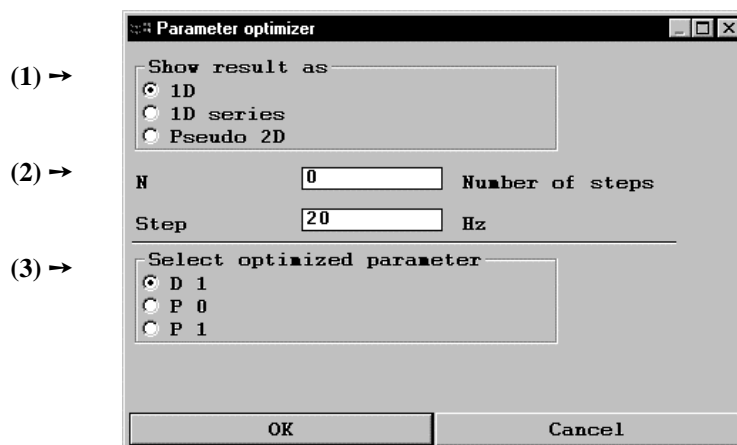
Fig. 4.20:   Parameter optimizer dialog box.

It is possible to choose between different display representation (1) for the simulated spectra. In pulse duration type experiments the 1D spectrum display is the recommended option whilst, because of the serious signal overlap that would occur in a 1D spectrum, the 1D series or pseudo 2D display are the best option to show the influence of a delay on a coupling pattern. The next three *Check its* show the main applications of the parameter optimizer routine.

A typical problem that can be solved by the parameter optimizer is the determination of the pulse duration for a given pulse power level and tilt angle.

4.2.1.4 Check it in NMR-SIM

Load the configuration file *ch4214a.cfg* using the **File│Experiment Setup│Load from file…** command. In the **Options│NMR-SIM settings…** dialog box toggle the **Output File** to *User defined* and check the **Modify RF fields** option. Select the **Go│Optimize Parameter** command and in the parameter optimizer dialog box select the **Show results as** *1D* option, set the **Number of steps N** to *40*, the **Step** size to *20* Hz, and the **Select optimized parameter** *p1*. Click on the **OK** button. In the **Set the optimized parameter** dialog box set the value of **p1** to *0* µs and **inp0** to *1* µs. Click on the **OK** button. Enter an appropriate output filename and process the data in 1D WIN-NMR using an exponential window function with **LB** = *1* Hz. The excitation profile of signal intensity against pulse length is shown in Fig. 4.22.
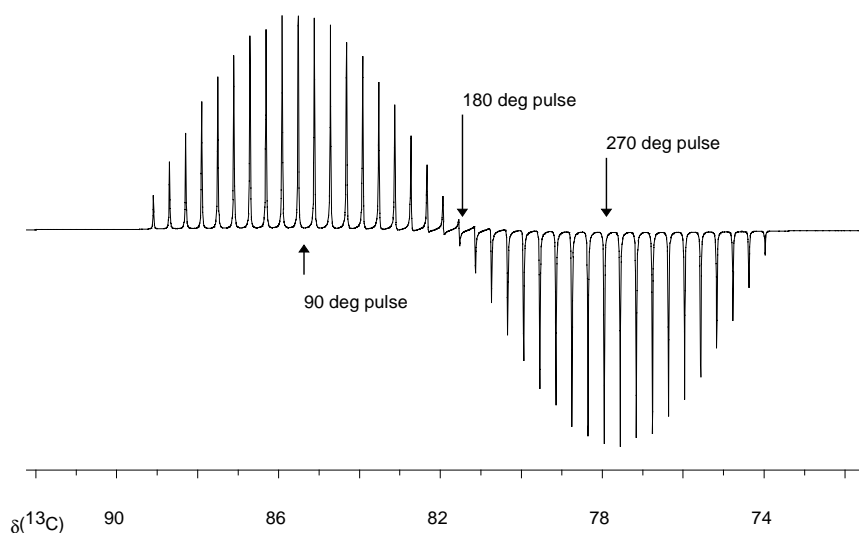
Fig. 4.20:   Optimization of a pulse duration, using the *Show the results* as 1D option, starting at 0 µs in 1 µs steps.

Many pulse sequences use delay periods during which, for instance, the antiphase coherence due to $^1J_{CH}$ coupling evolves. This delay period would be easy to calculate if the value of all the $^1J_{CH}$ coupling constants where the same but unfortunately this is not true in practise and a compromise must be made. *Check it 4.2.1.5* illustrates this problem and uses the NMR-SIM optimizer to find a compromise delay period for a 1D HMQC experiment.

4.2.1.5 Check it in NMR-SIM

Load the configuration file *ch4215.cfg* using the **File**⎮**Experiment Setup**⎮**Load from file…** command. Select the **Go**⎮**Optimize Parameter** command. In the parameter optimizer dialog box select the **Show the results as** *1D series* option, the **Number of steps N** to *10*, the **Step** size to *20* Hz and the **Select optimized parameter** *d2*. Click on the **OK** button. In the **Set the optimized parameter** dialog box set **d2** to *0.0034* s and **in2** to 0.*2* ms. Click on the **OK** button. Enter an appropriate output filename and ensure that the **Exp No** is set to *1*. Click **OK** and 10 files with experiment numbers 1 to 10 will be calculated. After the simulation has been completed 1D WIN-NMR will be started and the FID of the last file will be loaded into the main window. Process all the files in the same way using the **File**⎮**Serial processing** command. In the **Automatic Serial Processing** dialog box change to the directory where the simulated files are stored and select all the files for processing by clicking the appropriate filename with the mouse. A list of files for processing dialog box will appear in the **List of selected Files** window. Click on the **Select common Job** button, change to the directory *...\nmrsim_session\config* and load the 1D WIN-NMR job file *paropt.job*. Click on the **Execute** button. The processed spectra will be saved in the same directory as the unprocessed data. When the serial processing is complete use the **Display**⎮**Multiple Display** command to display

The last example is a DEPT45 experiment where the d2 delay must be optimized for two different ^{1}J(C, H) coupling constants for a CH and a CH$_2$ group. *Check its 4.2.1.6(a)* and *(b)* show two alternative methods of displaying the results as a series of 1D spectra or as a pseudo 2D spectrum.

4.2.1.6(a) Check it in NMR-SIM

Load the configuration file *ch4216a.cfg* using the **File**⎮**Experiment Setup**⎮**Load from file…** command and in the **Options**⎮**NMR-SIM settings…** dialog box toggle the option *Output File* to *User defined*. Use the **Go**⎮**Optimize Parameter** command and in the **Parameter optimizer** dialog box select the **Show the results as** *1D series* option, the **Number of steps N** to *10* and the **Select optimized parameter** *d2*. Click on the **OK** button. In the **Set the optimized parameter** dialog box set the value of **d2** to *0.0014s* and **in2** to *0.2m*. Click on the **OK** button. Enter an appropriate output filename and ensure that the **Exp No** is set to *1*. Click **OK** and 10 files with experiment numbers 1 to 10 will be calculated. After the simulation has been completed 1D WIN-NMR will be started and the FID of the last file will be loaded into the main window. Process all the files in the same way using the **File**⎮**Serial processing** command. In the **Automatic Serial Processing** dialog box change to the directory where the simulated files are stored and select all the files for processing by clicking the appropriate filename with the mouse. A list of files for processing will appear in the **List of selected Files** window. Click on the **Select common Job** button, change to the directory *...\nmrsim_session\config* and load the 1D WIN-NMR job file *paropt.job* from *....\nmrsim_session\jobs*. Click on the **Execute** button. The processed

spectra will be saved in the same directory as the unprocessed data. When the serial processing is complete use the **Display│Multiple Display** command to display the processed spectra.

4.2.1.6(b) Check it in NMR-SIM

To represent the optimization results as a pseudo 2D spectrum repeat the procedure of *Check it 4.2.1.6(a)*. However, in the parameter optimizer dialog box select the option Show the results as *pseudo 2D series* and the Number of steps **N** to *16* (in 2D WIN-NMR the number of experiments must be a multiple of 8). Enter the same output filename as in the previous *Check it* but ensure that **Exp No** is set to an unused number e.g. *20*. When the simulation is complete 2D WIN-NMR is started automatically and the serial file of the pseudo 2D spectrum should be loaded ready for processing. If the serial file is not loaded automatically use the **File|Open…** command to open the file manually. Select the pull-down menu command **Process│General parameter setup│edp** and change the value of **SI(F1)** from *8* to *16*, check that the parameters **STSI(F1)**, **STSI(F2)**, **TDEFF(F1)** and **TDEFF(F2)** are all 0. Click **Save** to close the dialog box. Start the processing in the f2 dimension using the **Process│Transform of F2 rows** (xf2) command. To represent the results as stack plot click the **Stack show** button on the left hand side of the main 2D WIN-NMR display window. To improve the appearance of the spectrum click the Manual button and in the **Set Stack Show colors** dialog box set **Sampling** to *2* and **Alpha** to *60*. Alternatively click the **Grid** button and adjust the display manually for the best appearance.

Both representations illustrate the phase distortion that occurs because it is impossibility to optimize the d2 value for two different $^1J(C, H)$ coupling constants. An acceptable compromise is to use the arithmetic mean of the optimum delay for each coupling constant.

4.2.2   Editing Processing Parameters

For a set of simulated data it would be desirable to be able to process all the data using the same processing parameters, such as zero filling or window function. It is possible to define a limited number of processing parameters in NMR-SIM and have these parameters transferred directly to 1D WIN-NMR or 2D WIN-NMR with the simulated experimental data. It is then possible to process the simulated data utilizing the parameters defined in NMR-SIM using all the standard processing commands in 1D WIN-NMR and 2D WIN-NMR.

The pull-down menu **Options|Processing parameter…** opens the dialog box shown in Fig. 4.21 displaying all the processing parameters that may be set in NMR-SIM.
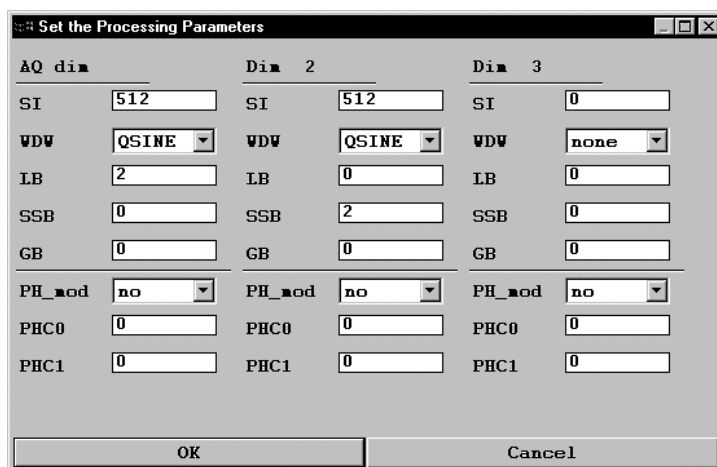
Fig. 4.21: Set the Processing Parameters dialog box.

The key parameters in the **Set the Processing Parameters** dialog box are explained briefly in Table 4.7. A complete introduction to data processing is given in number of textbooks [3.1, 3.2] as well as in the companion volume in this series *NMR Spectroscopy: Processing Strategies* [4.1].

The dialog box contains three columns labelled **AQ dim**, **Dim 2** and **Dim 3**. In a 1D experiment AQ dim corresponds to the standard time domain for the detected nuclei. Similarly in a 2D experiment AQ dim, or the f2 dimension, is again the standard time domain for the detected channel while Dim 2, or f1 dimension, is the frequency axis generated by the increment in d0. Dim 3 is reserved exclusively for 3D experiments which is only allowed in the full version of NMR-SIM.

Table 4.7: Input fields of the Set the Processing Parameters dialog box.

The parameter **SI** defines the number of data points in the spectrum. **TD**, the number of data points in time domain, can be different from the value of SI and the procedure of zero filling (see ref. [4.1]) enables a SI value greater than TD to be used in the data processing.

WDW `EM`

Fourier transformation of a FID, which has not decayed to zero intensity causes a distortion ("wiggles") at the base of peaks in the spectrum. By applying a suitable window function **WDW** the FID will decay smoothly to zero. A variety of window functions options are available, none, exponential **EM**, gaussian **GM**, sine **SINE**, squared sine **QSINE** and trapezoidal **TRAP** function. The best type of window function depends on the appearance of the FID and the resulting spectrum. Consequently where possible it is best to fit the window function interactively.

LB `2`

SSB `0`

GB `0`

The variables **LB**, **SSB** or **GB** can vary the overall effect of the window function. The type of window function determines the parameter and range of values used:

EM function: LB > 0, GM function: LB <0, GB > 0, QSINE / SINE function: SSB > 0; TRAP function: TM0,..., TM3 values can only be set in 1D or 2D WIN-NMR.

PH_mod `no`

Depending on the detection mode the appropriate phase mode has to be chosen. The possible options are **no**, **pk**, **mc** and **ps** for no phasing, phase correction using phase constants **PHC0** and **PHC1**, magnitude and power spectrum calculation respectively. For further information on these parameters see section 3.2.3.3.

PHC0 `0`

PHC1 `0`

A phase correction has to be applied for two reasons:
The zero-order phase correction **PHC0** arises because of the phase difference between the receiver and the detection pulse. Additional frequency dependent phase deviations arising from chemical shift evolution in the short delay between the last pulse and the signal detection can be compensated by a first-order phase correction **PHC1!**.

4.3   Using the Bloch Simulator

4.3.1   A Classical and Pictorial Approach

The Bloch Simulator is based on the BLOCH equations, named after FELIX BLOCH, one of the pioneers of NMR. The underlying mathematical approach used by BLOCH to understand the phenomenon of the resonance experiment was based upon the concept of

the macroscopic magnetization vector. The effect of a rf pulse on a spin system and the subsequent relaxation back to the equilibrium state can be described by the behaviour of this vector. The macroscopic magnetization vector can also be visualized from a microscopic point of view. The nuclei of the same NMR active isotope can be described by spin vectors where the "spins" represent the magnetic moment of each nucleus. The spin vectors precess about the static magnetic field B_o at the NMR resonance frequency and because the BOLTZMANN distribution favours the lower energy state there are slightly more vectors aligned with the magnetic field than against. Using basic vector addition it is possible to combine all the spins to generate a **net macroscopic magnetization vector** aligned along the static magnetic field B_0.

This classical mechanic approach is often used to illustrate NMR, the concept of a 90° pulse being easily visualised using the macroscopic magnetization vector. However this theory neglects all quantum mechanic effects and is based on the assumption that the magnetization vector can only be defined for ensembles of independent and uncoupled nuclei. The single magnetization vector cannot explain phenomena such as coupling evolution or the existence of multiple quantum states and therefore is unsuitable for understanding modern pulse sequences. Consequently NMR-SIM uses a quantum mechanical approach to simulate the effect of a pulse sequence based on the LIOUVILLE space equation and density matrix methods. Details about the theoretical background of NMR-SIM are given in section 2.2.

The Bloch Simulator is used primarily to calculate and visualize the basic effects of different types of pulses and small pulse sequence fragments using a purely classical macroscopic magnetization approach. To simplify the calculations the simulator ignores the relaxation processes that formed part of the original BLOCH equations. There are three main applications for the Bloch simulator:

- The simulation of shaped pulses
- The simulation of composite pulses which are defined as pulse sequence fragments
- The simulation of rudimentary pulse sequence units such as spin echoes

The simulator offers several different calculation modes designed to display a particular property of a pulse or sequence fragment in the most appropriate manner. The application of the different calculation modes is summarized below.

representation	available for: shaped pulses	pulse sequence fragments
Time evolution	✔	✔
Excitation profile	✔	✘
Rf field profile	✔	✘
Waveform analysis (particularly for adiabatic pulses)	✔	✘

The **Time evolution** calculation displays the movement of the magnetization vector in the rotating coordinate system. Several magnetization vectors with different rf offsets can be calculated simultaneously, the rf offset corresponding to the frequency difference between either the individual magnetization vector and the on-resonance magnetization vector or to the rotation frequency of the coordinate system. By clicking the **Movie** button the time evolution is demonstrated as a slow motion animated video. This type of representation is best suited to study the effect of rf pulses or short pulse sequence fragments and the relationship between experimental parameters such as pulse shape, phase error or delays and different rf offsets.

There is a difference in appearance between the representation of the magnetization vectors in NMR-SIM and the classical literature approach. Because NMR-SIM is an interactive process, it is possible to simplify the display. The movement of each magnetization vector is indicated by a line drawn out on the surface of a sphere by the tip of the magnetization vector as a function of time. In the literature with a static diagram the same process would be indicated by a vector in the initial position and final positions with the movement of the magnetization vectors being denoted by dotted arrows. Fig. 4.22 shows the same pulse sequence fragment in the two different representations.
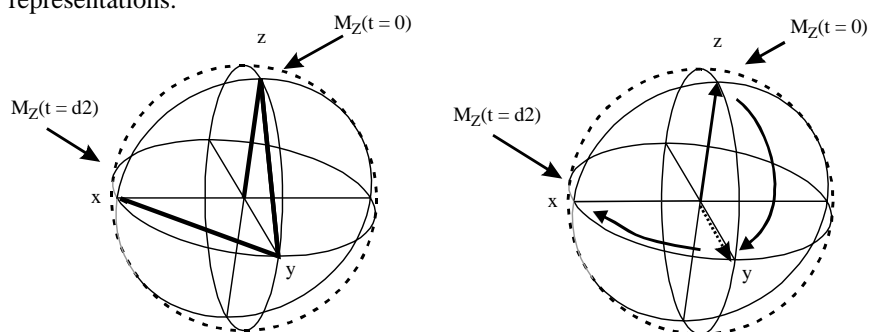

Fig. 4.22: The evolution of $M_Z(0)$ after a $90°_X$ pulse and a delay d2 - the NMR-SIM representation (left side) and the usual literature representation (right side).

Clicking the **XY View** button changes from a spherical display to a three dimensional figure where the axis represent time, rf offset and one CARTESIAN coordinate. This change consists of an internal transformation from a spherical to CARTESIAN coordinate system.

The calculation of the **Excitation profile** displays the effect of a shaped pulse on several magnetization vectors with different rf offsets. The result is a two dimensional graph of either one CARTESIAN or a combination of CARTESIAN coordinates as function of the relative offset. From the appearance of the graph the uniformity of the phase and the excitation of the magnetization may be determined within the frequency domain (frequency window of interest).

The **Rf field profile** calculation shows the effect of a shaped pulse on a single magnetization vector as a function of the pulse power. The magnetization vector does not have to be on-resonance.

Adiabatic pulses may be studied using the **Waveform analysis**. These pulses can either be frequency or phase swept pulses but during the frequency sweep the adiabatic condition must always be met. For an estimation of this condition an effective B_1 field is represented by the angles θ_M and $\theta_{eff}(B_1)$, the calculation then displays the angles θ_M and $\theta_{eff}(B_1)$, a further quality factor and the frequency sweep as function of time in as a series of graphs. Adiabatic pulses are discussed in more detail in section 5.3.1.

4.3.2   General Experiment Setup

Selecting the correct calculation method and the relevant options

The Bloch simulator is started using the pull-down menu command **Utilities|Bloch module...** The main display window is shown in Fig. 4.23. The different representation modes are available from the corresponding commands of the **Calculate** pull-down menu opening particular dialog boxes. The **File|Copy to clipboard** function offers the possibility to transfer the current graphical representation in the main display window to the Windows clipboard and then into other Windows programs.
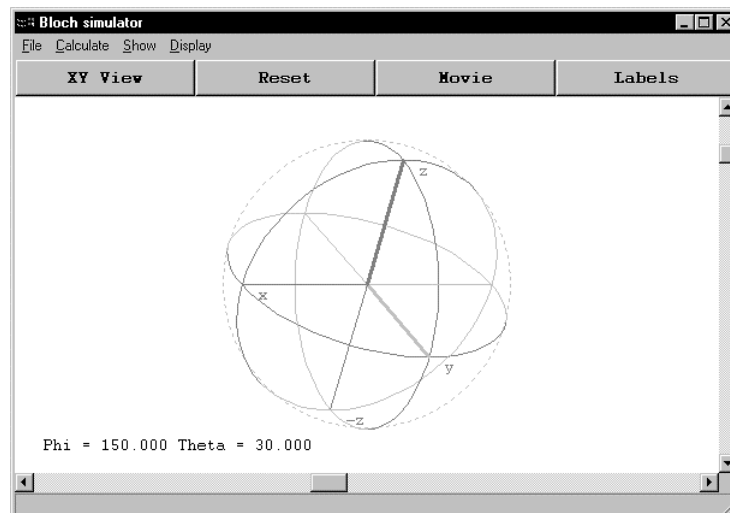

Fig. 4.23:   Default main display window of the Bloch simulator.

The most important function is the **Calculate** menu bar command where the four different calculation methods of the Bloch simulator can be selected. Each type of calculation opens a dialog box containing the parameters relevant to the selected

calculation mode and the calculation method. The menu bar command **Show** allows the user to toggle between the selected calculated representations.

When using the Bloch simulator the first step is to determine the calculation mode. The pull-down menu command **Calculate|Setup...** opens the dialog box shown in Fig. 4.24. The **Calculation mode** is selected by choosing either the *Shaped pulse* or *Sequence fragment* option. Both the shaped pulse **SPNAM0** and the pulse sequence fragment **Segment** are selected using standard Windows list boxes. Before it can be used, the pulse sequence fragment must be created and stored using either the pulse program editor of NMR-SIM or any standard ASCII text editor.
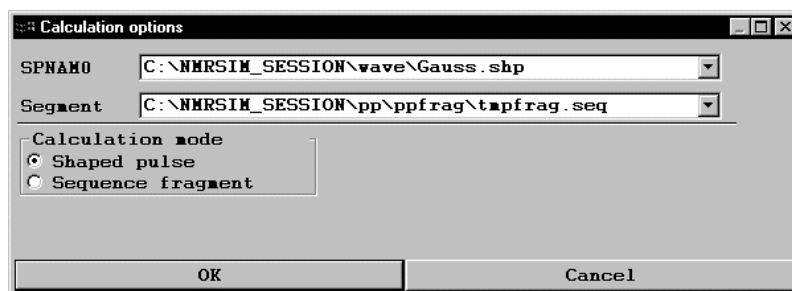

Fig. 4.24: The pull-down menu command **Calculate|Setup** dialog box.

How to simulate the different representations

After selecting the calculation mode the calculation method is chosen using the pull-down menu commands **Calculate|Time evolution**, **Excitation profile** or **RF field profile**. The entries listed in the **Check the experiment parameters** dialog box depend upon both the calculation mode and calculation method, but since these three calculation methods are based upon the concept of macroscopic magnetization they share a number of common parameters. The coordinates of the initial magnetization vector **Mx(0)**, **My(0)** and **Mz(0)** shown in Fig. 4.25 are common to all three calculation methods and have to be specified before the start of any calculation. The definition Mx(0), My(0) and Mz(1) represents the vector aligned to the positive z-axis, some other possible initial orientation are illustrated in the Fig. 4.25. The equilibrium state may be denoted as either Mx(0), My(0), Mz(0) or Mx(0), My(0), Mz(1). The second parameter common to the time evolution and excitation profile calculation methods is the **TSlice** option. Normally the Bloch simulator calculates, samples, the magnetization coordinates at the end of each rectangular pulse. (This also applies to shaped pulses, which are composed of a large number of rectangular pulses.) Sometimes it is not convenient to sample the magnetization only at the end of the pulse and the TSlice parameter is used to define the maximum time between sampling points. TSlice is defined as the pulse length divided by the required number of sampling points. The value "0" denotes that the magnetization is sampled at the end of each rectangular pulse. Because the process is time consuming it is only used in sequence fragment calculations and not in the study of shaped pulses.
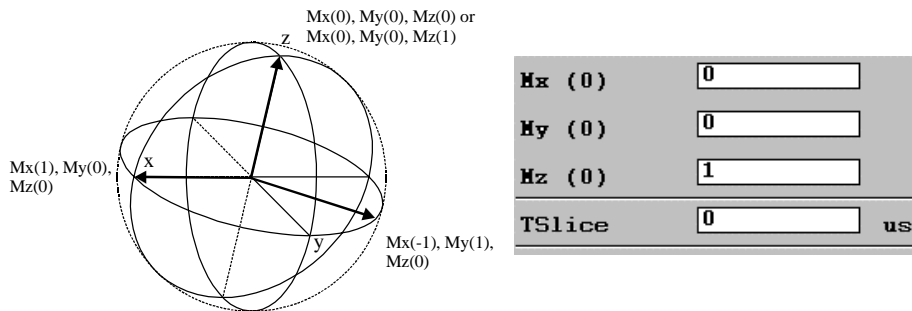
Mx(0), My(0), Mz(0) or
Mx(0), My(0), Mz(1)

Mx(1), My(0), Mz(0)

Mx(-1), My(1), Mz(0)

Mx (0)	0
My (0)	0
Mz (0)	1
TSlice	0	us

Fig. 4.25:   The initial position of the magnetization vector.

Depending on the calculation mode the upper part of the **Check the experiment parameters** dialog box will display either the pathway to the shaped pulse or the pulse sequence fragment in a text editor window mode. For the pulse sequence fragment, the contents of the text window may be scrolled using the sliders at the edge of the frame but the pulse fragment cannot be edited in any way. The pulse parameters also depend on the calculation mode; variable defined pulses, delays and power levels are requested for the sequence fragment calculation and pulse power **SPi** and pulse length **Pi** for the shaped pulse calculation. Pulses may be specified in two different ways. If the pulse power is defined and a normalized pulse is defined by specifying a pulse angle in degrees, the Bloch Simulator calculates the corresponding pulse duration in µs. Alternatively if the pulse power is defined and the pulse length is specified as a duration in µs, the magnetization vector is tilted through the appropriated angle.

TSlice	0	us
P 1	90d	us
PL 1	100000	Hz

4.3.2.1(a) Check it in NMR-SIM

Load the cfg file *ch4321.cfg* open the Bloch Simulator (**Utilities|Bloch module**) and in the **Calculate|Setup** dialog box toggle the *Sequence fragment* option. Close the dialog box

OK. In the **Calculate|Time Evolution** dialog box scroll through the displayed pulse sequence fragment and examine the parameters **d2**, **p1** and **pl1**. Click **Cancel** to close the dialog box.

4.3.2.1(b) Check it in NMR-SIM

| P 0 | 100 | us |
| SP 0 | 5000 | Hz |

Loading the file *ch4321.cfg* set the **Calculation mode** to Shaped pulse in the **Calculate|Setup** dialog box and in the **SPNAM0** filename box enter the filename *...\wave\gauss.shp*. Close the dialog box **OK**. In the **Calculate|Time evolution** dialog box check the shaped pulse parameters pulse duration **P0** and power level **SP0**. Click **Cancel** to close the dialog box.

For the **Time evolution** and the **Excitation profile** calculation the pulse power level is fixed, the rf offset is varied and the components of the macroscopic magnetization vector calculated for each rf offset. In the sequence fragment calculation mode the rf offset is generated by using a loop in the pulse sequence fragment, increments of **HS1** being added to the starting rf offset value **HV1**; both HV1 and HS1 have to be defined in Hz. The overall rf offset calculated depends upon the step size HS1 and the pulse sequence fragment loop counter.

L 1	9	
HV 1	-0.8	Hz
HS 1	0.2	Hz

4.3.2.1(c) Check it in NMR-SIM

Repeat *Check it 4.3.2.1(a)* and compare the entries in the **Calculate│Time Evolution** dialog box with the screenshot shown on the left.

The **RF field profile** and **Excitation profile** calculations can only be used for shaped pulses. The RF field profile calculation differs from the time evolution and excitation profile simulations because it is the pulse power level that is varied while the rf offset is held constant. The resulting graph displays the magnetization components along the CARTESIAN axis as a function of the rf pulse power level. Starting with a rf pulse power level value **Start** a series of **N** calculations are performed, the rf field intensity being incremented by the value **Step** for each new calculation. Using the parameter **Offset**, it is possible to perform calculations where the macroscopic magnetization vector is no longer exactly on-resonance.

Start	50000	Hz
N	9	
Step	100	Hz
Offset	0	Hz

4.3.2.1(d) Check it in NMR-SIM

Using the file *ch4321.cfg* open the Bloch Simulator (**Utilities|Bloch module…**) and in the **Calculate│Setup** dialog box toggle the *Shaped pulse* option and enter for **SPNAM0** the filename *...\wave\gauss.shp*. Close the dialog box **OK**. Compare the entries in the **Calculate│Rf field profile** dialog box with the screenshot shown on the left.

How to start a waveform analysis calculation

The **Waveform analysis** is designed specifically for use with adiabatic pulses. Different graphical representations are used to illustrate how well a given shaped pulse fulfils the adiabatic condition during its execution. A number of different parameters are calculated as a function of time. The time axis is defined indirectly and is given by the number of points into which the pulse shape is divided, the only other parameters

required are the pulse duration **P0** value in µs, the power level of the shaped pulse **SP0** in Hz and the rf **Offset** in Hz.

P 0	10	us
SP 0	50000	Hz
Offset	0	Hz

4.3.2.2 Check it in NMR-SIM

After loading the file *ch4321.cfg* open the Bloch Simulator (**Utilities|Bloch module…**) and in the **Calculate│Setup** dialog box toggle the *Shaped pulse* option and enter for **SPNAM0** the filename *...\wave\chirp.shp*. Close the dialog box **OK**. Compare the entries in the **Calculate│ Waveform analysis** dialog box with the screenshot shown on the left.

4.3.3   Analysing Shaped Pulses

In the literature hard pulses and shaped pulses are usually treated as different entities such that any phase or amplitude modulation of hard pulses is neglected or assumed to be negligible whereas the phase and amplitude variation of a shaped pulse is always emphasized. The truth is that even hard pulses can have a significant phase and amplitude variation particularly at the extremes of their excitation bandwidth. For a comprehensive discussion the reader is referred to section 5.3.1.

The following *Check its* will use the Bloch simulator module of NMR-SIM to study and analyse a number of different shaped pulses. **Time Evolution**, the **Excitation Profile** and the **Rf field profile** simulation are illustrated using a 90° GAUSSIAN pulse while an adiabatic CHIRP pulse is used for the **Waveform analysis**.

Check it 4.3.3.1 calculates the **Time Evolution** representation of a 90° GAUSSIAN pulse for a number of different rf offsets and displays the results as a set of lines on the surface of a sphere.

4.3.3.1 Check it in NMR-SIM

Open the Bloch Simulator (**Utilities|Bloch module…**) and in the **Calculate│Setup** dialog box toggle the *Shaped pulse* option and enter for **SPNAM0** the filename *...\wave\gauss.shp*. Close the dialog box **OK**. In the **Calculate│Time Evolution** dialog box set **M(x)**: *0*, **M(y)**: *0*, **M(z)**: *0*; **p0**: *90d*, **SP0**: *5000*, **N**: *11*, **Start**: *-2500* and **Step**: *500*. Close the dialog box with **OK**. The resulting graph should be similar to the one in the result file. Use the scroll bars at the sides of the window to adjust the view and to get the three-dimensional impression of the sphere.

In contrast to an ideal pulse that generates magnetization along only one CARTESIAN axis, the off-resonance magnetization vector has components along all three CARTESIAN axes making the spherical representation difficult to interpret. It is possible to simplify the display and to represent the effect of the GAUSSIAN pulse on the magnetization

vectors of the different rf offsets by plotting the magnetization components along the individual CARTESIAN axis as a function of time.

4.3.3.2 Check it in NMR-SIM

Repeat *Check it 4.3.3.1* and after the spherical representation is generated click on the **XY View** button in the option bar. Click the **X** button in the new option bar to display the x-component of the magnetization for the individual offsets as a 3D graph. Now click the **Projections** button to simplify the display further to a 2D graph. The 3D and 2D representations should be similar to graphs in *result.pdf* file.

The x, y and z **Projections** of the **XY view** illustrate more clearly than the 3D spherical representation the different effects of the GAUSSIAN shaped pulse on the three components of the magnetization vector. For a GAUSSIAN pulse the x-component shows a strong deviation from zero as the offset is varied in contrast to the y- and z-components which show a gradual change. As an additional exercise, *Check it 4.3.3.2* can be repeated but starting with the magnetization in a non-equilibrium state.

The **Excitation Profile** calculation displays information similar to the time evolution calculation but the units for the x-axis is now the rf offset instead of time. It also shows the phase modulation of the magnetization vectors derived from the projection of the 3D spherical representation into the x,y-plane. With the exception of the **Phase** and **Phase range** display options, the y-axis is scaled in relative units.

4.3.3.3 Check it in NMR-SIM

Open the Bloch module using the **Uitilities│Bloch module**… command. In the **Calculate│Setup** dialog box toggle the *Shaped pulse* option and enter for **SPNAM0** the filename *...\wave\gauss.shp*. Close the dialog box **OK**. In the **Calculate│Excitation profile** dialog box set **M(x)** = *0*, **M(y)** = *0*, **M(z)** = *0*; **p0** = *90d*, **SP0** = *5000*, **N** = *21*, **Start** = *-5000* and **Step** = *500*. Close the dialog box with **OK**. Using the buttons in the option bar toggle between the different representations. The graph obtained by clicking the **X,Y** button is shown in the result file also.

The effect of a shaped pulse depends upon both the duration and the rf field intensity of the pulse. Normally the duration of a shaped pulse is adjusted to give the desired excitation range and then the rf field altered to obtain the desired tilt angle. As a rule of thumb the excitation range (selectivity) of shaped pulse in Hz is proportional to the reciprocal of the pulse duration. The **RF field profile** simulation can be used to study the effect of a shaped pulse and the rf field intensity of the pulse as function of the rf offset. Because of the correlation of pulse duration and tilt angle, the simulation does not accept normalized pulses instead the tilt angles of the individual magnetization vectors are calculated as a function of the rf field intensity of a specific rf offset.

4.3.3.4 Check it in NMR-SIM

Open the Bloch module using the **Uitilities**⎮**Bloch module**… command. In the **Calculate**⎮**Setup** dialog box toggle the *Shaped pulse* option and enter for **SPNAM0** the filename *…\wave\gauss.shp*. Close the dialog box **OK**. In the **Calculate**⎮**RF field profile** dialog box set **M(x)** = *0*, **M(y)** = *0*, **M(z)** = *0*; **p0** = *10.000 u*, **N** = *41*, **Start** = *0* and **Step** = *10*. Close the dialog box with **OK**. Clicking the **Z** and then **X,Y** button in the option bar the graphs shown in the result file should be obtained.

An adiabatic pulse is a special type of shaped pulse where either a frequency or a phase sweep occurs during the pulse duration. Adiabatic pulses are discussed in detail in section 5.3.1. So far the simulations involving the Bloch module have not considered the exact time related frequency sweep of a shaped pulse yet it is this factor that determines if each point in the pulse shape obeys the adiabatic condition. Using an adiabatic chirp pulse *Check its 4.3.3.5* and *4.3.3.6* will examine various aspects of adiabatic pulses starting with the time evolution and the graphical representation of the amplitude and phase modulation.

4.3.3.5 Check it in NMR-SIM

Open the Bloch module using the **Utilities**⎮**Bloch module**… command. In the **Calculate**⎮**Setup** dialog box toggle the *Shaped pulse* option and enter for **SPNAM0** the filename *…\wave\chirp2.shp*. Close the dialog box **OK**. In the **Calculate**⎮**Time Evolution** dialog box set **M(x)** = *0*, **M(y)** = *0*, **M(z)** = *0*; **p0** = *50u*, **SP0** = *50000Hz*, **N** = *5*, **Start** = *-1000* and **Step** = *500*. Close the dialog box with **OK**. For a view similar to the one shown in the result file use the scroll bars to set **Phi** = *10.000* and **Theta** = *340.000*. For the waveform representation use the **Show**⎮**Waveform** command in the main menu bar and then click the **Amplitude-Phase** button in the option bar.

The time evolution representation shows how well the magnetization vectors with different rf offsets are tilted to the same degree by the adiabatic pulse. *Check it 4.3.3.6* examines a number of different quality factors of the pulse to determine how well the pulse fulfills the adiabatic condition.

4.3.3.6 Check it in NMR-SIM

Repeat *Check it 4.3.3.5* but this time select the **Calculate**⎮**Waveform analysis**. In the dialog box enter the parameters **p0** = *50* [us], **SP 0** = *50000* [Hz] and **Offset** = = *0* [Hz]. Closing the dialog box by clicking the **OK** button starts the calculation and the three graphs of the particular angles of the B_1(effective) field, the quality factor **Q** and the frequency sweep as a function of time are calculated and displayed.

The significance of these representations is described in section 5.3.1 as part of the introductory discussion of shaped pulses and adiabatic pulses.

4.3.4   Analysing Pulse Sequence Fragments

Because the Bloch simulator is based on a classical approach rather than a quantum mechanical approach to the NMR phenomena its use in analysing pulse sequence fragments is somewhat restricted. Nevertheless, as will be illustrated in the next three examples, in spite of these restrictions the Bloch simulator is a very powerful aid in visualizing what is happening in a pulse sequence fragment and consequently is an extremely valuable teaching and research tool.

Example 1: Most discussions involving the Bloch model introduce the concept of the rotating frame. The concept of a rotating coordinate system is a familiar one because in real life positions and motion are referred to the earth, a coordinate system that is rotating. Similarly rather than refer the motion of the magnetization vectors to the fixed laboratory coordinate system, it is simpler to refer their motion to a rotating frame of reference which rotates at the NMR transmitter frequency of the nucleus under study.

4.3.4.1 Check it in NMR-SIM

Open the Bloch Simulator (**Utilities|Bloch module...**) and in the **Calculate│Setup** dialog box toggle the *Pulse sequence fragment* option and enter for **Segment** the filename *...\ppfrag\chshev.seq*. Close the dialog box **OK**. In the **Calculate│Time Evolution** set **M(x)**: *0*, **M(y)**: 0, **M(z)**: *0*, **TSlice**: *0*, **D1**: *1* s, **p1**: *90d*, **PL1**: *1e+007*, **L1**: *8*, **HV1**: *0* and **HS1**: *0.125*.
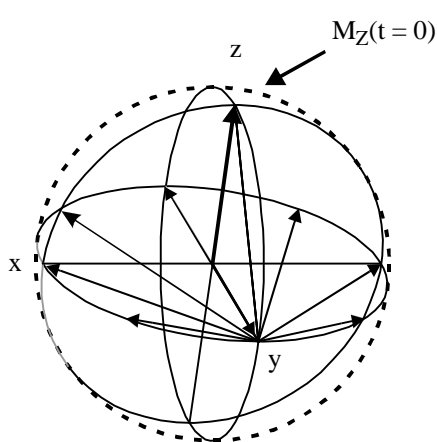

Close the dialog box with **OK**. The resulting graph should be similar to the one shown on the left hand side of this *Check it*. Use the scroll bars at the sides of the window to adjust the view and to get the three dimensional impression of the sphere.

The simulation in *Check it 4.3.4.1* illustrates how the magnetization vectors with different chemical shifts evolve in a simple 90° pulse - delay - sample pulse sequence fragment. At the start of the sequence the magnetization $M_Z(0)$ is aligned along the positive z-axis of the sphere, the 90° pulse tilts the magnetization so that it is aligned along the positive y-axis irrespective of any rf offset. During the delay d1 the magnetization evolves, the final position of the magnetization vector depending upon its

frequency (or offset) with respect to the rotational frequency of the rotating frame. In this example the frequency of each magnetization vector is defined by the parameters **L1**, **HV1** and **HS1**. Eight vectors are defined (L1: 8) starting with the on-resonance magnetization vector with an offset 0 (HV1: 0) with an increasing offset frequency 0.125, 0.25, 0.5, ... Hz (HS1) which evolve during the delay d1. In the NMR-SIM representation the lines in the x,y-plane show the final position of the magnetization vector after the delay period. The on-resonance magnetization stays aligned along the +y-axis during d1 but the other vectors precess by increasing amounts (L1 • HS1/360 degrees) until for the magnetization vector with an offset of 1 Hz, the precession is one complete revolution and it is again aligned along the +y-axis.

Example 2: A hard pulse is often called a perfect or ideal pulse; due to the high rf field strength the 90° pulse length is very short and the pulse can excite nuclei uniformly over a wide frequency range without any phase or amplitude modulation. Consequently the radio frequency offset between the frequency of the pulse and the resonance frequency of the observed magnetization is not particularly relevant provided that it is less than the reciprocal of four times the 90° pulse length. However if the radio frequency strength is reduced the frequency range over which the magnetization is excited uniformly is reduced and indeed this procedure was often used to generate soft pulses before the use of shaped pulses became widely available. The Bloch simulator can illustrate these effects using the time evolution calculation. A rectangular shaped hard pulse can be analysed using the same excitation profile and rf field profile calculation as for a shaped pulse.

$M_Z(t = 0)$
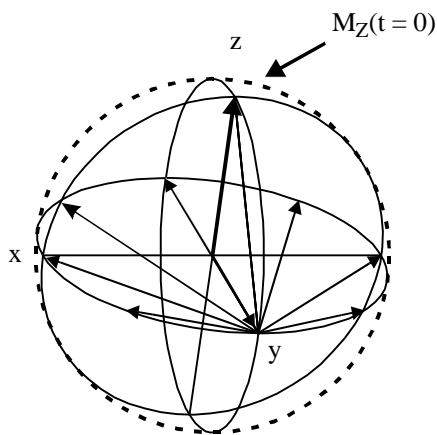
- simulated at a power level of pl1 = 100 Hz

4.3.4.2 Check it in NMR-SIM

Open the Bloch Simulator (**Utilities|Bloch module…**) and in the **Calculate⎢Setup** dialog box toggle the *Pulse sequence fragment* option and enter for **Segment** the filename *...\ppfrag\hpsp.seq*. Close the dialog box **OK**. In the **Calculate⎢Time Evolution** dialog box enter the following parameters: **M(x)**: *0*, **M(y)**: *0*, **M(z)**: *0*, **TSlice**: *0*, **p1**: *90d*, **PL1**: *10.000 Hz*, **L1**: *10*, **HV1**: *0* and **HS1**: *1000*. Close the dialog box with **OK**. After the calculation has finished click the **Movie** button to see a slow motion video of the time evolution. Repeat this *Check it* with different values of **PL1**: *10 Hz*, *1000 Hz*, *10000 Hz* and *1000000 Hz*.

By increasing pl1 from low power levels to higher power levels the soft pulse gradually approaches an ideal hard pulse which excites nuclei uniformly over a wide range of frequency offsets, i.e. sweep width.

Example 3: Composite pulses are designed to overcome the imperfections of "ideal hard pulses". The Bloch simulator is a suitable tool to illustrate the superiority of a composite 180° pulse inversion compared to a standard 180° pulse. The application of composite pulses in decoupling techniques is discussed in sections 5.3.2 and 5.5.3. In *Check it 4.3.4.3* the composite 180° pulse $90_x/180_y/90_x$ (the indices x and y denote the pulse phase) is demonstrated. These simulations reveal how effective a composite 180° inversion pulse is for different rf offsets.

4.3.4.3 Check it in NMR-SIM

(a) Open the Bloch Simulator (**Utilities|Bloch module…**) and in the **Calculate│Setup** dialog box toggle the *Pulse sequence fragment* option and enter for **Segment** the filename *...\ppfrag\p180.seq*. In the **Calculate│Time Evolution** dialog box enter the following parameters: **M(x)**: *0*, **M(y)**: *0*, **M(z)**: *0*, **TSlice**: *0*, **p1**: *180d*, **PL1**: *10000*, **L1**: *10*, **HV1**: *0* and **HS1**: *1000*. Close the dialog box with **OK**.

(b) For the simulation of the composite pulse experiment replace the pulse sequence fragment file in the **Calculate│Setup** dialog box by the file *...\ppfrag\cp121.seq*. In the **Calculate│Time Evolution** dialog box set **p1**:*90d*, **p2**: *180d* and **p3**: *90d*. In both cases use the scroll bars at the sides of the window to adjust the view and determine how close to the –z-pole the magnetization vectors are. The results of both simulations are shown below.

180° pulse at a power level of 10000 Hz
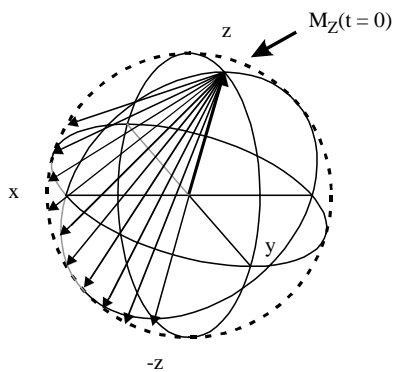
Composite Pulse $90_x/180_y/90_x$ at the same power level
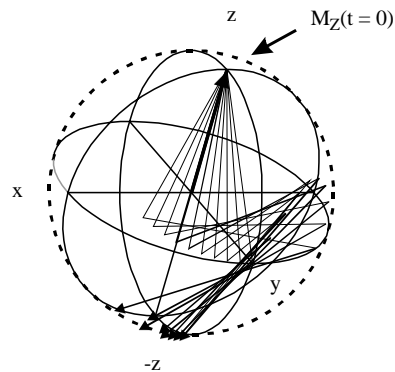
In the left hand side of the figure the strong defects in a single 180° pulse can be seen, the magnetization inversion gets progressively worse the greater the rf offset. In contrast the composite 180° pulse using the same pulse power is no so nearly as sensitive to the rf offset as a 180° pulse. As an additional exercise *Check it 4.3.4.3* can be repeated

using a $80_x/160_y/80_x$ composite pulse, which would represent the situation where the decoupler power level and pulse length have not been calibrated correctly, and then a $90_x/240_y/90_x$ sequence which is often the preferred 180° composite pulse.

4.4   References

[4.1] Bigler, P., *NMR Spectroscopy: Processing Strategies*, Weinheim, WILEY-VCH, 2nd Ed, 2001.
[4.2] Hoch, J. C., Stern, A. S., *NMR Data Processing*, New York, WILEY-Lyss, 1996.

5   Complete Sequences, Elements and Building Blocks

Hundreds of pulse sequences [5.1 – 5.4] have been developed and every month improvements and new combinations of sequence units are published. For a number of different reasons there is no systematic nomenclature for the naming of pulse sequences. A name based on the exact combination of sequence units used in a pulse sequence would be very unwieldy whilst spectrometer manufacturers have built up their own pulse sequences library using their own nomenclature system. In addition the number and type of characters in the name depends upon the spectrometer operating system.

The object of this chapter is the analysis of a wide range of pulse sequences by separating the building blocks of a particular sequence into the underlying sequence units and basic elements. Sections 5.1.1, 5.1.2 and 5.1.3 are a guide for the reader new to NMR to give an impression of the variety of pulse sequences, how pulse sequences are constructed and their application. The number of sequence units is finite and improvements in a pulse sequence arise by implementing a known sequence unit in a new or novel way. As shown in Fig. 5.1 and listed in Table 5.1 it is possible to categorize the components of a pulse sequence into basic element, sequence unit and building blocks. The effect of each of these categories may be simulated using NMR-SIM allowing the dependence on structural parameters or incorrectly set experimental parameters to be examined and verified.

Pulse, delay   *Spin echo*   *INEPT unit*
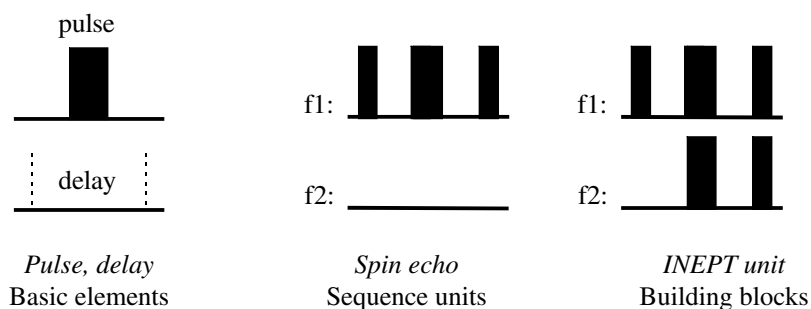Basic elements   Sequence units   Building blocks

Fig. 5.1: The NMR spectroscopist's "toolkit" for the design of pulse sequences.

The basic elements summarized in Table 5.1 are usually described by their overall effect on the spin system such that a ^1H cp decoupling sequence is described as the suppression of the $^nJ(^nX, {}^1H)$ coupling during the FID acquisition on the ^nX channel.

Sometimes sequence units can be mixed up so to avoided confusing a BIRD unit and a INEPT sequence it is important that all pulse sequences are analysed starting with the first pulse to trace the coherence evolution.

Table 5.1: Basic elements, units and building blocks of pulse sequences.

Basic elements:	Hard/shaped pulse, soft pulse, DANTE pulse train, composite pulse, cw-irradiation, cp decoupling sequence, spinlock, constant or incremented delay
Sequence units:	Spin echo, double quantum, multiple quantum filter, low-pass filter, relay step, BIRD filter, WATERGATE
Building blocks:	*Evolution*: INEPT, DEPT unit, *refocusing* period, *modulation*: t1 evolution period, constant-time t1 evolution period, ACCORDION-evolution, *detection* period with/without decoupling

It is common practise to separate NMR experiments according to dimensionality, this approach is not absolute because it is possible to convert a 2D experiment into a 1D experiment without changing the basic principles, correlation mechanism, sensitivity enhancement or coherence pathway selection by using selective pulses. The experiments in this chapter are divided into three parts using the following criteria:

- Single pulse and simple multi-pulse experiments
- Homonuclear correlation experiments
- Heteronuclear correlation experiments

Section 5.2 covers simple pulse experiments including selection of pulse angle and the influence of relaxation on repetition rate in multi-scan experiments and serves as an introduction for readers who have never before used a spectrometer or who have only obtained a spectrum by following a "written recipe". Section 5.3 *Building Blocks and Elements – Part One* give further insight the basic principles of NMR. Homonuclear correlation experiments are discussed in section 5.4. *Building Blocks and Elements – Part Two* in section 5.5 examines coherence transfer problems and delay incrementation. Heternonuclear correlation using direct or indirect detection is discussed in section 5.6 and 5.7 respectively. The final section 5.8 *Building Blocks and Elements – Part Three* examines BIRD related sequence units and filter elements. Each section follows a similar format starting with the basic experiment and discussing the advantages and disadvantages of the technique and how the experiment can be improved. In all cases simulations demonstrate the purpose and application of the experiments.

5.1   The Philosophy of Pulse Sequences

5.1.1   Pulse Sequences as Combination of Building Blocks

It is not possible to describe the basic experiment structure of one dimensional and n dimensional experiments using a single scheme but they may be described using three

schemes as shown in Fig. 5.2. The order of the building blocks can be interchanged for the evolution and modulation unit. Sometimes a substantial separation of excitation and refocusing is impossible because of simultaneous evolution. The **excitation** unit mostly consists of a single pulse that might be unselective or selective. A more complex excitation unit is given if multiple selective excitation or a DANTE sequence is wanted. The **thermal equilibrium setting** unit, which is often called the preparation period or relaxation delay, is particularly relevant in multi-scan experiments to ensure that the excited spin system has returned to the equilibrium state prior to the next scan. When observing ^nX nuclei it is also possible during this sequence period to apply noise or cp decoupling to ensure the build-up of the NOE enhancement or alternatively turn off the decoupling to allow the NOE to decay to zero.
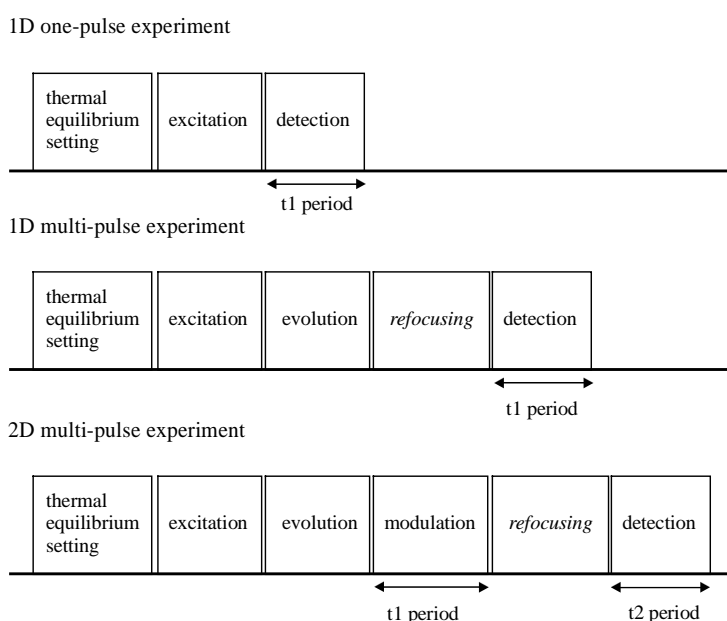
1D one-pulse experiment

thermal equilibrium setting	excitation	detection

t1 period

1D multi-pulse experiment

thermal equilibrium setting	excitation	evolution	*refocusing*	detection

t1 period

2D multi-pulse experiment

thermal equilibrium setting	excitation	evolution	modulation	*refocusing*	detection

t1 period   t2 period

Fig 5.2:   General scheme for 1D and 2D experiments as a combination of several building blocks. The refocusing element written in italics is optional.

The processes that occur during the **evolution** period are probably the most important in describing the effect of the complete pulse sequence. During this period coherence can evolve, coherence can be selectively manipulated or coherence transfer can occur. Coherence manipulation can be the inversion of the coherence order (WATERGATE experiment) or in a I_nS spin system a phase shift depending upon signal multiplicity (APT or SEMUT experiment). In the case of heteronuclear IS spin systems the creation of antiphase coherence and subsequent polarization transfer using a INEPT or a DEPT unit can be used in multiplicity edited experiments or heteronuclear 2D correlation experiments. In transient NOE experiments such as ROE and TROESY, coherence

transfer is achieved via cross relaxation using a spinlock field. If the evolution period is placed prior to the excitation pulse cw irradiation (NOE difference experiments) or the selective inversion of a single transition (SPI experiment) can be applied. For homonuclear spin systems a spin echo with a 90° pulse at the centre (homonuclear COSY experiment) to achieve polarization transfer or a spinlock field that matches the HARTMANN-HAHN condition for isotropic mixing (TOCSY experiments) and cross polarization can also form part of the **evolution** period.

The **modulation** part is the main part to create n dimensional experiments. During this period coherences evolve under free precession due to the chemical shift or coupling of a particular kind of nucleus like ^{13}C nucleus in an ^{1}H, ^{13}C COSY experiment. If only chemical shift evolution is allowed a shift resolved COSY spectrum results whilst a J-resolved experiments is obtained if only coupling evolution is permitted. Incrementing the delay between experiments modulates this evolution which after Fourier transformation generates the second frequency dimension. In a further step several modulation units can be implemented to create n dimensional spectra where each dimension is assigned to an individual nucleus or a particular type of coupling.

Initially the **detection** period might appear as the least important part of the pulse sequence. However for nD experiments the selection of the appropriate detection mode can have a significant effect on the experiment sensitivity; thus the magnitude detection mode results in broad signals which compared to spectra recorded using phase-sensitive detection, have a lower signal-to-noise ratio and resolution.

5.1.2   Two different Approaches to Pulse Sequence Classification

There are two approaches to pulse sequence classification depending on the user's occupation. For the chemist who has to solve a structural question or characterize a new compound it is the spectra obtained from the pulse sequence that is of primary importance. The NMR spectroscopist is usually more concerned with the pulse sequence structure and choice of experimental parameters and whether a particular pulse sequence can be improved or modified to solve a specific problem. These two different approaches lead to confusion in pulse sequence nomenclature such that names are often a combination of the purpose of the experiment and the sequence layout. For example the commonly used acronyms HMQC, HSQC and HMBC imply a consistent abbreviation system yet HMQC and HSQC describe the coherence state during the evolution time whilst HMBC denotes an experiment to correlate nuclei using multiple bond heteronuclear scalar coupling.

Table 5.2 attempts to categorize NMR experiments from a chemist's point of view based upon the structural parameters that can be obtained using different experiments. Structural analysis usually depends upon the identification of small structural units and the combination of these units to generate the complete molecular skeleton. Further information might be required to determine the conformation or stereochemistry of the unknown compound.

Table 5.2:   A chemist's requirements of pulse sequences.[1]

Nuclei	Multiplicity	Coupling constants	Relaxation times
Number and types of isotopes. Functional groups using chemical shift correlation charts	Number of sensitive nuclei bonded to a insensitive nucleus	Exaction of scalar coupling constant and determination of the coupling constant sign	Measurement of T_1 and T_2

Connectivity's

Homonuclear correlation	Heteronuclear correlation
Detection of neighbouring I and I or S and S nuclei through 1, 2 or 3 bonds	Detection of neighbouring I and S nuclei through 1, 2 or 3 bonds
Steric interaction	**Dynamic phenomena**
Detection of homonuclear or heteronuclear dipolar interactions	Analysis of chemical equilibria monitoring of slow reactions

[1]This overview does not claim to be complete.

On the other hand the NMR spectroscopist is more interested in the pulse sequence construction, the underlying coherence evolution and the possible transfer to specific quantum states. In addition they are also concerned with selecting the correct values of delays, spectrometer routing, pulse lengths, detection mode and gradient strengths.

Table 5.3:   Pulse sequences in order of acquisition principles[1]

One-pulse and multi-pulse experiments

Experiments without signal enhancement	Signal enhancement by NOE	Signal enhancement by polarization transfer
One pulse experiment, SPI experiment	APT, SEMUT experiment	INEPT, DEPT experiment

Multi-pulse correlation experiments

Correlation experiments by polarization transfer

Homonuclear correlation experiments

Coherence transfer by polarization transfer	Coherence transfer by isotropic mixing
1D/ 2D ^{1}H COSY experiment, relayed ^{1}H COSY experiment	TOCSY experiment

Heteronuclear correlation experiments

	Variable time experiment	Constant-time experiment
Direct detection		
MQ coherence during t1 period	^1H, ^{13}C HETCOR experiment	^1H, ^{13}C COLOC experiment
SQ coherence during t1 period	-	-
Indirect detection		
MQ coherence during t1 period	^{13}C, ^1H HMQC, ^{13}C, ^1H HMBC experiment	^{13}C, ^1H CT-HMBC experiment
SQ coherence during t1 period	^{13}C, ^1H HSQC experiment	

Coherence transfer by homo-/ heteronuclear cross-relaxation (a) steady state NOE, (b) transient NOE	**Coherence transfer by chemical exchange**	**Coherence transfer by heteronuclear cross-polarization**
(a) 1D NOE, 2D NOESY, 2D HOESY experiment (a) 1D ROE, 2D ROESY, 2D TROESY experiment	ACCORD-COSY, EXSY experiment	

[1]This selection is limited but probably reflects the pulse programs commonly used by the average NMR spectroscopist.

Table 5.3 gives a better sequence review because the NMR spectroscopist has the expertise in selecting the experiment and experimental parameters and appreciating the limitations of a particular technique. So when measuring the ^nX spectrum of a dilute sample an experiment like DEPT or INEPT, which gives signal enhancement and the possibility for multiplicity assignment, would be selected. Similarly the NMR spectroscopist can decide between an EXSY experiment or a COSY experiment or even a ACCORD-COSY experiment if the molecule should be analysed for slow chemical exchange and bond connectivities using scalar coupling.

5.1.3   Pulse Sequence Nomenclature

There is no standard pulse sequence nomenclature so that the system adopted in this book is a combination of the acronyms used in literature and the relevant adjectives to highlight the differences between similar experiments. A pulse sequence name must convey the following information:

- Dimensionality
  The usual letters like 1D or 2D are prefixed.
- Decoupled nucleus during acquisition
  The decoupled nucleus is given in brackets.
- The nucleus observed during the acquisition period (t2 period)
  The directly detected nucleus is given as the last nucleus so the expressions ^{13}C, ^1H COSY indicates a ^1H detected experiment.
- Coherence selection based on phase cycling or gradient selection
  The complete expression or the abbreviations ps: phase cycled or gs: gradient selected.
- Common acronyms for specific pulse sequence units
  Well-known sequence elements like DEPT, TOCSY or BIRD are added without any further comment,
- n dimensional experiments: detection mode
  The quadrature detection mode is given as a suffix to the main sequence name: mc: magnitude calculated, TPPI: time proportional phase increment, E/A: Echo / Antiecho
- Selective pulses
  The term "selective" is reserved exclusively for sequences using selective pulses. If selectivity is achieved using other methods this is defined using a different term.

5.2 Single Pulse and Simple Multi-Pulse Experiments

A simple one-dimensional spectrum is always recorded at the start of any structural analysis. Small modifications to the 1D pulse sequence enables the selection of groups of signals or singlet signals, the separation of multiplets for determining coupling constants or multiplicity and the determination of molecular parameters such as relaxation times or diffusion constant. In addition 1D pulse sequence can also be converted into 2D sequences (and vice versa) enabling homonuclear and heteronuclear correlation. Table 5.4 gives an overview of the different types of simple experiments:

Table 5.4:   Single pulse and simple multi-pulse experiments.

Selection of

Nuclei for 1D ^1H or ^nX experiments	➜ ^1H spectrum, ^nX spectrum
Single line or multiplet excitation experiment	➜ Selective excitation by a shaped pulse
Single line or multiplet suppression experiment	➜ Selective solvent suppression
Single line perturbation experiment	➜ Spin tickling experiment

Separation of
    Signals with different multiplicities   ➜ DEPT experiment
    Multiplet pattern   ➜ 2D J-resolved experiment
Determination of
    Relaxation time   ➜ Inversion recovery experiment

In this section the simple one-pulse experiment and different multi-pulse 1D experiments and the 2D coupling resolved experiment will be discussed. By means of the one-pulse experiments several concepts are introduced such as pulse length calibration or delay calculation which must be kept in mind when successfully setting up an n dimensional experiment. The J-resolved 2D experiment is included in this section because it is based on the simple but extremely useful spin echo unit whereby the chemical shift evolution is refocused by a 180° pulse applied in the centre of the free precession evolution.

5.2.1   One-pulse 1D ^{1}H and ^{n}X Experiments

The one-pulse 1D ^{1}H or ^{n}X experiment provides the first insight into molecular structure as well as being the basis for determining whether more demanding experiments, such as selective or 2D experiments, are necessary. In addition to indicating the number of observed nuclei, which are chemically and/or magnetically different, the 1D spectrum displays additional information that can be used to characterize the molecule under investigation. Thus chemical shifts, scalar coupling constants, isotope shifts of non-abundant isotopomers and non-first-order multiplet splittings, can be used to assign characteristic functional groups, cis-/trans-isomers or imply a molecular symmetry. Line-broadening which is not due to a small, unresolved coupling may indicate a dynamic molecular process. In which case the lineshape analysis of a series of spectra measured at different temperatures enables the determination of activation energies. Slow chemical reactions can be monitored by a series of spectra measured at specific time intervals. A wealth of information can often be obtained by the detailed interpretation of a 1D spectrum and the choice of further NMR experiments often depends upon the analysis of a simple 1D spectrum.

Some extensions to the one-pulse sequence can be made without changing the basic principle of an excitation pulse followed immediately by data acquisition. Decoupling and presaturation of unwanted signals such as solvent signals, are techniques that can be easily appended to the recording of 1D spectra. Decoupling is recommended for the measurement of ^{n}X nucleus spectra to remove the multiplets that arises from heteronuclear coupling which reduces the signal-to-noise. Thus for ^{1}H, ^{13}C spin systems ^{1}H decoupling collapses all the signals in a ^{13}C spectrum into singlets. The various types of heteronuclear decoupling off-resonance, inverse-gated and gated decoupling as well as homonuclear decoupling have been discussed briefly in section 2.3.2. Solvent presaturation is just one of a variety of techniques to suppress intense solvent signals which adversely effects the dynamic range of the rf detector. Solvent presaturation using cw irradiation is the simplest and most debatable method; for a detailed discussion of the

advantages and disadvantages of the various solvent suppression methods the reader is referred to section 5.2.3.

Sequence features:

Purpose / principles:	Primary detection of chemical shifts, coupling interaction and constants including multiplet structure to verify concentration, constitution, conformation or symmetry of one or mixture of compounds; kinetic, exchange or chemical equilibria information can be obtained by recording a series of spectra as a function of time or temperature.
	Basic sequence consists of an excitation pulse followed immediately by data acquisition
Variants:	Experiments with various decoupling techniques [5.1], with solvent presaturation [5.1], or selective population inversion of a singlet transition [5.1]

The simple one-pulse experiment is shown below, the delay d1 is called the **relaxation delay** and it ensures that in a multi-scan experiment the spin system has returned to equilibrium before the next pulse (see *Check it 5.2.1.5*). The delay d10 is not normally part of the ordinary sequence scheme and represents the pre-acquisition delay (Bruker nomenclature: de1, de2). This delay is automatically inserted to enable time for switching between transmit and receive mode to minimize pulse breakthrough. For further aspects the reader is referred to section 3.2.3.4 (*Check its 3.2.3.4* and *3.2.3.6*).

Pulse Sequence Scheme
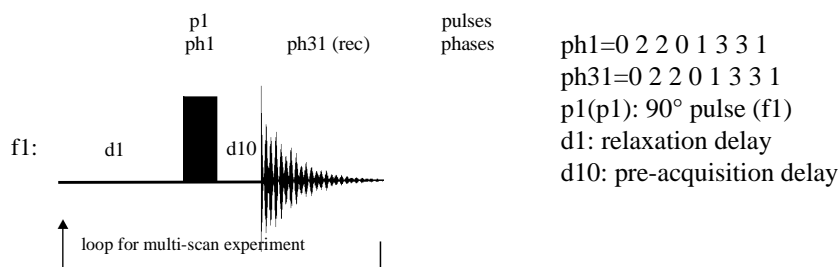
The 1D one-pulse experiment.

The rest of this sub-section is subdivided into three parts:

(a) Spectra characteristics of sensitive and insensitive NMR active isotopes
- ^1H and ^{19}F spectra - the most sensitive nuclei of high natural abundance
- ^{31}P and ^{29}Si spectra - examples of spin-1/2 isotopes of high natural abundance/low receptivity (^{31}P) and low abundance/low receptivity (^{29}Si)
- ^{11}B spectrum - example of a non-spin-1/2 nucleus

(b) Pulse calibration
  • Direct and indirect pulse calibration
(c) Experimental parameters and the relaxation process
  • The relaxation delay
  • The optimum excitation pulse
  • The dummy scans

Part (a) is aimed primarily at people new to the field of NMR spectroscopy whilst parts (b) and (c) which deal with the more technical aspects and spectrometer related problems, are aimed at readers who have already recorded spectra and are used to the basics of NMR spectral interpretation.

(a) Spectra characteristics of sensitive and insensitive NMR active isotopes

^1H and ^{19}F spectra - the most sensitive nuclei of high natural abundance

NMR active isotopes are normally divided into the ^1H nucleus and ^nX or heteronuclei. This somewhat misleading differentiation can be traced back to the spectrometer design and the nuclear properties of the NMR active isotopes as outlined in Table 5.5. With regard to the spectrometer design the desire for optimum ^1H sensitivity has resulted in a specific channel for ^1H observation and an extremely fine-tuned ^1H rf coil in the probehead. The channel for heteronuclear observation is broadband and the ^nX rf coil in the probehead can be tuned over a wide frequency range. This arrangement is also necessary because ^nX nuclei are usually observed using broadband proton decoupling. Using this approach the ^{19}F nucleus has been historically treated as an ^nX or heteronucleus. However as shown in Table 5.5 from the theoretical viewpoint the nuclear receptivity and natural abundance of the ^1H and ^{19}F isotope are very similar and a better description for both isotopes would be sensitive nuclei (Experimentally with a modern probehead the ^1H coil can often be tuned between the ^1H and ^{19}F frequencies without any major loss in sensitivity.).

Table 5.5:   Classification of spin-1/2 nuclei into sensitive and insensitive nuclei.

Sensitive nuclei		**Insensitive nuclei**	
High receptivity, high natural abundance	*Low receptivity, high natural abundance*	*Low receptivity, low natural abundance*	
^1H [1.00, 98.9%][1]	**^{31}P** [0.067, 100%]	**^{13}C** [$1.76 \cdot 10^{-4}$, 1.1%]	
^{19}F [0.834, 100%]		**^{15}N** [$3.85 \cdot 10^{-6}$, 0.37%]	
		^{29}Si [$3.69 \cdot 10^{-4}$, 4.7%]	

[1][(Receptivity on the basis of the ^1H nucleus = 1.0), (natural abundance [%])].

Theoretically all the pulse sequences developed for ^1H observation should also be applicable for ^{19}F based experiments provided that the larger ^{19}F chemical shift range

(around 350 ppm) and different coupling interactions or mechanisms do not cause any experimental problems. For instance the large ^{19}F spectral width causes experimental difficulties with spinlock-based sequences. In *Check it 5.2.1.1* the simulated ^{1}H and ^{13}C spectra of ethyl iodide are compared with the simulated ^{19}F and ^{13}C spectra of perfluoroethyl iodide. As would be expected, except for differences in the magnitude of the homonuclear and heteronuclear scalar coupling constants the spectra are very similar and this similarity extends to the appearance of the ^{13}C satellites in the ^{1}H and ^{19}F spectra. As a consequence of the large chemical shift range ^{19}F spectra generally have a low digital resolution.

5.2.1.1 Check it in NMR-SIM

(a) Load the configuration files *ch5211a.cfg* (^{1}H spectrum) and *ch5211b.cfg* (^{13}C spectrum) one after the other to simulate the ^{1}H and ^{13}C spectra of ethyl iodide (**File│Experiment setup│Load from file...**). Run the simulations (**Go│Run experiment**) saving the files as **Exp No.**: *1* and *2* respectively (**User**: *ch521*, **Name** *5211*). Process the FIDs using zero filling and apodization (**EM**, **LB**: *1.0* Hz). Phase the spectrum and store the data (**File|Save as…**). In the ^{1}H spectrum inspect the ^{13}C satellites and using the **Analysis|Multiplet** mode measure the separation of both satellites, which are symmetrical about the main ^{1}H signal of the ^{12}C isotopomer, to determine the value of ^{1}J (^{13}C, ^{1}H).

(b) Simulate the ^{19}F and ^{13}C spectra of pentafluoroethyl iodide using the corresponding files: *ch5211c.cfg* (^{19}F spectrum) and *ch5211d.cfg* (^{13}C spectrum). Run the simulation, process the FIDs and save the phase corrected spectra. Inspect the ^{19}F spectrum for the ^{13}C satellites of the CF$_2$ group. Because of the negligible difference in natural abundance and receptivity the intensity of the ^{13}C satellites of the CH$_2$ and CF$_2$ groups are comparable. In addition to the different coupling constant values a new effect can be observed - the **primary isotope effect**. Whilst the ^{13}C satellites are symmetrical about the main ^{1}H signal of the ^{12}C isotopomer for the CH$_2$ group, they are unsymmetrical for the CF$_2$ signal. Investigate the ^{13}C spectra for the two compounds and use the **Analysis|Multiplet** mode to measure the values of ^{1}J (^{13}C, ^{1}H) and ^{2}J (^{13}C, ^{1}H) for the ^{13}CH$_2$ and ^{13}CH$_3$ groups and of ^{1}J (^{13}C, ^{19}F) and ^{2}J (^{13}C, ^{19}F) for the ^{13}CF$_2$ and ^{13}CF$_3$ group.

(a) $CH_3 \longrightarrow CH_2 \longrightarrow I$ (b) $CF_3 \longrightarrow CF_2 \longrightarrow I$

  (a) Ethyl iodide, (b) Pentafluoroethyl iodide

[31]P and [29]Si spectra - examples of spin-1/2 isotopes with high abundance/low receptivity (^{31}P) and low abundance/low receptivity ([29]Si)

At first sight ^{31}P and [29]Si are typical examples of heteronuclei, their low receptivity and necessary multi-scan data accumulation consquently mean that the experiment times for ^{31}P and [29]Si spectra are longer compared to ^{1}H or ^{19}F spectra. Like most [n]X spectra they are measured using ^{1}H broadband decoupling to increase the overall signal intensity by removing the splitting due to scalar [n]X ^{1}H coupling. However as shown in Table 5.5 the ^{31}P isotope is separated from the other heteronuclei because although it has a low receptivity, it has 100% natural abundance. In *Check it 5.2.1.2a* the ^{1}H spectrum of methylphosphine oxide is simulated and illustrates that the effect of coupling between the 100% spin 1/2 ^{31}P nucleus and the ^{1}H nucleus is similar to the homonuclear ^{1}H, ^{1}H or ^{19}F, ^{19}F coupling. In contrast the ^{1}H spectrum of bromomethyl silane shows the doublet due to coupling with the low abundant [29]Si isotopomer as satellites superimposed upon the main ^{1}H signals of the highly abundant NMR-inactive [28]Si isotopomer.

5.2.1.2 Check it in NMR-SIM

(a) Simulate the ^{1}H, ^{31}P and ^{13}C spectra of methylphosphine oxide using the configuration files: *ch5212a.cfg* (^{1}H spectrum), *ch5212b.cfg* (^{31}P spectrum) and *ch5212c.cfg* (^{13}C spectrum). Run the simulation saving the FIDs as **Exp. No.**: *1*, *2*, *3* (**User**: *ch521*, **Name**: *5212*). For processing of the FIDs choose correct phase correction to obtain spectra as given in the result file. Observe the doublet for the PH group in the ^{1}H spectrum due to ^{31}P, ^{1}H coupling and the doublet for the [13]CH$_3$ signal in the ^{13}C spectrum due to ^{31}P, ^{13}C coupling. Note the triplet of quartets in the ^{31}P spectrum due to [1]J (^{31}P, ^{1}H) and [2]J (^{31}P, ^{1}H).

(b) The ^{1}H, [29]Si and ^{13}C spectra of bromomethyl silane can be simulated using the configuration files *ch5212d.cfg* (^{1}H spectrum), *ch5212e.cfg* ([29]Si spectrum) and *ch5121f.cfg* (^{13}C spectrum). For improved spectral appearance the FIDs should be processed by zero filling and apodization (**SI** = 2 • TD, wdw function: **EM**, **LB**: *3.0* [Hz]). If necessary phase correct the spectra for pure absorption lineshapes. In the ^{1}H spectrum note that the [29]Si satellites of the [29]SiH$_2$ group are more intense than the ^{13}C satellites of the [13]CH$_3$ group. In contrast to the ^{13}C spectrum of methylphosphine oxide note that there is no heteronuclear coupling in the ^{13}C spectrum of bromomethyl silane due to the relative low abundance of the [29]Si, ^{13}C isotopomer (0.05% probability). Similarly the [29]Si spectrum only displays splitting due to [1]J ([29]Si, ^{1}H) and [2]J ([29]Si, ^{1}H).
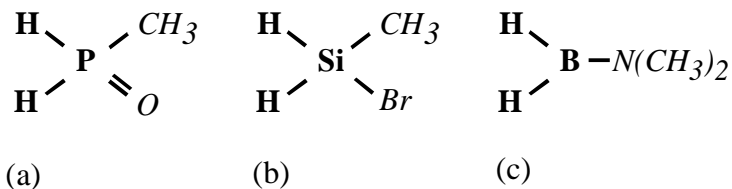
(a) Methyl phosphine oxide (*Check it 5.2.1.2 (a)*)
(b) Bromomethyl silane (*Check it 5.2.1.2 (b)*)
(c) Dimethyl amino borane (*Check it 5.2.1.2 (c)*)

It is obvious that the coupling interaction between two spin 1/2 nuclei ^nX and ^mY results in a doublet in both the ^nX and ^mY spectrum. However it is extremely important to consider the natural abundance of both the NMR active and NMR inactive isotopes and to calculate the probability of an isotopomer containing one or more NMR active isotopes. So for a two spin system it would be necessary to calculate the probability of the isotopomers ^nXY, X^mY and $^nX^mY$.

^{11}B spectrum - example of a non-spin-1/2 nucleus

^{11}B is a quadrupolar nucleus with a nuclear spin quantum number of 3/2, a high natural abundance (around 80%) and a receptivity which is twice as large as the receptivity of the ^{31}P isotope. In *Check it 5.2.1.2 (c)* the ^{1}H, ^{11}B and ^{13}C spectrum of dimethylamino borane is simulated to illustrate the effect of a quadrupolar nucleus coupling with a spin 1/2 nucleus. Due to the high natural abundance of ^{11}B this effect is similar to the ^{31}P isotope in methylphosphine oxide rather than the ^{29}Si satellite spectra in bromomethyl silane.

5.2.1.2 (c) Check it in NMR-SIM

Simulate the ^{1}H, ^{11}B and ^{13}C spectrum of dimethylamino methyl borane using the files: *ch5212g.cfg* (^{1}H spectrum), *ch5212h.cfg* (^{11}B spectrum) and *ch5212i.cfg* (^{13}C spectrum). Because of the high relative natural abundance of the ^{11}B isotope (80% abundance) and, as a consequence of having a nuclear spin, s = 3/2, the ^{1}H signal of the ^{11}BH$_2$ unit is split into four lines of equal intensity separated by ^{1}J (^{11}B, ^{1}H). The ^{11}B spectrum is a triplet, ^{1}J (^{11}B, ^{1}H), with ^{13}C satellites, coupling due to ^{2}J (^{11}B, ^{1}H) is not observed. The ^{13}C spectrum, like the ^{13}C spectrum of the methyl phosphine oxide, displays coupling interaction with two heteronuclei: ^{1}J (^{11}B, ^{1}H) of 120 Hz and ^{2}J (^{13}C, ^{11}B) of 45 Hz.

From this brief discussion comparing the effect on NMR spectra of the nuclear receptivity, natural abundance and spin quantum number, all be it for a small restricted variety of NMR-active isotopes, it is obvious that it is misleading to categorize experiments into ^{1}H and heteronuclear experiments. When discussing pulse sequences,

particularly experiments that utilize polarization transfer, a better definition is to classify nuclei on the basis of either their sensitivity or insensitivity to the NMR experiment irrespective of the natural abundance.

(b) Pulse length calibration

The pulse length relates to the angle by which the z-magnetization or the z-coherence component is rotated from its original direction. The pulse phase determines the new orientation of the magnetization vector with respect to the x,y-plane. In addition to sample properties such as the gyromagnetic ratio of the observed nucleus, solvent susceptibility, concentration and temperature the pulse length for a particular rotation depends upon the probehead design and spectrometer properties. Changing the general experiment setup by applying a pulse on the transmitter/receiver channel instead of the decoupler channel can influence the pulse length. The transmit/receive mode involves switching from the transmitter channel to the receiver channel prior to data acquisition. For the decoupler channel pulses can be transmitted during double resonance experiments or decoupling applied during data acquisition without any switching. Fig. 5.3 is a schematic diagram showing the routing and internal switching corresponding to recording a ^{1}H decoupled ^{n}X spectrum. Because of the different ways the rf signal is routed from source to probehead the pulse power will be attenuated differently and consequently the 90° pulse must be calibrated for both the transmitter and decoupler channel.
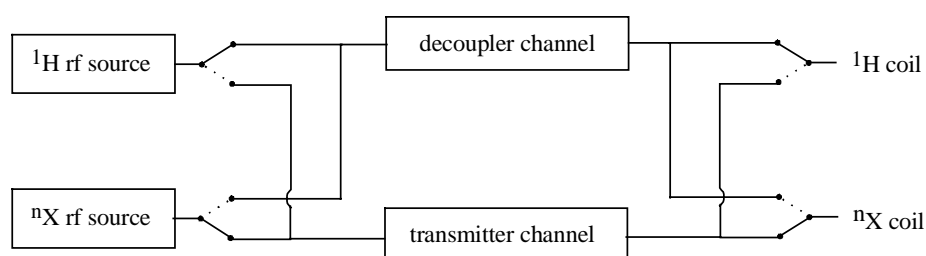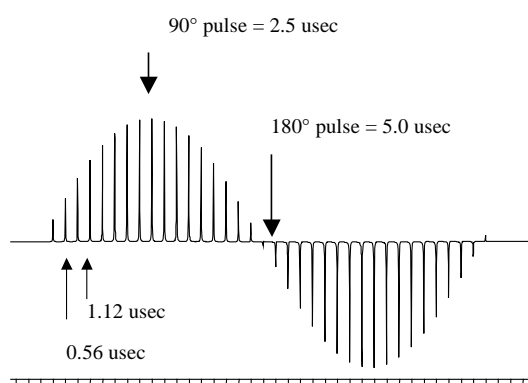

Fig. 5.3:   The spectrometer routing as source of pulse length changes.

The pulse calibration can be performed in two possible ways which are often called *direct* and *indirect calibration*. Pulses on the transmitter channel can be easily calibrated using a standard one-pulse sequence either with or without ^{1}H decoupling. Because the pulse and detected signal are transferred and received on the same channel this method is called *direct calibration*. The procedure is based on recording a series of spectra and comparing the signal intensity as the pulse length is gradually increased. Starting with a pulse length that is obviously shorter than the 90° pulse, the spectrum with the most intense signal corresponds to excitation by a 90° pulse. Ideally the sample used should display a single resonance and there should be a small offset from the transmitter frequency. To verify the 90° pulse length a spectrum can be recorded using a pulse
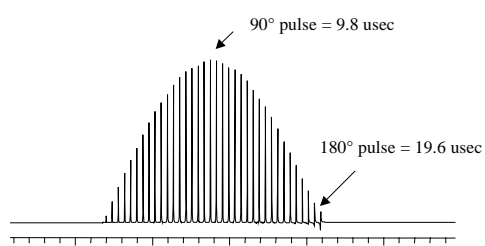
which is either twice or four times as long as the measured 90° pulse. The 180° or 360° pulse aligns the z-magnetization along the –z- and +z-axis respectively which cannot be detected giving a spectrum of nearly zero-intensity.

In *Check its 5.2.1.3(a)* and *(b)* the determination of ^{1}H and ^{13}C 90° pulse length is illustrated. *Check it 5.2.1.3(b)* also illustrates that the pulse length is a function of the gyromagnetic ratio and understanding this concept is very important when using NMR-SIM (see also section 3.2.2, *Check it 3.2.2.2*). Using the **Go|Optimize Parameter** routine a series of spectra can be calculated automatically with increasing pulse length. The routine also automatically shifts the resonance frequency and combines the spectra into a single 1D display giving a sinusoidal trace of pulse length against signal intensity.

^{1}H pulse calibration.

5.2.1.3 Check it in NMR-SIM

(a) ^{1}H pulse calibration
To determine the ^{1}H 90° pulse length, load the configuration file *ch5213.cfg*. Select **Go⎮Optimize parameter** and in the parameter optimizer dialog box select the **Show results as** *1D* option and **p1** for optimization. Click on the **OK** button. In the next dialog box enter the start value **p1**: *0.28u* [s] and increment size **inp0**: *0.28u* [s]. Click on the **OK** button. Process the FID (zero filling **SI(r+i)**: *32k*, apodization **EM**, **LB**: *1.0* [Hz]) prior to Fourier Transformation. Note that the 90° pulse length has the maximum signal intensity while the 180° pulse length has zero signal intensity.

^{13}C pulse calibration.
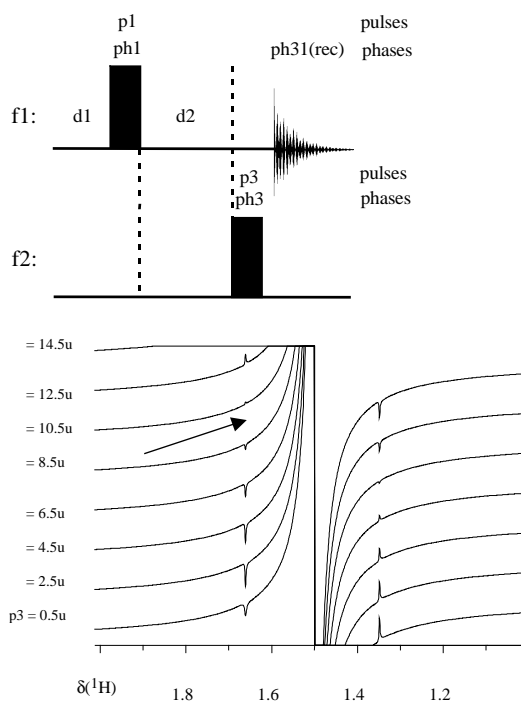
(b) ^{13}C pulse calibration
If not already done as part of the simulation to calibrate the ^{1}H pulse, load the file *ch5213.cfg*. Set the **F1** channel selection box to *C 13*. Load the single ^{13}C nucleus spin system *sglcarbon.ham* (**File⎮Spin system...**) and in the **Options⎮NMR-Sim settings...** dialog box select the **Modify RF field** option. In the (**Go⎮Check Experiment Parameters** dialog box change **SW**: *60* [ppm]. Use the Parameter Optimizer to optimize the p1 pulse length enter **p1**: *0.28u* (start value) and **inp0**: *0.56u* (pulse length increment). Process the data (zero filling **Si(r+i)**: *32k* and apodization **EM**, **LB**: *1.0* [Hz]). The 90° ^{13}C pulse length corresponds to the most

intense signal in the Fourier transformed spectrum.

The pulse calibration on the decoupler channel cannot be performed using the direct method since the pulse which is to be calibrated is transmitted on a different rf channel and resonance frequency to the observed nucleus. To calibrate the rf pulse on the decoupler channel it is necessary to determine the pulse length from the effect the pulse has on the nucleus observed on the transmitter/receiver channel. This *indirect calibration* is achieved by using a coupled IS spin system and transferring the detectable antiphase coherence $S_x I_z$ to the undetectable multiple quantum coherence $-S_x I_y$ ($S_x I_z \xrightarrow{\pi/2\,I_z}$ $S_x I_y$). The antiphase coherence $S_x I_z$ is generated using the pulse sequence shown in *Check it 5.2.1.4*. Again the 90° pulse length is determined using a series of spectra, but this time the 90° decoupler pulse length corresponds to the spectrum with zero-intensity corresponding to the perfect transfer to multiple quantum coherence.

In *Check it 5.2.1.4* the calibration of the ^{13}C decoupler pulse is demonstrated using a CH fragment. Experimentally CHCl$_3$ (S = ^{13}C, I = ^{1}H) would be a suitable test sample.

Stack plot of the 1D spectrum series of the indirect pulse calibration of p3 and pulse sequence scheme (upper part). The arrow denotes the transition of p3 < 90° to p3 > 90°.

5.2.1.4 Check it in NMR-SIM

Load the file *ch5214.cfg* (**File│Experiment setup│Load from file...**). Check the pulse lengths of **p1**: *2.5u* (90° pulse) and **p3**: *0.5u* (4.5° pulse) (**Go│Check Experiment Parameters**). In the **Options│NMR-Sim settings...** dialog box select the **Modify RF field** option. To simulate the decoupler pulse calibration, open the parameter optimizer dialog box (**Go│Optimize parameter**). Select the **Show results as** *1D series*, **N**: *8* and **p3** for optimization. Click on the **OK** button. In the next dialog box enter the start value **p3**: *0.5u* and increment size **inp0**: *2.0u.* Click on the **OK** button and enter then the path and name for the calculated and saved files. Run the series of simulations. In 1D WIN-NMR the last simulated FID will be automatically loaded into the spectrum window. Process the FID (zero filling **SI(r+i)**: *16k*, apodization **EM**, **LB**: *1.0* [Hz]) amd save the Fourier transformed spectrum. Process the remaining FIDs in exactly the

same way. Load all spectra using the **Display**|**Multiple Display** mode and zoom the spectra until the ^{13}C satellites either side of the dispersion signal of the main ^{12}C isotopomer are visible. The display should be similar to the printed figure shown above.

Because of the low abundance of the ^{13}C isotope the ^{1}H spectrum of the antiphase ^{13}C coherence signal is dominated by the intense ^{1}H signal of the abundant ^{12}C isotopomer. The 90° ^{13}C pulse length corresponds to the spectrum with zero-intensity ^{13}C satellites.

(c) Experimental parameters and the relaxation process

As discussed in section 3.2.1 one-pulse experiments are usually performed as multi-scan experiments because the signal-to-noise ratio is proportional $\sqrt{\text{number of scans}}$. It would appear that the most efficient use of spectrometer time would be to acquire as many scans as quickly as possible in the available time. However this approach ignores the relaxation processes that must always be taken into consideration when acquiring data. The longitudinal relaxation time T_1 is the time it takes the magnetization to return to its equilibrium value after perturbation of the spin system. After the first pulse and data acquisition in a multi-scan experiment, the second scan can only have the same magnetization value if the spin system has relaxed back completely to the equilibrium state between scans. So in the absence of incomplete longitudinal relaxation and if no experimental modifications to incorporate extra delays periods are made, a multi-scan experiment must be described as evolution to a steady-state system. During the first scan the thermal equilibrium z-magnetization is rotated by the 90° excitation pulse into the x,y-plane. Due to the relative long longitudinal relaxation time there is incomplete recovery of the magnetization and consequently there is a smaller z-coherence component to be excited, so that after several scans a steady-state balance evolves. A combination of interleaved relaxation delay, usually called d1, a modified excitation pulse angle, the so-called ERNST angle, and dummy scans can be used to overcome this and other undesirable relaxation effects in multi-scan experiments.

The relaxation delay

Increasing the length of the interleaved relaxation delay d1 is probably the easiest way to gain higher signal intensity if two experiments with the same number of scans are compared although the overall experiment time increases by d1 • (number of scans) (It should be pointed out that the total time between pulses is the sum of the acquisition time plus the relaxation delay.). *Check it 5.2.1.5* examines the signal intensity of a single quaternary ^{13}C nucleus as a function of the relaxation delay d1.
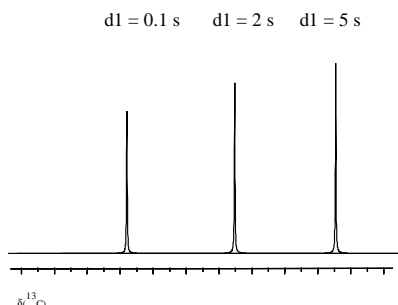
Signal intensity using different d1 relaxation delays.

5.2.1.5 Check it in NMR-SIM

Load the configuration file *ch5215.cfg* corresponding to the ^{13}C spectrum of a single quaternary carbon atom. Simulate three spectra (**Exp No.**: *1* to *3*) using **d1**: *0.1s*, *2s* and *5s*. Prior to each simulation change the value of **d1** in the **Experiment parameter** dialog box (**Go│Check Parameters & Go**). Process the FIDs (zero filling **Si(r+i)**: *64k*, apodization **EM**, **LB**: *1.0* [Hz]) and save the spectra after Fourier transformation. Display all three spectra using the **Multiple Display** mode of 1D WIN-NMR. Select the **Mouse grid** button in the button panel and holding down the left mouse button drag the grid until the spectra appear as in the figure above. With d1 = 3 • T_1 , as often proposed, the optimum in signal intensity is guaranteed because certainly all spins have relaxed completely prior to the next excitation pulse.

The optimum excitation pulse

Ideally each scan in a multi-scan experiment should start with the magnetization in thermal equilibrium although if the relaxation time of the nuclear spin system is comparable or longer than the duration of a single scan, this condition cannot be meet. However if the rotation angle of the one-pulse experiment is reduced from 90° the spin system should be able to return to thermal equilibrium during the duration of the scan such that the next scan starts with nearly the maximum z-magnetization M_0. If a pulse rotates the thermal equilibrium magnetization ($M_{z,0} = M_0$, $M_{x,0} = 0$, $M_{y,0} = 0$) by an angle α, the magnetization generated in the x,y-plane is $M_x = M_0 • \sin \alpha$.

Assuming irreversible decay of transverse coherence during each scan and negligible offset dependence, the optimum angle is a function of the longitudinal relaxation time T_1 and the duration of a single scan T_p (also called the repetition rate) as shown in equation [5-1], [5.5, 5.6]. Ernst and his co-workers first proposed this approach and consequently this optimum pulse angle is referred to as the ERNST angle. Taking the offset dependence and transverse relaxation time T_2 into consideration a more complex relationship can be derived equation [5-2].

ERNST angle as a function of the longitudinal relaxation time

$$\cos\beta_{opt} = \exp[-(T_p / T_1)]$$ [5-1]

T_1 = longitudinal relaxation time; T_p = repetition rate

ERNST angle as a function of the longitudinal and transverse relaxation times and offset dependence

$$\cos\beta_{opt} = \frac{E_1 + E_2 \bullet E_2\text{'}/E_2\text{''}}{1 + E_1 \bullet E_2 \bullet E_2\text{'}/E_2\text{''}}$$ [5-2]

$E_1 = \exp[-(T_p / T_1)]$; $E_2 = \exp[-(T_p / T_2)]$;

$E_2\text{'} = (\cos\phi - E_2)]$; $E_2\text{''} = (1 - E_2 \bullet \cos\phi)$,

T_2 = transverse relaxation time, $\cos\phi$ describes the offset dependence.

The relative enhancement of the signal intensity using the optimum angle relation depends very strongly on the T_p/T_1 ratio. For simplicity in *Check it 5.2.1.6* T_2 and offset effects have been ignored. Furthermore it has been assumed that $T_1 \gg T_2$. The two sets of simulations in *Check it 5.2.1.6* show that for a low T_p/T_1 ratio (a long T_1 relaxation time compared with T_p) there is a considerable advantage in not using a 90° pulse excitation pulse. In contrast for a high Tp/T_1 ratio the optimum pulse angle is close to 90° with more than 95% of the equilibrium magnetization being rotated into the x,y-plane for $T_p \geq 3 \bullet T_1$ [5.3].

Check it 5.2.1.6 also shows that it is possible to include relaxation induced effects into simulations which might be a source of perturbation in a real experiment. The overall pulse sequence time, especially in the long sequences used in nD experiments, becomes a very important, restrictive variable in the development of new pulse sequences. For fast relaxing molecules such as macromolecules the overall pulse sequence time is crucial because if the nuclei start to relax before the data acquisition there will be a loss in signal intensity. It is also important that for maximum signal intensity the spin system returns to thermal equilibrium between scans.

T1 = 20 sec:

Tp / T1 = 2.33 / 20

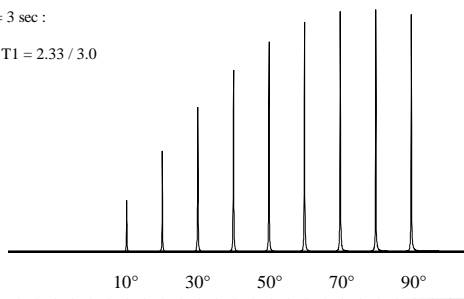10°   30°   50°   70°   90°
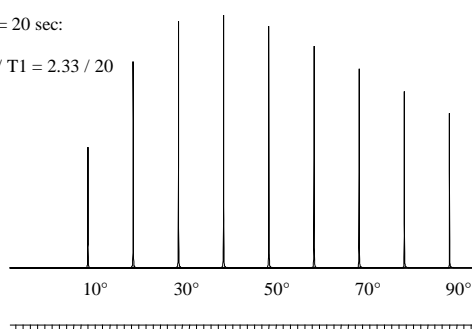
ERNST angle determination "profile".

5.2.1.6 Check it in NMR-SIM

Load the configuration file *ch5215.cfg*. Simulate nine ^{13}C spectra numbers (**User**: *ch521*; **Name**: *5215a* **Exp No.**: *1* to *9*) incrementing the pulse **p1** from *10d* to *90d* in *10d* steps. Process the FIDs (zero filling **Si(r+i)**: *64k*, apodization **EM**, **LB**: *2.0* [Hz]) and save the spectra after Fourier transformation. Display all spectra in 1D WIN-NMR using the option

for a T_p/T_1 ratio of 2.33 / 20.

T1 = 3 sec :

Tp / T1 = 2.33 / 3.0

10°   30°   50°   70°   90°

3D mode of the **Multiple Display** (**Display│Multiple Display**). Use the **Mouse Grid** button of the button panel to tilt the 3D representation corresponding to the figures on the left side. In a second session replace the spin system by the *c13t13.ham* to simulate again nine ^{13}C spectra of faster relaxing carbon atoms to obtain the lower figure on the left side processing and displaying the calculated FIDs as before.

Representation of the ERNST angle determination for a T_p/T_1 ratio of 2.33 / 3.

Check it 5.2.1.6 assumes that all the nuclear spins have the same or comparable longitudinal relaxation times, an assumption not necessarily true in practice. In this situation it is necessary to base the calculation of the ERNST angle upon the T_1 relaxation times of the most significant signals and accept a possible loss of signal intensity for other nuclei with a different relaxation time.

The dummy scans

The efficiency of phase cycling in suppressing unwanted coherences is usually based on the assumption that subsequent scans are acquired for the same initial z-magnetization. The combination of excitation pulse and receiver phase programs ensure that in consecutive scans the unwanted coherences are inverted without change in intensity such that the signals accumulate, ideally, to zero-intensity. However if the steady-state equilibrium is not reached with the first scan the phase cycling fails because the intensity of the unwanted coherences is different in consecutive scans and no longer adds destructively to zero-intensity. One method to reach the steady-state equilibrium prior to data acquisition is the use of dummy scans whereby the pulse program is executed normally but without data acquisition. The experiment proper starts after the dummy scans.

Check it 5.2.1.7 demonstrates the effect of dummy scans on the efficiency of the phase cycling in suppressing the unwanted coherence of a quaternary carbon in the DEPT45-$^{13}C\{^1H\}$ experiment. Because $T_1 \gg$ acquisition time, the initial magnetization before each scan depends upon the number of dummy scans and the relaxation delay d1. With no dummy scans or relaxation delay the initial magnetization is changing before each scan so that the destructive accumulation of the quaternary carbon coherences during the phase cycle fails.

experiment 1:

DS = *0*, **d1** = *0*

5.2.1.7 Check it in NMR-SIM

Load the configuration file *ch5217.cfg*. The spin system contains individual CH, CH_2 and CH_3 groups

experiment 2:

DS = *8*, **d1** = *0*

experiment 3:

DS = *0*, **d1** = *10s*

Experiment parameters for the three simulations of *Check it 5.2.1.7*

and a single quaternary carbon. Simulate the DEPT45-^{13}C{^{1}H} spectrum using **DS**: *0* and **d1**: *0s* saving the data as **Exp No.**: *1*. Set **DS**: *8* (**Go│Check Parameters & Go**) and repeat the simulation saving the data **Exp No.**: *2*. For the third simulation set **DS**: *0* and **d1**: *10s* and run the calculation as **Exp No.**: *3*. Process the FIDs (zero filling **Si(r+i)**: *64k*, apodization **EM**, **LB**: *1.0* [Hz]) and save the spectra after Fourier transformation. Compare the spectra using the **Display│Multiple Display** option and notice the variation in residual signal intensity for the quaternary carbon at 78 ppm.

Variations in the initial magnetization become very important for the phase cycles in experiments such as double quantum filtered COSY or BIRD filtered HMBC where coherences of ^{12}C isotopomers are filtered out by a relaxation driven BIRD unit. Relaxation can also cause artefacts in the detected FID. Normally the phase cycling used in a pulse sequence cancels out any undesirable coherences in subsequent scans by transferring these coherences to a particular axis in the rotational coordinate system. Transverse relaxation might effect these coherences such that they are no longer aligned along the correct axis of the rotational coordinate systems. Thus the phase cycling fails.

5.2.2   Single Line or Multiplet Excitation Experiment

As described in the previous section, a simple one-pulse experiment would normally be performed using a standard set of acquisition parameters such as sweep width and observation frequency. By reducing the acquired frequency range new spectral limits can be chosen, but the spectrum may contain fold-over peaks if digital filtering and oversampling become insufficient to discriminate signals from outside of the chosen frequency range. A comprehensive discussion of these phenomena form part of section 3.3.1 and *Check it 3.3.3.1*. Instead of reducing the acquisition range, a frequency selective pulse could be used to excite a specific line or multiplet. It is not feasible to use such an approach in a standard experiment, as it would be necessary to measure the desired frequency range in several increments in an experiment that is akin to a CW type NMR experiment with respect to both the measurement time and the information obtained.

However, selective pulses often form part of complex pulse sequences. They may be used in converting a 2D experiment into its 1D analogue and in a 2D heteronuclear COSY spectrum to reduce the frequency range of the indirectly detected f1 dimension without the risk of fold-over signals and thereby increasing the digital resolution. Both applications allow a higher digital resolution of the relevant frequency range. In addition selective pulses can also be used to suppress solvent signals (section 5.2.3) and to selectively perturb the equilibrium magnetization of a multi-spin system (section 5.2.4).

In section 5.3.1 there is a short introduction to shaped pulses, which also includes a discussion on how the frequency selectivity of pulses is achieved. There is an extensive

review of shaped pulses in the literature and so by necessity in a book of this nature there are a number of topics missing from section 5.3.1 including a comparison of the advantages and disadvantages of selective shaped pulses.

In this current section the use of amplitude and phase modulation of the pulse shape to achieve frequency selectivity is examined.

Sequence features:

Purpose / principles:	Experiments for selectively studying or suppressing the influence of individual spins to a complex spin system recording the one-pulse ^{1}H or ^{n}X spectrum
Examples:	Solvent signal suppression experiment [5.7], selective COSY experiment [5.8], selective TOCSY experiment [5.9], selective J-resolved experiment (SERF) [5.10], SPT experiment [5.11]

Pulse Sequence Scheme
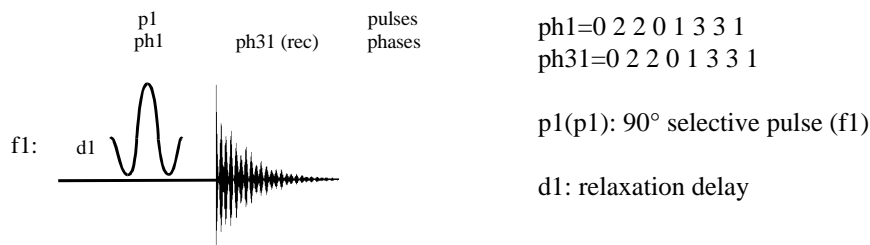
1D selective excitation experiment.

The basic 1D selective excitation experiment is illustrated in the scheme above. It is important to remember that the duration of a shaped pulse is typically 50 to 200 msec and between 7 to 40 usec for a hard pulse. A PO formalistic description would show that because of the relatively long duration of a shaped pulse coupling interaction and chemical shift evolution during the pulse can no longer be neglected leading to a phase and intensity modulation over the excited frequency range. Furthermore relaxation sets an upper limit for the length of the selective pulse.

Check its 5.2.2.1 to *5.2.2.4* examines various properties of selective pulses with the aim of obtaining "the perfect" selective pulse to use as a 90° excitation pulse and a 180° inversion pulse. Section 5.3.1 has a more comprehensive discussion regarding the imperfections of selective pulses and the non-trivial problems concerning the implementation of selective pulses in multi-pulse sequences.

To be able to understand the effect of a shaped pulse, it would be useful to represent the excitation profile of a shaped pulse as a spectrum. This may be easily achieved in NMR-SIM by using a variable spin system. Since the application of a selective pulse creates a mixture of x- and y-transverse magnetization components over its excitation range, a phase distorted profile would be generated (*Check it 5.2.2.1(a)*). Thus, a specific

pulse sequence must be created to separate the x- and y-transverse component of the excitation profile as shown in Fig. 5.4. Following the selective pulse the effects of the 90° hard pulses are illustrated for each component, which are denoted by the letters A and B. If the phase of the first hard pulse is increased by 90° it is possible to detect the other magnetization component.
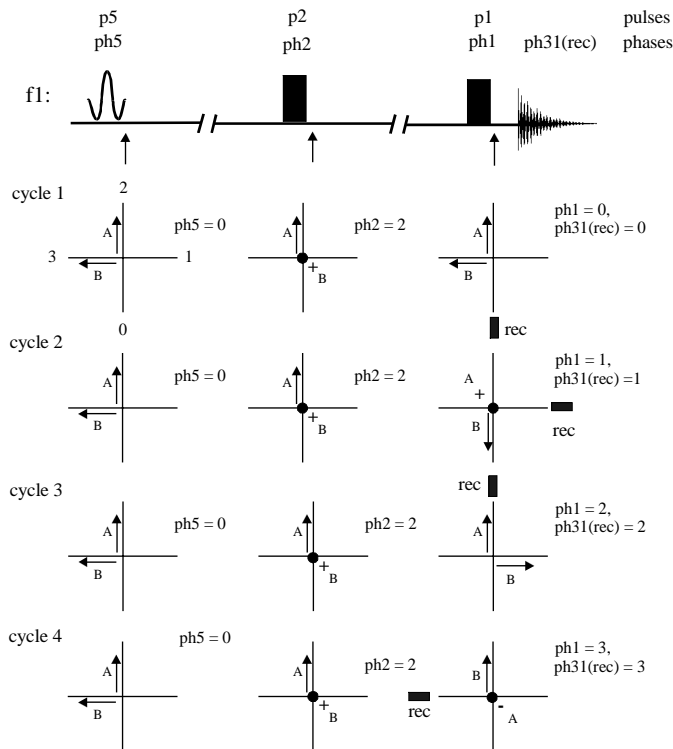

Fig. 5.4: Pulse sequence and resulting magnetization components displayed as vectors for each phase cycle.

In *Check it 5.2.2.1(b)* the profiles of both components are simulated and compared using the multiple display mode of 1D WIN-NMR. The Bloch module excitation profile of the same GAUSSIAN pulse using the time evolution calculation illustrates in a very impressive way that the y-magnetization component for different offsets show a symmetrical evolution relative to the on-resonance magnetization whereas the x-magnetization shows an unsymmetrical evolution.

5.2.2.1 Check it in NMR-SIM

(a) Load the configuration file *ch5221.cfg*, replace the pulse sequence by the file *shape0.seq* and simulate the excitation profile without a separation of x-

and y-magnetization. Process the FID in 1D WIN-NMR using zero filling **SI(r+i)**: *16k* and apodization **EM**, **LB**: *1* [Hz]. Save the Fourier transformed spectrum.

(b) To simulate the y-magnetization excitation profile, reload the configuration file *ch5221.cfg*. In the **Go│Check Experiment Parameters & Go** dialog box set the parameters **p5**: *20000u* , **L1**: *301*, **HV1**: *-150* [Hz] and **HS1**: *10* [Hz]. Start the calculation. Process the data in exactly the same way as for part (a). To detect the x-magnetization, using the **File│Pulse Program...** command replace the current pulse program with the sequence *...\pp\shape2.seq* containing the modified phase cycle **ph2=1**. Compare the two sequences using the **Edit│Pulse Program** command. Process the data in exactly the same way as for part (a). Compare the excitation profiles using the **Display│Multiple Display** mode as shown on the left side of Fig. 5.5.

(c) To calculate the time evolution sphere shown on the right side of Fig. 5.5 open the Bloch module using the **Utilities│Bloch module**... command and start the time evolution calculation (**Calculate│Time Evolution**).
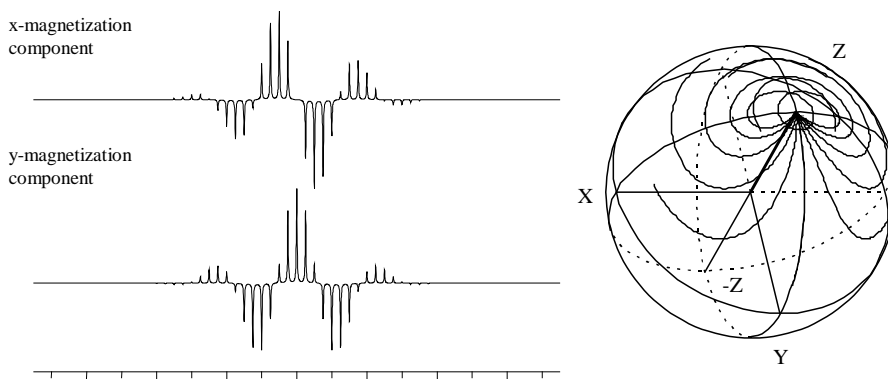

Fig. 5.5:   Magnetization components generated by a 20 msec GAUSSIAN pulse (left), the Bloch module time evolution spherical representation of the same GAUSSIAN pulse (right).

A shaped pulse must fulfil two main criteria; it must be selective and it must generate the required tilt angle e.g. 90° or 180°. The selectivity of a shaped pulse, which is related to the excitation range, is inversely proportional to the pulse length. Selectivity also depends upon the shape of the pulse. Unlike hard pulses, the pulse length and the pulse shape are pre-determined by the desired excitation profile. Thus, the pulse power must be adjusted to the desired title angle of the selective pulse. The relationship between these parameters is complex but may be broken down into three steps and examined using either a spectral representation or the tools of the Bloch module of NMR-SIM.

Step 1. The selectivity may be estimated by the rule of thumb:

$$\Delta v \text{ (excitation range) [Hz]} \propto 1 / \text{(pulse length) [sec]}$$

How applicable this rule is can be demonstrated in NMR-SIM by simulating the excitation profile of the pulse as a spectrum. This may be achieved in two possible ways; by using a spin system which consists of several individual proton spins with increasing frequency offset with respect to the observation frequency or alternatively using a spin system containing a single proton with a variable chemical shift. In the latter case the excitation profile is measured as a function of the frequency difference or offset between the spin's chemical shift and the observation frequency.

5.2.2.2 Check it in NMR-SIM

Load the configuration file *ch5222.cfg*. In the **Parameters⏐Shapes** dialog box check that the **SPNAM0** waveform has the filename *…\shape\eburp28.shp*. In the **Go⏐Check Experiment Parameter** dialog box set **p0**, **SP0**, **HV1** and **HS1** to the values given in Table 5.6 for simulation 1. Execute the simulation and in 1D WIN-NMR process the FID using zero filling **SI(r+i)**: *16k* and apodization **EM**, **LB**: *1* Hz. Do **not** apply a DC-Correction as recommended by 1D WIN-NMR. Before plotting the spectrum toggle the x-axis into Hz using <Ctrl X>. Repeat the simulation for parameter sets 2 and 3. Change the **SPNAM0** waveform filename to *…\shape\gauss129.shp* and repeat the process for parameter sets 4, 5 and 6.

Table 5.6: Simulation Parameters.[1]

	Pulse shape: *E1BURP128.shp*				Pulse shape: *GAUSS129.shp*		
	p0 [msec][2]	sp0 [Hz][3]	$\Delta\nu$ [Hz][4]		p0 [msec][2]	sp0 [Hz][3]	$\Delta\nu$ [Hz][4]
1	5	750	200	4	5	125	200
2	20	225	50	5	20	25	50
3	50	65	20	6	50	12	20

[1]Adjust the parameters HV1 and HS1 to obtain adequate resolution: HV1 = -500 (simulation 1, 4), -250 (simulation 2, 3, 5, 6) and HS1 = 10 (simulation 1, 4), 5 (simulation 2, 3, 5, 6). [2]Pulse length [3]Pulse power level: The optimum pulse power corresponding to the pulse length (90° tilt angle) and pulse shape were determined as described in step 2. [4]Expected selectivity using $\Delta\nu$ (excited frequency range) [Hz] $\propto$ 1 / (pulse length) [sec].

These simulations reveal two interesting facts; the selectivity of the E1BURP pulse shape does not follow the rule of thumb as given above and the GAUSSIAN pulse could not be used for very small excitation ranges because of the very dominant side lobes that invert the magnetization. Since the choice of pulse shape and pulse length depends upon the type of sample and problem being investigated specific pulse shapes have been developed for a particular application such as excitation (90° tilt angle) or inversion (180° tilt angle) of longitudinal (I_z) or transverse (I_x, I_y) magnetization.

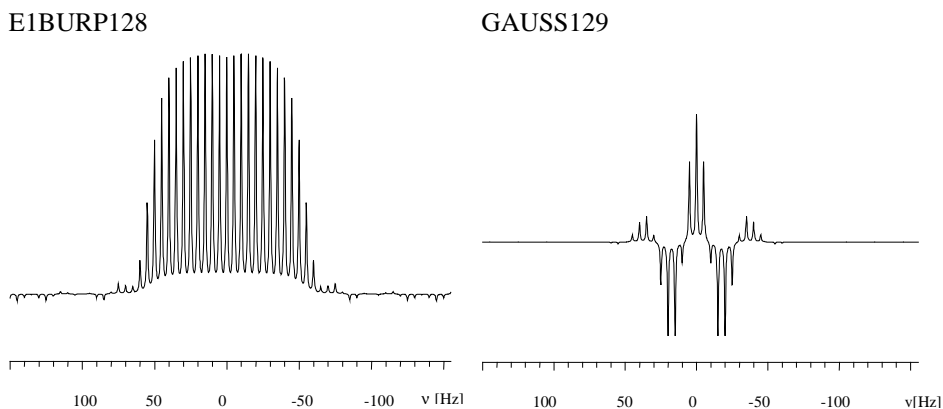E1BURP128   GAUSS129

Fig. 5.6:   Selectivity of a E1BURP 90° and a GAUSSIAN 90° pulse, each has a pulse length of 50 msec.

Step 2: For a shaped pulse the pulse length determines the selectivity and the pulse power the tilt angle. This is in contrast to a hard pulse where the pulse length is adjusted to obtain the required tilt angle. The interaction between pulse length and tilt angle can displayed graphically using the **RF field profile** calculation in the Bloch module of NMR-SIM.

5.2.2.3 Check it in NMR-SIM

Load the configuration file *ch5223.cfg*. Open the Bloch module using the **Uitilities│Bloch module**… command. In the **Calculate│Setup** dialog box toggle the *Shaped pulse* option and enter for **SPNAM0** the filename *…\wave\gauss129.shp*. In the **Calculate│RF field profile** dialog box set **M(x)**: *0*, **M(y)**: *0*, **M(z)**: *0*; **p0**: *5000u*, **N**: *50*, **Start**: *0*, **Step**: *10* and **Offset**: *0*. Close the dialog box with **OK**. The Rf field profile should be the same as in Fig. 5.7. As an additional exercise calculate the Rf field profiles for the shaped pulses used in *Check it 5.2.2.1* changing the **SPNAM0** filename and modifying the parameters **N**, **Start** and **Step** accordingly.
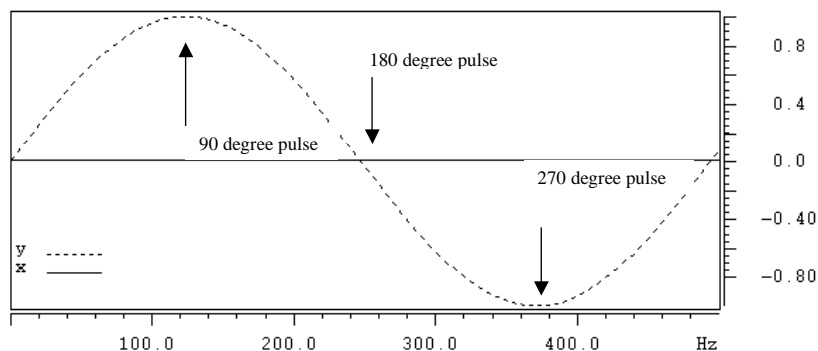
Fig. 5.7: Rf field profile of a 5 msec GAUSSIAN pulse (129 data points).

Step 3: To determine the optimum pulse shape the excitation profile should be calculated. The excitation profile can be simulated using either the **Excitation Profile** option of the Bloch module or as in *Check it 5.2.2.1* a 1D spectrum. The Bloch module can display both transverse magnetization components on the same graph while 1D WIN-NMR can only show either the x- or the y-component (see *Check it 5.2.2.1*).

5.2.2.4 Check it in NMR-SIM

(a) Load the configuration file *ch5224a.cfg*. Open the Bloch module using the **Utilities│Bloch module**… command. In the **Calculate│Setup** dialog box toggle the *Shaped pulse* option and enter for **SPNAM0** the filename *...\wave\gauss129.shp*. In the **Calculate│Excitation profile** dialog box set **M(x)**: *0*, **M(y)**: *0*, **M(z)**: *0*; **p0**: *20000u*, **SP0**: *25* [Hz], **N**: *81*, **Start**: *-200* [Hz] and **Step**: *5* [Hz]. Click the **OK** button to display the excitation profile.

(b) Load the configuration file *ch5224b.cfg*. In the **Go│Check Experiment Parameters & Go** dialog box set the parameters **p5**: *20000u*], **L1**: *101*, **HV1**: *-500* [Hz] and **HS1**: *10* [Hz]. Start the spectrum calculation (**Go│Run Experiment**) and save the data with a suitable filename. Process the FID in 1D WIN-NMR using zero filling of **SI(r+i)**: *16k* and apodization **EM**, **LB**: *1* Hz. After Fourier transformation the obtained spectrum should resemble the representation in the result file.

5.2.3   Single Line or Multiplet Suppression Experiments

The main application of selective signal suppression is solvent signal suppression [5.12]. Although a solvent signal may be a good reference signal, two problems can arise particularly when studying dilute samples. The first, and most obvious, problem is that the solvent signal can overlap with the sample signals whilst the second is a more subtle experimental hardware problem relating to the dynamic range of the digitizer used to

convert the analogue NMR signal intensities into binary representation. The large signal from the solvent dominates the FID filling the digitiser; superimposed upon the solvent signal are the very much weaker sample signals that are poorly digitised which leads to a overall reduction in signal-to-noise ratio for the sample signals. Solvent suppression is extremely important particularly when studying biological samples such as blood, urine and body fluids or compounds such as peptides or sugars which are only soluble in water.

Depending on the type of sample and spectrometer configuration there are three main selective signal suppression methods:

- Solvent presaturation
- Jump-and-return
- WATERGATE

The simplest method is solvent presaturation where the solvent signal is selectively saturated prior to data acquisition. The major drawback with this method are protons that belong to functional groups such as OH and NH that can exchange with the solvent; these exchangeable protons are also saturated and the signals might disappear. The jump-and-return method is based on an evolution method where all nuclei evolve under the influence of chemical shift and coupling interaction. The transmitter frequency is set exactly at the solvent resonance frequency so that after the initial 90° pulse the solvent coherence is static in the rotating frame coordinate system. A second 90° pulse sends the solvent coherence back to its equilibrium magnetization enabling other coherences to be detected. The disadvantage of this method is that signal intensities are affected in a complicated non-uniform manner and there is a 180° phase change at the solvent frequency giving a dispersive shape for the residual solvent signal, which disturbs the spectrum and diminishes the intensity of weak signals. The WATERGATE experiment is probably the most sophisticated method, combining selective pulses and gradient coherence selection. The sequence is based on pulsed field gradients that refocus required coherences while destroying unwanted coherences. After the first field gradient pulse the combined application of non-selective and selective pulses inverts the sample signals which are then refocused by the second field gradient pulse to give a gradient echo whereas the non-inverted solvent signal remains dephased and is not detected. The solvent is unaffected by the selective pulse and the field gradients combine to destroy any solvent coherence.

Sequence features:

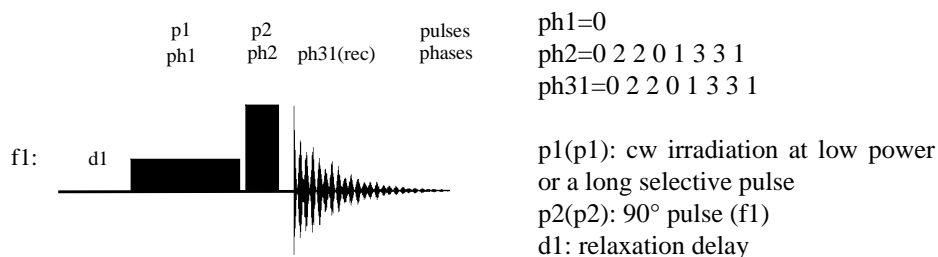|	
Purpose / principles:	Selective suppression of a single line or a multiplet which belongs to a high concentration compound, particularly solvents or by-products
	Different principles are used: (1) presaturation method: presaturation of the signal, (2) jump-and-return method: excitation of all signals followed by transfer of solvent coherence into not-detectable equilibrium magnetization of the solvent, (3) WATERGATE: gradient driven destruction of solvent coherence

Variants: Presaturation technique [5.13], jump-and-return technique [5.14], WATERGATE [5.15], DPFGSE-WATERGATE [5.16]

The presaturation method

As discussed in the introduction to this section, the presaturation method is the simplest experiment since the suppression is based on either cw irradiation or a shaped selective pulse. The method is not recommended for solvents such as water or methanol if protons of the compound under investigation exchange with the presaturated protons of the solvent, since the resonance signal of these protons would also be presaturated and disappear. Consequently the presaturation method should not be used for sugars, proteins etc. if the amid, imid or hydroxyl protons are of particular interest.

Most pulse sequences can be easily modified to include a presaturation unit provided that the detection of exchangeable protons is not the major purpose.

Pulse Sequence Scheme

ph1=0
ph2=0 2 2 0 1 3 3 1
ph31=0 2 2 0 1 3 3 1

p1(p1): cw irradiation at low power or a long selective pulse
p2(p2): 90° pulse (f1)
d1: relaxation delay

The presaturation experiment.

In *Check it 5.2.3.1* the ^{1}H spectrum of peracetylated β-D-glucose (1%) in water (99%) is simulated with and without solvent presaturation. To reduce the calculation time only the ^{1}H signals of the protons H-3, H-4, H-5 and H-6/H-6' are considered initially. The signals of the remaining protons H-1, H-2 and acetyl CH$_3$ signals are all well removed from the solvent signal.


R = CH$_3$OCO
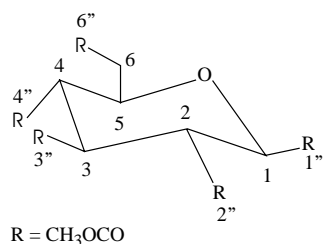
Structure of peracetylated β-D-glucose

5.2.3.1 Check it in NMR-SIM

Load the configuration file *ch5231.cfg*. Start the calculation. Process the FID in 1D WIN-NMR using zero filling (**SI(r+i)**: *32k*) and apodization **EM**, **LB**: *1.0* [Hz]). After Fourier transformation examine the small residual water signal at 4.6 ppm. Using the **File⏐Pulse program...** command replace the current pulse program with the sequence *zg.seq* and calculate the ^{1}H spectrum without water suppression. Compare the two spectra with respect

to the efficiency of the water suppression. It is also possible to calculate the ^{1}H spectrum of the complete spin system. Using the **Edit‖Spin system** command edit the file *bDglucos.ham* and delete the semicolon (;) and the term *(optional)* in each line containing the word *(optional)*. Save the modified spin system (**File|Save As…**) using a suitable name e.g. *bDgluall.ham*. Load the new spin system using the **File‖Spin system...** command and repeat the simulation. Note: depending upon the speed of the computer this calculation will take several minutes.

It is also possible to use the presaturation method with solvents and solvent mixtures where it is necessary to suppress several solvent signals with different chemical shifts. The presaturation of several singlets or multiplets can be achieved by using either multi-selective pulses or by using a cycle of soft pulses with different offset frequencies. Normally in ^{1}H COSY experiments such as ^{1}H gradient selected COSY or double quantum filtered COSY the filter functions used suppress extremely well singlet peaks such as solvent signals although additional solvent suppression methods are necessary when working with very low concentrated solutions such as biological samples. In *Check it 5.2.3.2* the ^{1}H COSY spectrum of the nucleoside uridine is simulated using presaturation of the solvent signal; presaturation may be used in this particular case because the exchangeable proton signals are not important. *Check it 5.2.3.2* also shows that it is possible to achieve a high degree of solvent suppression using the simple presaturation method without recourse to the more complicated double quantum filter or gradients experiments.
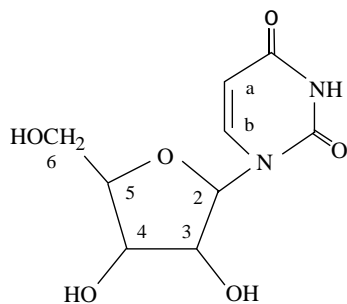
Structure of uridine

δ(H-2) = 5.9; δ(H-3) = 4.35; δ(H-4) = 4.25; δ(H-5) = 4.15; δ(H-6) = 3.82; δ(H-6') = 3.92; δ(H-a) = 5.90; δ(H-b) = 7.87

5.2.3.2 Check it in NMR-SIM

Simulate the ^{1}H spectrum of uridine using the configuration file *ch5232a.cfg*. Process the FID in 1D WIN-NMR using zero filling (**SI(r+i)**: *32k*) and apodization (**EM**, **LB**: *1.0* [Hz]). Save the spectrum. Simulate the ^{1}H COSY spectrum without water presaturation using the configuration file *ch5232b.cfg* and with water presaturation using the configuration file *ch5232c.cfg*. In the **Go‖Check Parameters & Go** dialog box check that **nd0**: *1*. Process the 2D data sets using the processing parameters stored in the configuration files Examine the small residual solvent signal of the ^{1}H COSY spectrum simulated with presaturation.
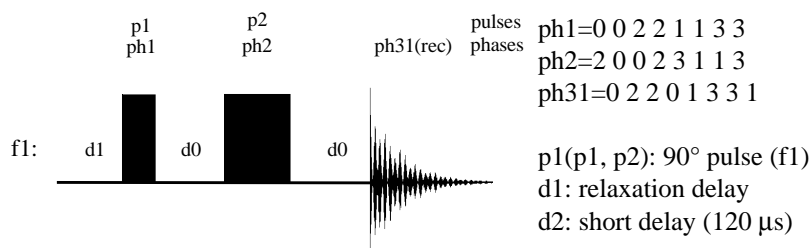
The jump-and-return method

The theory behind the jump-and-return method is simply illustrated using the rotating coordinate system. The transmitter frequency is first adjusted to be exactly on-resonance for the single solvent signal. After the initial 90° pulse all the coherences lie along the y-axis, during the fixed delay period d2 the coherences evolve under the influence of chemical shift differences and coupling interaction except for the solvent coherence which is static in the rotating frame co-ordinate system. The second 90° pulse brings the solvent coherence back to the z-axis while all the other coherence components, which are orthogonal to the pulse phase, are left unchanged and are detected as transverse coherences during the subsequent acquisition. There are several major drawbacks for the jump-and-return method:

- There is a 180° phase shift across the spectrum.
- The method requires the pulse to be exactly 90°.
- It is not possible to suppress several solvent signals simultaneously.
- The spectrum must be centred on the solvent resonance signal.

Despite these disadvantages the jump-and-return method is a useful technique if the overall experiment time should be kept as short as possible.

Pulse Sequence Scheme

1D jump-and-return method experiment.

As shown in *Check it 5.2.3.3* in the jump-and-return method it is very critical that the hard pulse p1 and p2 are exactly 90° because an error of as little as 0.5° can cause a large residual solvent signal.

5.2.3.3 Check it in NMR-SIM

Load the configuration file *ch5233.cfg*. To illustrate the sensitivity of the jump-and-return method to variations in the 90° pulse angle, simulate the spectrum three times varying the pulse angle **p1**: *90d*, *89.9d* and *89.5d* in the **Go│Check Experiment Parameters & Go** dialog box. Process the FID in 1D WIN-NMR using zero filling (**SI(r+i)**:*32k*) and apodization (**EM**, **LB**: *1.0* [Hz]). Save the spectrum. Use the **Display│Multiple Display** option to compare the spectra.

The jump-and-return method can also be implemented in 2D experiments in a similar manner to the presaturation method. *Check it 5.2.3.4* shows the jump-and-return method as part of a 2D homonuclear COSY experiment for peracetylated β-D-glucose.

5.2.3.4 Check it in NMR-SIM

Simulate the ^{1}H spectrum to use as the projection files using the configuration file *ch5234a.cfg*. Process the FID in 1D WIN-NMR using zero filling (**SI(r+i)**: *8k*) and apodization (wdw-function: **EM**, **LB**: *2.0*). Save the spectrum. Simulate the ^{1}H COSY spectrum (**nd0**: *1*) using the configuration file *ch5234b.cfg* (^{1}H jump-return-COSY spectrum) and *ch5234c.cfg* (^{1}H COSY spectrum). Process the data set in 2D WIN-NMR checking that in the **Process|General parameter setup|edp** dialog box that **SI** (F1 and F2**)**: *1024*, **WDW** (F1 and F2): *SINE* and **SSB** (F1 and F2): *0*. Set the **MC2**-option to *qf*, **PH-mod** (F1): *mc* and **PH-mod** (F2): *no*. Select the **Utilities**-button in the button panel to add the projections on each dimension (**ext**-button (f1-axis and f2-axis)).

The WATERGATE method

The WATERGATE (**WATER** suppression by **GrA**dient-**T**ailored **E**xcitation) experiment [5.15] is a pulsed field gradient spin-echo experiment and consists of a sequence **S** enclosed by two gradient pulses of the same strength and same sense. It may be represented as (excitation) **... G1 - S - G2 ...** (acquisition). The sequence **S** does not effect the water or more generally the solvent coherence so that the net rotation of the solvent magnetization is zero in contrast to the coherences of all other protons, which are inverted by 180°. The two gradients dephase and then rephase the coherences inverted by the sequence **S** giving a gradient echo but cumulatively destroys the solvent coherence, which effectively bypasses the sequence **S** and is no longer detected during the acquisition period.

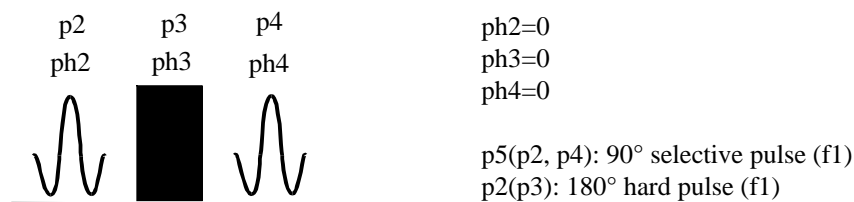Ideally the WATERGATE sequence should have the following characteristics:

- The sequence S must be highly selective to discriminate between the wanted coherence and solvent coherence.
- There should be little or no change in intensity for signals close to the suppressed solvent signal(s).
- Spectrum distortions such as baseline roll or phase distortions should be negligible.

However no pulse sequence is ideal and as discussed in the following *Check its* there has been several modifications to the original WATERGATE sequence to try and achieve the optimum solvent suppression experiment.

Pulse Sequence Scheme

ph1=0 0 1 1 2 2 3 3
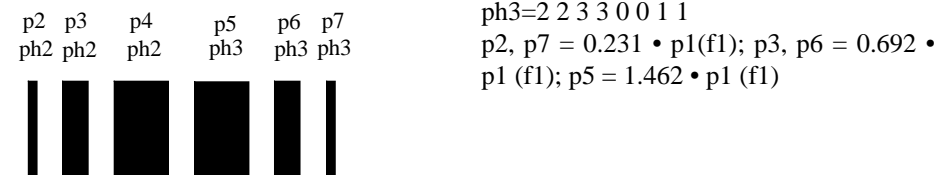ph31=0 0 1 1 2 2 3 3

p1(p1): 90° pulse (f1)
d1: relaxation delay
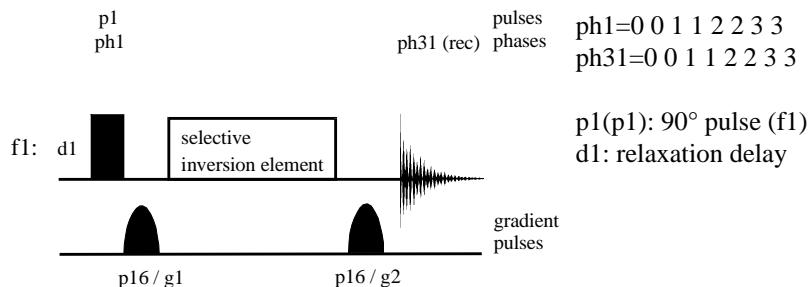
The WATERGATE experiment.

The selective inversion element:

(a) a pulse composite of selective 90° pulses and a hard 180° pulse [5.15]
(WATERGATE-1)

ph2=0
ph3=0
ph4=0

p5(p2, p4): 90° selective pulse (f1)
p2(p3): 180° hard pulse (f1)

(b) a binomial pulse 3-9-19 [5.17]
(WATERGATE-2)

ph2=0 0 1 1 2 2 3 3
ph3=2 2 3 3 0 0 1 1
p2, p7 = 0.231 • p1(f1); p3, p6 = 0.692 •
p1 (f1); p5 = 1.462 • p1 (f1)

   In the original WATERGATE-1 experiment, using selective inversion element (a), a net rotation of zero for the solvent magnetization is achieved while the $180°_x$ pulse inverts all the other coherences. In *Check it 5.2.3.5* the efficiency of the WATERGATE-1 sequence is demonstrated for the ^{1}H spectrum of uridine (1%), a nucleoside of uracil and ribose, in water (99%).

5.2.3.5 Check it NMR-SIM

Load the configuration file *ch5235.cfg* and simulate the ^{1}H spectrum of uridine without solvent suppression. Process the FID in 1D WIN-NMR using zero filling (**SI(r+i)**: *32k*) and apodization (**EM**, **LB**: *1.0* [Hz]). Load the configuration

file *ch5236.cfg* and simulate the WATERGATE-1 ^{1}H spectrum. Process the FID in the same way as the previously calculated data. Compare both spectra using the multiple display option in 1D WIN-NMR.

A comparison of the spectra with and without the WATERGATE-1 sequence shows how efficient the sequence is in suppressing the residual water signal. Less desirable is the loss in intensity for the signals close to the residual solvent signal; this effect is particularly noticeable for the triplet at 4.35 ppm. One reasonis that the shaped pulse is not perfectly selective which decreases the intensity of signals nearby to the excited region. The effect of a finite excitation range will be discussed later. In *Check it* 5.2.3.6 the effect of varying the tilt angle of the shaped pulse on the residual water signal is examined.

5.2.3.6 Check it in NMR-SIM

Load the configuration file *ch5236.cfg* and perform a set of simulations varying the power level of the shaped pulse: **sp0**: *61*, *62.5* (optimum for a 90° tilt angle), *64* and *68* [Hz]. Process the set of data in 1D WIN-NMR in exactly the same way; zero filling of **SI(r+i)**: *32k* and apodization **EM**, **LB**:*1.0* [Hz]. Compare the spectra using the 1D WIN-NMR multiple display mode.

Check it 5.2.3.7 illustrates that for the successful suppression of the water signal the shaped pulse power is critical and the power level must correspond very closely to a 90° tilt angle. Unfortunately the quality of a shaped pulse is strongly dependent on both the type of sample and the experimental conditions such as salt concentration, solvent dielectricity and temperature. Consequently to ensure optimum solvent suppression it is necessary to adjust the shaped pulse parameters on a sample to sample basis. This continuous parameter adjustment is rather tedious. Consequently the WATERGATE-2 experiment using a binomial combination of hard pulses [5.17] has been proposed. Binomial pulses are discussed in detail in section 5.3.1. In *Check it 5.2.3.7* the so-called (3-9-19) binomial combination - derived from an extended binomial pulse [5.18] - for solvent suppression is introduced. However the hard pulse application does have its disadvantages, the binomial pulse sequence decreasing further the intensity of signals close to the suppressed solvent. In the second part of *Check it 5.2.3.7* the insensitivity of the binomial pulse sequence to the value of the hard pulse tilt angle is illustrated by replacing the 90° hard pulse with an 80° pulse. Only a small loss in intensity is observed while the solvent suppression remains perfect illustrating quite clearly the superior of this sequence particularly when experiment conditions such as temperature or sample properties are changed.

5.2.3.7 Check it in NMR-SIM

(a) Load the configuration file *ch5237.cfg* and simulate the ^{1}H spectrum with WATERGATE solvent suppression using the (3-9-19) binomial pulse sequence. Process the FID using zero filling of **SI(r+i)**: *32k* and apodization **EM**, **LB**: *1.0* [Hz].

(b) Repeat the simulation but in the **Go│Check Parameters & Go** dialog box check set **p1**: *80d*. Process the FID. Using the dual display window option compare both spectra, in particular the region 3.5 to 4.5 ppm.

Comparing the signals at 4.15, 4.25 and 4.35 ppm in the ^{1}H spectrum simulated using the WATERGATE-1 and the WATERGATE-2 sequence the greater loss of signal intensity close to the solvent signal for the WATERGATE-2 sequence is evident. Nevertheless as the second simulation in *Check it 5.2.3.7* has shown the binomial pulse sequence is a very effective method for solvent suppression. In practise the WATERGATE 2 sequence is extremely easy to implement so that the loss of signal intensity is a minor consequence.

Although the (3-9-19) sequence is the most commonly used binomial pulse sequence other sequences have been developed called W4 and W5 [5.19]. Only the W5 sequence will be considered here. The W5 sequence consists of a five hard pulse train, each pulse length being calculated to give the optimum excitation profile. In the first part of *Check it 5.2.3.8* the ^{1}H spectrum with WATERGATE-3 (W5-binominal pulse sequence) is simulated and the results compared with *Check it 5.2.3.7a*. In the second part of this *Check it* the excitation profiles of three different WATERGATE sequences are calculated and compared.
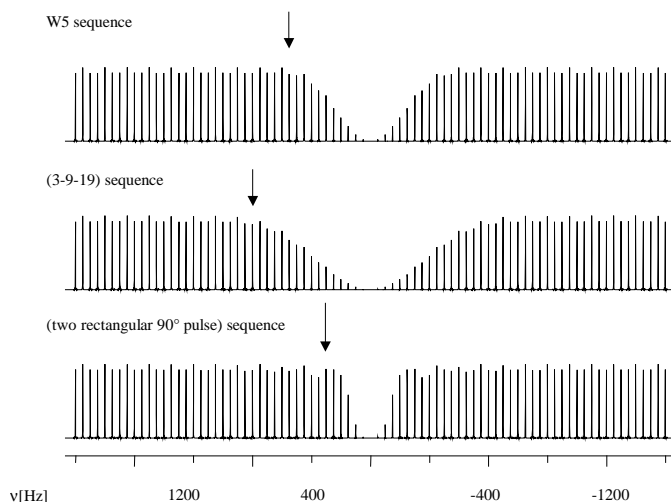

Fig. 5.8:   Suppression profiles of different sequence units S in the WATERGATE element. The arrow denotes the first offset relative to the on-resonance frequency where no attenuation can be assumed.

5.2.3.8 Check it in NMR-SIM

(a) Load the configuration file *ch5238.cfg*. Process the FID using zero filling **SI(r+i)**: *32k* and apodization **EM**, **LB**: *1.0* [Hz]. Save the spectrum and compare the results from *Check it 5.2.3.7a* using the multiple display window of 1D WIN-NMR.

(b) To calculate the excitation profiles of the different WATERGATE sequences load sequentially the configuration file *ch5238a.cfg* (WATERGATE-1), *ch5238b.cfg* (WATERGATE-2) and *ch5238c.cfg* (WATERGATE-3). Process the FIDs using zero filling **SI(r+i)**: *32k* apodization **EM**, **LB**: *1.0* [Hz]. Save the spectra. Compare the results using the multiple display window.

It is interesting to contrast the results of *Check it 5.2.2.1* and *Check it 5.2.3.8b*. In the former a shaped pulse was used to give a very narrow excitation range with no excitation over most of the spectral width. In the latter the converse is true, a pulse sequence is used to give a very wide excitation range with a well-defined notch where there is no excitation. The suppression profile of the W5 sequence is similar to the profile obtained for the original WATERGATE-1 sequence indicating that the binomial and the original pulse sequence have comparable suppression characteristics. However on a practical basis the hard pulse train sequence is favoured because it is easier to use.

From the practical viewpoint it might be surprising that the WATERGATE sequence is usually applied with the transmitter frequency exactly on-resonance with the solvent signal. The reason for this approach is that it minimizes radiation damping, which decays the transverse magnetization. Because NMR-SIM is based on an ideal spectrometer this radiation damping decay mechanism cannot be simulated.

A further improvement can be made using excitation sculpting [5.16], which essentially consists of two pulsed field gradient spin echo units and may be represented as (excitation) **... G1 - S - G1 - G2 - S - G2 ...** (acquisition). The effect of the second pulsed field gradient spin echo unit is to cancel out any remaining phase errors to give a pure phase selective excitation profile that only depends on the inversion properties of the *S* element. To prevent the accidental refocusing of any unwanted magnetization *G1* and *G2* have different gradient strengths. Excitation sculpting is a general procedure, which uses selective excitation such as shaped pulses or the DANTE-sequences and may be used as a building block in many pulse sequences. The theory of excitation sculpting is discussed in more detail in section 2.3.3. When used for solvent suppression the **D**ouble **P**ulsed **F**ield **G**radient **S**pin **E**chos (DPFGSE) acts like a "super-spin echo", refocusing the effects of chemical shift and distorsions introduced by the element S and producing spectra with less phase errors and baseline distortion.

In *Check it 5.2.3.9* the efficiency of the excitation sculpting for the WATERGATE experiment is demonstrated. Using a $180°_{-x}$(selective) - $180°_{-x}$ *S* element in the **... G - S - G ...** sequence the phase profile of the *S* element is examined using the Bloch module of NMR-SIM and the effects of this phase behaviour on the ^{1}H spectrum of uridine in water illustrated. The spectrum is then simulated using the DPFGSE-WATERGATE experiment and the results compared with that from the standard WATERGATE experiment.

5.2.3.9 Check it in NMR-SIM

Load the configuration file *ch5239.cfg* and simulate the ^{1}H spectrum without water signal suppression (**Go**⎪**Run experiment**). Process the FID using zero

filling **SI(r+i)**: *32k* and apodization **EM**, **LB**: *1.0* [Hz]. Save the spectrum. Now consider the phase behaviour on the whole spectrum of the rectangular pulse. Load the configuration file *ch5239a.cfg*. Open the Bloch module using the **Uitilities⎮Bloch module**… command. To check the power level for the 180° selective pulse open the **Calculate⎮RF field profile** dialog box and set the following parameters; the initial magnetization **M(x)**: *0*, **M(y)**: *-1*, **M(z)**: *0*; the pulse parameters **SPNAM0**...*\wave\rect.shp* and **p0**: *2200u* and the calculation range **Start**: *0* , **N**: *100* and **Step**: *10*. Close the dialog box with **OK**. Click the **Z** and then **X,Y** button in the option bar to confirm that for an offset of 0 Hz a rf power level of 210 Hz corresponds to a 180° pulse. At this power level the on-resonance magnetization is transferred from initially being aligned along the -y-axis to be aligned along the y-axis in both cases $M_z(t) = 0$ and $M_x(t) = 0$. Using the **Calculate⎮Excitation profile** command, calculate the excitation profile for different frequency offsets using the parameters **Start**: *-1000*], **N**: *201* and **Step**: *10*. Close the dialog box with **OK**. Clicking on the **X**, **Y** and **Z** buttons in the window option bar confirm the complex phase behaviour of the magnetization components. It is the phase properties of the selective pulse that introduces the phase distortions in the final spectrum. If not already loaded, load the configuration file *ch5239a.cfg* (^{1}H WATERGATE experiment with 180°$_x$(selective) - 180°$_x$ sequence). Simulate the spectrum and process the data using zero filling **SI(r+i)**: *32k* and apodization **EM**, **LB**: *1.0*. Try to phase the spectrum, it will be impossible to phase all the signals correctly. Load the configuration file *ch5239b.cfg* (^{1}H DPFGSE-WATERGATE experiment with 180°$_x$(selective) - 180°$_x$ sequence) and repeat the simulation. Compare the results of the single pulsed field gradient spin echo experiment and the double spin echo version.

Although the double spin echo spectrum can be phased and the solvent suppression is excellent there is a further reduction in the intensity of the detected signals. This reduction in signal intensity is a function of the gradient field strength used for the second spin echo unit and in *Check it 5.2.3.10* this relationship is examined.

5.2.3.10 Check it in NMR-SIM

Load the configuration file *ch52310.cfg*. Simulate the ^{1}H spectrum with DPFGSE-WATERGATE suppression (**Go⎮Run experiment & Go**). Process the FID using zero filling of **SI(r+i)**: *32k* and apodization **EM**, **LB**: *1.0* [Hz]. Save the spectrum. Repeat the simulation for the different gradient field strength combinations shown in Table 5.7.

Even at very low gradient strengths (G3 : G4 = 0.5 : 0.5) there is only a small residual water signal which is acceptable but there has not been any dramatic increase in the intensity of the signals close to the water signal. The sequence **S** in the WATERGATE unit has a major influence on the coherence selection, the signal intensity and the phase behaviour of the final spectrum. It may be considered to be a non-ideal filter, which effectively removes the solvent signal but also has the undesirable side

effect of reducing the intensity of signals that have a chemical shift similar to the suppressed solvent signal.

Table 5.7:   Gradient intensities for the ^{1}H DPFGSE-WATERGATE spectrum.

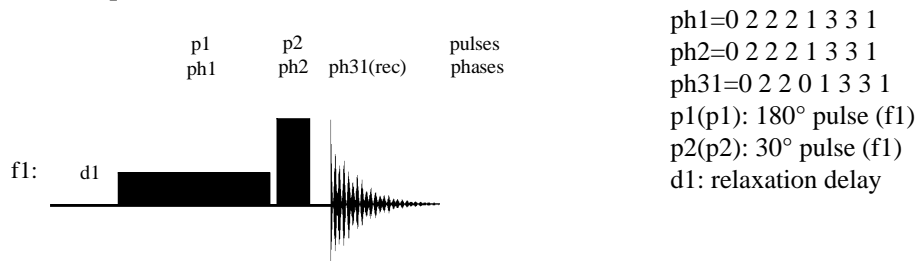| GPZ1 : GPZ2	GPZ3 : GPZ4
10 : 10	0.5 : 0.5
10 : 10	3 : 3
10 : 10	5 : 5
10 : 10	9 : 9

5.2.4   Single Line Perturbation Experiment

Scalar coupling constants possess sign and magnitude. Both parameters depend upon the stereochemistry of a molecule and the number and type of chemical bonds between coupling partners. Consequently coupling constants are extremely useful in signal assignment and determining detailed molecular structures. Experiments for determining the magnitude of scalar coupling constants will be discussed in the next section, in this section one of the methods available for determining the relative signs of coupling constants will be examined. Knowledge of the relative signs of coupling constants is extremely important in spin system analysis.

Single line perturbation experiments such as spin-tickling or internuclear double resonance (INDOR) have been performed on continuous wave (CW) NMR spectrometers whereas selective population transfer (SPT) or selective population inversion (SPI) may also be performed on both CW and pulse FT spectrometers. These types of experiments do not depend on the magnitude of the coupling constants involved. This is in contrast to the homonuclear COSY type experiments which are very sensitive to the value of the coupling constants involved and where it has been necessary to develop experiments specifically for studying long-range scalar couplings.

Sequence features:

Purpose / principles:	Determination of the relative sign of scalar coupling constants, general detection of coupling interaction. The perturbation of a single transition shows intensity changes on related transitions.
Variants:	Spin-tickling experiment [5.20, 5.11], (90°sel.-90°hard)-SPT [5.21], (135°sel.-45°hard)-SPT [5.21], INDOR [5.11]

Pulse Sequence Scheme (homonuclear)

ph1=0 2 2 2 1 3 3 1
ph2=0 2 2 2 1 3 3 1
ph31=0 2 2 0 1 3 3 1
p1(p1): 180° pulse (f1)
p2(p2): 30° pulse (f1)
d1: relaxation delay

Single-line saturation experiment.

The **S**elective **P**opulation **T**ransfer (SPT) experiment is usually used in spin system analysis with a FT spectrometer. Normally the experimental SPT spectra are compared with calculated SPT spectra simulated using different combinations of coupling constant signs. In common with many textbooks the AMX spin system 2,3-dibromopropionic acid will be used to introduce the concepts behind the SPT experiment. The ^{1}H spin system parameters for 2,3-dibromopropionic acid are shown below. The only difference between *Spin System A* and *Spin System B* is the sign of the coupling constant [3]J(H(2), H(3)), the results of SPT experiments will be used to distinguish between the two possible spin systems.

Spin system file	*ch524.ham*	*ch524pos.ham*
	Spin system A	*Spin system B*
	$\delta(H(1)) = 3{,}87$	$\delta(H(1)) = 3{,}87$
	$\delta(H(2)) = 3{,}37$	$\delta(H(2)) = 3{,}37$
	$\delta(H(3)) = 2{,}85$	$\delta(H(3)) = 2{,}85$
	$^3J(H(1), H(2)) = 11$ [Hz]	$^3J(H(1), H(2)) = 11$ [Hz]
	$^3J(H(1), H(3)) = 5$ [Hz]	$^3J(H(1), H(3)) = 5$ [Hz]
	$\mathbf{^3J(H(2), H(3)) = -10}$ **[Hz]**	$\mathbf{^3J(H(2), H(3)) = 10}$ **[Hz]**

In this particular instance the relative sign of this [3]J(H, H) coupling constant does not effect the appearance of the ^{1}H spectrum and this is confirmed in *Check it* 5.2.4.1 where the spectrum for each spin system is simulated. These simulated spectra will also used for comparing the effects of the SPT experiment. In the spin systems *ch524.ham* and *ch524pos.ham* the **nucleus** statement contains three *identifiers* a, m and x; these identifiers are used to label the nuclei.

H(1)

H(2)

C

Br — C   COOH

H(3)   Br
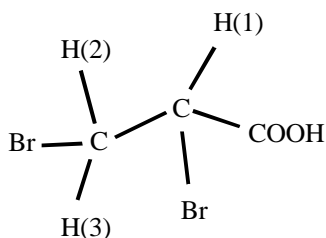
Structure of
2,3-dibromopropionic acid.

5.2.4.1 Check it in NMR-SIM

Load the configuration file *ch5241.cfg* that uses the spin system file *ch524.ham*. Using the **Edit│Spin system** command confirm the sign of the ^{3}J(H(2), H(3)) spin coupling constant: *couple m x -10*. Simulate the ^{1}H spectrum and process the data using zero filling **SI(r+i)**: *32k* and apodization **EM**, **LB**: *1.0* [Hz]. Save the spectrum. Using the **File│Spin System** command load the spin system *ch524pos.ham*; confirm the entry *couple m x 10*. Simulate and process the data. Compare the spectra in the dual display mode of 1D WIN-NMR (**Display│Dual Display**).

In an SPT experiment one spectral line which belongs to a single transition of the spin system is irradiated and the effects on the spectrum observed. To understand the effect of a SPT experiment the energy levels of the spin system must first be calculated. NMR-SIM has the option to generate an energy level scheme of a spin system and to display the results either as a list or in graphical representation.

5.2.4.2 Check it in NMR-SIM

Load the configuration file *ch5241.cfg*. In the **Utilities│List energy levels** dialog box set the spectrometer frequency **SF**: *400* MHz. Click on the **OK** button. The **Spin System Energy Levels** window opens showing the energy levels, transition frequencies and the eigenvectors and eigenvalues. To compare the energy level values for the two spin systems of 2,3-dibromopropionic acid assuming a different sign of the coupling constant use the **File│Save as...**command to store the listing as a simple text file using the filename *systema.txt*. Close the window (**File│Close**). Using the **File│Spin system...** command replace the current spin system by the ham-file *ch524pos.ham*. Calculate the energy levels for the second spin system and save the listing under the filename *systemb.txt*. To display a graphical representation of the energy levels use the **Utilities│Show energy levels** option. Print both text files. Sketch the energy levels and then mark the transitions between the various spin states as listed in the **Lines** section of the energy level files. The diagram should be the similar to Fig. 5.9. Draw the predicted spectrum marking each line with the spin states involved in the transition e.g. 2 -> 1. Starting with the line at lowest frequency label the signals 1 to 12.

Using the calculated energy level list the complete energy level scheme can be deduced as shown in Fig. 5.9. In this figure each energy level is labelled with a number in parenthesis, corresponding to the numbering used by NMR-SIM. Each transition is labelled with a number from 1 to 12 that correlates with a specific spectral line. Thus the

transitions denoted by "12" correlates the highest frequency line in the ^{1}H spectrum to the transition between energy levels (2) and (1).
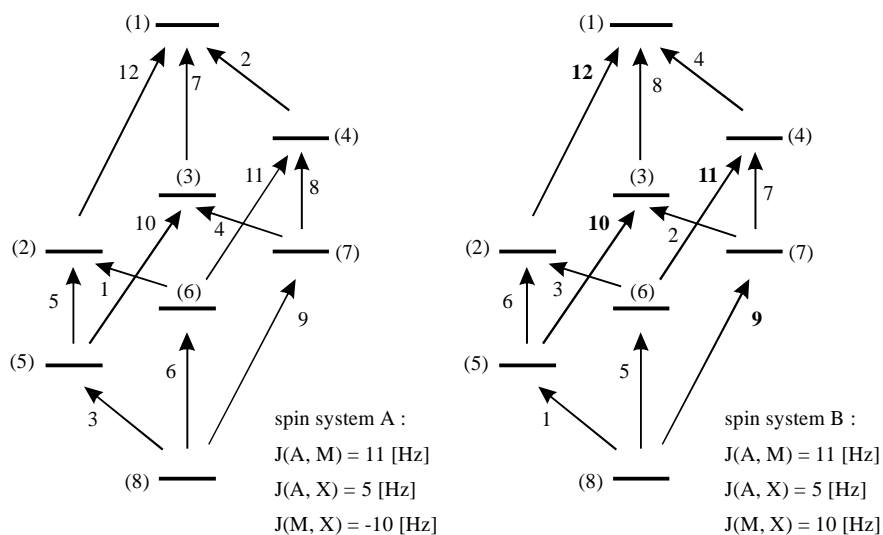

Fig. 5.9: Spin system energy level scheme of the alternative AMX spin systems A and B which vary in the sign of the ^{3}J(H(2), H(3)) coupling constant.

From Fig. 5.9 it is apparent that the 12 transitions of an AMX spin system correspond to the edges of a cube. Four transitions slope from right to left, 1, 2, 3 and 4; four transitions are vertical, 5, 6, 7 and 8; four transitions slope from left to right, 9, 10, 11 and 12. The effect of the relative sign J(M, X) is obvious in the comparing spin systems A and B; transitions 9, 10, 11 and 12 are unaffected but the other transitions are exchanged in pairs, 1 with 3 and 2 with 4, 5 with 6 and 7 with 8.

The effect of a selective 180° inversion pulse on transition 12, for instance, will invert the populations of energy levels (2) and (1) and consequently alter the signal intensity of the transitions associated with these two energy levels. Transitions connected to energy level (1) will decrease in intensity because energy level (1) is "over-populated" compared to the equilibrium value whereas transitions connected to the "under-populated" energy level (2) will increase in intensity.

According to the two energy level schemes shown in Fig. 5.9 for case A the intensity of transition 1, 5 will increase and 2, 7 decrease while for case B transition 3, 6 increases and 4, 8 decreases. This prediction may be confirmed in *Check it 5.2.4.3*.

5.2.4.3 Check it in NMR-SIM

Load the configuration file *ch5243.cfg* and simulate the SPT experiment for spin system A (*ch524.ham*). Process the data using zero filling of **SI(r+i)**: *32k* and apodization **EM**, **LB**: *1.0* [Hz]. Save the spectrum. Repeat the simulation for spin system B (*ch524pos.ham*) (**File│Spin system…**). Process the spectrum in exactly the same way as for spin system A. Use the multiple

display option of 1D WIN-NMR (**Display│Multiple Display**) to compare the results of the SPT experiment with the original ¹H spectrum.
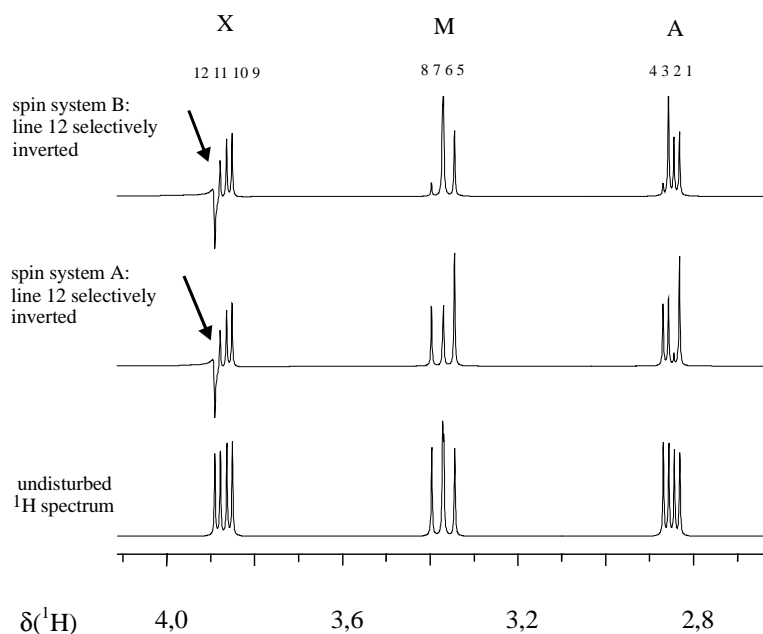
The experimental data shows the same effects as for system A. Based on these observations it may be proposed that the ^{3}J(H(2), H(3)) coupling constant is of opposite sign compared to the other coupling constants.

Prior to the development of 2D homonuclear COSY experiments, the SPT experiment was used to unravel coupling networks. The use of SPT experiments to trace coupling interactions of a spin system has two advantages which even today makes this technique superior to the selective 1D COSY experiment.

- The SPT effect and hence the detection of coupled spins is independent of the magnitude of the scalar coupling constant.
- In a SPT experiment single lines rather than multiplets are perturbed resulting in a higher sensitivity which is particularly beneficial in overcrowded spectra.

The method of tracing coupling interactions by spin-tickling experiments is based essentially on difference spectra, which are generated either by the subtraction of a SPT spectrum from a unperturbed control spectrum or by the type of pulse sequence used in the SPT experiment. With the latter approach only the signals effected by the SPT experiment appear in the difference spectrum.

In *Check it 5.2.4.4* two SPT experiments are simulated for a ^{31}P-3-spin system [5.21]. In the first simulation the "original" 180°/30° SPT pulse sequence (180°(selective) - 30°(unselective) is used and the difference spectrum is obtained by subtracting the unperturbed control spectrum. In the second simulation a 90°/90° variant (90°(selective) - 90°(unselective)) is used which generates the difference spectrum directly without the

need of any further processing. Both experiments achieve population inversion by selective excitation of a specific spectral line; in the 180°/30° SPT experiment a 180° selective pulse is applied, whereas for the 90°/90° experiment a combination of a 90° selective and a 90° unselective pulse is used. In the 180°/30° SPT experiment it is possible that because of coupling evolution during the selective pulse both single quantum and multiple quantum coherence components could be generated. The unwanted single quantum coherences detected by a 90° detection pulse would distort the spectrum while the unwanted multiple quantum coherences reduce the signal intensity. Consequently only a 30° detection pulse can be incorporated in the pulse sequence and the 90°/90° pulse sequence is superior to the 180°/30° pulse sequence due to the higher observed signal intensity.
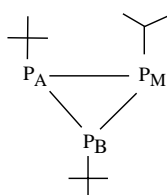
$\delta(A) = -111,5$
$\delta(B) = -108,2$
$\delta(M) = -98,3$

Structure of the ^{31}P-spin system [5.21]

5.2.4.4 Check it in NMR-SIM

Load the configuration file *ch5244a.cfg*. Simulate the ^{31}P spectrum and process the data using zero filling **SI(r+i)**: *32k* and apodization **EM**, **LB**: *2.0* [Hz]. Save the spectrum. Repeat the procedure for the configuration files *ch5244b.cfg* (180°/30° SPT experiment) and *ch5244c.cfg* (90°/90° SPT experiment). To get the 180°/30° SPT-difference spectrum load the processed 180°/30° SPT spectrum into 1D WIN-NMR. In the **Process│File Algebra** dialog box enter the filename of the original ^{31}P spectrum. Close this box using the **Ok** button. In the main display window the ^{31}P spectrum (upper spectrum), the SPT spectrum (middle spectrum) and the SPT-difference spectrum (lower spectrum) are displayed. Select the **Execute** and then the **Return** buttons in the button panel. The file algebra window is closed and the difference spectrum is displayed in the main window. Using the **File│Save as...** command save this difference spectrum with a filename. Compare the results using the **Display│Multiple Display** option.

The results of *Check it 5.2.4.4* can be summarized as follows:

- In the 90°/90° SPT experiment the signal intensity are greater because the 30° pulse is replaced by a 90° pulse, however the relative sign can no longer be determined because of excitation of active and passive lines.
- Because of the phase cycling and the number of scans being a multiple of two, the 90°/90° SPT experiment generates by default the difference spectrum.
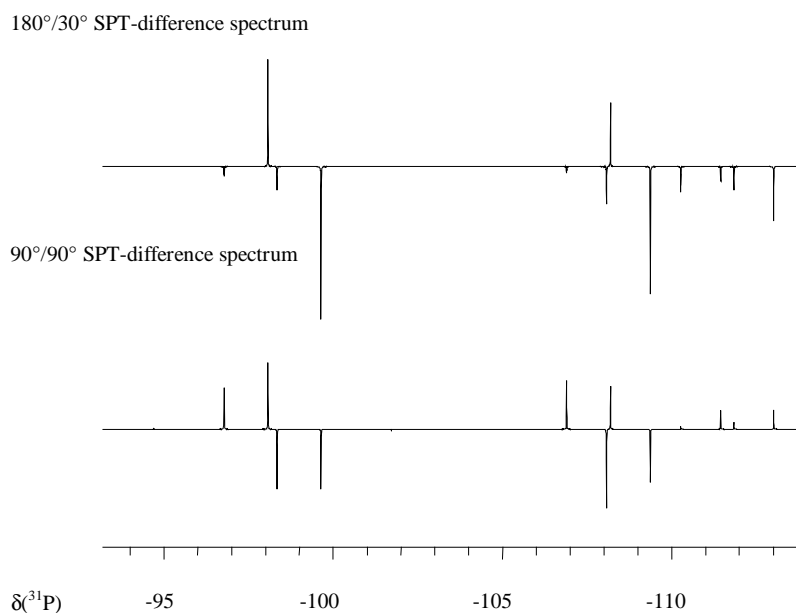
180°/30° SPT-difference spectrum

90°/90° SPT-difference spectrum

δ(^{31}P)   -95   -100   -105   -110

Fig. 5.10:   Comparison of the difference spectra from a 180°/30° SPT and a 90°/90° SPT experiment.

The 90°/90° SPT experiment can also be used to determine the individual coupling networks in a binary mixture. In *Check it 5.2.4.5* the single line at 3.69 ppm is irradiated and all the signals of the spin system which are connected by scalar coupling to the irradiated line can be determined.

5.2.4.5 Check it in NMR-SIM

To simulate the unperturbed ^{1}H spectrum load the configuration file *ch5245a.cfg*. Process the data using zero filling **SI(r+i)**: *32k* and apodization **EM**, **LB**: *1.0* [Hz]. Save the spectrum. Repeat the simulation for the 90°/90° SPT experiment using the configuration file *ch5245b.cfg*. When compared using the **Display|Dual display** mode of 1D WIN-NMR the results should be similar to Fig. 5.11.

In Fig. 5.11 the results of *Check 5.2.4.5* are shown. From a comparison of the simulated spectra the two spin systems can be assigned. Unfortunately because the selectivity of the shaped pulse is limited, irradiation of the line at 3.69 ppm also excites lines of spin system A at 3.69 ppm so that in addition to the expected responses, small artefacts from the second spin system A can also be observed in the SPT experiment.
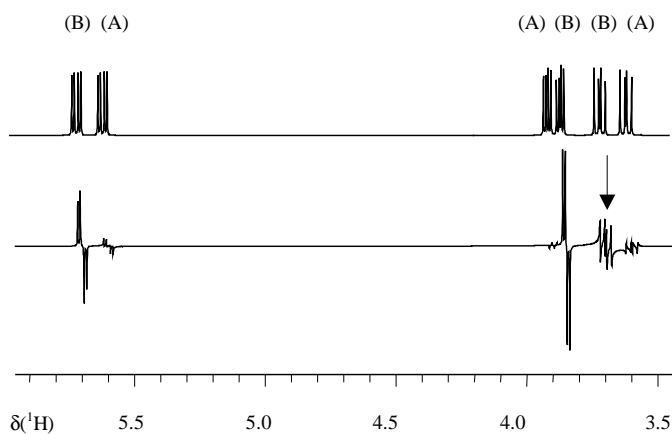
Fig. 5.11: ^{1}H spectrum and 90°/90° SPT difference spectrum of a binary mixture. The arrow denotes the saturated line of spin system B.

5.2.5   2D Shift and Coupling Resolved Experiments (JRES, SERF, SELRESOLV)

Often the 1D ^{1}H spectra of hydrocarbons and organic compounds are difficult to interpret because of severe signal overlap which precludes the determination of coupling constants even using a simple first order analysis. In these cases the 2D shift and coupling resolved experiment and variants may provide a solution. Of particular interest is the determination of the scalar long-range ^{3}J(H, H) and ^{3}J(X, H) coupling constants (X = ^{13}C, ^{15}N etc.) where the magnitude of the coupling constant can help with signal assignment or support proposals for the conformational orientation of a molecular structure. In unsaturated hydrocarbon the ^{3}J(H, H) coupling constant can be used to differentiate between trans and cis-oriented protons because ^{3}J(trans) > ^{3}J(cis) whilst in cyclohexane derivatives it is possible to differentiate between axial, axial(aa) and equatorial, equatorial (ee) protons because ^{3}J(aa) > ^{3}J(ee). Another important application is the approximation of the dihedral angle along a peptide bond, for instance, using the experimental value of the ^{3}J(X, H) coupling constant. Fig. 5.12 shows some of the possible relationships between structure and ^{3}J coupling constants.

^{3}J(trans) > ^{3}J(cis) ^{3}J(N, H): dihedral angle

^{3}J(H$_a$, H$_a$) > ^{3}J(H$_e$, H$_e$) ^{3}J(C, H): dihedral angle

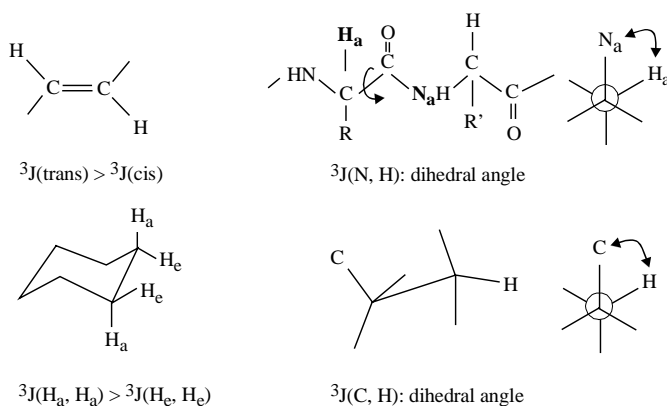**Fig. 5.12:**   Selected structural units whose dihedral angle, bond angle or conformation can be deduced from a ^{3}J(H, H) or ^{3}J(X, H) coupling constant.

In addition to the J-resolved experiments several other enhanced chemical shift correlated experiments are available for determining coupling constants. A short overview and classification is given in Table 5.8. Some experiments like the P.COSY or E.COSY experiment are explained in more detail in section 5.4.1.1.

Table 5.8:   Experiments for the determination of scalar coupling constants.

Exclusive scalar coupling evolution

Homonuclear	J(H, H)-resolved exp. (JRES) [5.22], ^{n}X INEPT J(H, H)-resolved exp. [5.23], 2D selective J(H, H)-resolved exp. (SERF) [5.10] ACT-J(H, H)-resolved exp. [5.24]
Heteronuclear	J(X, H)-resolved exp. [5.25], 2D selective. J(X, H) resolved exp. [5.26], semi-sel. J(X, H)resolved exp. [5.27], 2D selective J(H, H)(f1) /J(X, H)(f2)-resolved exp. (SELRESOLV) [5.28], 2D ACT-J(X, H)-resolved exp. [5.24], 2D selective. HSQC like J(X, H)-resolved exp. [5.29], 2D ^{n}X DEPT J(X, H)-resolved exp. [5.30], 2D selective ^{n}X INEPT J(X, H)-resolved exp. [5.31]

Selected scalar coupling and chemical shift evolution

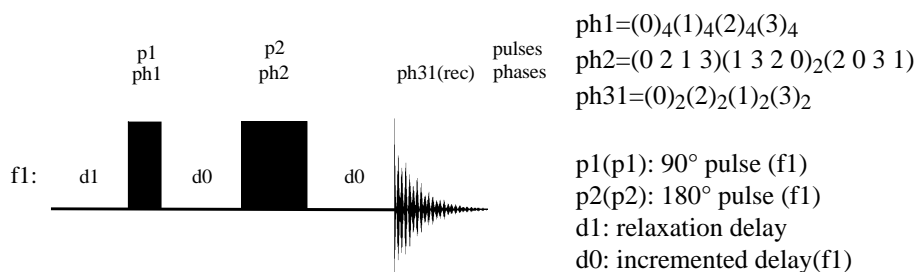|	
Homonuclear	HECADE exp. [5.32], E.COSY[5.33], P.E.COSY [5.34], P.COSY exp. [5.35]
Heteronuclear	ExSc TOCSY HMQC exp[1] [5.36], modified HSQC-TOCSY exp. [5.37], 1D selective long-range HSQC exp. [5.38, 5.39], EXSIDE exp. [5.40] [1]ExSc = Excitation Sculpting

The J-resolved experiment is based upon a spin echo and an incremented delay d0 that occurs before and after the spin echo. It is the incrementation of the spin echo time that generates the second time domain and subsequently the f1 dimension. How the spin

echo and incremented delay are implemented depends upon the type of experiment; J-resolved experiments may be broadly classified as homonuclear, heteronuclear, ^{n}X selective and ^{1}H selective. A homonuclear J-resolved experiment consists of a 180° pulse sandwiched between two d0 delays, the second delay allowing the chemical shift evolution to be refocused. In a heteronuclear ^{n}X J-resolved experiment a 180° ^{n}X pulse is applied simultaneously with the 180° ^{1}H pulse. Modified versions using selective pulses can use either a selective excitation pulse or a selective 180° refocusing pulse as part of the spin echo. Furthermore, the basic sequence may be modified to include polarization transfer steps to increase the experiment's sensitivity for nuclei with a low receptivity to the NMR experiment. A full description of the various J-resolved experiments is given in the introduction to the following *Check its*.

Sequence features:

Purpose / principles:	2D experiments to separate overlapping multiplets, exclusive coupling evolution in a spin echo using the incrementation of the spin echo time to create a f1 dimension
Variants:	2D J(H, H)-resolved exp. (JRES) [5.22], 2D J(X, H)-resolved exp. [5.25], 2D ^{n}X INEPT J(H, H)-resolved exp. [5.23], 2D ^{n}X DEPT J(X, H)-resolved exp. [5.30], 2D selective J(H, H)-resolved exp. (SERF) [5.10], 2D selective ^{n}X RINEPT J(H, H)/J(X, H)-resolved exp. (SELRESOLV) [5.28], 2D selective ^{n}X INEPT J(X, H)-resolved exp. [5.31], 2D selective ^{n}X J(X, H)-resolved exp. [5.26]

Pulse Sequence Scheme

$ph1=(0)_4(1)_4(2)_4(3)_4$
$ph2=(0\ 2\ 1\ 3)(1\ 3\ 2\ 0)_2(2\ 0\ 3\ 1)$
$ph31=(0)_2(2)_2(1)_2(3)_2$

p1(p1): 90° pulse (f1)
p2(p2): 180° pulse (f1)
d1: relaxation delay
d0: incremented delay(f1)

2D shift and coupling-resolved experiment.

Table 5.9 categories the different types of J-resolved experiment used by the *Check its* in this section. The choice of experiment in each *Check it* has been chosen deliberately to illustrate a specific point; how coupling constants may be determined, how different type of artefacts arise and how these artefacts may be suppressed.

Table 5.9:   Section 5.2.5 *Check its* List [1]

J(H, H) resolved	J(C, H) resolved
Homonuclear	*Heteronuclear*
Check it 5.2.5.1:	*Check its 5.2.5.4* and *5.2.5.5:*
2D ^{1}H J-res. exp.	2D ^{13}C J-res. exp.
Homonuclear and selective	*Heteronuclear and selective*
Check it 5.2.5.2:	*Check it 5.2.5.6*
2D ^{1}H selective ^{1}H J-res. exp. (SERF)	2D ^{1}H selective ^{13}C J-res. exp.
	Check its 5.2.5.7 and *5.2.5.8*
	2D ^{1}H selective ^{13}C INEPT J-res. exp.
Heteronuclear	
Check it 5.2.5.3	*Check it 5.2.5.9*
2D ^{13}C INEPT J-resolved exp.	2D ^{13}C selective ^{13}C INEPT J-res. exp. (SELRESOLV)

[1] J-res. expt. = J-resolved experiment

Homo- and heteronuclear J(H, H)-resolved experiments

In *Check it 5.2.5.1* p-(2,2-dichloroethoxy)(2,2-dibromoethoxy)benzene is used to illustrate the situation where the 1D ^{1}H spectrum is quite complex but where there are no overlapping multiplets.

5.2.5.1 Check it in NMR-SIM

Simulate the ^{1}H spectrum using the configuration file *ch5251a.cfg* (**File│Experiment Setup│Load from file...**). Save the data with a suitable filename and then process the FID in 1D WIN-NMR using zero filling **SI(r+i)**: *16k* and apodization **EM**, **LB**: *0.2* [Hz]. Save the spectrum.

Simulate the ^{1}H J-resolved and the ^{1}H gs-COSY spectrum using the configuration files *ch5251.cfg* and *ch5251b.cfg* respectively. Prior to the simulation check the value of nd0 using the **Go│Check Parameters & Go** command. If necessary check the pulse program using the command **Utilities|Show pulse program…**. Save the data with a suitable filename and then process the 2D data (**Process│2D transform [xfb]**). Add the ^{1}H spectrum as projections to the 2D spectra (**Display│Layout│Spectrum...**). Examine the 2D spectra in particular the chemical shift and coupling evolution in the J-resolved spectrum.

H-a   H-b   H-e   H-d

H   H   H   H

Br$_2$ C ── C─O─⟨ ⟩─O─ C ── C Cl$_2$

H   H

H-c   H-f
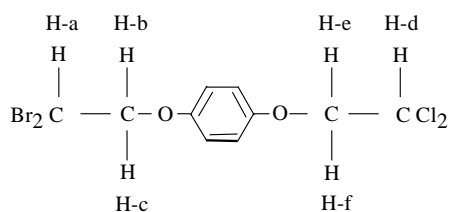
Structure of p-(2,2-dichloroethoxy) (2,2-dibromoethoxy)benzene.

^{1}H spectrum: *ch5251a.cfg*
^{1}H J-resolved spectrum: *ch5251.cfg*
^{1}H gs-COSY spectrum: *ch5251b.cfg*

A comparison of the ^{1}H gs-COSY and the ^{1}H J-resolved experiment shows that whilst the COSY spectrum enables coupling partners to be determined the J-resolved spectrum allows the individual coupling constants to be easily measured even if, in the original 1D spectrum, the multiplets overlap. A development of the standard J-resolved experiment is the selective refocusing or SERF experiment that uses two selective pulses. After the initial selective 90° excitation pulse, the selected proton exhibits coupling to all its coupling partners. The 180° refocusing pulse in the middle of the spin-echo sequence is optimized such that only the original proton plus one possible coupling partner is selected reducing the J-resolved spectrum to the interaction of only two proton spins. Using a double selective 180° refocusing pulse the mutual coupling constant between two protons can be easily obtained. In *Check it 5.2.5.2* three SERF experiments are simulated to determine all the H, H-coupling constants and coupling partners for the AMX spin system 1,2-dibromopropionic acid.

p1   p2   p3   pulses
ph1   ph2   ph3   ph31(rec) phases

f1: d1 ⋀⋀ [ ] d0 ⋀⋀ d0
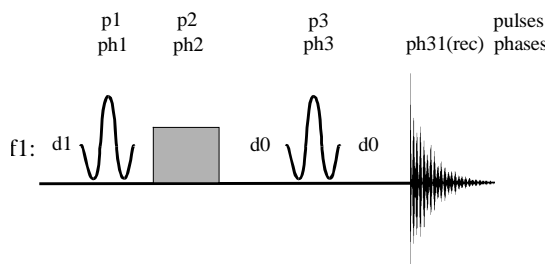
The SERF experiment (p2: trim pulse).

5.2.5.2 Check it in NMR-SIM

To determine and assign all the $^nJ(^1H, ^1H)$ coupling constants in 2,3-dibromopropionic acid it is necessary to perform three simulations representing all the possible correlation's between the protons. Calculate the standard ^{1}H spectrum for use as the f2 projection using the configuration file *ch5252.cfg*. Process the data in 1D WIN-NMR using **SI(r+i)**: *16k* and apodization **EM**, **LB**: *0.2* [Hz]. For the SERF experiments perform three simulations using the configuration files *ch5252a.cfg*, *ch5252b.cfg* and *ch5252c.cfg*, storing each data set with a different filename. Process the 2D data sets using the parameters stored in the configuration files and compare the results.

cfg file	interaction of	p1: selective 90° excitation pulse on	p3: selective 180° refocusing pulse on
ch5252a	H-a/H-m	H-a	H-a H-x
ch5252b	H-a/H-x	H-a	H-a H-x
ch5252c	H-m/H-x	H-m	H-m H-x

Another method to separate overlapping multiplets in ^{1}H spectra and simplify the measurement of H, H coupling constants is the 2D ^{13}C INEPT-J(H, H)-resolved experiment [5.23]. In this experiment ^{13}C spectra are acquired in the f2 dimension and the H, H-coupling is detected indirectly in the f1 dimension using the ^{1}J(C, H) coupling interaction. Because the ^{13}C chemical shift range is large compared with the ^{1}H chemical shift range there is little or no signal overlap in a ^{13}C spectrum and consequently the multiplets that overlapped in the ^{1}H spectrum are well resolved in the 2D ^{13}C INEPT-J(H, H)-resolved spectrum. A modification of the original experiment has been to include a simultaneous 180°(^{13}C)/180°(^{1}H) pulse as part of the refocusing spin echo which suppresses unwanted modulation and artefacts in the f1 dimension. In *Check it 5.2.5.3* the 2D ^{13}C INEPT-J(H, H)-resolved spectrum is simulated for both the original (*hjresinp.seq*) and the modified sequence (*hjresinp1.seq*) and the improvement of the latter is illustrated by comparing the spectra using the same contour plot level scale.

5.2.5.3 Check it in NMR-SIM

(a) Using the configuration file *ch5253b.cfg* (**File│Experiment Setup│Load from file...**) simulate the ^{1}H spectrum. Save the data with a suitable filename and then process the FID in 1D WIN-NMR using zero filling **SI(r+i)**: *16k* and apodization **EM**, **LB**: *0.2* [Hz]. Examine the signal overlap in the ^{1}H spectrum. In a similar manner simulate the ^{13}C{^{1}H} spectrum using the configuration file *ch5253c.cfg* and the 1D WIN-NMR processing parameters: zero filling **SI(r+i)**: *16k* and apodization **EM**, **LB**: *2.0* [Hz]. Save the spectrum using a suitable name to use as the f2 projection for the 2D spectra.

(b) Load the configuration file *ch5253.cfg* file and simulate the ^{13}C INEPT J(H, H)-resolved experiment. Fourier transform the data in 2D WIN-NMR using the **Process│2D transform [xfb]** command and the processing parameters defined in the configuration file. Scale the spectrum by clicking the **Change all** button and then the **Options>>** button in the Change all levels dialog box, set the **Lowest level** and **Factor** to optimum values.

(c) For the modified sequence load, if necessary, the file *ch5253.cfg*. Open the pulse program (**Edit│Pulse program**) and replace the line *d4*2* and extend the phase cycling program for the phases *ph7=0* and *ph8=0* as shown in Fig. 5.13. Using the **File│Save as...** option save the modified pulse program under the new name *hjresinp1.seq*. Load the new pulse program (**File│Pulse program...**) and run the simulation. Process and scale the data in 2D WIN-NMR in the exactly the same way as described for the original pulse sequence.

A comparison of the spectrum obtained with and without the simultaneous 180°(^{13}C)/180°(^{1}H) pulses illustrates quite clearly the superiority of the modified sequence in suppressing artefacts in this J-resolved experiment and why it should always be used in preference to the original sequence.
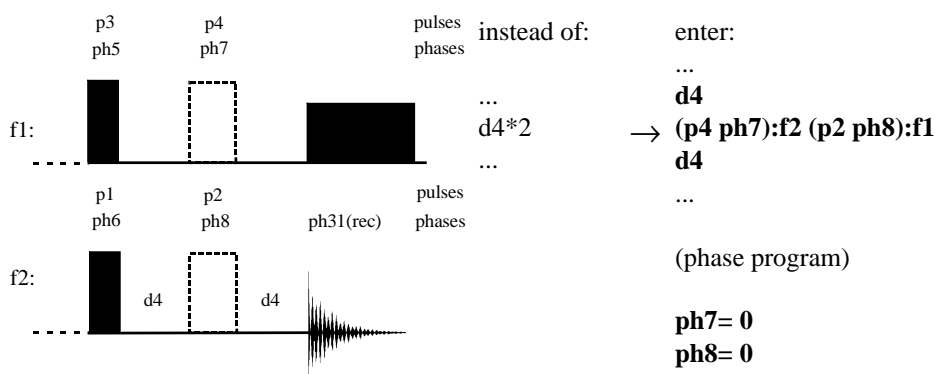

Fig. 5.13: Optional 180°(^{13}C)/180°(^{1}H) pulse combination (dotted pulses) to the INEPT-J(H, H)-resolved experiment (left), additional pulse program lines for the pulse combination (right).

Heteronuclear J(X, H)-resolved experiments

There are several heteronuclear 2D ^{n}X J(X, H)-resolved experiments for the determination of ^{n}J(X, H) coupling constants all based upon a heteronuclear spin echo which refocuses the chemical shift evolution of the ^{n}X nucleus but which let through the
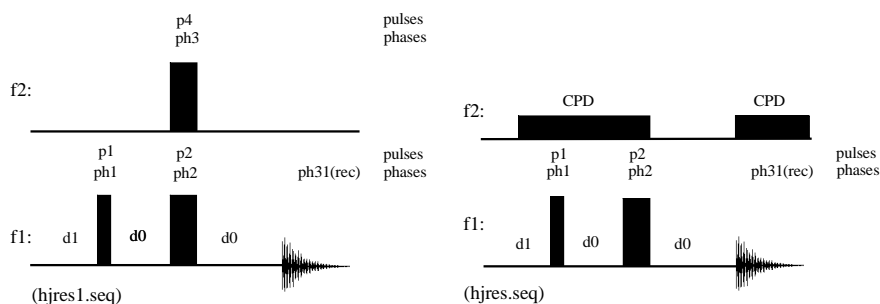
Fig. 5.14: Two variants of the 2D ^{n}X J(X, H)-resolved experiment. The sequence of the left-hand side uses the "spin-flip" method whilst the sequence of the right-hand side uses the "gated-decoupling" method.

coherence due to X, H coupling interactions. The pulse sequences for the two most common experiments are shown in Fig. 5.14. Initially the pulse sequence on the right hand side of Fig. 5.14 might not be recognized as spin echo but the application of a decoupling sequence during the first delay d0 is equivalent to a ^{1}H 180° pulse between the two d0 periods. However in this gated decoupling experiment the splitting in the f1 dimension of the 2D spectra is only half the true coupling constant value.

In addition to these two variants in the early days of J-resolved spectra a further experiment was proposed which included a polarization transfer step to enhance signal intensities [5.25]. The sequence starts with a 90° ^{1}H pulse, the ^{1}J(C, H) coupling evolves during the incremented delay d0 after which a spin echo 180°(^{1}H)/180°(^{13}C) refocusing pulse combination is applied. At the end of the second delay period d0 simultaneous 90° ^{1}H and 90° ^{13}C pulses generate the polarization transfer. *Check it 5.2.5.4* examines the "spin-flip", "gated decoupling" and polarization transfer variants of the ^{n}X J(X, H)-resolved experiment. Because the magnitude of the splitting in the f1 dimension depends upon of the type of experiment a simple ^{1}H, ^{13}C spin system bromomethane is used. As an additional exercise *Check it 5.2.5.4* can be repeated replacing the bromomethane spin system with more complex bromoethane spin system, stored in the file *ethylbr.ham*.

5.2.5.4 Check it in NMR-SIM

(a) Load the configuration file *ch5254a.cfg* and simulate the ^{13}C, ^{1}H coupled spectrum of bromomethane that is to be used as a projection for the 2D spectra. In 1D WIN-NMR process the data using zero filling of **SI(r+i)**: *16k* and an exponential window function with **LB**: *2.0* [Hz].

(b) To simulate the 2D ^{13}C J(C, H)-resolved spectrum of bromomethane obtained using the gated decoupler pulse sequence *hjres.seq*, load the configuration file *ch5254b.cfg*. Process the calculated 2D data set using the processing parameters defined in the configuration file. In the **Change all levels** dialog box, set the **Lowest level** and **Factor** to an optimum representation. Toggle the f1 dimension to the Hz scale and measure the peak separation in the observed quartet. The separation of 76 Hz is half the true value of ^{1}J(C, H).

(c) Load the configuration file *ch5254c.cfg* and simulate the 2D ^{13}C J(^{13}C, ^{1}H)-resolved spectrum obtained using the spin flip pulse sequence *hjres1.seq*. Run the simulation and process the calculated 2D data. Toggle the f1 and f2 dimension to the Hz scale and measure the peak separation of the tilted quartet (contour plot; optimum **Lowest level** and **Factor**). The separation of 152 Hz is the true value of ^{1}J(C, H).

(d) Load the configuration file *ch5254d.cfg* to simulate the 2D ^{13}C J(^{13}C, ^{1}H)-resolved spectrum obtained using the polarization transfer pulse sequence *hjres2.seq*. Check the pulse sequence using the pulse sequence viewer of NMR-SIM (**Utilities│Show pulse program...**). Start the simulation and process the 2D data set, toggle the f1 and f2 dimension to the Hz scale and

measure the quartet separation in the f2 dimension and the doublet separation in the f1 dimension using a sufficient **Lowest level** and **multiply factor** for the contour plot. In both cases the separation should be 152 Hz, the value of $^1J(C, H)$.

The results of *Check it 5.2.5.4* are summarized below.

Sequence	Splitting in f1 dimension	Splitting in f2 dimension
hjres.seq	Multiplet obeying the (n+1) rule, peak separation equal to half the value of $^1J(C, H)$	None
hjres1.seq	Multiplet obeying the (n+1) rule, peak separation equal to $^1J(C, H)$	Multiplet obeying the (n+1) rule, peak separation equal to $^1J(C, H)$
hjres2.seq	A doublet with a separation equal to $^1J(C, H)$	Multiplet obeying the (n+1) rule, peak separation equal to $^1J(C, H)$

Repeating *Check it 5.2.5.4* using the bromoethane spin system, *ethylbr.ham*, the results are similar for the gated decoupler and spin flip experiments. However for the polarization transfer experiment there is an additional splitting in the f1 dimension which can be attributed to the homonuclear H, H scalar coupling between the CH_3 and CH_2 groups.

The 2D ^nX J(X, H) resolved experiment has been studied extensively and there has been a number of major improvements in the pulse sequence. The spin echo is very sensitive to imperfections in the 180° pulse angle but the use of composite pulses [5.41] reduces this sensitivity and also the rf offset dependence. The suppression of different types of artefacts called "ghosts" and "phantoms" [5.42] as well as an additional category of unnamed artefacts [5.43] may be overcome using phase cycling and an important development has been the EXORCYCLE phase cycling procedure [5.42]. *Check it 5.2.5.5* is split into three parts: part (a) illustrates the artefacts generated as a consequence of pulse imperfections, part (b) uses the EXORCYCLE procedure for artefact suppression and part (c) examine the use of composite pulses to minimize pulse imperfections.

5.2.5.5 Check it in NMR-SIM

(a) If the ^{13}C, ^1H coupled spectrum of bromomethane is not already calculated simulate the spectrum to be used as a projection for the 2D spectra as described in *Check it 5.2.5.4a*. Load the file *ch5255a.cfg* and in the **Go|Check Experiment Parameters** dialog box enter the perfect pulse lengths for the 180° pulses: **p2**: *180d* and **p4**: *180d*. Start the simulation and process the 2D data using the processing parameters defined in the configuration file. Repeat the simulation using incorrect pulse angles **p2**: *160d* and **p4**: *160d*. The spectrum should be similar to Fig. 5.15. To examine the origin of the different artefacts simulate the spectrum again

with only the 180° ^{1}H pulse incorrectly set **p4**: *160d*. The resulting spectrum should only show the "ghost" peaks.

(b) To examine the effectiveness of the EXORCYCLE phase cycling for the pulse p2(^{13}C) and the receiver phase ph31, load the file *ch5255b.cfg* and repeat *Check it 5.2.5.5a*. Scale the contour plot in 2D WIN-NMR to the same lowest level. Only the "unnamed" artefacts should be clearly visible, the "ghost" and "phantom" peaks should have nearly zero intensity.

(c) To simulate the 180° ^{13}C composite pulse experiment, load the configuration file *ch5255c.cfg* and repeat *Check it 5.2.5.5a*. Scale the contour plot to the same level as in *Check it 5.2.5.5a* and examine the plot for the suppression of any artefacts. Load the pulse program *hjes1cp.seq* (**File│Pulse program...**) containing both the EXORCYCLE phase cycling and composite pulse procedure. Run a simulation and process and scale the data. Note the slight signal suppression of the unnamed artefacts U.
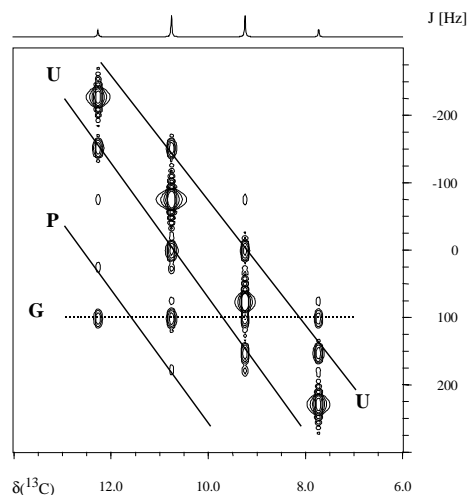
Fig. 5.15:   Contour plot of the ^{13}C J(C, H) resolved spectrum of bromomethane using a minimum phase cycling and incorrectly set 180° (^{1}H, ^{13}C) pulses (G = ghost peaks, P = phantom peaks and U = unnamed artefacts).

Heteronuclear selective J-resolved experiments

So far the 2D heteronuclear ^{n}J(C, H) J-resolved experiments have only allowed the determination of ^{1}J(C, H) coupling constants and have ignored the long-range CH couplings which are of more use in spectrum analysis. There have been two different approaches to this problem of selecting individual, long-range heteronuclear coupling interactions; the selective ^{1}H pulse experiment and the reverse INEPT type SELRESOLV experiment. Using a selective ^{1}H pulse the coupling of a single ^{1}H nucleus can be traced to all the ^{13}C nuclei, which are coupled to it by replacing the refocusing

180° ^{1}H pulse of the spin echo by a selective 180° ^{1}H pulse. This experiment is illustrated in *Check it 5.5.2.6*.
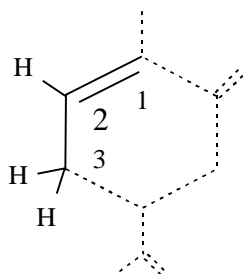
Carvone structure
fragment

5.2.5.6 Check it in NMR-SIM

(a) Using the configuration file *ch5256a.cfg* simulate the ^{1}H spectrum for use as the f2 projection. In 1D WIN-NMR process the data without any zero filling and a slight apodization (exponential window function with **LB: = *0.5*** [Hz]). Save the processed ^{1}H spectrum using a suitable name.

(b) To obtain the ^{13}C{^{1}H} spectrum replace the nucleus in the combo box of the rf channel menu bar : **F1**: *C 13* and **F2**: *H 1*. Using the **File⏐Pulse program...** command select the one-pulse decoupled experiment *zgdc.seq*. In the **Go⏐Check Experiment Parameters** dialog box modify the experiment parameters: **O1**: *75*, **O2**: *4.0* and **SW**: *160*. Fourier transform the FID using zero filling of **SI(r+i)** = *16k* and an exponential window function with **LB**: 3.*0* [Hz]. Save the spectrum using a suitable name.

(c) To measure all the ^{2}J(C, H) and ^{3}J(C, H) coupling constants it is necessary to simulate the ^{13}C selective J-resolved spectra three times using different offsets for the selective 180° pulse on the F2 channel (^{1}H). Load the configuration file *ch5256b.cfg* and in the **Go⏐Check Experiment Parameters** dialog box check the O2 offset **O2**: *6.8* (H-2). Perform a simulation and Fourier transform the data set in 2D WIN-NMR using the processing parameters loaded by the configuration file. Change the f1-axis to Hz and calibrate the f1 dimension setting the centre to zero. The ^{2}J or ^{3}J(C, H) coupling constants can be measured from the splitting in the f1 dimension by using the **Distance** button in the button panel. Repeat the simulation for the other two protons using offset values of *2.4* (H-3a) and *2.1* (H-3b).

To improve the sensitivity the selective J-resolved pulse sequence may be combined with a refocused INEPT polarization transfer experiment. In contrast to the original heteronuclear J-resolved experiment the first excitation pulse is executed on the F2 channel with the spin-echo sequence sandwiched between two incremental delay. Coupling evolves during the second incremental delay before the refocused INEPT unit creates in-phase coherence for the ^{13}C nuclei which are coupled to the selected proton nucleus allowing decoupling on the F2 channel during data acquisition.
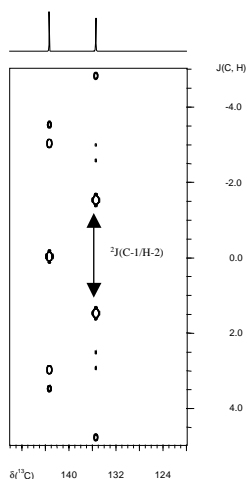
5.2.5.7 Check it in NMR-SIM

Load the configuration file *ch5257.cfg*. Before starting the simulation check in the **Go⏐Check Experiment Parameters** dialog box that **nd0** is set correctly. Using the same method as *Check it 5.2.5.6* perform three simulations

corresponding to an **O2** value of *6.80* (H-2), *2.40* (H-3a) and *2.1* (H-3b). Save the data sets with suitable names. Process the 2D data in 2D WIN-NMR using the parameters in the configuration file. Toggle the f1 frequency axis to Hz scale and measure the $^{n}J(C, H)$ coupling constants using the **Distance** button in the button panel.

Because of the conceivable imperfections of pulses in contrast to the original reference [5.23] a composite 180° ^{13}C pulse was proposed in the INEPT unit. However upon closer examination it is apparent that this four-pulse combination constitutes a selective BIRD filter. The effect of a simultaneous hard and selective pulse cannot be calculated explicitly by NMR-SIM but because both pulse lengths are short relative to the delays in the BIRD sequence, the selective BIRD filter can be represented by a sequential 180° ^{13}C and selective 180° ^{1}H pulse.

In *Check it 5.2.5.8* the different types of artefacts that can appear in a selective J-resolved experiment are examined in detail.

5.2.5.8 Check it in NMR-SIM

Load the configuration file *ch5258.cfg*. Before starting the simulation check in the **Go│Check Experiment Parameters** dialog box that **nd0** is set correctly. Process the data set in 2D WIN-NMR using the parameters stored in the configuration file. Using the **File│Spin system…** command repeat the simulation for the two additional spin systems *carvone1.ham* (all values of $^{1}J(C, H)$ set to zero) and *carvone2.ham* (all values of $^{n}J(H, H)$ set to zero). Process the data sets in exactly the same as for the first data set. Plot all three 2D spectra using the same settings and compare the three simulations with respect to the type of artefacts.

Fig. 5.16:   The partial ^{13}C selective INEPT J-resolved spectrum of a spin system based on carvone, H-2 was selectively inverted by the 180° pulses of the sequence.

A comparison of the results obtained for the previous two *Check its* shows immediately the superiority of the composite 180° ^{13}C pulse used in *Check it 5.2.5.7* in suppressing artefacts over the simple 180° ^{13}C pulse used in *Check it 5.2.5.8*. Figure 5.16 shows two types of artefacts: the first arises from the effects of $^{1}J(C, H)$ and the second from $^{n}J(H, H)$. From the splitting in the f1 dimension carbon C-2 at 143.3 ppm displays a long range coupling to H-2 yet an examination of the spin system *carvone.ham* shows that this long-range coupling is zero. Coherence caused by $^{1}J(C, H)$ are folded back to generate ghost peaks and an apparent coupling to H-2 as confirmed by the second simulation in *Check it 5.2.5.8* where all values of $^{1}J(C, H)$ are set to zero. The second

simulation also shows artefacts that can be attributed to homonuclear coupling $^nJ(H, H)$ as confirmed by the third simulation which generates a spectrum without these artefacts.

A complete different approach is used in the SELRESOLV selective J-resolved experiment. SELRESOLV is an inverse experiment, the ^1H spectrum is acquired directly and the ^{13}C detected indirectly. A carbon signal is selectively excited and all the $^nJ(^{13}C, ^1H)$ coupling interactions associated with the specific carbon spin are traced out in the J-resolved spectrum. Of course, only the ^1H signals that are coupled to the selectively excited carbon are detected. The projection in the f1 dimension shows the individual proton resonance split by $^nJ(H, H)$ coupling whilst the projection in the f2 dimension shows the individual proton resonance split by both $^nJ(H, H)$ and $^nJ(C, H)$ coupling. Analysis of the appropriate rows and columns enable both $^nJ(H, H)$ and $^nJ(C, H)$ to be determined. The experiment has two major disadvantages. Firstly the signals in the f1 dimension are split by homonuclear H, H coupling causing a dramatic loss in intensity. Secondly because the value of $^nJ(X, H)$ is relatively small, to get sufficient digital resolution in the f2 dimension several experiments must be performed, using a small sweep width and different ^1H observation frequencies.

5.2.5.9 Check it in NMR-SIM

Load the configuration file *ch5259.cfg*. To measure all the $^nJ(^{13}C, ^1H)$ coupling constants it is necessary to perform four simulations using different combinations of ^1H frequency range and selective ^{13}C pulses. Before starting the first simulation check in the **Go│Check Experiment Parameters** dialog box that the values of **O1** and **O2** correspond to the first combination in the table shown on the left side of this *Check it*. Store the data with a suitable filename. Repeat the simulation of the other O1/O2 combinations shown in the table. Process the data sets in 2D WIN-NMR. To measure the $^nJ(H, H)$ and $^nJ(C, H)$ coupling constants change the f1 and f2 dimension into Hz scale and use the **Distance** button in the button panel.

Using the simulation parameters

simulation:	**1**	**2**	**3**	**4**
O1=	6.7	6.7	2.25	2.25
O2 =	135.4	31.4	135.4	143.3

By necessity the discussion of the J-resolved experiment in this section is not as comprehensive as in most textbooks. Nevertheless the most salient points of the main types of experiments have been discussed and the spin systems and methodology used in this section may be used as a basis for using NMR-SIM to study specific J-resolved experiments not covered.
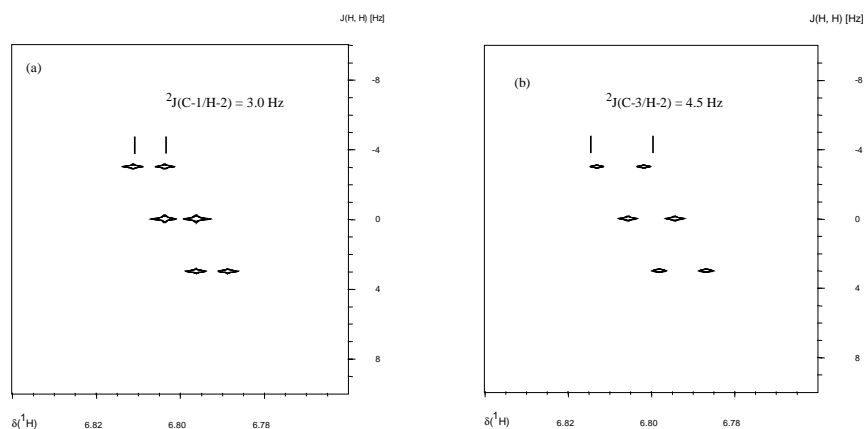
Fig. 5.17:   Partial SELRESOLV spectra using the parameters in the configuration file *ch5259.cfg*: (a) Selective excitation of C-1; (b) Selective excitation of C-3.

5.2.6   Multiplicity-Edited Experiments (APT, SEMUT, DEPT, POMMIE, INEPT and PENDANT)

Multiplicity edited experiments are very useful tools for the analysis of highly substituted organic compounds. Multiplicity refers to the number of magnetically equivalent atoms I, which are bonded to an atom S to form an I_nS group. Normally I is a NMR sensitive nucleus such as ^1H or ^{19}F and S is a NMR insensitive nucleus such as ^{13}C or ^{15}N. All experiments are characterized by a time period when only the coupling evolution is allowed, the chemical shift evolution being refocused by a 180° pulse. Different multiplicities can be recognized by the relative phase of the signals. Since these experiments are used to determine the number of NMR sensitive atoms I bonded in a SI_n group to a NMR insensitive nuclei such as ^{13}C or ^{31}P sensitivity enhancement using either heteronuclear Overhauser enhancement or polarization transfer would be advantageous. Consequently there are two categories of multiplicity edited experiments:

• Simple Spin-Echo (SE) based experiments
- which use heteronuclear Overhauser enhancement for sensitivity gain and
• DEPT or INEPT like experiments
- where the signal intensity is enhanced by polarization transfer

By varying the pulse angles (SEMUT and DEPT experiments) or coupling evolution delays (INEPT experiment) sets of spectra can be obtained which can be manipulated to generate a set of subspectra which only display signals of a specific multiplicity. Using these editing experiments signals from CH, CH_2 and CH_3 groups can be separated and displayed as separate spectra.

Table 5.10:   Selection of pulse programs for multiplicity assignment.

Simple SE based experiments	SEFT [5.44, 5.45, 5.46], APTSE [5.47][1]), APTDE [5.48][1]), ESCORT [5.49], CAP1, 2, 3 [5.50] SEMUT [5.51], SEMUT-GL [5.52, 5.53]
INEPT based experiments	INEPT [5.54, 5.55], R-INEPT [5.56] selective R-INEPT [5.57], selective INEPT [5.58], INEPT+ [5.59], off-resonance optimized INEPT [5.60], Broadband INEPT [5.61], INEPT-CR [5.62] PENDANT [5.63], improved PENDANT [5.64]
DEPT based experiments	DEPT [5.65], DEPT+/DEPT++ [5.59], off-resonance optimized DEPT [5.60], inverse DEPT [5.66], DEPTQ [5.67], 2D DEPT J-resolved [5.30], 2D DEPT-HMQC [5.68]

[1])Nomenclature proposed by the authors: APTSE = single spin echo APT, APTDE = double spin echo APT experiment.

Besides the INEPT step is a general unit for the effective creation of antiphase coherence for later polarization transfer the DEPT sequence can be extended to 2D experiments for the purpose of decoding coupling evolution or the chemical shift to the new f1 dimension. For a more comprehensive discussion see section 5.6.

Sequence features:

Purpose / principles:	Determination of magnetically equivalent sensitive nuclei which are scalar coupled to an insensitive, non-abundant nucleus like ^{13}C or ^{15}N, extended spin echo sequences for signal enhancement by nuclear Overhauser effect (APT, SEMUT) or polarization transfer (DEPT, INEPT, etc).
Variants:	APT [5.47, 5.48], DEPT [5.65], DEPT++ [5.59], POMMIE [5.69] INEPT [5.54, 5.55], INEPT+ [5.59], PENDANT [5.63]

The SEFT/APT and SEMUT experiments

A comparison of the pulse sequence schemes shown in Fig. 5.18 shows a marked similarity between the SEFT and APT experiment, the only difference between the sequences being whether ^1H decoupling occurs during the first or the second part of the spin echo. By coincidence these similar sequences, which give identical results, where developed and named independently by two different research groups. This type of sequence is also referred to as JMOD (*J-MOD*ulated) ^nX spectra. The discrimination of signals by their multiplicity depends upon the delay period d2; the subspectra of signals of selected multiplicity being obtained using linear combinations of experiments measured using suitable d2 delays.

SEFT experiment   **SE-APT experiment**
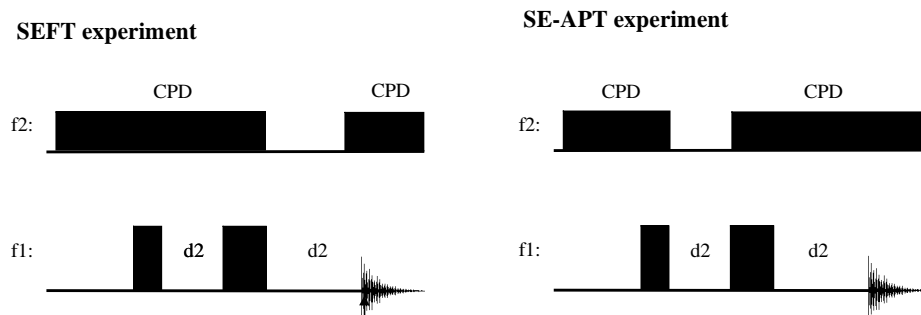
Fig. 5.18:   Pulse sequence schemes of the SEFT experiment and the basic APT experiment.

In this section the advantages and disadvantages of delay or pulse length variation for multiplicity selection will be examined. Improvements to a variety of pulse sequences as implied by the names in Table 5.10, will also be considered.

The APT sequence

The APT sequence was the first experiment to decode the sign of the signal amplitude as a function of I_nS multiplicity. Because of the hardware restrictions in early NMR spectrometers, particularly applying simultaneous pulses on both the acquisition and second channel, emphasis was made on making the pulse sequence as simple as possible. The sequence only requires a 90° pulse and 180° pulse on the acquisition channel, which may be easily determined, and a simple decoupler switch-on/off on the second channel. Nevertheless the experiment is still included in modern pulse program libraries; the experiment seems to be very robust and in contract to DEPT or INEPT type experiments quaternary carbon atoms can also be detected by the same experiment.
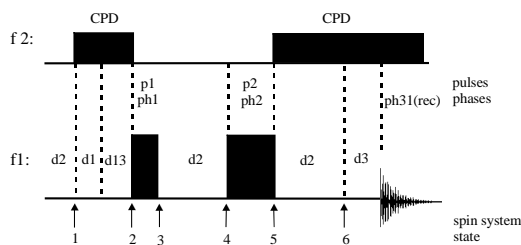
The APTSE experiment.

5.2.6.1 Check it in NMR-SIM

(a) Load the configuration file *ch5261.cfg*. The spin system file *ch5261a.ham* contains three CH_n groups: CH, $^1J(C, H) = 160$ Hz; CH_2, $^1J(C, H) = 140$ Hz and CH_3, $^1J(C, H) = 120$ Hz. Simulate the APTSE $^{13}C\{^1H\}$ spectrum and process the FID (**Si(r+i)**: *32k*, wdw: **EM**, **LB**: *2.0*) and transform the data. Observe that the quaternary carbon at 140 ppm and the CH_2 group at 45 ppm have the same phase while the CH at 110 ppm and CH_3 group at 10 ppm have the opposite signal phase.

(b) Replace the spin system file by the file *ch5261b.ham* and simulate the APT $^{13}C\{^1H\}$ spectrum for the variety of CH_n groups listed in Table 5.11 (**File**|**Spin system...**). Run the calculation (**Go**|**Run Experiment**) and process the data as in (a). Because the delay d2 is based on a typical $^1J(C, H)$ value of 120 to 140 Hz the results of the APTSE experiment can be misleading if a CH group has a value of $^1J(C, H) > 210$ Hz. The different signal intensities arise from the widely different values of $^1J(C, H)$.

As shown in Table 5.11 a wide range of $^1J(C, H)$ coupling constants can be observed for C, H spin systems and one aim of an improved APT based sequence is to reduce the effect of these different coupling constants. The d2 delay can only be optimized to one specific value of $^1J(C, H)$ and in the following discussion this coupling constant is referred to as the nominal coupling constant $J_{nominal}$.

Table 5.11: Example spin systems for a range of $^1J(C, H)$ arranged by CH_n group.

CH_3	example	CH_2	example	CH	example
120	$(CH_3)_4Si$	120	cyclohexane	160	benzene
130	CH_3COOH	145	tetrahydrofurane	210	$CHCl_3$
150	CH_3Cl	180	CH_2Cl_2	250	C_2H_2

In the basic ATP sequence the combination of 90° excitation pulse and high repetition rates leads to intensity loss due to the incomplete relaxation. Therefore before discussing specific extensions to the APT sequence it is of interest to consider replacing the 90° excitation pulse with a pulse adapted to the ERNST angle condition in a similar manner as for one-pulse experiments. However simply replacing the 90° pulse by an ERNST pulse angle fails because the spin echo is based on a complete transfer of the z-magnetization into x- or y-coherence. Consequently it is necessary to append a second

spin echo. *Check it 5.2.6.2* demonstrates the signal intensity gain by the double spin echo APT experiment in comparison to the single spin echo APT sequence.
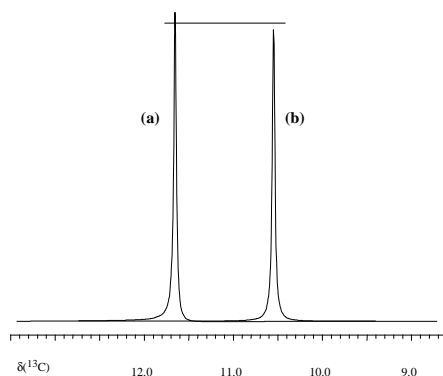
Relaxation optimized APT experiment, (a) double spin echo APT experiment, (b) single spin echo APT experiment.

5.2.6.2 Check it in NMR-SIM

Simulate the APTSE-^{13}C{^{1}H} spectrum of the CH$_n$ groups in the spin system file *ch5262.ham*. The CH$_n$ groups all have the same longitudinal relaxation time 2 sec but different values of ^{1}J(C, H): ^{13}CH (120 Hz), ^{13}CH$_2$ (140 Hz) and ^{13}CH (160 Hz). Prior to the simulation check in the **Options⎮NMR-Sim settings…** dialog box that the *Full relaxation* option is selected. Save the data as **Exp No.:** *1*. Repeat the simulation using the optimum ERNST angle for this experiment (d1 = 0 sec, AQ = 0.81 sec) **p1**: *48d* (**Go|Check Parameters & Go**) saving the data as **Exp No.:** *2*. Finally calculate the APTDE-^{13}C{^{1}H} spectrum using the pulse sequence *aptde.seq* (**File⎮Pulse program...**) and the ERNST angle for **p1**: *48d* saving the data as **Exp No.:** *3*. Process all three FID similarly (**Si(r+i)**: *32k*, wdw: **EM**, **LB**: *1.0* [Hz]) and compare the Fourier transformed spectra using the Display|**Multiple Display** option.

As described in reference [5.48] the combination of a double spin echo and ERNST angle pulse (see section 5.2.1) guarantees higher signal intensity than the single spin echo sequence. Also *Check it 5.2.6.2* shows that even with the ERNST angle the signals in the single spin echo APT experiment have lower intensity than the standard 90° - d2 - 180° ATP sequence. Consequently it is only the double spin echo and ERNST angle combination that gives the maximum signal intensity. Of course the ERNST angle assumes that all the carbon atoms in the different CH$_n$ group have the same or similar longitudinal relaxation times, a condition not necessarily true in practise.

An extension of the basic APT experiment are the CAPT sequences [5.70, 5.50], designed to reduce the susceptibility of the multiplicity selection to variations in the value of ^{1}J(^{n}X, ^{1}H). These sequences are more complex involving pulses on both the observation and F2 channel and uses a BIRD sequence (see section 5.8.1) in the centre of the preparation period to refocus the unwanted coherences generated by (^{n}X^{1}H) groups with ^{n}X, ^{1}H coupling constants considerably different from J$_{nominal}$. *Check it 5.2.6.3* demonstrates these improvements for several CH$_n$ groups and illustrates the possible of combining the CAPT3 sequence and the ERNST angle for higher signal intensity.

Experimental parameters:

5.2.6.3 Check it in NMR-SIM

|	
Exp No.: 1	**CAPT3**
p1 = 90d	**d2 = 3.57 msec,**
Exp No.: 2	**d9 = 1.79 msec**
p1 = 48d	

Load the configuration file *ch5263.cfg*. Simulate two CAPT3 $^{13}C\{^1H\}$ experiments using **p1** values of *90d* (**Exp No.**: *1*) and *48d* (**Exp. No.**: *2*) (**Go**|**Check Parameters & Go**). Process the FIDs (**Si(r+i)**: *64k*, wdw: **EM**, **LB**: *2.0*) and save the Fourier transformed spectra. Then replace the pulse program by the sequence *aptde.seq* (**File**|**Pulse program...**) and simulate the

Exp No.: 3	**APTDE**
p1 = 48d	**d2 = 7.14 msec**

APTDE $^{13}C\{^1H\}$ experiment **(Exp No.**: *3*) using **p1**: *48d* and **d2**: *7.14m*. Use the same processing strategy as before and save the Fourier transformed spectrum. Use the **Display|Dual display** command to compare pairs of spectra using the **Move trace** button to shift the second trace appropriately.

(a) Comparing experiment 1 and 2 higher signal intensity for the CAPT3 experiment can be achieved by using an excitation pulse related to the ERNST angle condition.

(b) Comparing experiment 2 and 3 the CAPT3 experiment is less susceptible to variations in the value of $^1J(C, H)$ than the APTDE experiment. The CAPT3 experiment always gives the expected signal phase although there is some loss on signal intensity. Whereas in the APTDE experiment there is both a considerable loss in signal intensity for the CH group ($^1J(C, H) = 220$ Hz) and a phase inversion ($^1J(C, H) = 210$ Hz). As shown in Table 5.11 there is a wide range of $^1J(C, H)$ values and these phenomena may occur with other CH_n groups depending upon the molecular structure.

An advantage of NMR-SIM simulations compared to experimental results is the ability to calculate an "excitation profile" to analyze how the intensity enhancement for the improved CAPT3 sequence, for instance, varies as a function of coupling constant. In *Check it 5.2.6.4* this excitation profile is calculated for three CH_n spin systems (*jspreadn.ham*, $n = 1$, 2 and 3). In each spin system the value of $^1J(C, H)$ is incremented from 80 Hz to 200 Hz in 20 Hz steps; to help in the analysis the chemical shift for each signal is the same as the value of $^1J(C, H)$. So for instance the ^{13}C signal at 200 Hz is related to a CH group with a $^1J(C, H)$ coupling constant of 200 Hz.

(a)

(b)

$^1J(^{13}C, {}^1H)$ 200   180   160   140   120   100   80
[Hz]
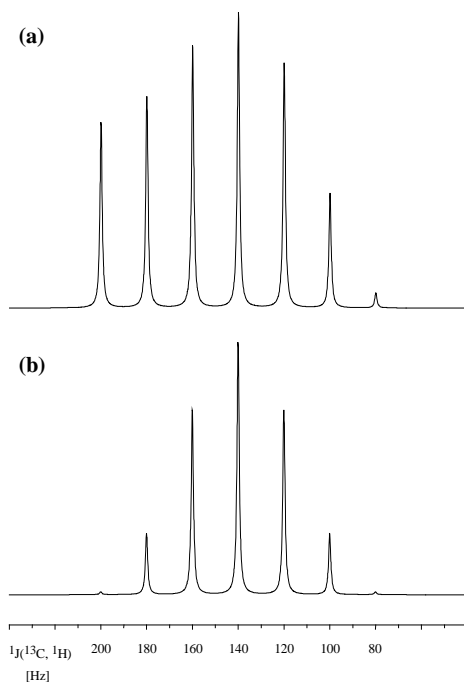
(a) CAPT3 experiment for different CH groups ($^1J(C, H)$ = 80 to 200 Hz) the "chemical shift" in Hz corresponds to the magnitude of $^1J(C, H)$ for each CH group. (b) Corresponding APT-DE experiment with the same spin system file.

5.2.6.4 Check it in NMR-SIM

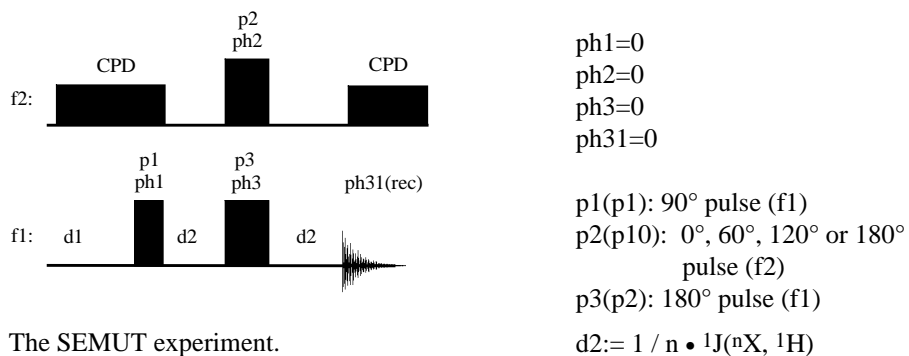Load the cfg file *ch5264.cfg* to simulate the CAPT3 $^{13}C\{^1H\}$ spectrum for the CH only spin system *jspread1.ham*. Run the simulation saving the data as **Exp No.:** *1*. Process the FID (**Si(r+i)**: *32k*, wdw: **EM**, **LB**: *1.0* [Hz]) and save transformed spectrum. To calculate the APT spectrum replace the current pulse program by *aptde.seq* (**File│Pulse program...**). Prior to the calculation set **d2**: *7.14m* (**Go│Check Parameters & Go**). Use the **Dual Display** command in 1D WIN-NMR to compare the results of the CAPT3 and APTDE simulation. There is a signal maximum at ν = 140 Hz (ν = $^1J(C, H)$) in both sequences but unlike the APTDE sequence the CAPT3 profile is not symmetrical about this maximum. Consequently with the CAPT3 sequence the nominal coupling constant might be set to a value smaller than the average value of $^1J(C, H)$. To confirm similar profiles for the other CH_n groups (n = 2 or 3) repeat the simulations using the files *jspread2.ham* (CH_2 groups) and *jspread3.ham* (CH_3 groups) (**File│Spin system...**).

Further development of APT related experiments have been curtailed by the higher intensity gain obtained using polarization transfer experiments such as DEPT or INEPT. However the simplicity of the APT sequences plus the possibility of obtaining all ^nX signals, even quaternary carbons, is an important advantage which is only achieved by the DEPTQ and the PENDANT sequence (see *Check its 5.2.6.10(1)* and *5.2.6.14(1)*).

The SEMUT sequence

Initially the SEMUT experiment (*SEMUT S*ubspectral *E*diting using a *MU*ltiple quantum *T*rap) may appear to be an advanced APT experiment. However it differs from the ATP experiment in that it was developed to produce a series of subspectra which only display signals of a chosen multiplicity such as quaternary C atoms, CH, CH_2 or

CH_3 groups. The subspectra are obtained by varying the pulse p2(p10) in a specific manner and taking linear combination of the resulting spectra. An overview of all the necessary experiments and the subsequent linear combination to calculate the CH_n subspectra are listed in Table 5.12.

ph1=0
ph2=0
ph3=0
ph31=0

p1(p1): 90° pulse (f1)
p2(p10): 0°, 60°, 120° or 180° pulse (f2)
p3(p2): 180° pulse (f1)

The SEMUT experiment.

$d2 := 1 / n \cdot {}^1J({}^nX, {}^1H)$

Table 5.12: Subspectra editing of the four SEMUT experiments.

Spectrum	p2 (p10)	Linear combinations	Selected multiplicity	Subspectra	Selected multiplicity
A	0°	X = A + B	CH, CH_2	U - 0.25 • X	C
B	180°	Y = A - B	CH_3, CH	V - 0.125 • Y	CH
C[1)]	60°	U = C + D		X - U	CH_2
D[1)]	120°	V = C - D		0.5 • Y - V	CH_3

[1)] The optimum pulse angle would be C = 54.74° (magic angle) and D = 180 - 54.74°. However the pulse was set to 60° and 120° respectively to obtain simple constants for the linear combination of subspectra [5.51].

In *Check it 5.2.6.5* spectrum A and B are simulated and the linear combination X and Y obtained using the file algebra function of 1D WIN-NMR. The linear combinations reveal the presence of the J cross-talk artefacts. J cross-talk is the term used in the original SEMUT experiment to describe the residual signals of other CH_n groups that appear in the subspectra of a selected CH_n group. J cross-talk artefacts occur when the value of ${}^1J(C, H)$ is markedly different from the $J_{nominal}$ used in the experiment.

5.2.6.5 Check it in NMR-SIM

To simulate the SEMUT-A $^{13}C\{^1H\}$ spectrum using the pulse sequence *semuta.seq* load the configuration file *ch5265a.cfg*. In the sequence *semuta.seq* the pulse p10 corresponding to p10 = 0° is omitted. Run the simulation saving the data as **Exp No.:** *1*. Process the FID (**Si(r+i)**: *64k*, wdw: **EM**, **LB**: *2.0* [Hz]) and save the spectrum after Fourier transformation. Load the file *ch5265b.cfg* and repeat the simulation for the SEMUT-B spectrum using the pulse sequence *semutb.seq*. Check the experiment parameters for **p10**: *180d* (**Go**│**Check Parameters & Go**). Start the calculation saving the data as **Exp No.:** *2*. Process the FID as the SEMUT-A spectrum and save the spectrum. Select the **Process**│**File Algebra** command and choose the SEMUT-A spectrum file as the second file. Click the **Ok** button. In the **File Algebra** window the three traces are visible: the SEMUT-A (middle trace), SEMUT-B (upper trace) and the CH, CH_3 only spectrum Y (A - B, lower trace). By clicking the **Add./Sub.** button the lower trace can be switched to the C, CH_2 only spectrum X (A + B) which is inverted by a 180° phase shift compared to the conventional representation. Toggle back to the spectrum Y calculation and click on the **Execute** and **Return** buttons to return to the main spectrum window displaying the linear combination A - B. Use the **File|Save as…** command to save the Y spectrum with a new filename e.g. *001002.1r*.

The effects of the J cross-talk are already apparent with residual C and CH_2 signals appearing in the CH and CH_3 only subspectrum and vice versa. These residual signals may be substantially reduced by using the SEMUT-GL sequence which incorporates a BIRD sequence to scale the coupling evolution to the same extent irrespective of the $^1J(C, H)$ values.

5.2.6.6 Check it in NMR-SIM

Simulate the SEMUT-GL $^{13}C\{^1H\}$ spectra A and B using the configuration files *ch5266a.cfg* (spectrum A) and *ch5266b.cfg* (spectrum B) saving the data as **Exp No.:** *1* and *2* respectively. Process the FIDs as in *Check it 5.2.5.6* (**Si(r+i)**: *64k*, wdw: **EM**, **LB**: *2.0* [Hz]). Save the spectra after Fourier transformation and perform a slight phase correction, particularly for spectrum B. Use the **File Algebra** command of 1D WIN-NMR to obtain spectrum X and Y and compare these spectra to the corresponding spectra of *Check it 5.2.6.5*.

Check its 5.2.6.5 and *5.2.6.6* demonstrate the signal enhancement of the wanted coherences by incorporating the BIRD element as part of the SEMUT-GL sequence. However the results of the subspectra editing is conflicting because although the residual CH_2 signals are of lower intensity the residual signals of the quaternary carbon atoms are more pronounced.
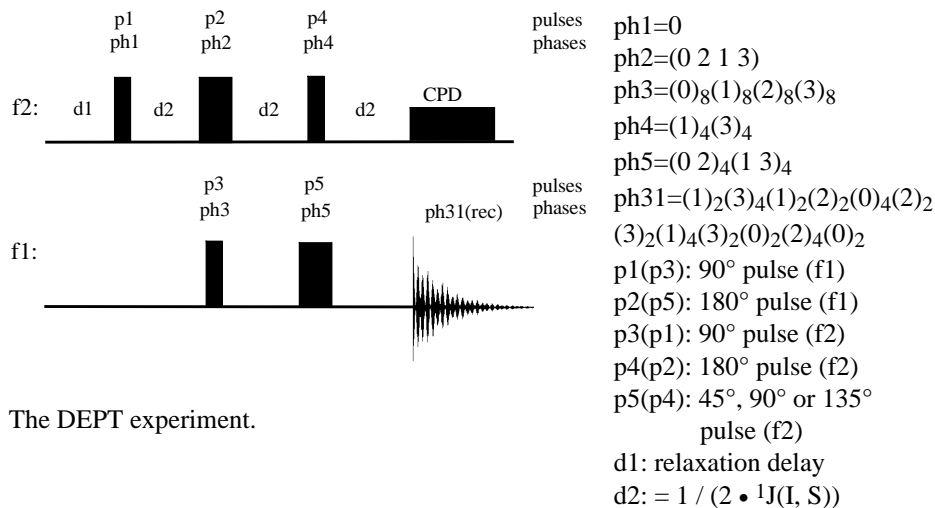
The SEMUT experiments have never been as popular as the DEPT or INEPT experiment for spectral editing. It is probably because it is necessity to measure four experiments that must then undergo extensive spectral editing coupled with the low signal enhancement in comparison to the polarization transfer experiments such as DEPT and INEPT. With the development of modern NMR spectrometers the APTSE or APTDE experiments have been nearly forgotten because there is no longer any hardware restrictions regarding applying pulse to both the observe and F2 channels simultaneously.

The DEPT sequence

The DEPT sequence shown below was introduced to overcome problems associated with the INEPT sequence [5.65]. Further development have led to the inverse DEPT sequence [5.66] used in ^{1}H detected 2D experiments [5.68] in addition to direct detection ^nX 2D experiments [5.71, 5.72, 5.73]. The advantage of the DEPT experiment compared to the INEPT sequence is that it is less sensitivity to variations in the $^1J(X, H)$ coupling constants. DEPT primarily uses the magnitude of the ^{1}H pulse p4(p5) to determine the signal amplitude and the signal phase of the different ^nXH_n group signals whereas INEPT uses the d4 delay (see scheme) for multiplicities selection. Consequently a ^nXH_n group which has a $^1J(X, H)$ coupling constant different from the value used to calculate the optimum d4 delay (d4 = $1/(4 \cdot \, ^1J(X, H)))$ appears as a phase distorted multiplet structure in the INEPT-^nX experiment. It will also have a reduced signal intensity in the ^{1}H decoupled INEPT-$^nX\{^1H\}$ spectrum. The signal intensity in the DEPT spectrum is also related to the magnitude of the $^1J(X, H)$ but to a less degree than the INEPT sequence.

There have been several improvements to the basic DEPT experiment to achieve nearly the maximum theoretical enhancement for the polarization step. These improvements have included better refocusing prior to acquisition and decoupling, the so-called DEPT$^+$ and DEPT^{++} [5.59], and a lower dependence on pulse imperfections such as off-resonance effects and incorrectly set pulse lengths [5.60, 5.74, 5.75].

Before using a CH_n spin system to demonstrate the various DEPT experiments it is worthwhile to look at the theory behind the polarization step and to examine the main features of the sequence which has led to its popularity. The DEPT experiment is not limited to CH_n groups but can be applied to any group IS_n of spin 1/2 nuclei that exhibit scalar coupling e.g. CF_n, SiH_n/SiF_n, TeH_n/TeF_n. The enhancement factor is independent of any relaxation mechanism and is a function of the gyromagnetic ratio of the coupled nuclei. The theoretical enhancement factor is a function of the multiplicity and, assuming an optimum delay d2, can be calculated for the decoupled spectrum using equation [5-4] [5.56, 5.76]. Table 5.13 lists the maximum enhancement for a number of IS_n groups where I represents a NMR sensitive nuclei like ^{1}H, ^{19}F or ^{31}P and S a NMR insensitive nuclei like ^{13}C, ^{15}N, ^{29}Si.

Pulse Sequence Scheme

The DEPT experiment.

ph1=0
ph2=(0 2 1 3)
ph3=$(0)_8(1)_8(2)_8(3)_8$
ph4=$(1)_4(3)_4$
ph5=$(0\ 2)_4(1\ 3)_4$
ph31=$(1)_2(3)_4(1)_2(2)_2(0)_4(2)_2$
$(3)_2(1)_4(3)_2(0)_2(2)_4(0)_2$
p1(p3): 90° pulse (f1)
p2(p5): 180° pulse (f1)
p3(p1): 90° pulse (f2)
p4(p2): 180° pulse (f2)
p5(p4): 45°, 90° or 135°
        pulse (f2)
d1: relaxation delay
d2: = 1 / (2 • ^{1}J(I, S))

$$\Theta_{opt} = \arcsin n^{-1/2} \quad \text{(p4(p5) in the sequence scheme)} \qquad [5\text{-}3]$$

$$E_{opt} = \left(\frac{\gamma_S}{\gamma_I}\right) n^{1/2} (1 - 1/n)^{(n-1)/2} \qquad [5\text{-}4]$$

γ_S = gyromagnetic ratio of the insensitive nuclei S, γ_I = gyromagnetic ratio of the sensitive nucleus I, n = multiplicity, the equation is only defined for n ≠ 1, n = multiplicity of I_nS group.

Table 5.13: Enhancement factor E_{opt} assuming an optimum d2 delay and a optimum pulse Θ_{opt} (= p4(p5) in the sequence scheme).

E_{opt}	IS_2	IS_3
I = ^{13}C, S = ^{1}H	3.97	4.59
I = ^{13}C, S = ^{19}F	3.74	4.31
I = ^{15}N, S = ^{1}H	-9.86	-11.39
I = ^{29}Si, S = ^{1}H	-5.03	-5.81

The following parameters were used: $\gamma(^1H)$ = 26.7520, $\gamma(^{13}C)$ = 6.7283, $\gamma(^{19}F)$ = 25.181, $\gamma(^{15}N)$ = -2.712, $\gamma(^{29}Si)$ = -5.318 ($\gamma/10^7$ rad T^{-1} s^{-1}). The optimum pulse angle Θ_{opt} corresponds to p5 in the pulse sequence above and is calculated: $\Theta_{opt}(IS)$ = π/2, $\Theta_{opt}(I_2S)$ = π/4 and $\Theta_{opt}(I_3S)$ = 0,196 • π [5.65].

In the first *Check it* the enhancement effect of the DEPT experiment and the general editing of ^nX spectra as a function of the last proton pulse p4(p5) prior to the FID acquisition is examined. In contrast to the apriori theoretical descriptions of equations [5-

3] and [5-4] the simulations illustrate visually the basic factors that are important for the enhancement and spectral appearance.

5.2.6.7 (1) Check it in NMR-SIM

Consecutively load the configuration files *ch5267a.cfg* and *ch5267b.cfg* and calculate the $^{13}C\{^1H\}$ and the DEPT45-$^{13}C\{^1H\}$ spectrum of the compound dimedone saving the data as **Exp No.**: *1* and *2* respectively. Process the data (zero filling: **Si(r+i)**: *32k*, wdw: **EM**, **LB**: *3.0* [Hz]) and save the Fourier transformed spectra. If necessary adjust the phase (**Process|Phase Correction**). Perform two additional simulations setting **p5**: *90d* (**Exp No.**: *3*) and *135d* (**Exp No.**: *4*) in the **Go│Check Experiment Parameters & Go** dialog box. Use the **Display|Multiple Display** mode to compare all four spectra. Note that the spin system is restricted to only $^1J(^{13}C, {}^1H)$ coupling interactions all other homonuclear and heteronuclear scalar interactions are excluded.
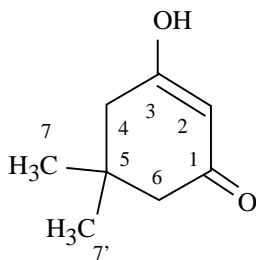
5,5-dimethyl-1,3-cyclohexane-dione (dimedone, enol tautomer).

The DEPT45, 90 and 135 $^{13}C\{^1H\}$ spectra enable the spectrum of dimedone to be edited to only show signals with the selected multiplicity. However there are signal artefacts and phase anomalies of the signals that are related to the NMR characteristics of the investigated compound and to imperfections in the pulse sequence. *Check it 5.2.6.7 (2)* examines the effect of variations in coupling constants and multiplicity using a set of virtual CH_n groups. Alternatively the **Parameter Optimizer** can be used to investigate the influence of incorrectly set delays and pulse lengths.

5.2.6.7 (2) Check it in NMR-SIM

(a) Load the configuration file *ch5267b.cfg* as used in *Check it 5.2.6.7 (1)*. Use the **Edit│Create new│Spin system** command to create the spin system file *mychngrp.ham* containing the entries listed below. These entries consists of three examples for each type of CH_n multiplicity using typical values of $^1J(C, H)$ taken from Table 5.11. Simulate the DEPT45-$^{13}C\{^1H\}$ spectrum and process the FID (zero filling of **Si(r+i)**: *64k* and wdw: **EM**, **LB**: *2.0* [Hz]). Note the very strong intensity decrease for the CH groups when the value of $^1J(C, H)$ is very different from the nominal coupling constant ($J_{nominal} = 140$ Hz, d2 = $1/(2 \cdot 140)$). Similarly note that for the same value of $^1J(C, H)$ the intensity enhancement is a function of the signal multiplicity.

; filename : mychngrp.ham[1]

molecule ch3groups 1.00	**molecule ch2groups 1.00**	**molecule chgroups 1.00**
carbon a 5 t2=2.0	**carbon a 35 t2=2.0**	**carbon a 80 t2=2.0**
carbon b 10 t2=2.0	**carbon b 40 t2=2.0**	**carbon b 85 t2=2.0**
carbon c 15 t2=2.0	**carbon c 45 t2=2.0**	**carbon c 90 t2=2.0**
proton 3*d 0.2 t2=2.0	**proton 2*d 0.2 t2=2.0**	**proton d 0.2 t2=2.0**
proton 3*e 0.5 t2=2.0	**proton 2*e 0.5 t2=2.0**	**proton e 0.5 t2=2.0**
proton 3*f 1.0 t2=2.0	**proton 2*f 1.0 t2=2.0**	**proton f 1.0 t2=2.0**
weak a d 120	**weak a d 120**	**weak a d 180**
weak b e 130	**weak b e 140**	**weak b e 210**
weak c f 150	**weak c f 180**	**weak c f 250**
endmol	**endmol**	**endmol**

[1]All statements have to be entered on sequential lines in a single column.

; filename : mychn.ham

carbon a 30 t2=2.0
carbon b 40 t2=2.0
carbon c 50 t2=2.0
proton 3*d 0.2 t2=2.0
proton 2*e 0.5 t2=2.0
proton f 1.0 t2=2.0
weak a d 140
weak b e 140
weak c f 140

(b) Use the configuration file from part (a). Edit the spin system file *mychngrp.ham* (**Edit**⎮**Spin System**) and convert the spin system to a single molecule expression corresponding to one CH_n group each with a $^1J(C, H)$ value of 140 Hz. Use the **File**⎮**Save as…** option to store the new spin system file as *mychn.ham*. Replace the current spin system file with the new spin system (**File**⎮**Spin system...**). Set the experiment parameters **SW**: *30* and **O1**: *40*. Select the Parameter Optimizer (**Go**⎮**Optimize Parameter**). Select the **Show results as** *1D series*, **N**: 10, **Step**: *40* [Hz] and **d2** for optimization. Click on the **OK** button. In the next dialog box enter the start value **d2**: *0.001s* and increment size **in2** = *0.5m* [s]. Click on the **OK** button. Process the FID (zero filling **Si(r+i)**: *64k* and wdw: **EM**, **LB**: *1.0* [Hz]) and Fourier transform the FID. Apply a slight numerical phase correction **phc0**: *6.00* and **phc1**: *-11.25* (**Process**⎮**Phase Correction**, and click the **Numerical** button in the button panel). From the "profiles" of each CH_n group it is apparent that the enhancement for the CH_3 group is relative insensitive to variations in the value of d2 (broad profile) in contrast to the CH group.

Since the DEPT experiment is an ^nX detected experiment large spectral widths are required in comparison with the relative small frequency range for ^1H spectra. To be successful DEPT requires homogenous excitation over the complete spectral width and finite pulse power gives rise to off-resonance effects. The DEPT experiment has been improved to overcome these effects using a combination of composite pulses, especially for the refocusing 180° ^{13}C pulse, and phase cycling [5.60]. This improved sequence is illustrated in *Check it 5.2.6.8(b)*.

5.2.6.8 Check it in NMR-SIM

(a) Using the configuration file *ch5268.cfg* simulate the $^{13}C\{^1H\}$ spectrum (**Exp No.**: *1*) of five individual CH groups with chemical shifts of 150, 125, 100, 75 and 50 ppm. Replace the pulse program by the file *deptorig.seq* (**File│Pulse program...**) and simulate the DEPT45-$^{13}C\{^1H\}$ spectrum using the original pulse sequence with a minimum phase cycle (**Exp No.**: *2*). Process both spectra, and all subsequent spectra in this *Check it*, (zero filling: **Si(r+i)**: *128k*, wdw: **EM**, **LB**: *2.0* [Hz]). Compare both spectra using the **Display│Dual Display** representation in 1D WIN-NMR. Note that as a consequence of the polarization transfer the intensity in the DEPT spectrum is nearly four times higher. Run the simulation of a DEPT45 spectrum again after changing pulse **p2**: *120d* to study the effect of an incorrectly set180° ^{13}C pulse (**Exp No.**: *3*). A comparison of experiments 2 and 3 shows a loss of signal intensity. This effect can be minimized by replacing the refocusing 180° pulse with a composite pulse. Therefore replace the current pulse program (**File│Pulse program...**) by *deptcp.seq* (deptcp = dept + composite pulse) which uses a composite 180° ^{13}C pulse. Repeat the simulation using **p2**: *120d*. (**Exp No.**: *4*). Use the **Multiple Display** mode to compare all four spectra and confirm that the signal intensity can be regained by the use of a composite pulse.

(b) Load the configuration file *ch5268b.cfg* and simulate three experiments using the spin system *choffset.ham*. (**Exp No.**: *5*) a DEPT45-$^{13}C\{^1H\}$ spectrum using the pulse program *deptorig.seq*, (**Exp No.**: *6*) a DEPT45-$^{13}C\{^1H\}$ spectrum with a 180° ^{13}C composite pulse using the pulse program *deptcp.seq* and (**Exp No.**: *7*) a DEPT45-$^{13}C\{^1H\}$ spectrum with a 180° ^{13}C composite pulse and an appropriate phase cycling using the pulse program *deptcpof.seq*. Prior to simulation (6) and (7) replace the current pulse programs (**File│Pulse program...**). To be certain that the off-resonance effects will be visible the ^{13}C channel (f1) pulse power must be set to **pl1**: *20000* [Hz] (**Go│Check Experiment Parameters**). Process the FIDs as described in section (a). Compare the results using the **Dual Display** option of 1D WIN-NMR. Use the **Move Trace** button in the button panel to shift the second trace for a better representation.

A product operator analysis of the observable coherences for the standard DEPT sequence [5.59] shows that in addition to the wanted coherence S_x (where S_x is the x-component of the S spin product operator and S is the non-abundant ^{13}C spin) several other single quantum coherences are generated. These terms such as I_zS_x lead to phase distortions in the ^1H coupled spectra because signals which could be assigned to either the S_x or S_y state are overlapped by antiphase signals from coherences like I_zS_y. Consequently the signal intensity of the related decoupled spectrum is reduced by these coherences. In the DEPT++ sequence only the required single quantum coherences S_x (or

S_y) contribute to the detected FID because the unwanted coherences have been previously transfer of to an undetectable multiple quantum state [5.59].

In *Check it 5.2.6.9* the effectiveness of the improved DEPT++ experiment is shown by comparing the results from a ^1H coupled ^{13}C DEPT experiment with those obtained using the DEPT++ sequence. The ^1H coupled experiments in the most effective way of illustrating this improvement because in the broadband ^1H decoupled each CH_n group is a singlet and phase and intensity anomalies are reduced to minor intensity changes.

DEPT

(p5 ph3):f2 (p2 ph5 d2):f1

...

DEPT++

(p5 ph3):f2
d4
(p4 ph4):f2 (p2 ph5):f1
d4
(p3 ph6):f2
d4
(p4 ph7):f2
d4

...

ph6 =0 2
ph7 =0

DEPT and the DEPT++ sequence differences.

5.2.6.9 Check it in NMR-SIM

Load the file *ch5269a.cfg*. Calculate the $^{13}C\{^1H\}$ spectrum of a virtual spin system containing an ethyl and ethylene skeleton. Run the simulation (**Go**⏐**Run Experiment**) saving the data as **Exp No.**: *1*. Process the FID (**Si(r+i)**: *64k*, wdw: **EM**, **LB**: *2.0* [Hz]), Fourier transform the FID and save the phase corrected spectrum. Then load the *ch5269.cfg* file and simulate the DEPT45-$^{13}C\{^1H\}$ spectrum of the same spin system saving the data as **Exp No.**: *2*. Process the FID and save the properly processed spectrum. Prior to the calculation of the DEPT++ spectrum open the DEPT pulse program file by the pulse program editor (**Edit**⏐**Pulse program**) and save the file as *mydeptpp.seq* (**File**⏐**Save as…**). Replace the current pulse program for the new program *mydeptpp.seq* (**File**⏐**Pulse program…**). Using the pulse program editor replace the statement **(p5 ph3):f2 (p2 ph5 d2):f1** by the lines printed in bold on the left side of this *Check it*. Extend the phase program to include ph6 and ph7. Modify the comments in the pulse program prior to saving the modified file (**File**⏐**Save**). In the **Go**⏐**Check Parameters & Go** dialog box change **p5**: *135d* and **d4**: *1.786m* and save the calculation as **Exp No.**: *3*. Process the FID in a similarly manner to the other spectra. In 1D WIN-NMR compare all three spectra by using the **Multiple Display** mode and clicking on the **Stack plot** button in the button panel.

As interesting variant of the standard DEPT experiment is the DEPTQ experiment [5.67] which enables the detection of ^nX groups such as quaternary carbons atoms which are not directly bonded to a sensitive NMR nucleus. These types of group are not enhanced by the polarization transfer step and are usually missing from the standard DEPT spectrum. Consequently if quaternary carbon are part of the molecule skeleton in a structural determination it is necessary to record both the broadband ^1H decoupled ^{13}C spectrum and multiplicity edited DEPT135-$^{13}C\{^1H\}$ spectrum. However the DEPTQ

experiment enables the signals of quaternary carbon atoms to be observed, without of course signal enhancement, with the enhanced CH_n groups signals in a polarization transfer experiment. The authors of DEPTQ proposed that for the assignment of quaternary carbon atoms a combination of DEPTQ [5.67] and $C_{quaternary}$ optimized SEMUT-90 should be used. Unlike the other spectral editing experiments APT or SEMUT which also display quaternary carbon signals, this approach is relatively insensitive to variation in $^1J(C, H)$ and pulse imperfections.

Check it 5.2.6.10 (1) shows the differences between the DEPT and the DEPTQ experiment by converting the standard DEPT pulse sequence into the DEPTQ sequence. The spin system used to illustrate these differences is a reduced spin system similar to caffeine.

1...

   ...

3 **(p1 ph6):f1**

  d2

  (p4 ph2):f2 **(p1 ph7):f1**

  ...

exit

ph5=...

ph6 = 1 1 1 1 3 3 3 3 0 0 0 0

2 2 2 2 3 3 3 3 1 1 1 1 2 2 2 2

 0 0 0 0

ph7 = 0 2 1 3

ph31=...

DEPTQ sequence: Additional lines and commands to the conventional DEPT experiment are shown in bold letters (Note: The pulse phases have to be entered on the same line.).

5.2.6.10 (1) Check it in NMR-SIM

Load the file *ch52610.cfg*. Create the new pulse sequence file by loading the DEPT sequence into the editor window (**Edit│Pulse program**). Save the unchanged pulse sequence with the new filename *mydeptq.seq* using the **File│Save As...** option. Replace the current pulse program with *mydeptq.seq* (**File│Pulse program...**). Using the pulse program editor convert the program to the DEPTQ sequence by inserting the lines printed in bold on the left side of this *Check it*. Save the modified pulse program. Now check the program using the NMR-SIM internal pulse program viewer (**Utilities│Show pulse program...**). Simulate the DEPTQ spectrum of the caffeine based spin system and process the data (zero filling **Si(r+i)**: *32k*, wdw: **EM**, **LB**: *3.0* [Hz]). For comparison run a second simulation using the DEPT135 experiment and display both spectra using the **Display│Multiple Display** option.

The effect of the additional pulses in the DEPTQ experiment can be understood by analysing the coherence evolution of the quaternary carbon atom in the standard DEPT experiment.

ph1=0 ;...
ph2=0 ;...
ph3=1 ;...
ph4=0 ;...
ph5=0 ;...

5.2.6.10 (2) Check it in NMR-SIM

Load the configuration *ch52610.cfg*. Modify the phase program **phi** of *dept.seq* (**Edit|Pulse program**) by placing a semicolon between the first and second phase value for each phase program as shown on the left side. Save the

ph31=1 ;...   new sequence as *mdeptph1.seq*. Load the new sequence *mdeptph1.seq* (**File⏐Pulse program...**). Run a calculation for the reduced spin system of caffeine and process the FID (**Si(r+i)**: *32k*, wdw: **EM**, **LB**: *3.0* [Hz]). Compare the results with the *result.pdf* file.

In the conventional DEPT experiment the quaternary carbon coherence is generated but the phase cycling destroys it. The additional two pulses in the DEPTQ experiment re-establishes these coherences and simultaneous generates a pure absorption lineshapes for the signals of the other CH_n groups by transferring all the coherences to the same relative phase in relation to the rotational co-ordinate system.

The POMMIE sequence

An alternative to the DEPT experiment for assignment of odd and even multiplicities I_nS groups is the POMMIE sequence (*POMMIE = Phase Oscillations to MaxiMIze Editing*) [5.77]. Again CH and CH_3 signals are inverted with respect to the signals of CH_2 groups. Both sequences are similar but in the DEPT sequence the decoding of the signal phase as a function of the multiplicity depends upon the pulse angle of the final ^1H pulse (45°, 90° or 135°) whereas in the POMMIE sequence it is the phase of this pulse. Experimentally the DEPT experiment has been easier to implement just requiring pulse length calibration and 90° phase shifts in contrast to the POMMIE sequence where the pulse phase generation must be an exact multiple of 45°. However spectrometer hardware has improved in the last few years and exact pulse phase generation is no longer a problem and the POMMIE method has been successfully implemented in both 2D [5.78] and inverse detection experiments [5.69]. As shown in Table 5.14 in contrast to the DEPT and INEPT experiments full editing of ^{13}C spectra into individual CH_n subspectra is not possible in the POMMIE experiment. However the results from the DEPT135-$^{13}C\{^1H\}$ and POMMIE135 experiment are similar, the sign of the signals of the CH and CH_3 groups being opposite to signals of the CH_2 groups. With respect to identify multiplicities of XH_n groups the DEPT135-$^{13}C\{^1H\}$ and POMMIE135-$^{13}C\{^1H\}$ experiments are equivalent.

In *Check it 5.2.6.11* the POMMIE sequence is used for editing $^{13}C\{^1H\}$ of a number of CH_n with a variety of $^1J(C, H)$ coupling constant values and as expected the signal intensity depends upon the value of $^1J(C, H)$. The d2 delay (d2 = 1 / (2 • $^1J(C, H)$)) used in the polarization transfer and the refocusing prior to acquisition and decoupling can only be optimized to a single value or a mean value based upon the expected range of coupling constants for the analysed compound.

5.2.6.11 Check it in NMR-SIM

Simulate the POMMIE135-$^{13}C\{^1H\}$ spectrum of several CH_n groups, n = 1, 2, 3, as defined in the spin system file *cJspread.ham* using the cfg-file *ch52611.cfg*. Replace the sequence file by the pulse program file *pommie225.seq* (**File⏐Pulse program...**). Run the simulation again saving

the FID with a different filename. Process both spectra in the same way. Phase correct the spectra for pure absorption lines paying particular attention to the CH and CH_3 signals which have a negative signal amplitude in both spectra. With the POMMIE225 spectrum in the main display window select the **Process|File Algebra** command and choose the POMMIE135 spectrum file as the second file. Click the **Ok** button. In the **File Algebra** window three spectra appear, the POMMIE225 spectrum (upper section), the POMMIE135 spectrum (middle section) and the linear combination of both POMMIE spectra (lower section). By clicking the **Add./Sub.** button in the button panel the linear combination in the lower trace can be toggled between addition and subtraction displaying the spectrum of either CH_2 groups or CH and CH_3 groups. Select the linear combination for the CH_2 group and click on the **Execute** and **Return** buttons to return to the main spectrum window. Use the **File|Save as…** command to save the CH_2 group spectrum with a new filename.
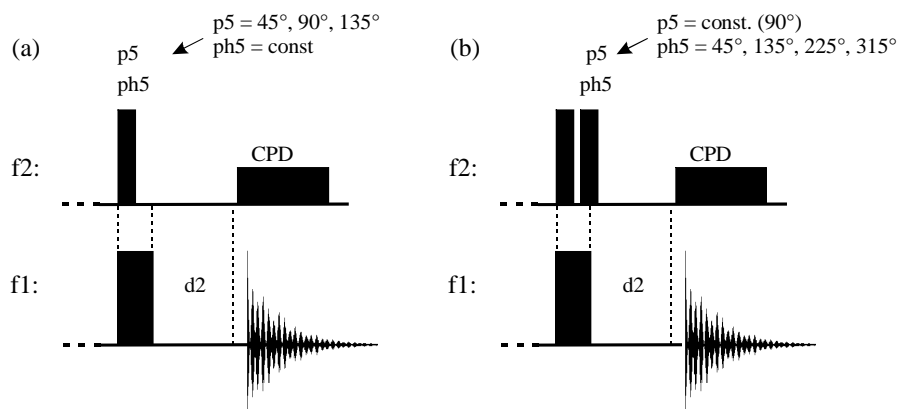
Fig. 5.19:   Partial pulse sequence scheme (a) DEPT experiment (b) POMMIE experiment.

The CH_2 group only difference spectrum shows small artefacts for the CH group signals with a $^1J(C, H)$ coupling constant which differs from the nominal coupling constant ($J_{nominal} = 140$ Hz). More apparent are the CH_3 artefacts, which are readily, observed when the value of $^1J(C, H)$ differs by more than 20 Hz from $J_{nominal}$. Fortunately these simulations are made using the very extreme variations for $^1J(C, H)$ so that experimentally the artefacts should not be as large. Nevertheless this point must be kept in mind for ^nX, ^1H experiments where a wide range of coupling constants for the same substance might be possible. In conclusion the standard POMMIE135 experiment is a useful technique in identify ^nXH_n group multiplicities, the spectrum being relatively free of artefacts.

Table 5.14:   Relative signs of the signal amplitude for $^{13}CH_n$ groups (n = 1, 2 and 3) as a function of pulse length p5 and pulse phase ph5.

	DEPT-^{13}C{^{1}H}experiment				POMMIE-^{13}C{^{1}H} experiment			
p5 =	45°	90°	135°	**ph5 =**	45°	135°	225°	315°
CH	+	+	+		+	-	-	+
CH$_2$	+	2)	-		-	+	-	+
CH$_3$	+	2)	+		+	-	-	+

[1])The pulse p5 and the pulse phase ph5 correspond to the partial pulse sequence scheme of Fig 5.19. [2])Signals of this multiplicity are not detected.

The INEPT sequence

The INEPT sequence was the first non-specific polarization transfer experiment and subsequently the INEPT unit has becomes an important part of heteronuclear correlation spectroscopy as in the ^{13}C, ^{1}H HSQC experiment. The INEPT sequence creates antiphase magnetization for a heteronuclear spin system with an optimum reduction in chemical shift evolution that can then be effectively transferred by a coherence transfer step for signal enhancement. The results obtained with the INEPT unit are very sensitive to the delay periods used in the sequence. Nevertheless it is possible to use the refocused INEPT experiment in a similar manner to the DEPT experiment to produce a series of multiplicity selected subspectra such as CH/CH$_3$- or CH$_2$ only.

ph1=(0)$_8$(2)$_8$
ph2=0 2
ph3=0 2
ph4=1 1 3 3
ph5=(0)$_4$(1)$_4$(2)$_4$(3)$_4$
ph31=0 0 2 2 1 1 3 3

p1(p5): 90° pulse (f1)
p2(p3): 180° pulse (f1)
p3(p1, p4): 90° pulse (f2)
p4(p2): 180° pulse (f2)
d1: relaxation delay
d2: = 1 / (4 • J(^{13}C, ^{1}H))
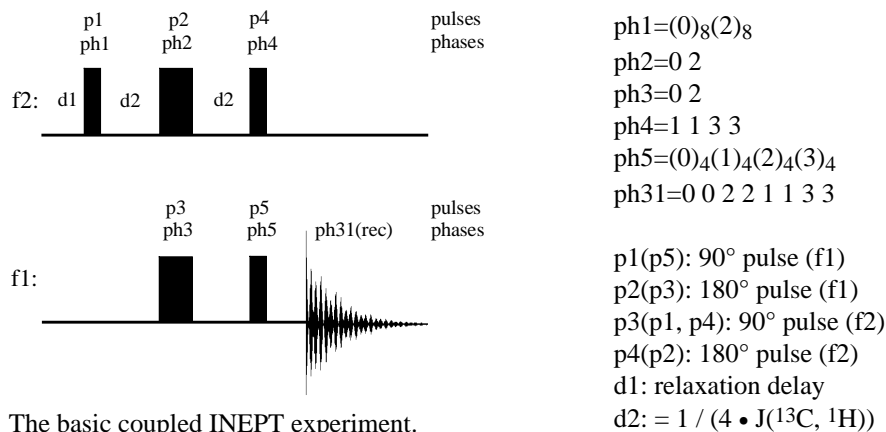
The basic coupled INEPT experiment.

The basic INEPT sequence does not allow ^{1}H decoupling during data acquisition and the ^{1}H refocused INEPT sequence incorporating an reverse INEPT unit has been developed. Essentially the sequence has two functional parts: The first INEPT unit creates antiphase coherence ($I_z \rightarrow I_yS_z$) and polarization transfer ($I_yS_z \rightarrow I_zS_y$). The overall signal enhancement depending upon the difference in value between ^{1}J(C, H) and the optimum coupling constant $J_{nominal}$ (d2 = 1 / (4 • $J_{nominal}$)). The second, reverse

INEPT unit refocuses the antiphase coherence $(I_zS_y \rightarrow S_x)$. The detected signal intensity is correlated with the effective polarization transfer and can be reduced by the underlying I_zS_y antiphase coherence if the refocusing is not prefect. In the ^1H coupled spectrum these antiphase coherences produce multiplet anomalies.

The following scheme reflects the complex relationship between signal enhancement, multiplicity, optimum delay and nominal coupling constant [5.56, 5.61] for the refocused INEPT experiment. Compromise delays are given if particular CH_n groups are required. The signal enhancement dependence on θ' causes particular problems for CH_3 groups because of the opposing effects of $\sin\theta'$ and $\mathrm{cosine}\theta'$ as shown in the table below.

^nX group	Enhancement of the observable signals[1]	Optimum refocusing delay τ'	Compromise delay [5.61]
IS	$= \sin\theta'$ [2]	$\tau' = (2 \bullet J_{nom})^{-1}$	CH/CH_2: $\tau' = (3 \bullet J_{nom})^{-1}$
I_2S	$= 2\sin\theta'\cos\theta' = \sin2\theta'$	$\tau' = (4 \bullet J_{nom})^{-1}$	
I_3S	$= 3\sin\theta'\cos^2\theta'$	$\tau' = (5 \bullet J_{nom})^{-1}$	$CH/CH_2/CH_3$: $\tau' = 3(10 \bullet J_{nom})^{-1}$

[1]The enhancement is also related to the gyromagnetic ratio, for example $E(CH) = (\gamma_I/\gamma_S) \bullet \sin\theta'$. [2]$\theta' = \pi J\tau'$, τ' corresponds to $2 \bullet d3$ of *Check it 5.2.6.12*.

The following *Check it* demonstrates that the refocusing unit as an extension of the simple coupled INEPT experiment causes severe multiplet anomalies which can be simply circumvent by applying an additional 90° pulse to the I spin. This new sequence is called INEPT[+]. The complete discussion of the INEPT[+] sequence and the product operator analysis of the refocused INEPT are described elsewhere [5.59]. The results for the observable coherences without the underlying intensity factors are summarized for the refocused INEPT and the INEPT[+] experiment in Table 5.15.

Table 5.15: Refocusing delay parameters for multiplicity related signal phase.

d3 =		Positive signal amplitude	Negative signal amplitude
	$1 / (6 \bullet {}^1J(X, H))$	XH, XH_2, XH_3	
	$1 / (4 \bullet {}^1J(X, H))$	XH	
	$1 / (3 \bullet {}^1J(X, H))$	XH, XH_3	XH_2
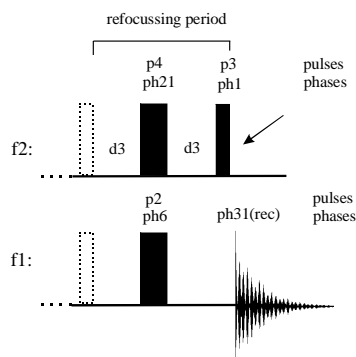
Refocusing period of the INEPT⁺ experiment, the arrow denotes the additional pulse (purge pulse) in comparison to the refocused INEPT sequence.

5.2.6.12 Check it in NMR-SIM

Load the configuration file *ch52612.cfg*. The spin system has three CH$_n$ groups (n = 1, 2 and 3) each with a value of $^1J(^{13}C, {}^1H) = 140$ Hz. Simulation the coupled INEPT spectrum saving the data as **Exp No.**: *1*. Process the spectrum, inspect the multiplet structure of the CH$_n$ groups and note the missing central line for the CH$_2$ group. Replace the current pulse program by the refocused INEPT experiment *ineptref.seq* (**File│Pulse program...**). Repeat the simulation (**Exp No.**: *2*) and process the FID as before. Phase correct the spectrum as best as possible. Convert the INEPT sequence (**Edit│Pulse program**) into the INEPT+ sequence by adding the line *(p3 ph1):f2* before the **go=2 ph31** line. Save the new sequence as *myineptp.seq*. Prior to the simulation replace the current pulse sequence by the newly created INEPT+ sequence. Run a third simulation (**Exp No.**: *3*). Use the **Display|Multiple Display** mode to compare all three spectra.

To overcome problems arising from coupling constants which deviate strongly from the nominal coupling constant two similar improvements to the INEPT⁺ sequence called Broadband-INEPT [5.61] and INEPT-CR [5.62] have been developed. In the Broadband-INEPT experiment [5.61] the improvement relates to the creation of antiphase coherence prior to the polarization transfer and refocusing which is largely independent of the value of $^1J(C, H)$. In the second approach [5.62] the refocusing period is optimized by the inclusion of a BIRD sandwich (see section 5.8.1). The sequence was called INEPT-CR⁺ (**CR** = **C**omposite **R**efocusing) because of its dependence on the conventional 180° composite pulse ($90°_y/180°_x/90°_x$).

In *Check it 5.2.6.16* the INEPT-CR⁺ and INEPT⁺ sequences are compared. A disadvantage of the INEPT-CR+ sequence is the 45° phase shift of the CH$_2$ groups relative to the CH and CH$_3$ groups. This 45° phase shift requires the spectrum to be phase corrected twice and is probably the reason why this sequence has never become popular. Nevertheless the simulation does show how effective this approach is and demonstrates the importance of a BIRD filter as a refocusing tool for coupling evolution for a wide range of $^1J(C, H)$ values.

5.2.6.13 Check it in NMR-SIM

Load the configuration file *ch52613a.cfg* to simulate the ^{1}H coupled INEPT$^+$-^{13}C{^{1}H} spectrum of several individual CH$_n$ groups with a range of ^{1}J(C, H) values (120, 140 and 160 Hz). Run the simulation, process the FID (**SI(r+i)**: *32k*, wdw: **EM**, **LB**: *2.0* [Hz]) and Fourier transform the data. Phase correct the spectrum to obtain pure absorption lines for signals 1b, 2b and 3b which have ^{1}J(C, H) = 140 Hz. Simulate the ^{1}H decoupled spectrum replacing the current pulse program with *ineptpdc.seq* (**File|Pulse program...**). Load the configuration file *ch52613b.cfg*. Using the pulse programs *ineptcr.seq* and *ineptcrd.seq* respectively, simulate the ^{1}H coupled and ^{1}H decoupled INEPT-CR$^+$ spectra. Process the calculated FIDs in the same way as before and phase correct the spectrum to obtain pure absorption lines for the CH (1b) and CH$_3$ (3b) signals.

The ^{1}H coupled INEPT$^+$ spectrum can be nearly phased to pure absorption lines for all the CH$_n$ groups except for the CH group with a ^{1}J(C, H) coupling of 160 Hz which is not detected. In the ^{1}H coupled INEPT-CR$^+$ experiment the multiplets have greater intensity but there is severe phase distortion. Comparison of the ^{1}H decoupled INEPT$^+$ and INEPT-CR$^+$ sequences shows a tremendous gain in signal intensity for the INEPT-CR$^+$ such that even the signal of CH group with ^{1}J(C, H) = 160 Hz can be detected. The $45°$ phase shift between the CH and CH$_3$ groups and the CH$_2$ groups is more obvious in the ^{1}H coupled spectra and may be confirmed by setting the value of phc0 in the Numerical phase dialog box to -45°.

As an additional exercise the reader might investigate the dependence of the Broadband-INEPT sequence on off-resonance effects and incorrectly set pulse lengths as well as the sensitivity enhancement for different values of ^{1}J(C, H).

The PENDANT sequence

The PENDANT sequence is an extended version of the INEPT sequence for the detection of quaternary carbon atoms in a similar way that the DEPTQ sequence is an extension of the standard DEPT sequences. Initially the only difference between PENDANT and the refocused INEPT sequence is an extra 90° ^{13}C pulse executed simultaneously with the first 90° ^{1}H pulse. Upon closer inspection a second difference is apparent, the refocusing period delay d3 in the INEPT sequence is $3/(8 \cdot {}^1J(C, H))$ and $5/(8 \cdot {}^1J(C, H))$ for PENDANT. Compared to the DEPT sequence, the modifications necessary to detect quaternary carbon atoms are easier to implement in the refocused INEPT sequence. The refocused INEPT sequence has two periods for refocusing ^{13}C chemical shift evolution so that the quaternary carbons atoms coherences which are generated by the initial 90° ^{13}C pulse evolve under the chemical shift evolution during the free precession periods and are refocused immediately before the acquisition period. In contrast the DEPTQ sequence requires an additional coherence evolution delay

compared to the standard DEPT sequence. A major disadvantage of the PENDANT sequence is the strong dependence on the value of the coupling constant used to calculate the time for the antiphase coherence evolution prior to the polarization transfer. This dependence is a common feature of INEPT type transfer and does not occur with DEPT experiments.

Pulse Sequence Scheme

pulses
phases
ph1, ph2=$(0)_8(2)_8$
ph3, ph4, ph7, ph8=0 2
ph5, ph6=1 1 3 3
ph31=$(2)_8(0)_8$

pulses phases
p1(p2, p6): 90° pulse (f1)
p2(p4, p8): 180° pulse (f1)
p3(p1, p5): 90° pulse (f2)
p4(p3, p7): 180° pulse (f2)

d1: relaxation delay
d4: =$1 / (2 \bullet J(C, H))$
d3: = $5 / (8 \bullet J(C, H))$
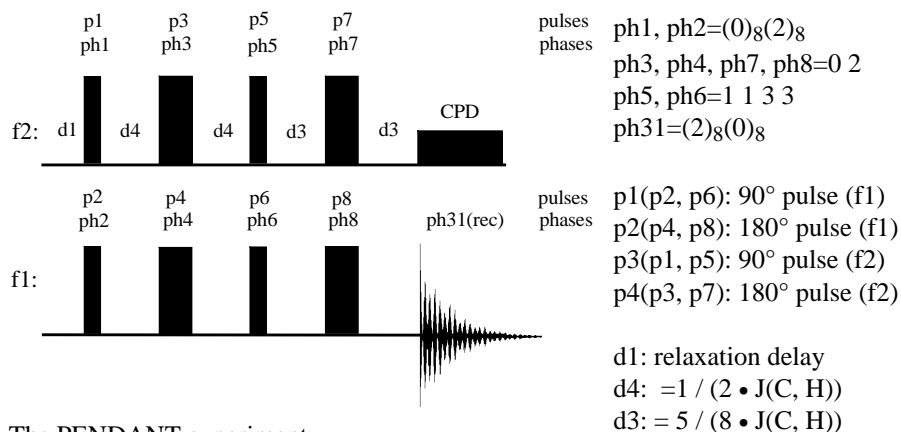
The PENDANT experiment.

Check it 5.2.6.14 focuses on the optimum d3 delay as described in the literature [5.64] using the NMR-SIM Parameter Optimizer tool.
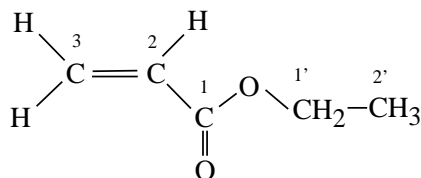
Ethyl acrylate
experimental parameters:
d4 = $1/(4 \bullet J(C, H))$
d3 = $5/(8 \bullet J(C, H))$

5.2.6.14 (1) Check it in NMR-SIM

Load the configuration file *ch52614.cfg* and simulate the ^{1}H decoupled PENDANT-^{13}C{^{1}H} spectrum of ethyl acrylate. Save the data as **USER**: *ch526*, **Name**: *52614* and **Exp No.**: *1*. Process the FID (**SI(r+i)**: *64k*, wdw: **EM**, **LB**: *2.0* [Hz]). Apply a slight phase correction and then examine the spectrum for the sign of the signal amplitude.

Note the phase distortions for the overlapping signals of C-2 and C-3. Unfortunately the original references [5.63, 5.64, 5.79] did not contain any comments on the susceptibility of the sequence to complex coupling interactions and the PENDANT experiment was validated using a simple spin system, ethyl benzene. The authors did propose using a delay d3 = $5/(8 \bullet J(C, H)$ rather than $3/(8 \bullet J(C, H))$ for the corresponding d3 delay in the refocused INEPT experiment. Using the *Parameter Optimizer* tool it is possible to use NMR-SIM to study the influence of values of d3. In

Check it 5.2.6.14(2) the signal intensity of the CH, CH$_2$ and CH$_3$ groups are calculated as a function of d3 ranging from d3 = 2/(16 • J(C, H)) to 15/(16 • J(C, H)) using a value of ^{1}J(C, H) of 140 Hz.

new experiment parameters:
O2 = 0 ppm
SW = 40 ppm
Parameter Optimizer
parameters:
N = 14
Step: 40
incremented parameters
d3 = 0.893m
in3 = 0.4465m

5.2.6.14 (2) Check it in NMR-SIM

Load the configuration file *ch52614.cfg* and replace the current spin system file by file *chgroup.ham* (**File│Spin system...**). Start the parameter optimizer (**Go│Optimize parameter**). Select the **Show results as** *1D*, **N**:*14*, **Step**: *40* and **d3** for optimization. Click on the **OK** button. In the next dialog box enter the start value **d3**: *0.893m* and increment size **in3**: *0.4465m*. Click on the **OK** button and save the calculated FID as **Exp No.**: *2*. Repeat the simulation for the CH$_3$ (*ch3group.ham*) and CH$_2$ group's (*ch2group.ham*) replacing the current spin system file with the corresponding files and saving the data as **Exp No.**: *4* and *5*. Process the FIDs (zero filling **SI(r+i)**: *64k*, wdw: **EM**, **LB**: *2.0* [Hz]). Compare the spectra using the **Stack plot** option in the **Multiple Display** mode of 1D WIN-NMR.

Comparing the results of the simulation the only difference between using a d3 value of 3/(8 • J(C, H)) instead of 5/(8 • J(C, H)) is an overall phase inversion of the signals.

The PENDANT experiment can also be used for polarization transfer using long-range coupled I$_n$S groups as shown in *Check it 5.2.6.15*. This proposal is based on the intrinsic chemical shift refocusing of the INEPT step. The two 180° pulses in the centre of the spin echo prior to the coherence transfer guarantee the refocusing of the chemical shift evolution. This becomes very important if the spin echo is adapted for the antiphase coherence evolution using long-range coupling constants. Because these coupling constants are generally small the evolution delays are long and there is progressive shift evolution. A major drawback of the sequence is that it does not suppress the signals arising from the antiphase coherence related to the short-range I$_n$S coupling constants (I = sensitive nuclei, like ^{1}H, ^{19}F, S = insensitive nuclei, like ^{13}C, ^{29}Si etc).

$J(H, H) = 3$
$J(H, Si) = 10$

$\delta(^{29}Si) = 2$

$J(H, H) = 3$
$J(H, Si) = 10$

$\delta(^{29}Si) = 10$

$J(H, H) = 3$
$J(H, Si) = 10$

$\delta(^{29}Si) = 20$
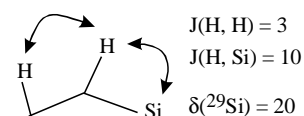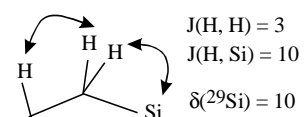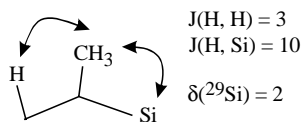
Structure units representing the spin systems of the file *simult.ham*.

5.2.6.15 Check it in NMR-SIM

Load the configuration file *ch52615.cfg*. The spin system file *simult.ham* corresponds to the ^{1}H, ^{29}Si the structural fragments shown on the left. Run the calculation for the PENDANT sequence based on the long-range ^{1}H, ^{29}Si coupling saving the data as **Exp. No.:** *1*. Process the (zero filling **SI(r+i)**: *32k*, wdw: **EM**, **LB**: *1.0* [Hz]). Phase correct the spectrum so that the Si(H$_2$) signal at 10 ppm is negative. Save the Fourier transformed spectrum (Note: After the initial Fourier transformation the phase of the spectrum is inverted because of the negative gyromagnetic ratio of ^{29}Si). Edit the spin system (**Edit│Spin system**) and change the magnitude of the homonuclear H, H coupling for each molecule definition to: **weak a b 10**. Save the modified spin system as *simula.ham* (**File│Save as…**). Replace then the current spin system with the modified file (**File│Spin system...**). Repeat the simulation saving the data as **Exp No.:** *2*. Process the FID as before. Use the **Dual display** option of 1D WIN-NMR to show both calculated spectra in the same window: first trace = first spectrum (J(H, H) = 3 Hz) and second trace = the second spectrum (J(H, H) = 10 Hz). To observe any signal for the second trace use the **Options…** button in the button panel and set the **Factor** (of the **Second Trace**) to *1000* closing the window with the **Ok** button.

The results of *Check it 5.2.6.15* shows that when the homonuclear H, H coupling constant is set equal to the long-range ^{29}Si, ^{1}H coupling constant the signal intensity in the ^{29}Si is considerably diminished. The reason for this reduction in signal intensity is that the H, H coupling and chemical shift evolution is not refocused by the INEPT unit. The overall evolution of the coherences in the x,y-plane is such that the antiphase coherence is aligned along the direction of the subsequent 180° ^{1}H and ^{29}Si pulses so that these pulses are either ineffective or rotate the coherence in the wrong sense. In addition the simulations have also impressively demonstrated that the proposal [5.64] to use the PENDANT sequence for multiplicity edited spectra based on long-range I, S coupling is not feasible if the magnitude of homonuclear coupling J(I, I) is comparable to the heteronuclear long-range coupling J(I, S).

In the style of the DEPT$^+$ and INEPT$^+$ sequence a ^{1}H purge pulse prior to the acquisition period is proposed as an advantage for coupled PENDANT ^{n}X spectra. The following *Check it 5.2.6.16* examines the advantages of the so-called PENDANT$^+$ sequence which has been developed to reduce the phase anomalies in coupled spectra.

Simulations

(a) spin systems (*ch3ch2ch.ham*):
individual CH$_n$ groups
with ^{1}J(C, H) = 140 Hz
(b) spin systems (*ch3ch2jv.ham*):
individual CH$_n$ groups
with ^{1}J(C, H) = 130, 140, 150 Hz
(c) spin systems (*ch3h2.ham*):
CH$_3$ groups
with ^{1}J(C, H) = 130, 140, 150 Hz
and additional H, H coupling to
two equivalent protons

Spin systems for studying the effect of a ^{1}H 90° purge pulse prior to data acquisition

5.2.6.16 Check it in NMR-SIM

Load the configuration file *ch52616.cfg*. Run the simulations for the PENDANT (*pend.seq*) and the PENDANT$^+$ sequence (*pendp.seq*) using the spin system file *ch3ch2ch.ham*. Save the data as **Exp No.**: *1* and *2* respectively. Process the FID (**Si(r+i)**: *32k*, wdw: **EM**, **LB**: *2.0* [Hz]), and phase correct the Fourier transformed spectra. Save the spectra. To investigate the influence on ^{13}C signals which have a value of ^{1}J(C, H) different from the nominal one used to calculate the d4 and d3 value load the spin system *ch3ch2jv.ham*. Repeat the simulations saving the data as **Exp No.**: *3* and *4*. Process and Fourier transform the FIDs and phase correct the calculated spectra similarly. Finally to study the influence of homonuclear coupling on the re-focusing period and the effect of the ^{1}H purge pulse load the spin system *ch3ch2.ham* and repeat the *pend.seq* and *pendp.seq* simulation saving the experiments as **Exp No.**: *5* (*pend.seq*) and *6* (*pendp.seq*). Use the **Dual Display** option of 1D WIN-NMR (**Display│Dual Display**) to compare the different simulations by loading the PENDANT$^+$ experiments (**Exp No.**: *2*, *4* and *6*) into the main spectrum window and selecting the corresponding PENDANT experiment (**Exp No.**: *1*, *3* and *5*) as the second trace. Compare the line intensities in the spectra by clicking the **Move Trace** button in the button panel and while holding down right mouse button move the mouse horizontally to shift the second spectrum.

The results for some very simple spin system units are shown in the following list. Whilst the changes between the PENDANT and PENDANT$^+$ pulse sequence are small, *Check it 5.2.6.16* once again illustrates another advantage of NMR-SIM compared to experimental measurement, the comparison is based upon changes in a single spin system parameter which cannot be achieved experimentally.

Varied spin system parameter	Effect on PENDANT$^+$ spectrum in comparison to the standard PENDANT experiment
Ideal coupling constant for each CH$_n$ group (J$_{nominal}$ = J$_{individual}$ = 140 Hz)	A minor improvement can be observed.
Different coupling constant for each CH$_n$ group (J$_{nominal}$ = 140 Hz, J$_{individual}$ = 130, 140, 150 Hz	No overall improvement can be observed, there may even be a small loss in signal intensity.

Different coupling constants for CH_3 ($J_{nominal} = 140$ Hz, $J_{individual} = 130, 140, 150$ Hz and homonuclear H, H coupling interaction	A small enhancement in signal intensity for the CH_3 group whose $^1J(C, H)$ coupling constant is different from the nominal $^1J(C, H)$ coupling constant.

Check it 5.2.6.16 also illustrates that the PENDANT$^+$ sequence should be used for coupled spectra of CH_n groups which exhibit homonuclear $^nJ(H, H)$ coupling. In contrast to the PENDANT$^+$ experiment, under these conditions the conventional PENDANT ^{13}C spectrum displays considerable lineshape distortion that cannot be corrected. These lineshape distortions can be traced back to underlying antiphase zero quantum coherences of the order I_zS_x or I_zS_y ($I = {^1H}$, $S = {^{13}C}$) which are transferred by the ^1H purge pulse of the improved sequence to undetectable multiple quantum coherences. Broadband ^1H decoupling during acquisition destroys this antiphase coherence such that only very minor differences are apparent when comparing the decoupled versions of the experiment.

5.2.7 Relaxation Time Measurement Experiments

The relaxation times of individual spins in the same compound may vary over a wide range. The underlying relaxation mechanism depends upon a number of different variables such as the molecular structure and symmetry, solvent viscosity and temperature. From the basic 1D ^1H spectrum to the calculation of the correct delay for use in the BIRD-d7 filter in a ^{13}C, ^1H HMQC or HMBC experiment (section 5.8.2) knowledge of even an approximate time constant is necessary for obtaining the optimum results. As shown in sections 5.2.1 and 5.2.6 knowledge of the relaxation time is required when calculating the ERNST angle for the optimized excitation pulse. Usually the longitudinal relaxation time is the most relevant, but the transverse relaxation time also plays a major role in the signal evolution during a pulse sequence and is responsible for introducing undesired artefacts or an overall loss in signal intensity.

The early investigations of BLOCH [5.80, 5.81] established two directly detectable macroscopic relaxation processes which where not related to any explicit molecular mechanism. BLOCH assumed that longitudinal and transverse relaxation could be treated as a first-order process with the time constants T_1 and T_2 respectively. Both relaxation processes relate to the decay of the magnetization either along or perpendicular to the external magnetic field. In NMR-SIM longitudinal relaxation is implemented using the BLOCH approach. Selecting the *Acquisition* relaxation option in the NMR-SIM options dialog box, the transverse relaxation time T_2 is used to simulate natural lineshapes (linewidth at half-height = $(1/\pi \cdot T_2)$. Alternatively if the *Full Relaxation* option is enabled the transverse relaxation is considered as an independent process during evolution of transverse coherence during free precession.

Sequence features:

Purpose / principles:	A pseudo 2D experiment to measure the longitudinal (T_1) or transverse (T_2) relaxation time constant
Variants:	Inversion recovery method [5.82], CARR-PURCELL-MEIBOOM-GILL experiment [5.83]

A comprehensive discussion of relaxation time measurement experiments are given in [5.84], in the following *Check its* only the inversion recovery method and the CARR-PURCELL-MEIBOOM-GILL experiment are considered. As shown in section 5.2.1 the pulse length in a one-pulse experiment can be optimized for the relaxation times of the observed nuclei. However even if the maximum signal intensity is not the main goal the NMR spectroscopist must keep in mind that if the relaxation delay is too short, the signals will not integrate correctly.

5.2.7.1 Check it in NMR-SIM

Using the configuration file *ch5271.cfg* simulate the spectrum of four individual proton nuclei with different T_1 values. Process the FID (wdw: **EM**, **LB**: *3.0* [Hz]). Integrate the signals and compare the integration values as a function of the relaxation time.

Check it 5.2.7.2 demonstrates the experimental T_1 determination using the inversion recovery method as a pseudo 2D experiment and the separation of the resulting serial file into the corresponding 1D files.

5.2.7.2 Check it in NMR-SIM

To simulate the experimental T_1 data for the four protons defined in the spin system file *ch527.ham* recorded as a pseudo 2D experiment, load the configuration file *ch5272.cfg*. Run the simulation saving the file as **USER**: ch527, **Name**: *1* and **Exp No.**: *1*. In 1D WIN-NMR and use the **File│Filecopy & Convert** command to separate the serial file *…\ch527\001001.ser* into eight separate FIDs. Open the **Serial Processing** dialog box (**File│Serial Processing**) and select the split FIDs in the scroll windows. Using the job *relax.job* in the *…NMRSIM-Session\jobs* directory (**Select common job**) execute the automatic serial processing of all files by clicking on the **Execute** button. Use the **Display|Multiple Display** mode and inspect the spectra in the 3D representation for zero-intensity signals.

ph1(ph2)=
$(0)_2(2)_2(1)_2(3)_2$
ph2(ph1)=(0 2)$_4$
ph31=$(0)_2(2)_2(1)_2(3)_2$

p1(p2): 90° pulse (f1)
p2(p1): 180° pulse (f1)
d1: relaxation delay,
d2: incremented delay
  (pseudo f1 dimension)
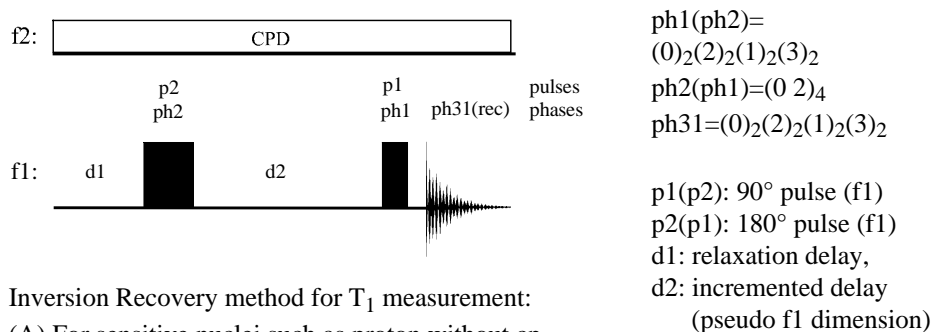
Inversion Recovery method for T_1 measurement:
(A) For sensitive nuclei such as proton without cp
decoupling on the F2 channel; (B) For heteronuclei with
cp decoupling on the F2 channel.

The T_1 value of an individual signal can be estimated from the spectrum using the delay d2 corresponding to zero-signal intensity: $d2 \approx T_1 \ln 2 = 0.693 \bullet T_1$. As an additional exercise use the configuration file *ch5272a.cfg* to simulate the individual FIDs of the pseudo 2D experiment using the **Go|Check Parameters & Go command**.

Since the present NMR-SIM version also consider transverse relaxation as a proper process, it is possible to simulate the common T_2 measurement experiment using the CARR-PURCELL-MEIBOOM-GILL sequence.

5.2.7.3 Check it in NMR-SIM

Load the file *ch5273.cfg*. Run five simulations using different loop values **l2**: *1, 2, 4, 8, 16* (**Go|Check Parameters & Go** command) saving the data with **Exp No**: *1* to *5*. Process the FID (no zero filling, wdw: **EM**, **LB**: *1.0* [Hz]). Inspect the spectra in the 3D representation of 1D WIN-NMR.

ph1=$(0)_2(2)_2(1)_2(3)_2$
ph2=$(1\ 3)_2(0\ 2)_2$
ph31=$(0)_2(2)_2(1)_2(3)_2$

p1(p1): 90° pulse (f1)
p2(p2): 180° pulse (f1)
d0: incremented delay
(pseudo f1 dimension)
d2: spin echo evolution delay
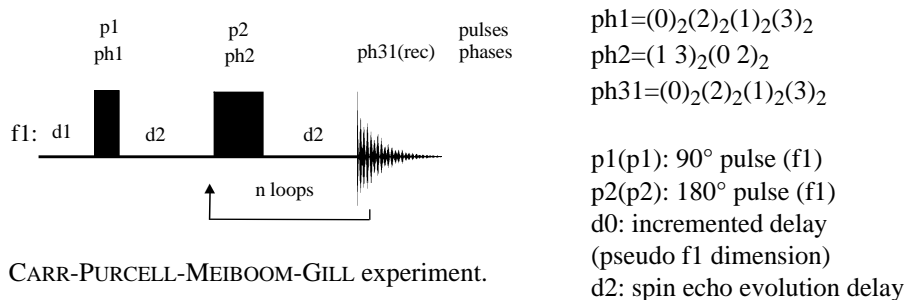
CARR-PURCELL-MEIBOOM-GILL experiment.

Strictly speaking the result of the T_2 measurements must be corrected for the longitudinal relaxation. Taking T_1 relaxation into account, the signal amplitude of an individual signal decreases in the series of repeated spin echos in the CARR-PURCELL-MEIBOOM-GILL pulse sequence because of the T_2 relaxation. Any field inhomogenity, chemical shift or coupling evolution effects being cancelled by the spin echos. The signal

intensity is proportional to the T_2 relaxation time $I \propto \exp(-t/T_2)$ and this information can be used to analyze a series of spectra and determine the value of T_2.

5.3   Building Blocks and Elements - Part One

Pulses are naturally the basic prerequisite of pulsed FT NMR spectroscopy. There are many categories of pulses varying from the hard or "ideal" pulse to selective and adiabatic pulses. In addition combinations of pulses such as composite pulses or the DANTE pulse train, are often discussed as a single "virtual pulse". NMR-SIM offers the possibility, based upon the classical BLOCH description, to study the magnetization evolution in the rotating coordinate system from using such pulses and to calculate the excitation profiles. In the remaining part of this section various aspects of pulses will be examined including the use of combinations of hard pulses to create composite pulses that minimize the imperfections of a single "ideal" hard pulse and the use of the DANTE sequence as an alternative to selective pulses. The spin echo [5.85, 5.83] is the simplest combination of pulses and delays and probably most widely applied pulse sequence unit. Finally in section 5.3.4 the importance of the spin echo for tailored coherence evolution is discussed.

5.3.1   Pulse Types and Pulse Properties

There is a large number of pulse sequences in the literature representing a vast combination of pulses and delays. Many of these pulse sequences often contain the same combination of pulses and delays such as a INEPT polarization transfer unit and so form a loosely related family of sequences. In addition pulse sequences are modified to achieve a specific selectivity or to overcome the imperfections of the ideal hard pulse. Basically pulses may be subdivided into non-selective or hard pulses and selective or shaped pulses. The ideal hard pulse provides a wide uniform excitation profile without any intrinsic intensity loss or signal phase distortion over a specified frequency range. Selective pulses however are applied to a specific frequency range; the frequency selectivity is a function of the pulse shape so that selective pulses are synonymous with shaped pulses. Hard pulses also have shape and are usually rectangular. Selective pulses can be categorized as follows according to the selectivity and whether the shape generation is by amplitude or phase modulation:

- frequency selective pulses
- band selective pulses
- phase or amplitude modulated shaped pulses
- adiabatic pulses

Binomial pulses, which are predominantly used in signal suppression sequences, such solvent signal suppression experiments will be discussed as a special category.

Hard and soft pulses

The basic pulse for excitation, inversion and rotation around any arbitrary axis of the rotating frame is the hard pulse. Hard pulses are of very high power and very short duration and are characterized by uniform excitation and pure phase excitation over a wide frequency range which is generally much larger than the chemical shift range for a particular nucleus. Real rectangular pulses have strong sidelobes aside the effective excitation range that can null or even invert a signal. These sidelobes are generally only relevant for heteronuclei such as ^{19}F, ^{31}P or ^{195}Pt that have a large chemical shift range.
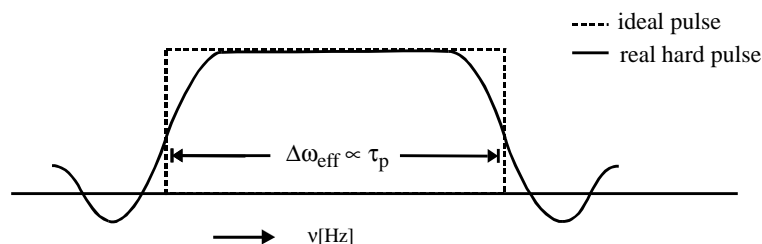
Fig. 5.20:   Schematic excitation range of a hard pulse.

Because the excitation range $\Delta\omega_{eff}$ is inversely proportional to the pulse length τ_p, if the pulse power of a hard pulse is reduced the pulse length increases and the effective excitation range decreases. Using this approach hard pulses can be converted into so-called soft pulses which where the first type of selective pulse. However this approach introduces significant excitation outside the effective excitation range and non-linear phase behaviour and consequently compares very unfavourable with the correctly shaped pulses that can be generated by modern a NMR spectrometer.

5.3.1.1 Check it in NMR-SIM

Load the file *ch5311.cfg*. Run three simulations using different pulse power **pl1** values of *10e5*, *1000* and *100* [Hz] (**Go|Check Parameters & Go** command) to represent the conversion from a hard to a soft pulse. Save the data as **Exp No**: *1* to *3*. Process the FIDs (no zero filling, wdw: **EM**, **LB**: *4.0* [Hz]). Examining the pulse profiles even a pulse of 1000 Hz whose pulse length is adapted to a 90° rotation for on-resonance magnetization excites a frequency range of 4000 Hz in a uniform way although there is a phase distortion of off-resonance magnetization because of chemical shift evolution. However a 100 Hz pulse, which corresponds to a pulse length of 2.5 ms with 90° on-resonance rotation, becomes selective with an excitation range of approximately 400 Hz.

Spin pinging [5.86] has been proposed as a method of using rectangular pulses in 2D homonuclear COSY experiments for tailored excitation. Using spin pinging it would be possible to select regions of overlapping multiplets which are not defined sufficiently in a standard 2D COSY spectrum because of the restricted number of data points. Probably

due to the extended phase cycling and the resulting increase in experiment time this ingenious approach is currently of only academic interest [5.7, 5.87]. The method is based on the combination of a hard excitation pulse and a selective 180° inversion pulse. The cancellation of the unwanted excited off-resonance signals is achieved by shifting the selective pulse phase and the receiver phase in 90° and 180° increments in subsequent experiments. *Check it 5.3.1.2* compares the excitation profile of the spin pinging sequence with a soft pulse derived from a hard pulse.

5.3.1.2 Check it in NMR-SIM

Load the configuration file *ch5312.cfg* to simulate the excitation profile of an ^{1}H spectrum with selective excitation of the on-resonance signal using the spin pinging sequence. Process the FID (no zero filling, wdw: **EM**, **LB**: *4.0* [Hz]). Replace the current pulse sequence with the pulse program *zgihc.seq* and change **p1**: *5m* and **pl1**: *100* [Hz]. Simulate the spectrum and compare the results.

Frequency selective Pulses

Selective pulses are widely used in many pulse sequences [5.88, 5.89], not just for solvent signal suppression. The transformation of an n dimensional experiment into a (n-x) dimensional experiment by the application of x selective pulses not only reduces experiment time but it also keeps the acquired data matrix to a minimum. The implementation of selective pulses can be easily incorporated into pulse sequence design but the choice of selective pulse and associated parameters depends upon the current problem under investigation. When implementing pulse sequences that use selective rf pulses the following aspects must be considered:

- Selective pulses which are amplitude and/or frequency modulated during their duration are not phase coherent with hard pulses using the same experimental setup. This phase difference arises because the shaped pulse and hard pulse are derived from different electronic sources. Consequently a phase correction factor must be determined and applied, this phase correction often depends on the experimental parameters.
- The pulse calibration procedure for a selective pulse is more difficult than for a hard pulse. In calibrating a particular flip angle the pulse length is kept constant while the pulse power is varied.
- If a selective pulse is applied to bring an on-resonance magnetization vector to a given final state it must be always considered that off-resonance magnetization vectors might be transferred to a different state.
- The pulse length of a selective pulse should be kept as short as possible to minimize relaxation loss. Nevertheless chemical shift and coupling evolution during the selective pulse must always be considered.
- The excitation profile of a selective pulse must be subdivided in different regions of effective excitation that depends upon the resonance offset and the pulse shape. The excitation region is described by the parameters in Table 5.16.

Table 5.16:   Descriptive parameters of selective pulses.

$\Delta w_e/\Delta w_t$ Ratio excitation versus transition range with Δw_e : width of excitation range and Δw_t : width of transition range
Excitation range: 95 - 100% intensity
Transition range: 5 - 95% intensity
Suppression range: 0 - 5% intensity

$\Delta \omega \bullet \Delta T$ Selectivity or bandwidth factor with $\Delta \omega$: frequency range for intensity > 70.8 % (3 dB point) and ΔT: pulse length

The application of pulse sequences using selective pulses is an interesting development in multi-pulse experiments. It is worthwhile to consider in a little more detail the GAUSSIAN pulse family which represent the "classic" selective pulse and how the members of this family have been adapted for particular applications.

The Gaussian pulse family
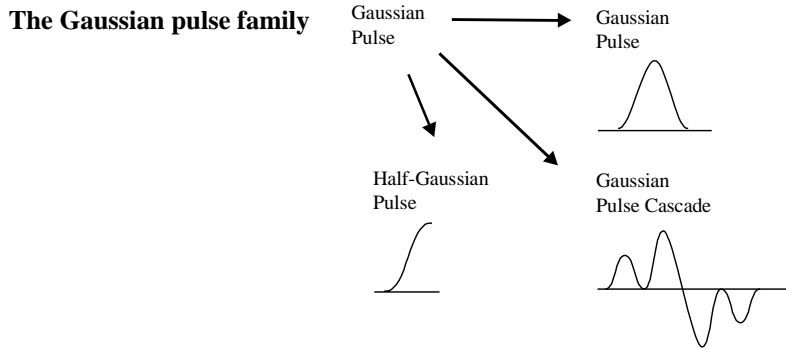
There are a two main problems associated with using low power rectangular pulses; unfavourable excitation profile that creates phase distortions across the excited frequency range and sidelobes of excitation adjacent to the main excitation region. The GAUSSIAN shaped pulse belongs to a series of pulse shapes, which try to overcome these problems. The application of a GAUSSIAN shape is based on the assumption that the frequency domain response of a GAUSSIAN pulse is simply another GAUSSIAN shape because at least for small flip angles, they are a Fourier pair [5.90]. The 90°GAUSSIAN excitation pulse is superior to the rectangular pulse having a higher selectivity, missing outer sidelobes and an approximately linear phase deviation across the excited frequency range. The disadvantage of a GAUSSIAN pulse is that there are two dominant sidelobes close to the main excitation range. If a 270° GAUSSIAN pulse is used instead of a 90° [5.91], the phase deviation across the excited frequency range is reduced since all the properties which increase the phase error in a 90° GAUSSIAN pulse serves to reduce the phase error in a 270° GAUSSIAN pulse. The Half-GAUSSIAN pulse does not exhibit the two flanking sidelobes of a full GAUSSIAN pulse [5.92] but is a compromise with an excellent excitation profile for the y-component after a 90° rotation from longitudinal

magnetization obtained at the expense of a much wider M_x profile. Finally the GAUSSIAN pulse cascades [5.93] have been developed for selective inversion and in-phase excitation and have nearly ideal offset dependence. *Check its 5.3.1.13* and *5.3.1.4* illustrate these improvements.

5.3.1.3 Check it in NMR-SIM

Use the Bloch simulator (**Utilities|Bloch module…**) to compare the behaviour of several magnetization vectors with offsets ranging from +10 to +80 Hz in 10 Hz steps which are rotated by a 90° and then a 270° GAUSSIAN pulse. Load the configuration file *ch5313.cfg* and use the **Calculate⎮Time evolution** command to display the magnetization vectors. Change the pulse power **sp0**: *15* Hz (90° pulse angle) to *45* Hz (270° pulse angle) and repeat the calculation. The spherical representation shows some interesting aspects:

As expected the on-resonance magnetization vector is rotated to the y-axis (90° pulse angle) and –y-axis (270°) as required. In addition the 270° pulse rotates the magnetization with an offset of 10 Hz by nearly the same amount as the on-resonance vector, the 90° pulse does not achieve this. Finally the 270° pulse rotates the magnetization vectors with an offset of +40, +50 and +60 Hz back almost to their initial position; again the 90° pulse does not achieve this.

For a different perspective simulate the 1D selective excitation ^{1}H spectra of dibromopropionic acid with a 90° and a 270° GAUSSIAN pulse on the proton resonance at 2.85 ppm. Start the simulations using the previously loaded configuration file changing the value of **sp0** to *15* Hz (90° pulse angle) and *45* Hz (270° pulse angle) and store the data with different **Exp No**. Process the FIDs (**Si(r+i)**: *64k*, wdw: **EM**, **LB**: *1.0* [Hz]). Apply a numerical zero-order phase correction of 270° (90° pulse angle) and 90° (270° pulse angle) before comparing the spectra.

The multiplet at 2.85 ppm has a severe phase distortion after excitation by a 90° pulse whereas the 270° pulse generates a multiplet signal of uniform phase.

In *Check it 5.3.1.4* the x- and y-profiles of the transverse magnetization for a 270° GAUSSIAN pulse [5.91], a 90° half-GAUSSIAN pulse [5.92] and a 90° GAUSSIAN Pulse Cascade G4 [5.93] are compared. Finally the ^{1}H spectra of dibromopropionic acid with selective excitation of the proton at 2.85 ppm is simulated for all three shaped pulses.

5.3.1.4 Check it in NMR-SIM

(a) Calculate the x- and y-profiles of the 270° GAUSSIAN pulse, 90° half-GAUSSIAN pulse and 90° GAUSSIAN Pulse Cascade G4 [5.93] with the same pulse length **p0** of *33* ms. Load the configuration file *ch5314a.cfg*. The profiles are calculated using the pulse sequence *exctspy.seq* (y-profile) and *exctspx.seq* (x-profile). In the **Go|Check Parameters & Go** dialog box set the pulse shape **spnam0** and pulse power **sp0**: *…\wave\gauss.shp* and *45*

Hz (270° GAUSSIAN pulse), *…\wave\halfg128.shp* and *17.5* Hz (90° Half-GAUSSIAN pulse), *…\wave\gcas128.shp* and *139* Hz (90° GAUSSIAN Pulse Cascade). Process the FIDs (**Si(r+i)**: *64k*, wdw: **EM**, **LB**: *1.0* [Hz]) and compare the profiles for the phase alternation from a positive to a negative offset frequency.

(b) Using the file *ch5314b.cfg* simulate the 1D selective excitation ^{1}H spectra for each of the GAUSSIAN pulses and inspect the multiplet at 2.85 ppm for phase errors and line intensities compared to the standard ^{1}H spectrum. Finally simulate the 1D selective excitation spectrum using a 200 ms 90° GAUSSIAN Pulse Cascade with a power level of **sp0**: *24* [Hz].

The results of *Check it 5.3.1.4* displays the superior quality of the GAUSSIAN pulse cascade for the 90° selective excitation of the multiplet at 2.85 ppm. Compared to the hard pulse spectrum the 270° GAUSSIAN and the half-GAUSSIAN spectra display both phase and line intensity distortions. From the simulated profile of the GAUSSIAN pulse cascade it is evident that the superior excitation profile is achieved at the expense of selectivity. To achieve the same selectivity as with a 270° GAUSSIAN pulse the pulse length must be increased. Even with a pulse length four times greater the GAUSSIAN pulse cascade has a comparable excitation range and possesses a superior performance provided that relaxation effects are neglected. Based on the results of *Check it 5.3.1.4* the GAUSSIAN pulse variants may be ordered: GAUSSIAN pulse cascade > 270° GAUSSIAN pulse > half-GAUSSIAN pulse > 90° GAUSSIAN pulse for decreasing performance.

A second point to consider is the use of GAUSSIAN shaped pulses as a 180° inversion pulse. *Check it 5.3.1.5* compares a 180° half-GAUSSIAN pulse with a 180° GAUSSIAN pulse to determine whether the half-GAUSSIAN pulse is superior in this context.

5.3.1.5 Check it in NMR-SIM

Compare the x-, y- and z-profiles of a 180° Gaussian and a 180° half GAUSSIAN pulse in the Bloch module (**Utilities**⏐**Bloch module...**). Load the configuration file *ch5315.cfg*. Determine the power required for a 100 ms GAUSSIAN and half GAUSSIAN pulse to invert the y-magnetization by using the **Calculate**⏐**RF field profile** option. (The 180° pulse power corresponds to the first point where the y-profile has a value of -1). Using these pulse powers calculate the excitation profiles for both shaped pulses with **N**: *40*, **Start**: *-50* and **Step**: *2.5* (**Calculate**⏐**Excitation profile**). Clicking the **x**, **y** or **z** buttons in the button panel, inspect the different profiles.

Obviously the half-GAUSSIAN pulse is better for 90° excitation but when used for a 180° inversion of y- to –y-magnetization there is a severe phase distortion over a wide offset frequency range as demonstrated by the $(x^2 + y^2)$-profile. Even the z-profile is characterized by a dominant amplitude modulation. In contrast the GAUSSIAN pulse shape has a very distinctive (x^2+y^2)-profile with the z-profile displaying limited amplitude modulation indicating that the common GAUSSIAN pulse is a better choice for generating a 180° inversion pulse. Table 5.17 lists a number of selective pulse shapes and it is left to the reader as an additional exercise to analyze these examples.

Table 5.17: Pulse shapes of frequency selective, band selective and adiabatic pulses.

Pulse name	Filename	Shape modulation
Frequency selective pulses		
GAUSSIAN pulse [5.90]	GAUSS129	am
Half-GAUSSIAN pulse [5.94]	HALFG128	am
GAUSSIAN pulse cascade [5.93.5.95]	GCAS128	am
Rectangular pulse [5.96]	RECT	am
TOPHAT pulse	TOPHAT128	am/pm
Hermite pulse [5.97]	HERM367	
Band selective pulses		
EBURP pulse [5.98]	E1BURP128	am/pm
REBURP pulse [5.98]	REBURP128	am/pm
IBURP pulse [5.98]	IBURP128	am/pm
Adiabatic pulses		
Chirp pulse [5.99]	chirp2	am/pm
Wurst pulse [5.100]	wurst	am/pm

Band-selective Pulses

Most selective pulses are designed to have a specific frequency range of excitation, which allows the rotation of a whole multiplet without perturbing the nearby signals from different nuclei. However the family of BURP pulses (*B*and-selective, *U*niform *R*esponse, *P*ure-phase) offers uniform and pure phase excitation over a specific bandwidth [5.98]. They can only be transformed into selective pulses with a narrow excitation band by considerable increasing the pulse length. The BURP pulse family can be subdivided into four categories based upon the magnetization rotation required.

Z-magnetization specific excitation or inversion

EBURP pulse   90° excitation pulse for magnetization transfer M_z to M_x or M_y

IBURP pulse   180° inversion pulse for magnetization transfer M_z to M_{-z}

General 90° or 180° rotation

UBURP pulse   Universal 90° rotation pulse such as M_y to M_{-z}

REBURP pulse   Universal 180° refocusing pulse such as M_y to M_{-y}

The excitation profile of the EBURP pulse has already been simulated in section 5.2.2 and the reader may check the profile in *Check it 5.2.2.2*. To achieve the desired excitation profile the number of data points used to digitize the pulse shape is critical [5.98]. In *Check it 5.3.1.6* this digitization problem is demonstrated by comparing the excitation profiles of four EBURP-1 pulses.

5.3.1.6 Check it in NMR-SIM

To calculate the excitation profiles of four EBURP-1 pulse shapes, each digitized with a different number of data points, load the configuration file *ch5316.cfg*. Open the Bloch module (**Utilities│Bloch module...**). Use the **Calculate│RF field profile** option to determine the power required for a 10 ms EBURP-1 pulse to rotate the z-magnetization by 90° for the following shapes: *ebp4.shp* (4 data points), *ebp16.shp* (16 data points), *ebp64.shp* (64 data points) and *ebp128.shp* (128 data points). Use these pulse powers to calculate and compare the excitation profiles of the four EBURP-1 pulse shapes over the frequency range +400 to -400 Hz (**Calculate│Setup** and **Calculate│Excitation profile**).

For studying organic macromolecules pulse sequences have been developed which permit the measurement of 2D experiments over a small region of the complete ^{1}H frequency range. This type of experiment increases the digital resolution in both dimensions without dramatically increasing the size of the data matrix. In the following *Check it 5.3.1.7* a partial 2D COSY experiment is simulated using EBURP and UBURP pulses which are particularly suitable for this type of experiment.

5.3.1.7 Check it in NMR-SIM

Load the configuration file *ch5317a.cfg*. Using the current pulse sequence as a template, create the pulse sequence shown below saving the file with the name *mycosysf.seq*. Use commands such as *(p11:sp3 ph2):f1* to implement the shaped pulses. Test the sequence with the spin system *1habcmx.ham*. The detected peak has an E.COSY pattern that enables the coupling constants to be determined. To simulate the complete ^{1}H COSY(mc) experiment for the *1Habcmx.ham* spin system, load the configuration file *ch5317b.cfg*.

Soft-COSY pulse sequence [5.101].

$ph1=(0)_4(1)_4(2)_4(3)_4$
$ph2=(0\ 1\ 2\ 3)$
$ph3=(0\ 1\ 2\ 3)$
$ph31=(0\ 2)_2(3\ 1)_2(2\ 0)_2(1\ 3)_2$

p10(p1): on-resonance selective 90°
EBURP pulse (f1)
p11(p2): 90° on-resonance
selective 90° UBURP pulse (f1)
p12(p3): on-resonance 90°
UBURP pulse (f2)
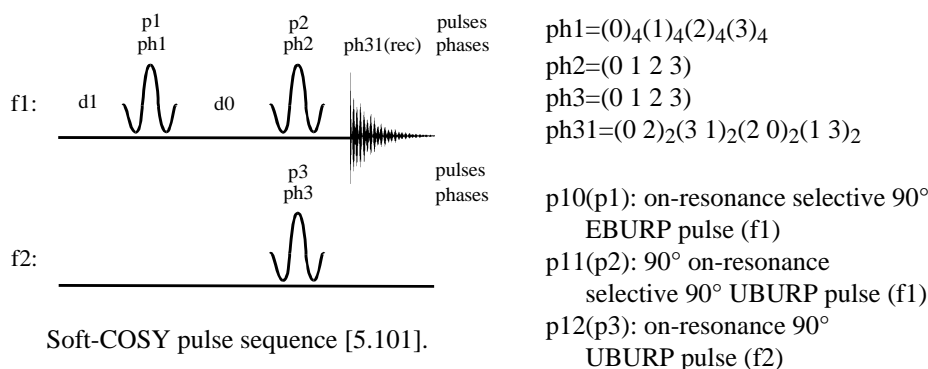
Adiabatic Pulses

Selective adiabatic pulses have the following characteristics: they are less sensitive to rf field inhomogeneity and frequency offsets and they dissipate the same or in favourable cases less thermal energy into the sample than conventional pulses. Currently the main application for selective adiabatic pulses is MRI (*M*agnetic *R*esonance *I*maging) [5.102, 5.103] and adiabatic pulse decoupling [5.104, 5.102, 5.105]. In MRI the sensitivity to rf field inhomogeneity is a major problem for surface coils used in *in vivo* NMR. The adiabatic pulse decoupling sequences are superior to common cpd sequences because of the lower energy dissipation in the sample. Moreover the wide uniform inversion profile guarantees an equal decoupling effect over a large frequency range and is particularly suited to modern high field spectrometers with frequencies in excess of 600 MHz.

Adiabatic pulses are generated by amplitude and/or frequency (or equivalent phase) modulation. For a short overview of the different shaping procedures the reader is referred to reference [5.104]. The rf amplitude $B_1(t)$ and frequency modulation $\Delta\omega(t)$ are the most relevant parameters of all selective pulses. Moreover the **adiabatic condition** must hold during the whole pulse duration. For an adiabatic pulse applied to the magnetization M the adiabatic condition occurs if the amplitude and frequency modulation are such that the effective field B_{eff} varies slowly enough for the magnetization vector M to follow the orientation of B_{eff} [5.106]. The effective field B_{eff} is the vector sum of the rf amplitude and rf offset. In mathematical terms the adiabatic condition can be described in terms of the velocity of the B_{eff} or by the adiabaticity factor Q where Q >> 1. For a detailed discussion the reader is referred to references [5.102, 5.107].

The adiabatic condition:

$$|(d\theta/dt)| << \omega_{eff}$$ $\omega_{eff} = \gamma \bullet B_{eff}$ and is the effective field expressed in angular frequency units

$(d\theta/dt) =$ velocity of B_{eff} inclined at an angle θ to an

$$Q > \omega_{eff} / |(d\theta/dt)|$$ arbitrary chosen coordinate axis i.e. x

Q = adiabaticity factor

Adiabatic pulses differ from other selective shaped pulses by one characteristic to permit 90° excitation by adiabatic half-passage (AHP) or 180° inversion by adiabatic full passage (AFP). In addition a pulse sequence cannot be converted into a selective experiment simply by replacing a hard pulse with an adiabatic pulse. The effect of a hard pulse on the M_x and M_y magnetization depends upon the pulse phase so that a $90°_x$ pulse will rotate M_y to M_z keeping M_x unchanged. However an adiabatic pulse will effect both the M_x and M_y magnetization because the frequency shift that occurs during the pulse duration will not keep the so-called rotation axis constant and both M_x and M_y will be tilted by differents angle simultaneously. Consequently an adiabatic pulse can not be

used to rotate a one single transverse components the M_x or M_y into M_z, M_{-z} or M_{-x} without changing the other transverse component.

In the next *Check it* the use of the NMR-SIM Bloch module to analyze the adiabatic condition for a 180° full passage CHIRP pulse is demonstrated.

5.3.1.8 Check it in NMR-SIM

Load the file *ch5318.cfg*. Open the Bloch module (**Utilities|Bloch module**) and determine the necessary pulse power for a 50 ms CHIRP pulse **p0**: *50* ms, **N**: *300*, **Start**: *0*, **Step**: *5* and **Offset**: *0* (**Calculate|RF profile**). Clicking the **x**, **y** and **z** buttons in the button panel, determine the point where the x and y intensity is 0 and the z-profile is -1. Use the waveform analysis tool to inspect the pulse shape **p0**: *50m*, **sp0**: *210* Hz and **Offset**: *0* (**Calculate⎪Waveform analysis**) and then calculate the excitation profile for **N**: *61*, **Start**: *-1500* and **Step**: *50* (**Calculate⎪Excitation profile**). Repeat the calculation for a pulse power of 160 Hz and compare the results.

The results of the waveform analysis show that for a pulse power of 210 Hz "theta B1" and "theta M" obey the same functional relation during the pulse duration, the characteristic of a well-behaved adiabatic pulse. The excitation profile reveals for the x- and y-components intense flanks at +/- 1000 Hz either side of zero while the z profile has a value of -1 over a range of +/- 750 Hz either side of zero. With a pulse power of 160 Hz the excitation profile changes very little, the intensity of the flanks for the x- and y-components is reduced while the z-component is virtually unchanged. However the wave form analysis shows a deviation between "theta B1" and "theta M" for the latter period of the pulse duration. "Theta M" corresponds to an oscillating function which describes an envelope of "theta B1" indicating that at this pulse power the 50 ms CHIRP pulse does not fulfil the requirements of a good adiabatic pulse.

Binomial pulses

Binomial pulses are another interesting category of pulses [5.108, 5.109, 5.110] although strictly speaking a binomial pulse is a short pulse train rather than a single individual pulse. The excitation profile of such a series of pulses is closely approximated by the Fourier transformation of the pulse sequence. For a pulse train with a delay τ between preceding pulses, Fourier transformation results in a cosine like excitation profile. The effective flip angle of the series is simply the sum of the flip angles of the individual components. There are zero excitation regions at $1 / (2 \bullet \tau)$ relative to the transmitter frequency. The zero regions can be shifted to give a null point at the transmitter frequency by phase inversion of alternate pulses. Furthermore as the number of pulses increases the zero excitation regions becomes flatter. In mathematical terms a sequence of n pulses each with a pulse length τ derived from the coeffients of the binomial series generates an excitation profile of the analytical form $\cos^n\Theta$. Accordingly an endless series of binomial pulses of the form 11, 121, 1331 or 14641 is conceivable. The notation used to describe the binomial pulse relates to the relative pulse length ratio of the individual pulses in a train. So a 90° binomial pulse $22.5° – \tau– 45° – \tau – 22.5°$ would be represented by the notation 121. A π phase shift is indicated by the overbar symbol as in $1\overline{1}$. The development of binomial pulses has been driven by the search for selective solvent signal suppression, particularly for the suppression of water in biological samples. For such samples the transmitter frequency is set on-resonance with the water signal and a binomial pulse is used to excite all frequencies except the resonance frequency of water.

In *Check it 5.3.1.9* the excitation profile of the $1\overline{1}$ pulse sequence is simulated with and without the π phase shift of the second pulse. The π phase shift of the second pulse changes the excitation profile from a cosine to a sine function.

```
; filename  : ...
; referred to: ..
1 ze
2 d1
   (p1 ph1):f1
   d2
   (p1 ph2):f1
   go=2 ph31
   ihc
   lo to 2 times l1
  wr #0
exit

ph1=0
ph2=0
ph31=0
```

5.3.1.9 Check it in NMR-SIM

Load the configuration file *ch5319.cfg*. Open the pulse sequence template and add the lines shown on the left to create the $1\overline{1}$ pulse sequence. Save the pulse sequence with the name *mybinpul.seq*. Note the use of the increment command **ihc** to calculate the excitation profile using a spin system file with a **var** chemical shift. Run two simulation: the first with the original phase program and a second with **ph2=2**. Process the FIDs (no zero filling, wdw: **EM**, **LB**: *4.0* [Hz]). After phase correction compare the spectra for the over all phase alternation and the position of the zero-intensity region.

An interesting question is which binomial pulse sequence gives the most uniform excitation over a wide frequency range combined with a well defined notch with zero excitation. This question is not purely of academic interest as such as sequence would be extremely useful for biological sample where the water resonance is characterized by a broad signal. The zero excitation region around the null point of the overall sine or cosine modulated excitation profile depends upon the binomial pulse sequence. In *Check it 5.3.1.10* the profiles of the 121, 1331 and 14641 pulse sequences are simulated. A comparison of the profiles indicate why symmetric binomial pulses and pulses of less than five pulse components, in particular the 1331 sequence, are preferred experimentally. Symmetric binomial pulses are less critical of the pulse length having a degree of internal error compensation such that the pulse lengths do not have to obey exactly the coefficients of the binomial series [5.111].

5.3.1.10 Check it in NMR-SIM

Modify the pulse sequence in the *Check it 5.3.1.9* for the schemes shown below saving each modified sequence with a suitable new name e.g. *bnp121.seq*. Calculate the excitation profile for all three sequences and process the FIDs (no zero filling, wdw: **EM**, **LB**: *2.0* [Hz]). Use the Multiple Display option to compare the magnitude calculated profiles (**Process│Magnitude Calculation**) as a function of pulse train length.

$1\bar{2}1$ sequence

ph1=0
ph2=2
0.25*p1(p1): 22,5° pulse (f1)
0.5*p1(p2): 45° pulse(f1)

$1\bar{3}3\bar{1}$ sequence

ph1=0
ph2=2
0.125*p1(p1): 11.25° pulse (f1)
0.375*p1(p2): 33.75° pulse(f1)

$1\bar{4}6\bar{4}1$ sequence

ph1=0
ph2=2
0.0625*p1(p1): 5.625° pulse (f1)
0.25*p1(p2): 22.5° pulse(f1)
0.375*p1(p3): 33.75° pulse(f1)
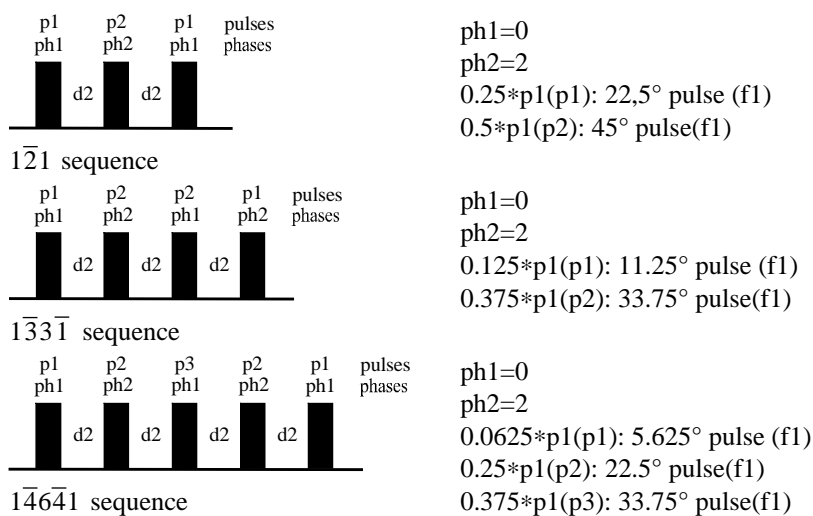
A considerable disadvantage of the binomial pulse is the linear phase change that occurs over the frequency range centred either side of the excitation null. In an ideal situation it should be possible to correct this phase change with a large first order phase correction but if the excitation band is extended by a longer sequence this is no longer possible [5.112]. In an attempt to overcome this phase problem the NERO sequence (*N*onlinear *E*xcitation with *R*ejection *O*n-resonance) has been developed [5.113, 5.114].

In contrast to the original binomial pulses the delays between adjacent pulses vary and the pulse lengths are no longer related to the coefficients of the binomial series. As shown in *Check it 5.3.1.11* the delays are related to the excitation range $\Delta\omega$ which relates to the frequency difference between the solvent signal which is to be suppressed and the centre of the excitation band. As also shown in *Check it 5.3.1.11* the excitation bands are symmetrical about the solvent signal.

5.3.1.11 Check it in NMR-SIM

Load the configuration file *ch53111.cfg*. Open the pulse program editor (**Edit│Pulse program**) and change the template sequence into the NERO sequence shown below. Make sure to add the incrementation and loop commands to simulate the excitation profile using a proton with a variable chemical shift. Run two simulations using a value for $\Delta\omega$ of 250 Hz and 1000 Hz to calculate *d2*, *d3* and *d4*.

NERO-1 pulse sequence [5.113].

ph1=0
ph2=2
ph31(rec)=0
p1(p1): 120° pulse (f1)
p2(p2): 115° pulse (f1)
d1: relaxation delay
d2: = 0.139 / ($\Delta\omega*2\pi$)
d3: = 0.625 / ($\Delta\omega*2\pi$)
d4: = 0.428 / ($\Delta\omega*2\pi$)
d5: = 0.222 / ($\Delta\omega*2\pi$)
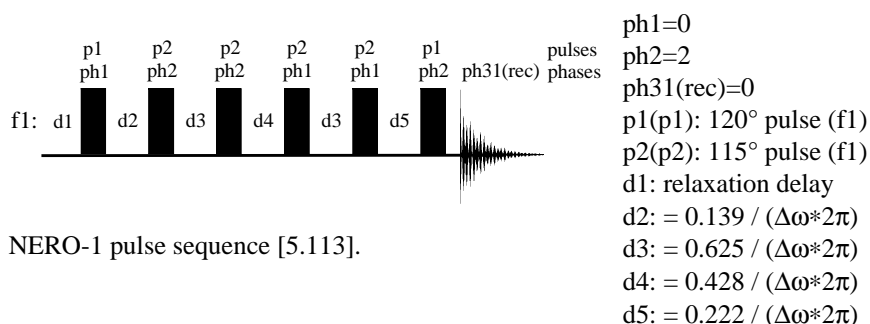
5.3.2   Composite Pulses

Although hard pulses are often thought as being ideal for wideband and homogenous excitation, even these "prefect" pulses are limited in their application. Apparent pulse imperfections introduce reduced signal intensity, phase errors and artefacts to the processed spectrum. The underlying reasons may be rf field inhomogenity in the macroscopic sample and the limited excitation or inversion range of a pulse; effects which are often summarized as off-resonance effects.

Composite pulses [5.115, 5.116] have been developed as a way of reducing these problems by using a short series of closely spaced high power pulses instead of a single pulse. The interval between pulses is kept as short as possible to minimize relaxation and free precession evolution although in certain sequences this precession forms part of the compensation procedure. A common feature of composite pulses is that they have the same nominal flip angle as the single pulse they replaced but are more tolerant to field inhomogeneity and off-resonance effects.

Several composite pulse schemes as substitutes for 90° and 180° high power pulses have been proposed and in a similar manner to selective pulses, there is no composite pulse scheme that can not be used for any purpose. Table 5.18 categorizes composite

pulses according to the nominal pulse angle, properties of the composite pulse and the type of pulse imperfection that must be minimized. Category A pulses can be used as an ideal pulse without any restriction. On the other hand the state of the magnetization before and after the pulse and the pulse imperfections which still arise despite the composite pulse determines the application for a category B pulse.

Table 5.18: (a) Composite Pulse Classification
(b) Examples of simple Composite Pulses [5.116, 5.115].

Class	Description
A	These composite pulses act as an ideal pulse independent of the initial spin system state.
B	The pulses in this category do not nutate the magnetization in the same way as a perfect pulse. These pulses might cause an overall phase shift due to pulse imperfections. Some pulses in this category provide an improvement for only one particular initial magnetization state such as longitudinal or transverse magnetization.

Imperfection	Nominal pulse angle	Category A	Category B
a	90°		$90_{300}180_{60}$, $90_{0}90_{90}$
	180°	$180_{0}180_{120}180_{0}$	
b	90°	$10_{2}100_{0}$	$385_{0}320_{180}25_{0}$
	180°		$90_{0}180_{180}270_{0}$
c	90°	$360_{0}270_{180}90_{90}$	
	180°		$90_{90}180_{0}90_{90}$

a = rf field compensation, b = resonance offset compensation, c = simultaneous rf field and resonance offset compensation, [1] Further composite pulses are given in reference [5.116].

The most common application for composite pulses is the substitution of 180° heteronuclear pulses, which are very sensitive to off-resonance effects and rf field inhomogenity, as the element of cpd and pulsed spinlock sequences. In *Check its 5.3.2.1* and *5.3.2.2* the advantages of a 90° composite pulses are illustrated using the Parameter Optimizer routine and Bloch Simulator module. The use of the Bloch simulator to study a composite 180° pulse, the $90°_x180°_y90°_x$ sequence, has been discussed in section 4.3.4

In *Check it 5.3.2.1* the influence of rf field inhomogenity on the excitation profile is simulated. The field inhomogenity in a macroscopic experimental sample means that to achieve the same 90° rotation the pulse length is dependent upon the position of the spins in the sample. Consequently a 90° pulse will not rotate all the spins in the sample from longitudinal magnetization to transverse magnetization and there will be a residual z-magnetization. However some experiments, such as accurate T_2 measurements experiment, require nearly zero z-magnetization after a 90° pulse. In these situation a

composite pulse $90°_x90°_y$ with a nominal 90° flip angle has been proposed to reduce residual z-magnetization. In *Check it 5.3.2.1* the field inhomogeneity of this type of composite pulse is simulated using the Parameter Optimizer routine as the nominal flip angle is incremented.

5.3.2.1 Check it in NMR-SIM

(a) Load the configuration file *ch5321a.cfg*. Calculate the excitation profile of the high power 90° pulse using the **Go│Optimize parameter** command. Select **Show results as** *1D*, **N**: *25*, **p1** for optimization, the start value **p1**: *0.01u* and increment size **inp0**: *0.02u*. To calculate the excitation profile of the $90°_x90°_y$ composite pulse, replace the current pulse program by the program *zgcp1.seq*. Compare the processed FIDs (no zero filling, wdw: **EM**, **LB**: *2.0* [Hz]). The composite pulse introduces a strong phase deviation that masks any obvious advantages.

(b) The advantage of the $90°_x90°_y$ composite pulse compared to the high power 90° pulse is the smaller residual z-magnetization when the longitudinal magnetization is transferred into transverse magnetization by a non-optimum excitation pulse. Using the simple pulse sequence shown below the z-profile can be calculated using the parameter optimizer routine. To calculate the z-profiles load the configuration file *ch5321b.cfg*. Proceed as in part a replacing the current pulse program with the sequence *zgcp3.seq*. The processed z-profiles show two effects. The residual z-magnetization is smaller for a wide range of incorrectly set 90° pulses if the 90° composite pulse is used. And in addition there is no phase change in the z-profile of the composite pulse experiences as the pulse length changes from being less to greater than the optimum pulse length.

p1   p2   pulses
ph1   ph2   ph31(rec) phases

f1:   d1

p1: represents the 90° pulse or 90° composite pulse whose z-profile is detected
p3(p2): 90° pulse
d1: relaxation delay

ph1=0
ph2=1 3
ph31=1 3

Pulse sequence to measure the profile of the residual z-magnetization.
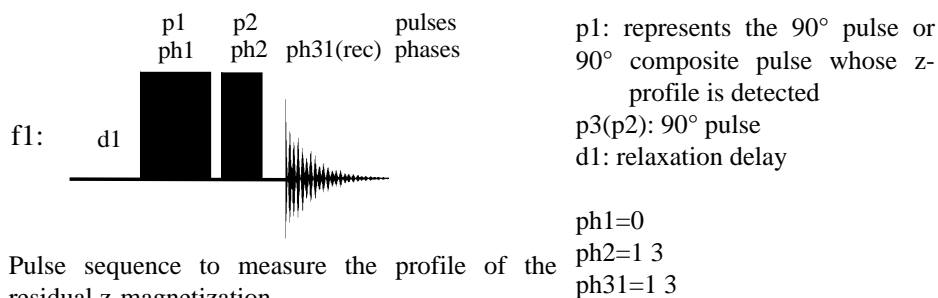
Off-resonance effects which contribute to frequency dependent phase distortion can be minimized using a 90° composite pulse $10°_x60°_{-x}140°_x$. Thus if an excitation pulse with phase x is applied to several longitudinal magnetization vectors, each with a different rf offset, the signals detected along the y-axis will have different phase distortions. In the first part of *Check it 5.3.2.2* the generation of phase deviation by off-resonance effects and the compensation using a composite pulse is shown using the Bloch module. The final position of the magnetization vectors with the composite pulse

are nearly at the same position resulting in this compensation being called "spin knotting" [5.115]. The second part of *Check it 5.3.2.2* displays the results as a series of spectra. The composite pulse used in this *Check it* is an example that utilizes the free precession evolution that occurs during the delays between two pulses for compensation.

5.3.2.2 Check it in NMR-SIM

(a) Bloch Module
Load the configuration file *ch5322a.cfg* and calculate the time evolution profile of a one pulse experiment for several magnetization vectors with offsets in the range of +8000 to -8000 Hz (**Calculate|Time evolution**). To compare the spherical representation with the profile of the 90° composite pulse $10°_x/60°_{-x}/140°_x$ replace the sequence fragment with the segment *C:\NMRSIM_SESSION\pp\ppfrag\cp1614.seq* (**Calculate ⎮ Setup...**).

(b) Frequency Spectrum
For a different insight into the off-resonance effect calculate the ^{13}C spectra for a common one-pulse experiment and a 90° composite pulse experiment using the configuration file *ch5322b.cfg* and the pulse program files *zg.seq* and *zgcp1614.seq*. Compare the processed FIDs (no zero filling, wdw: **EM**, **LB**: *2.0* [Hz]) for the offset related phase deviations. The non-perfect pulse creates a mixed state of transverse components for the off-resonance magnetization that results in phase distorted for these signals. The composite pulse creates primarily one transverse component which is independent of the offset and which only has a minor out of phase component. Thus the phase corrected spectra reveals the advantage of using the 90° composite pulse to excite magnetization components with a large offset.

5.3.3   DANTE pulses - a different way for selective excitation

A series of m equal hard pulses with a small flip angle $\alpha << \pi/2$ and a constant delay τ between the pulses is known as the DANTE sequence (**D**elay **A**lternating **N**utation **T**ailored **E**xcitation) [5.117, 5.118]. The DANTE sequence provides the possibility of selective excitation using hard pulses. In addition to the on-resonance excitation, the excitation profile of such a pulse train is characterized by excitation sidebands at N/τ [Hz], where N is an integer. A further feature of the DANTE sequence is that each excitation range resembles the profile of a soft pulse although noticeable sidelobes are evident. The selectivity of the pulse train can be improved by increasing the number *m* of pulses for a fixed total flip angle m • α. The superposition of several regular pulse trains with different periods τ can be used to excite more than one specific frequency range [5.117, 5.98], and is applied in the DOUBLE-DANTE sequence [5.119].

Besides the main excitation sidebands, a disadvantage of the DANTE sequence is an overall sinc oscillation of the excitation range. To increase the selectivity and the

uniformity of the excitation profile the width, phase and amplitude of the rf pulses can be modified and there are several variants of the basic DANTE sequence. Placing a "half" pulse or a "half" delay before and after the pulse train a more accurate π/2 DANTE pulse can be generated. Shaped DANTE pulse trains achieve comparable excitation with GAUSSIAN or half-GAUSSIAN pulses. The shaped DANTE sequence is obtained by modulation of the pulse lengths and delays whilst keeping the total duration of the pulse train constant.

In *Check it 5.3.3.1* first the original DANTE sequence and the corresponding x-, y- and z-excitation profiles are simulated to show how the improved DANTE-Z sequence [5.120] was developed.

5.3.3.1 Check it in NMR-SIM

(a) Using the configuration file *ch5331a.cfg* simulate the ^{1}H spectrum of the spin system file *dante.ham* which consists of seven individual protons with a chemical shift from 1 ppm to 7 ppm in 1 ppm steps. Due to the selective excitation only the on-resonance signal at 4.0 ppm gives rise to a signal in the processed FID. This signal has an extremely large phase distortion.

(b) To calculate the excitation profiles aligned along the x- and y-axis and residual z-component load the configuration file *ch5331b.cfg*. Run three simulations using the pulse programs *dante_x.seq*, *dante_y.seq* and *dante_z.seq*. A comparison of the different profiles reveals that the z-profile actually would provide a better selective excitation profile of uniform phase.

The improved DANTE-Z sequence only differs from the original sequence by an additional pulse whose phase is cycled by a π phase shift and a final 90° pulse to transfer the z-magnetization to detectable transverse magnetization. In *Check it 5.3.3.2* the modification to the phase cycling in the original DANTE sequence is examined and the results of selective excitation using the DANTE1-1 and DANTE363 sequence compared.

5.3.3.2 Check it in NMR-SIM

$(p10_x - d10 - p10_x)_n$

dantez1 sequence

$(p10_x - d10 - p10_{-x})_n$

dantez2 sequence

Load the file *ch5332a.cfg*. Calculate two FIDs for the *danteprf.ham* spin system file using the *dantez1.seq* and *dantez2.seq* pulse sequence. Process the FIDs (zero filling **SI(r+i)**: *64k*, wdw: **EM**, **LB**: *1.0* [Hz]) and obtain the difference spectrum using the **Process│File Algebra** command. Using the configuration file *ch5332b.cfg* compare the selective excitation of the nucleus at 4.0 ppm using the DANTE1-1: *dante11.seq* and DANTE363: *dante363.seq* sequences.

From the results of *Check it 5.3.3.2* in the *dantez1.seq* there is a 180° phase shift between the selected magnetization and the sidebands. A simple phase change for the second p10 pulse in the dantez2.seq results in a normal spectrum similar to that obtained

with a hard pulse. A DANTE sequence that uses a combination of phase programs used in these sequences would provide high frequency selectivity and pure phase over the excitation range. The profile for this sequence no longer has the characteristic sawtooth profile of the standard DANTE sequence. The weak sidebands in the second part of *Check it 5.3.3.2* illustrates the high selectivity of the DANTE363 sequence.

As a final example *Check it 5.3.3.3* simulates the 1D selective COSY experiment using the DANTE-Z sequence [5.120, 5.121].

5.3.3.3 Check it in NMR-SIM

Simulate the 1D selective COSY spectrum of glucose using the configuration file *ch5333.cfg*. The experiment uses a DANTE-Z element for the selective excitation of the proton at 3.9 ppm. Note: depending upon the computer speed this simulation may take several minutes.
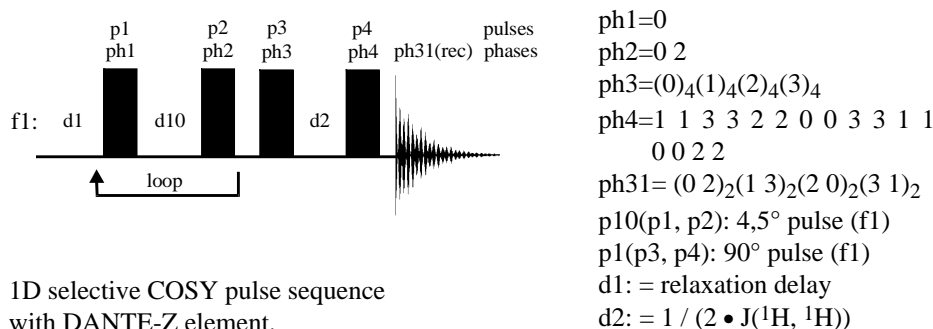
1D selective COSY pulse sequence with DANTE-Z element.

$ph1=0$
$ph2=0\ 2$
$ph3=(0)_4(1)_4(2)_4(3)_4$
$ph4=1\ 1\ 3\ 3\ 2\ 2\ 0\ 0\ 3\ 3\ 1\ 1$
$0\ 0\ 2\ 2$
$ph31=(0\ 2)_2(1\ 3)_2(2\ 0)_2(3\ 1)_2$
$p10(p1, p2)$: 4,5° pulse (f1)
$p1(p3, p4)$: 90° pulse (f1)
d1: = relaxation delay
$d2: = 1 / (2 \bullet J(^1H, {}^1H))$

5.3.4 Spin Echo - the first step to sequences

Spin echos are extremely common in pulse sequences although they may not always be obvious. In contrast to early discussions [5.85] nowadays a spin echo is a sequence of two delays with a 180° pulse between them. Spin echos are a universal tool that takes advantage of free precession evolution during the two delay periods. In combination with a 180° pulse chemical shift evolution is refocused whereas coupling evolution and transverse relaxation are not. The most obvious advantage of a spin echo is to reduce rf field inhomogenity effects for a macroscopic sample. However by varying the free precession periods it is possible to generate specific coherence states such as antiphase magnetization for homonuclear or heteronuclear spin systems which are subject to modulation by the chemical shift evolution.

5.3.4.1 Check it in NMR-SIM

(a) Load the configuration file *ch5341a.cfg* and start the parameter optimizer using the current parameters (**Go│Optimize parameter)**. Ensure that **d2** is selected for optimization Process the FID (no zero filling, wdw: **EM**, **LB**: *2.0* [Hz]). Inspect the "profile" for the antiphase state of the ^{1}H AX-

spin system which is characterized by a 90° phase shift of the multiplet relative to the in-phase state for the calculation with d2 = 0s.

(b) Simulate the heteronuclear spin echo d2 - [180°(^{1}H); 180°(^{n}X)] - d2 using the file *ch5431b.cfg*. The spin system is composed of a $^{12}C^1$H and $^{13}C^1$H group. The 180° phase difference between the ^{1}H signals of the two groups forms the basis of the BIRD-d7 filter element (see section 5.8.1).

5.4 Homonuclear Correlation Experiments

Homonuclear correlation experiments are not just restricted to the standard COSY experiment, but also include the TOCSY and INADEQUATE experiments. The separation of TOCSY and INADEQUATE from the homonuclear COSY experiment is based on the different coherence evolution and transfer processes involved. Thus the TOCSY experiment is based on cross-polarization in contrast to the polarization transfer used in the homonuclear COSY experiments. INADEQUATE experiments are characterized by the double quantum state of two scalar-coupled nuclei during the t1 period such that the second dimension (f1) is scaled into a double quantum frequency. Nevertheless these experiments can all be considered together because they are based on homonuclear scalar coupling and the f1 and f2 dimension of the corresponding 2D spectra are related to the same nucleus.

Table 5.19:   Types of homonuclear correlation experiments.

Homonuclear COSY experiments	Homonuclear polarization transfer and coherence detection which evolve due to the chemical shift of one nucleus in the t1 period
TOCSY experiments	Cross polarization and coherence detection which evolve due to the chemical shift of one nucleus in the t1 period
INADEQUATE experiments	Polarization transfer and detection of coherences which evolve due to the chemical shift of two coupled nuclei in the t1 period (double quantum frequency in f1)

In contrast to homonuclear COSY experiments in 2D heteronuclear correlation experiments the two frequency dimensions are assigned to different nuclei. The term COSY is often used to imply homonuclear correlation and in particular ^{1}H, ^{1}H correlation. Consequently heteronuclear correlation experiments either have a specific name related to the processes involved such as ^{13}C, ^{1}H HMQC or simply have the words "COSY experiment" appended to the detected nuclei as in ^{1}H, ^{13}C COSY experiment.

5.4.1   Homonuclear COSY Experiments

5.4.1.1   2D COSY Experiments

The standard homonuclear ^{1}H COSY experiment is probably the most popular 2D experiment and is used for the detection of scalar coupling interaction in spin systems of abundant NMR active nuclei. From a ^{1}H COSY experiment it is possible to assign ^{1}H signals to individual ^{1}H substituents in a molecular structure and using the dominant ^{2}J, ^{3}J and ^{4}J(H, H) coupling constants the coupling interaction can be interpreted to describe the whole molecular structure. The next step is the phase decoding of the correlation peaks into active and passive couplings such that the structure of cross peaks can be analyzed and the magnitude of coupling constants determined. For the analysis of mixtures the COSY experiment is a useful tool enabling mixtures of either isomers or different compounds to be successfully investigated.

The COSY experiment does have some disadvantages. The magnitude mode of the standard sequence causes relatively broad cross and diagonal peaks making the determination of coupling constants as well as the differentiation of direct and indirect coupling impossible. In addition the intensive diagonal peaks can overlap with the cross peaks arising between signals with a small chemical shift difference. The intensity of cross peaks involving small coupling constants might be diminished if the delay, during which the chemical shift and coupling evolution takes place, is too short.

Different variants of the COSY experiment have been developed to overcome these problems. The long-range COSY experiment for instance has an extra delay so that the correlation's involving small coupling constant are enforced resulting in a increase in the intensity of the cross peaks. The problem of overlapping peaks due to poor digital resolution can be solved in two ways. The application of selective pulses reduces the experiment to a 1D spectrum that can be recorded with more time domain data points to obtain a higher digital resolution. Alternatively the 2D experiment can include a double quantum filter (DQF) or even a triple quantum filter (TQF) which reduces the intensity of the diagonal peaks such that cross peaks very near to the spectrum diagonal are better resolved. If a phase sensitive acquisition mode is chosen direct and indirect coupling can be obtained from the analysis of the cross peaks. E.COSY, P.COSY and z-filtered COSY experiments tailor the appearance of the cross peaks. In these experiments the cross peaks always have a distinctive appearance with the splitting due to remote coupling interaction being suppressed. These types of experiment have enable procedures for automatic spectral analysis to be developed. A further improvement is the use of pulse field gradients that reduce phase cycling procedures and the number of signal artefacts.

Sequence features:

Purpose / principles:	Homonuclear correlation of signals using scalar homonuclear ^{3}J and/or ^{n}J coupling. The experiment is limited to sensitive nuclei with high natural abundance like ^{1}H and ^{19}F.
Variants:	COSY90 [5.122, 5.123, 5.124], COSY45 [5.22, 5.125], long-range COSY [5.125], DQF-COSY [5.126], E.COSY [5.33, 5.127, 5.128,

5.129], P.COSY [5.35, 5.34], z-filtered COSY [5.130], relayed
COSY (H-X-H) [5.131, 5.132], ACCORD-COSY [5.133]

Homonuclear COSY experiments may be broadly classified as follows, although as
will become apparent from the following discussions some experiments fall into both
categories:

Tailored correlation detection

In these types of experiment the selection of the correlated nuclei depends upon
the magnitude of the homonuclear coupling constant involved.

- COSY90 experiment for detection of scalar interaction
- Long-range COSY experiment for detection of small coupling constants

Tailored cross and diagonal peaks

In these types of experiment the cross and diagonal peak structure are tailored
to correlate the relative signs of coupling constants and to suppress passive
coupling or unwanted coherences. In addition from the appearance of the cross
peaks it is possible to determine the coupling constants.

- COSY45 experiment
- Multiple quantum filtered COSY experiments
- E.COSY experiments
- Z-filtered COSY experiments

Some aspects of the COSY experiments have already been discussed in sections
2.3.1, 2.3.3 and 5.2.3. Section 2.3.1 examined the superior spectral representation
obtained using phase sensitive quadrature detection mode, section 2.3.3 the use of
gradients for recording phase sensitive spectra and reducing data acquisition times and
section 5.2.3 solvent suppression.

Tailored correlation detection

The homonuclear COSY experiment is designed for nuclei with high magnetic
receptivity and natural abundance such as ^{1}H and ^{19}F. The spectra of these types of
nuclei are dominated by homonuclear scalar coupling interaction although depending on
the nucleus, heteronuclear scalar coupling interaction can also be observed. Nuclei with
low natural abundance such as ^{13}C, in samples of natural isotope distribution, display
only satellite spectra with low intensity which can not be detected in the experimental ^{1}H
COSY spectra. *Check its 5.4.1.1* and *5.4.1.2* introduce the basic COSY experiment and
the long-range COSY variant designed to detect small coupling constants. In both *Check
its* the test spin system is the four proton spin system shown in Fig. 5.21 which is a
common molecular fragment. The chemical shifts and coupling constants have been
arbitrarily selected to demonstrate the COSY spectra for a range of ^{n}J(H, H) values from
0.5 to ±15 Hz and with different signs.

$\delta(H_a) = 2.0$, $\delta(H_b) = 2.6$,
$\delta(H_c) = 4.0$, $\delta(H_d) = 1.5$

$J_{ab} = -15$, $J_{ac} = 12$, $J_{bc} = 6$,
$J_{ad} = -0.9$, $J_{bd} = 0.8$, $J_{cd} = 7$ [Hz]
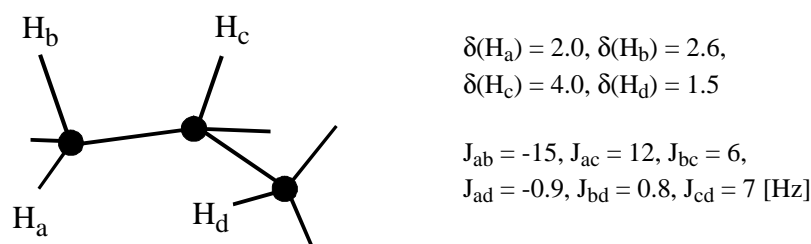
Fig. 5.21:   Molecular fragment of test spin system *4halkane.ham*.

5.4.1.1 Check it in NMR-SIM

(a) Using the configuration file *ch5411a.cfg* simulate the ^{1}H COSY(mc) spectrum of the test spin system. Process the spectrum. Note the weak intensity of the cross peaks due to the small coupling constants J_{ad} and J_{cd}. Furthermore observe the low resolution of the cross peak arising from the coupling of H_a and H_b with H_c.and H_d.

(b) Using the configuration file *ch5411b.cfg* calculate the phase sensitive ^{1}H COSY(TPPI) spectrum (**nd0**: *1* and **in0**: *SW*). The processed spectrum displays very dominant diagonal peaks with wide ridges made up of superimposed dispersive signals. In contrast cross peaks are very detailed and it might be possible to extract the coupling constants from the peak pattern. Note how the small number of increments in the time domain (TD1: 256) results in a lower digital resolution in the f1 dimension compared to the f2 dimension. To simulate the ^{1}H spectrum for the projections and to examine the coupling patterns use the configuration file *ch5411c.cfg*.

$ph1=(0_4(1)_4(2)_4(3)_4$
$ph2=(0\ 1\ 2\ 3)$
$ph31=(0\ 2)_2(3\ 1)_2(2\ 0)_2(1\ 3)_2$

p1(p1, p2): 90° pulse (f1)
d0: incremented delay (f1)
d1: relaxation delay
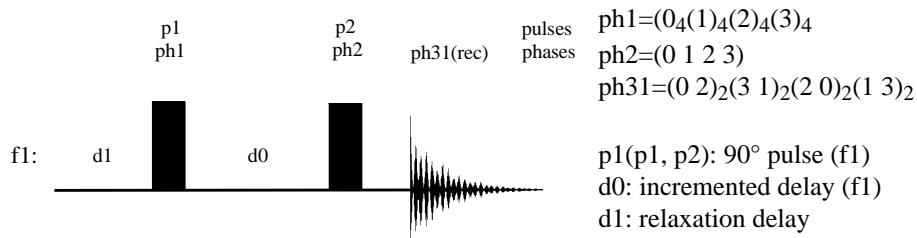
Basic COSY pulse experiment.

The detection of small coupling constants can be very helpful in the assignment of molecular structural units. Long-range coupling constants can be used to distinguish the spin systems of the alcohol and acid component of an ester for instance. The expected small ^{5}J coupling constants between the ^{1}H spin systems of the alcohol and acid usually leads to a decrease in the intensity of the intense cross peaks. The optimized long-range COSY experiment increases the intensity of these cross peaks by inserting two additional

delays before and after the second 90° pulse which ensures that the coherence evolves into nearly perfect antiphase coherence.

5.4.1.2 Check it in NMR-SIM

Load the configuration file *ch5412.cfg*. Modify the basic ^{1}H COSY experiment for the improved detection of small coupling constants. Using the pulse program editor (**Edit│Pulse program**) add the delay **d6** before and after the second 90° pulse, called p2 in the scheme below. Save the new pulse program as *mycosylr.seq*. Load the new pulse program and run the simulation for the test spin system. Compare the processed spectrum with the basic ^{1}H COSY90(mc) spectrum simulated in *Check it 5.4.1.1*.

Long-range COSY experiment.

$ph1=(0)_4(1)_4(2)_4(3)_4$
$ph2=(0\ 1\ 2\ 3)$
$ph31=(0\ 2)_2(3\ 1)_2(2\ 0)_2(1\ 3)_2$

p1(p1, p2): 90° pulse (f1)
d0: incremented delay
d1: relaxation delay
$d6:=1/(2 \bullet {}^nJ(H, H))$
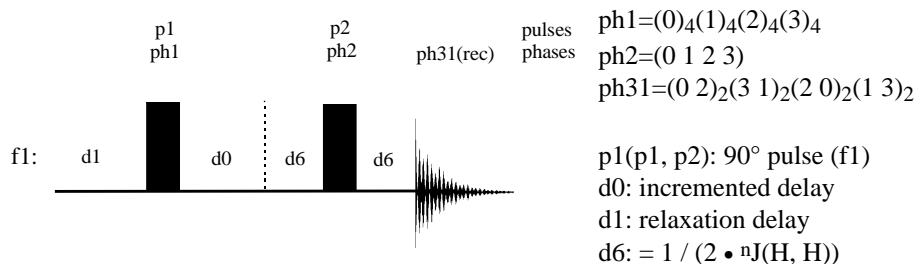
Tailored cross and diagonal peak structure

The relative sign of coupling constants can be determined by means of a COSY45 experiment. The pulse sequence differs from the common COSY90 experiment by replacing the second 90° pulse by a 45° pulse. As well as a reduction in the intensity of the dialogonal peaks, the pattern symmetry of the cross peaks changes which enables the relative signs of the underlying coupling constant to be determined.

5.4.1.3 Check it in NMR-SIM

Load configuration file *ch5413.cfg* with the COSY45 pulse program and the test spin systems *h4alkane.ham*. Run the simulation and compare the pattern of the cross peaks of protons: H_a/H_b, H_a/H_c and H_b/H_c. Inspect the symmetry of the H_a/H_b cross peak in comparison with the other cross peaks. The H_a/H_b cross peak is parallel to the diagonal whilst the other cross peaks are perpendicular implying that $J(H_a,H_b)$ is of opposite sign to $J(H_a,H_c)$ and $J(H_b,H_c)$ as shown in Fig. 5.21.

The correlation peaks in a basic homonuclear COSY experiment arise from both directly and remotely connected transitions and as such does not allow the measurement of coupling constants in complex spin systems [5.130, 5.134]. To try and rectify this problem the COSY45 experiment can be extended to include a DQF. In addition to

tailoring the cross peaks to help in the extraction of coupling constants the multiple quantum filter (MQF) can also be used for [5.126]:

- The suppression of singlets, such as solvent signals
- The reduction in the intensity of the dominant diagonal peaks
- The selection or suppression of specific coupling patterns

Check it 5.4.1.4 (a) demonstrates the effect of a DQF in reducing the intensity of the dominant diagonal peaks and in disentangling the cross peak coupling patterns.

5.4.1.4(a) Check it in NMR-SIM

To simulate the DQF ^{1}H COSY spectrum for the spin system *h4alkane.ham*, load the configuration file *ch5414.cfg*. Run the simulation checking that **nd0**: *1*. Inspect the well-resolved diagonal and cross peaks of the spectrum and compare the results with the phase sensitive COSY(TPPI) spectrum of *Check it 5.4.1.1 (b)*.

DQF COSY experiment.

$ph1=(1)_4(0)_4$
$ph2=(0)_4(1)_4$
$ph3=(1\ 2\ 3\ 0)(2\ 3\ 0\ 1)$
$ph31=(0\ 3\ 2\ 1)(3\ 2\ 1\ 0)$
p1(p1, p2, p3): 90° pulse (f1)
d0: incremented delay (f1),
d1: relaxation delay,
d13: switch delay,
d20: short DQ filter
        enhancement delay
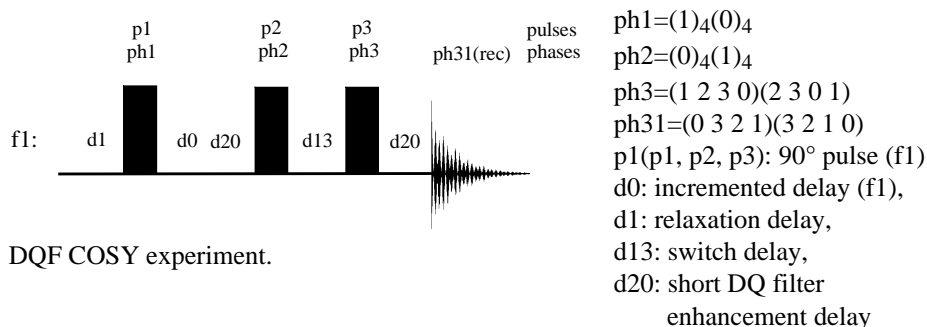
The TQF ^{1}H COSY enhances the cross peak structure, but again reduces the intensity of diagonal peaks such that even doublet diagonal peaks might decrease to a very low intensity. The TQF is achieved by using an extended phase cycling program as shown in the *Check it 5.4.1.4(b)*.

ph1=(12) 0 6 4 10 8 2 3 9 7 1 11 5
     6 0 10 4 2 8 9 3 1 7 5 11
     6 0 10 4 2 8 9 3 1 7 5 11
     0 6 4 10 8 2 3 9 7 1 11 5
ph2=(12) 0 6 4 10 8 2 3 9 7 1 11
     5 6 0 10 4 2 8 9 3 1 7 5 11
ph3=(12) 0 0 0 0 0 0 3 3 3 3 3 3
     6 6 6 6 6 6 9 9 9 9 9 9
ph31=0 2 0 2 0 2 1 3 1 3 1 3
     2 0 2 0 2 0 3 1 3 1 3 1
     2 0 2 0 2 0 3 1 3 1 3 1
     0 2 0 2 0 2 1 3 1 3 1 3

5.4.1.4(b) Check it in NMR-SIM

Load the configuration file *ch5414.cfg*. Convert the DQF homonuclear COSY pulse program to the TQF variant. Open the pulse program *cosydq.seq* in the NMR-SIM editor (**Edit│Pulse program**) and modify the phase programs as shown on the left hand side. Save the pulse program with the filename *mycosytq.seq* (**File│Save as…**). Replace the current pulse program with the new pulse program (**File│Pulse program…**) and run a simulation with **NS**:

24, **nd0**: *1* and **in0**: *SW*. Inspect the spectrum. Note how the diagonal peak at 1.5 ppm has nearly vanished while the cross peak at 4.0 ppm (f2) / 2.6 ppm (f1) is a doublet in each dimension. Repeat *Check it 5.4.1.4(a)* setting **NS**: *24* and compare the results of the DQF and TQF experiments.

It is apparent from *Check it 5.4.1.4* that a DQF or TQF COSY experiments require extensive phase cycling and hence a large number of scans per increment with the related increase in acquisition time. As discussed in section 2.3.3 coherence selection can also be achieved using gradients and MQF experiments can also take advantage of gradient selection. By incorporating two 180° pulses to create an additional spin echo flanked by two gradients the new sequence unit can be toggled between a DQF or TQF by changing the gradient ratio. In contrast to the phase cycled MQF COSY experiment the phase program is considerable simpler and there is no need for extra time-consuming scans.

5.4.1.5 Check it in NMR-SIM

Load the configuration file *ch5415a.cfg*. Using the **Edit│Pulse program** command open the pulse program *cosydptq.seq* and convert the sequence to the gradient selected MQF COSY experiment using the sequence scheme below. Store the new sequence in the file *mycosydg.seq* (**File│Save as…**). Replace the current pulse program with the new sequence. Run the simulation using the test spin system file (*amxsolv.ham*) which consists of a singlet solvent signal at 7.24 ppm and an AMX spin system. For comparison replace the current pulse program with *cosygs.seq* and calculate the magnitude COSY spectrum setting **GPZ1 : GPZ2** to *10 : 10*. Note the large solvent signal. Alternatively use the configuration file *ch5415b.cfg*.

Gradient selected DQF COSY experiment.

ph1=0 2
ph2, ph2, ph3,
ph4=0
ph31=0 2

p1(p1, p2, p4):
90° pulse (f1)

p2(p3, p5):
    180° pulse (f1)
p16: gradient pulse
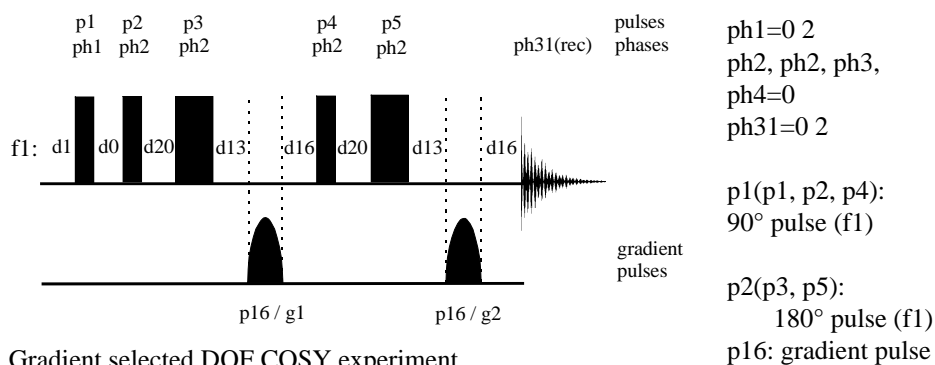
Delays:
d0: incremented delay (f1), d1: relaxation delay, d13: switch delay, d16: gradient recovery delay, d20: d(p16)

Gradient ratio:
(g1 : g2) = (20 : 40)   DQF
(g1 : g2) = (20 : 60)   TQF

The solvent signal at 7.24 ppm is representative of all single quantum transitions that fall on the diagonal. So the MQF based on gradients selection has the same effect as the DQF phase cycled experiment in *Check it 5.4.1.4(a)*.

The E.COSY group of experiments E.COSY [5.33, 5.127, 5.128], P.E.COSY [5.34] and P.COSY [5.35] have been developed to achieve the same quality of cross peak as a DQF spectra, but with the restriction that the cross peaks relate only to those transitions involving the nucleus directly. Whilst in a DQF COSY experiment the structure of the cross peaks is related to the active and passive coupling, in a E.COSY experiments the passive couplings are suppressed.

The E.COSY experiment uses extensive phase cycling and in an effort to reduce the long acquisition times the P.E.COSY and P.COSY techniques have been developed. However these techniques require excessive post-processing of the data and consequently only the E.COSY experiment will be illustrated in *Check it 5.4.1.6*. For a comprehensive review of the other techniques the reader is referred to the literature [5.34, 5.35].

The E.COSY experiment can be described as a weighted DQF COSY experiment that discriminates between the active and passive coupling [5.127]. As shown in Fig. 5.22 this discrimination can be achieved using either a variable pulse length p2 or variable pulse phase ph1. Of the two possible sequences phase discrimination is the better choice because the same pulse lengths and delays are used for successive scans.

Variable pulse length   Variable pulse phase
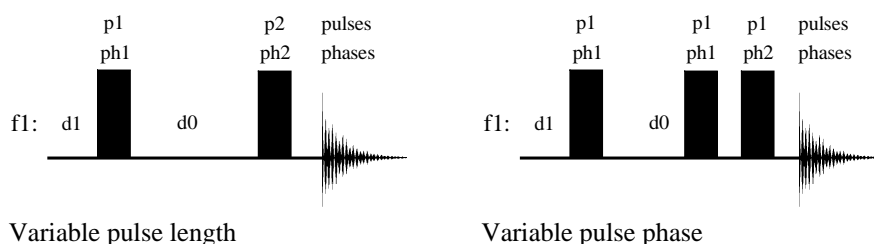
Fig. 5.22:   Alternative E.COSY pulse sequences [5.127].

In *Check it 5.4.1.6* the E.COSY sequence using variable pulse phase for coherence selection is written and tested by simulating the ^{1}H E.COSY spectrum of 2,3-dibromopropionic acid.

5.4.1.6 Check it in NMR-SIM

Using the configuration file *ch5417.cfg* convert the pulse sequence *cosydptq.seq* into the phase cycled E.COSY experiment (**Edit**|**Pulse program**). As shown below add the lines in bold to the sequence and modify the phase programs. Store the new sequence as *myecosy.seq* (**File**|**Save as…**). Run the simulation. Replace the current pulse program with either *cosydqtp.seq* or the pulse program from *Check it 5.4.1.4 (a)* and repeat the simulation. Compare the appearance of the cross peaks in the E.COSY and DQF spectrum.

```
1 ze                              ph1=(12) 3 3 3 3 5 5 5 7 11 1 1 1
2 d1                              ph2=(12) 0 0 0 0 2 2 2 4 8 10 10 10
  d11*2                           ph3=2
3 (p1 ph1):f12                    ph31=1 1 1 1 3 3 3 1 1 3 3 3
  ...
  d1 wr #0 if 0 id0 ip1 zd
  d11 ip1
  d11 ip1
  lo to 3 times td1
exit
```

Phase cycled E.COSY pulse sequence.

Coherence selection using gradients is usually associated with reducing the number of scans per increment in a 2D experiment and hence minimizing the effects of external experimental parameters, such as magnetic field drift and temperature changes. With its long phase program the E.COSY experiment can also be converted into a gradient version [5.129]. If required this conversion can be done as an additional exercise.

An alternative approach to tailor the cross peaks is the z-filtered COSY spectrum (z-COSY) [5.130]. In *Check it 5.4.1.7* the "small-flip angle COSY" spectrum of 2,3-dibromopropionic acid, the basic sequence of the ^{1}H z-COSY spectrum, is simulated. As such a z-COSY spectrum can not be calculated because the randomly changing delay which is the major part of the z-filter can not be simulated in the current version of NMR-SIM. A comparison of the results of *Check it 5.4.1.7* and the E.COSY spectrum of the same spin system calculated in *Check it 5.4.1.6* shows that due to the small flip angles the diagonal peaks of the z-COSY spectrum are reduced in intensity while the cross peaks are very similar.

5.4.1.7 Check it in NMR-SIM

Using the configuration *ch5417.cfg* simulate the "small-flip angle COSY" spectrum of 2,3-dibromopropionic acid. Inspect the cross peak structures and compare the results with E.COSY spectrum of the same compound (see *Check it 5.4.1.6*).

Table 5.20 summarizes the main characteristics of the commonly used COSY90, COSY45 and DQF-COSY experiments.

Table 5.20: Cross and diagonal peak structure in homonuclear COSY experiments

Experiment	Diagonal peaks	Cross peaks
COSY90 magnitude	Peaks have positive absorption lineshape obtained by magnitude calculation.	Peaks have positive phase only with large ridges at the base due to the magnitude calculation.

COSY90 phase sensitive	Peaks have mixed lineshapes.	Peaks have pure absorption lineshape.
COSY45 phase sensitive	Peaks have mixed lineshapes.	In comparison to the COSY90 experiment the cross peaks are tilted depending on the relative sign of the coupling constant. Cross peaks arising from scalar couplings with the same sign will have the same tilt angle.
DQF-COSY phase sensitive	Peaks have a pure absorption lineshape but the intensity peaks is reduced compared to the COSY90 experiment. The DQ filter suppresses solvent and other signals peaks not split by scalar homonuclear coupling.	For the structure of the cross peaks it is possible to determine the active and passive coupling. Lines of a cross peaks arising from the active coupling are out-of-phase or antiphase to each other while lines arising from the passive coupling are in-phase.

5.4.1.2 Selective 1D COSY experiments

The homonuclear 2D COSY experiment has two major disadvantages:

- Because of the low digital resolution and spectral representation the multiplet structure of respective cross peaks are not sufficiently resolved. Moreover the relevant coupling constants can not be determined from the multiplet structure.
- The recording of a 2D experiment usually requires long experiment times because of the extensive phase cycling or because of the number of increments necessary to obtain suitable resolution in the f1 dimension.

In the majority of cases these disadvantages may be overcome by using a 1D COSY experiment which to a first approximation resembles a cross section through the corresponding 2D spectrum [5.8]. The 1D COSY experiment can be recorded using the same digital resolution as a basic 1D experiment allowing the resolution of multiplet structures and the extraction of coupling information. In addition the 1D COSY experiment has a short experiment time. It is possible to consider a selective 1D COSY experiment as a 2D COSY sequence where the first 90° hard pulse has been replaced by a selective pulse. However this is approach is only partly true especially for gradient selected versions of the 1D COSY experiments which are not necessarily based on a selective excitation pulse. As shown in Fig. 5.23 there are two possible schemes and these will be explained in connection with gradient based coherence selection.
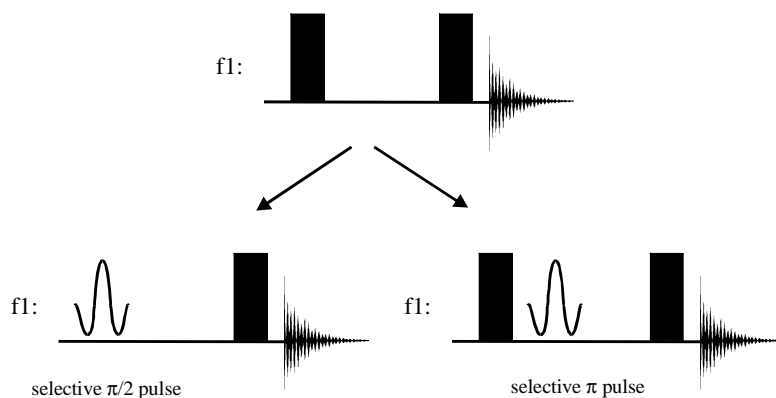
Fig. 5.23: Possible selective pulse schemes to generate a 1D COSY experiment.

However some new problems arise with the implementation of selective pulses:

- Depending on the pulse sequence the selective 90° or 180° pulse introduces phase distortions because of its inherent excitation profile.
- Ideally the selective pulse should be calibrated for each sample.

The pulse program development of 1D COSY experiments is driven by the need for a nearly pure absorptive lineshapes in the final spectrum and for the experiment to be tolerrant of imperfect selective pulses. The use of gradients not only reduces the number of scans necessary but field gradients are superior at suppressing unwanted coherences. The gradient selection has two functions. On the one hand gradients can assist the selectivity introduced by the selective pulse and other hand phase distorsion which is apparent for the excited range can be minimized (see *excitation sculpting*).

1. One class of selective 1D COSY experiments relies upon a selective excitation pulse corresponding to the non-gradient 1D selective COSY experiments (left hand scheme in Fig 5.24).
2. The second class of gradient-selected, selective 1D experiments is based on a selective spin-echo-unit which consists of a 180° selective pulse flanked by two gradients with the same or of opposite sign (see *Check it 5.4.1.10*).

Listed below a number of different types of 1D COSY experiment with and without gradient selection are summarized. By necessity the following discussion can give only a short description of the development of the selective 1D COSY experiment starting with the basic experiment and ending with the 1D DPFGSE selective COSY experiment.

Sequence features:

Purpose / principles:	Homonuclear correlation of signals using scalar homonuclear ^3J and/or ^nJ coupling. The experiment is limited to sensitive nuclei with high natural abundance. The 1D analogous experiment of the 2D COSY experiment.
Variants:	1D selective COSY [5.8, 5.88], 1D MQF selective COSY [5.8], 1D selective z-filtered, refocused COSY [5.8], 1D gradient selected COSY with selective excitation pulse [5.135, 5.136] or selective refocusing pulse [5.137, 5.138], 1D DPFGSE selective COSY [5.139, 5.89]

The remaining *Check its* in this section use a test spin system based on a structural fragment of brucine which is typical of the type of molecule analyzed using the selective 1D COSY experiment in a routine laboratory. The ^1H spin system is reduced to the protons shown in the figure below with the bold lines indicating the structural fragment of interest. The coupling constants and chemical shifts are based on the experimental data of brucine.

5.4.1.8 Check it in NMR-SIM

Load the configuration file *ch5418.cfg*. Simulate the ^1H spectrum of the test spin system based on a structural fragment of brucine. Process the FID and save the processed spectrum.
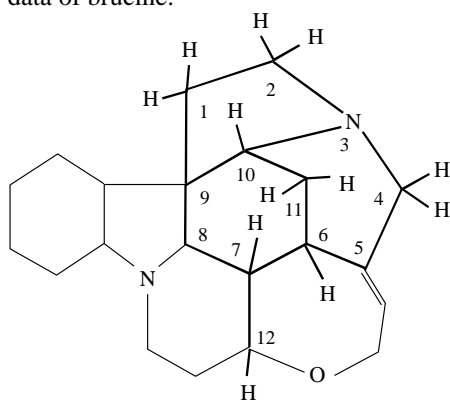
Structural fragment of brucine showing the protons corresponding to the spin system *brucinpt.ham*.

The signal of proton H-11a at 1.35 ppm is well separated and is an ideal candidate for excitation by a selective pulse. In the following *Check its* the selective pulse(s) is always set on-resonance to the H-11a proton. Thus the corresponding selective 1D COSY experiments must show responses to protons H-11b 2.30 ppm, H-6 3.05 ppm and H-10 3.90 ppm. In *Check it 5.4.1.9* the 1D selective COSY experiment is derived and tested using the test spin system.

5.4.1.9 Check it in NMR-SIM

Load the configuration file *ch5419.cfg*. Using the **Edit**⎪**Pulse program** command, create the selective 1D COSY experiment shown in the scheme and syntax below. Save the pulse program with the name *mycosysl.seq* (**File**⎪**Save as…**). Run a simulation with new pulse program using the parameters contained in the configuration file. Process the data and inspect the spectrum obtained if proton H-11a is selectively excited in the COSY spectrum. Note the response of H-12 that does not couple with H-11a. Because the excitation of the shaped pulse is not perfect the shaped pulse also excites H-7 which is coupled to H-12.
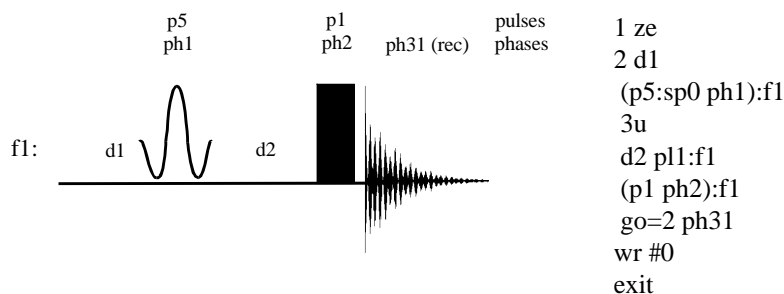

```
1 ze
2 d1
  (p5:sp0 ph1):f1
  3u
  d2 pl1:f1
  (p1 ph2):f1
  go=2 ph31
  wr #0
  exit


ph1=1 3 3 1 2 0 0 2
ph2=0 2 0 2 1 3 1 3
ph31=0 2 2 0 1 3 3 1
```

1D selective COSY experiment.

In *Check it 5.4.1.10* gradients are used in the 1D selective COSY experiment to try and improve the selectivity of the selective 90° excitation pulse.

5.4.1.10 Check it in NMR-SIM

Using the configuration file *ch54110.cfg* edit the 1D selective COSY pulse program according to the scheme below. Save the program with the new name *mycosys2.seq*. Using the loaded parameters simulate the gradient selected 1D COSY spectrum of the structural fragment of brucine used in *Check it 5.4.1.9*. Compare the processed spectrum with the result *of Check it 5.4.1.9*. The intensity of the signals for H-6 and H-10 has increased but some small artefacts have been introduced. These artefacts can be removed as shown in *Check it 5.4.1.11*.

p5(p1): selective 90°
     pulse (f1)
p1(p2): 90° pulse (f1)

ph1=0 0 1 1 2 2 3 3
ph2=1 3 2 0 3 1 0 2
ph31=2 2 3 3 0 0 1 1
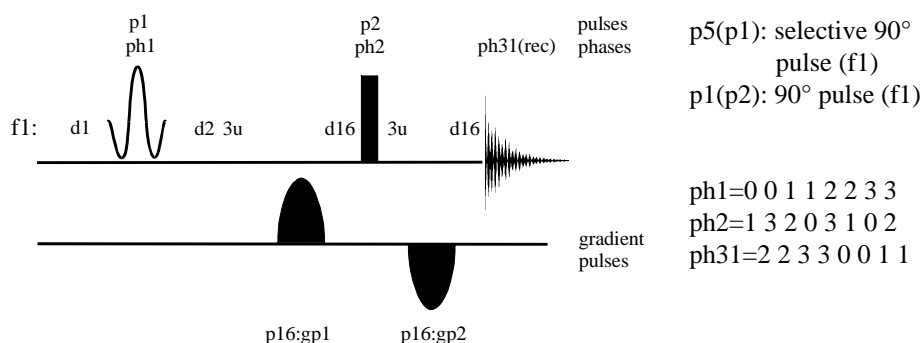
1D selective COSY experiment with a selective excitation
pulse and gradient pulses.

In *Check it 5.4.1.11* the improved selective 1D COSY experiment using a selective
refocusing π pulse are calculated. These category of selective COSY experiments based
on a gradient flanked selective spin echo generate less artefacts and are superior to the
1D COSY pulse sequences with a selective excitation pulse. Essentially the flanking
gradients cancel the artefacts in a similar manner as a "perfect EXORCYCLE" scheme
[5.140].

5.4.1.11 Check it in NMR-SIM

Using the configuration files *ch54111a.cfg* to *ch54111c.cfg* simulate the 1D
gradient selected COSY experiments using three slightly different pulse
sequences with a selective refocusing π pulse and without and with an
excitation sculpting unit. Process the data and compare the spectra for
artefacts, intensity loss and the apparently pure absorption lineshape
obtained with all these sequences. Sequence c [5.89] differs from sequence
b by the missing 180° pulse p2 and the fifth and sixth gradient now flank the
second 90° pulse p1. The delay d2 = 1 / (2 • J(^{1}H, ^{1}H)) precedes this unit.
Little if any intensity differences can be observed for these spectra.

Important note: These simulations take a lot longer than other calculations
and depending on the speed of the computer can take over 6 minutes.

Sequence a [5.137]
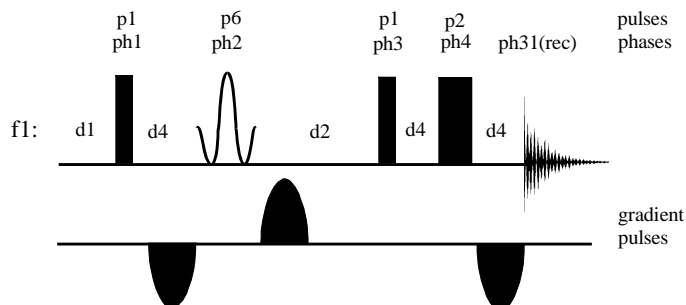
Sequence b [5.139]
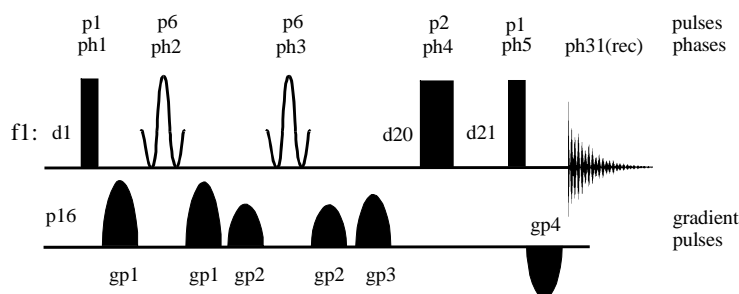
5.4.1.3   Relayed COSY Experiments

Relayed COSY experiments are used to establish a link between separate homonuclear spin systems either via a heteronuclear relay step (left side of Fig. 5.24) or in H, H spin systems a homonuclear relay step (right side of Fig. 5.24). In the latter case correlation peaks are generated for protons which are not directly coupled together but form part of the same spin systems. Correlation's can arise using the small value long-range coupling constants $^4J(H, H)$ and $^5J(H, H)$.

Similar results can be obtained using the TOCSY experiment. TOCSY has the advantage that the experiment can be tailored to a specific purpose by varying the mixing time. To a first approximation the mixing time is inversely proportionally to the magnitude of the coupling constant so that short mixing times lead to correlation's with the nearest neighbouring protons. As the mixing time increases, information about the spin system is relayed through the molecule and correlation's between protons further and further apart appears. In spite of the obvious advantage of a tailored mixing time the relayed experiment is not completely redundant. Because of the limited power of the spinlock field the excitation range is restricted and TOCSY experiments cannot be used for nuclei such as ^{19}F which have a large spectral width. For these nuclei the relayed COSY experiment is the only option.

Heteronuclear relay step   Homonuclear relay step
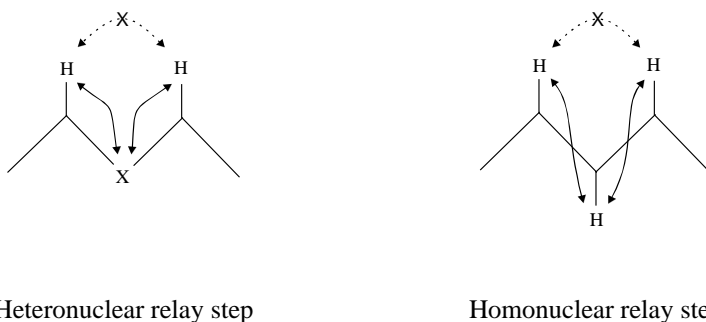
Fig. 5.24:   Heteronuclear and homonuclear relay step. The dotted arrows denote missing scalar coupling of the corresponding protons.

Even though ^{1}H coherences are assigned to both dimensions, heteronuclear relay COSY experiments can be helpful in the indirect detection of heteronuclear functional group. Often from the relay cross peak the functional group acting as a bridge between two spin systems can be deduced.

Sequence features:

Purpose / principles:	Homonuclear correlation of signals which are not directly related by a scalar homonuclear coupling, experiment limited to sensitive nuclei like ^{1}H and ^{19}F, implementation of a relayed magnetization transfer
Variants:	H-H-H relay COSY [5.141, 5.142], H-X-H relay COSY [5.132, 5.131], H-C-C relay ^{13}C detected COSY [5.143], H-H-C relay ^{13}C detected COSY [5.144, 5.145, 5.146], C-H-H relay ^{1}H COSY [5.147, 5.148], relay [n]X, ^{1}H HMQC [5.149], relay 1D selective COSY experiment [5.137, 5.140]

Crotonaldehyde has been used in the literature to test the homonuclear and heteronuclear relayed COSY experiment [5.142]. In the following *Check its* a spin system based on crotonaldehyde will also be used but because the maximum number of coupled spins in a cluster is restricted to nine, see section 1.2, and to speed up the calculation the CH_3 group has been replaced by a CHX_2. Two spin systems have also been created for this crotonaldehyde type molecule: one for a pure ^{12}C isotopomer and a second with the natural ratio of ^{12}C and ^{13}C isotopomers the latter being used for pulse sequence with relay transfer through the ^{13}C nucleus.
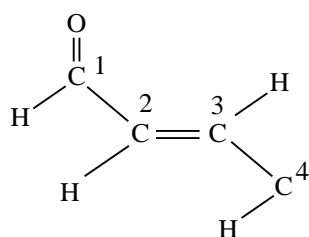
chemical shifts:
δ(H-1) = 9.43, δ(H-2) = 6.11, δ(H-3) = 6.57, δ(H-4) = 1.91
δ(C-1) = 193, δ(C-2) = 135, δ(C-3) = 154, δ(C-4) = 19.

Fig. 5.25:   Molecular structure of the relay COSY experiment test spin system.

The test spin system corresponds to an ^{1}H AKMX system. H-1 has a single coupling to H-2 while H-2, H-3 and H-4 couple with each other with an observable scalar coupling. So in the ^{1}H homonuclear relay COSY experiment proton H-1 should exhibit connectivity to either H-3 or H-4 or both.

5.4.1.12 Check it in NMR-SIM

Load the configuration file *ch54112.cfg*. Using the current 2D pulse program template create the H-H-H relay COSY(mc) pulse sequence shown below. Save the new pulse program with the filename *mycosyrl.seq*. Replace the current pulse sequence with the new relay sequence and run a simulation. Repeat the simulation using the basic ^{1}H COSY(mc) sequence. Note the additional cross peaks due to the relay transfer step in the relayed ^{1}H COSY spectrum. Repeat both simulations after replacing the current spin system with *rel2sppsy.ham* (**File|Spin system...**).
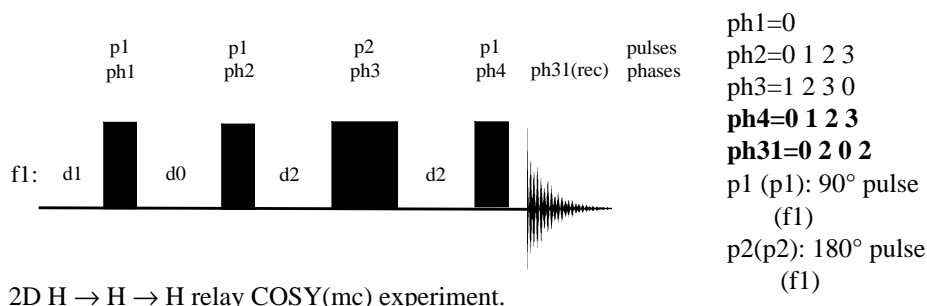
2D H → H → H relay COSY(mc) experiment.

The H-X-H relay COSY experiment enables the verification that two apparently isolated ^{1}H spin systems belongs to the same molecule. The experiment is based upon the detection of a heteronuclear coupling interaction between at least two protons from each spin system to the same bridging heteronucleus such as a ^{13}C atom in a carbonyl functional group. By default the experiment is not very sensitive, the relay cross peak depending on the magnetization transfer to a ^{13}C atom with low natural abundance.

5.4.1.13 Check it in NMR-SIM

Load the configuration file *ch54113.cfg* and run the simulation of the 2D ^{1}H-

¹³C-¹H relay COSY experiment of the crotonaldehyde type spin system. In this modified spin system the coupling between H-1 and H-2 is excluded to show the relay transfer from H-1 to H-2 trough C-1. Compare the result with the basic ¹H COSY spectrum. Repeat both simulations using the spin system *relcspsy.ham*. Note however that in this spin system the ¹³C nucleus is 100% abundant.
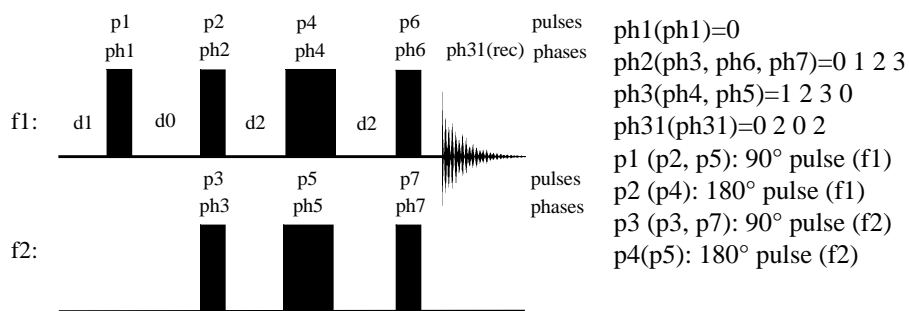
2D H-X-H relay COSY experiment.

As shown in the list of relay COSY experiments heteronuclear correlation experiments are possible. In *Check it 5.4.1.14* the H-H-X relay ¹H, ¹³C COSY experiment for the crotonaldehyde type spin system is calculated. Implementing a relay step to a heteronucleus enables complex ¹H COSY spectrum to be disentangled by including a heteronuclear polarization transfer to link the ¹H signals to the heteronuclear chemical shift dimension. Fig. 5.26 illustrates this schematically for two spin systems. Since $\delta(H_a) = \delta(H_d)$ and $\delta(H_b) = \delta(H_e)$ at least two ¹H, ¹H relay cross peaks which belong to two different relayed spin systems overlap in the ¹H, ¹H spectrum. However because $\delta(C_c) \neq \delta(C_f)$ these peaks may be separated if the correlation peaks can be related to the heteronucleus which has a different chemical shift for each peak.

¹H COSY spectrum   ¹H-¹H-¹³C relay ¹H, ¹³C COSY spectrum
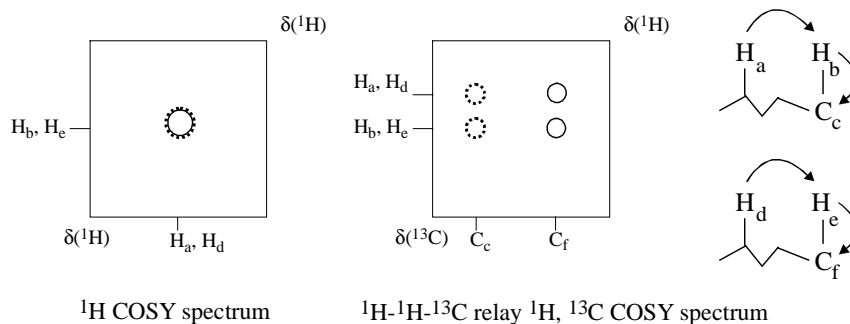
Fig. 5.26:   ¹H-¹H-¹³C relay COSY spectrum to separate ¹H, ¹H correlation peaks with similar chemical shift.

5.4.1.14 Check it in NMR-SIM

Run the ^{1}H-^{1}H-^{13}C relay ^{1}H, ^{13}C COSY experiment (*hhxrcosy.seq*) for the *ccrotal.ham* spin system used in *Check it 5.4.1.13* using the configuration file *ch54114.cfg*. Inspect the processed ^{1}H, ^{13}C correlation spectrum for the additional relay cross peaks in addition to the ^{1}J(C, H) correlation peaks. Compare the result with the analysis in the *result.pdf* file.

ph1=0
ph2=(0)$_4$(2)$_4$
ph3=0 2 1 3
ph4=0 2 1 3 2 0 3 1
ph5= (0 2 1 3)$_2$
    (2 0 3 1)$_2$
ph6=0
ph31= (0 2 1 3)$_2$
    (2 0 3 1)$_2$

p1(p6): 90° pulse (f1)
p2(p2): 180° pulse (f1)
p3(p1, p3, p5): 90° pulse (f2)
p4(p4): 180° pulse (f2)
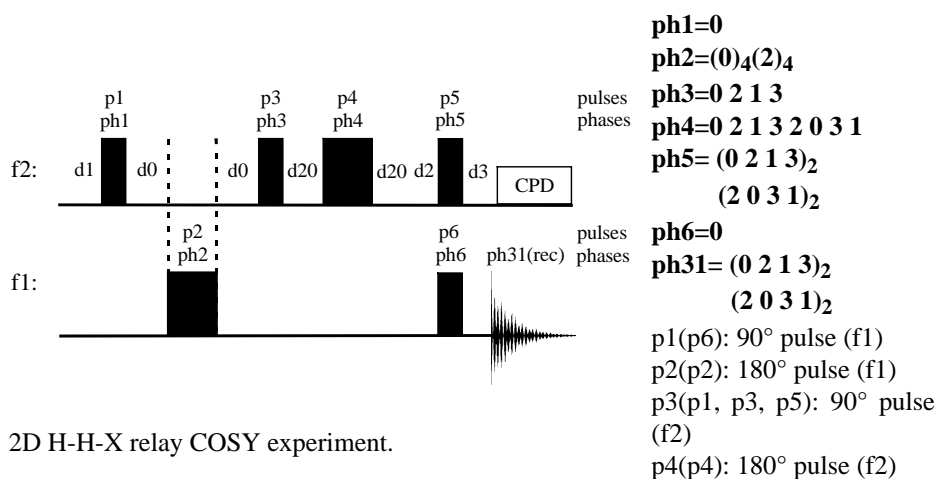
2D H-H-X relay COSY experiment.

An alternative to the H-H-X relay COSY experiment is the X-H-H relay COSY experiment [5.148], which has the advantage that it is based on the detection of the sensitive nucleus [5.3]. In *Check it 5.4.1.15* the X-H-H relay COSY sequence is created and then various aspects of the phase cycling examined to illustrate how the original phase cycling proposed in the literature must be adapted to give quadrature detection in f1 [5.148] using NMR-SIM.

5.4.1.15 Check it in NMR-SIM

(a) Load the configuration file *ch54115.cfg*. Using the **Edit│Pulse program** command write the ^{n}X-^{1}H-^{1}H relay COSY pulse program using the sequence scheme below. Rationalize the pulse sequence by replacing p5 and p9 with p1 as shown on the right hand side of the pulse scheme. Save the new pulse program with the name *mxhhcosy.seq* (**File│Save as…**). Check the pulse sequence (**Utilities|Show pulse program…**) and then calculate the ^{13}C-^{1}H-^{1}H relay COSY spectrum of the test spin system *ccrotal.ham*. Compare the result with the spectrum of *Check it 5.4.1.14*.

(b) The proposed minimum number of scans is four. To understand the reasoning and the underlying phase cycling simulate four spectra with the following phase combinations of the phases **ph6** and **ph31**. All other phase programs are run with phase 0.

(1) ph6=0, ph31=0   **(3) ph6=0 2, ph31=0 2**

(2) ph6=0 1, ph31=0 3   **(4) ph6=3 1, ph31=1 3**

2D ^nX-^1H-^1H relay COSY experiment.

ph1, ph2, ph3, ph4,
ph5, ph7, ph8, ph9
=0
ph6=0 1 2 3
ph31=0 3 2 1
p1(p5, p9):
   90° pulse (f1)
p2(p2, p3, p7):
   180° pulse (f1)
p3(p6):
   90° pulse (f2)
p4(p4, p6):
   180° pulse (f2)
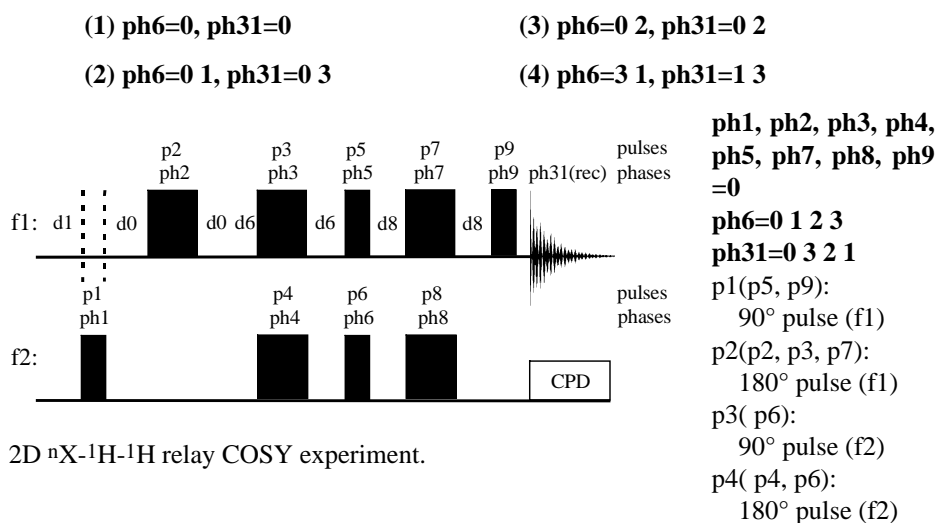
From *Check it 5.4.1.15* it is possible to understand the phase cycling of the X-H-H relay COSY sequence and hence the basic phase cycling of other heteronuclear correlation experiments. The results of *Check it 5.4.1.15* can be summarized:

(1)   With no phase cycling of the pulse phase ph6 and the receiver phase ph31 there is no coherence suppression and no frequency discrimination in the f1 dimension because of the missing co-addition of the cosine and sine modulated response during the t1 period (see section 2.3.3).

(2)   Phase cycling the pulse phase ph6 in 90° steps enables the co-addition of cosine and sine modulated response to obtain frequency discrimination in the f1 dimension. Due to the internal co-addition procedure the receiver phase ph31 must be shifted by 3 • 90° which is equivalent to -90° steps.

(3)   Phase cycling the pulse phase ph6 and the receiver phase ph31 in 180° steps suppresses unwanted coherences arising from imperfectly refocused coherences during d0, which effects folded correlation peaks centred about O2.

(4)   The four-step phase cycle gives the required performance of artefact suppression and frequency discrimination in the f1 dimension.

5.4.2 TOCSY Experiments

The HOHAHA or TOCSY experiment [5.150, 5.151] has proved a popular alternative in many applications to the main homonuclear correlation experiment for sensitive nuclei, the basic COSY experiment. Both the HOHAHA and the TOCSY experiment are based on the principal of isotropic mixing but differ in the type of spinlock sequence used. Nevertheless they may be considered together and for convenience in the following discussion the expression TOCSY experiment will be used for both sequences. The TOCSY experiment uses cross polarization for the coherence

transfer process in contrast to the COSY experiment which uses polarization transfer. A 2D TOCSY spectrum has the following advantages over a basic COSY spectrum:

- The diagonal and cross peaks have a pure absorptive lineshapes for the optimum spinlock conditions of optimum spinlock time and perfect spinlock sequence.
- Cross polarization produces a net magnetization transfer over the whole spin system such that an individual proton in a large proton spin system will exhibit cross peaks to all the other protons in the same system. Cross peaks will be observed for both very small coupling constants and in similar manner to a relay experiment for protons not directly coupled.
- The relay COSY experiments has to contend with reduced signal intensity during the long relay step. In contrast in a TOCSY experiment because of the different effective rate constant during the spinlock period relaxation effects are minimized [5.143] and TOCSY experiments can be successfully performed on fast relaxing molecules such as polymers or organic macromolecules.
- The duration of the mixing time determines to some extent how far the coherence is transferred from an initial spin along the coupling network.

The spinlock sequence is an integral part of the TOCSY experiment since the success of the experiment depends upon isotropic mixing which depends upon the spinlock sequence. The spinlock sequence generates a strong rf field perpendicular to the B_0 field along one of the orthogonal axis of the rotating frame coordinate system. The effect of the spinlock field can be depicted as all the spins in the transverse plane aligned along either the x- or y-axis of the coordinate system. If the Hartmann-Hahn condition is fulfilled the spinlocked spins experience no chemical shift evolution and exchange energy with each other behaving as an infinitely coupled system. To obtain this "collective spin mode" [5.151] a cpd sequence is often applied with the choice of cpd pulse sequence limited by its excitation range. Since the rapidly repeated pulses, even at low power, dissipate thermal energy into the sample causing thermal gradients and degrading spectral quality it is not possible to increase the power of the spinlock sequence to achieve a wider excitation range. Consequently some ingenious pulse sequences and spinlock sequences have been developed to overcome this problem and the prerequisites of such sequences are discussed in *Check it 5.4.2.2* using an MLEV-17-based 1D TOCSY sequence [5.143].

Sequence features:

Purpose / principles:	The homonuclear correlation of direct and relayed connected nuclei is established by isotropic mixing and cross polarization, The isotropic mixing is achieved by a cw field (HOHAHA experiment) or a multi-pulse spinlock sequence (TOCSY experiment).
Variants:	1D selective TOCSY / HOHAHA [5.152, 5.149, 5.153], 2D TOCSY [5.143, 5.154, 5.151, 5.150], gradient selected 1D selective / 2D TOCSY [5.140, 5.9, 5.155, 5.156], TOCSY ^{13}C, ^{1}H HMQC [5.157, 5.158, 5.159]

In *Check it 5.4.2.1* the 1D selective COSY, 1D selective relayed COSY without and with z-filter and a 1D selective TOCSY spectrum are simulated for the same spin system and the results compared. As already mentioned the spinlock for isotropic mixing can be generated in different ways and this has lead to the development of improvements and elements being added to the spinlock sequence. Of these improvements the trim pulse and z-filter, adapted to the spinlock sequence [5.154], are the most popular.

coupling   relay   relay

H(a)   H(b)   H(c)   H(d)

$\delta(H(a)) = 4,5; \delta(H(b)) = 3,5;$

$\delta(H(c)) = 2,5; \delta(H(d)) = 1,5$
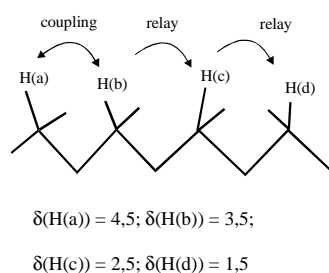
Test spin system *4Hchain.ham*

5.4.2.1 Check it in NMR-SIM

Load the appropriate configuration file and using the identical experiment parameters simulate the following spectra for the spin system *4Hchain.ham*. In all cases H(a) at 4.5 ppm is selectively excited. (a) *ch5421a.cfg* 1D selective COSY experiment, (b) *ch5421b.cfg* 1D selective relay COSY experiment, (c) *ch5421c.cfg* z-filtered 1D selective relay COSY experiment, (d) *ch5421d.cfg* 1D selective TOCSY experiment. Process the FIDs in the same way and inspect the different effects due to generating coherence transfer using either a relay step or a cross polarization with isotropic mixing. Run the 1D TOCSY experiment twice with **L1**: *10* and **L1**: *20* to increase the mixing time to allow coherence transfer from the selectively excited proton to the more remote protons H(c) and H(d) in the spin system. As predicted by theory in addition to probing the spin system further, the longer spinlock period gives an increase in signal intensity. To see the effect of the purge pulse **p17** repeat the simulation for both values of **L4** changing the value from *2.5u* to *2500u.*
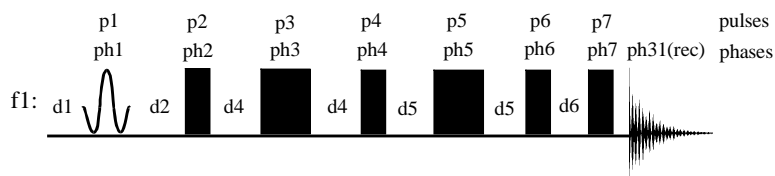
z-filtered 1D selective relay COSY experiment.

Originally it was proposed that a series of 180° pulse should be used for the spinlock sequence but this has now been superseded by more efficient sequences. Although other spinlock sequences can be implemented [5.154] the most popular sequence is MLEV-17 with z-filter [5.143] which enables lower pulse power levels to be used with less lineshape distortion. *Check it 5.4.2.2* examines several spinlock sequences.

5.4.2.2 Check it in NMR-SIM

(a) Simulate three 1D selective TOCSY experiments using different spinlock sequences and configuration files. (a) A simple 180° low power pulses *ch5422a.cfg*, (b) a composite 180° (90°$_x$/180°$_y$/90°$_x$) pulse *ch5422b.cfg* and (c) the MLEV-16 sequence *ch5422c.cfg*. Process the FIDs in an identical way and compare the results for offset dependency and the overall signal intensity.
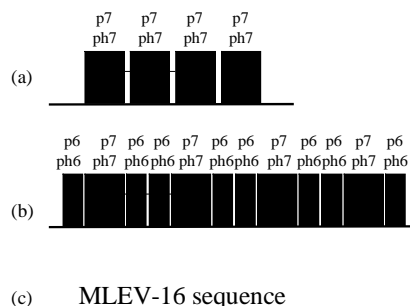
Several "simple" spinlock sequences.

(b) The superior MLEV-17 spinlock sequence can also contain the appropriate z-filter to suppress the coherence that distorts the signals. The efficiency of the z-filter can be simulated using the configuration file *ch5422d.cfg*. Simulate the z-filter experiment **L4**: *10* and then the basic MLEV-17 spinlock sequence **L4**: *1*. The second simulation does not implement the z-filter because only one variable delay vd is used because the loop counter L4 is set to one (see sequence scheme below).

p17: trim pulse,
p5: 60° pulse,
p6: 90° pulse,
vd: random delay from a delay list
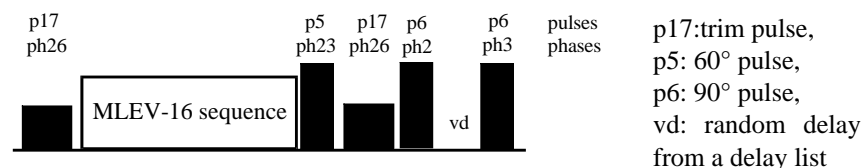
MLEV-17 spinlock sequence with z-filter and trim pulses.

In part (b) of *Check it 5.4.2.2* the z-filter function was shown in combination with the MLEV-17 sequence. The basic principle of the z-filter [5.160] is to transfer the wanted coherences into z-magnetization at the beginning of the filter sequence letting all the unwanted coherences undergo chemical shift or coupling constant evolution in the following period. The wanted coherences are then brought back into the x,y-plane for detection. The z-filter works by accumulating several subexperiments with randomly changing evolution periods such that the unwanted coherences accumulate destructively while the wanted unmodulated coherences are accumulate constructively. The z-filter mainly eliminates phase anomalies that arise from in-phase dispersive lines caused by using non-optimum mixing times.

Whilst the z-filter helps to eliminate experimental phase errors further spectral distortions can be suppressed by using two trim pulses and an additional pulse in the MLEV-17 pulse sequence. There are two main sources for these distortions:

- Ideally the excitation pulse and the spinlock pulses should be phase coherent. However this is not a trivial problem because the same spectrometer device does not necessarily generate the high power pulses and low power spinlock pulses.
- The pulse phase shifting is not perfect or there is a transmitted power imbalance on the different quadrature detection channels.

In the MLEV-17 sequence a 180° pulse (or a 60° pulse) is appended to the MLEV-16 sequence. The additional 180° pulse inverts the magnetization that is not perfectly aligned with a particular axis of the rotating frame so that after an even number of MLEV17 cycles the magnetization is perfectly aligned. Any residual magnetization which is not perfectly parallel to the selected axis to which the spins are locked are defocused by the two trim pulses.

The 1D TOCSY pulse sequence can be converted into a 2D experiment by inserting an incremented delay between the excitation pulse and the spinlock sequence as shown in the scheme below. In *Check it 5.4.2.3* the 2D ^{1}H TOCSY experiment is calculated and the results compared with the corresponding ^{1}H COSY experiment without and with relay step to highlight the additional correlation peaks in the TOCSY spectrum.

5.4.2.3 Check it in NMR-SIM

Compare the 2D ^{1}H COSY, the ^{1}H relay COSY and ^{1}H TOCSY spectra of the test spin system *ch524.ham* using the configuration files *ch5423a.cfg*, *ch5423b.cfg* and *ch5423c.cfg* respectively. Use the configuration file *ch5423d*.cfg to simulate the ^{1}H to use for the projections.

Note: depending upon the speed of the computer the calculation of the TOCSY experiment can take more than 8 minutes.
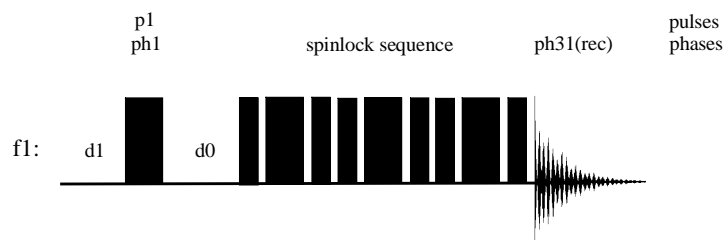
2D TOCSY experiment.

The advantages of the TOCSY experiment have led to the implementation of spinlock sequences in heteronuclear correlation experiments to detect additional homonuclear coupling interaction. In the ^{13}C, ^{1}H TOCSY-HMQC experiment in addition to cross peaks from one-bond connectivities between a ^{13}C and a ^{1}H nucleus there are correlation peaks to protons which are coupled to the primary proton by homonuclear H, H coupling. The advantage of this method is that it allows the differentiate between overlapped ^{1}H signals of different spin systems provided that the spin systems differ by the carbon shift of at least one carbon atom. This approach is shown by the simulations in the *Check it 5.4.2.4*.

5.4.2.4 Check it in NMR-SIM

First simulate the ^{13}C, ^1H HMQC experiment using the configuration file *ch5424a.cfg* to detect the one-bond ^{13}C, ^1H correlation peaks of H(a) and C(c). Then calculate the ^{13}C, ^1H TOCSY-HMQC experiment, *ch5424b.cfg*, and inspect the spectrum for the additional correlation peaks due to $^nJ(H(a), H(b))$. Simulate the 1D spectra to use for the projection: ^1H spectrum ch5424c.cfg, $^{13}C\{^1H\}$ spectrum *ch5424d.*cfg.

Note: depending upon the speed of the computer the calculation of the TOCSY-HMQC experiment can take in excess of 30 minutes.
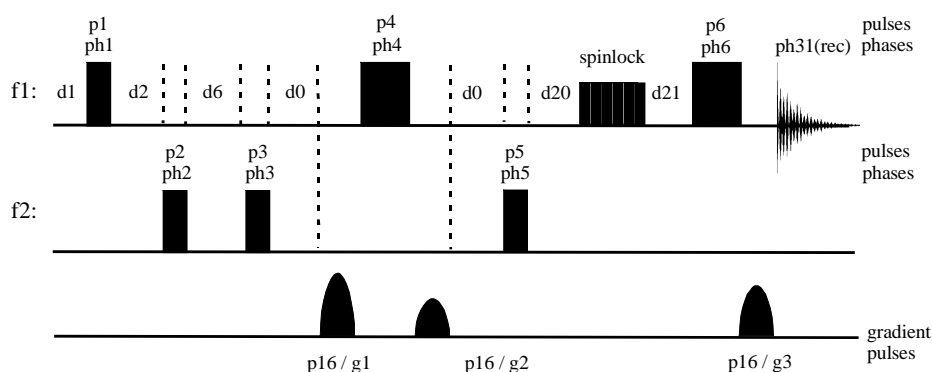
2D TOCSY-HMQC experiment.

5.4.3 INADEQUATE Experiment

The INADEQUATE experiment (**I**ncredible **N**atural **A**bun**D**anc**E** **QUA**ntum **T**ransfer **E**xperiment) [5.161] plays a minor role in everyday NMR spectroscopy even though it is the only direct method to investigate the backbone of a molecule. The analysis of an ^1H, ^1H or ^1H, ^{13}C correlation experiment is based on a number of assumptions and from this information the molecular structure is determined indirectly. For instance a correlation peak in a homonuclear ^1H COSY spectrum is assumed to be the result of $^2J(H, H)$ or $^3J (H, H)$ scalar coupling between neighbouring nuclei yet the number and type of nuclei taking part in the coupling interaction is normally based upon the supposed structure. Similarly long-range ^{13}C, ^1H correlation experiments do not permit a correlation peak to be assigned unambiguously to a $^2J(C, H)$ or $^3J(C, H)$ coupling. Both of these experiments depend upon the magnitude of the coupling constant and cannot differentiate between different coupling interaction on the basis of coupling pathways. In a typical organic compounds often $^2J(H, H)$ is comparable to $^3J(H, H)$ and $^2J(C, H)$ to $^3J(C, H)$. However the INADEQUATE experiment is based upon scalar coupling between directly bonded nuclei in the molecular skeleton.

There are several experimental problems that have prevented this correlation experiment from becoming a routine method for determining the backbone of a molecule. In the analysis of organic molecules in addition to the ^{13}C nucleus having a low magnetic receptivity, its abundance of 1% means that there is a probability of 0.01% that there will be two neighbouring ^{13}C nuclei in the same molecule. In addition small sample quantities and low concentration preclude any attempt to analyze the carbon backbone by this experiment. Apart from the sample the INADEQUATE experiment also makes great demands on the spectrometer which must guarantee nearly ideal experimental conditions. It is essential that the phase settings are perfect during the course of the experiment and the extensive phase cycling programs of the pulse sequence, which are necessary to suppress the signals of the single ^{13}C substituted isotopomers. The ^{1}H decoupling on the second rf channel must be prefect to prevent line broadening and decreased intensity for $^{13}C^{1}H_n$ group signals due to incomplete decoupling. There must also be no thermal gradients in the sample. There have been a number of different approaches to minimizing phase imperfections and to overcoming the inherent insensitivity of the experiment. The implementation of coherence transfer based on a INEPT [5.162] or DEPT [5.163] polarization transfer or cross polarization (CP) [5.164], indirect detection in 2D experiments and the application of gradients [5.165].

Sequence features:

Purpose / principles:	Homonuclear correlation of nuclei of with low natural abundance, spin-echo sequence for scalar coupling evolution, DQF to suppress unwanted coherences, a double quantum frequency scaled dimension in 2D spectra
Variants:	1D INADEQUATE [5.166, 5.60], 1D/2D INEPT-INADEQUATE [5.162], DEPT-INADEQUATE [5.163], 2D INADEQUATE [5.167, 5.168], SELINQUATE [5.169], 1D/2D CP INADEQUATE [5.164], gradient selected 2D ^{13}C, ^{1}H INADEQUATE [5.165]

Fig. 5.27 shows the structure and ^{13}C NMR related parameters of 1,2-oxazole which is the test spin system used in the following *Check its*.

δ(^{13}C):
δ(C-3) = 150, δ(C-4) = 100, δ(C-5) = 159

J(^{13}C, ^{1}H) [Hz]:
J(C-3 / H-3) = 188, J(C-4 / H-4) = 185,
J(C-5 / H-5) = 203

J(^{13}C, ^{13}C) [Hz]:
J(C-3 / C-4) = 50,
J(C-4 / C-5) = 65
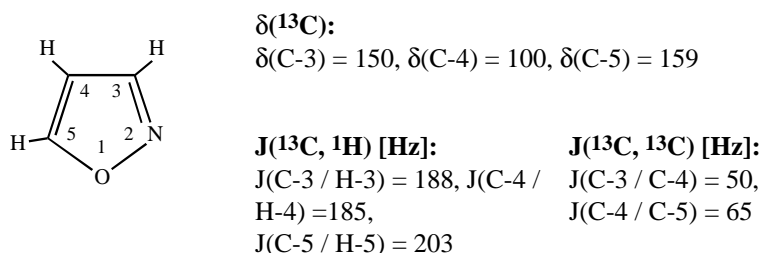
Fig. 5.27:   1,2-oxazole - the test spin system for the INADEQUATE spectra.

Starting with the basic INADEQUATE experiments the simulation focuses on the inherent disadvantage of homonuclear correlation experiments on nuclei with low natural abundance.

5.4.3.1 Check it in NMR-SIM

(a) Load the configuration file *ch5431a.cfg* and simulate and compare the ^{13}C spectra of the spin system files *isoxa1.ham* and *isoxa2.ham*. The file *isoxa1.ham* describes 1,2-oxazole with a variety of natural abundance ^{13}C isotopomers whilst *isoxa2.ham* describes a mixture of double ^{13}C substituted isotopomers. The second spin system is the reduced test spin system used for simulating the time-consuming 2D INADEQUATE experiments. Notice how the ^{13}C signals of the ^{13}C, ^{13}C isotopomers are nearly lost in the baseline of the ^{12}C, ^{13}C isotopomer signals.

(b) Using the configuration file *ch5431b.cfg* simulate the unrefocused (*inade1.seq*) and refocused 1D INADEQUATE experiment (*inade1rf.seq*) for the spin system file *isoxa2.ham*. Check the suppression of the ^{12}C, ^{13}C isotopomer signals and note how the signals in the refocused INADEQUATE experiment no longer have a pure absorptive lineshape.

1D unrefocused INADEQUATE experiment.

$ph1=(0)_4(1)_4(2)_4(3)_4(2)_4$
$\quad (3)_4(0)_4(1)_4$
$ph2=[(0)_4(1)_4(2)_4(3)_4]_2$
$\quad [(2)_4(3)_4(0)_4(1)_4]_2$
$ph3=(0)_4(1)_4(2)_4(3)_4$
$ph4=(0\ 1\ 2\ 3)$
$ph31=(0\ 1\ 2\ 3\ 2\ 3\ 0\ 1)_2$
$\quad (2\ 3\ 0\ 1\ 0\ 1\ 2\ 3)_2$

p1(p3, p4): 90° pulse (f1)
p2(p2): 180° pulse (f1)
d1: relaxation delay,
d2: $= 1 / (4 \bullet J(^nX, {}^nX))$
d3: switch delay
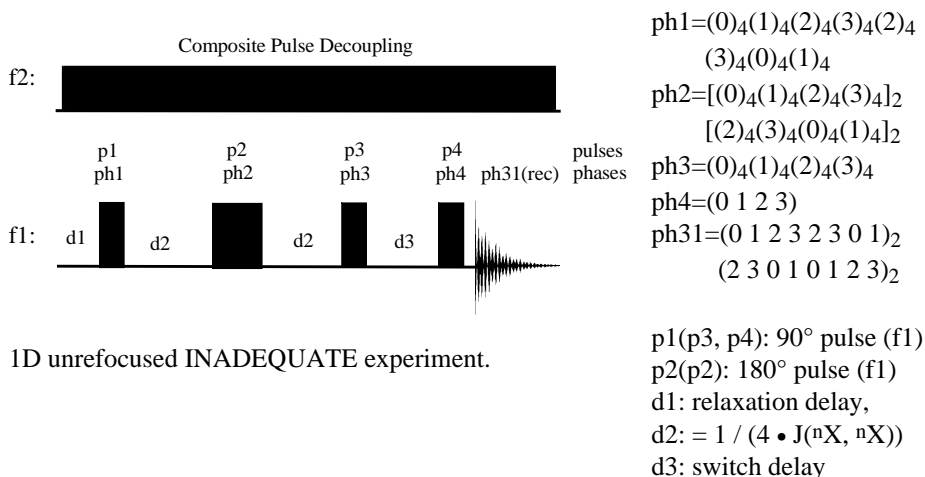
The first step in increasing the signal intensity in INADEQUATE experiments is to implement a polarization transfer step. The INEPT-INADEQUATE experiment [5.162] starts with the INEPT sequence creating antiphase coherence for the sensitive nucleus with a subsequent coherence transfer step before continuing the basic INADEQUATE experiment. In *Check it 5.4.3.2* the INEPT-INADEQUATE pulse sequence is created and the results compared with the unrefocused 1D INADEQUATE experiment.

5.4.3.2 Check it in NMR-SIM

Load the configuration file *ch5432.cfg*. Write the 1D INEPT-INADEQUATE pulse sequence using the pulse sequence scheme shown below. Save the pulse sequence with the new filename *myininad.seq* (**File|Save as…**). Replace the current pulse program with the newly created sequence and simulate the experiment. Simulate the unfocused 1D INADEQUATE experiment by replacing the pulse program with the sequence file *inade1.seq*. Compare the signal intensities.
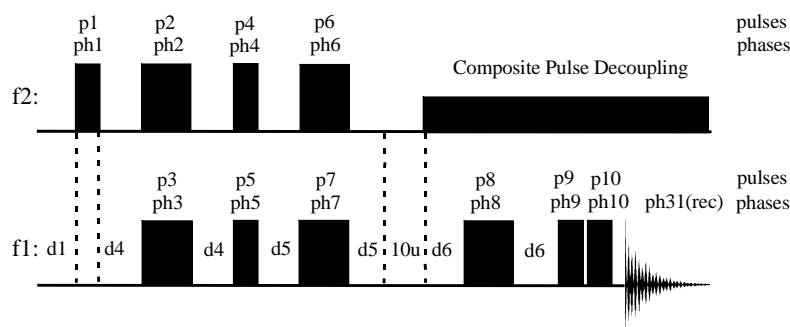
1D INEPT-INADEQUATE experiment.

Pulses and delays:
p1(p5, p9, p10): 90° pulse (f1); **p2**(p3, p7, p8): 180° pulse (f1); **p3**(p1, p4): 90° pulse (f2); **p4**(p2, p6): 180° pulse (f1); d4: = $1 / (4 \bullet {}^1J({}^{13}C, {}^1H))$, d5: = $1 / (4 \bullet {}^1J({}^{13}C, {}^{13}H))$; d6: = $[1 / (4 \bullet {}^1J({}^{13}C, {}^{13}C))] - d5$

Phase cycles:
ph1, ph2, ph3, ph5, ph6=0; ph4=1; ph5, ph7=3, ph8=$(0)_8(1)_8$,
ph9=$(0)_4(2)_4(0)_4(2)_4$, ph10=0 1 2 3, ph31=(0 3 2 1)(2 1 0 3)$_2$(0 3 2 1)

2D INADEQUATE experiments are also possible and these type of experiments are unique in that the f1 dimension does not correspond to single quantum coherence frequency but to a double quantum coherence frequency. These double quantum coherences are observed because homonuclear coupling and chemical shift evolve simultaneously during the d0 period and can not be suppressed. In *Check its 5.4.3.3* and *5.4.3.4* two alternative 2D INADEQUATE experiments are demonstrated. Both reveal the same connectivities, but the second experiment displays a COSY like spectrum.

5.4.3.3 Check it in NMR-SIM

Simulate the original 2D ${}^{13}C$, ${}^{13}C$ INADEQUATE spectrum of the oxazole test spin system using the configuration file *ch5433.cfg*. Inspect the f1 dimension and try to analyze the signal assignment of coupled carbon nuclei consulting the *result.pdf* file if necessary.

The COSY like 2D INADEQUATE experiment differs not only in the signal pattern but there is a possibility that the proposed sequence might also enhance signal intensity [5.168, 5.161]. As shown in the pulse sequence scheme below the basic difference is the additional delay d0 after the pulse p4. Because there are now two d0 delays the value of d0 is halved compared to the original 2D INADEQUATE sequence in *Check it 5.4.3.3*.

5.4.3.4 Check it in NMR-SIM

Run the alternative 2D ^{13}C, ^{13}C INADEQUATE experiment [5.168] using the configuration file *ch5434.cfg*. Compare the result to the spectrum from *Check it 5.4.3.3*.
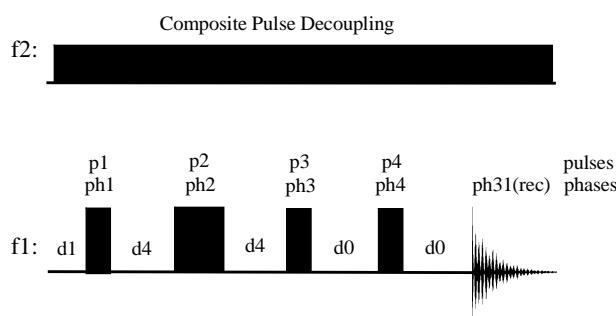
COSY like 2D INADEQUATE experiment.

5.5 Building Blocks and Elements - Part Two

This section focuses on the coupling evolution that occurs during the pulse sequences of heteronuclear correlation experiments. Because polarization transfer is a requirement of intensity optimized heteronuclear correlation spectroscopy this section also acts as a short introduction to coherence transfer by polarization transfer. A coherence transfer from a sensitive nucleus, e.g. ^{1}H in most experiments, to a ^{n}X nucleus contributes a gain of signal intensity. To obtain the required antiphase coherence for the transfer step the coherence must evolve exclusively by heteronuclear coupling during a free precession periods. This can only be assumed in theoretical spin systems. In real samples three aspects make this ideal approach more difficult:

- During free precession periods both coupling evolution and chemical shift evolution occurs. This evolution may be refocused using a refocusing 180° pulses after the half period, see section 5.3.4, but 180° pulse are sensitive to pulse imperfections.
- The antiphase coherence state generated is a function of the underlying coupling constant. In a ^{n}X, ^{1}H correlation experiments the optimum evolution period is given by $1/(2 \bullet J(^nX, {}^1H))$. However in a real sample there will be a variety of values for $J(^nX, {}^1H)$ for different ^{1}H, ^{n}X spin groups so a
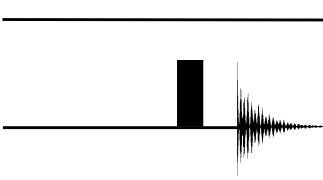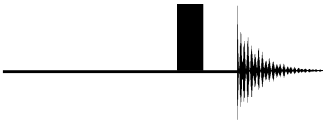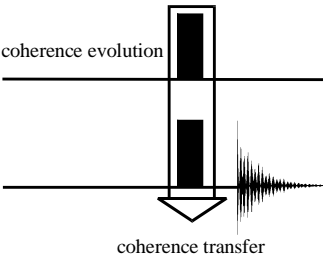
compromise must be made or special sequence elements added, see section 5.5.2.

- Homonuclear coupling evolution must also be taken into consideration. There are two types of heteronuclear correlation experiments: one bond and multiple bond correlation and homonuclear coupling becomes a serious problem with the latter. The periods of antiphase coherence evolution are noticeably different between these two types of experiment. In the one bond correlation experiment the evolution period is very short and homonuclear coupling evolution occurs to a negligible extent. However during the multiple bond correlation experiment the evolution period is relatively long and both antiphase coherence and homonuclear coupling evolution takes place. The reason is that for ^{13}C, ^{1}H spin systems the homonuclear coupling constants $^{n}J(H, H)$ is comparable in magnitude to the heteronuclear multiple bond coupling constants $^{2/3}J(C, H)$. However it also depends upon the nuclei in the spin system. Thus for one bond ^{19}F, ^{13}C correlation experiments homonuclear coupling evolution must be taken into account because $^{2}J(^{19}F, ^{19}F)$ is comparable to $^{1}J(^{19}F, ^{13}C)$.

5.5.1   Coherence Transfer Problems

As outlined in the introduction the maximum sensitivity gain shown in Table 5.13 for direct or ^{n}X detection experiments and Table 5.21 for indirect detection experiments cannot be guaranteed for a real sample.

Table 5.21:   Comparative sensitivity gain by coherence transfer in heteronuclear correlation spectroscopy [5.3].

$$\gamma(S)^{5/2} \bullet (1-\exp(-T/T^{S}_{1}))$$

$$\gamma(I) \bullet \gamma(S)3/2 \bullet (1-\exp(-T/T^{I}_{1}))$$

In the following *Check its* the possible deficiencies of the heteronuclear coherence transfer step in combination with the preparative evolution step are shown. In an attempt to represent a real sample a number of different values for $^nJ(C, H)$ are used to simulate the simultaneous chemical shift and homonuclear coupling evolution.

Bandwidth of coupling constants

5.5.1.1 Check it in NMR-SIM

Use the configuration file *ch5511.cfg* and edit the pulse sequence template according to the scheme below (**Edit│Pulse program**). Save the new sequence with the name *myhetco1.seq*. Replace the current pulse program with the new sequence. Simulate the ^{13}C spectrum for the spin system file *ch5511.ham* that contains a range of values for $^1J(^{13}C, ^1H)$ from 120 Hz to 200 Hz in 20 Hz increments. The value of **d2**: $1/(2 \bullet 140) = 0.00357s$. Inspect the processed spectrum and note how the intensity and antiphase coherence depends upon the coupling constant. To study the same effects for $^nJ(^{13}C, ^1H)$ replace the current spin system with the spin system file *ch5511b.ham* which has values from 2.5 Hz to 12.5 Hz in 2.5 Hz increments. Change the value of **d2**: $1/(2 \bullet 8) = 0.0625s$ and repeat the simulation.


```
            p1        p2        pulses          ph1=0
            ph1       ph2       phases          ph2=1
                                                ph3=0
f2:    d1         d2                            ph31=0


                   p3          pulses
                   ph3 ph31(rec) phases         p1(p3): 90° pulse (f2)
                                                p3(p1, p2): 90° pulse (f1)
f1:
```
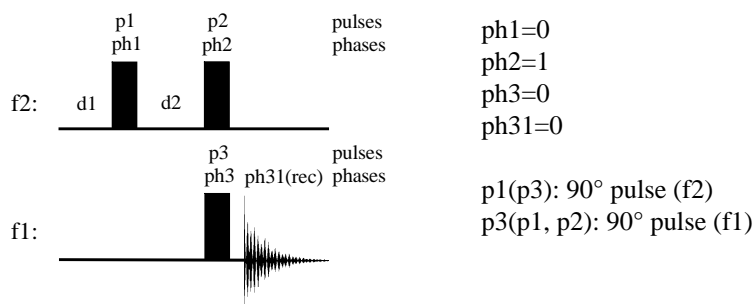
Chemical Shift evolution

5.5.1.2 Check it in NMR-SIM

Using the configuration file *ch5512.cfg* simulate the ^{13}C spectrum using the pulse sequence from previous *Check it 5.5.1.1*. To investigate the effect of ^1H chemical shift evolution during the d2 delay on the effectiveness of the coherence transfer change $J(^{13}C, ^1H)$ to *8* Hz which is a typical value for a two bond coupling (**Edit│Spin system**). Set **d2** to *0.0625*s and run a simulation. Modify the pulse sequence as shown below and run the simulation again after setting **d4**: $1 / (4 \bullet 140) = 1.78m$. Compare the results and note how the two 180° pulses (p2 and p3) refocus the chemical shift evolution.

ph1=0
ph2=0
ph3=0
ph4=1
ph5=0
ph31=0

p1(p5): 90° pulse (f1)
p2(p3): 180° pulse (f1)
p3(p1, p4): 90° pulse (f2)
p4(p2): 180° pulse (f2)
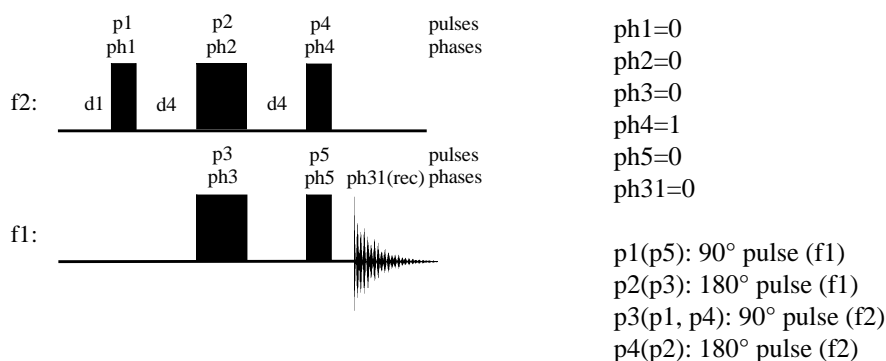
Homonuclear Coupling evolution

5.5.1.3 Check it in NMR-SIM

Load the configuration file *ch5513.cfg*. The spin system file contains different $^{13}C^1H(a)$-$^1H(b)$ groups where $J(^{13}C, {}^1H(a))$ is fixed at 140 Hz and the value of $J(^1H(a), {}^1H(b))$ varies over a range of 2 to 60 Hz. Run the simulation. Change the value of $J(^{13}C, {}^1H(a))$ to 8 Hz which corresponds to a typical $^nJ(^{13}C, {}^1H)$ coupling by editing the spin system and modifying the line: *weak a b 8*. Set **d4**: 1 / (4 • 8 [Hz]) = *0.03125s* and repeat the simulation.

5.5.2 Delay Incrementation - Constant Time Principle and Accord-Principle

Delay incrementation is a prerequisite of n-dimensional NMR spectroscopy. During a selected free precession period, called the t_1 period in a 2D experiment, either coupling or chemical shift evolution of a particular NMR-active species i.e. ^1H, ^{13}C occurs. In a J-resolved (JRES) experiment the coupling evolves whilst in a chemical shift resolved (COSY) experiments the chemical shift evolves. The selected free precession period is then incremented in subsequent experiments to generate a modulation of the directly detected response during the t2 period.

During the t1 period of heteronuclear COSY experiments homonuclear ^1H-^1H coupling can also evolves resulting in the correlation peaks in the processed data being split due to coupling in the f1 dimension. This splitting decreases the signal intensity and thus the sensitivity of the experiment and also precludes the differentiation between correlation peaks with similar chemical shift. The purpose of the constant time principle [5.170], is to overcome this homonuclear coupling whilst allowing signal modulation during the t1 period. Two delays are included in the pulse sequence before and after the t1 period that are decremented simultaneously with the incrementation of the t1 period. Thus, the homonuclear coupling evolves to the same degree in all experiments and the Fourier transformation in the f1 dimension neglects this constant modulation. The

constant time strategy is particularly important in heteronuclear multiple-bond correlation experiments. It was first introduced in the COLOC sequence [5.170] and has also been proposed for "inverse" detected HMBC experiments [5.171] to record spectra with higher sensitivity and sharp correlation peaks making spectra easier to interpretation.

The Constant-Time HMBC experiment
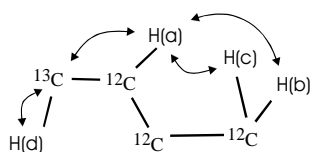
5.5.2.1 Check it in NMR-SIM

To compare the constant time and ^{13}C, ^{1}H HMBC experiment using the test spin system shown on the left load the configuration file *ch5521.cfg*. The arrows in the figure denote homonuclear and heteronuclear coupling. Simulate the gradient selected HMBC experiment. Replace the current pulse program with the pulse program file *ghmbc2ct.seq* and repeat the simulation. The decrement of d3 has to be equal to in0 and d3 > in0 • td1.
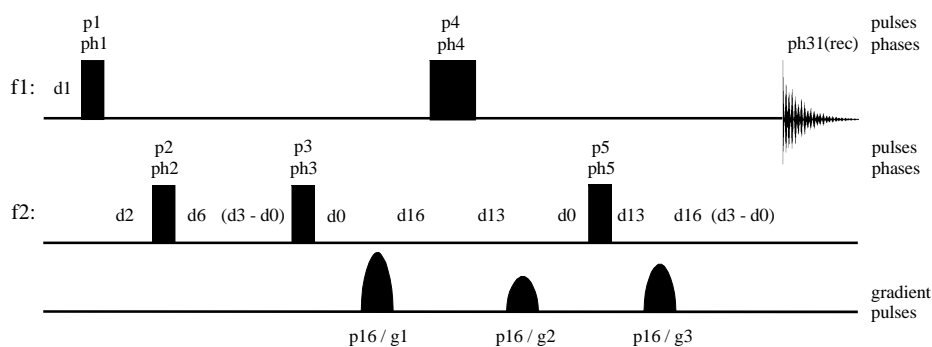
The constant-time HMBC experiment [5.171].

A perennial problem with coherence transfer experiments is the choice of coupling constant to use for calculating the free precession period prior to the coherence transfer step. The same problem arises when calculating the refocusing delay after a coherence transfer step prior to data acquisition under decoupling.

It is possible to perform homonuclear COSY experiment kinetic studies by introducing an additional delay incrementation into the pulse program to create the ACCORDION experiment [5.133]. The ACCORD-HMBC [5.172] experiment has been proposed as a method of overcoming the need for an exactly defined delay period. Because of the wide range of long-range ^{13}C, ^{1}H coupling constants correlation peaks which might be valuable for signal assignment are diminished in intensity due to the delay period being inappropriate for the particular value of $^{n}J(C, H)$. Only if the delay and coupling constant match will perfect antiphase coherence evolve in the common

HMBC experiment. However as already discussed decreasing the corresponding free precession period prior to the coherence transfer reintroduces splitting due to ^{1}H, ^{1}H coupling in the f1 dimension. So alternative experiments such as IMPEACH-HMBC and CIGAR-HMBC experiment have been designed to suppress this splitting [5.173, 5.174, 5.175].

In *Check it 5.5.2.2* the ACCORD-HMQC experiment is simulated [5.176]. This experiment is characterized by a low sensitivityof resulting signals to varying ^{n}X, ^{1}H coupling constants, but an unwanted modulation in the f1 dimension that is a function of the incrementation and the underlying heteronuclear coupling constant. The ACCORD-HSQC experiment [5.177] has been suggested to overcome this modulation in the f1 dimension.

The ACCORD-HMQC experiment

5.5.2.2 Check it in NMR-SIM

Using the configuration file *ch5522.cfg* run the simulation of the ^{13}C, ^{1}H ACCORD-HMQC experiment for a spin system of four ^{13}C^{1}H groups with different ^{n}J(^{13}C, ^{1}H) values: 1, 2.5, 7.5 and 14 Hz. For comparison simulate the common gradient selected ^{13}C, ^{1}H HMBC experiment.
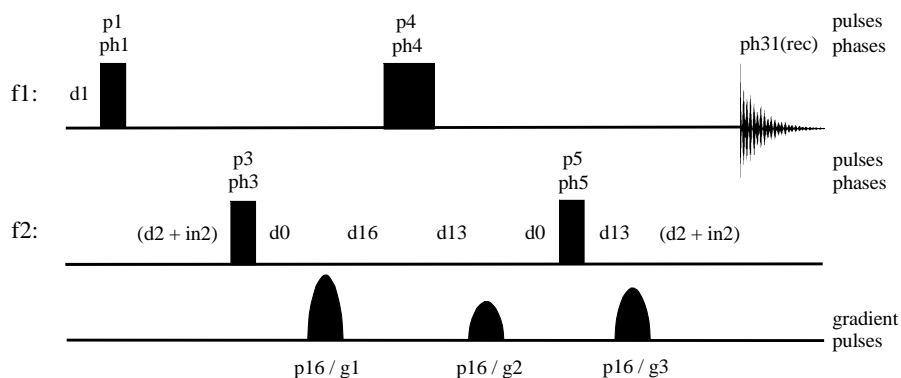
The ACCORD-HMQC experiment.

Using *Check it 5.5.2.2* as a basis investigate the ACCORD-HMBC experiment using the pulse sequence enclosed in the file *gachmb2.seq*.

5.6 Heteronuclear Correlation Experiments I - ^nX Detected Experiments

The discussion of heteronuclear correlation experiments is overdue with many of the requirements being already covered in earlier chapters. The main tools can be summarized as follows:

> Coherence transfer: The basic steps of heteronuclear coherence transfer units such as INEPT or DEPT have been outlined in section 5.2.6 on multiplicity edited experiments. Sensitivity gain by coherence transfer has been discussed in section 5.5.1.
>
> Coherence selection by phase cycling and gradients: The theoretical aspects and the resulting commands for delay incrementation, phase cycling and choice of gradient strength are included in section 2.3.3

The following discussions on heteronuclear correlation experiments in sections 5.6.1, 5.6.2 and 5.6.3 relate to ^1H, ^{13}C spin systems, but the discussions are also valid for ^{19}F as a sensitive nucleus and for all other heteronuclei instead of the ^{13}C isotope.

5.6.1 ^1H, ^nX HETCOR Experiment

The heteronuclear correlation experiment offers further possibilities to verify the proposed structure of an unknown sample. Organic compounds in particular are widely analysed by heteronuclear ^1H, ^{13}C correlation experiments but nowadays ^1H detected experiments are preferred because of their higher sensitivity to the NMR experiment of ^1H which reduce substantially the experiment time.

Both ^nX detected experiments as well as ^1H detected experiments are classified according to the structural information obtained. Based on the experimental knowledge that the coupling constant between nuclei decreases significantly the heteronuclear correlation experiment can be operated to detect either correlation peaks between directly bonded nuclei or between remote nuclei in the molecular structure. A delay period is set to permit the coherence evolution of only one of these connectivities.

The HETCOR experiment is designed primarily for one-bond detection with direct detection of the heteronuclei in the t2 acquisition period. After an excitation pulse, ^1H nuclei evolve under coupling and chemical shift influence in the t1 period. During a longer second period ^1H antiphase coherence is created. The following transfer by two rf pulses generates ^{13}C antiphase coherence which may be detected directly or after a refocusing period converted into in-phase coherence. Only in-phase coherence can be detected using broadband decoupling.

Sequence features:

Purpose / principles: Correlation of ^1H and ^nX signals by scalar $^1J(^1H, ^nX)$ coupling, ^{13}C detection, intensity enhancement by single polarization transfer

Variants: HETCOR [5.178], HMQC-DEPT [5.73], BIRD-HETCOR [5.179, 5.180, 5.181]

This section on the HETCOR experiments focuses on the susceptibility of the pulse sequence to the "refocusing delay", which is necessary for decoupling during acquisition, and for the suppression of ^1H, ^1H coupling evolution in the t1 period. The alternative DEPT-HETCOR experiment is introduced to emphasize that the coherence transfer and the preceding coherence preparation are obtained using the two common steps outlined in section 5.5.1.

Chemical shifts
$\delta(^1H)$: H(1): 2.0; H(4): 4.0; H(5): 5.0
$\delta(^{13}C)$: C(1): 36; C(3): 180;, C(4): 60; C(5): 40
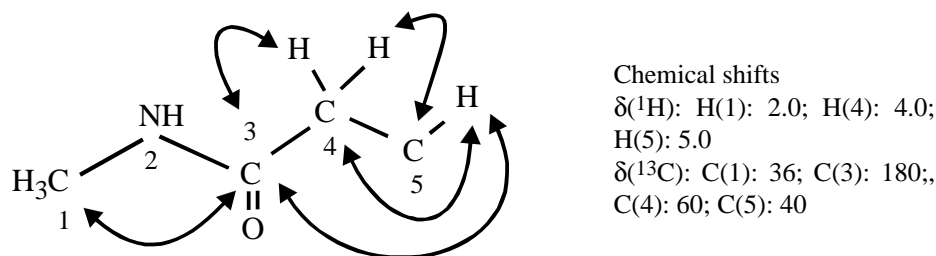
Fig. 5.28: Test spin system for the HETCOR experiments. The arrows denote the long-range heteronuclear coupling.

The test spin system for all the HETCOR experiments is the carbonic acid amide skeleton shown in Fig 5.28. Two spin system files are involved: the file *ch561.ham* which considers only H, H coupling and $^1J(C, H)$ coupling and the file *ch561lr.ham*, which also includes the long-range heteronuclear coupling as shown in the figure.

In the following *Check its* the reader will be instructed to write their own HETCOR pulse program and to simulate both the one-bond and multiple-bond ^{13}C, ^1H correlation experiments.

5.6.1.1 Check it in NMR-SIM

Load the configuration *ch5611a.cfg* and edit the ^{13}C, ^{1}H HETCOR pulse program according to the scheme given below. Save the pulse progam with the name *myhxco.seq*. Run a simulation using the spin system *ch5611.ham*. Then load the configuration file *ch5611b.cfg* to simulate the HETCOR experiment using the multiple-bond ^{13}C, ^{1}H coupling. The new configuration file sets the correct delay parameters and the spin system file *ch5611lr.ham*. Using the configuration files *ch5611c.cfg* and *ch5611d.cfg* calculate the corresponding ^{1}H and $^{13}C\{^{1}H\}$ spectra to use as projections.

The HETCOR experiment.

pulses phases
$ph1=0$
$ph2=(0)_4(2)_4$
$ph3=0\ 2\ 1\ 3$
$ph4=(0)_8(1)_8(2)_8(3)_8$
$ph31=(0\ 2\ 1\ 3)_2$
$\quad\quad (1\ 3\ 2\ 0)_2(2\ 0\ 3\ 1)_2$
$\quad\quad (3\ 1\ 0\ 2)_2$
$p1(p4)$: 90° pulse (f1)
$p2(p2)$: 180° pulse (f1)
$p3(p1, p3)$: 90° pulse (f2)
d1: relaxation delay
d0: incremented delay
$d2: = 1 / (2 \bullet {}^{1}J(^{n}X, {}^{1}H))$
$d3: = 1 / (3 \bullet {}^{1}J(^{n}X, {}^{1}H))$
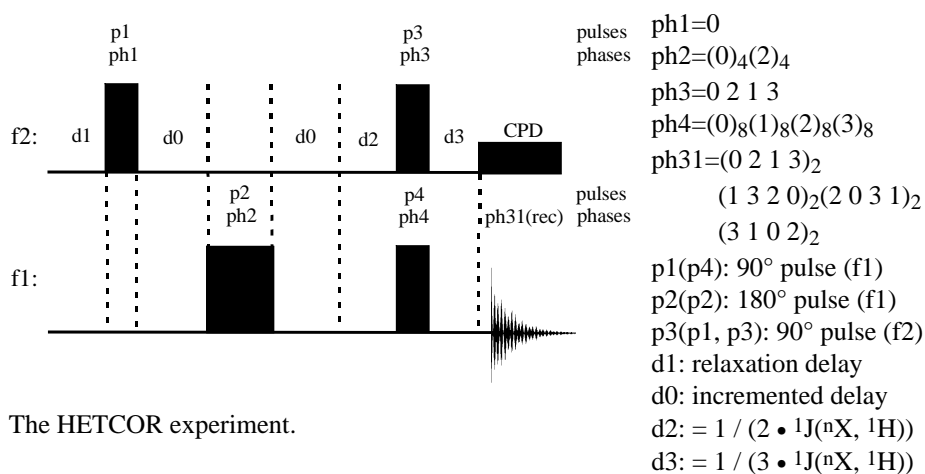
Because of the low sensitivity ^{n}X detected heteronuclear correlation experiments are invariable acquired using broadband decoupling. However after the coherence transfer step the coherence state must be refocused because simply switching on the decoupler for the antiphase coherence would result in a signal of zero intensity. Initially it may seem surprising that the delays before and after the coherence step are different. In the preparatory delay the antiphase coherence state is generated and reversed in the subsequent period. However, in both periods the evolving coherence is different: in the first period the ^{1}H coherence evolves while in the second period it is the ^{13}C coherence. Consequently, in the first period the multiplicity of the $^{13}C^{1}H_n$ group is irrelevant while in the second period the evolution of ^{13}C coherences of the $^{13}C^{1}H_n$ group is subject to the multiplicity. Thus the delay $d3 = 1/(3 \bullet {}^{1}J(C, H))$ is a simple compromise to achieve satisfactory intensity of any CH_n group.

5.6.1.2 Check it in NMR-SIM

Using the configuration file *ch5612.cfg* open the parameter optimizer (**Utilities│Optimize parameter**), select the options **Show result as**: *1D series*, **N**: *6*, **Step**: *10*, **Selected optimized parameter**: *d3*, **d3**: *0.002* and

in3: *0.2m* in the dialog boxes and start the calculation for the 1D HETCOR experiment. To compare the intensity modulation for each type of CH$_n$ group, change the multiplicity factor in the spin system for proton b from *3* to *2* to *1*.

A bigger problem in HETCOR experiments is the H, H coupling during the t1 period which produces a line splitting of the correlation peaks in the f1 dimension. In addition to enlarging the peak contour this unresolved splitting reduces signal intensity. Incorporation of a BIRD pulse [5.179] suppresses the H, H coupling evolution in the f1 dimension.
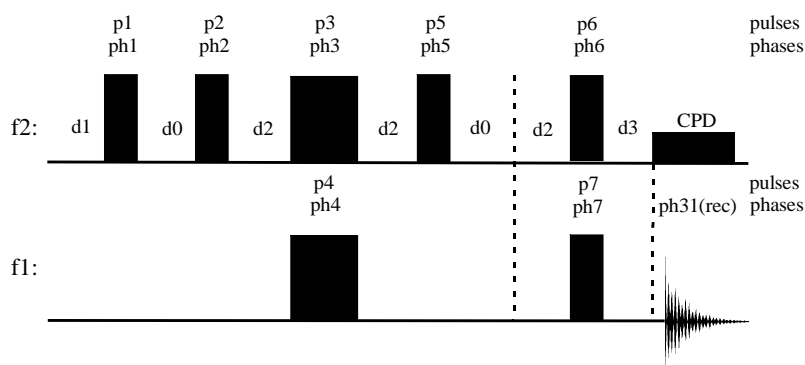
ph1=0
ph2, ph5= (1)$_4$(2)$_4$(3)$_4$(0)$_4$
ph3=(0)$_4$(1)$_4$(2)$_4$(3)$_4$
ph4=(0)$_4$(2)$_4$
p1(p1, p2, p5, p6): 90° pulse (f1)
p2(p3): 180° pulse (f1)

ph6=0 2 1 3
ph7=(0)$_8$(1)$_8$(2)$_8$(3)$_8$
ph31=(0 2 1 3)$_2$(1 3 2 0)$_2$
          (2 0 3 1)$_2$(3 1 0 2)$_2$
p3(p7): 90° pulse (f2)
p4(p4): 180° pulse (f2)

BIRD-HETCOR experiment.

5.6.1.3 Check it in NMR-SIM

Simulate the ^{1}H, ^{13}C HETCOR experiments for the basic HETCOR and the BIRD-HETCOR experiment which suppresses homonuclear coupling evolution during the t1 period. Use the configuration file *ch5613.cfg*. For the second simulation replace the current pulse sequence with the BIRD-HETCOR pulse program *hxcobi.seq* (**File│Pulse program...**). Compare the correlation peak at δ(^{13}C): 20 / δ(^{1}H): 1 for the resolved splitting due to ^{1}H, ^{1}H coupling in the f1 dimension in both spectra.

As an alternative method to achieve coherence transfer, the DEPT element can be implemented in the HETCOR experiment. This modification makes the HETCOR experiment a multiplicity selective method.

5.6.1.4 Check it in NMR-SIM

To examine the ^{1}H, ^{13}C DEPT-HETCOR(TPPI) experiment load the configuration file *ch5614.cfg*. Perform three simulations (**nd0**: *2*) with different pulses **p5**: *45d, 90d* and *135d*. Compare the spectra for the detected correlation and inspect the different signal phases of the CH$_2$ signal relative to other CH$_n$ groups in the experiment with **p5**: *135d*. Because of the phase sensitive detection the spectra can be phased correctly. Try to determine if the delay d2 prior to data acquisition might be defined as d3 using a duration as discussed in *Check it 5.6.1.2*.

The DEPT-HETCOR experiment.

ph1=0
ph2= 0 0 2 2
ph3=(0)$_4$(1)$_4$(2)$_4$(3)$_4$
ph4=0 0 2 2 1 1 3 3
ph5=1 3
ph31=(0 2)$_2$
     (1 3)$_2$(2 0)$_2$(3 1)$_2$
p1(p3): 90° pulse (f1)
p2(p4): 180° pulse (f2)
p3(p1): 90° pulse (f2)
p4(p2): 180° pulse (f2)
p5(p5): 45°, 90° or 180° pulse (f2)
d0: incremented delay
d1: relaxation delay
d2 : = $1/(2 \cdot {}^1J(^nX, {}^1H))$
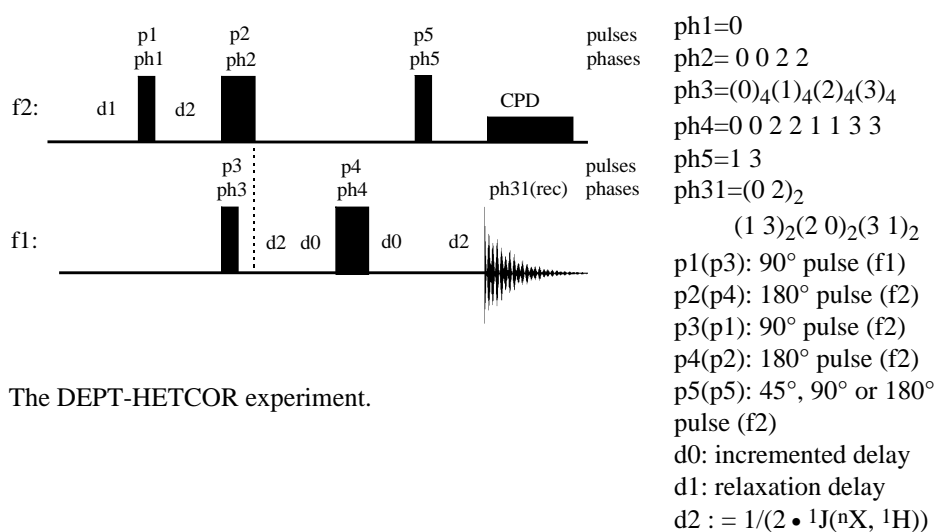
5.6.2 ^{1}H, ^{n}X COLOC Experiment

In most cases, structure analysis of organic molecules which is based exclusively on the proton, proton coupling network is ambiguous even if sophisticated ^{1}H, ^{1}H correlation experiments are applied. If quaternary carbon atoms or other heteronuclear atoms form part of the molecular skeleton the structural determination will fail if the proton scalar coupling cannot be traced beyond these atoms. Sometimes these is confusion over the assignment of ^{2}J(H, H) and ^{3}J(H, H) coupling constants which also effects the structural determination. More information is available from ^{1}H, ^{13}C correlation experiments, since the scalar coupling constants ^{1}J(^{13}C, ^{1}H) and $^{2/3}$J(^{13}C, ^{1}H) differ by a factor of ten. Pulse sequences have been developed to discriminate between correlation peaks that arise from a specific scalar coupling.

To overcome the imperfections of the HETCOR experiment (section 5.6.1) the COLOC sequence has been designed to detect long-range correlation peaks. The sequence is a constant-time experiment which suppresses peak splitting in the f1

dimension that arise from homonuclear H, H coupling. As described in section 5.5.2 the constant-time procedure relies on two incremented d0 periods during which the heteronuclear coherence evolves. As the delay d0 is incremented an addition delay d5 is decremented by twice the d0 increment to guarantee a constant time for each experiment. The overall result is the same ^{1}H chemical evolution of each experiment, e.g. signal modulation, which does not lead to a further signal splitting in the f1 dimension of the Fourier transformed spectrum.

The original COLOC sequence did not attempt to suppress [1]J(C, H) correlation peaks using a low-pass J filter, which is part of the HMBC experiment (section 5.8.3). The authors who proposed the COLOC sequence [5.170] stated that there would be no practical improvement using additional [1]J(C, H) suppression elements [2]. However, several modified COLOC experiments have been published to suppress [1]J(C, H) correlation peaks and spectrum artefacts that are introduced by pulse imperfections. The "BIRD-COLOC" sequence [3] uses two BIRD units to suppress the one-bond ^{1}H, ^{13}C correlation peaks [5.182]. The alternative "TANGO-COLOC" [5.183] is similar to the "BIRD-COLOC" experiment except that a TANGO unit replaces the first BIRD unit. The S-COLOC sequence [5.94] utilizes the COLOC-TANGO sequence plus an additional 180° [13]C pulse to enhance the constant-time procedure.
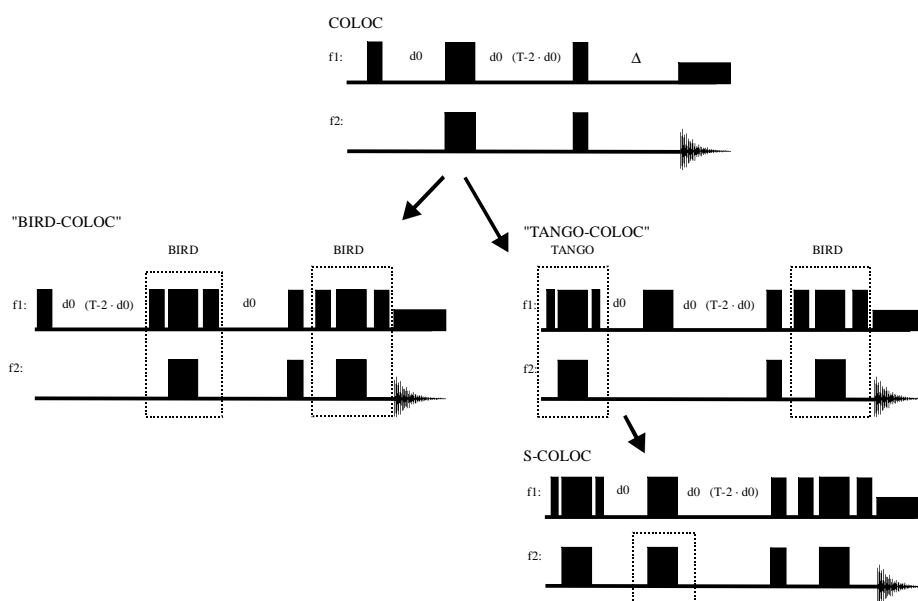
Fig. 5.29: "BIRD-COLOC", "TANGO-COLOC" and S-COLOC - modifications of the original COLOC experiment.

Sequence features:

Purpose / principles:	Correlation of ^1H and ^nX signals by scalar $^1J(^1H, ^nX)$ coupling, ^{13}C detection, intensity enhancement by single polarization transfer, constant time principle for homonuclear coupling suppression in the f1 dimension
Variants:	COLOC [5.170, 5.184], "BIRD-COLOC"[1] [5.182], "TANGO-COLOC"[1] [5.183], S-COLOC [5.94]

[1] The acronyms are not literature references, but they describe the modifications in comparison with the original sequence.

In *Check it 5.6.2.1* the basic COLOC sequence is written.

5.6.2.1 Check it in NMR-SIM

Load the configuration *ch5621a.cfg*. Edit the pulse program template (**Edit│Pulse program**) and enter the COLOC pulse sequence shown below. Add the necessary pulses, delays, phase programs and increment and decrement commands to the template, saving the new sequence with the name *mycoloc.seq*. Run a simulation using the spin system file *ch562*.ham.

The COLOC experiment.

p1(p1, p4): 90° pulse (f1)
p2(p2): 180° pulse (f1)
p3(p5): 90° pulse (f2)
p4(p3): 180° pulse (f2)

d0 = incremented delay
d1: relaxation delay
d2: definite value > td1 • in0
d3: = 1 / (3 • ^nJ(C, H))
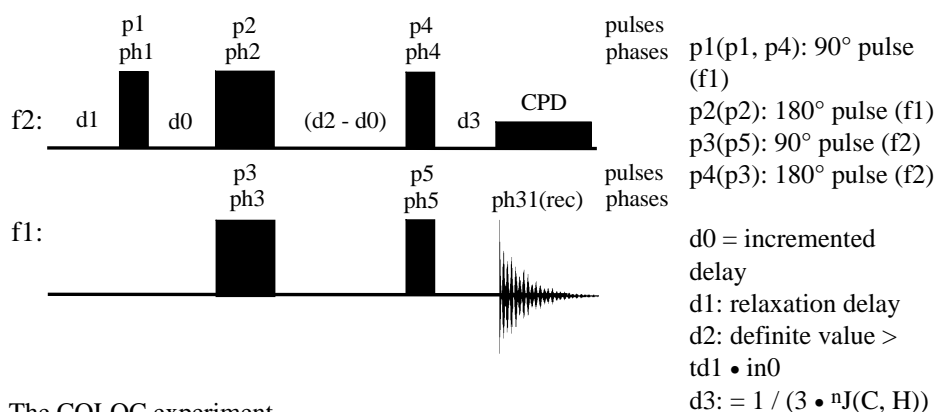
ph1=(0)$_8$(1)$_8$(2)$_8$(3)$_8$
ph2, ph3=(0 0 1 1 2 2 3 3)(1 1 2 2 3 3 0 0)(2 2 3 3 0 0 1 1)(3 3 0 0 1 1 2 2)
ph4=(0 2 1 3)$_2$(1 3 2 0)$_2$(2 0 3 1)$_2$(3 1 0 2)$_2$
ph31=(0 0 2 2)$_2$(1 1 3 3)$_2$(2 2 0 0)$_2$(3 3 1 1)$_2$

In the following *Check it* two alternative COLOC-related experiments "TANGO-COLOC" and S-COLOC versions are compared.

5.6.2.2 Check it in NMR-SIM

Open the configuration file *ch5622a.cfg* and simulate the TANGO-COLOC experiment. Use the file *ch5622b.cfg* to calculate the S-COLOC sequence spectrum.

5.7 Heteronuclear Correlation Experiments II - ^{1}H Detected Experiments

Heteronuclear correlation experiments with ^{1}H detection in the direct acquisition period t2 are often called inverse detected experiments. The term "inverse" is also used to describe probeheads that are constructed with the ^{1}H coil as the inner coil and the rf coil for the heteronuclear frequency as the outer coil. The outer coil has a lower sensitivity because of the lower fill factor. This term may also be used to distinguish between two classes of experiments. The HETCOR and COLOC experiments belong to the class of direct detection experiments with take advantage of the coherence transfer from the sensitive nucleus to the relatively insensitive heteronucleus. This type of experiment is illustrated by the first entry in Table 5.22. However experiments in this category are no longer popular and have been superseded by inverse detected experiments, shown in the second entry in Table 5.22. In a comparison of the different types of experiments the ^{1}H detected heteronuclear correlation experiments have three distinct advantages over the ^{n}X detected experiment:

- The population difference between the spin states oriented parallel and antiparallel to the B_0 field is a function of the gyromagnetic ratio of the observed nucleus. Since ^{1}H has the highest gyromagnetic ratio, ^{1}H detection is more sensitive than the detection of any other NMR-active nucleus.
- Generally the sensitivity of the NMR experiment, excluding population difference, is a function of the gyromagnetic ratio of the observed nucleus increasing the sensitivity of ^{1}H detection.
- Because the ^{1}H nuclei have shorter relaxation times than most heteronuclei, higher pulse rates can be used in heteronuclear ^{1}H detected correlation experiments.

Table 5.22:   Sensitivity of "inverse" detected experiments under ideal conditions [5.3].

$\gamma(I)^{3/2}\,\gamma(S) \bullet (1-\exp(-T/T^{S}_1))$

$\gamma(I)^{5/2} \bullet (1-\exp(-T/T^{I}_1))$

[1]H detected heteronuclear experiments has two main disadvantages:

- Homonuclear ^{1}H, ^{1}H coupling can evolve with the first ^{1}H excitation pulse.
- NMR-active heteronuclei are often only the minor component in the isotope mixture of an element. Consequently the ^{1}H coherences from several isotopomers, which do not contain the NMR-active isotope, contribute to the ^{1}H detected signal and these often strong signals must be suppressed.

5.7.1   [n]X, ^{1}H HMQC Experiment

The main effort in developing [n]X, ^{1}H HMQC pulse sequence to use with organic compounds has been the suppression of coherence which belongs to ^{12}C isotopomers. The most effective method for suppressing ^{12}C isotopomer coherence is gradient selection but two other techniques have been proposed using a BIRD or a TANGO sandwich. The latter is based on a pulse combination which acts as a 360° pulse for ^{1}H coherence which evolve under ^{1}H, ^{13}C coupling whilst acting as a 90° pulse for ^{1}H coherence without ^{1}H, ^{13}C interaction as in a ^{12}C isotopomer. The BIRD sequence is based on selective inversion of the ^{1}H magnetization associated with the ^{12}C isotopomer combined with a longitudinal relaxation period that forms part of a pulse sequence. The overall result is that the pulse combination acts as a 90° pulse for the ^{1}H, ^{13}C coherence

whilst the ^1H magnetization of the ^{12}C isotopomer is reduced in intensity nearly to zero. The main disadvantages of the BIRD unit is that it relies on ^1H longitudinal magnetization having the same or similar T_1 relaxation times and that the applied relaxation delay generally reduces the signal intensity.

Sequence features:

Purpose / principles:	Correlation of ^1H and ^nX signals by scalar $^1J(^1H, {}^nX)$ coupling, ^1H detection, intensity enhancement by polarization transfer
Variants:	HMQC [5.185, 5.186, 5.187], BIRD-HMQC [5.188], relayed HMQC [5.189], DEPT-HMQC [5.68], gs-HMQC [5.190, 5.191, 5.192], TANGO-SL-HMQC, HMQC-TOCSY [5.193]

In *Check it 5.7.1.1* the basic structure of the 1D HMQC experiment is introduced. The limits of ^1H coherence suppression of ^{12}C isotopomers, the so-called ^{12}C coherence, by phase cycling is shown and the use of the BIRD-d7 filter element as one solution to this problem is illustrated.

5.7.1.1 Check it in NMR-SIM

(a) Open the configuration file *ch5711a.cfg*. Use the NMR-SIM editor to write the pulse sequence shown below adding the phase programs. Start the simulation for the given spin system.

(b) To inspect the limits of the phase cycling driven suppression of ^{12}C coherence, change the receiver phase program of the pulse program to the following and run the simulation again.

ph31=(360) 0 271 180 90 179 90 0 270


```
ph1(ph1)=0
ph2(ph3)=0
ph3(ph2)=0 1 2 3
ph4(ph4)=(0)4(2)4
ph31=0 3 2 1 2 1 0 3

p1(p1): 90° pulse (f1)
p2(p3): 180° pulse (f1)
p3(p2, p4): 90° pulse (f2)
d1: relaxation delay
d2: = 1 / (2 • 1J(nX, 1H))
```
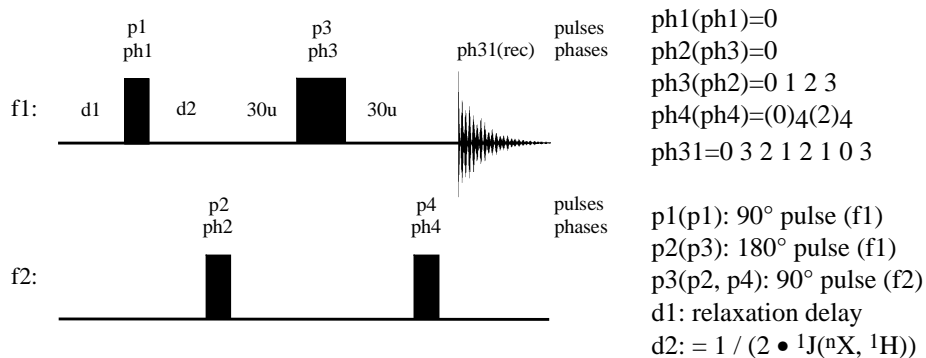
1D HMQC experiment.

(c) The BIRD-HMBC sequence is one alternative method for suppressing ^1H, ^{12}C coherence. The BIRD element selectively inverts the unwanted ^1H coherence that then undergoes T_1 relaxation during the d7 delay period to

zero amplitude in the z-direction. To assess the effectiveness of the BIRD element in suppressing ^{1}H, ^{12}C coherence run two simulations using different values for d7. Load the configuration file *ch5711b.cfg* and run the first simulation with a delay **d7**: *30u*. In the spin system file the relaxation time T_1 and T_2 of all the ^{1}H spins is set to 0.5s so in the second simulation use a delay **d7**: *0.34s*. The delay d7 corresponds to t_{null} = T_1 • ln2 = 0.5 • ln2 = 0.34s. Even when the receiver phase cycling is not optimum with the BIRD element there is extremely good ^{1}H, ^{12}C coherence suppression.

ph31=(360) 0 175 180 5.

(d) Repeat the simulations for the corresponding two dimensional experiments with decoupling during acquisition and compare the t1 noise. Use the configuration files *ch5711c.cfg* and *ch5711d.cfg* and change the optimum phase cycling program of the receiver phase for instance and the **d7** parameter of the 2D BIRD-HMQC experiment.

The results of *Check it 5.7.1.3* illustrate a number of important points about suppressing ^{1}H, ^{12}C coherence. Extensive phase cycling suppresses this coherence but increases the overall experiment time whilst being susceptible to minor variations in the receiver phase settings. Sequences such as the BIRD element are effective and relatively insensitive to phase minor variation but they prolong the time before the data acquisition starts. Hence signal loss due to relaxation must be accepted and the sensitivity of the pulse sequences is reduced. Coherence suppression using gradient selection is an effec-
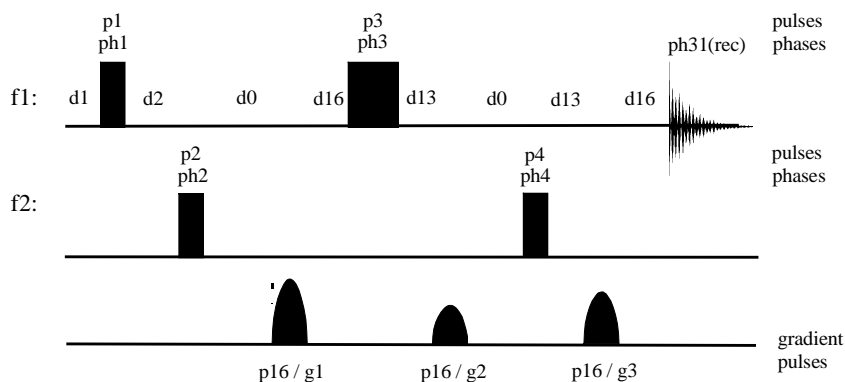
The gradient selected HMQC(mc) experiment.

ph1=0	p1(p1): 90° pulse (f1)	d0: incremented delay (f1)
ph2=0	p2(p3): 180° pulse (f2)	d1: relaxation delay
ph3=(0 2)	p3(p2, p4): 90° pulse (f2)	d2: = 1 / (2 • ^{1}J(C, H))
ph4=(0)$_2$(2)$_2$		d13: switch delay
ph31=(0 2 2 0)		d16: gradient recovery delay

tive method of reduce phase cycling and thus experiment time, although the gradient selection in itself reduces the sensitivity. Gradient selection is based on destroying the unwanted coherences by dephasing in a gradient field whereas phase cycling is based on the constructive and destructive accumulation of signal intensities along different coherence pathways. Consequently in a phase cycled experiment the acquired signal can consist of coherences from several pathways whilst in the gradient selection experiment the acquired signal is from one specific pathway only.

5.7.1.2 Check it in NMR-SIM

The gradient selected 2D HMQC(mc) experiment can be run with one scan per increment in comparison to the minimum of four scans per increment for the phase cycled HMQC experiments. Therefore, simulate the HMQC experiment using the configuration file *ch5712.cfg* with **NS**: *1*.

The HMQC sequence does not necessarily have to be based on the coherence transfer step shown in the sequence scheme above. The coherence transfer can also be generated by a DEPT element which has the advantage in a phase sensitive experiment of labelling the signal phase according to the multiplicity of the ^nX, ^1H spin groups.

5.7.1.3 Check it in NMR-SIM

Load the configuration file *ch5713.cfg* and simulate four experiments with different values of pulse **p4**: *60d*, *90d*, *120d* and *180d*. Inspect the processed 2D experiment for the changing sign of the signal amplitude and suppressed ^{13}C signals of particular multiplicity (p4: 90°).
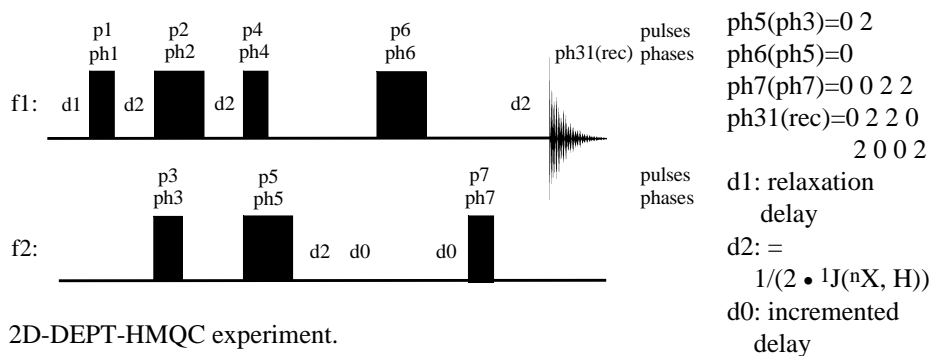
2D-DEPT-HMQC experiment.

ph5(ph3)=0 2
ph6(ph5)=0
ph7(ph7)=0 0 2 2
ph31(rec)=0 2 2 0
                2 0 0 2
d1: relaxation
    delay
d2: =
    $1/(2 \cdot {}^1J(^nX, H))$
d0: incremented
    delay

p1(p1): 90° pulse (f1)   p4(p5): 180° pulse (f1)
p2(p2, p6): 180° pulse (f1)   p5(p4): 60°, 90°, 120° or 180° pulse (f1)
p3(p3, p7): 90° pulse (f2):

Pulse p4 in the above scheme is the pulse that determines the signal detection and the signal phase as a function of the ^nXH_n multiplicity.

p4	positive	negative signal amplitude
$60°$ pulse	^nXH	$^nXH_2$, $^nXH_3$
$90°$ pulse	$^nXH_2$ only	
$120°$ pulse	$^nXH_3$	^nXH, $^nXH_2$
$180°$ pulse	$^nXH_2$	^nXH, $^nXH_3$

The advantages of relay coherence in assigning signals in the same molecule have already been discussed in section 5.4.1.3 in some detail. Briefly the connectivities of remote protons which do not couple can be proved by the coupling of each proton to a third coupling partner, which may be either the same or a different isotope (homonuclear and heteronuclear relay step). This relay element can also be implemented in HMQC experiments and in *Check it 5.7.1.4* the HMQC and relay-HMQC experiments for signal assignment using a heteronuclear relay step are compared.

5.7.1.4 Check it in NMR-SIM

Load the file *ch5714.cf*g and simulate the ^{13}C, ^1H relay HMQC and the basic ^{13}C, ^1H HMQC experiment. Replace the current pulse program with the common HMQC experiment *hmqc2nd.seq* and repeat the calculation. Inspect the processed spectra for the additional relay correlation peaks in the relay HMQC experiment.
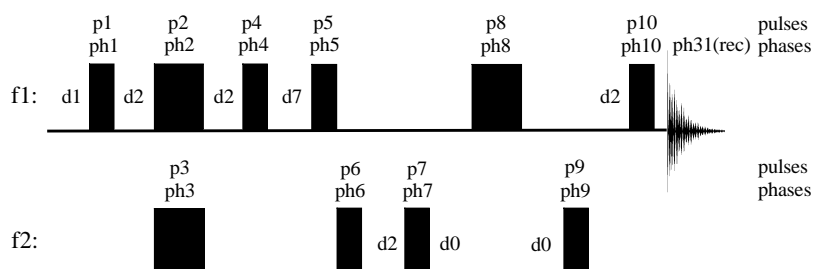
The relay HMQC pulse sequence with BIRD-d_7 element.

As discussed in section 5.4.2, TOCSY experiments also provide the same proof of remote connectivities in homonuclear spin systems as relay experiments. Hence the relay-HMQC experiment is also equivalent to the TOCSY-HMQC experiment, introduced in *Check it 5.4.2.4*.

5.7.2 ^nX, ^1H HSQC Experiment

A major drawback of the HMQC sequence is the H, H coupling-induced splitting of each correlation peak in the f1 dimension. As shown for the BIRD-HETCOR experiment in section 5.6.1 this splitting can cause broader lineshapes, if the splitting is unresolved,

such that the correlation peaks which belong to different spin groups but with similar chemical shifts cannot be identified. The origin of this splitting is the H, H coupling evolution of the double quantum coherence, such as I_xS_y ($I = {}^1H$, $S = {}^nX$), after the first coherence transfer during the t1 period. In the HSQC experiment the single quantum coherence arises after the coherence transfer and is generated by an additional 90° ^1H pulse that is not part of the coherence transfer step.

Particular improvements to the HSQC experiment has been the implementation of phase sensitive echo/antiecho-detection in combination with gradient coherence selection. Further variants include the sensitivity-enhanced HSQC experiment [5.194] and experiment developed for long-range coupling detection and J-scaled experiments (for references see sections 5.2.5 and 5.7.3).

Of course, the HSQC experiment is not the perfect solution for the detection of one-bond correlation spectra, since artefacts can also be observed. Some studies have determined the cause of these artefacts which can be assigned to off-resonance effects of the 180° ^nX pulses and H, H coupling [5.195, 5.196].

Sequence features:

Purpose / principles:	Correlation of ^1H and ^nX signals by scalar $^1J(^1H, {}^nX)$ coupling, evolution of single quantum IS coherence during the t1 period
Variants:	HSQC [5.197], sensitivity enhanced HSQC [5.194], α/β HSQC [5.198, 5.199], EXSIDE [5.40], HSQC-TOCSY [5.37], excitation sculpted HSQC [5.200]

Check it 5.2.7.1 introduces the phase cycled HSQC experiment.

5.7.2.1 Check it in NMR-SIM

Using the configuration file *ch5721.cfg* create the phase sensitive HSQC experiment with decoupling during acquisition The pulse sequence scheme is given below. The template incorporates the necessary commands for TPPI detection. Save the new sequence with the name *myhsqc2n.seq* and test the sequence with the current spin system.
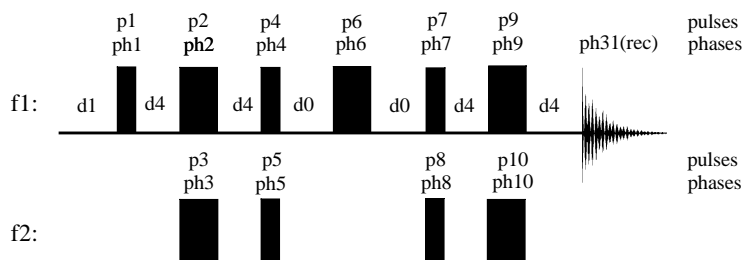
The HSQC(TPPI) experiment.

ph1(ph1)=0

ph2(ph2, ph6, ph9)=0

ph3(ph4)=1

ph4(ph7)=1

ph5(ph3, ph10)=$(0)_4(2)_4$

ph6(ph5)=(0 2)

ph7(ph8)=$(0)_2(2)_2$

ph31=(0 2 2 0)

p1(p1, p4, p7): 90° pulse (f1)

p2(p2, p6, p9): 180° pulse (f1)

p3(p5, p8): 90° pulse (f2)

p4(p3, p10): 180° pulse (f2)

d0: incremented delay

d1: relaxation delay

d4: = $1 / (4 \cdot {}^1J(C, H))$

A further improvement is the gradient selected HSQC experiment that can be run like the gradient selected HMQC experiment with one scan per experiment. In the following *Check it* an experiment with decoupling during acquisition is simulated and compared with the other HSQC experiments which differ in the detection mode and the sensitivity enhancement.

5.7.2.2 Check it in NMR-SIM

(a) Gradient selected HSQC(E/A) experiment
Load the configuration file *ch5722a.cfg* and run a simulation. Run several simulations using different values of d21. This delay in conjunction with the delay d20 has an important effect on the experiment sensitivity. Because both gradients are applied during one part of the refocusing spin echo element for optimum signal intensity the 180° pulse p11 must be applied in the middle of the element. To achieve this timing delays d20 and d21 must be adapted to the gradient pulse length p16 and the delay d4.

(b) Gradient selected HSQC(TPPI) experiment
Load the configuration file *ch722b.cfg* and run a gradient selected HSQC experiment with TPPI detection. Compare the result with the similar HSQC experiment under echo/antiecho (E/A) detection, i.e. with the same number of scans and same experimental parameters. Extract the rows containing the correlation peaks.

(c) Sensitivity enhanced HSQC(E/A) experiment
Load the configuration file *ch5722c.cfg* that includes the sensitivity enhanced HSQC experiment. Study the signal enhancement of this pulse sequence as an additional exercise.
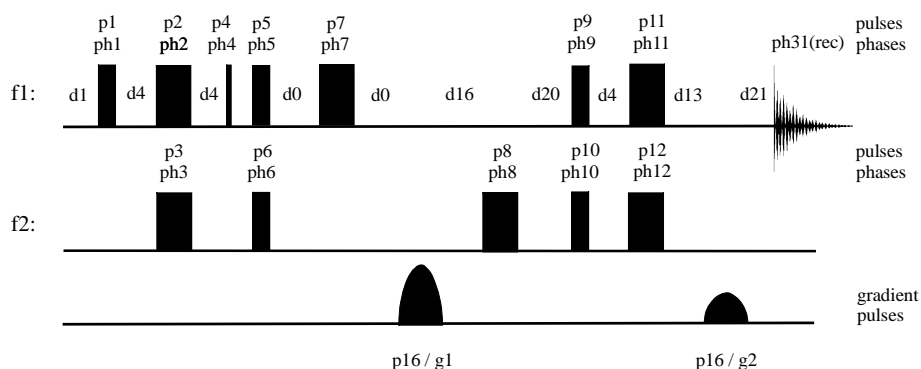
The gradient selected HSQC(E/A) experiment.

ph1(ph1, ph2, ph3, ph4, ph9, ph11,   p1(p1, p5, p9): 90° pulse (f1)
   ph 12)=0   p2(p2, p7, p11): 180° pulse (f1)
ph2(ph5)=0   p3(p6, p10): 90° pulse (f2)
ph3(ph6)=(0 2)   p4(p3, p8, p12): 180° pulse (f2)
ph4(ph8, ph10)=(0)$_4$(2)$_4$ p16: gradient pulse
ph5(ph7)=(0)$_2$(2)$_2$ p20(p4): trim pulse, ~ 1 ms (f1) (This
ph31=(0 2)$_2$(2 0)$_2$ pulse is omitted in the enclosed sequence
                                           file)

d0 = incremented delay (f1), d1 = relaxation delay, d4 = 1 / (4 • ^{1}J(C, H));
d13 = switch delay, gradient recovery delay, d20 = d(p16) + d16 + d(p2) + 2 • d0,
d21 = d4 - d(p16) - d13

gradient ratio:	constants	nuclei
(g1 : g2)(g1 : g2)	(80 : 20)(80 : -20)	^{13}C/^{1}H
(g1 : g2)(g1 : g2)	(80 : 8)(80 : -8)	^{15}N/^{1}H

5.7.3 ^{n}X, ^{1}H HMBC Experiment

The heteronuclear correlation experiment to detect connectivities between protons and ^{n}X nuclei separated by one bond is only the first step of a structure analysis. The next step is to obtain information about the connectivity of these individual CH$_n$ groups using the HMBC experiment. In addition to suppressing ^{1}J(^{n}X, H,) correlation signals this experiment also shows connectivities to non-proton bearing ^{n}X nuclei such as quaternary carbon atoms which were not detected by a ^{1}J(^{13}C, ^{1}H) correlation experiment. If gradient selection is not used in the experiment a BIRD sequence is implemented to suppress the signals from the ^{12}C isotopomers with have nearly the same proton resonance as the ^{13}C isotopomer. Unfortunately, the residual t1-noise of the ^{12}C magnetization often prevents analysis of dilute samples. Gradient selection completely removes the signals of the ^{12}C isotopomers making the BIRD filter unnecessary. In addition gradient selection removes the need for time-consuming phase cycling and

converting the experiment to a one scan per increment experiment. In real molecules $^1J(H, C)$ has a range of values which cause artefacts due to partially unsuppressed ^1J correlation signals. One possible improvement suggested is the ACCORD-HMBC experiment [5.172].

Nowadays, structure analysis also requires the accurate determination of long-range coupling constants. However in the standard HMBC experiment signals in the f1 dimension are modulated by H, H coupling and new improved sequences that bypass this modulation have been developed. In the GSQMBC [5.201] sequence homonuclear coupling which evolves during evolutionary delay periods are refocused using 180° refocusing pulses. The CT-HMBC [5.171] bypasses homonuclear coupling effects in a different way by expanding the sequence by two delays to generate a constant-time experiment. Although the t1 period is incremented, the sequence length is held constant by two variable delays. The constant time for homonuclear coupling evolution in different experiments leads to signals in the f1 dimension, which are not split by homonuclear coupling.

Sequence features:

Purpose / principles:	Correlation of ^1H and ^nX signals by scalar long range $^nJ(^1H, ^nX)$ coupling, n = 2, 3, low-pass filter to suppress $^1J(^1H, ^nX)$ coupling, ^1H detection, intensity enhancement by polarization transfer
Variants:	HMBC [5.202], J-HMBC [5.203], TANGO-SL-HMBC [5.204], CT-HMBC [5.171], GSQMBC [5.201], ACCORD-HMBC [5.172], IMPEACH-HMBC and CIGAR-HMBC [5.173, 5.174, 5.175]

With respect to the pulse sequence layout, the HMBC experiment is essentially a HMQC experiment incorporating a low-pass filter to suppress the one-bond correlation peaks. The low-pass filter, consists of a delay $d2 = 1/(2 \bullet {}^1J(C, H))$ and a 90° ^{13}C pulse, which transfers the $^1J(C, H)$ coherence into a multiple quantum state. In a second period coherences which are generated by $^nJ(C, H)$ evolution are also transferred to a multiple quantum state by a 90° ^{13}C pulse but with a different phase in relation to the first 90° ^{13}C pulse of the low-pass filter. A combination of appropriate receiver phase cycling and pulse phase cycling enables the exclusive detection of $^nJ(C, H)$ correlation peaks in the 2D experiment.

5.7.3.1 Check it in NMR-SIM

Open the configuration file *ch5731.cfg*. Create the HMBC pulse sequence as shown in the scheme below saving the new sequence files with the name *myhmbc2.seq*. Check the new pulse sequence using the test spin system *chlongrg.ham* (calculation time approximately 3 minutes).
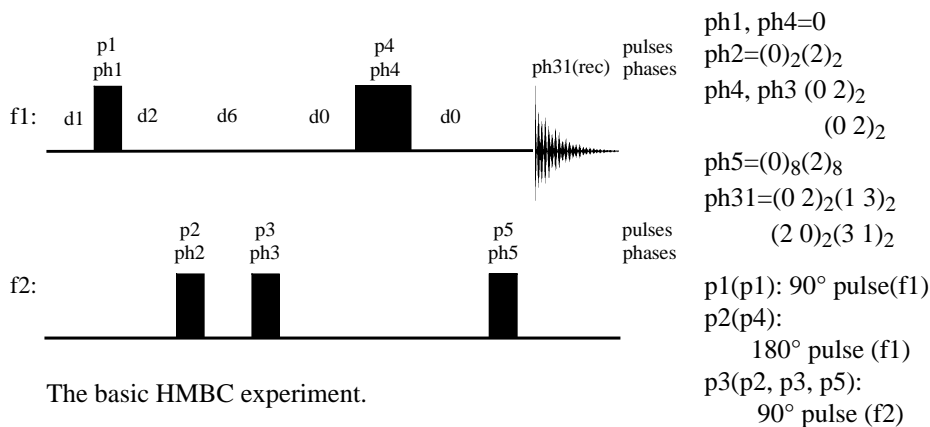
The basic HMBC experiment.

ph1, ph4=0
ph2=$(0)_2(2)_2$
ph4, ph3 $(0\ 2)_2$
$\quad\quad\quad (0\ 2)_2$
ph5=$(0)_8(2)_8$
ph31=$(0\ 2)_2(1\ 3)_2$
$\quad\quad\quad (2\ 0)_2(3\ 1)_2$

p1(p1): 90° pulse(f1)
p2(p4):
$\quad$ 180° pulse (f1)
p3(p2, p3, p5):
$\quad$ 90° pulse (f2)

d0: incremented delay (f1), d1: relaxation delay, d2: = $1 / (2 \bullet {}^1J(C, H))$; d6: = $1 / (2 \bullet {}^nJ(C, H))$,

Gradient selection can be implemented in the HMBC experiment in an analogous manner to the HMQC experiment.

5.7.3.2 Check it in NMR-SIM

Load the configuration file *ch5732.cfg* and run a simulation. Inspect the spectrum for residual ${}^1J(C, H)$ correlation peaks and compare their intensity with the same peaks of the phase cycled HMBC experiment of *Check it 5.7.3.1*.
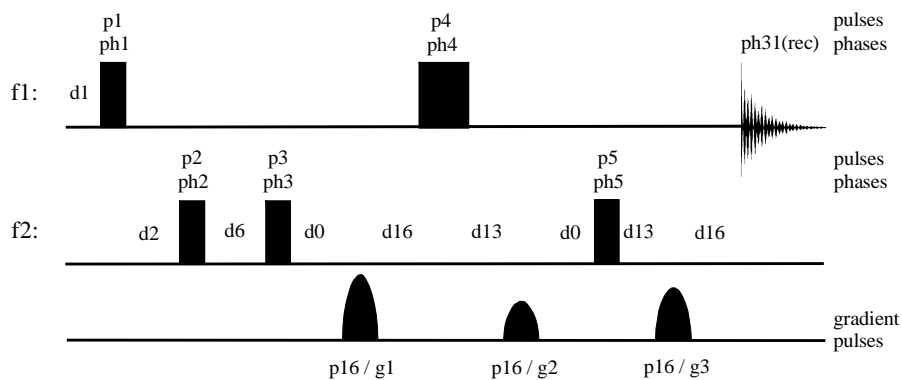
The gradient selected HMBC experiment.

ph1(ph1) =0	ph4(ph3)=(0 2)	p1(p1): 90° pulse (f1)
ph2(ph4)=0	ph5(ph5)=0	p2(p4): 180° pulse (f1)
ph3(ph2)=0	ph31=(0 2)	p3(p2, p3, p5): 90° pulse (f2)

d0: incremented delay (f1), d1: relaxation delay, d2: = $1 / (2 \bullet {}^1J(C, H))$; d6: = $1 / (2 \bullet {}^nJ(C, H))$, d13: switch delay, d16: gradient recovery delay

gradient ratio:	constants	nuclei
(g1 : g2 : g3)	(50 : 30 : 40)	$^{13}C/^1H$
(g1 : g2 : g3)	(70 : 30 : 50)	$^{15}N/^1H$

5.8 Building Blocks and Elements - Part Three

This last section on building blocks will examine BIRD related sequence units and filter elements. It might appear strange to separate the BIRD and TANGO sequence element from other filters but the BIRD element is an extremely versatile element being used for both filter and purging elements and as such merits a section in its own right.

5.8.1 BIRD, TANGO and BANGO as members of the same family

The combination of pulses and delays shown in Fig. 5.30 is a very versatile unit or "sandwich" which has been used for a variety of different purposes [5.205, 5.206, 5.207]. If the value of the delay d2 is based on a specific scalar coupling constant the combination serves as an INEPT unit for the evolution of multiple quantum coherence starting from longitudinal magnetization. If the unit is extended by an additional delay d3, which corresponds to the apparent relaxation time the BIRD-d7 element is obtained This element can be used to discriminate coherences which evolve during both the d2 delays from magnetization which are not influenced by coupling. An early application of this unit was in ^{13}C, ^1H correlation experiments, especially HMBC experiment to suppress ^1H magnetization of ^{12}C isotopomers. The BIRD filter can also be used for suppression of multiple quantum coherence so that in ^{13}C detected ^1H, ^{13}C correlation experiment the homonuclear coupling is suppressed. Another modification which is used in several pulse sequences is to substitute pulse p3 by a 45° pulse which enables a phase selection of coherences that have evolved during the d2 delays and the transverse magnetization which has remained unchanged during the whole sequence except for a phase shift. This modification creates the well-known TANGO sequence.
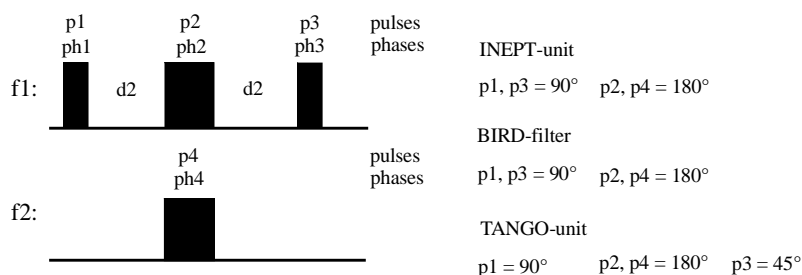
Fig. 5.30: The building block: INEPT-, BIRD- and TANGO-unit.

A more theoretical description using CARTESIAN product operators is given in Table 5.23.

Table 5.23:   The sequences BIRD and TANGO(1), (2).

	pulses	phases	spin system	
			inital state	**final state**
BIRD	p1 = p3 = 90°	ph1 = 0; ph2 = 0; ph3 = 0; ph4 = 0	Iz	-Iz
			Iz + Sz	Iz
TANGO-(1)[1]	p1 = 135°; p3 = 45°	ph1 = 0; ph2 = 0; ph3 = 0; ph4 = 0	Iz	Iz
			Iz + Sz	Iy
TANGO-(2)[1]	p1 = p3 = 45°	ph1 = 0; ph2 = 1; ph3 = 2; ph4 =0	Iz	-Iz
			Iz + Sz	-Iy

[1]The labels TANGO-(1) and -(2) are only used in the present discussion.

NMR-SIM is an extremely well equipped to study the performance of such sequence units and to examine the limitations and possible improvements of such elements.

The TANGO sequence unit
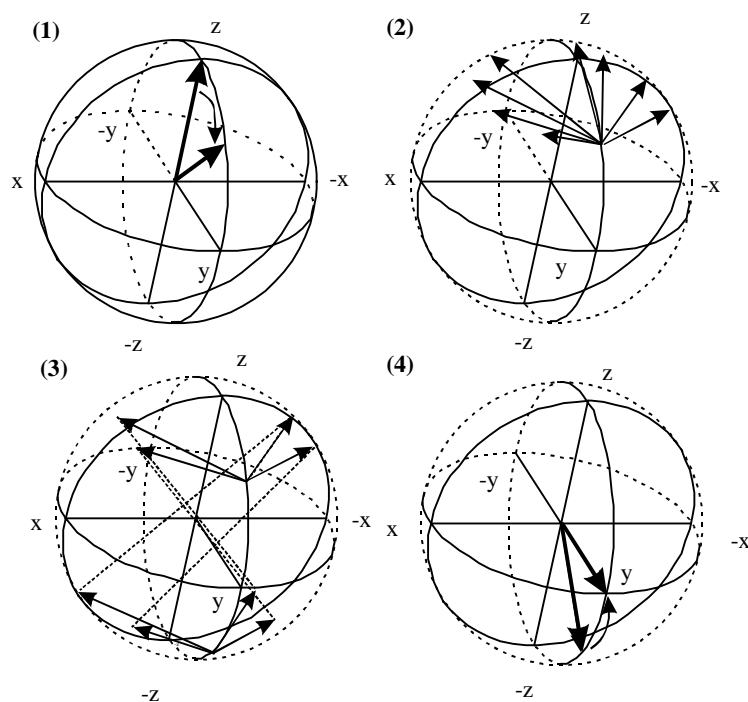
Fig. 5.31:   TANGO-45 pulse sequence unit evolution of $^{13}C^1H$ spin groups (1) after the first 45° ^1H pulse, (2) after the first 180° ^1H pulse, (3) evolution after the 180° ^{13}C pulse, (4) after the second 45° ^1H pulse.

5.8.1.1 Check it in NMR-SIM

Study the TANGO135 sequence using several $^{13}C^1H$ groups with different values of $^1J(^{13}C, ^1H)$. Define a spin system for each group (molecule statement) and include the ^1H signal of the ^{12}C isotopomer. Use the configuration file *ch5811.cfg* which loads the TANGO sequence.

ph1(ph1, ph2, ph4)=0 0 2 2 1 1 3 3
ph2(ph3)=0 2 2 0 1 3 3 1
ph31(rec)=0 0 2 2 1 1 3 3

p1(p1): 135° pulse (f1)
p2(p2): 180° pulse (f1)
p3(p4): 45° pulse (f1)
p4(p3): 180° pulse (f2)

The TANGO-135 sequence unit.

d1: relaxation delay
d2: = $1/(2 \cdot {}^1J(C, H))$
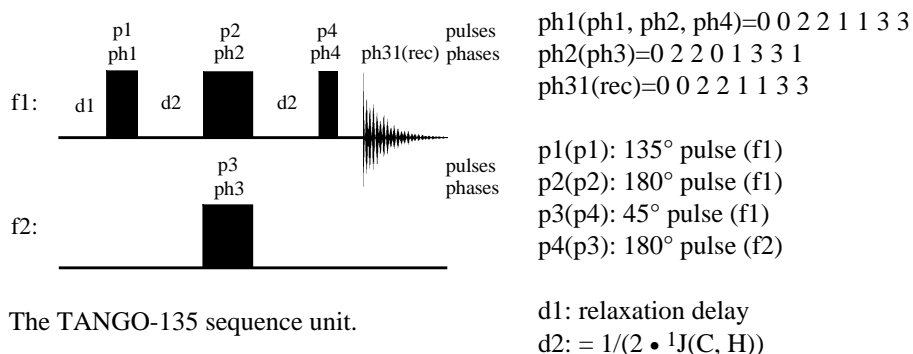
The BIRD-pulse

5.8.1.2 Check it in NMR-SIM

Using the configuration file *ch5812.cfg* as basis, write a pulse sequence according to the scheme shown below. Run a simulation to test the efficiency of the ^{12}C coherence suppression for several protons with a variety of T_1 relaxation times.

p1(p1, p4, p5): 90° pulse (f1)
p2(p2): 180° pulse (f2)
p4(p3): 180° pulse (f2)

d1: relaxation time
d2: = $1 / (2 \cdot {}^1J(^{13}C, {}^1H))$
d7: ≈ T_1(approx.) • ln2
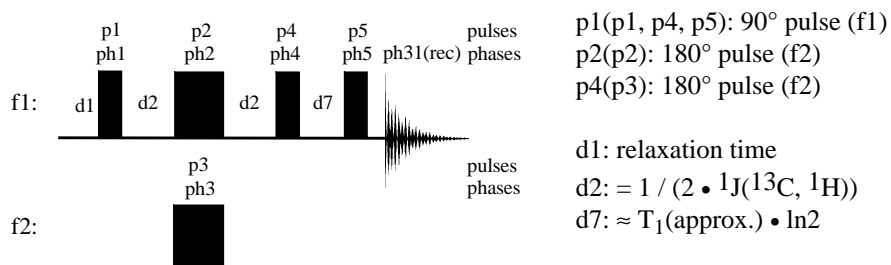
The BIRD-d_7 element

5.8.2 Filter elements: z-Filter, Multiple quantum Filter and Low-Pass Filter

Filters play an important part in pulse sequences and throughout this course a variety of filters has been introduced and their performance tested. Enhancing signal intensity is worthless if strong artefacts are also present.

- The double quantum filter: In homonuclear COSY the DQF plays an important role for phase sensitive spectra filtering out the dispersive coherence contribution to diagonal peaks.
- The z-filter: In spinlock sequences and selective 1D COSY experiments the z-filter improved the artefact suppression of accumulated experiments.
- The low-pass filter: Without the low-pass filter HMBC spectra would be very overcrowded by one-bond correlation peaks.

The last two *Check its* reveal that the efficiency of these filters depends upon the experimental and spin system parameters.

The low-pass filter

5.8.2.1 Check it in NMR-SIM

Load the configuration file *ch5821.cfg*. Edit a spin system file consisting of five $^{13}C^1H$ groups with values of $^1J(^{13}C, {}^1H)$ of 200, 180, 160, 140 and 120 Hz. Set the ^{13}C chemical shifts to 10, 20, 30, 40 and 50 ppm and the chemical shift of the associated ^1H nuclei to 0 ppm. Define a $^{13}C^1H$ group where both the ^{13}C and ^1H chemical shift is 0 ppm and with a ^{13}C, ^1H coupling constant of 8 Hz typical of a long-range $^2J(^{13}C, {}^1H)$ coupling constant. Save the spin system with a suitable filename. Amend the pulse sequence from *Check it 5.8.2.1* by adding an 90° ^1H pulse p4 which is executed simultaneously with pulse p3. Modify the phase cycling to obtain the best results for the new sequence.

ph1(ph1)=0
ph2(ph2)=0 2
ph3(ph3)=1
ph4(ph4)=0
ph31=0

p1(p1, p3): 90° pulse (f2)
p2(p2, p4): 90° pulse (f1)
d2: = $1/(2 \cdot {}^1J(^{13}C, {}^1H))$
d3: = $1/(4 \cdot {}^nJ(^{13}C, {}^1H))$
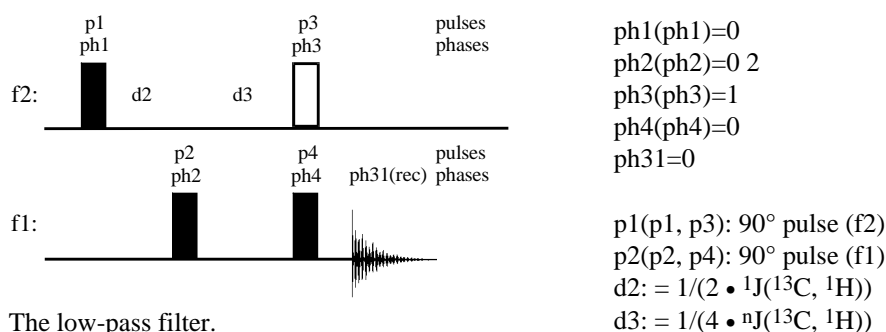
The low-pass filter.
(Pulse p3 is not part of the proper low-pass filter.).

The zz-gradient filter [5.208, 5.209]

5.8.2.2 Check it in NMR-SIM

Edit a pulse sequence according to the scheme below. Test the new pulse sequence with a spin system containing a combination of $^{13}C^1H$ and $^{12}C^1H$ groups.

ph1(ph1, ph2, ph3, ph5)=0
ph2(ph 4)=1
ph31=0

p1(p1, p4, p5): 90° pulse (f1)
p2(p2): 180° pulse (f1)
p4(p3): 180° pulse (f2)
p16: gradient pulse

d1: relaxation delay
d2: = $1/(4 \cdot {}^1J(^nX, {}^1H))$
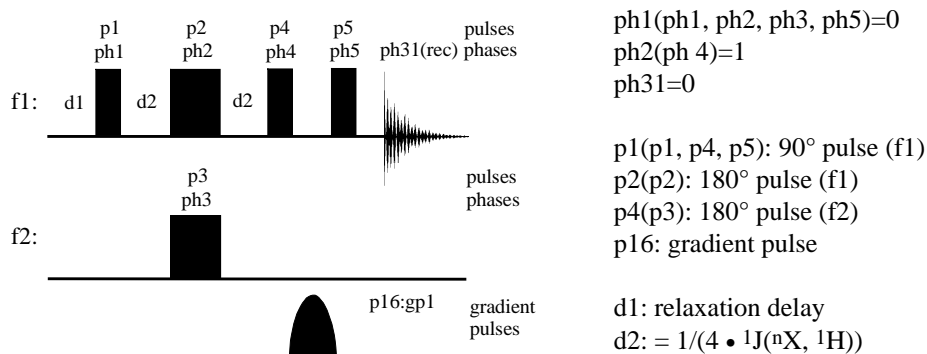
The zz-gradient filter.

5.9   References

[5.1] Braun, S., Kalinowski, H. O., Berger, S., *150 and More Basic NMR Experiments*, 2nd Ed., Weinheim, Wiley-VCH, 1998.

[5.2] Cavanagh, J., Fairbrother, W. J., Palmer, A. G. III, Skelton, N. J*., Protein NMR Spectroscopy - Principles and Practice*, San Diego, Academic Press, 1995.

[5.3] Ernst R. R., Bodenhausen, G., Wokaun, A., *Principles of Nuclear Magnetic Resonance in One and Two Dimensions*, Oxford, Clarendon Press, 1994.

[5.4] Harris, R. K., *Nuclear Magnetic Resonance Spectroscopy*, Harlow, Longman Scientific & Technical, 1986.

[5.5] Ernst, R. R., Anderson, W. A., Rev. Sci. Instrum. 1966, *37*, 93.

[5.6] Jones, D. E., Sternlicht, H., J. Magn. Reson. 1972, *6*, 167 - 182.

[5.7] P. Xu, Wu, X.-L., Freeman, R., J. Magn. Reson. 1989, *84*, 198 - 203.

[5.8] Kessler, H., Oschkinat, H., Griesinger, C., Bermel, W., J. Magn. Reson. 1986, *70*, 106 -133.

[5.9] Dalvit, C., Bovermann, G., Magn. Reson. Chem. 1995, *33*, 156 - 159.

[5.10] Fäcke, T., Berger, S., J. Magn. Reson. Ser. A, 1995, *113*, 114. - 117

[5.11] v. Philipsborn, W., Angew. Chem. 1971, *83*, 470 - 484.

[5.12] Guéron, M., Plateau, P., Decorps, M., Prog. NMR Spectrosc. 1991, *23*, 135 - 209.

[5.13] Patt, S. L., Sykes, B. D., J. Chem. Phys. 1972, *56*, 3182 - 3184.

[5.14] Guéron, M., Plateau, P., J. Am. Chem. Soc. 1982, *104*, 7310 - 7311.

[5.15] Piotto, M., Saudek, V., Sklenár, V, J. Biomol. NMR, 1992, *2*, 661 - 665.

[5.16] Hwang, T, L., Shaka, A. J., J. Magn. Reson. Ser. A, 1995, *112*, 275 - 279.

[5.17] Sklenár, V., Piotto, M., Leppik. R., Saudek, V., J. Magn. Reson. Ser. A, 1993, *102*, 241 - 245.

[5.18] Wang, Ch., Pardi, A., J. Magn. Reson. 1987, *71*, 154 - 158.

[5.19] Liu, M., Mao, X.-a., Ye, Ch., Huang, H., Nicholson, J. K., Lindon, J. C., J. Magn. Reson. 1998, *132*, 125 - 129.

[5.20] Pachler, K. G. R.., Wessels, P. L., J. Magn. Reson. 1973, *12*, 337 - 339.

[5.21] Koppelmann, S., Oimann, S., Hahn, J., GIT Fachz. Lab. 1994, *38*, 83 - 85.

[5.22] Aue, W. P., Karhan, J., Ernst, R. R., J. Chem. Phys. 1976, *64*, 4226 - 4227.

[5.23] Morris, G. A., J. Magn. Reson.1981, *44*, 277 - 284.

[5.24] Kozminski, W., Bienz, S., Bratovanov, S., Nanz, D., J. Magn. Reson. 1997, *125*, 193 - 196.

[5.25] Bodenhausen, G., J. Magn. Reson. 1980, *39*, 175 - 179.

[5.26] Bax, A., Freeman, R., J. Am. Chem. Soc. 1982, *104*, 1099 - 1100.

[5.27] Hricovini, M., Liptaj, T., Magn. Reson. Chem. 1989, *27*, 1052 - 1056.

[5.28] Ochs, M. Berger, S., Magn. Reson. Chem. 1990, *28*, 994 - 997.

[5.29] Liu, M., Farrant, R. D., Gillam, J. M., Nicholson, J. K., Lindon, J. C., J. Magn. Reson. Ser. B, 1995, *109*, 275 - 283.

[5.30] Coxon, B., J. Magn. Reson. 1986, *66*, 230 - 239.

[5.31] Jippo, T., Kamo, O., Nagayama, K., J. Magn. Reson. 1986, *66*, 344 - 348.

[5.32] Kozminski, W., Nanz, D., J. Magn. Reson. 1997, *124*, 383 - 392.

[5.33] Griesinger, C., Sorensen, O. W., Ernst, R. R., J. Am. Chem. Soc. 1985, *107*, 6394 - 6396.

[5.34] Müller, L., J. Magn. Reson. 1987, *72*, 191 - 196.

[5.35] Marion, D., Bax, A., J. Magn. Reson. 1988, *80*, 528 - 533.

[5.36] Xu, G., Evans, J. S., J. Magn. Reson. Ser. A 1996, *123*, 105 - 110.

[5.37] Kozminski, W., J. Magn. Reson. 1999, *137*, 408 - 412.

[5.38] Poppe, L., van Halbeek, H., J. Magn. Reson. 1991, *92*, 636 - 641.

[5.39] Poppe, L., van Halbeek, H., J. Magn. Reson. 1991, *93*, 214 - 217.

[5.40] Krishnamurthy, V. V., J. Magn. Reson. Ser. A, 1996, *121*, 33 - 41.

[5.41] Freeman, R., Keeler, J., J. Magn. Reson. 1981, *43*, 484 - 487.

[5.42] Bodenhausen, G., Freeman, R., Turner, D. L., J. Magn. Reson. 1977, *27*, 511 - 514.

[5.43] Bodenhausen, G., Turner, D. L., J. Magn. Reson. 1980, *41*, 200 - 206.

[5.44] Brown, D. W., Nakashima, T. T., Rabenstein, D. L., J. Magn. Reson. 1981, *45*, 302 - 314.

[5.45] Bendall, M. R., Doddrell, D. M., Pegg, D. T., J. Am. Chem. Soc. 1981, *103*, 4603 - 4605.

[5.46] Levitt, M. H., Freeman, R., J. Magn. Reson. 1980, *39*, 533 - 538.

[5.47] Le Cocq, Ch., Lallemand, J.-Y. J. Chem. Soc. Chem. Commun. *1981*, 150 - 152.

[5.48] Patt, S. L., Shoolery, J. N., J. Magn. Reson. 1982, *46*, 535 - 539.

[5.49] Madsen, J. Ch., Bildsoe, H., Jakobsen, H. J., J. Magn. Reson. 1986, *67*, 243 - 257.

[5.50] Torres, A. M., Nakashima, T. T., McClung, R. E. D., J. Magn. Reson. Ser. A., 1993, *101*, 285 - 294.

[5.51] Bildsøe, H., Dønstrup, S., Jakobsen, H. J., Sørensen, O. W., J. Magn. Reson. 1983, *53*, 154 - 162.

[5.52] Sørensen, O. W., Dønstrup, S., Bildsøe, H., Jakobsen,. H. J., J. Magn. Reson. 1983, *55*, 347 - 354.

[5.53] Sørensen, O. W., J. Magn. Reson. 1984, *57*, 506 - 512.

[5.54] Morris, G. A., Freeman, R., J. Am. Chem. Soc. 1979, *101*, 760 – 762.

[5.55] Freeman, R., Mareci, T. H., Morris, G., J. Magn. Reson. 1981, 42, 341 - 345.

[5.56] Burum, D. P., Ernst, R. R., J. Magn. Reson. 1980, 39, 163 - 168.

[5.57] Mohebbi, A., Gonen, O., J. Magn. Reson. Ser. A, 1996, *123*, 237 - 241.

[5.58] Bax, A., J. Magn. Reson. 1984, 57, 314 - 318.

[5.59] Sørensen, O. W., Ernst, R. R., J. Magn. Reson. 1983, *51*, 477 - 489.

[5.60] Schenker, K. V., v. Philipsborn, W., J. Magn. Reson.1986, *66*, 219 - 229.

[5.61] Wimperis, S., Bodenhausen, G., J. Magn. Reson. 1986, *69*, 264 - 282.

[5.62] Sørensen, O. W., Madsen, J. Ch., Nielsen, N. Ch., Bildsoe, H., Jakobsen, H. J., J. Magn. Reson. 1988, 77, 170 - 174.

[5.63] Homer, J., Perry, M. C., J. Chem. Soc. Chem. Commun. *1994*, 373 - 374.

[5.64] Homer, J., Perry, M. C., J. Chem. Soc. Perkin Trans. I, *1995*, 533 - 536.

[5.65] Doddrell, D. M., Pegg, D. T., Bendall, M. R., J. Magn. Reson. 1982, *48*, 323 - 327.

[5.66] Bendall, M. R., Pegg, D. T., Doddrell, D. M., Field, J.,J. Magn. Reson. 1983, *51*, 520 - 526.

[5.67] Burger, R., Bigler, P., J. Magn. Reson. 1998, *135*, 529 - 534.

[5.68] Kessler, H., Schmieder, P., Kurz, M., J. Magn. Reson. 1989, *85*, 400 - 405.

[5.69] Bulsing, J. M., Brooks, W. M., Field, J., Doddrell, D. M., Chem. Phys. Lett. 1984, *104*, 229 - 234.

[5.70] Torres, A. M., McClung, R. E. D., Nakashima, T. T., J. Magn. Reson. 1990, *87*, 189 - 193.

[5.71] Bigler, P., Kamber, M., Chimia, 1986, *40*, 51 - 54.

[5.72] Köver, K. E., Batta, G., Magn. Reson. Chem. 1989, *27*, 68 - 71.

[5.73] Bendall, R. M., Pegg, D. T., J. Magn. Reson. 1983, *53*, 144 - 148.

[5.74] Bendall, M. R., Pegg, D. T., J. Magn. Reson. 1984, *59*, 237 - 249.

[5.75] Pegg, D. T., Bendall, M. R., J. Magn. Reson. 1984, *60*, 347 - 351.

[5.76] Pegg, D. T., Doddrell, D. M., Bendall, M. R., J. Magn. Reson. 1983, *51*, 264 - 269.

[5.77] Bulsing, J. M., Brooks, W. M., Field, J., Doddrell, D. M., J. Magn. Reson. 1984, *56*, 167 - 173.

[5.78] Schmieder, P., Leidert, M., Kelly, M., Oschkinat, H.,J. Magn. Reson. 1998, *131*, 199 - 202.

[5.79] Homer, J., Perry, M. C., Palfreyman, S. A., J. Magn. Reson. 1994, *125,* 20 - 27.

[5.80] Bloch, F., Hansen, W. W., Packard, M. E., Phys. Rev. 1946, *49*, 127.

[5.81] Bloch, F, Phys. Rev. 1946, *70*, 460 - 474.

[5.82] Gupta, R. K., Ferretti, J. A., Becker, E. D., Weiss, G. H., J. Magn. Reson. 1980, *38*, 447 - 452.

[5.83] Carr, H. Y., Purcell, E. M., Phys. Rev. 1954, *94*, 630 - 638.

[5.84] Kingsley, P. B., Concepts Magn. Reson. 1999, *11*, 29 - 40.

[5.85] Hahn, E. L., Phys. Rev. 1950, *80*, 580 - 594.

[5.86] Wu, X.-L., Xu, P., Freeman, R., J. Magn. Reson. 1989, *83*, 404 - 410.

[5.87] Xu, P., Wu, X.-L., Freeman, R., J. Magn. Reson. 1992, *99*, 308 - 322.

[5.88] Kessler, H., Mronga, S., Gemmecker, G., Magn. Reson. Chem. 1991, *29*, 527 - 557.

[5.89] Berger, S., Prog. NMR Spectr. 1997, *30*, 137 - 156.

[5.90] Bauer, Ch., Freeman, R., Frenkiel, T., Keeler, J., Shaka, A. J., J. Magn. Reson. 1984, *58*, 442 - 457.

[5.91] Emsley, L., Bodenhausen, G., J. Magn. Reson. 1989, *82*, 211 - 221.

[5.92] Friedrich, J., Davies, S., Freeman, R., J. Magn. Reson. 1987, *75*, 390 - 395.

[5.93] Emsley, L., Bodenhausen, G., Chem Phys. Lett. 1990, *165*, 469 - 476.

[5.94] Krishnamurthy, V. V., Casida, J. E., Magn. Reson. Chem. 1987, *25*, 837 - 842.

[5.95] Lunati, E., Cofrancesco, P., Villa, M., Marzola, P., Osculati, F., J. Magn. Reson. 1998, *134*, 223 – 235.

[5.96] Nuzillard, J.-M., Freeman, R., J. Magn. Reson. Ser A, 1994, *110*, 253 - 256.

[5.97] Warren, W. S., J. Chem. Phys. 1984, *81*, 5437 - 5448.

[5.98] Geen, H., Freeman, R., J. Magn. Reson. 1991, *93*, 93 - 141.

[5.99] Boehlen, J.- M., Bodenhausen, G., J. Magn. Reson. Ser. A, 1993, 102, 293 - 301.

[5.100] Kupce, E, Freeman, R., J. Magn. Reson. Ser. A, 1995, *115*, 273 - 276.

[5.101] Brüschweiler, R., Madsen, J. C., Griesinger, C., Sørensen, O. W.,Ernst, R. R., J. Magn. Reson. 1987, *73*, 380 - 385.

[5.102] (a) De Graaf, R. A., Nicolay, K., Concepts Magn. Reson. 1997, *9*, 247 - 268 (b) Tannus, A., Garwood, M., NMR in Biomed. 1997, *10*, 423 - 434.

[5.103] Slotboom, J., Bovée, W. M. M. J., Concepts Magn. Reson. 1995, *7*, 193 - 217.

[5.104] Kupce, E., Freeman, R., J. Magn. Reson. Ser. A, 1995, *117*, 246 - 256.

[5.105] Kupce, E, Freeman, R., J. Magn. Reson. Ser. A, 1996, *118*, 299 - 303.

[5.106] Slotboom, J., Bovee, W. M. M. J., Concepts Magn. Reson. 1995, *7*, 193 - 217.

[5.107] Goelman, G., Leigh, J. S., J. Magn. Reson. Ser. A 1993, *101*, 136 - 146.

[5.108] Sklenar,V., Starcuk, Z., J. Magn. Reson. 1982, *50*, 495 - 501.

[5.109] Turner, D. L., J. Magn. Reson. 1983, *54*, 146 - 148.

[5.110] Hore, P. J., J. Magn. Reson. 1983, *55*, 283 - 300.

[5.111] Hore, P. J., J. Magn. Reson. 1983, *54*, 539 - 542.

[5.112] Dickinson, N. A., Lythgoe, R. E., Waigh, R. D., Magn. Reson. Chem. 1987, *25*, 996.

[5.113] Levitt, M. H., Roberts, M. F., J. Magn. Reson. 1987, *71*, 576 - 581.

[5.114] Levitt, M. H., J. Chem. Phys. 1988, *88*, 3481 - 3496.

[5.115] Freeman, R., Kempsell, S. P., Levitt, M. H., J. Magn. Reson. 1980, *38*, 453 - 479.

[5.116] Levitt, M. H., Progr. NMR Spectrosc. 1986, *18*, 61 - 122.

[5.117] Bodenhausen, G., Freeman, R., Morris, G. A., J. Magn. Reson. 1976, *23*, 171 - 175.

[5.118] Morris, G. A., Freeman, R., J. Magn. Reson. 1978, *29*, 433 - 462.

[5.119] Geen, H., Wu, X.-L., Friedrich, J., Freeman, R., J. Magn. Reson. 1989, *81*, 646 - 652.

[5.120] Boudot, D., Canet, D., Brondeau, J., Boubel, J. C., J. Magn. Reson. 1989, *83*, 428 -.439.

[5.121] Flood, T. A., Concepts Magn. Reson. 1996, *8*, 119 - 138.

[5.122] Jeener, J., Ampere International Summer School, Basko Polje, Yugoslavia, 1971.

[5.123] Aue, W. P., Bartholdi, E., Ernst, R. R., J. Chem. Phys. 1976, *64*, 2229 - 2246.

[5.124] Bax, A., Freeman, R., Morris, G., J. Magn. Reson. 1981, *42*, 164 - 168.

[5.125] Bax, A., Freeman, R., J. Magn. Reson. 1981, *44*, 542 - 561.

[5.126] Piantini, U., Sorensen , O. W., Ernst, R. R., J. Am. Chem. Soc. 1982, *104*, 6800 - 6801.

[5.127] Griesinger, C., Sorensen, O. W., Ernst, R. R., J. Chem. Phys. 1988, *85*, 6837 - 6852.

[5.128] Griesinger, C., Sorensen, O. W., Ernst, R. R., J. Magn. Reson. 1987, *75*, 474 - 492.

[5.129] Willker, W., Leibfritz, D., Kerssebaum, R., Lohmann, J., J. Magn. Reson. Ser. A, 1993, *102*, 348 - 350.

[5.130] Zektzer, A. S., Quast, M. J., Linz, G. S., Martin, G. E., McKenney, J. D., Johnston, M. D., Castle, R. N., Magn. Reson. Chem. 1986, *24*, 1083 - 1088.

[5.131] Neuhaus, D., Wider, G., Wagner, G., Wüthrich, K., J. Magn. Reson. 1984, *57*, 164 - 168.

[5.132] Delsuc, M. A., Guittiet, E., Trotin, N., Lallemand, J. Y., J. Magn. Reson. 1984, *56*, 163 - 166.

[5.133] Bodenhausen, G, Ernst, R. R., J. Am. Chem. Soc. 1982, *104*, 1304 - 1309.

[5.134] Anderson, W. A., Freeman, R., Reilly, C. A., J. Chem. Phys. 1963, *39*, 1518.

[5.135] Mutzenhardt, P., Brondeau, J., Canet, D., J. Magn. Reson. Ser. A, 1995, *117*, 278 - 284.

[5.136] Bernstein, M. A., Trimble, L. A., Magn. Reson. Chem. 1994, *32*, 107 - 110.

[5.137] Dalvit, C., J. Magn. Reson. Ser. A, 1995, *113*, 120 - 123.

[5.138] Willker, W., Leibfritz, D., Magn. Reson. Chem. 1994, *32*, 665 - 669.

[5.139] Xu, G., Evans, J. S., J. Magn. Reson. Ser. B, 1996, *111*, 183 - 185.

[5.140] Dalvit, C., Ko, S. Y., Böhlen, J. M., J. Magn. Reson. Ser. B, 1996, *110*, 124 - 131.

[5.141] Wagner, G., J. Magn. Reson. 1983, 55, 151 - 156.

[5.142] Eich, G., Bodenhausen, G., Ernst, R. R., J. Am. Chem. Soc. 1982, *104*, 3731 - 3732.

[5.143] Kessler, H., Bermel, W., Griesinger, C., J. Magn. Reson. 1985, *62*, 573 - 579.

[5.144] Bolton, P. H., Bodenhausen, G., Chem. Phys. Lett. 1982, *82*, 139 - 144.

[5.145] Bax, A., J. Magn. Reson. 1983, *53*, 149 - 153.

[5.146] Bolton, P. H., J. Magn. Reson. 1982, *48*, 336 - 340.

[5.147] Bolton, P. H., J. Magn. Reson. 1985, *63*, 225 - 229.

[5.148] Field, L. D., Messerle, B. A., J. Magn. Reson. 1985, *62*, 453 - 460.

[5.149] Edwards, M. W., Bax, A., J. Am. Chem. Soc. 1986, *108*, 918 - 923.

[5.150] Davis, D. G., Bax, A., J. Am. Chem. Soc. 1985, *107*, 2820 - 2821.

[5.151] Braunsweiler, L. Ernst, R. R., J. Magn. Reson. 1983, *53*, 521 - 528.

[5.152] Davies, D. G., Bax, A., J. Am. Chem. Soc. 1985, *107*, 7197 - 7198.

[5.153] Bax, A., Davies, D. G., J. Magn. Reson. 1985, *65*, 355 - 360.

[5.154] Rance, M., J. Magn. Reson. 1987, *74*, 557 - 564.

[5.155] Fäcke, T., Berger, S., J. Magn. Reson. Ser. A, 1995, *113*, 57 - 299.

[5.156] Hurd, R. E., J. Magn. Reson. 1990, *87*, 422 - 428.

[5.157] Crouch, R. C., Davis, A. O., Martin, G. E., Magn. Reson. Chem. 1995, *33*, 889.

[5.158] Davis, D. G., J. Magn. Reson. 1989, *84*, 417 - 424.

[5.159] Spitzer, T., Kuehne, M. E., Bornmann, W., J. Magn. Reson. 1989, *84*, 654 - 657.

[5.160] Sørensen, O. W., Rance, M., Ernst, R. R., J. Magn. Reson. 1984, *56*, 527 - 534.

[5.161] Buddrus, J., Bauer, H., (a) Angew. Chem. Int. Ed. Engl. 1987, *26*, 625 - 643; (b) Angew. Chem. 1987, *99*, 642 - 659.

[5.162] Sørensen, O. W., Freeman, R., Frenkiel, T. A. , Mareci, T. H., Schuck, R., J. Magn. Reson. 1982, *46*, 180 - 184.

[5.163] Sparks, S. W. Ellis, P. D., J. Magn. Reson. 1985, *62*, 1 - 11.

[5.164] Dalvit, C., Bovermann, G., J. Magn. Reson. Ser. A, 1994, *109*, 113 - 116.

[5.165] Weigelt, J., Otting, G., J. Magn. Reson. Ser. A, 1995, *113*, 128 - 130.

[5.166] Bax, A., Freeman, R., Kempsell, S. P., J. Am. Chem. Soc. 1980, *102*, 4849 - 4851.

[5.167] Bax, A., Freeman, R., Frenkiel, T. A., J. Am. Chem. Soc. 1981, *103*, 2102 - 2104.

[5.168] Turner, D. L., J. Magn. Reson. 1982, *49*, 175 - 178.

[5.169] Berger, S., (a) Angew. Chem. Int. Ed. Engl. 1988, *27*, 1196 – 1197; (b) Angew. Chem. 1988, *100*, 1198 - 1199.

[5.170] Kessler, H., Griesinger, C., Zarbock, J., Loosli, H. R., J. Magn. Reson. 1984, *57*, 331- 336.

[5.171] Furihata, K., Seto, H., Tetrahedron Lett. 1998, *39*, 7337 - 7340.

[5.172] Wagner, R., Berger, S., Magn. Reson. Chem. 1998, *36*, 844 - 846.

[5.173] Martin, G. E., Hadden, C. E., Crouch, R. C., Krishnamurthy, V. V., Magn. Reson. Chem. 1999, *37*, 517 - 528.

[5.174] Hadden, C. E., Martin, G. E., Krishnamurthy, V. V., Magn. Reson. Chem. 2000, *38*, 143 - 147.

[5.175] Krishnamurthy, V.V., Russell, D. J., Hadden, Ch. E., Martin, G. E., J. Magn. Reson. 2000, *146*, 232 - 239.

[5.176] Zangger, K., Armitage, I. M., Magn. Reson. Chem. 2000, *38*, 452 - 458.

[5.177] Hadden, Ch., E., Angwin, D. T., Magn. Reson. Chem. 2001, *39*, 1 - 8.

[5.178] Bax, A., Morris, G. A., J. Magn. Reson. 1981, *42*, 501 - 505.

[5.179] Bax, A., J. Magn. Reson. 1983, *53*, 517 - 520.

[5.180] Wilde, J. A., Bolton, P. H., J. Magn. Reson. 1984, *59*, 343 - 346.

[5.181] Rutar, V., J. Magn. Reson. 1984, *58*, 306 - 310.

[5.182] Reynolds, W. F., Hughes, D. W., Perpick-Dumont, M., J. Magn. Reson. 1985, *63*, 413 - 417.

[5.183] Bauer, C., Freeman, R., Wimperis, S., J. Magn. Reson. 1984, *58*, 526 - 532.

[5.184] Kessler, H., Bermel, W., Griesinger, C., J. Am. Chem. Soc. 1985, *107*, 1083 - 1084.

[5.185] Müller, L., J. Am. Chem. Soc. 1979, *101*, 4481 - 4484.

[5.186] Bax, A., Griffey, R. H., Hawkins, B. L., J. Magn. Reson. 1983, *55*, 301 - 315.

[5.187] Tolman, J. R., Clung, J., Prestegard, J. H., J. Magn. Reson. 1992, *98*, 462 - 467.

[5.188] Bax, A., Subramanian, S., J. Magn. Reson. 1986, *67*, 565 - 569.

[5.189] Lerner, L., Bax, A., J. Magn. Reson. 1986, *69*, 375 - 380.

[5.190] Hurd, R. E., John, B. K., J. Magn. Reson. 1991, *91*, 648 - 653.

[5.191] Ruiz-Cabello, J., Vuister, G. W., Moonen, C. T. W., van Gelderen, P., Cohen, J. S., van Zijl, P. C. M., J. Magn. Reson. 1992, *100*, 282 - 302.

[5.192] Willker, W, Leibfritz, D., Kerssebaum, R., Bermel, W., Magn. Reson. Chem. 1993, *31*, 287 - 292.

[5.193] Kövér, K. E., Prakash, O., Hruby, V. J., J. Magn. Reson. 1992, *99*, 426 - 432.

[5.194] Kay, L. E., Keifer, P., Saarinen, T., J. Am. Chem. Soc. 1992, *114*, 10663 - 10665.

[5.195] Shaw, G. L., Stonehouse, J., J. Magn. Reson. Ser. B, 1996, *110*, 91 - 95.

[5.196] Turner, C. J., Connolly, P. J., Stern, A. S., J. Magn. Reson. 1999, *137*, 281- 284.

[5.197] Bodenhausen, G., Ruben, D. J., Chem. Phys. Lett. 1980, *69*, 185 - 188.

[5.198] Sattler, M., Schleucher, J., Schedletzky, O., Glaser, S. J., Griesinger, C., Nielsen, N. C., Sørensen, O. W., J. Magn. Reson. Ser. A, 1996, *119*, 171 - 179.

[5.199] Hu, H., Shaka, A., J. Magn. Reson. 1999, *136*, 54 – 62.

[5.200] Heikkinen, S., Rahkamaa, E., Kilpeläinen, I., J. Magn. Reson. 1997, *127*, 80 - 86.

[5.202] Bax, A. Summers, M. F., J. Am. Chem. Soc. 1986, *108*, 2093 - 2094.

[5.203] Willker, W., Leibfritz, D., Magn. Reson. Chem. 1995, 33, 632 - 638.

[5.204] Mattila, S., Koskinen, A. M. P., Otting, G., J. Magn. Reson. Ser. B, 1995, *109*, 326.

[5.205] Sørensen, O. W., Bull. Magn. Reson. 1994, *16*, 49 - 53.

[5.206] Briand, J., Sørensen , O. W., J. Magn. Reson. 1997, *125*, 202 - 206.

[5.207] Burger, R., Schorn, C., Bigler, P., Magn. Reson. Chem. 2000, *38*, 963 - 969.

[5.208] Otting, G., Wüthrich, K., J. Magn. Reson. 1988, *76*, 569 - 574.

[5.209] Wider, G., Wüthrich, K., J. Magn. Reson. Ser. B 1993, *102*, 239 - 241.

Glossary

ADC	Analog-to-Digital converter
AQ	AcQuisition time
CPD	Composite Pulse Decoupling
CP	Composite Pulse
CW	Continuous Wave
DPFGSE	Double Pulsed Field Gradient Spin Echo
DQ(F)	Double Quantum (Filter)
E/A	Echo/Antiecho
EM	Exponential Multiplication
FID	Free Induction Domain
fn	frequency domain in the nth dimension
Fn	nth radiofrequency channel
FT	Fourier Transformation
GB	GAUSSIAN Broadening factor
GM	GAUSSIAN Multiplication
GL	GAUSSIAN multiplication Line factor
HR	High Resolution
LB	Line Broadening factor
LP	Linear Prediction
NOE	Nuclear Overhauser Enhancement
PO	Product Operator (formalism)
ppm	parts per million
PW	Pulse Width
QSINE	sQuared SINE bell weighting function
Rf, rf	Radio Frequency
SI	frequency domain data SIze
SINE	SINE bell weighting function
SQ	Single Quantum
S/N	Signal-to Noise
SSB	Shift factor of Sine Bell wdw function
TD	Time Domain data size
t_m	mixing time
t_n	time domain in the nth dimension
TRAP	TRAPedoizal window function
wdw function	WinDoW function (apodisation function)

Index